UNIVERSITÀ DEGLI STUDI DI PALERMO

Ingegneria Civile Ambientale – Indirizzo Infrastrutture Viarie
Dipartimento di Ingegneria Civile, Ambientale, Aerospaziale, dei Materiali- DICAM
Ingegneria Civile e Architettura – Strade, ferrovie e aeroporti - ICAR/04

CHARACTERIZATION OF RUBBERIZED ASPHALT FOR RAILWAY SUBBALLASTS

IL DOTTORE
FERNANDO MARTINEZ SOTO

IL TUTOR
Prof. Ing. Gaetano Di Mino

IL COORDINATORE
Prof. Ing. Mario Di Paola

CICLO - XXIX
ANNO CONSEGUIMENTO TITOLO 2017



UNIVERSITÀ DEGLI STUDI DI PALERMO

UNIVERSITÀ DEGLI STUDI DI PALERMO
Ingegneria Civile Ambientale – Indirizzo Infrastrutture Viarie
Dipartimento di Ingegneria Civile, Ambientale, Aerospaziale, dei Materiali - DICAM
Ingegneria Civile e Architettura – Strade, ferrovie e aeroporti - ICAR/04

CHARACTERIZATION OF RUBBERIZED ASPHALT FOR RAILWAY SUB-BALLASTS

IL DOTTORE
FERNANDO MARTINEZ SOTO

IL TUTOR
Prof. Ing. Gaetano Di Mino

IL COORDINATORE
Prof. Ing. Mario Di Paola

CICLO - XXIX
ANNO CONSEGUIMENTO TITOLO 2017

UNIVERSITÀ DEGLI STUDI DI PALERMO
Ingegneria Civile Ambientale – Indirizzo Infrastrutture Viarie
Dipartimento di Ingegneria Civile, Ambientale, Aerospaziale, dei Materiali - DICAM
Ingegneria Civile e Architettura – Strade, ferrovie e aeroporti - ICAR/04

CHARACTERIZATION OF RUBBERIZED ASPHALT FOR RAILWAY SUB-BALLASTS

CARATTERIZZAZIONE DELL'ASFALTO MODIFICATO CON GOMMA RICICLATA PER LO STRATO DI SUB-BALLAST FERROVIARIO

Ph.D. candidate
FERNANDO MARTINEZ SOTO

Supervisor
Prof. Ing. Gaetano Di Mino

Thesis submitted to the University of Palermo for the degree
of Doctor of Philosophy

Palermo, 2017-2018

CICLO - XXIX
ANNO CONSEGUIMENTO TITOLO 2017

UNIVERSITÀ DEGLI STUDI DI PALERMO

CHARACTERIZATION OF RUBBERIZED ASPHALT FOR RAILWAY SUB-BALLASTS

IL DOTTORE
FERNANDO MARTINEZ SOTO

IL TUTOR
Prof. Ing. Gaetano Di Mino

IL COORDINATORE
Prof. Ing. Mario Di Paola

CICLO - XXIX
ANNO CONSEGUIMENTO TITOLO 2017

TABLE OF CONTENTS

Abstract ..... **i**
Acknowledgments ..... **ii**
Author agreement. Declaration ..... **iii**
Financing statement. Certificate of award Marie Curie ..... **iv**
Compendium of publications ..... **v-x**
Chapter 1 - Introduction **1**
1.1. Background 2
1.2. Problem statement 4
1.3. Research methodology 5
1.4. Thesis Layout 7
Chapter 2 – State of the Art **9**
List of Figures Chapter 2 10
2.1. Rail Tracks Structures 11
2.1.1. Track forces and geometry quality 14
2.1.2. Track deterioration 15
2.1.3. Vertical track stiffness 17
2.1.4. Damping vibrations 18
2.1.5. Distresses: ground-borne vibrations and fatigue 19
2.2. Sub-ballast properties 20
2.2.1. Permeability 21
2.2.2. Bearing capacity and stress reduction 21
2.2.3. Requirements 22
2.3. Bituminous sub-ballast 22
2.3.1. Introduction 23
2.3.2. Bituminous mixes in railway construction 23
2.3.3. Properties and advantages 24
2.3.4. Types of bituminous layer railway track 24
2.3.5. Functions and design 25
2.3.6. International asphalt track-bed applications 26
2.3.7. Other studies 28
2.3.8. Inconvenient and Disadvantages 29
2.4. Rubberized Asphalt Sub-ballast 29
2.4.1. Introduction 29
2.4.2. Literature review 30
2.4.3. Rubberized asphalt 31
2.4.4. Crumb Rubber Modifier 33
2.4.5. Historical Use of rubber in Asphalt materials 34
2.4.5.1. Wet process 35
2.4.5.2. Dry process 35
2.4.6. Technologies and production 37
2.4.7. Dry method of adding crumb rubber modifier 38
2.4.8. Evaluation of Rubber Modified Asphalt Concrete mixes 39
2.4.9. Benefits and drawbacks of RUMAC mixtures 40
2.4.10. Other applications of End-of-Life tires in railways 40
2.4.11. Conclusions of Rubberized Asphalt Sub-ballast 42
2.4.12. Life-Cycle Cost Analysis for RUMAC 42
2.4.12.1. Tools LCA for rail infrastructure 43
2.5. Conclusions of the State of the Art 44
Chapter 3 – Research objectives **45**
3.1. Abstract 46
3.2. Introduction 47
3.3. Scope of the study 47
3.4. Purposes of the research 48
3.5. Main objectives pursued 49

3.6. Secondary objectives 50
Chapter 4 – Methodology 51
List of Figures Chapter 4 52
List of Tables Chapter 4 54
4.1. Introduction 55
4.2. Constituent Materials 57
4.3. Technical aspects of bituminous sub-ballast: a review 59
4.4. Materials: Aggregates 60
4.5. Materials: Bitumen [composition and structure] 68
4.5.1. Bitumen Rheology 69
4.5.2. Performance grade of Bitumen 69
4.5.3. Penetration & "Ring-and-ball" Softening point tests 70
4.5.4. Viscosity. Brookfield viscometer 71
4.5.5. Thermal parameters for Superpave 72
4.5.6. Bitumen-filler and Dust/Asphalt ratio 74
4.6. Materials: Crumb/Ground rubber modifier 75
4.7. Bituminous asphalt mixtures 79
4.7.1. Classification of asphalt mixture according to grading 79
4.7.2. Conventional Hot-Mix-Asphalt (HMA) 80
4.7.3. Plusride mixtures 81
4.7.4. Generic dry mixtures (RUMAC) 81
4.7.5. Description of final mixtures studied 82
4.8. Methods 85
4.9. Methodology 01: "Volumetric Mixture design" 85
4.9.1. Superpave system: a literature review 85
4.9.2. Characterization of the mixtures: "SGC mix-design" 87
4.9.3. Specifications of the gyratory compactor 88
4.9.4. Adjusting the Energetic parameters: Ndesign 89
4.9.5. Air Temperature 91
4.9.6. Traffic levels (ESAL) 92
4.9.7. Bulk specific gravity and Maximum Density 92
4.9.8. Air voids, Va 95
4.9.9. Voids in the Mineral Aggregates, VMA 96
4.9.10. Voids Filled with Asphalt, VFA 96
4.9.11. Effective Binder content, Vbe 97
4.9.12. Laboratory protocol of execution 98
4.9.13. Densification curves [%Γmm-LogN] 101
4.9.14. Quantitative extraction of Asphalt binder 101
4.10. Methodology 02: "Marshall mix-design" 102
4.10.1. Comparison SGC with Marshall methodology 102
4.10.2. Performance test: Water Sensitivity (ITSR) 103
4.11. Methodology 03: "Asphalt Slab Roller Compactor" 105
4.11.1. Equipment for Roller Compacted slabs 105
4.11.2. Sample production. Types of mixtures 106
4.12. Methodology 04: "Fatigue cracking resistance" 108
4.12.1. Equipment: UGR_FACT 108
4.12.2. Test conditions of the UGR_FACT Test Method 109
4.12.3. Fatigue Testing plan 110
4.12.4. Sample characteristics 111
4.13. Methodology 05: "NDT-FFRC" 111
4.13.1. Determining Stiffness, Poisson and Shear modulus from NDT-FFRC test 111
4.14. Work plan 113
4.15. Conclusions and expectations 114
Chapter 5 – Mechanistic Structural design for railways 115
List of Figures Chapter 5 116
List of Tables Chapter 5 116
5.1. Introduction 117
5.2. Scope 118
5.3. A review of model factors 118
5.4. Framework of rail modelling 120

5.5. Materials properties 120
5.6. Damage analysis: Fatigue cracking model 121
5.7. Assumptions from modelization 122
5.8. Design criteria of the HMA mix-design for the sub-ballast layer 123
5.8.1. KENPAVE. A computer package for Pavement Analysis and Design 123
5.8.2. KENTRACK. A Railway Trackbed structural design program 123
5.8.2.1. Parameters of Kentrack. Reference values 124
5.8.2.2. Axial load position concerning to the rail 125
5.8.2.3. Finite Element division (FEM) of the crosstie 126
5.9. "Volumetric Mix-Design" system in railways 126
5.9.1. Comparison between sub-ballast-base road stresses 127
5.9.2. Simulations with Kenpave – Kentrack software 128
5.9.1.3. A Predictive model of temperature 130
5.9.3.1. Environmental conditions 132
5.9.4. Railway Equivalent Single-Axle load, R_{ESAL} 134
5.9.4.1. Conversion of traffic spectrum in n° of R_{ESALs} 135
5.9.4.2. Definition of N_{design} as a function of traffic-T^a 137
5.9.10. "SupeRail." Evaluation and conclusions 138
Chapter 6 – Results (Laboratory Testing). Discussion 139
List of Figures Chapter 6 140
List of Tables Chapter 6 142
6.1. Introduction 144
6.2. Phase 1: Volumetric mix-design 144
6.2.1. Evaluating compacted HMA trial mixtures 145
6.2.2. Mix-design of "optimal HMA recipes." 149
6.3. Phase 2: Marshall method 151
6.3.1. Determination of Water Sensitivity (ITSR) 151
6.4. Phase 3.1. Mix-design of Dry rubberized mixtures 155
6.4.1. Substitution of rubber into a granulometric curve 155
6.4.2. Evaluating compacted DRY 1.5% trial mixtures 156
6.4.3. Optimization of the DRY manufacturing process 159
6.4.3.1. Introduction 159
6.4.3.2. Analysis of rubber-bitumen interaction 159
6.4.3.3. Swelling and Expansion of STR in rubberized mixes 160
6.4.3.4. Rebounding effect by the recovery of storage energy 161
6.4.4. An empirical approach for the mix-design 163
6.4.4.1. Problem statement 163
6.4.4.2. Empirical approach: Methodology 163
6.4.4.3. Empirical approach: Results 165
6.5. Phase 3.2. Mix-design of DRY1.5%, Ndes.152, b.*5-5,5% 168
6.6. Phase 3.3. Mix-design of DRY 2.0%, Ndes181, b*6.0-6.5% 170
6.7. Phase 3.4. Mix-design of DRY3.0%, Ndes.291, b.6,5% 172
6.7.1. Final results from SGC "Volumetric mix-design" 174
6.8. Phase 4: Results with Asphalt Roller compactor (ASRC) 176
6.8.1. A comparison between SGC and Slab Roller compactor 178
6.9. Phase 5: Fatigue cracking (mechanical characterization) 180
6.9.1. Load (kN) vs. Nf (Whöler curves) 183
6.9.2. Dissipated energy (ωi) [Hysteresis loops] 185
6.9.3. Dissipated energy (ωi) vs. Geometry variation 188
6.9.4. Effect of frequency, temperature and loading 191
6.10. Phase 6: Non-Destructive testing (FFRC). Elastic modulus 191
6.10.1. Effect of frequency on Nf vs. Young's modulus 194
6.10.2. Empirical approach: Results 196
Chapter 7 – Conclusions and future lines 197
7.1. Overall conclusion 198
7.2. Conclusions of the mix design and methodology "SupeRail" 198
7.3. Conclusions from Mechanical characterization 200
7.4. Overall rating 201
7.5. Future lines of research 202

Bibliography ..... **A-V**
Glossary of terms ..... **I-VI**
Annexes ..... **VII**
Annex 1. Complex and Stiffness modulus VIII
1.1.1. Complex modulus VIII
1.1.2. Stiffness modulus VIII
Annex 2. Densification data file (SGC) X
Annex 3. Framework of rail modeling XII
3.1. Kentrack theory XII
3.1.1. Multilayer modellization XIV
3.1.2. Superposition principle XVI
Annex 4. Kenpave computer program XVI
4.1. Kenpave. A computer package for Pavement Analysis XVI
4.2. Kenpave. Example XVII
Annex 5. Kentrack computer program XX
5.1. Example of an "output-file" with Kentrack software XX
Appendix .....
Appendix 01. Fellow individual research project (ESR8, SUPRITN) ..... A
Appendix 02. Secondment plan ..... B
02.1. First letter of admission as visiting student.
02.2. Secondment certificates.
Appendix 03. Overview of the research project ESR8 SUPRITN C
3.1. An overview of the project and significant accomplishments.
3.2. Detail research activities pursued. Results.
Appendix 04. ESR8 Research Timeline ..... D
Appendix 05. Main full contributions ..... E
Appendix 06. Report of APA citations ..... F

ABSTRACT

SCRAP tire rubber (STR) can be incorporated into asphalt mixtures in two different methods, which are referred to as the wet-dry process. The blending of recycled rubber (CRM) with asphalt has been used for years, and several manufacturing processes have been developed in Europe as well as in the USA. The use of a bituminous sub-ballast layer has been pointed out as an exciting alternative to the granular sub-ballast design traditionally applied in most railroad tracks. Frequently, unbound granular materials are replaced by bituminous sub-ballast that provide additional benefits to the subgrade protection.

Much research has been conducted on finding other alternative material to be used as a modifier in asphalt mixes to improve its properties. Rubberized asphalt mixtures (RUMAC) are regarded as a proper solution for improving the strength of the rail-track section. In comparison with traditional granular sub-ballast, these materials allow an increase in bearing capacity and excellent protection of the substructure.

The recycled rubber has become a significant enhancer of the modified bituminous mixtures, and in this work, it has been shown as a sustainable improvement option in hot mix asphalt (HMA) mixes due to the elastic behavior exposed by the rubber particles especially in reducing the fatigue cracking potential.

This thesis presents a laboratory evaluation of the performance of HMA-DRY mixes to study its application as sustainable bituminous sub-ballast manufactured from scrap tires at the end of their service life. To this end, the procedures developed in the Department of Civil Engineering of the University of Palermo during 2014 to 2017, were focused on evaluating the mechanical behavior of bituminous materials in comparison to that presented by conventional sub-ballast. Mechanical performance was examined concerning the primary requirements that need these materials (resistance to energy dissipation, fatigue-cracking strength and, waterproof properties) for their use in railway tracks.

Inside the SUP&R ITN project, enrolled as an ESR-8 fellow, the primary purpose of this laboratory research was the application of ambient crumb rubber (0.2mm to 0.4mm) and ground rubber (2mm to 4mm) recycled from discarded truck tires. CRM was processed at a standard temperature (20°C) inside hot bituminous mixtures (160-220 °C) as a substitute for 1.5%, 2% and 3% by weight of the total aggregates using the Volumetric Mix-Design gyratory compactor (SGC) and Asphalt Slab Roller Compactor (ASRC).

The impact of temperature on the mechanical properties and thermal susceptibility of the railway bituminous sub-ballast layer has served as motivation to develop the advanced measurement of the thermal cycles inside the rail track. Different simulations following the AASHTO Mechanistic calibrated model with *Kentrack* and *Kenpave* software (Univ. Kentucky) were developed to be effective with the best mix-design for railways. Thermal cycles in this layer and, an evaluation of the characteristic parameters were found. A chapter was then included on the application of the AASHTO mechanistic-empirical pavement design approach to railways, to calculate first strain and deformation parameters, resulting in a rationale for the definition of a Railway Equivalent Standard Axle Load (RESAL) and a design number of gyrations for use with SGC.

CRM incorporated into asphalt mixes by using "dry process" method which refers to technology that mixes the fine-ground rubber with the aggregate before mixing it with asphalt binder. Two aggregate gradations were considered under this investigation, dense-graded (asphaltic concrete with 22.4mm nominal maximum aggregate size) and gap-graded (stone mastic asphalt with 31.5mm maximum aggregate size). For each particle size distribution, of an aggregate sieve, the percentages of CRM added varied from 1 to 3% by weight of the total aggregates. RFI Italian standard as grading curve and Superpave gyratory compactor technique as mix-design were used.

The UGR_FACT device investigated that RUMAC mixes had shown a higher resistance to fatigue cracking compared to the conventional blend as a performance indicator. The results proved that the rubberized sustainable solution studied can offer advantages such as reducing greenhouse emissions, fuel consumption and, a suitable performance for railways tracks from a mechanical behavior point of view. The purpose of using rubber modifiers in HMA to obtain a stiffer-elastic sustainable material has been achieved for the assessment of its behavior in the sub-ballast layer. The better overall performance and fatigue results obtained were with an amount of 2% of crumb rubber and a 6% of bitumen added.

Keywords: Railway, Bituminous sub-ballast, Granular sub-ballast, Hot mix asphalt, Superpave, Crumb rubber; Temperature profile; ESAL; Traffic spectrum; RUMAC; Marshall; Roads; Compaction; Elasticity; Tensile strain; Fatigue; Swelling and Rebounding effect; Plusride-Generic mixtures.

ACKNOWLEDGMENTS

This research was conducted under the supervision of Professor Gaetano Di Mino, to whom I sincerely express my gratitude for his guidance, assistance, and inspiration during the last three years at the University of Palermo.

Thanks also to Laboratory of Construction Engineering (LabIC.ugr) for giving expert advice and time to this project during my Secondment. A special dedication to Miguel del Sol, Raúl Tauste, Luca, Pooyan Ayar, Fernando Moreno, Mayca Rubio and the whole Granada team for adapting their times to my needs. Thanks for the secondment.

I would also like to thank Professor Rafael Gallego Sevilla (UGR) for his presence and guidance encouraging despite the distance, during all my doctoral training research.

The research presented was made possible by the financial assistance from the Marie Curie Initial Training Network (ITN) action, FP7-PEOPLE-2013-ITN. This project, commonly known as SUP&RITN. To all the partners, I offer my thanks. I hope this project could contribute to the research development.

Special thanks go to friends and co-workers at the Department of Civil, Environmental, Aerospace, Materials Engineering (DICAM) at the University of Palermo (UNIPA), for their suggestions in all aspects of the research including personal matters. Thanks, must also go to all friends at the laboratory of Transportation Infrastructures (Roads, Railways, and Airport), especially the engineering colleagues whom I had the pleasure of co-tutoring.

Thanks, are also due to the colleagues at SIIV (*Società Italiana Infrastructure Viarie*) for including me in their association and become part of their events, with an immense appreciation for my work and dedication.

Finally, I would like to thank my family for their constant support, understanding, sacrifice, encouragement, and your love. To my children, who have proven that despite their youthful age, they have resisted without my fatherly presence these years, because if it were not for you, I would not have been able even to take the step of traveling abroad.

Characterization of rubberized asphalt for railway sub-ballast

Fernando Martínez Soto
Ph.D. Researcher, Department of Civil Engineering, University of Palermo, Italy.
E-mail: fernando.martinezsoto@unipa.it

AUTHOR AGREEMENT. DECLARATION

Report presented by Mr. Fernando Martinez Soto to obtain a Ph.D. from the University of Palermo, with a mention of European International Doctorate.
I declare that this project report entitled "Characterization of rubberized asphalt for railway sub-ballast" is the result of my study except as cited in the references. The project report has not been accepted for any degree (bachelor's, master's or, doctorate mention) and, is not concurrently submitted in the candidature of any other academic degree.
The doctorate Mr. Fernando Martínez Soto and the thesis director Professor Gaetano Di Mino guarantees by signing this document, which the work presented to obtain the degree of Doctor has been done in its totality by the doctoral student under the direction as tutor and director.
As far as the knowledge reaches, during the development of the work the rights of other authors cited in the section of bibliography, when their results or publications have been used, have been respected.

Signed by doctoral candidate and supervisor as follows:





Fernando Martinez Soto

Gaetano Di Mino

FINANCING STATEMENT: CERTIFICATE OF AWARD

The research presented was carried out as part of the Marie Curie Initial Training Network (ITN) action, FP7-PEOPLE-2013-ITN. This project has received funding from the European Union's Seventh Framework Programme for research, technological development and demonstration under grant agreement number 607524.









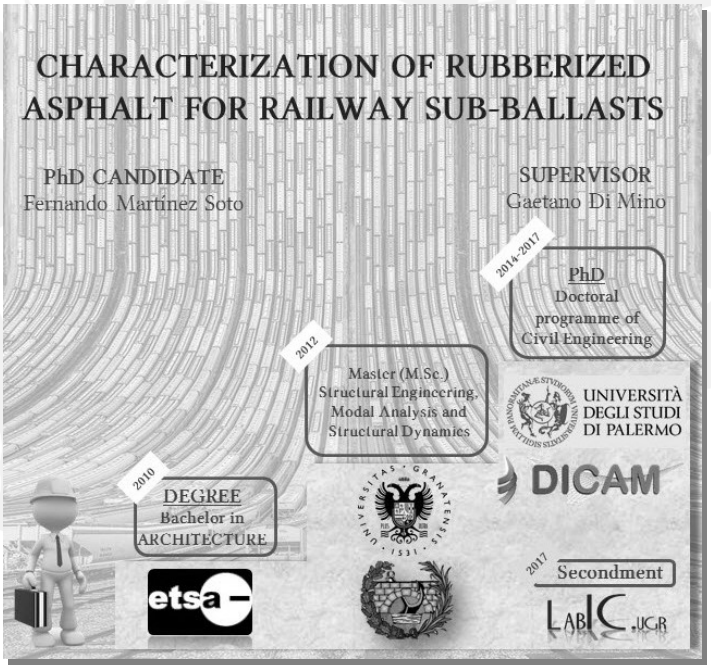


COMPENDIUM OF PUBLICATIONS

Report presented by D. Fernando Martinez Soto to obtain a Ph.D. from the University of Palermo, with a mention of European International Doctorate.
The following thesis consists of a "full thesis + publications (optional)," according to the University of Palermo ("Regolamento recante norme in materia di Dottorato di ricerca, Decreto nº 2521-2014 Ciclo XXIX") about sustainable rubberized asphalt in railways sub-ballast.
Also, this thesis is part of the European research project called "SUSTAINABLE PAVEMENTS & RAILWAYS INITIAL TRAINING NETWORK (SUP&R ITN)" with the research project ESR-8. Furthermore, the present thesis meets the requirements to qualify the International doctorate mention in according to the "Art. 21 Certificazione aggiuntiva di "Doctor Europaeus."

- The publications (in press) presented are eleven in total (peer reviewed and indexed in the International Science Index [Google Scholar, Scopus or Thomson Reuters]). At the time of delivery of this thesis, other manuscripts were submitted to international journals, which current state is "under review."
- As publications from conferences (indexed proceedings in the International Science Index, and submitted to Google Scholar, Scopus or Thomson Reuters) between 2014 to 2017, nine conferences as a delegate-oral presenter were developed.
- Future publications at international conferences and journals include general aspects of fatigue results in bituminous mixtures and non-destructive tests.

The Ph.D. student has contributed in all stages of development of all the articles, from the elaboration of the idea, literature search, experimental realization, analysis and interpretation of data, draft, preparation of the manuscript and, monitoring and final correction thereof according to the recommendations of the referees.
In the next pages, the summarize of all these contributions is shown as indexed citations:



Publications (incl. in press):

1. *(2015)* **"The resistance to fatigue of dry asphalt rubber concrete for the sub-ballast layer."** *Railway Gazette, Edinburgh, UK, (July 2015),*
   - *APA: Di Mino, G., Di Liberto, M., Noto, S., Soto, F. M., & Palermo, I. (2015). The resistance to fatigue of dry asphalt rubber concrete for the sub-ballast layer. In 15th International Conference of Railway Engineering. https://doi.org/10.13140/rg.2.2.11104.89606 ; http://superitn.eu/wp/wp-content/uploads/2017/08/2015-RW-ID1517-ESR8-Fatigue-DARC-Subballast-layer.pdf*

2. *(2016)* **"Evaluation of Dry Asphalt Rubber Concrete in Railway Sub-Ballast using the Four Point Bending Test,"** *Proceedings of the 3rd International Conference on Railway Technology: Research, Development, and Maintenance, Civil-Comp Press, Stirlingshire, UK, Paper 37, 2016. doi:10.4203/ccp.110.37.*
   - *APA: F. Martinez Soto, G. Di Mino, C.M. Di Liberto, "Evaluation of Dry Asphalt Rubber Concrete in Railway Sub-Ballast using the Four Point Bending Test", in J. Pombo, (Editor), "Proceedings of the Third International Conference on Railway Technology: Research, Development and Maintenance", Civil-Comp Press, Stirlingshire, UK, Paper 37, 2016. doi:10.4203/ccp.110.37.*

3. *(2017)* **"Effect of temperature and traffic on mix-design of bituminous asphalt for railway sub-ballast layer,"** *International Journal of Pavement Engineering (IJPE), CRC Taylor & Francis group (RN 196.1462313407).*
   - *APA: Soto, F. M., Di Mino, G., & Acuto, F. Effect of Temperature and traffic on mix-design of bituminous asphalt for railway sub-ballast layer. Loizos, A., Al-Qadi, I., & Scarpas, T. (Eds.). (2017). Bearing Capacity of Roads, Railways, and Airfields: Proceedings of the 10th International Conference on the Bearing Capacity of Roads, Railways and Airfields (BCRRA 2017), June 28-30, 2017, Athens, Greece. CRC Press.*

4. *(2017)* **"Increased Stability of Rubber-Modified Asphalt Mixtures to Swelling, Expansion and Rebound Effect during Post-Compaction,"** *World Academy of Science, Engineering and Technology, International Journal of Transport and Vehicle Engineering Vol: 4, N°7, 2017, Scholar.waset.org/1999.59/73683.*
   - *APA: Soto, F. M., Mino, G. D. (2017). 'Increased Stability of Rubber-Modified Asphalt Mixtures to Swelling, Expansion and Rebound Effect during Post-Compaction.' World Academy of Science, Engineering and Technology, International Science Index, Transport and Vehicle Engineering, 11(7), 334. DOI: 10.1999/1307-6892/73683; http://thedigitaluniversity.org/Abstracts/transport-and-vehicle-engineering?&page=3; https://waset.org/abstracts/73683*

5. *(2017)* **"Empirical Superpave Mix-Design of Rubber-Modified Hot-Mix Asphalt in Railway Sub-Ballast,"** *World Academy of Science, Engineering and Technology, International Journal of Civil and Environmental Engineering Vol: 4, N°9, 2017; Scholar.waset.org/1999.20/69025.*
   - *APA: Soto, F. M., & Di Mino, G. (2017). Empirical Superpave Mix-Design of Rubber-Modified Hot-Mix Asphalt in Railway Sub-Ballast. World Academy of Science, Engineering, and Technology. International Journal of Civil and Environmental Engineering, Vol. 4, N°(9). urn:doi:10.1999/1307-6892/69025 https://waset.org/abstracts/civil-and-environmental-engineering/69025*

6. *(2017)* **"Procedure for a temperature-traffic model on rubberized asphalt layer for roads and railways,"** *(JTTE-E 20170721-1) Journal of Traffic and Transportation Engineering, ISSN: 2328-2142, DOI: 10.17265/2328-2142/2017.04.001, David Publishing Company, Valley Cottage, NY, USA [Volume 5, N°4, July-August 2017, pp.171-202].*
   - *APA: Soto, F. M., & Di Mino, G. (2017). Procedure for a Temperature-Traffic Model on Rubberized Asphalt Layers for Roads and Railways. Journal of Traffic and Transportation Engineering, 5, 171-202. DOI: 10.17265/2328-2142/2017.04.001. David Publishing Company, Valley Cottage, NY, USA [Volume 5, N°4, July-August 2017, pp.171-202]. https://www.davidpublisher.org/Public/uploads/Contribute/59acc527f2050.pdf http://www.davidpublisher.org/Article/index?id=32566.html*

7. *(2017)* **"Optimization of a mix-design system for the sub-ballast railroad,"** *(JTTE-E 20170721-2) Journal of Traffic and Transportation Engineering, ISSN: 2328-2142, DOI: 10.17265/2328-2142/2017.05.002, David Publishing Company, Valley Cottage, NY, USA [Volume 5, N° 5, Sept-Oct 2017, pp.246-259].*
   - *APA: Soto, F. M., & Di Mino, G. (2017). Optimization of a mix-design system for the sub-ballast railroad. Journal of Traffic and Transportation Engineering, 5, 246-259. DOI: 10.17265/2328-2142/2017.05.002. David Publishing Company, Valley Cottage, NY, USA [Volume 5, N° 5, Sept-Oct 2017, pp.246-259]. http://www.davidpublisher.org/Public/uploads/Contribute/59f2aba3819bc.pdf http://www.davidpublisher.org/index.php/Home/Article/index?id=33178.html*

8. *(2018)* **"Eco-Sustainable optimization of the mix-design methodology in modified bituminous mixtures with a high percentage of recycled tire rubber,"** *(GJESRM/A008/18) Global Journal of Engineering Science and Research Management, ISSN: 2349-4506, DOI: 10.5281/zenodo.1156460 [Volume 5, Issue 1, N°5, pp. 37-59, January 2018].*

➢ *APA: Soto, F. M. (2018) "Eco-Sustainable optimization of the mix-design methodology in modified bituminous mixtures with a high percentage of recycled tire rubber," (GJESRM/A008/18) Global Journal of Engineering Science and Research Management, ISSN: 2349-4506, DOI: 10.5281/zenodo.1156460 [Volume 5, Issue 1, N°5, January 2018] https://doi.org/10.5281/zenodo.1156460 ; http://www.gjesrm.com/January-2018.html http://www.gjesrm.com/Issues%20PDF/Archive-2018/January-2018/5.pdf*

9. *(2018)* **"Volumetric Mix-Design optimization of bituminous rubber-mixtures in railway sub-ballast,"** *(IJESRT/Q080/17) International Journal of Engineering Sciences and Research Technology, Coden: IJESS7, ISSN: 2277-9655, DOI: 10.5281/zenodo.1158653 [Volume 7, Issue 1, N°61, pp. 483-507, January 2018].*

➢ *APA: Soto, F. M. (2018). "Volumetric Mix-Design optimization of bituminous rubber-mixtures in railway sub-ballast," (IJESRT/Q080/17) International Journal of Engineering Sciences and Research Technology, Coden: IJESS7, ISSN: 2277-9655, DOI: 10.5281/zenodo.1158653 [Volume 7, Issue 1, N°61, pp. 483-507, January 2018] https://zenodo.org/record/1158653 ; http://www.ijesrt.com/January-2018.html http://www.ijesrt.com/issues%20pdf%20file/Archive-2018/January-2018/61.pdf*

10. *(2018)* **"Characterization of rubberized asphalt for railways,"** *(IJESRT/R067/17) International Journal of Engineering Sciences and Research Technology, Coden: IJESS7, ISSN: 2277-9655, DOI: 10.5281/zenodo.1173468 [Volume 7, Issue 2, N°41, pp. 284-303, February 2018].*

➢ *APA: Soto, F. M., Di Mino, G. (2018). "Characterization of rubberized asphalt for railways," (IJESRT/R067/17) International Journal of Engineering Sciences and Research Technology, Coden: IJESS7, ISSN: 2277-9655, DOI: 10.5281/zenodo.1173468 [Vol. 7, Iss. 2, N°41, pp. 284-303, February 2018]. https://zenodo.org/record/1173468 http://www.ijesrt.com/issues%20pdf%20file/Archive-2018/February-208/41.pdf*

11. *(2018)* **"Improvements in the mix-design, performance features and rational methodology of rubber modified binders for the thermal evaluation of the railway sub-ballast,"** *(IJRSM/F09/17) International Journal of Research Science and Management, ISSN: 2349-5197, DOI: 10.5281/zenodo.1175219 [Volume 5, Issue 2, N°7, pp. 90-108, February 2018].*

➢ *APA: Soto, F. M., & Di Mino, G. (2018). "Improvements in the mix-design, performance features and rational methodology of rubber modified binders for the thermal evaluation of the railway sub-ballast", (IJRSM/F09/17) International Journal of Research Science and Management, ISSN: 2349-5197, DOI: 10.5281/zenodo.1175219, Volume 5, Issue 2, N°7, pp. 90-108, February 2018]. http://www.ijrsm.com/issues%20pdf%20file/Archive-2018/February-2018/7.pdf https://doi.org/10.5281/zenodo.1175219*

Conferences (as a delegate - oral presenter):

1. Railway Engineering RW2015, paper entitled ***"The resistance to fatigue of dry asphalt rubber concrete for the sub-ballast layer,"*** 13th International Conference (Edinburgh, UK, 1st July 2015).
2. COMPRAIL 2016, 15th International Conference on Railway Engineering Design and Operation, abstract submission entitled: ***"Characterization of rubberized asphalt for railway sub-ballast,"*** (19-21 July 2016, Madrid, Spain).
3. CCP: 110 Civil-Comp. Press: Railways 2016, 3rd International Conference on Railway Technology, Research, Development and Maintenance, paper entitled: ***"Evaluation of Dry Asphalt Rubber Concrete (DARC) in railway sub-ballast using the 4PBFT",*** (Cagliari, Sardinia, IT, 5-8 April 2016).
4. World Conference on Pavement and Asset Management, WCPAM 2017, ID-470, poster entitled: ***"Effective parameters to define an optimal mix design system for the sub-ballast railroad"*** (13th June 2017, Milan, Italy).
5. Railway Engineering 2017, 14th International Conference, paper entitled: **"*Criteria for a new mix-design system for railway sub-ballast*"** (Edinburgh, Scotland, 21st-22nd June 2017).
6. BCRRA-2017, 10th International Conference on the Bearing Capacity of Roads, Railways and Airfields, paper entitled: ***"Effect of temperature and traffic on mix-design of bituminous asphalt for railway sub-ballast layer,"*** ID 196.1462313407 (28th-30th June 2017, Athens, Greece).

7. ICRE-2017, 19th International Conference on Railway Engineering, paper entitled: **"*Empirical Superpave mix-design of rubber-modified hot-mix asphalt in railway sub-ballast,*"** (London, UK 21st -22nd Sept. 2017).
8. ICRT-2017, 19th International Conference on Rail Transportation, paper entitled: **"*Increased Stability of Rubber-Modified Asphalt Mixtures to Swelling, Expansion and Rebound Effect during Post-Compaction,*"** (Rome, 17-18th July 2017).
9. WIT Urban Transport 2017, 23rd International Conference on Urban Transport and the Environment, paper entitled: ***"Optimization of the manufacturing process-compacting layers of sub-ballast rail through modified bituminous mixtures with rubber tires"*** (Rome, 5-7th September 2017).

Dissemination (moving forward):

A. Abstract submitted to Rubberized Asphalt Rubber 2018 (RAR2018) in South Africa at Protea Hotel Kruger Gate, September 25-28th, 2018;
B. TRA2018, 7th European Transport Research Conference Paper submitted entitled "Mechanical characterization of dry-rubberized asphalt in railway sub-ballast" (ID959), topic SP-7 Transport Infrastructure (16th-19th April 2018) at Vienna;
C. Paper acceptance entitled "Development of dry-rubberized asphalt mixtures for railway sub-ballast using Free-Free resonant frequency technique (FFRC)" to COMPRAIL 2018 16th International Conference on Railway Engineering Design, 2-4th July 2018, Lisbon Portugal).

Seminars - Workshops presentations:

[1]. SIIV 2015, Summer school on Management & maintenance of civil infrastructures at the University of Sapienza (Rome), Italian paper entitled "Caratterizzazione di Dry Asphalt Rubber concrete per Sub-Ballast ferroviario" (7th-11th September 2015).
[2]. SYB2015, 8th International RILEM Symposium, pre-conference workshops on "Testing and Characterization of Sustainable & Innovative Bituminous Materials" (Ancona, 6th October 2015, Italy).
[3]. TRA2016, 6th EUROPEAN Transport Research conference; Marketplace Rail session, ID 1587 entitled "Characterization of rubberized asphalt for railway sub-ballast" (Poster session n°11090), topic Transport infrastructure, mode B Rails (18th-21st April 2016, Warsaw, Poland).
[4]. Eurkind GCW 2016 Conference in Universitat Politècnica de València - Centro de Formación Permanente (Valencia, Spain, 24th-28th June 2016).
[5]. SIIV Arena 2016, Spazio di confronto SSD ICAR/04 "Strade, Ferrovie e Aeroporti" (DICAM-UNIBO), Università di Bologna (Italy), Italian presentation entitled "Indagine sperimentale sul Dry Rubberized Asphalt per strato di sub-ballast ferroviario (Un nuovo approccio sul MIX DESIGN)" (29th November 2016).
[6]. JTR2017, Journees Techniques Route by IFFSTAR, Nantes. Poster and discussion session entitled "Sustainable Pavements and Railways, SUP&R H2020/ITN", (http://jtr.ifsttar.fr/programme/), (7th-8th Feb. 2017, Nantes, France).
[7]. MCAA General Assembly & Annual Conference 2017 (Marie Curie Alumni association), poster session "Characterization of rubberized asphalt for railways sub-ballast" (24th-25th March 2017, Salamanca, Spain).
[8]. Green Pavements IRF/RAF Rubberized asphalt mixtures, entitled "Cost-effective pavement today for a greener tomorrow," Lisbon 24th-25th May 2017 (Portugal).
[9]. "Thermo-rheological behavior of bituminous materials and focus on Linear Viscoelasticity," about Study of Fatigue mechanical behavior of bituminous mixtures, by Professor H. Di Benedetto (University of Lyon) at Laboratory of Construction Engineering, University of Granada (29th May 2017).
[10]. 1st International InterUniversity Symposium on Infrastructure Management (IISIM), WCPAM 2017, entitled: "Characterization of rubberized asphalt for roads and railways" (12th June 2017, Baveno, Milan, Italy).

Workshops and courses:

- "Introduction to Sustainable Development" & "The Age of Sustainable development" by Columbia University (July-August 2015).

- "How Green Is That Product? An Introduction to Life Cycle Environmental Assessment" by Northwestern University (16th June 2015, nine weeks).
- "Learning for Sustainability: Developing a personal ethic" (22nd June -26th July 2015).
- "Learning How to Learn: Powerful mental tools to help you master tough subjects" by University of California, San Diego (2016).
- "Mastering bitumen for better roads and innovative applications" (Ecole des Ponts Paris Tech. France; 4 weeks, July-August 2016).

Official SUP&R ITN dissemination events:

[1]. (2014) Nottingham Training Week 2014, *"Scientific Introduction on Sustainable roads and railways,"* (8th-12th September 2014, University of Nottingham, UK).
[2]. (2015) Nottingham (UK) Complementary skills (12th-15th January 2015, A02 Highfield House, University of Nottingham).
[3]. (2015) Dublin Training week 2015, "Winter workshop on Railway Engineering" (2nd-6th March 2015, Irish rail & UCD, Newstead Building, University College Dublin, Belfield).
[4]. (2015) Palermo Summer School 2015, "Sustainable assessment of transport infrastructures" (16th-23rd September 2015, University of Palermo, Italy).
[5]. (2016) Granada Winter school 2016, "From research to Sustainable Pavement and Railway to implementation in Practical engineering Projects" (8th-12th February 2016, LaBiC at the University of Civil Engineering of Granada, Spain).
[6]. (2016) Madrid & Huelva Summer school 2016, "Bituminous products for sustainable asphalt technologies" (3rd-7th October 2016, Repsol Technology center in Madrid, Chemical Dpt. Pro2tes at the University of Huelva, Spain).
[7]. (2017) Nantes Winter school 2017, "Road and railways European research" by IFFSTAR in parallel with JTR2017, *Journees Techniques Route* (23rd-27th January 2017, France).

- ## Other training/courses:

  - Italian course B2 level, 40h (Itastra winter school, UNIPA, Palermo).
  - English Upper-Intermediate, level B2, 220h (APEW, Palermo).
  - English Advance, Level C1, 60h (APEW A Piece of English world, Palermo).

- ## Secondment plan:

Host university (period abroad): *University of Granada, Spain.*

Laboratory of Materials & Engineering Construction (LabIC.ugr). Department of Construction and Engineering Projects and inside the Department of Structural Mechanics and Hydraulic Engineering. Higher Technical School of Civil Engineers, Canals and Ports (ETSICCP, UGR, GRANADA).

Local Supervisor: Mª. Carmen Rubio Gamez (Duration period: 26th March – 26th June 2017, three months).

- ### Research Skills and techniques acquired:

- Fundamental presentation, and capacity to formulate tough research questions.
- The process of writing an academic paper (the structure and writing style required).
- To communicate in the context of research to a specialist or non-specialist audience.
- The critical components of selecting and summarizing academic papers of relevance.
- Develop and advance scientific theories. Appreciate the role of models in science.
- Determine criteria for the desired communication with an audience.
- Apply standard techniques to achieve satisfactory performance in writing and presentation skills within an engineering and scientific community.

- ### Techniques:

- Design methodologies and experiments to test bituminous asphalt materials.
- Use of sustainable resources and materials to apply to bituminous rubberized asphalt mixes for roads and railways.
- Laboratory development of mechanical characterization of asphalt material.
- Study of resources to obtain an optimal mix-design through different compaction techniques (gyratory, slab-roller, and impact-hammer compactors).

- Display an improved ability to communicate research findings to non-specialist audiences through computer presentations, posters sessions and conferences.

- **Communication skills:**

- Explain of technical concepts (meeting proposals with a peer mentor, mini-presentations, library research activity, technical reports, and presentations).
- Oral communication (speeches/public speaking, seminars, workshops, interviewing, telephoning, role play, discussions, and debates).

- **Other professional training (course work, teaching activity):**

- Co-tutoring activity (Thesis title: "*Il progetto di miscele bituminose innovative per strato di subballast ferroviario. Un nuovo approccio e indagini sperimentali*", Unipa student (DICAM), Francesco Acuto (October 2016).
- Thesis degree co-tutoring: *"Studi di Lyfe cycle assessment nell'ambito delle tecnologie SUP&R ITN"*, Corso di Laurea in Ingegneria Civile Magistrale – Infrastrutture viarie e Trasporti, University of Palermo, Engineer student, Antonino Scaffidi Abbate (2016).

- **Other activities with professional relevance:**

- Reviewer member of the Committee Member of WASET (World Academy of Science, Engineering, and Technology), Scientific & Technical Editorial Review Board on Civil and Environmental Engineering.
- Chairman Session at the ICRT, 19th Conference on Rail Transportation (Rome, July 2017).
- Ordinary member of SIIV since 2015 (Società Italiana Infrastrutture Viarie).
- Group-Member and follower of the "Marie Curie Alumni Association" (MCAA, https://www.mariecuriealumni.eu/).

Date & Signature of fellow:



Date & Signature of supervisor:



2017

Chapter 1

INTRODUCTION

PH.D. FERNANDO MARTÍNEZ SOTO



Chapter 1 - Introduction

1.1. Background

Growth and development of countries, while increasing scarcity of energy resources, population growth without sustainable thinking and eco-environment with long-term consequences are all factors that arise from the development model that will generate adverse effects for future generations. Performance overhaul of railway superstructures, due to increased traffic volumes, loads transmitted to the system and the vibrational phenomenon, are factors that contributed more to the search for new materials and approaches.

In particular, with the advent of high speed, in recent years, several studies have shown that the bituminous conglomerate with natural rubber from recycled tires has found extensive use thanks to its excellent physical-mechanical properties.

The incorporation of elastic elements in structures of the railway is a technique increasingly used by different railway administrations to respond to a series of problems associated with the movement of trains through the pathway. The main elastic components are rail pads, soft under sleeper pads, fastenings system, stiff-mat under the ballast and blankets under the sub-ballast, and an over round formation layer [*Sol-Sánchez, M., et al. 2016*].

However, the increase in train speeds and traffic loadings, modifications of the track section have been developed with the purpose of obtaining higher bearing capacity and durability of the track system [*López Pita, 2006*].

Modern tracks have used other configurations such as track over asphalt layer (used as sub-ballast) in the new railway's lines [*López Pita et al. 2001; López-Pita, Andres, et al. 2007; Rose Jerry G., et al. 2009*], which is commonly used to reduce the deterioration of the infrastructure, fatigue cracking and degradation of its components. With the same objective, other solutions could be developed, such as a bituminous sub-ballast layer instead of the conventional granular sub-ballast, which also provides the track with higher bearing capacity as well as for mitigating the phenomena of transmission of waves and noise caused by the passage of vehicles.

Due to the rapid growth and development of countries, the mistake is to think that resources are unlimited without long-term consequences for the environment, a factor that arises from our development model that will generate adverse effects for future generations. In reality, resources are limited, the environment can absorb a certain amount of waste and naturally eliminate them from the environmental system, and the social and economic differences between the developed countries are enormous. That is means that in recent years has begun to pose a new social and economic development model: Sustainable Development.

The sustainability is a huge concept, and surely can be easier to understand than to define. In any case, there are many definitions of similar principles. One of the most quoted is the one issued by the

United Nations World Commission on Environment and Development, which states that sustainable development "meets the needs of the present without compromising the ability of future generations to meet their own needs" [*Brundtland, G. H., & Mansour, K., 2010*]-[*Soimakallio, S., et al. 2011*].

The sustainability is based on three primary factors such as economic, social and environmental sustainability in equal harmony [*Santoyo-Castelazo, E., & Azapagic, A. 2014*]. This fact may be illustrated with a sustainability Venn diagram, as shown in Figure 1.



Figure 1. Diagram of sustainable development

- **Environmental sustainability** *is the ability to preserve over time the three functions of the environment: the role of supplier of resources, waste receptor function and the direct source of utility. To live in real environmental sustainability, we have to make sure to consume natural resources sustainably.*
- **Economic Sustainability** *: requires that a business or country use its resources efficiently and responsibly so that it can operate sustainably to produce an operational profit consistently. Without acting responsibly and using its resources efficiently, a company will not be able to sustain its operations in the long term.*
- **Social sustainability** *is the capacity of society to achieve a satisfactory level of social welfare, which ensures that can be maintained in the long term.*

Critical areas of environmental sustainability are:

- Industrial Ecology, which is concerned with developing industrial process;
  - ♦ Efficient use of energy;
  - ♦ De-carbonization & technological improvement;
  - ♦ Eco-design into current systems & development of eco-industrial parks;
  - ♦ Green Engineering: involves embedding into infrastructure the following:
    - management of stormwater
    - recycling and reuse of drinking water
    - water treatment & green engineering practices
    - Ecological Engineering[1]

At the center of these definitions lies its applicability to three elements of life: economic consideration, environmental protection, and community-individual human welfare. However, our lifestyle requires resources and ecosystem services well above the rate of resources regeneration. The social and economic differences are increasing between countries and environmental effects promote even more these differences [*Assessment, M. E. 2005*].

[1] http://www.mpsaz.org/mtnview/staff/mrsandomir/apes/syllabus/apes/env/sus4/

In this context, it is estimated that the construction industry is one of the activities that have the most influence on climate change since it employs about half of the resources that man consumes from nature. It is believed that about 25 - 30% of waste material comes from construction and demolition [*Esin, T., et al. 2007*], and a 70% of global energy moves this sector [*Oteiza, I., et al. 2007*]-[*Alarcón 2005*].

However, in recent years, in the construction sector, the sustainability has become one of the highest priorities to manage natural resources and at the same time develop new techniques that allow the reuse of waste material generated in the environment. Mainly, road engineering has already adopted these new techniques in through various ways such as pavement recycling, use of waste material in bituminous mixes, low-temperature mixes that reduce emissions and energy consumption [*Ibrahim, I. M., et al. 2015; Silva H., et al. 2010; Kim H., et al. 2011*].

Even the railway sector (Figure 2), has been directed towards development committed to the future through the implementation of sustainable construction techniques and utilization of waste materials [*Presti D. L., et al. 2017; Lastra-González, P., et al. 2017*]. The railroad could have a vital role to play in the sustainability of our country, as it has the potential to reinvigorate our community, to support regeneration and generate local employment. The railway has already taken steps to become greener, more efficient and more sustainable.

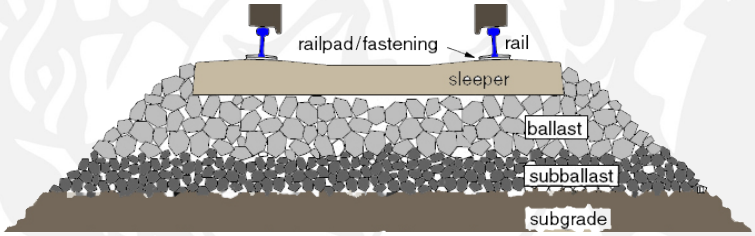


Figure 2. Railway track as thesis theme

However, it must do more if it is to realize its potential fully. From this point of view, the use of crumb rubber [*Crockford W.W., 1995; Kök, B. V., et al. 2011; Marais, H. I., et al. 2017*] could be a feasible means of modifying the mechanical performance of ballasted track to avoid critical changes in stiffness along the track. Also, the mechanical performance of CRM mixtures [*Feiteira Dias J L., et al. 2014; Fontes L., et al. 2006*] enhances the benefits of the track, obtaining lower degradation of track geometry (ballast settlement) as well as a higher capacity of dissipated energy from train passage [*Shen & Carpenter 2007*].

1.2. Problem statement

Pavement engineering, for decades, has sought innovative ways to design and build road surfaces, layers of rail, more flexible and more durable, with excellent absorption and drainage. In another aspect, it has focused on the improvement of modified materials in an attempt to extend the lifecycle of the structures.

Bearing capacity and impermeability are the principal functions of the sub-ballast layer that must be ensured to lengthen the service life of the infrastructure and reduce its maintenance costs. Thicker layer and better drainage in sub-ballast railway layers may be used to extend rail track's life.

For a mixture of bituminous hot mix asphalt, a conventional method of improving performance is to use modifiers as rubber from scrap tires to enhance the properties of the mixtures, which can be added to the mixes directly with a substitution of a part of aggregates. The result is an improvement of field performance, which means reducing or delaying the main distresses: permanent deformation such as rutting or shoving, cracking from repeated loads (fatigue) or cold-temperature contraction.

Rubber from discarded tires, one of the generic asphalt additives types, has been promoted and used to decrease all these distresses [*Shu, X., & Huang, B. 2014; Ganiron Jr, T. U. 2014*]. In this context, the use of HMA to replace the granular sub-ballast is a solution that has the potential to ensure the required bearing capacity and impermeability, while simultaneously reducing the thickness of the layer to 12 - 15 cm, compared with the 22-25 cm used in the conventional granular design.

From earlier studies [*Rose & Walker, 2002; Rose & Teixeira, 2010*], it was possible to understand that the adoption of bituminous layers, may bring significant benefits to railroad track performance, compared to those offered by the granular one. This alternative solution has also allowed a substantial attenuation of vibration and noise. Further, it could be able to improve the bearing capacity and at the same time reducing the thickness of the layer. From an investment/cost viewpoint, it has been proved that the use of bituminous sub-ballast is more appropriate than granular material when high transport distances from the quarry [*Sol-Sánchez M., et al. 2015; Di Mino, G. et al. 2012*].

The frequent use of recycled materials within the road and railway infrastructures is now an irreversible trend. In this area, the use of Dry Asphalt Rubber Concrete (DARC) in sub-ballast layer seems to be a suitable technique to reach high mechanical and environmental performance even if such material should be analyzed over a long time horizon [*F. Martínez-Soto, G. Di Mino, et al. 2015*].

It has been found that fatigue performance of Dry rubber asphalt mixtures is broadly comparable to other mixes, making them a desirable material regarding technical and economic skills. [*Moreno-Navarro F., et al. 2014*].

The purpose of this thesis is to develop new mixtures environmentally competitive and with an adequate mechanical behavior, in replacement of conventional materials. In that case, the primary objective has been to conduct a workshop focused on the capacity of using crumb or ground rubber from discarded tires as elastic aggregate substituted in volumetric proportion inside a bituminous mixture by dry-process in the sub-ballast layer.

1.3. Research methodology

The research activity includes the mix-design of rubber asphalt, temperature-traffic predictive modellization [*Calderon, A. E. U. 2013; Martinez-Soto, F., et al. 2017*], the characterization, and performance of the rail regarding mechanical behavior and vibration damping within the Railway technology. The experimental study presents the results of detailed investigations in the laboratory. The evaluation of the performance of hot mix asphalt (HMA) using recycled crumb rubber as an additive to fundamentally characterize the laboratory performance of conventional mixtures (standard hot mix asphalt) and mixtures modified with crumb rubber added using dry process limited to hot mix asphalt (HMA) applications [*Lastra-González, P., et al. 2016*]. The fine crumb rubber incorporated into asphalt mixes by using 'dry process' method refers to technology that mixes the crumb rubber with the aggregate before mixing it with asphalt binder.

In the field of railway application, technological processes involved in the use of crumb rubber are the wet/dry processes. The mechanical characterization of the asphalt concrete regarding the fatigue resistance is necessary to review the methodology in volumetric mix-design of railways materials [*Soto, F. M., et al. 2016; Martinho, F. C. G., et al. 2017*].

Such material (dry asphalt rubber concrete) is less known and investigated than the wet process, even if its application implies peculiar economic and environmental advantages such as no specialized equipment or significant plant modifications and a lot of recycled waste tires compared to the wet process [*Siddique, R., & Naik, T. R. 2004; Huang, Y., et al. 2007*].

Therefore, after exposing the criteria that lead to the decision to innovate with dry-technology, one of the most important aspects is to develop a new methodology of volumetric mix-design by the existing one for roads and flexible pavements, but elaborated, in this case, exclusively for railway lines. That is, to make feasible the use of the technology of mixing by Superpave and Marshall [*Sousa, J. B., et al. 1995; Habib, A., et al. 1998; Jiang, R. N., et al. 2016*] at the level of bituminous mixtures for rail sub-ballast.

Despite the importance of the presence of the bituminous sub-ballast to conceive the construction and rehabilitation of sustainable infrastructure, in literature, there is only fragmentary information regarding the definition of benchmark criteria for their mix design. The Volumetric Mix-Design approach is applied systematically to the railway domain, without it been adjusted for the different load configuration of the rail track system. This research aims at defining the target parameters for adopting a new approach methodology to the optimization of the bituminous sub-ballast.

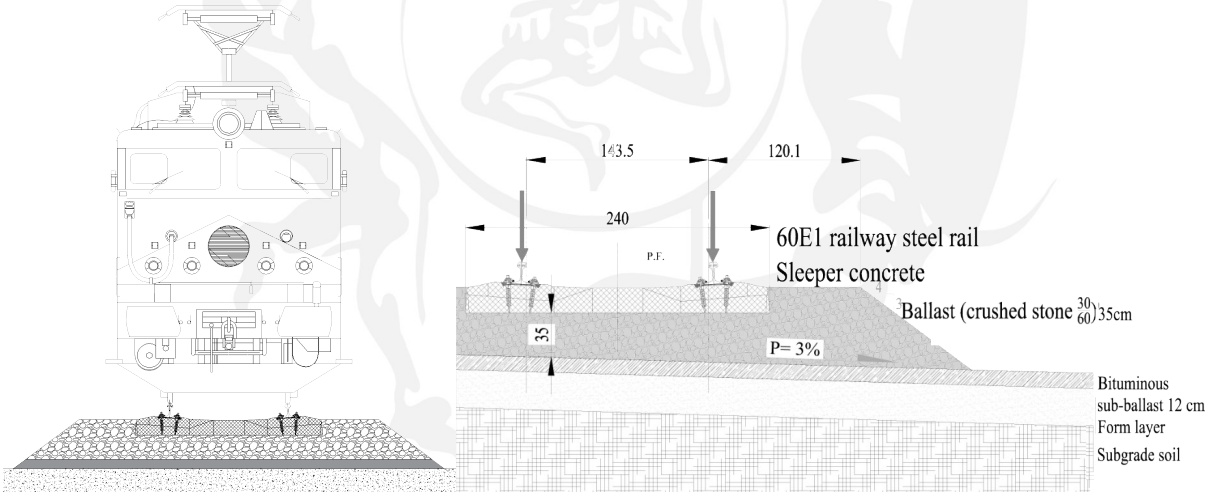


Figure 3. (a)Bituminous sub-ballast section studied in Italian rail lines; (b) Section through railway track showing the sub-ballast and formation layers.

The rail equivalent single axle load (RESAL) will be defined, and the traffic spectra of the track lines will be transformed into "number of RESALs," to calculate the N_{Design} as a function of the rail high-speed traffic level (Figure 3). Additional research is needed to overcome certain limitations which remain unsolved as the fluctuations in temperatures and traffic spectrum, which significantly affect the pavement stability or the different conductivity and density of the materials [*Barber E. 1957; Crispino M., et al. 1998; Norouzi, A., et al. 2017*].

Different kinds of test are used in experimental work such as bending tests or uni-axial tests, but they do not give the same answer [*Soto, F. M., Di Mino, G., & Di Liberto, C. M. 2016*]. In this work,

the mechanical characterization was carried out using UGR_FACT fatigue device test, focused on the mechanical cracking behavior of rubber modified asphalt mixtures by a dry process with different rubber content by weight of the aggregates.

The cracking resistance of hot-mix asphalt (HMA) mixtures is directly related to the fatigue performance of flexible pavements. As is related by N. Thom [2008] in "Principles of Pavement Engineering," fatigue cracking is one of the critical design issues for asphalt pavement. Therefore, the laboratory characterization of the fatigue behavior of HMA mixtures has been a topic of intensive study for many years *[Thom N., 2006-2008]*. It may be defined by the relationship between the number of cycles to failure and initial stress [*Ghuzlan, K., & Carpenter, S. 2000*].

Fundamental mechanical properties based on fatigue cracking will be the final objective of this thesis to evaluate the optimal rubberized mixtures for the sub-ballast layer [*Norouzi, A., et al. 2017*].

1.4. Thesis Layout

This thesis is divided into eight chapters, conclusions, future lines and, an appendix with five annexes. The following is a summary of the remaining chapters.

In **Chapter 1**, a broad *introduction* describing the issue of environmental sustainability in the railway sector, the general purpose of this research and the theme of the project were mentioned. Problems related to the methodology of using recycled rubber as a sustainable material are analyzed instead of the conventional granular sub-ballast layer. The determination of choice the solution of underlayment with mixtures modified with rubber by the dry process constitutes the primary objective of the thesis.

Chapter 2 it focuses on the study of *state of the art* conducted to review the knowledge related to the railway infrastructure and its response to traffic loading, thermal changes as well as the key features, functions, and experiences of the bituminous sub-ballast layer. In detail, it was conducted on recycled materials, such as crumb rubber from scrap tires, and dry-technology of manufacturing. Also analyzing the key features and brief experiences in the railway sector, and evaluating the feasibility of using them to manufacture sustainable asphalt to be used as sub-ballast in railways tracks. Subsequently, the sustainable solution, the central theme of this thesis, is described with precision, the sub-ballast modified with the recycled rubber of discarded tires (technique, problems, advantages, conclusions and other applications).

Chapter 3 presents the *objectives* pursued in this research, established from the revision of state of the art. Also, some specific targets and other secondary objectives, parallel to the development of investigation work, were formulated to achieve the general purpose.

Chapter 4 explain the *methodology* based on experimentation with the *volumetric mix-design* carried out, with the aim of manufacturing rubberized sustainable asphalts to be used as sub-ballast in railway tracks. Therefore, this chapter contains description and properties of the materials concisely to characterize the mixtures both conventional and those modified with recycled rubber. After describing the physical and mechanical properties of the materials, the different methods studied [Volumetric Gyratory compactor (SGC), Marshall test, ITSR Water Sensitivity test, Indirect Tensile Strength (IDT) test, Asphalt Slab Roller Compactor (ASRC), and mechanical performance by Fatigue

cracking UGR device and Non destructive Free-Free Resonant Column test] are elaborated step by step in a rigorous way.

Chapter 5, as an *original approach about mix-design in railways*, based on AASHTO Calibrated mechanistic-empirical pavement design procedure for flexible layers, the improvement of the method for the rail case is justified. The sub-section of this chapter includes a new methodology, which we will call "SupeRail," using Kenpave and Kentrack software to calculate principal strain and deformation parameters. A new approach is resulting for the definition of a Railway Equivalent Standard Axle Load (RESAL) and a design number of gyrations for use in the gyratory compactor to enhance the mix-design for railway sub-ballast. It will be explained a procedure (Protocol) that serves as a nexus between roads and railways, at the level of stress-deformation parameters to design of mixtures.

Chapter 6 presents the *results of the laboratory testing of asphalt mixtures for each method*. In this case, it develops the whole procedure established in the laboratory (Mix design with SGC and ASRC techniques, optimization of methodology, and results to *mechanical characterization to fatigue cracking* and elastic modulus). The different approaches to characterize fatigue (Whöler curves, Hysteresis loops, and damage-dissipation energy), the test criteria and a laboratory work plan (enhancing parameters, frequency-temperature selection, loads and deformation levels) are analyzed. The results are presented from fatigue life point of view. Also, a new section at the scientific level, after the comparison of the SGC, Marshall, and Roller compactor methodologies was carried out to understand the swelling, rebound and interaction effect of bitumen-rubber in laboratory specimens. Finally, another essential aspect is developed as a result of Volumetric optimized mix-design, an *empirical approach* to justify the required compaction energy (N_{des}) on the design of the rubber-modified mixtures. Again, the volumetric mix-design system is submitted to evaluation judgment.

Chapter 7, based on the *conclusions* derived from the results of different mixtures of the sub-ballast layer, in line with the experimental procedures of the optimal rubberized solution.

Future lines exhibit a series of *potential studies* that could be conducted to improve the development of the sustainable bituminous sub-ballast. From the results, a list of recommendations is proposed.

Bibliography, all references consulted and supported during the development of each chapter are listed in APA citation format.

Annexes, technical concepts related to Chapters 4 and 5 are developed widely. Aspects such as complex modulus, stiffness modulus, densification curves of the volumetric mixing method and computational development with Kenpave-Kentrack have been studied as a separate chapter.

Appendix. In this last section, we mention the technical and academic aspects necessary for the development of the research project during the three years of the doctorate. The period of stay abroad, the objectives and achievements are some of the sections developed. The last part comprises the chrono-program during each annual period of the activities carried out and the links to the main contributions at the scientific level.

2017

Chapter 2

STATE OF THE ART

PH.D. FERNANDO MARTÍNEZ SOTO

List of Figures Chapter 2

Figure 1. Railroads tracks in railways (Adapted from Pirozzolo, L. [2017]) 11
Figure 2. Ballasted track section [Pirozzolo, L. 2017]. 12
Figure 3. (a) Fastening system ; (b) Sleepers in railway superstructure 13
Figure 4. Standard configurations in conventional and high-speed tracks (Adapted from López Pita A., 2010). ...13
Figure 5. (a) Three main directions of loads acting on track (Adapted from Selig and Waters, 1994); (b) Sub-ballast as a stress reducer (Adapted from Sol-Sánchez, M., 2014] 14
Figure 6 (b). Wheel load distribution into the track structure (Adapted from Selig, E. & Waters, J. 1994). 15
Figure 7. (a) Spatial Cartesian coordinate system adopted; (b) Track gauge (Adapted from Chen, Q. 2015). 15
Figure 8. Longitudinal Level....16
Figure 9. Horizontal alignment (Adapted from Profillidis, V. [2000]) 16
Figure 10. Cross-level [EN 13848-1] 16
Figure 11. Track twist [Teixeira, 2010] 16
Figure 12. Deterioration of ballasted track geometric quality associated with the granular layers 17
Figure 13. Vertical track stiffness (Adapted from Teixeira 2003). 17
Figure 14. Vibrations produced by the railway infrastructure 18
Figure 15. (a) Long life concept in flexible pavements (Newcomb. 2010); (b) Fatigue in railway lines under tensile strains (Adapted from Li et al. 2013) 19
Figure 16. (a) Sub-ballast shedding water from the surface; (b) from subgrade (Adapted from Selig et al. 1994). 21
Figure 17. Freezing conditions without an insulating (Adapted from Selig and Waters, 1994). 21
Figure 18. Schematic illustration of track drainage system [Adapted from Indraratna, B. et al. 2006]. 22
Figure 19. Sub-ballasted track rail section with asphalt layer 23
Figure 20. (a) Variability of a granular sub-ballast cost with distance from the quarry; (b) Sensitivity of bituminous sub-ballast cost to variations in the bitumen price (Teixeira et al., 2009). 24
Figure 21. (a) Asphalt Underlayment track-bed without granular sub-ballast layer; (b) Asphalt Combination track-bed containing both asphalt and sub-ballast layers 25
Figure 22. Ballastless trackbed is containing thickened asphalt and sub-ballast layers 25
Figure 23. (a) Cross section of Italian trackbed (Buonnano, 2000); (b) Italian rail lines. 26
Figure 24. German Getrac A1 Cross-Sectional Profiles [Adapted from Frenzel J. 2010] 27
Figure 25. (a) Track design with bituminous sub-ballast for Spanish high-speed lines; (b) Bearing capacity (Adapted from Teixeira, P.F. 2009) 27
Figure 26. (a) Liquid Saturation evolution along five years (Extended Bituminous cross-section); (b) Control points [(Ferreira et al., 2007]. 28
Figure 27. (a) Vertical accelerations: time signals in ballast for 300 km/h; (b) maximum values at different track levels for 300 and 350 km/h (right), comparing two tracks with different sub-ballast 29
Figure 28. (a) Configuration of perpetual pavement [Perpetual Bituminous Pavements, 2001]; (b) Evolution of ELTs recovery rates in significant tire markets, adapted from [ETRMA ELTs, 2015]. 32
Figure 29. (a) The step of the wet process [Epps, 1994]; (b) Wet process, adapted from Hassan et al. [2014]. 35
Figure 30. (a) The step of the dry process [Epps, 1994]; (b) Dry process, adapted from Hassan et al. [2014]. 36
Figure 31. Asphalt rubber and Rubber modified asphalt concrete mixtures manufacturing 36
Figure 32. Qualitative performance of viscosity with time (Brookfield viscometer) 39
Figure 33. Use of recycled rubber from scrap tires (CRM) in asphalt [adapted from Soto, F.M. 2017] 39
Figure 34. Dry-Rubberized asphalt mixtures (CRM 1.5%, binder 5%, Superpave vs. Roller) [Soto, F. et al. 2017]40
Figure 35. (a) Embedded rail system (Sistem MLG); (b) Elastic elements for railway high-speed 41
Figure 36. Railroad sleeper made of a rubber-plastic composite (TieTek LLC of Houston, Texas). 41
Figure 37. New uses and applications of rubber according to grain size 42
Figure 38. Summary table of the environmental advantages of using rubber asphalt 42
Figure 39. (a) Flowchart of the service life of a tire; (b) Tire contribution of noise reduction [Rimondi, 1995] 43

Chapter 2 – State of the Art

2.1. Rail Tracks Structures

The rail network is one of the most vital transportation systems in everyday life. It is designed to provide a safe, efficient, and durable transit route for cargo and passengers. In this context, high-quality railway services are needed to withstand the increasing numbers of passengers as well as to relieve the already congested roads. The superstructure is made up of its classic rail configuration, traverses and joints and the supporting layers on which it rests (ballast and sub-ballast). There are two types of railroad tracks in use today: slab tracks and ballasted tracks. This research will be focused on the ballasted track structure (Figure 1).

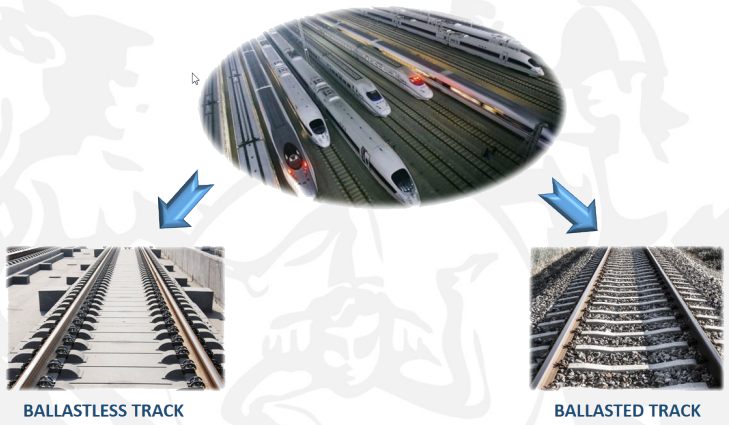


Figure 1. Railroads tracks in railways (Adapted from Pirozzolo, L. [2017])

In the slab track, the ballast layer is replaced by a concrete or asphalt surface which supports the rails above that can be directly attached to concrete sleepers with a behavior stiff and brittle. Hence the required elasticity can be obtained by inserting elastic components below the rail or/and below the sleeper [Lichtberger B., 2005]. The significant advantages of slab track are low maintenance, high availability, low structural weight, and its high resistance against lateral loading [Esveld C., 2001]. Furthermore, maintenance costs are relatively low if the structure has sufficient strength and resiliency to prevent cracking [Esveld C., 2003]. For this reason, these tracks are more suitable for high-speed rail lines, where shut-down for maintenance would impact the users considerably. Also, recent life cycle studies have shown, that from the cost point of view, slab track might be very competitive [Giunta, M. et al. 2017]. The slabs tracks are divided into two broad categories, discrete rail support systems, and continuous rail support systems [Bastin R. 2005; Martínez-Casas, J. et al. 2016]. Further, these two fall into subcategories (Table 1).

TABLE 1. DIFFERENT SLAB TRACK SYSTEMS (BASTIN, 2005; ESVELD, 2001; MIODRAG).

SLAB TRACK SYSTEMS					
DISCRETE RAIL SUPPORT				CONTINUOUS RAIL SUPPORT	
With sleepers or blocks encased in concrete	Sleepers on top of the asphalt-concrete roadbed	Prefabricated concrete slabs	Monolithic design	Embedded rail structure (ERS)	Clamped and continuously supported rail

The main components of ballasted track structures can be grouped into two broad categories: superstructure and substructure (Figure 2), both are mutually important in ensuring the safety of passengers and quality of the ride [Li, D., & Selig, E. T. 1995]. The superstructure receives the load stress from the rolling stock and transmits it to the substructure, and includes the rails, fastening system, sleepers, ballast and so increasingly common elastic elements, such as rail-pads. The substructure supports the components of the superstructure, and it must be capable of supporting the track structure above it and remaining stable under traffic loads. The substructure is associated with a geotechnical system, made up of supporting layers as sub-ballast, as well as form-layer and subsoil.

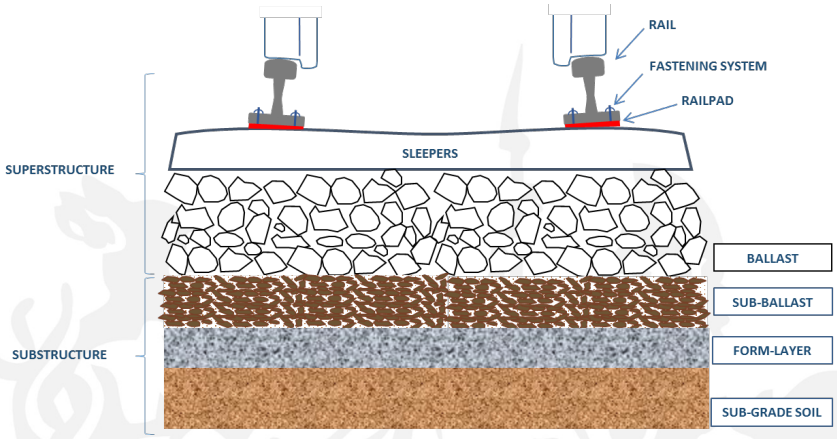


Figure 2. Ballasted track section [Pirozzolo, L. 2017].

Rails are longitudinal steel members that are placed on spaced sleepers [Kaewunruen, S. et al. 2010] and are in contact with the train wheels. One of their primary functions is to accommodate and transfer the wheel/axle loads to the sleepers. Also, their strength and stiffness must be sufficient to maintain a constant shape and smooth track configuration [Selig & Waters, 1994]. Dynamic responses of the railway track and its components are the keys to evaluate the structural capacity of railway track and its components [Kaewunruen, S. et al. 2017].

The rails UIC54 and UIC60, are the most used type in Europa. However, high-speed lines adopted the rail UIC60 which weighs 60 kg/m, due to the need to increase the inertia. Thereby increasing its resistance to bending, to be able to withstand higher stresses without compromising the geometric quality of the track [Ruano, 2007; Dahlberg, 2010].

Railway sleepers are an essential element of railway track structures, which functions are to provide supporting and fixing for the rail and fastenings, to transfer wheel loads from the rails to the underlying ballast foundation, and to be resistant to mechanical influences and weathering over a long time [Kaewunruen, S. et al. 2009]. Currently, the sleepers most used in European new track are the concrete sleepers. They can be grouped into two groups [Rezaie, F. et al. 2012]: twin-block sleeper, which consists of two blocks of reinforced concrete connected by a coupling rod or pipe, and the mono-block sleeper, which is heavier and low susceptibility to cracking [Sadeghi, J., et al. 2006].

Fastenings are all the materials whose function is to connect the rail to the sleeper structurally. The fastenings used in concrete sleepers must be resilient [Giannakos, 2014], presenting elasticity in both tension and compression. They clamp the rail gauge and absorb forces from the rails and transfer them to the sleepers (Figure 3). Fasteners are typically classified into rigid and elastic [Smutny J. 2004; Romero, M. J. G., et al. 2010; Sadeghi J. et al. 2017]. There are diverse types and techniques of

fastening systems from manufacturers such as *Vossloh* (mostly used in Germany and Spain), *Nabla* (developed and applied in French railway network, including high-speed lines) and *Pandrol* (used for example in the new high-speed LGV-East: Paris-Strasbourg) [Delaplace, M., et al. 2014].

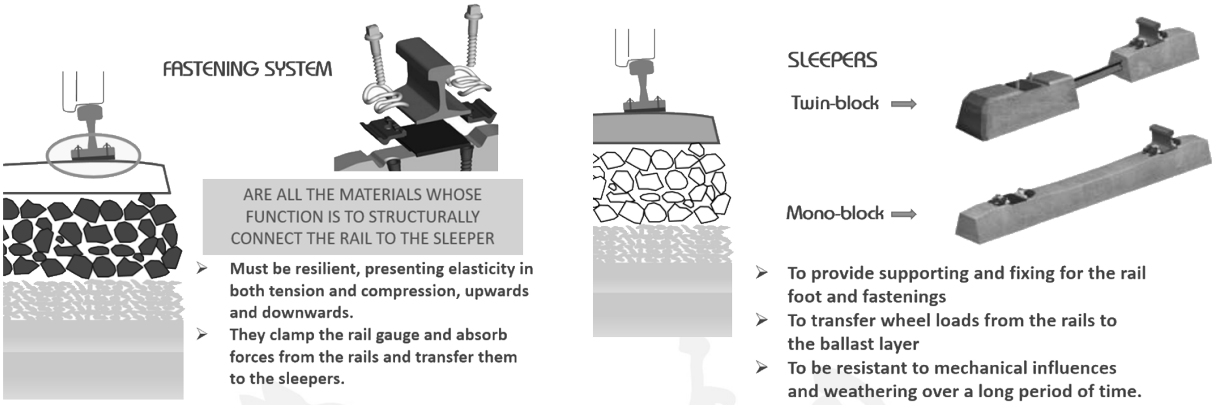


Figure 3. (a) Fastening system ; (b) Sleepers in railway superstructure

The fastening system also includes rail pads, which are placed on the rail seat to filter and transfer the dynamic forces from rails and fasteners to the sleepers [Gautier, P. 2015]. The use of this component improves load distribution and better conservation of the superstructure.

The ballast layer is formed by a crushed granular material that should be resistant and hard, resistant to weather conditions, to water absorption and to crushing by passing trains, it should be sufficiently elastic and have diameters varying between 22,4 to 60,0 mm. It not only provides support but also resists to vertical, lateral, and longitudinal forces applied to the sleepers and provide for transferring them to the substructure. For this purpose, the layer should have an adequate thickness, which is in general of 30 to 35 cm for high-speed lines [Connolly, D. et al. 2013].

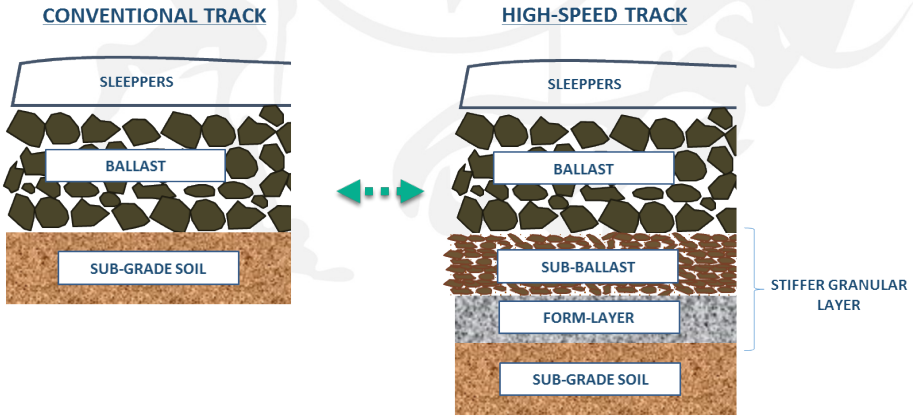


Figure 4. Standard configurations in conventional and high-speed tracks (Adapted from López Pita A., 2010).

In recent decades, the development of high-speed railway and the increases in train speed, as well as the load transported by modern trains, produce an increase in the dynamic forces transmitted to the track [Sol-Sánchez, M., 2014]. Because of this, it was necessary to add a stiffer granular layer under the ballast to increase the bearing capacity of high-speed tracks and lengthening the service life of the track, reducing its maintenance costs (Figure 4).

2.1.1. Track forces and geometry quality

For the study of the behavior of the various components of the railway infrastructure [Esveld, C. 2003], it is essential to know the transmission of loads from the train to the sub-grade soil. The main forces, generated by train's vehicles, which must be supported by railway tracks may be distinguished in forces in the vertical, lateral, and longitudinal directions (Figure 5, a).

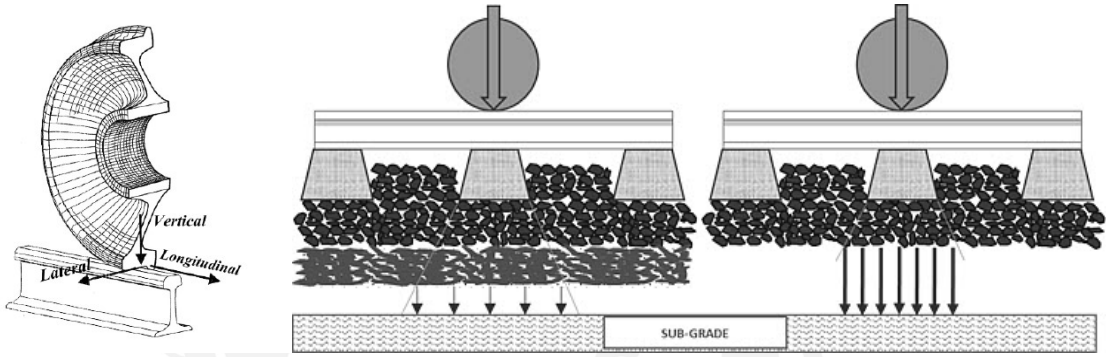


Figure 5. (a) Three main directions of loads acting on track (Adapted from Selig and Waters, 1994); (b) Sub-ballast as a stress reducer (Adapted from Sol-Sánchez, M., 2014]

The vertical force can be subdivided into the downward and upward force. In reaction to the downward force, the upward force is induced by the rail as shown in Figure 5 (b) [Li & Selig 1998]. The downward force is a combination of a static load and a dynamic component Figure 6 (a).

The static component is the weight of the train, which in Europe the part of the static axle load related to the train gravity load is limited to 225 kN. Axle loads usually take values below 150 kN for passenger coaches and between 200 kN for freight wagons and modern locomotives able to circulate at speeds up to 200 km/h. However, when circulating at speeds over 250 km/h, the maximum axle loads must be significantly reduced to nearly 170 kN/axle to contain track damage[1] [Zhai, W. et al. 2015].

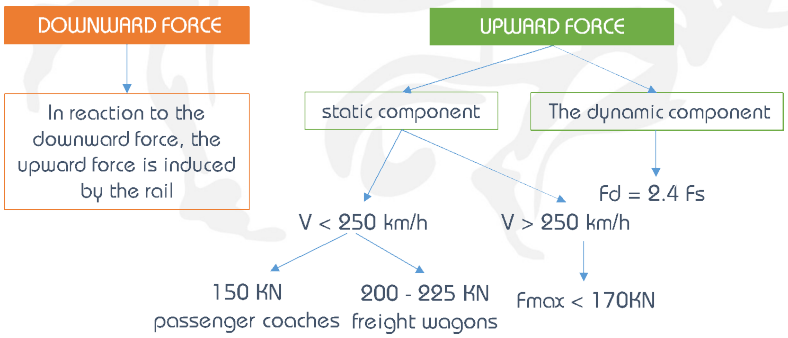


Figure 6 (a). Scheme of the track forces induced in railways

It is the dynamic component that usually causes an adverse effect on the track, as it can be much larger than the static load. According to Li, D., & Selig, E. T. (1995), the magnitude of the dynamic component can be up to 2.4 times the static load. In Figure 6 (b), a wheel load distribution is showed as an example of influence into the rail-track.

[1] In the last century, the operation speeds of high-speed trains in the world were rarely more than 300 km/h. After the start of the 21st century, with the rapid development of high-speed railway technology, a number of new high-speed railway lines were put into service, where operation speeds are commonly at 300 km/h and occasionally up to 350 km/h, heralding a new era of high-speed railway.

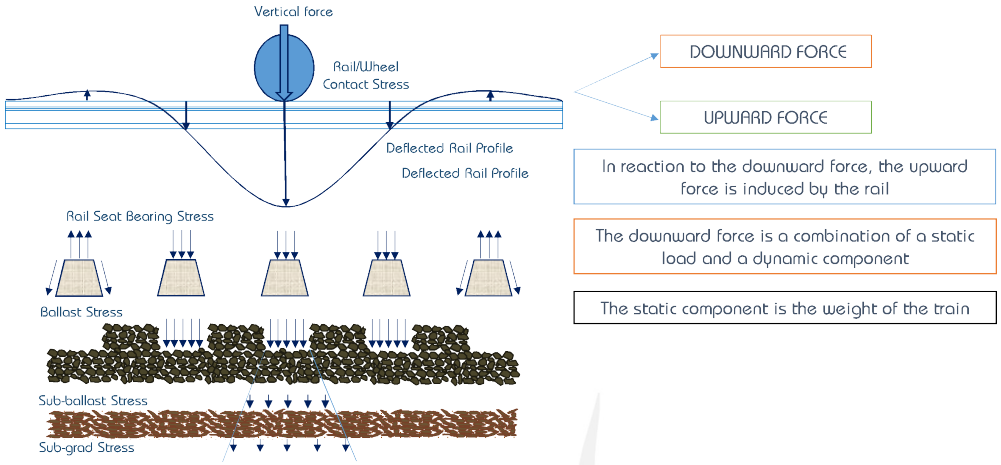


Figure 6 (b). Wheel load distribution into the track structure (Adapted from Selig, E. & Waters, J. 1994).

The curving of the freight equipment introduces lateral forces which act upon the track structure, the development of lateral instabilities or the response of the vehicle to lateral track irregularities [Yang, L. A., et al. 2009; De Man, 2002]. During curving, track anomalies can cause lateral loading. The amount of lateral force generated depends on the amplitude and shape of the defect, the speed of the vehicle and the track and vehicle characteristics [Zhang Z. et al. 2016].

Previous studies have shown that the track curvature primarily controls the lateral forces induced within a track [Larsson, D. 2004]. If these lateral force values exceed the inherent lateral resistance of the tracks, derailment and road instability may occur. The underlying ballast layer provides the lateral frictional resistance for the train under the previously mentioned loadings [Di Pilato M.A. et al. 1983]. Thus, ballast conditions are essential to resist and handle any lateral forces induced.

The longitudinal forces act parallel to the long axis of the rail and are caused by four different effects (thermal expansion, the acceleration the train along with its cars, rails shrink after continuously welded rail installation, and track creep of the underlying ballast layer and embankment) [Ionescu D. 2004]. Overall, longitudinal forces within the track system create a third axis of ballast loading [Tzanakakis, K. 2013] (vertical, lateral, and longitudinal vectors). This system of several variable forces on all axes creates a highly dynamic loaded environment that is favorable to abrasion and breakdown of the ballast in all directions [Rose, J. G., et al. 2015].

2.1.2. Track deterioration

The European standard EN 13848-1 established five main parameters to evaluate the geometry quality of the track, which is related to vertical and horizontal geometry [Li et al. 2009]. Following a spatial Cartesian coordinate system, where the X-axis is parallel to the rolling direction, the Y-axis is horizontally perpendicular to the rails, and the Z-axis is vertically perpendicular to the track grid, (Figure 7a).

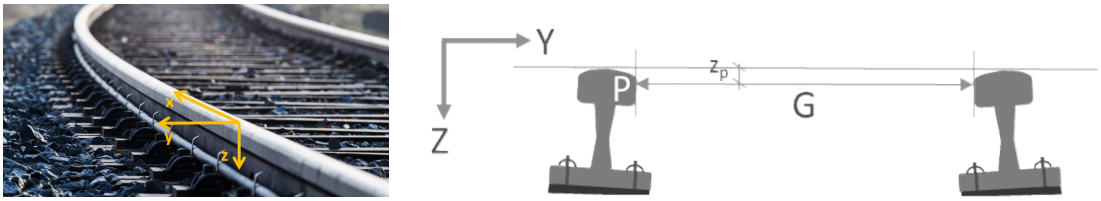


Figure 7. (a) Spatial Cartesian coordinate system adopted; (b) Track gauge (Adapted from Chen, Q. 2015).

The different parameters include track gauge (Fig. 7b), longitudinal level (Fig. 8), horizontal alignment (Fig. 9), cross-level (Fig. 10) and track-twist [European Committee for Standardization, 2008; International Union of Railways, 2005]:

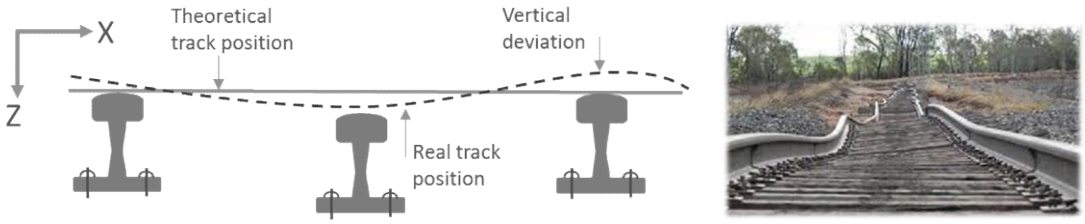


Figure 8. Longitudinal Level

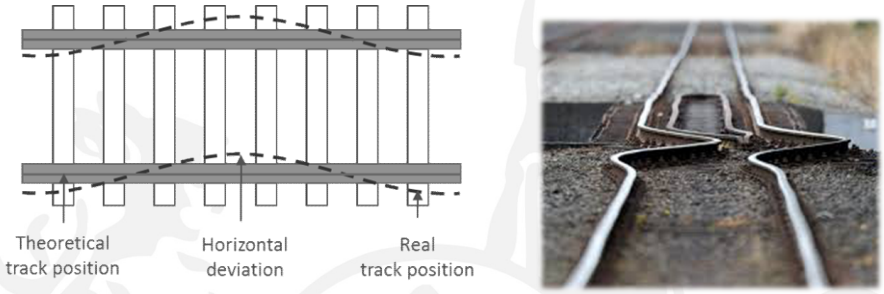


Figure 9. Horizontal alignment (Adapted from Profillidis, V. [2000])

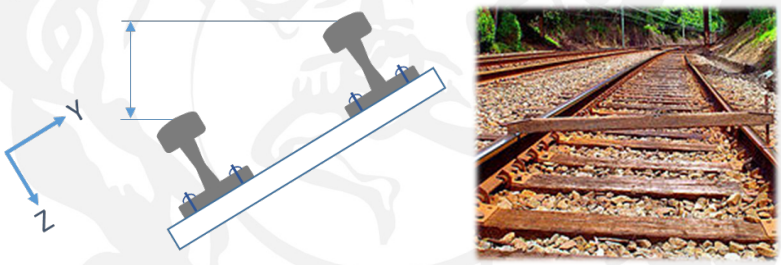


Figure 10. Cross-level [EN 13848-1]

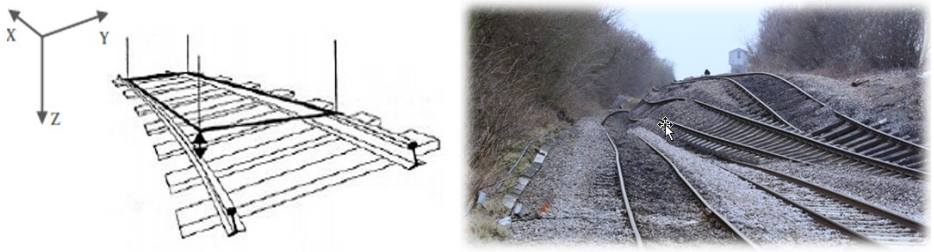


Figure 11. Track twist [Teixeira, 2010]

Track geometry quality decreases as the rolling stock transmit static and dynamic loads into the track structure through wheel-rail contact [Rhayma N. et al. 2013; Jovanovic S., 2006]. It is recognized that vertical track stiffness interacts with the mass, velocity, spring and damping characteristics of the train [Sun, Y. Q., 2002]. An increase in the dynamic forces on the wheel-rail interface and downwards to the sleepers and ballast, affect the condition of the track's components [Berggren E., 2009]. The cyclic train loads submit the particles of the ballast layer under stress, crushing them and leading to the decrease of its shear strength [Indraratna B. et al. 2011; Horvát F. et al. 2013; Rhayma N. et al. 2013]. Thus, maintenance operations are essential to extend the life cycle of the track itself [Guler H.

2011]. In this context, there are many results such as the use of Geogrid to minimize the settlement of the ballast layer [Brown S.F. 2006; Thom N., 2007].

Other solution could be the use of bituminous sub-ballast to keeping the railroad geometry unaltered thanks to its high stiffness. In this case, the settlement can be considered null allowing for reductions in the overall mean settlement of the track. The increase in granular sub-ballast height leads to increase in settlement. *Equation 1* represents a quantitative of this situation:

$$S_t = s_b + s_{sb} + s_f \rightarrow s_b = 0.026 \cdot h_b \cdot T^{0.21}\ ; \quad s_{sb} = 0.017 \cdot h_{sb} \cdot T^{0.16}\ ; \quad s_f = 1.4 \cdot T^{0.25} \tag{1}$$

Where:

- S_t = *total settlement of the track (mm);*
- s_b = *Settlement of the ballast layer (mm);*
- s_{sb} = *Settlement of the sub-ballast layer (mm);*
- s_f = *Settlement of the track formation.;*
- h_b = *the thickness of the ballast layer (mm);*
- h_{sb} = *the thickness of the sub-ballast layer (mm), and;*
- T = *cumulative traffic (10^6 tons).*

From equation 1, it can be assumed that increases in sub-ballast thickness will increase the settlement. From this perspective, it can be deduced that increasing ballast support-bearing capacity using stiffer layers without deformities (e.g., bituminous sub-ballast) will result in reduced levels of track settlement. Finally, as a resume of these points, Figure 12 shows a scheme about the deterioration of ballasted track geometry quality associated with the granular layers.

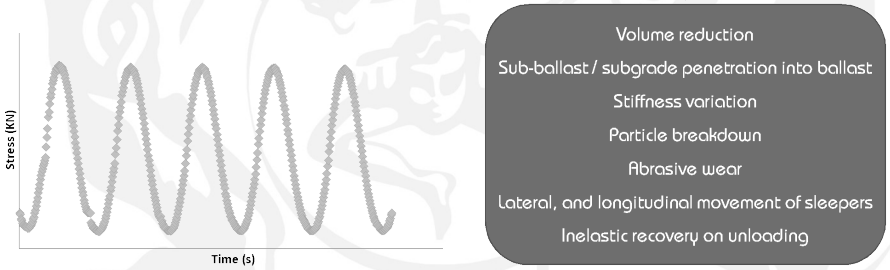


Figure 12. Deterioration of ballasted track geometric quality associated with the granular layers

2.1.3. Vertical track stiffness

Winkler (1867) was the first researcher to make breakthroughs in the study of the mechanical behavior of the railway track [Sheng, X. et al. 2004]. Talbot (1918) made different approach respect to Winkler, regarding the behavior of the track by defining the track modulus (u) for characterizing the track support by a unit of length of the rail (N/mm^2).

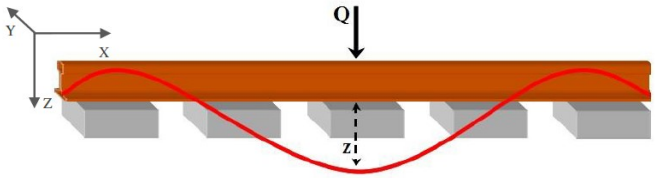


Figure 13. Vertical track stiffness (Adapted from Teixeira 2003).

There was also another approach for the definition of the effect of the vertical support provided by the track structure, which was based on the resulting displacement of the ballast layer due to the load transmitted by the sleeper (Figure 13). The stiffness coefficient represents the vertical resistance

provided by each sleeper, and it is defined as a "spring coefficient" that embodies the contribution of each layer to the total track stiffness coefficient (kN/mm). The approach of static vertical stiffness can be considered as an evolution towards better modeling of the track. Static vertical track stiffness, K (kN/mm), may be defined as the ratio between the concentrated loads applied on the rail, Q (kN) and the maximum deflection of the track structure, Z (mm), Equation 2 [Kerr, A. 1972].

$$K = {Q}/{Z} \tag{2}$$

The static vertical stiffness is the most accessible parameter to obtain as it only requires the measurement of the maximum deflection due to a wheel load at a given point [Pita & Teixeira, 2004]. When a train starts moving, the load changes immediately from static to dynamic [Berggren E., 2009]. The response given by the track structure to the dynamic vertical movements created by the rolling stock on the rail is the dynamic vertical stiffness, and it varies as a function of time, t (sec). For dynamic vertical stiffness studying purposes in the frequency domain, f (Hz), it is preferable to use its inverse, the dynamic vertical flexibility, α (m/kN), Equation 3:

$$K_t = {Q_t}/{Z_t} \rightarrow \alpha(f) = {z_t}/{q_t} \tag{3}$$

The problem is that those components present a non-linearity stiffness and this fact leads to a nonlinear behavior of the track. The nonlinear behavior can also be explained by the ballast tightening when submitted to load stresses, which increases the contact area between the stones leading to higher stiffness of the layer [Hosseingholian M., 2009].

2.1.4. Damping vibrations

Extensive research has carried out a series of theoretical analysis and numerical simulation to investigate the ground vibration caused by railway transportation [Tomioka, T. et al. 2017]. Particularly in recent decades, there has been growing interest in artificially induced vibrations in the soil, such as vibrations by machine foundations, or road and rail traffic (Figure 14). In particular, vibrations are studied in the soil to analyze their impact on people and buildings. Vibrations are distinguished at low frequencies, and at high frequencies, about 80-250 Hz.

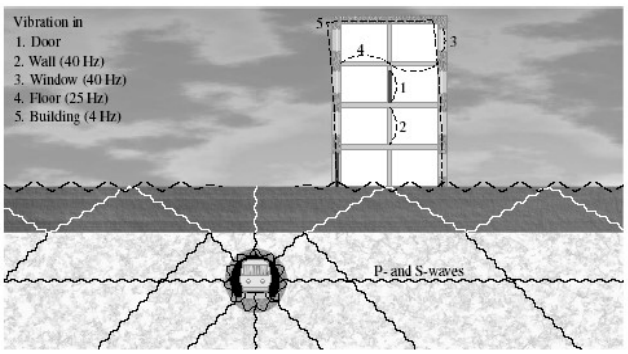


Figure 14. Vibrations produced by the railway infrastructure

Most of the studies carried out over the last twenty years mainly concerned stiffness measures; less attention has been devoted to the determination of dissipative properties [Andersson, A., et al. 2015; Wei K. et al. 2017].

The interpretation of the results of the laboratory tests for the determination of the damping factor is based on the linear viscoelastic model (Kelvin-Voigt model) [Nishiura, D. et al. 2017; RFI 2016]. Experiences conducted by R.F.I. (2016) on regular speed lines have shown that the presence of sub-ballast in bituminous conglomerate also allows a decrease in the vibrations transmitted to the ground.

In recent years, several studies have demonstrated the possibility of obtaining a higher attenuation of earth-borne vibrations using sub-ballasts made of a bituminous conglomerate of asphalt rubber.

2.1.5. Distresses: ground-borne vibrations and fatigue

Ground-borne vibrations resulting from the railway traffic have become an important environmental issue which has aroused a great deal of public attention [Yang, Y. B., et al. 2006; Gupta S. et al. 2009]. The primary method of vibration reduction is to use different stands or to interrupt the connection between the various structures with damping materials. Experience has shown that to obtain meaningful results; the base is "floating," i.e., there are entirely no hard contact points with the underlying ground and with the concrete foundation of the armament. The damping material to be used must meet the following requirements:

- Compression resistance depending on the loads it will have to withstand;
- Low dynamic modulus, variable with load, and close to the static elastic modulus.
- Lower the frequency of the binary action, adopting less rigid elastomeric supports; but beyond a certain limit it cannot get off, as long as an excessive deformation of the track, to the detriment of the regularity of the march of the convoys;
- Increase the oscillating mass, but in this case, too, it is not possible to push beyond certain limits, because too large wagons would require excessive space in the tunnel and would be difficult to move.

Fatigue is a significant issue affecting safety and quality of service in the railway industry. The phenomenon of fatigue-cracking is one of the leading causes of deterioration of the superstructure. It manifests itself at first in the degradation of the bonded layers of the package and the damage to the entire layer structure (Figure 15). Fatigue, therefore, must be adequately understood and studied to ensure proper structural design also in railways [Smith, R. A. 2005]. The phenomenon of cracking is a common pathology of roads, but of similar consequences in the railway field, although less studied due to the generalized use of granular sub-ballast in which the lateral tensions are smaller due to the distribution of stresses between the aggregates.

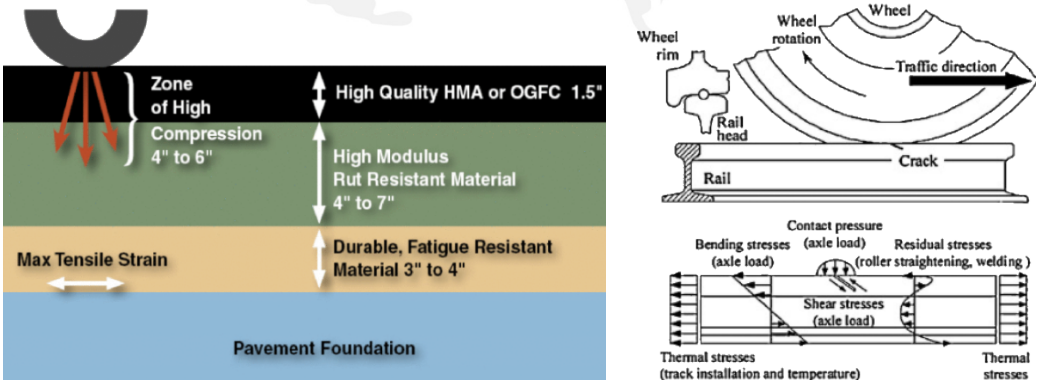


Figure 15. (a) Long life concept in flexible pavements (Newcomb. 2010); (b) Fatigue in railway lines under tensile strains (Adapted from Li et al. 2013)

Concern at rail level focuses on the specific fatigue problems of the rail industry, i.e., those adjacent to the wheel-rail interface and the design of the wheels-rails leads to a discussion of the importance of dynamically induced loads. Vehicle shells, accessories and internal components should be examined, followed by a review of infrastructure problems, including bridges, signs and power supply components [Robinson, M. 2009]. These are some of the reasons why, despite its long history, fatigue remains a problem, a review, and study in this thesis.

Fatigue in the railway infrastructure is a significant pathology responsible for maintaining the infrastructure, as well as the analysis of the propagation of cracks, formation during the life cycle of the sub-ballast layer and mode of propagation (bottom-up) [Rose, J. et al. 2016]. Among other aspects, the following issues will be discussed in depth, as to analyze fatigue cycles in different bituminous mixtures prepared for a service life of 30 to 60 years as a rail sub-ballast; dissipated energy cycles during the cracking-fracture, and the behavior depending on frequency, load, and temperature. The conventional ballasted railway track is designed to deflect elastically under train loadings, both from the total mass and from localized frequency-induced axle deflections [Palikowska, K. 2014]. As in any elastic system, two mechanisms can cause fatigue failure. The first is the number and load of transiting axles, which flexes the sleepers, creating an accumulation of fine particles by ballast grinding and changing the track bed properties, which become less elastic and more rigid. The second comes when the elastic limit of the ballast drops below the maximum axle load.

These fatigue failure modes become accelerated when water is entrapped, creating lubrication that allows the aggregate and particles to flow and so reducing the adequate depth of ballast, thus lowering further the elastic limit. The failure of sleepers is rarely a result of fatigue problems. The design of the whole rail track must be under review, not just for the physical make-up of the track but also for its geometric properties [Rose, J. G., Teixeira 2010].

2.2. Sub-ballast properties

The development of high-speed railway and the increase in the loading capacity of trains have led to the need for enhancing the track substructure by adding stiffer granular layers, such as sub-ballast between the subgrade and the ballast. Thus, the sub-ballast in railway infrastructures traditionally consists of a granular layer composed of a well-graded gravel-sand that is placed between the ballast and the sub-base of the substructure. This layer is usually used in modern high-speed routes to distribute and reduce the dynamic loads transmitted by the passage of trains to the rest of the infrastructure, as well as to protect it against climatic effects. In this way, the central demand for this material is a high load-bearing capacity (a range of 80 to 120 MPa) to extend the service life of the track and to reduce the need for frequent maintenance are usually required [Teixeira, F. et al. 2010].

The sub-ballast must shed water entering from the surface. It, then, serves as an underlying lower permeability boundary of the ballast to direct the water away from the subgrade (Figure 16a). Permits drainage of water that might be flowing upward from the subgrade includes draining water weeping up from the subgrade, including that produced by excess pore pressure generated from cyclic stress. The exceptions are when the subgrade is relatively permeable, such as natural sand or sand-gravel layer, or when no upward seepage is expected such as on an embankment (Figure 16b).

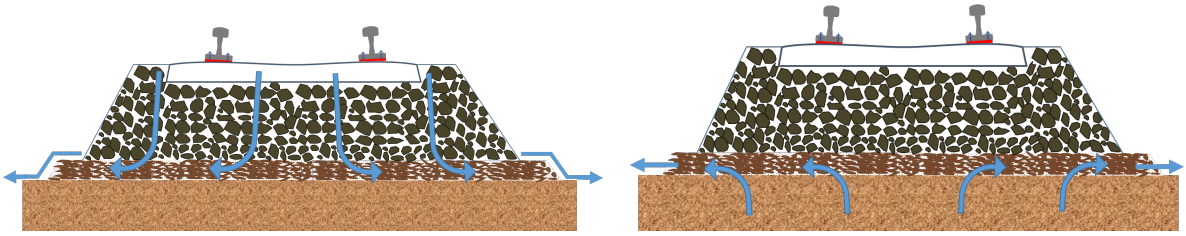


Figure 16. (a) Sub-ballast shedding water from the surface; (b) from subgrade (Adapted from Selig et al. 1994).

The sub-ballast must not be susceptible to frost; however, it must be protected by an insulating layer of ballast (Figure 17). Predicting the frost susceptibility of soil is difficult because of the complex thermodynamics and seepage processes involved. Overall experience shows that soils containing a high percentage of silt particles are the most susceptible and clays are the second most susceptible to frost.

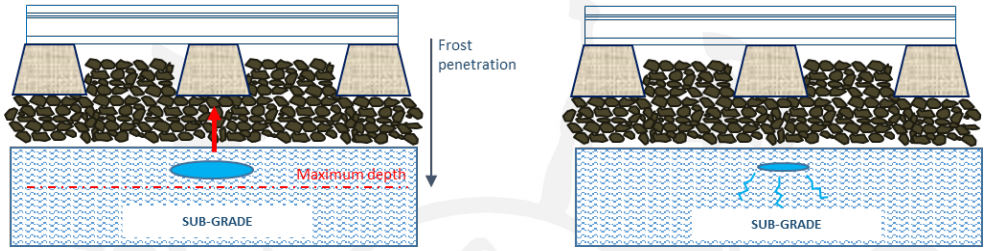


Figure 17. Freezing conditions without an insulating (Adapted from Selig and Waters, 1994).

Sands and gravels are not frost susceptible, thus when the frost level reaches the sub-ballast, a good rule of thumb is that the sub-ballast must have less than 5% silt and clay size particles.

2.2.1. Permeability

Drainage plays a significant role in the stability and safety of a track substructure [Indraratna, B. et al. 2006]. Because the ballast surface is open, precipitation falling onto the track will enter the ballast rather than run off the surface as will occur for intact road pavements. Adequate drainage for these sources of water is of the utmost importance to prevent or minimize substructure problems related to excess water. In this context, in the last decades, there has been a growing trend towards the use of bituminous sub-ballast made from hot mix asphalt (HMA), which allow reducing the thickness of the sub-ballasted layer 22-25 cm to 12-15 cm.

2.2.2. Bearing capacity and stress reduction

Bearing capacity and stress reduction are not economical to provide the entire stress reduction function by ballast alone because of the often-large required depth between the sleepers and the subgrade surface. To serve as a structural material, the sub-ballast must have a high enough resilient modulus and a stable plastic strain accumulation characteristic under repeated wheel load. The material must be permeable enough to avoid significant positive pore pressure build up under repeated load, must consist of durable particles, and must not be sensitive to moisture content. The durability must be adequate to resist breakdown and abrasion from the cyclic stresses produced by the train loading. Under dry conditions, the strength and settlement characteristics of the sub-ballast will be governed by the in-place density and the gradation of the material [Kazmee, H., et al. 2015].

The strength of sub-ballast is profoundly affected by the amount of moisture in the aggregate. In an unsaturated condition, water acts to lubricate the particles and increase both elastic and

permanent deformation, even without developing pore pressure. A high percentage of fines is undesirable since fines tend to both attract and retain moisture, which causes hydraulic problems due to low permeability and the possibility of retaining water at a high degree of saturation.

2.2.3. Requirements

The first requirement in achieving satisfactory track drainage is to maintain the ballast clean enough to ensure sufficiently high permeability for quick drainage. Secondly, the surface of the sub-ballast and subgrade should be sloped towards the sides. The third requirement in track drainage is to provide suitable means to carry away the water, as shown in Figure 18.

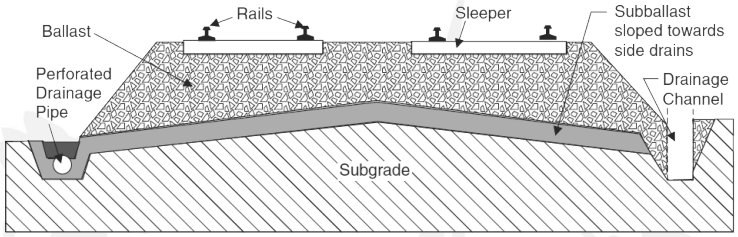


Figure 18. Schematic illustration of track drainage system [Adapted from Indraratna, B. et al. 2006].

Excess moisture within the roadbed was found to reduce the subgrade strength and provide easy access for fine grain soils to foul the open ballast. Proper drainage techniques combined with geotextiles are given special consideration [Raymond, G. P. 1984]. According to Fatahi B., et al. 2008, the use of Geosynthetics (flexible sheets manufactured from synthetic materials like polyethylene and polypropylene) is one of the most efficient methods to improve the stability and drainage of railway infrastructure. Alternatively, there is the use of hot mix asphalt as sub-ballast (object of this study) which provides an impermeable uniform drainage layer, and reduce the effects of freeze/thaw action and ballast fouling [Rose J.G. et al. 2002; Teixeira & Pita, 2006; Policicchio, 2008].

2.3. Bituminous sub-ballast

Bituminous sub-ballast, compared to conventional granular, not only reduces maintenance costs but also increases the load capacity and the impermeability of the subgrade [Teixeira, P.F. et al. 2009]. Due to this, improved viscoelastic properties can be achieved since a better reduction of vibration is provided. The sub-ballast layer (Figure 19) is commonly placed at the top layer of the substructure and consists of gravel and well-graded sand, which is suitable to carry out their functions within the track. It is employed in high-speed lines with the aim of distributing and reducing the cyclic loads transmitted to the underlying subgrade layer to an acceptable level of stress, and to protect the subgrade from climatic effects. Two main improvements are slower track degradation and much higher efficiency of the maintenance operation in resetting the track's quality [Cardona, J., 2016; Di Benedetto et al. 2016; Kraemer C., 2004].

The form-layer is placed between the sub-ballast layer and the sub-grade, and its function is to help support the weight of tracks and trains without any subsidence occurs. The subgrade is the last support, which bears and distributes the dynamic loading resultant downward along its infinite depth.

This thick layer must have sufficient bearing capacity, provide excellent drainage and yield a tolerably smooth settlement to prolong track serviceability.

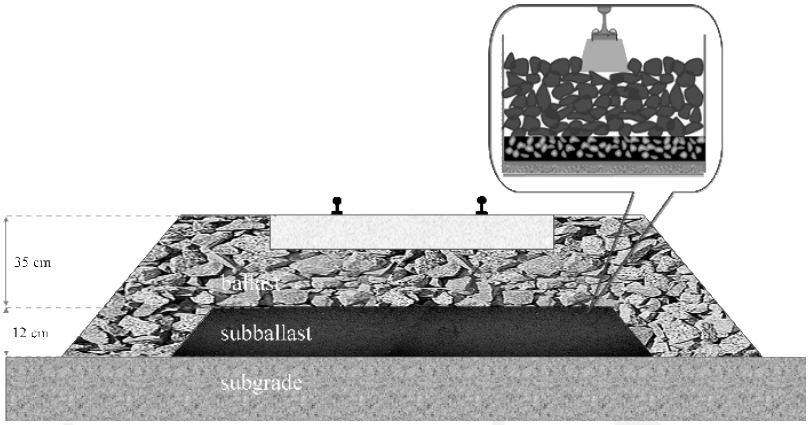


Figure 19. Sub-ballasted track rail section with an asphalt layer

2.3.1. Introduction

The mechanical properties of a bituminous mixture are dependent on nature and the amount of the components (mineral aggregates, asphalt binder, and eventually additives). It is essential to have suitable proportions of asphalt binder and aggregates to develop mixtures that have desirable properties associated with superior performance such as resistance to permanent deformation, fatigue cracking, and low-temperature cracking [Ozer, H., et al. 2018; Da Silva, L., et al. 2018].

Asphalt mixtures are composed by a mineral skeleton made from aggregates of different sizes (which provide the bearing capacity and the resistance to compressive efforts) and by a bituminous binder (which provide the cohesion needed and the resistance to shear and tensile efforts).

The amount of aggregate in asphalt concrete mixtures is 90 to 95% by weight and 75 to 85% by volume. Aggregates are primarily responsible for the load supporting capacity of a pavement [Tutumluer, E., & Al-Qadi, 2009], which are typically comprised of crushed rock, gravel, sand, or mineral filler according to grading curves. Occasionally, products from other industries, in that case, including crumb rubber may be recycled into asphalt pavement as aggregate [Van Kirk J. 1991].

Many studies have been carried out in the last years to offer information to make a more accurate choice of the binder during the rubberized asphalt mixture design. These studies have shown that the performance of these materials is influenced by the properties of the binder [Jensen, W. et al. 2006; Cao, W. 2007]. The deformation behavior of bitumen is well described with a system of springs and dashpots that represent the elastic, and viscous behavior respectively [Poel, V., & Der, C. 1954].

2.3.2. Bituminous mixes in railway construction

The bituminous asphalt has the potential to ensure the required bearing capacity and impermeability, while simultaneously reducing the thickness of the layer compared with the conventional granular design. However, studies concerning the long-term efficacy (drainage, bearing capacity, stress dissipation and durability) of bituminous sub-ballast are needed under the various service conditions expected in railway tracks. Also, it is essential to consider that temperature variations cause changes in the performance of asphalt mixtures (more elastic at low temperatures and more viscous at higher temperatures) [Hafez, I. H., 1994].

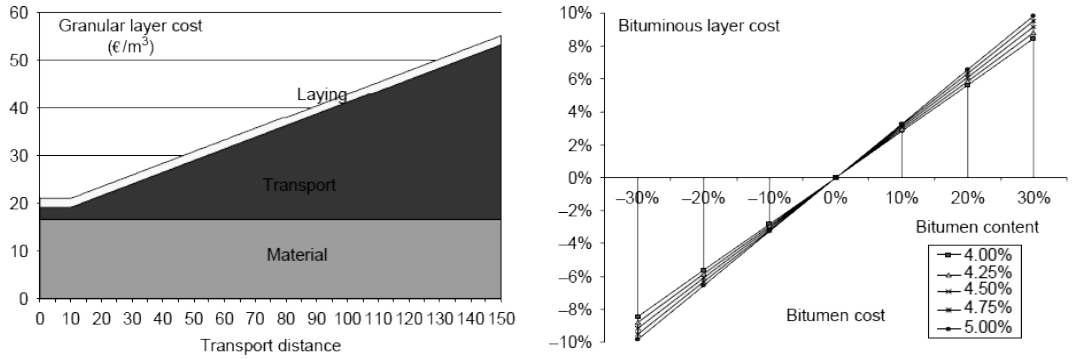


Figure 20. (a) Variability of a granular sub-ballast cost with distance from the quarry; (b) Sensitivity of bituminous sub-ballast cost to variations in the bitumen price (Teixeira et al., 2009).

From a cost viewpoint, it has been demonstrated that the transport distance is a critical factor in the cost of the granular sub-ballast, it is highly dependent on the local availability of quarries with materials that are suitable for high-speed tracks [Buonanno, A., 2003]. As it can see in Figure 20, the price of the granular layer can double for distances to quarry varying from 20 to 80 km.

Moreover, it has been confirmed that the use of a bituminous sub-ballast layer can lead to a reduction of around 200 m^3/km per track in the volume of ballast required. This decrease in ballast material needs is due to the waterproof characteristics of the bituminous sub-ballast layer, which enables the track lateral slope to be reduced from 5% to nearly 3% (as adopted in Italy for bituminous sub-ballast). This saving in ballast material can be equivalent to around 5% of the price of the bituminous sub-ballast layer, considering the average costs of the ballast material suitable for high-speed lines [Teixeira, P.F. et al. 2010]. In conclusion, using bituminous sub-ballast as a feasible alternative to all-granular layers for future high-speed ballasted tracks is possible (min. thickness of 12 cm to 14 cm of a conventional bituminous mix) [Teixeira, P.F.et al. 2009; Di Mino, G., et al. 2012].

2.3.3. Properties and advantages

The design of this bituminous mixture is commonly similar to that used for dense or semi-dense mixtures used as the base layer on road pavements [Hafez & Witzack 1994]. The difference is the slight increase in the binder strength to reduce the void index to values between 1-3%, allowing a higher permeability of the infrastructure [Rose, J., et al. 2000; Buonanno, A., 2003]. However, these types of bituminous mixtures also have drawbacks such as roads: fatigue and permanent deformation (rutting). The rapid decay of the railroad level with traditional ballast construction is due to the poor fatigue behavior of the ballast and to embankment settling [Elfgren, L. et al. 2015]. To get proper asphalt pavements that work well in service, during the design production and place phase, must include stability, durability, permeability, workability, flexibility, and fatigue resistance properties that contribute to the quality of asphalt mixtures [Bardesi A., 2000; Topal, A., et al. 2005].

2.3.4. Types of bituminous layer railway tracks

The design of the ballast and sub-ballast should be such that they can successfully transmit all the loads coming on the track superstructure to the subgrade without any failure [Tzanakakis, 2013]. Asphalt mixtures have been shown to provide excellent technical alternatives for several elements of traditional railway construction [Cominsky et al. 1994], providing a positive contribution to the bearing capacity of the structure, improving both the stability and the durability of the structure and

contributing to the reduction of maintenance activities. Also, the use of modified asphalt also helps to reduce vibration and noise [Lee, S. J., et al. 2008; Rose et al. 2011; Zhao, C. et al. 2018].

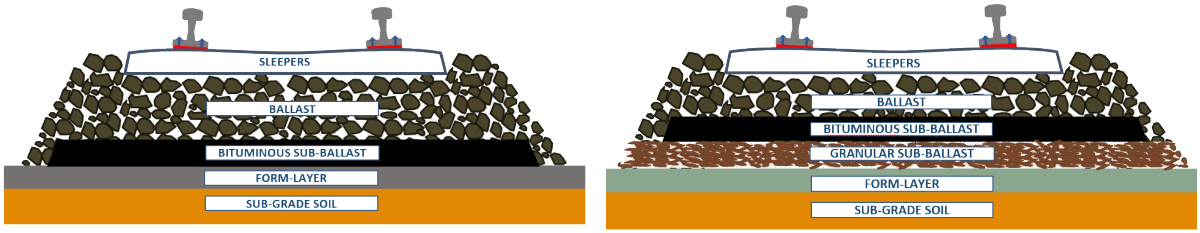


Figure 21. (a) Asphalt Underlayment track-bed without granular sub-ballast layer; (b) Asphalt Combination track-bed containing both asphalt and sub-ballast layers

Applications of asphalt in railway construction can be divided into sub-ballast layers and as full depth (asphalt) construction, also called ballast-less track. The first one is similar to the classic Granular track-bed but the asphalt layer used to replay the granular sub-ballast layer, maintaining the ballast downwards at the edges to cover the asphalt and prevent exposure of the asphalt to sunlight [Rose, J. G., et al. 2014) (Figure 21a). The track-bed can also include both the asphalt layer and the granular sub-ballast layer (Figure 21b). Less-track is a solution where the track frame of rail and sleepers is placed directly on an asphalt mix (Figure 22) with the aim to have a track structure with good elasticity, independent of the foundation stiffness. The advantages of these systems are the asphalt elasticity, the easiness of construction-maintenance and, the ability to carry out corrections without demolishing and reconstructing the base, in comparison to the conventional concrete solution.

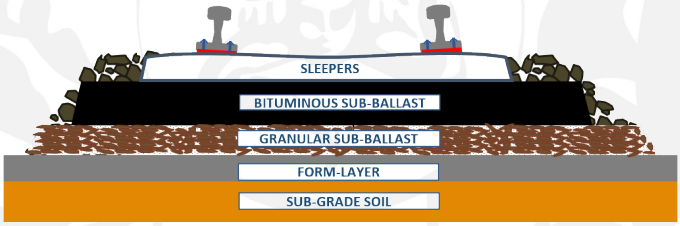


Figure 22. Ballastless trackbed is containing thickened asphalt and sub-ballast layers

The thickness of a granular sub-ballast layer is usually 150 to 200 mm thick. The typical asphalt mixture specification is dense-graded highway base mix having a maximum aggregate size of 25 to 37.5 mm. 0.5% above that considered optimum can increase the asphalt binder content for highway applications resulting in a low-elastic modulus and design air voids of 1 to 3%. This mix is more comfortable to densify to less than 5% in-place air voids and therefore facilitates adequate strength. Rutting is not a concern in the trackbed since the pressures are applied through the ballast over a wide area [Robinet A. 2010; Rose et al. 2011]. Bleeding and flushing are also of little concern since the wheels do not come in direct contact with the asphalt layer and the temperature extremes are minimized in the insulated track-bed environment [Hicks, R. G., et al. 2012].

2.3.5. Functions and design

The design, construction, and performance of the trackbed support are fundamental to control deflections and settlement [Shahraki et al. 2015]. These factors influence the long-term performance of the track to maintain geometric features and safe train operations. In any case, life cycle fatigue will depend on the daily load of trains as a factor depending on the design. In general, the load type is a

crucial requirement. In the case of the solid railway trackbed, loading frequency is at a lower level than with asphalt roads [EAPA 2003]. On highways, the actual distributed load results in a wheel load of 5.75 tons for a truck with an 11.5-ton axle, which works out to around 0.8 MPa for a surface area of around 710 cm^2. For railways, however, there is a considerable load distribution over the rail and the sleeper. The wheel load of 11.25 tons results in stress on the bottom of the sleeper of around 0.25 MPa, and thus only around one-third of the load experienced on roads.

Different types of railroad tracks are used successfully during the last decades, based on HMA instead of the all-granular ballasted track bed [Fang, M. et al. 2011] for numerous advantages. The underlayment HMA trackbed, well defined by the United States studies, in practice, is acceptable since there is a ballast layer as traditionally between the wood tie and sub-ballast HMA layer. The asphalt is designed to be permanent, environmentally sustainable, flexible and dense to avoid maintenance work and subsequent improvements, which are practically impossible. The lifetime of the solid railway trackbed has been estimated to be around 30 years [Rose J. G. et al. 2009].

2.3.6. International asphalt track-bed applications

Bituminous sub-ballast has been used in a few railway lines in diverse countries, although this solution is not very widespread, at least in European countries. The first experimental work was carried out at the end of 1960 in the USA (however, the use of bituminous sub-ballast layers, instead of crushed stone sub-ballast layers, developed in 1980; nowadays it is well spread due to less demand for maintenance of the rail track [Huang, Y. H., 1987; Rose J. G. 2000; Albalat, S. A., et al. 2011]. For performance-based design, the settlement of the track and fatigue damage to the asphalt are the primary considerations [Matthews, J. M., et al. 1993; Wang, H., et al. 2017].

In Japan, since 1970, the use of bituminous sub-ballast in the rail tracks is widespread for the construction of both convention and high-speed rail traffic with the aim to provide firm support for the ballast and to reduce track irregularities [Momoya, Y., et al. 2007]. The performance-based design is a ballasted track with a 15-60 cm thick of a well-graded crushed layer, a 5cm thick asphalt layer and a thickness of ballast beneath tie of 25-30cm. This design has been used for over 30 years in Japan. It is checked for track settlement, fatigue damage, cracking, and thermal stresses.

In European countries context, Italy began to use asphalt mixes in high-speed railway from the early 1970s [Buonanno, A., et al. 2000-2007; Celauro et al. 2003; D'Andrea A. et al. 2001-2007; Di Mino, G., et al. 2002-2008]. During the construction of the line Rome-Florence, the Italian Railway Company adopted a bituminous layer to achieve a minimum bearing capacity of 180MPa (Figure 23).

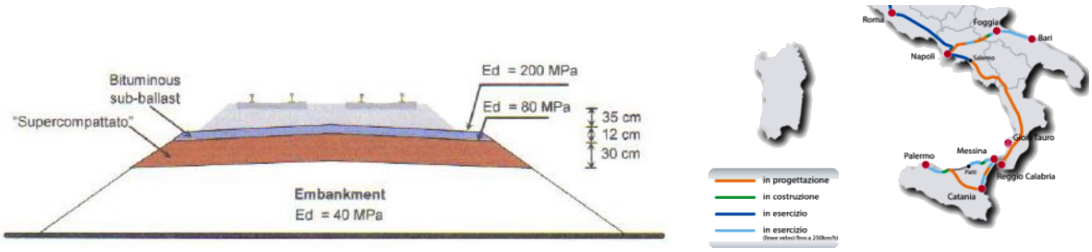


Figure 23. (a) Cross section of Italian trackbed (Buonnano, 2000); (b) Italian rail lines.

This layer was also adapted to carry out distinct functions, such as prevent rainwater from infiltrating the layers below the embankment; protect the upper part of the embankment from freeze/thaw action; gradually distribute static and dynamic stresses caused by trains and eliminate

ballast fouling. The Italian High-Speed Railway is a multi-layered system, consisting of an embankment, compacted sub-layer, asphalt sub-ballast, ballast, and rail-ties.

The embankment does not exceed 50cm in thickness and has a minimum specified bearing capacity of 40MPa, then is placed the sand/gravel mixture compacted layer and is placed on a cross slope of 3.5%. This layer can withstand the loads transmitted by the high-speed trains and at the same time can serve as an impermeable layer. It is applied with a thickness of around 30cm with and a minimum modulus of 80MPa. The asphalt sub-ballast layer, placed above the compacted layer, consists of an asphalt mixture with a maximum aggregate size of 25mm and a finished thickness of 12cm. The sub-ballast must have a modulus of 200MPa and compacted to 98% of maximum density.

In Germany, since 1970, bituminous ballast trackbed has been used to reduce maintenance costs and preserve environmental resources [Frenzel J. et al. 2010]. The main asphalt track (called A1) in use in Germany consists of concrete ties or slab track placed on a 26 to 30-cm thick layer (Figure 24).

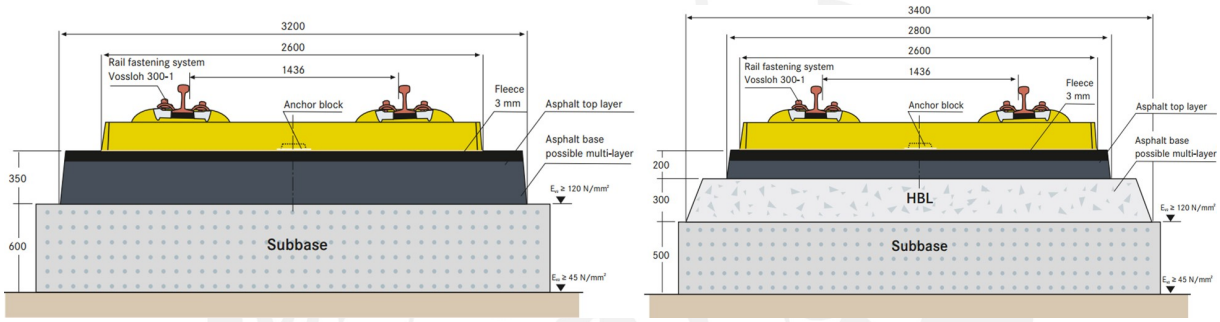


Figure 24. German Getrac A1 Cross-Sectional Profiles [Adapted from Frenzel J. 2010].

The A1 system is a ballastless track system with the direct support of the track panel on an asphalt supporting layer. The sleepers are made of prestressed-concrete [German railways, 1997]. The bituminous supporting layer is installed onto a load-bearing ballast layer or hydraulically bonded layer with a modulus greater than or equal to 120 N/mm^2.

Moreover, France started following this trend developing a 3km long test section containing an asphalt sub-ballast layer (Paris to Strasbourg). The traditional cross section consists of 30cm of ballast layer, 20cm of the sub-ballast layer, and a resting layer of limestone aggregate thick 50cm [UIC Code 719R, 2008; Bitumen Info, 2005]. The TGV-East line was opened in June 2007. In Spain, many researchers have developed research on this subject to understand the behavior of bituminous sub-ballast layers instead of crushed stone sub-ballast layers.

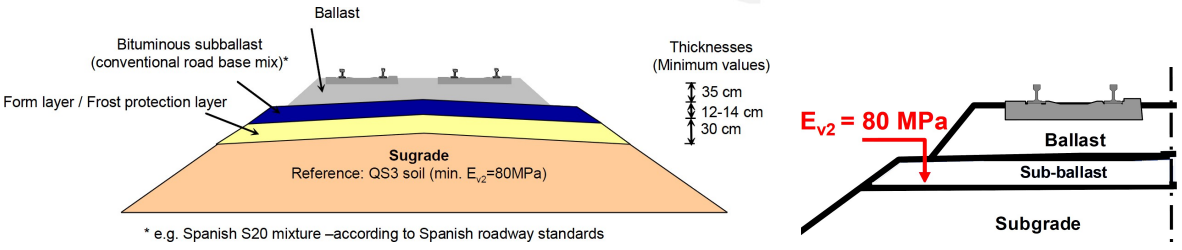


Figure 25. (a) Track design with bituminous sub-ballast for Spanish high-speed lines; (b) Bearing capacity (Adapted from Teixeira, P.F. 2009)

The Spanish Railways decided to use this solution in trial sections in four sites [Teixeira, P.F. et al. 2009-2010; López Pita, A. 2003; Rose, J. G., et al. 2011; Albalat, S. A., et al. 2012; Hidalgo-Signes, C. et al. 2016]. The structural design that supported the construction of these sections consists of a 12-14

cm of a bituminous sub-ballast layer. It is applied over a frost protection layer with a thickness of 30 cm with a bearing capacity of 80 MPa, as shown in Figure 25 [Spanish Ministry of Public Works, 2006; Peña M., 2003; Teixeira, 2009].

The bearing capacity parameter is usually assessed using the Static Bearing Plate Test [BS 1377-9, 1990], which for a sub-ballast layer is required [PF-7, 006; UIC 719R, 2008] to yield a deformation modulus value over 120 MPa and a second-first deformation modulus ratio under 2.2 MPa.

One specific parameter is the moisture content (as the humidity drops below its optimum value, the bearing capacity tends to increase) [Santiago E. et al. 2006; Teixeira, P.F. 2009].

Other countries, for example in India, the first high-speed corridor Mumbai–Ahmedabad will start in 2018 and is expected to complete by 2023, are involved to varying degrees with the development of asphalt trackbed technology, particularly for high-speed rail lines [Agarwal, M. et al. 2010].

2.3.7. Other studies

Several have been the studies and experiences about asphalt mix used into the railway's track to replace the conventional granular sub-ballast. From long-term deterioration of the sub-grade, [Rose, J. et al. 2016] found that the bituminous solution offers significant comparative advantages. Rose summarizes findings from a previous study, under a bituminous underlayment, the subgrade's moisture content is kept closer to optimum moisture content under bituminous sub-ballast after a 16-year monitoring plan.

Other advantages of using a bituminous sub-ballast layer are concerned with the differential settlement of the track. A first study carried out by the Centre for Innovation in Transport (CENIT, 2005) in collaboration with the University of Rome, analyzed the geometric quality deterioration records on sections with and without bituminous sub-ballast on the Rome–Florence HS line, as an attempt to evaluate the possible benefits of this solution. This study indicates a positive effect of using bituminous sub-ballast in the maintenance needs at transition sections (bridge embankment), one of the most significant problems of deterioration in high-speed lines [López Pita A. et al. 2007; Teixeira, P. F. et al. 2010; Teixeira, 2004]. Ferreira & Cardoso, in 2011, they analyzed theoretically the performance of bituminous sub-ballast against environmental actions regarding its seasonal variation as well as the capability of maintaining the moisture content of the year, as an alternative to the conventional sub-ballast layers. To reach an equivalent structural behavior of a granular sub-ballast layer with 30 cm of thickness, the sub-ballast layer designed with 12 cm.

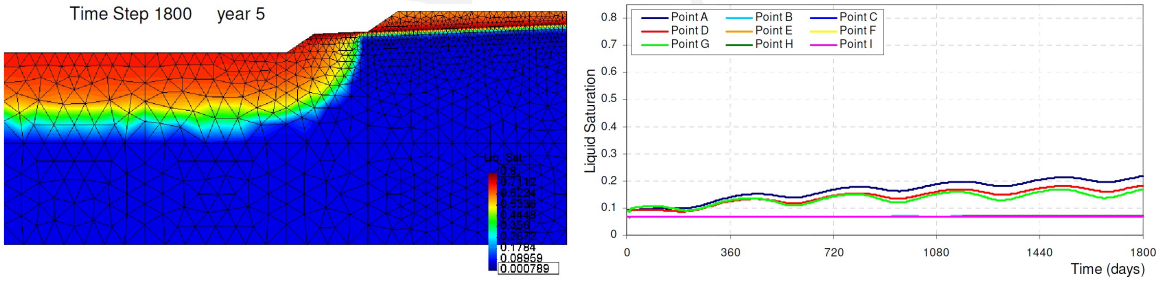


Figure 26. (a) Liquid Saturation evolution along five years (Extended Bituminous cross-section); (b) Control points [(Ferreira et al., 2007].

The comparison was made by recurring to the evolution of liquid saturation, vertical displacements and their amplitude in several points of control. Figure 26 presents the Liquid Saturation inside the embankments for the bituminous and granular cross sections at the end of the five years. It is possible

to see that the bituminous sub-ballast works as a barrier against water infiltration. Regarding liquid saturation, bituminous sub-ballast helps to maintain low levels of the moisture content of the year in opposition to the granular solution.

Another factor of track settlements where the bituminous sub-ballast can play an important part is related to the dynamic behavior of track deterioration [Lopez Pita et al. 2006]. Displacements and vibration accelerations within the track and sub-track generated by a two-wheel vehicle set traveling at 300-350 km/h were calculated using a dynamic finite-element model (Figure 27). Comparisons made for different types of sub-ballast in what concerns track dynamic behavior were performed. Bituminous sub-ballast can reduce vibration acceleration levels inside the track for the speed of 300 km/h, compared to those of a track with an all-granular trackbed. Thus, it seems reasonable that the use of bituminous mixtures in the sub-ballast layer enhances the dynamic performance at high-speed.

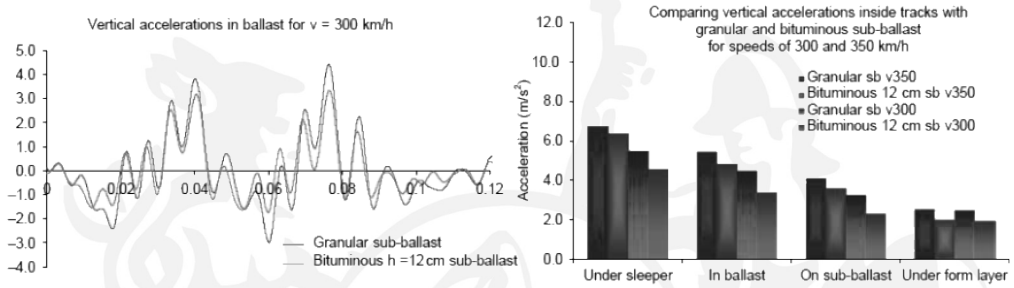


Figure 27. (a) Vertical accelerations: time signals in ballast for 300 km/h; (b) maximum values at different track levels for 300 and 350 km/h (right), comparing two tracks with different sub-ballast.

2.3.8. Inconvenient and Disadvantages

Considering the higher temperatures applied in HMA technologies, a few benefits-drawbacks can be expected. Fewer emissions, lower fuel consumption, longer haul distances, and better working conditions are the most significant advantages of these technologies [Vaitkus A. et al. 2009; Zaumanis et al. 2014]. However various concerns have not yet been resolved and need to be further studied. From an economic point of view, the benefits depend on the type of energy used in the production process, its cost, and pollution potential.

2.4. Rubberized Asphalt Sub-ballast

2.4.1. Introduction

End of life tires is among the most significant and problematic sources of waste, due to the large volume produced, their durability, and the fact they contain several components that are ecologically problematic. The utilization of crumb rubber in asphalt mixture has significantly evolved in the past few decades [Farouk, A.I. et al. 2016]. Nonetheless, the same characteristics that make waste tires problematic, their availability, bulk, and resilience, also make them attractive targets for recycling. One of the most promising options to deal with this issue is to use rubber shreds from scrap tires as raw material for construction, particularly in roads and railway lines [Hendriks, C. F. et al. 2000]. The shreds are either mixed with other materials or used as a standalone component to form some of the earthwork layers underneath the infrastructure. Thus, material recovered from waste tires, known as "crumb rubber," is being used in new tires, in tire-derived fuel, in molded rubber products, for

agricultural purposes, recreational and sports applications. For this reason, this doctoral thesis collects a concise description of the problem of the end-of-life-tires, as well as their properties and their applications in bituminous mixtures and the railway sector.

2.4.2. Literature review

This alternative has been studied with some depth in recent decades, especially on roads [Humphrey D.N. et al. 2010; Wolfe S.L. et al. 2004; Salgado R. et al. 2003; Yoon S. et al. 2005]. However, the use of tires in the construction of railway lines has been subtly studied and, mostly limited in bituminous mixtures [Buonanno A. et al. 2000]. There is also a remarkable experience mixing rubber particles with ballast [Wulandari, P.S. et al. 2017; Shen J. 2017; Feiteira J. et al. 2010; Z. Xie et al. 2016; Yu, M. et al. 2014; Nguyen, H.T. et al. 2017]. Utilization of scrap tire has been achieved through the production of crumb rubber modified binders and rubberized asphalt concrete. In this regard, end-of-life tires, which have found significant use in diverse applications in civil engineering [Moreno F., et al. 2011; Sol-Sánchez M. et al. 2015], particularly in the road and rail sector. Rubberized asphalt concrete has better stability and is highly resistant to permanent deformation, thermal cracking, and aging behavior. Therefore, pavements constructed with rubberized asphalt concrete are thought to be more durable, produce better drive quality and cost-effective to maintain [Heitzman, M. 1992; Huang, B., et al. 2002; Zhou, H., et al. 2014]. Waste tires crumb rubber has been one of the most studied recycled materials used as an additive in bituminous mixtures. The reason of this is that crumb rubber improves characteristics of the conventional bituminous mixtures such as viscosity, fatigue crack resistance and noise attenuation [Herráiz, T. R., et al. 2015; Way, G., et al. 2010; Ibrahim, M. R., et al. 2013]. In recent years, in the area of road engineering, there has been a change of social awareness that has resulted in the implementation of more sustainable construction processes, which argue the valorization and recycling of materials. To reduce the consumption of natural resources, energy and the impacts caused by emissions, ultimately railways allow the implementation of more tough materials that promote a reduction in the impact of their rehabilitation and conservation.

In this sense, the incorporation of out-of-use pneumatic powder to bituminous mixtures contributes to the improvement of its mechanical properties, allowing a more efficient response to fatigue and thermal susceptibility. Out of use tires, thanks to their deformability, load-damping, and resistance to external environmental agents can be recycled as secondary material in the construction or rehabilitation of railways, providing greater elasticity to them, while reducing vibration and transmission of loads. Thus, there are various practices in which materials formed from used tires have been used for their use as components of the railway structure [Buonanno A. et al. 2000; Albalat et al. 2011]. The technique commonly employed for obtaining elements from tires consists in the grinding of the material for use as rubber granules [Pehlken & Müller 2009; Torretta, V. et al. 2015].

The continuous and massive manufacture of tires and the difficulties to make them disappear once used is one of the most pressing environmental problems of the last decades. In addition to being an abundant waste, we must add the problem that it is a material that is resistant to degradation and the disposal of the same in a clean way. The direct burning of this type of waste causes, for example, the emission into the atmosphere of gases and harmful particles. Combustion in high-quality kilns that guarantee a minimum of emissions is very expensive, so year after year, tons of tires have finished their days abandoned in landfills. Buonanno & Mele (2000) considered the benefits already attained

using an asphalt sub-ballast layer might even be increased by adding rubber granulates into the bituminous mix, as it seems to improve further its tendency to dissipate energy.

In the case of the use of pneumatic powder in bituminous sub-soils, Zhong & Rose J.G. (2002) through laboratory studies, have shown that the use of these materials improves the dynamic behavior reducing the vibrations transmitted to the underlying layers. On the other hand, a study [Lee S. et al. 2014] indicates that the thickness of the bituminous layer with rubber could be reduced to values close to 9 cm, instead of the 12-14 cm used routinely for the bituminous layer. Similarly, Zhong and Rose (2002) showed that an asphalt mixture with 20% rubber content has an average damping ratio of about 9.5%, whereas without rubber it is approximately around 6%. Another study proves that the addition of rubber (up to 5 % by weight) increases the damping ratio and reduces vibration [Hidalgo, C. et al. 2017].

These research studies pointed out the propensity to dissipate the energy of this kind of composite material (as the loss factor increases with the increase in rubber content) and, thus, provided evidence of the right dynamic performance of rubber-modified asphalt when applied to sub-ballast layers of high-speed railway tracks. Furthermore, the authors believe that the use of this waste material, enhancing the track sub-ballast anti-vibrating properties, inclusive with an optimal mix-design and construction method, may result in an innovative mixture to be used in railway tracks in future.

Other researchers [Albalat, S. A. et al. 2011; Lee S. H. et al. 2014] evaluated the performance of moisture susceptibility and fatigue cracking in three asphalt concrete mixtures for railway track using different asphalt binders, crumb rubber modified (CRM), and styrene–butadiene–styrene (SBS). Dynamic modulus and uniaxial creep test were conducted to characterize the material properties of asphalt mixtures. Regarding resistance to cracking, the results of the repeated IDT test under dynamic loading showed that asphalt mixture with CRM asphalt had the highest fatigue resistance.

In addition to the laboratory work and modeling of the behavior of the track with rubberized bituminous sub-ballast, in a high-speed line in Italy (Turin-Milan) were measured the vibrations transmitted to the ground at the passage of the trains. The results, for a section of thickness 12 cm of a bituminous mixture with rubber powder, were compared with those obtained in an adjacent section with the same mixture but without rubber [D'Andrea et al. 2004, 2007, 2008]. The measurements were recorded with accelerometers, verifying that the bituminous layer incorporating rubber decreased the vibrations in the frequencies between 50 and 100 Hz.

About the used tires in the manufacture of sleepers, these residues put together with plastic materials to obtain lighter and more durable components, can reduce the maintenance costs of the tracks [Evans, A. 2006]. Also, this type of sleepers allows reducing the loads and vibrations transmitted to the ballast layer, while they increase the lateral resistance of the system.

2.4.3. Rubberized asphalt

The bituminous conglomerate with rubber (CRM) from recycled tires has found extensive use thanks to the physical-mechanical characteristics, especially with the arrival of high-speed [Wulandari et al. 2017; Nguyen et al. 2017; Wang S. et al. 2017; Zheng, X. 2005; Cao W. 2007; Di Mino G. 2002]. Some previous laboratory and small-scale tests have shown that rubber modified asphalt concrete (RUMAC) has high stiffness and damping ratio compared with conventional asphalt [Sol-Sánchez et al. 2017; Zeng, X. 2005]. It substantially reduced both the recorded amplitude and duration of vibrations compared with the conventional asphalt concrete underlayment [Tzanakakis, K. 2013].

These vibration attenuation characteristics have the likely to reduce maintenance costs and improve the long-term performance of the track structure [Zhao C. et al. 2018; Gmelin, H. et al. 2014; Zeng X. et al. 2001]. According to J. Rose [2011], rubber modified asphalt concrete mixtures (RUMAC) utilize one of the significant industrial wastes in the world, discarded rubber tires. Experience in the field showed that recycled rubber tires in highways have better durability and loading capacity [Epps, J. A. 1994]. However, the relentless increase in used tires has become a primary environmental concern. Different solutions have been proposed to improve the performance of the pavements, which use tire rubber at the end of its useful life to modify the asphalt concrete. The recycling of CRM offers considerable environmental benefits, such as less need for landfills and less air pollution from combustion.

Nowadays, there are several types of asphalt innovations in favor of sustainability, through methods that minimize energy consumption and encourage recycling of materials or by design that improve storm-water management. Among the critical innovations there are:

- Asphalt Reuse/Recycling: It is the part of paving material removed containing bitumen and aggregates. It is a useful alternative to virgin materials; in fact, it is used to replace mineral aggregates and bitumen in the production of asphalt pavement [Zaumanis M. et al. 2015].
- Pavement Aggregate Substitutes: Over 95% of the weight of the materials in a bituminous mix comes from aggregates. The asphalt industry annually consumes vast quantities of such materials. This amount is roughly 12,500 tons/km [Zoorob S. E. et al. 2000]. Since quarries are the source of most aggregate, this has a very negative impact on the environment and results in significant economic and energy losses.
- Perpetual Pavement [TRC, 2001]: is a type of pavement designed in successive layers of asphalt pavements that present an adequate level of flexibility and rigidity to avoid cracking and rutting. Perpetual pavements also prevent the inconvenience and environmental impacts from frequent resurfacing (Figure 28a).

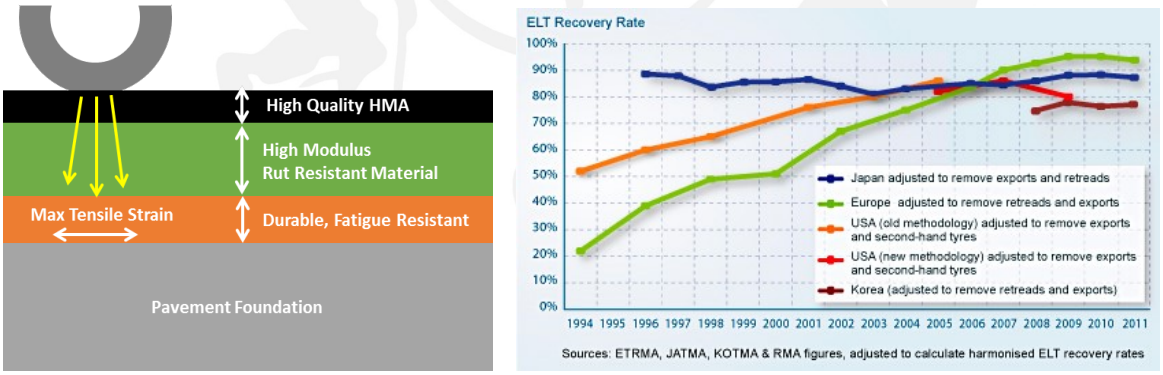


Figure 28. (a) The configuration of perpetual pavement [Perpetual Bituminous Pavements, 2001]; (b) Evolution of ELTs recovery rates in significant tire markets, adapted from [ETRMA ELTs, 2015].

In industrialized countries, the increasing number of vehicles generates millions of used tires every year. It is estimated that worldwide, every year, are sold around 1.5 billion tires and subsequently, at the end of their useful life, fall into the category end of life tires (ELTs) (Figure 28b) [ETRMA, 2015]. At the same time, the cost of recycling to the consumer has decreased due to both increased efficiency in management structures and new recovery routes. In detail in Europe, are produced 355 million tires, and this number represents about 24% of world production. Also, the severe problem is that the EU has millions of used tires that have been illegally dumped or stockpiled.

Most countries, in Europe and worldwide, have relied on landfilling to dispose of used tires but the limited space and their potential for reuse have led to many countries imposing a ban on this practice. Recovery rates demonstrate that ELTs management in Europe is allowing the progressive elimination of landfilling and raises the availability of Recycled Tyre Rubber to be recycled for other purposes. One of the most efficient recycling options for scrap tires is their use (in the form of ground-crumb rubber) in hot mix asphalt pavements. Literature has shown that rubberized asphalt increases resistance against aging, cracking, stripping and rutting. Moreover, rubberized asphalt creates more flexible and durable pavement [Fontes L. et al. 2006; Lo Presti D. 2013].

2.4.4. Crumb Rubber Modifier

In general, tires are composed of natural and synthetic rubber. From the material point of view, the tire is made up of rubber, carbon black, metal, and steel. The remaining materials are additives, which facilitate compounding, and vulcanization. Table 2 is a summarized version of general tire composition in cars and truck tires in the EU.

TABLE 2. COMPARISON OF PASSENGER CAR AND TRUCK TIRES

Material	Car	Truck
Rubber/Elastomers	48%	45%
Carbon Black	22%	22%
Metal	15%	25%
Textile	5%	-
Zinc oxide	1%	2%
Sulphur	1%	1%
Additives	8%	5%

The proportion varies according to the size and use of the tire. The accepted rule of thumb is that the larger the tire and the more rugged its intended use, the higher will be the ratio of natural to synthetic rubber. Engineering process is necessary to transform natural rubber into a product able to ensure performance, durability, and safety. In fact, natural rubber is sticky and can easily deform when heated up and, it is brittle when cooled down. In this state, it cannot be used to make products with a proficient level of elasticity [Vijayaram, T. R. 2009]. The second most important component of a tire is carbon black, that is not a generic product. The individual manufacturer uses extensive ranges of specific grades of carbon black. Carbon black is mainly used to enhance rigidity in tire treads to improve traction, control abrasion and reduce aquaplaning; in sidewalls to add flexibility and to reduce heat build-up [Shulman V.L. 2000]. The third largest component is steel that provides rigidity, and strength as well as flexibility to the casing. The most common traditional textiles used in rubber are nylon and polyester. In recent years, a range of new textiles, primarily aramid, which is an ultra-lightweight material, have been substituted for traditional materials.

In this process, the steel is removed by a magnet and the fiber is removed by aspiration. After that, the crumb rubber can be used. The size may range from as large as 460 mm to as small as 25 mm, with most particles within the 100 mm to 200 mm range, while the tire chips range from 76 mm down to approximately 13 mm. By further reducing the size of shreds and chips, it is possible to produce Ground and Crumb Rubber, also known as size-reduced rubber, which is suitable to be re-used in the asphalt industry. To produce crumb rubber, it is usually necessary to further reduce the size of the tire shreds or chips. The ambient and cryogenic processes are the two primary methods.

2.4.5. Historical use of rubber in Asphalt materials

Asphalt rubber (ARC) is a term used to indicate asphalt cement modified with Crumb rubber modifier (CRM), which is a general type of modified asphalt that contains scrap tire rubber. CRM is a general term to identify concepts that incorporate scrap tire rubber into mixtures by reacting the rubber with hot aggregates before mixing with asphalt (dry technology). Three methods of producing asphalt rubber concrete (ARC) have been used. The *wet process*, in which small-sized (Ø0–1 mm) rubber grains are added to bitumen, and after digestion, the period is used as a binder to produce an ARC. The *dry process*, used in this thesis, in which small-sized (Ø0.2–2mm) rubber grains are added directly to heated aggregates, and then bitumen is added, producing an ARC similar to the one obtained by the wet process. After a period of rubber digestion, it is laid down and compacted. Finally, *terminal blend rubber bitumen*, which is a binder prepared in refineries to be used to produce ARC in the same way as conventional asphalt concrete (AC) [Heitzman M. 1992].

Several studies addressing ARC compared with another type of mixtures have been executed in the last years. Sienkiewicz et al. [2017] presented an overview of methods for improving the storage stability at high temperature of rubber-modified bitumen and concluded that the increase in stability could be achieved by using CR surface-activated by furaldehyde or ground tire rubber treated by gamma irradiation or modified by a devulcanization process. H. Shao et al. [2017] proposed a novel mixing technique (double-drum mixing) and carried out a comparative study to investigate the effect on the performance of hot recycled asphalt mixtures. They verified that this process could reduce the air voids if the tensile strength, moisture damage, rutting, and low-temperature cracking resistance were improved to a certain extent.Lastra-González et al. [2016] analyzed a reference asphalt concrete separately, and four modified asphalt concrete with polymeric wastes. Xie and Shen [2012] investigated the dynamic modulus, rutting resistance, moisture susceptibility, and fatigue resistance of rubberized stone matrix asphalt (SMA) through laboratory performance tests. In this research was found that the introduction of CR may affect the high-temperature dynamic modulus and rutting resistance, while no significant influence on the moisture susceptibility and fatigue life was registered. Zhai, W. et al. [2015] evaluated the performance of CRM and concluded that the crumb rubber improved the mechanical properties of the control asphalt mixture. Shafabakhsh et al. [2014] show that the use of some wastes such as waste rubber powder in asphalt mixtures not only increases their lifetimes but also reduces production costs. About asphalt rubber mixtures, Kaloush [2014] summarizes findings from several research studies conducted at Arizona State University in the areas of binder and mixture performance.

In the wet process, the crumb rubber is added to hot bitumen before mixing it with the aggregates, modifying its properties as a modified binder. In the **dry process,** the particles of crumb rubber are added directly to the aggregates before the addition of the bitumen, as though it was another type of aggregate thus directly modifying the properties of the mix. Same meaning as a modified asphalt binder containing CRM is called "rubberized asphalt" (RB), which is a mixture whose response is primarily asphalted, although the responses are modified with rubber.

The **dry process** is usually used only with hot bituminous mixtures, whereas the wet process has been applied in crack sealants, surface treatments, and hot bituminous mixtures. Granulated, ground rubber and crumb rubber (Ø0.4 to 8 mm) are used as substitutes for a small portion of the fine aggregates (typically 1-3 % by mass of the total aggregate in the mixture). The rubber particles are blended with the aggregate before the addition of the bitumen. Historically, rubber in asphalt blends

has been used to improve the elasticity of binders and blends [Bloom E.F. et al. 2016]. However, the application of rubber in asphalt mixtures requires careful consideration as the rubber reacts with the bitumen at high temperatures, consequently changing the performance of the mixtures [Soto, F.M. et al. 2018]. Gawel et al. [2006] found that rubber particles can swell to thrice to five times their original size with rubber-bitumen interaction and may resist later compaction effort. This swelling effect can prevent the mixture from achieving its target density, consequently leading to premature cracking failure [Shen J. 2017; Wulandari et al. 2017; Wang S. et al. 2016; Hassan N. et al. 2014; Kumnuantip C. et al. 2003]. Both technologies are described, with focus on the dry-process, theme of the thesis.

2.4.5.1. Wet process

Asphalt rubber, "wet process," was developed by Charles McDonald in 1960's and refers to the modification of bitumen with 5-25% by mass of crumb rubber (between 0.075 and 1.2 mm) at an elevated temperature. The wet process includes the blending of crumb rubber with bitumen at high temperatures and produces a viscous fluid through rubber bitumen interaction. This reaction depends on temperature, size, and type of crumb rubber, aromatic type of asphalt binder [Presti, D.L. et al. 2014; Airey, G. et al. 2002]. The wet technology has the advantage that controls the binder properties because requires asphalt plants with another binder storage tank, that can handle more viscous modified binder than conventional asphalt. The mixing and laying temperatures are slightly higher due to increased bitumen viscosity. It should be noted that the blend of bitumen-rubber must be kept stirred or agitated to prevent stratification or separation of the crumb rubber modifier [Epps, J.a: et al. 1994]. The mixing temperatures range from 175-205°C, and the modified binder is then transferred to a heated reaction tank for 30-60 minutes at a temperature of 165-190°C (Figure 29).

Nowadays, these rubberized bitumen materials, obtained through the wet process, have spread worldwide as solutions for different quality problems (asphalt binders, pavements, the stress absorbing lays, and in roofing materials) with much different evidence of success demonstrated by roads built in the last 30 years.

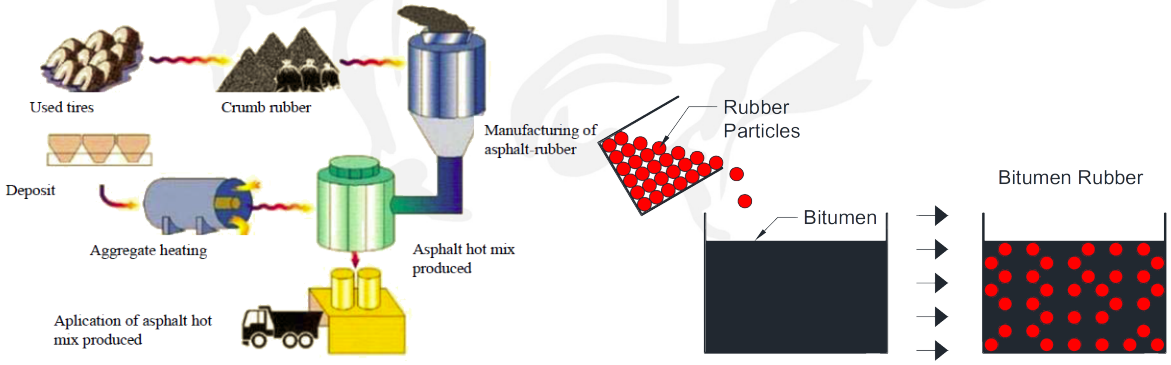


Figure 29. (a) The step of the wet process [Epps, 1994]; (b) Wet process, adapted from Hassan et al. [2014].

2.4.5.2. DRY process

The process was first developed in Sweden in the 1960s and widely known in Europe under the name "Rubit." It was then patented in the USA under the name "*PlusRide*" in 1978. The dry process is a process where rubber particles are added to pre-heated aggregates before binder mixing [Khan, N. et al. 2017; Zanetti, M.C. et al. 2015; Dong, D. et al. 2012; Huang et al. 2002]. In this process, CRM is added as a replacement of fine aggregate up to 5% by total weight of the mixture (Figure 30).

Between the two methods, the Dry process exhibited more significant potential for recycling scrap tires. Moreover, it is a more cost-effective method because it utilizes large quantities of rubber with less modification to the plant compared to the wet process [Hassan, N.A. et al. 2014].

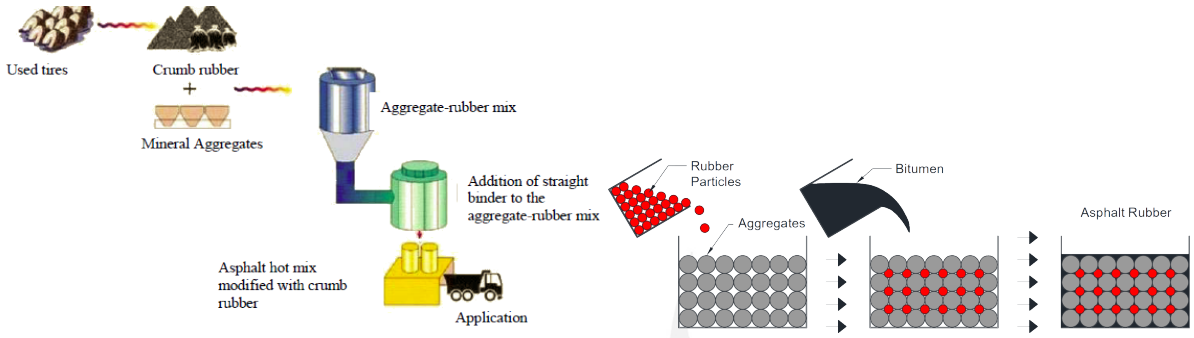


Figure 30. (a) The step of the dry process [Epps, 1994]; (b) Dry process, adapted from Hassan et al. [2014].

Wet process can accommodate dense-graded, gap and open-graded mix design. However, the dry process gives the best performance with gap-graded mixes. Gap-graded mixes do not only provide space for binder but also increase the resistance against fatigue cracking since more binder is introduced into an aggregate skeleton. Even though anti-oxidants are not thoroughly mixed with a binder, the dry process provides excellent skid resistance properties. In the dry process, there is little digestion of the rubber by the conventional binder. The time of contact binder-rubber is short and not enough to produce all necessary reactions between the two materials [Shen, J. et al. 2017; Dong, D. et al. 2012; Moreno, F. et al. 2011; Liang, R. et al. 1996].

Asphalt rubber products have been typically used in hot mix asphalt and spread applications. Instead, rubber modified asphalt mixes by a dry process (RUMAC) are gap-dense graded asphalt concrete mixes [Zhou, H. et al. 2014; Caltrans 2011; Takallou, H. et al. 1997] (Figure 31).



Figure 31. Asphalt rubber and Rubber modified asphalt concrete mixtures manufacturing

However, the dry process lost its popularity in the rubberized asphalt industry because of several unresolved issues, including the difficulty in achieving consistent performance about the swelling effect after compaction. Soto, F.M. et al. [2018] provided a manufacturing mix-design process to avoid swelling problems in the post-compaction phase characteristic of dry mixes. This *swelling effect* can prevent the mixture from achieving its target density, consequently leading to premature failures [Hang, L. et al. 2016; Gawel, I. et al. 2006]. The term ‘‘interaction’’ refers to the diffusion of the

lighter bitumen fraction (aromatic oils called maltenes) into rubber, thereby causing the rubber particles to swell [Hassan et al. 2014; Airey, G. et al. 2002; Peralta, E. J. F. 2009].

Also, the rubber–bitumen interaction is expected to increase the bitumen viscosity, thus imparting more excellent flexibility at low temperature while maintaining high stiffness at high temperature [Li, P. et al. 201; Kim, H. et al. 2011; Airey G. et al. 2003]. However, the rubber–bitumen interaction is often disregarded without being discussed extensively or documented in the study of dry mixed rubberized asphalt mixture, most likely because of the common assumption that interaction time before compaction is insufficient and can thus be ignored.

In practice, crumb rubber modified asphalt is stored at elevated temperatures after its production for easy handling and operation. However, due to the differences in specific gravity[2], crumb rubber particles dispersed in asphalt matrix tend to settle down to the bottom, resulting in the separation of crumb rubber and asphalt phases [Shu, X. et al. 2014]. This thesis carefully investigates the effects of varying mixture-design variables on the rubber–bitumen interaction, compaction effort, and target density. The mechanical properties of dry mixed rubberized asphalt mixture are also considered. An understanding of this swelling phenomenon in the dry process, in which crumb rubber expands after being exposed to bitumen, as well as the causes and measures that can be taken to achieve the target density and enhance the performance of rubberized asphalt mixture, will be developed in Chapter 6.

2.4.6. Technologies and production

There are two technologies in the dry method depending on the CRM and the aggregate gradation and distribution: *Plusride* and *Generic* dry technologies.

The *Plusride* technology modifies a conventional gap-graded aggregate gradation (Ø2.36-4 mm) with the elastic properties of the reclaimed tire rubber. It is necessary to create a gap in the aggregate gradation curve to provide space for the rubber particles, depending on the sieve chose and the grain size [Huang B. et al. 2002; Troy, K. et al. 1996; Newcomb, D. 1994; Bahia, H.U. et al. 1994].
The asphalt content is higher than that for a conventional mixture. Unlike conventional mix design methods, the only mix design criterion is an air void content in the range of 2 to 4 percent[3]. Instead, the *Generic-dry* technology uses an equivalent or slightly lower percentage of crumb rubber modifier. The CRM is smaller than that used in PlusRide. A conventional dense graded aggregate (Ø0.18-0.42 mm) is used with only slight modification. The gradation of CRM is adjusted to suit the aggregate gradation. The CRM passing the Nº40 (#0,40 mm) sieve reacts with the asphalt cement producing a modified binder and acts as an elastic aggregate. This technology has been used efficiently in USA [Huang et al. 2002; Gowda, G. et al. 1996] and other states [Epps, J.A. 1994; Page, G. 1989]

Recycled waste tires are used in asphalt paving mixtures in the form of crumb rubber with sizes ranging from Ø4.75 mm to Ø0.075 mm. Crumb rubber is produced by mechanically grinding shredded tire pieces to desired sizes under different conditions: ambient temperature, wet condition, high temperature, or cryogenic temperature. Ambient grinding is a process in which waste tire chips are crushed in fast running granulators or mills at ambient temperature. The wet grinding process at ambient temperature is introduced to spray water to crumb rubber to eliminate the temperature rise

[2] Specific gravity of rubber is approximately 1.151 while asphalt is about 1.033 g/cm^3
[3] On the basis of experience in laboratory developed at least three different aggregate gradations have been recommended for different layer thicknesses to serve different traffic levels.

due to milling. High-temperature grinding takes place at about 130ºC, resulting in granules of 1–6 mm [Shu, X. et al. 2014].

The Federal Highway Administration (FHWA) and many state agencies have conducted numerous field studies on the feasibility of using recycled rubber tire products in asphalt pavements. The National Cooperative Highway Research Programs[4] (NCHRP) provides a comprehensive review of the use of recycled rubber tires in highways [Bairgi, B.K. 2015; Hall, K. et al. 1996; Epps, J. et al. 1994].

2.4.7. Dry method of adding crumb rubber modifier

When crumb rubber is added with sufficient time and heat to the asphalt cement, it is slowly partially depolymerized [Swapna, V.P. et al. 2016]. Tthe asphalt used in the dry process needs to contain a relatively high percentage of light fractions, lower viscosity grade binder, contributing thus with aromatics for rubber reaction without removing asphalt components [Stroup-Gardiner et al. 1993]. A fine-dense gradation provides a higher surface area, and hence are more interactive with the asphalt [Sefidmazgi, N. R., 2014].

It is recommended, as a measure in this thesis, to resort to the use of industrial rubber mixed tires out of use of both light and heavy vehicles. Car tires are primarily a combination of synthetic rubber (approximately 26%) and natural rubber (approximately 20%). Industrial tires (truck, bus) are inherently natural rubber (approximately 33%) and only 20% synthetic rubber. The remainder of the tire is composed of carbon black, plasticizers, and other additives. Previous research has suggested that industrial tires produce a more stable and desirable reaction [Zanetti, M.C. et al. 2015].

Selection and acceptance of CRM for use in asphalt rubber classically relies upon requirements [Di Mino, G. et al. 2002]. These are expressed in terms of fiber content <0.5%; metal content <0.01%, moisture content <0.75%, density equal to 1.15 ± 0.05 g/cm^3 and maximum particle size Ø2.36 mm [M.C. Zanetti et al. 2014]. However, the ASTM D6114 standard [2009] also specifies that the exact size distribution of rubber powder should be agreed between producer and end-user.

In the case of the "dry" production technology, CRM can be employed with different size distributions, ranging from "ultrafine" (entirely passing the 0.3 mm sieve) to "coarse" (passing the 6 mm sieve and wholly retained on the 2.36 mm sieve) [Caltrans, 2005]. CRM is employed with a dosage of 1-3% (by weight of the total dry aggregates) or regarding volumetric substitution respect the weight of the total mixture (3-5%). Depending upon the type of plant or drum-mix, CRM is always added to the heated aggregates before coming in contact with bitumen, even though rubber particles are not digested in bitumen.

As mentioned earlier, the interaction between rubber and bitumen becomes tangible in the digestion phenomenon. Contact between the two constituents generates a chemical-physical reaction that takes place under precise temperature conditions and after a period. The high temperature, conjugated to the presence of aromatic oils and resins in the bitumen, allows the bulk of the rubber particles, which also arrive to duplicate their volume and the generation of a gel within the two elements in which the oils and resin are dispersed. During the inflation phase of the rubber particles, there is a sharp increase in the viscosity of the binder, which, after reaching a maximum value, is reduced due to the devulcanization[5] of the rubber (Figure 32).

[4] "Synthesis of Highway Practice 198 Uses of Recycled Rubber Tires in Highways"
[5] Rubber is "regenerated" to a chemical configuration close to that of the elastomer, thus allowing the solubility in the binder.

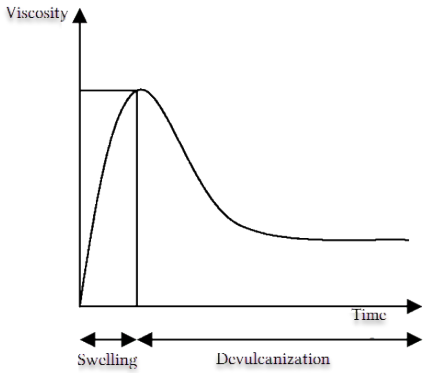


Figure 32. Qualitative performance of viscosity with time (Brookfield viscometer)

2.4.8. Evaluation of Rubber Modified Asphalt Concrete Mixes

The rubber granulates produced by the shredding process has a smooth surface that is less reactive with the bitumen present in the blend. Studies carried out in recent years have led to often conflicting results. It has found that elastic recovery capacity increases as the size of the granulate rubber increases. A study conducted by the Texas Transport Institute showed that swelling time increases with the radius of the rubber particle, requiring a PRM[6] particle of 0.075 mm per minute to react at a temperature of 163°C [Wayne, J. et al. 2006]. The swelling of the rubber particles is therefore only partial because only a portion of the fine fraction of the granulate entails some level of modification of the binder and consequently does not undergo substantial changes [Attia, M. et al. 2009].

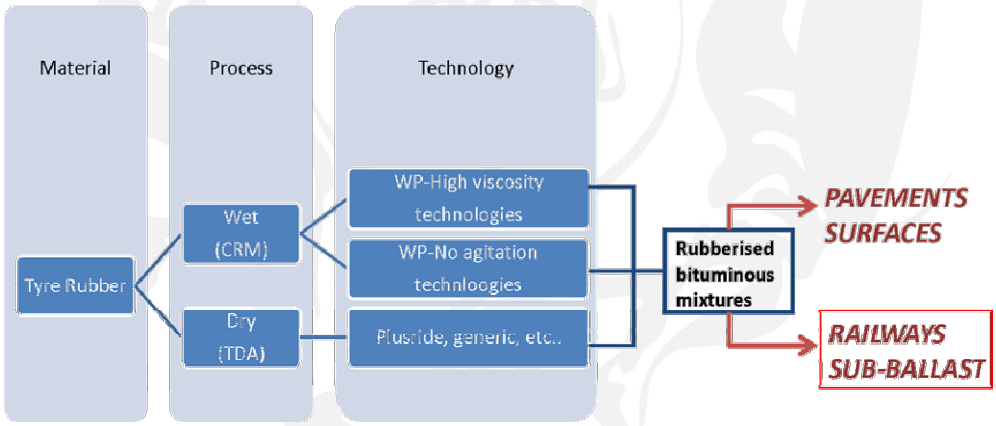


Figure 33. Use of recycled rubber from scrap tires (CRM) in asphalt [adapted from Soto, F.M. 2017]

The bitumen used has the same specifications as the one frequently used in conventional conglomerates. No significant changes to the standard hot-mix asphalt mixture plant are required, but a more accurate formulation of the granulometric curve and the digestion times are needed (Figure 33). The rheological and mechanical properties of the conglomerate with rubber depend strongly on the process used for its realization as well as the shape and granulometry of the granulated curve employed. A first differentiation between the wet-dry processes is comparing the equipment required for plant production. In fact, the rubber-bitumen reaction, until the obtained mixture shows a stable

[6] By the term, PRM, Powdered Rubber Modified, is meant a rubber powder was having granules of less than 0.24 mm, generally used in the production of modified bituminous binders. For granules of less than 0,075 mm, the term "ultra-thin dust."

viscosity, in the wet process, implies the use of sophisticated equipment at high temperatures, not necessary for the dry process, even it implies higher rubber consumption than wet [Kazi, T. 2017].

However, these considerations, are now in question, and constitutes this thesis research, proving the feasibility of using mixtures modified with rubber recycled by the dry-process. Following a protocol that leads to achieving the same benefits as in the traditional conglomerate, is possible to obtain best density results and target air voids percentages using the conventional procedure. As a preview of the samples well manufactured is shown in Figure 34. The difference, therefore, will depend on the mixing times, compaction, earlier digestion of the mixture, temperatures, post-compaction and method of adaptation (Marshall, Superpave or roller compactor).



Figure 34. Dry-Rubberized asphalt mixtures (CRM 1.5%, binder 5%, Superpave vs. Roller) [Soto, F. et al. 2017]

2.4.9. Benefits and drawbacks of RUMAC mixtures

From several studies and international experiences discussed above, when comparing with all-granular solutions, the use of rubberized HMA as sub-ballast can offer essential advantages at different points of view (Bearing capacity, Geometric quality, Vertical deformation, Drainage, Durability, and Environment reduction of noise-vibrations).

The performance of rubberized mixtures can be at least equivalent to the performance offered by traditional mixtures. Monitoring of traditional lines without sub-ballast compared with monitoring of lines with bituminous mix sub-ballast has proved that this layer has excellent damping properties.

Also, the concept of sustainable development embraces reduced consumption of raw materials, reduced emissions, and the possibility of increased recycling while still meeting development needs. In this way, the use of crumb rubber from scrap tires in bituminous mixes is a sustainable alternative to improve mix performance and, at the same time, allowing the valorization of waste products that developed countries generate in massive quantities. For these reasons, rubberized asphalt presents a high potential for their application as bituminous sub-ballast in railway tracks.

Bituminous mix also has disadvantages. A significant drawback with the use of crumb rubber modified asphalt is the resulting higher viscosity of the asphalt cement, which requires a relatively high temperature to pump the binder through the plant and efficiently coat the aggregates at temperatures of 160 °C or higher.

2.4.10. Other applications of End-of-Life tires in railways

In the last years, there have been several requests of crumb rubber (from the end of life tires) within the rail structure. Thanks to its capacity of deformation and attenuation of the loads and to its ability to withstand external environmental agents, this material has been used in the construction and rehabilitation of both superstructure and infrastructure, covering various tasks, such as providing

the structure of higher elasticity, reduce vibration problems or absorption of loads among others. Crumb rubber was used as the elastic element to mitigate the loads and reduce the stiffness of the track slab. Figure 35a shows an embedded rail system in a mixture of CRM and the polymeric matrix resin. This system emphasizes its level of vibration attenuation due to the presence of nearby buildings. According to the topic of development, crumb rubber has been used by various researchers to develop elastic element, such as rail pads, under sleeper pads and ballast mats [Carrascal I. et al. 2014; Sol-Sánchez, M. et al. 2014]. Figure 35b shows elastic elements for railway high-speed from the outer layer of deconstructed end-of-life tires to improve track mechanical performance.



Figure 35. (a) Embedded rail system (Sistem MLG); (b) Elastic elements for railway high-speed

This application would allow reducing construction costs as well as an abundant waste is reused. Results indicate the ability of tire pads to manufacture elastic elements (rail pads, under sleeper pads and ballast mats) to be used on high-speed tracks. Another application from a US company [Evans et al. 2006] has developed a railroad sleeper made of a rubber-plastic composite (Figure 36).



Figure 36. Railroad sleeper made of a rubber-plastic composite (TieTek LLC of Houston, Texas).

They are composed of a mixture of plastics, rubber from whole end-life-tires, rubber buffing from retreaters and other waste materials. They are lighter, impervious to insect and moisture damage, resistant to fungus, electrically non-conducive, resistant to chemical damage, and reduce vibration on track materials. Indian Railways have begun laying of composite sleepers in 10 railway zones across the country after successful testing at its laboratory and the partner's manufacturing plant in the USA. With increasing rail traffic and faster train speeds, railway boards across the globe are migrating to composite sleepers because of their increasingly evident benefits. As is illustrated in Figure 37, end-of-life tires have a broad range of use in the form of powders and granules; the primary applications of which are industrial floors, sports fields, children playgrounds, equestrian floors, molded pieces, and anti-vibratory mats [Brunner, P.H. et al. 2016].



Figure 37. New uses and applications of rubber according to grain size

2.4.11.Conclusions of Rubberized Asphalt Sub-ballast

In the infrastructure, the crumb rubber is used for bituminous sub-ballast improving the behavior of the track regarding bearing capacity, permeability, and vibrations among others. Some benefits of adding crumb rubber to the asphalt concrete layer in sub-ballast for railways are increased flexibility, skid resistance, fatigue life, as well as reduced crack reflection control, traffic noise, and aging.

There have been several applications in civil engineering try to solve the disposal of used tires problems, during the last years, especially in the road and rail sector. Notably, most of the studies assess the capacity of this material in vibration damping out of the dynamic loading and noise due to the transit of the trains since previous studies and field measurements on highways [Su, B. 2005].

As a result (Fig. 38), new lines are exclusively built using rubberized bituminous mixtures, in fact, there are not affected by freezing and are available as production facilities are located throughout the country. CRM is quick to settle and suitable for irregular surfaces. Also, it is waterproof and requires a lesser quantity of granular material leading to a saving of approximately 40% in the cost of aggregates in comparison with the mixed cement solution.



Figure 38. Summary table of the environmental advantages of using rubber asphalt

2.4.12.Life-Cycle Cost Analysis for RUMAC.

The life cycle of a consumer product is defined as the period of the product that serves the purpose for which it was created [Zaumanis M. 2018; Gmelin, H. et al. 2014]. The life of a tire is approximately 5-7 years during which a tire can be retreaded. It comprises three main periods: new, continuous use (continuous chain of utility) and shipment to a waste treatment system (end of the useful life of the tire). An out-of-use tire whose tire will be structurally stable from a depth of residual footprint suitable for the additional use of the road will be discarded and consigned to another use,

such as waste tires in road construction. Once the tire is removed from a vehicle, waste scrap tire can be usable in different forms, such as a whole tire, a slit tire, a shredded tire, and as ground-crumb rubber product. The short life cycle of a tire is shown in Figure 39a.

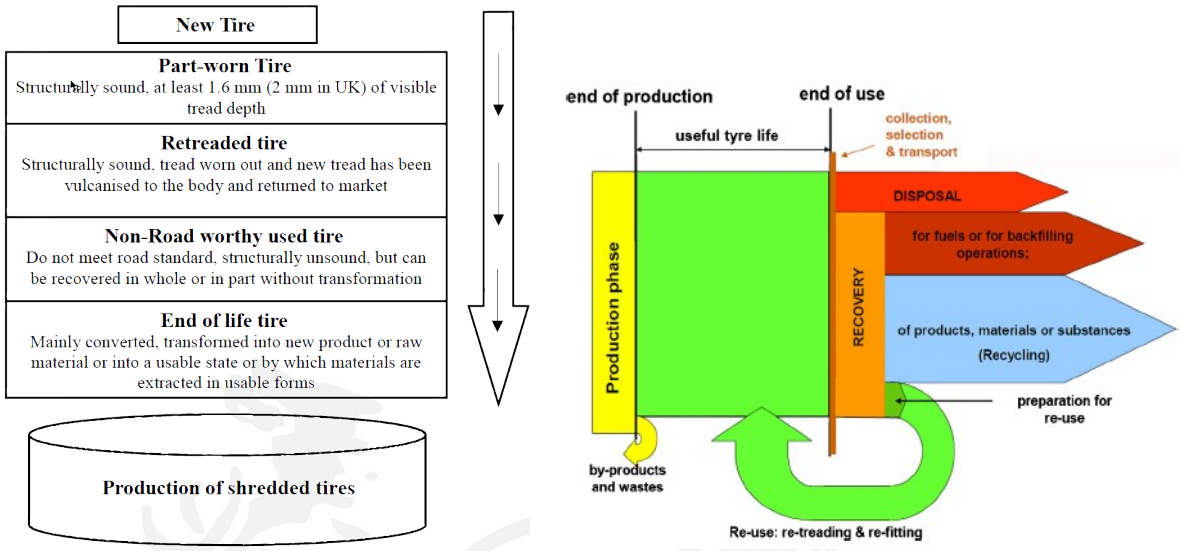


Figure 39. (a) Flowchart of the service life of a tire; (b) Tire contribution of noise reduction [Rimondi, 1995].

Worldwide, the Kyoto Protocol provides the lines to follow to the reduction of carbon dioxide (CO_2) and other so-called greenhouse gases. It was adopted by a consensus of the third session of the United Nations Framework Convention on Climatic Change. The Kyoto The protocol is designed to halt the concentrations of greenhouse gases that some people believe cause global warming. In this context in the construction sector, the sustainability has become one of the highest priorities to manage natural resources and at the same time develop new techniques. Figure 39b shows a simplified version of the tire cycle life. They can be summarized in five steps: extraction, consumption, collection, landfilling and recovery [Emery, 1995]. The most efficient method of measuring the cost-effectiveness of alternative designs is life-cycle cost analysis (LCCA) [Kerr, W. et al. 1987].

Farina et al. [2017] carried out a Life Cycle Assessment (LCA) of different types of road paving technologies based on the use of rubberized bituminous mixtures, considering different production, construction, and maintenance operations. LCA results, expressed regarding gross energy requirement and global warming potential, showed that the use of rubberized bituminous mixtures leads to significant benefits in comparison with standard paving solutions.

Some LCCA approaches can be employed to evaluate construction materials. However, the most appropriate method appears to be the MTO Asphalt Institute [Kerr, W. et al. 1987]. The life-cycle costing of the conventional HMA and RUMAC mixes assumed that routine maintenance activities would be provided on a regularly scheduled basis. A conventional asphalt concrete sub-ballast layer usually requires an overlay after about 30 years to extend its functional service life. The timing for significantly extended maintenance in railways required is about 60 years [Miura, S. et al. 1998].

2.4.12.1. Tools LCA for rail infrastructure.

Growth in demand for rail transportation across Europe is predicted to continue on existing lines that contain old infrastructure [Jensen. J.S. et al. 2014]. The impact of these interventions must be

minimized and will also need to take into account the need for lower economic and environmental impacts. There are currently commercially available several tools and specialized software dedicated to the study of LCA, meaning that is possible to model any product or service, but also specific to a particular scope. The tools analyzed refer to different databases, which lists:

- The CML 2001 (Center for Environmental Science of Leiden University) is a method of impact assessment developed by the Institute of environmental sciences, University of Leiden, Netherlands.
- The GREET MODEL (Greenhouse Gases, Regulated Emissions, and Energy Use in Transportation) aims to adequately assess the impact of energy and emissions of vehicles [Woertz, I.C. et al. 2014].
- The grid (Emissions & Generation Resource Integrated Database) is a comprehensive source of data on the environmental characteristics of almost all electrical power generated in the United States.
- Eurobitume Life Cycle Inventory: Bitumen bitumen paving describes the impact of production, modified bitumen and bituminous emulsions used in Europe.
- LCAT Project MainLine (MAINtenance, renewal, and Improvement of rail transport Infrastructure).

2.5. Conclusions of the "State of the Art."

The development of high-speed railway and the increase in the loading capacity of trains have led to the need to improve the track by adding a stiffer sub-ballast layer between the subgrade and the ballast. Its principal functions are bearing capacity, permeability and, among others, to protect subgrade from atmospheric actions. The granular configuration presents problems as the lack of quarries able to provide a material with appropriate characteristics for this layer, resulting in high transport costs from the quarry to the construction site with adverse consequences on the environment. Another problem is that to achieve the requested bearing capacity is necessary a higher thickness, with consequent use of a high amount of raw material.

Other limitations are related to the waterproofing ability through the presence of small aggregates in the granular material. However, some innovative solutions, such as the adoption of bituminous layers, may bring significant benefits on subgrade protection and railroad track performance. The use of asphalt mixtures in place of granular sub-ballast is a solution that must ensure the conditions required for bearing capacity [Thom, N.H. et al. 1987].

First results obtained with this material in other studies and experiences found in the literature show that it is worth further research on this topic, as it is necessary to optimize this solution, implementing recent technologies already developed in highways construction. Moreover, the solution of asphalt as sub-ballast used so far could be much improved compared to the asphalt used in the road sector; the design can be enhanced to obtain innovative solutions best performing. Furthermore, it is of great interest to study the feasibility of using crumb rubber from scrap tires with different sizes or scrap rubber particles, also include an amount diverse into mixtures, to manufacture sustainable asphalt to be used as sub-ballast. All this justifies the present research project[7].

[7] In addition, this research project is part of the European research project called "SUSTAINABLE PAVEMENTS & RAILWAYS INITIAL TRAINING NETWORK (SUP&R ITN) section "WP2 Railway's technologies" with the research project ERS8 "Characterization of rubberized asphalt for railway sub-ballast" which justifies its development.

2017

Chapter 3

RESEARCH OBJECTIVES

PH.D. FERNANDO M. SOTO

Chapter 3 – Research objectives

3.1. Abstract

The purpose of the experimental study is the performance evaluation of the traditional bituminous conglomerate according to Italian standard [RFI, 2016].

From the conclusion drawn in the study of state of the art, it was possible to understand that the adoption of bituminous layers, may bring essential benefits on subgrade protection and railroad track performance. Also, its advantages are the improvement of the requirements of bituminous conglomerate enriched with CRM rubber granules, derived from discarded lorry-tires, using a different proportion of rubber by the dry process in the sub-ballast layer (Fig. 1).

In this context, the primary aim of the present thesis is the optimization of bituminous sub-ballast in railways infrastructure under sustainability criteria through the reuse of end-of-life tires, by reducing energy consumption and gas emissions.

This technique needs further analysis, development and field verification for high-speed railways, since, however, in roadways, it is widely used. The analysis is carried out through a series of dynamic laboratory tests available for the determination of the stiffness modulus of a bituminous conglomerate (conventional and modified with ground rubber). The research has also been associated with the dissipative energy study of the materials, to build a complete picture of its physical and performance characteristics.

In the next chapters, the study of a Volumetric mix-design enhanced and the mechanical characterization to fatigue cracking distress, as well as the effects above of rebound-swelling in compacted specimens are the central topics of analysis [Soto, F.M. 2018].

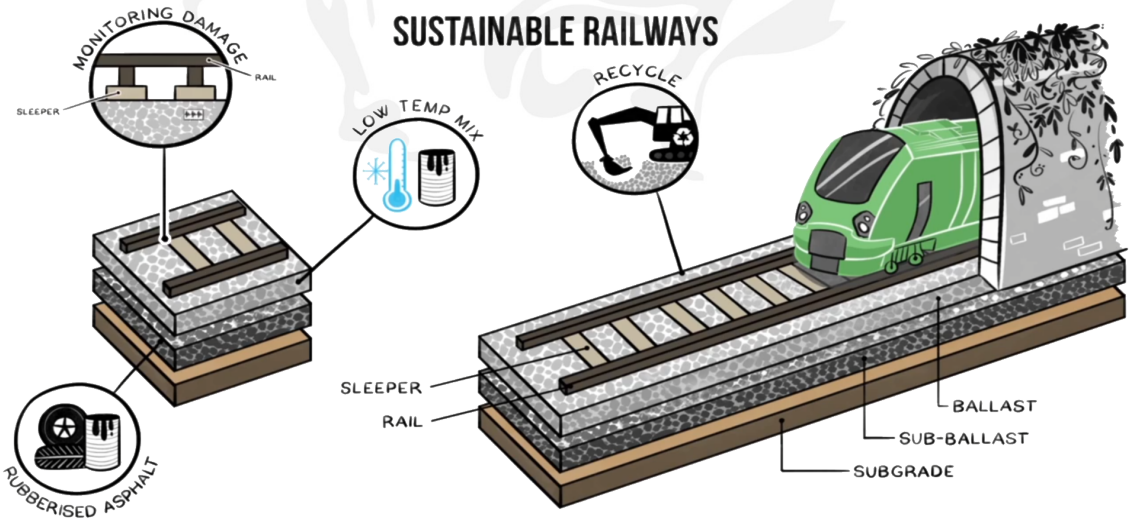


Figure 1. Graphical abstract of the scope of the thesis [adapted from SUP@R ITN[1] project as an ESR8 researcher, 2017]

[1] Sustainable Pavements & Railways Initial Training Network European Project (http://superitn.eu/wp/)

3.2. Introduction

The utilization of crumb or ground rubber in asphalt mixtures for base roads and railways sub-ballast has evolved in the last years increasing attention in many areas worldwide, especially CRM has attracted increasing attention in many regions worldwide. The recycled rubber (pneumatic out-of-use) shows an excellent recycling potential as a possible additive of the bituminous mixtures that require elasticity and resistance to long-life cycles. Although the modification through dry process method had been less used compared to the wet process, research conducted along this thesis, show that it is a viable technology, and industry should reconsider using the dry process in real projects.

The application of Rubberized mixtures requires attention due to the rubber-bitumen interactions [Airey, G.D. et al. 2002], which are considered a disadvantage since there appear effects like "swelling, rebounding effect and post-expansion" that affect the performance of the material [Putman, B.J. et al. 2010]. Therefore, adverse effects of the instability of rubber particles cause defects in the mixture. Thus it required an improved manufacturing process (mixing-compaction) [Soto, F.M. et al. 2017].

The Volumetric[2] mix design approach (designed as Superpave for roads [Cominsky, R.J. et al. 1994; Tashman, L. S., et al. 2000]) is applied systematically to the railway domain, without being adjusted for the different load configuration of the rail track system. Based on the dry technology, asphalt-rubber binders using devulcanized or natural rubber (truck and bus tread rubber), have been used to solve the problems generated during the Volumetric mix-design. As a target in rubber modified asphalt concrete mixes (RUMAC), we intend to enhance the workability by Superpave gyratory compactor (SGC) [Soto, F.M. et al. 2017].

3.3. The scope of the study

The **key aspects** covered in these years of research under the SUP@R ITN project are described:

- Study of "dry asphalt rubber" with the aim of increasing the duration of the sub-ballast layer.
- Optimization of bituminous sub-ballast, determining the optimal design of bituminous mixtures to be used as sub-ballast in railway tracks.
- Evaluation of recycled rubber asphalt to reduce the degradation of sub-ballast and reduce the stresses transmitted to the subsoil.
- The viability of using bituminous mixtures manufactured with crumb-ground rubber, as sub-ballast in railways track to obtain a sustainable and environmentally alternative to traditional asphalt products.

Project activities :

1. Evaluation of sustainable methods in the application of the Dry Rubber Asphalt Concrete (DARC), to decrease the vibrations in the sub-rail ballast.
2. Provide an experience of "mix-design volume" of bituminous mixtures and materials.
3. Investigate the optimal HMA mixtures of rubber granulates from disused tires.
4. DARC performance regarding mechanical behavior and ground vibrations.

[2] AASHTO M 323 Standard Specification for Superpave Volumetric Mix Design and, AASHTO R 35 Standard Practice for Superpave Volumetric Design for Asphalt Mixtures. American Association of State Highway and Transportation Officials. Standard specifications for transportation materials and methods of sampling and testing (30th ed.). Washington, DC: American Association of State Highway and Transportation Officials (AASHTO).

3.4. Purposes of the research

This thesis specifies the mix-design procedures developed in the Department of Civil Engineering of the University of Palermo during September 2015 to June 2017. Extensive integrated research has been carried out based on the sustainable search for improved modified asphalt mixes performed with coarse rubber from scrap tires as a sub-ballast layer in railways. In this context, the **aim** of the thesis is the optimization of bituminous sub-ballast in railways infrastructure under sustainability criteria through the reuse of end-of-life tires to obtain a solution economically competitive and with an adequate mechanical behavior, at least equivalent to that presented by the granular sub-ballast.

The following **specific purposes** have been established:

1. The mechanical design of the Railtrack through a three-dimensional model of finite elements (FEM), explaining the stress-strain behavior of the HMA trackbed underlayment interface with Kenpave-Kentrack software (AASHTO Methodology of calibrated mechanistic procedure for flexible layers)[Rose J. et al. 2014; Huang Y.H. et al. 1984].
2. The viability of using conventional (HMA) bituminous mixtures manufactured by high-temperature technology as sub-ballast in railway tracks by Superpave, Marshall, and Roller slab compactors.
3. The exhaustive fatigue-cracking study of the mixtures modified with rubber recycled by its recent acceptance in the use of roads and now, at rail level, as sub-ballast in railways track to obtain a sustainable and environmentally alternative to traditional asphalt products.

- This research aims at defining the parameters for adapting the gyratory compactor methodology to the bituminous sub-ballast mix-design [F. Martínez-Soto et al. 2017].
- After that, other parameters deal with the rail structure, as the *temperature* in the whole rail track formation, the *traffic*, and the *distresses* of the sub-ballast layer:
    - Regarding the evaluation of useful life of the railway, predictive models of temperature based on bibliography have been revised [Andrei, D. et al. 1999; Barber, E.S. 1957; Crispino M. et al. 1998].
    - The traffic spectrum is adapted to select the design parameters of the road-model adopted by Superpave. After defining the average seasonal temperatures interpolated by sinusoidal functions is calculated the elastic modulus of the asphalt layer.
    - A FEM modeling with the aim of representing the real conditions in railway trackbed. After that, it represents the volumetric mix-design criteria of the lab-mixtures using the Superpave gyratory and Roller slabs compactors [Lee S.J. et al. 2008].
- Fatigue cracking is explained to the mechanical characterization of the mixtures by using the UGR_FACT (Fatigue Asphalt Cracking Test)[3] device at different traffic loads and frequencies [Moreno, F. 2013-2014; F. M. Soto et al. 2015; Carpenter, S.H. et al. 2006].

[3] The fatigue tests were performed at the LabIC, Laboratory of Construction and Engineering at the University of Granada (Spain) with the test device called UGR_FACT, based on a device that produces controlled fatigue cracking process, makes possible to analyze the cracking propagation in the different phases (initiation, progression, and failure).

3.5. Main objectives pursued

- The first objective was to acquire a broad knowledge related to the dry-recycled rubber technique in road base layers and rail sub-ballast. It has been proposed a review of the known techniques, the design of mixtures, optimization and protocol of execution to avoid deformations and short-term maintenance;
- A second objective was to study the effect of environmental conditions such as temperature, bitumen aging and moisture damage on the mechanical properties of the conventional hot mix asphalt mixtures;
- The third objective is the study using Kenpave-Kentrack calculation software, determine the similarity between the road base layer and the sub-ballast layer regarding stresses, temperature (environmental conditions) and traffic (bearing capacity).
- The fourth objective is the development of dry mix blends in the laboratory that meets the minimum requirements for international rail sub-ballast standards (aggregates, bitumen, recycled rubber, methods, and techniques).
- The last objective of this study, it was to evaluate the fatigue-cracking resistance of the crumb rubber modified asphalt mixes compared to conventional asphalt mixes.

A graphical resume of this points is showed in Figure 2.

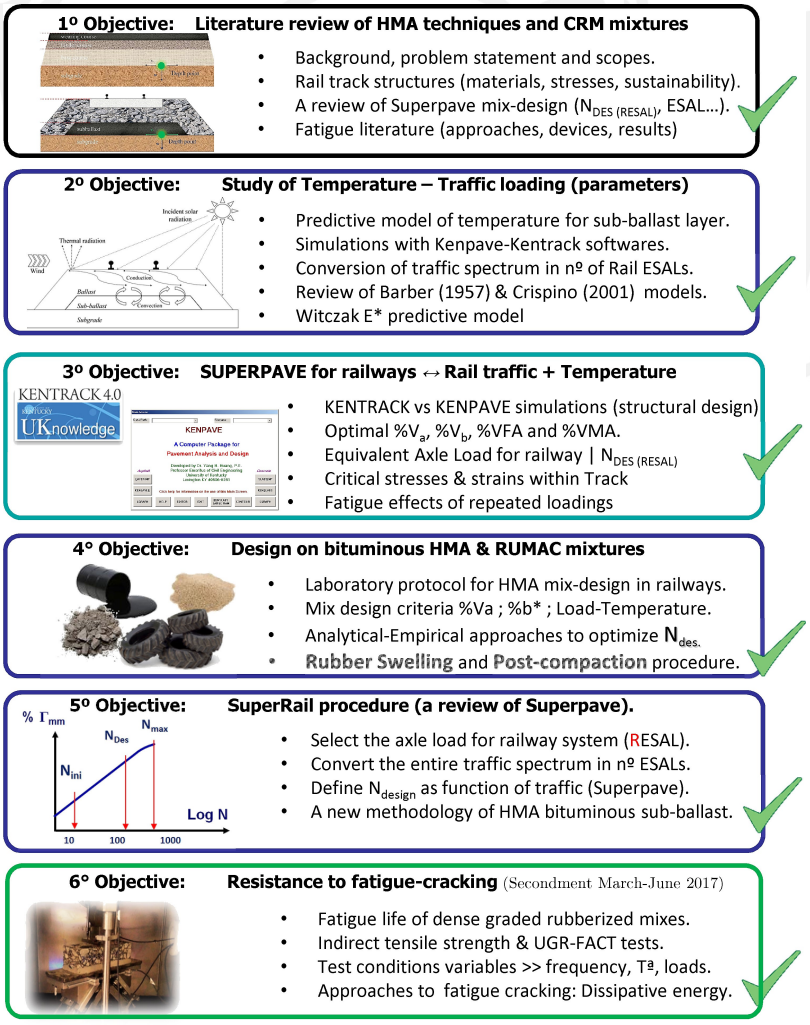


Figure 2. Objectives in a flow-chart graphical resume

3.6. Secondary objectives

During the development of the objectives mentioned above, new parallel lines of research emerged during laboratory work and review of the results. In some cases they have come to study in parallel for their scientific value and because they have motivated changes in final decisions.

Among these secondary objectives are:

- During 2015, inside the literature review done, a review of the resistance to fatigue of DARC materials was proposed, considering a previous work developed in the laboratory using the *fatigue device 4PBT* (Four-point bending test).
- During 2016, it was proposed a review of the flexural fatigue in railways and stiffness modulus by European standards EN 12697-24/26. A review of the *complex modulus* that relates stress to strain for linear viscoelastic material subjected to apply sinusoidal loading in the frequency domain continuously was considered.
- During 2016, an Empirical approach was proposed as a new methodology of mix-design based on the precision of the N_{des} parameter [Soto M. F. et al. 2017];
- In February 2017, a relationship between the Volumetric gyratory and the mechanical roller slabs compactors was studied after validating both techniques and parameters (pressure of loading, the number of cycles, the ratio of rotations/passages between SGC and Roller.
- Within the secondment period, a parallel investigation was carried out using the non-destructive technique FFRC [ASTM C215, 2014; Gudmarson, A. et al. 2012][4].
- Finally, during June 2017, after finishing the fatigue tests, the wastes derived from the fractured test specimens UGR_FACT, of dimensions 100x60x60mm, were cut into small cubes of 5x5cm for the realization of a *static compression test in a hydraulic pressure machine*. These tests, considered elastic because of their fastness at high compressive loads, determined the slope-strain curve that allows obtaining the dynamic modulus of the mixtures manufactured post-fatigue.

[4] The free–free resonant frequency (FFR) method as an attractive alternative for measuring the small-strain Young's modulus and shear modulus in prismatic samples of rubberized asphalt by dry process. The modal parameters (resonant frequency, modal damping and frequency response function) are measured. The dynamic modulus of elasticity, shear modulus of rigidity and, Poisson's ratio are derived.

2017

Chapter 4

METHODOLOGY

PH.D. FERNANDO M. SOTO

List of Figures Chapter 4

Figure 1. Work plan (methodology steps) 55
Figure 2. The confrontation between conventional and sustainable HMA sub-ballast in railways. 57
Figure 3. Materials description and methodology procedures 57
Figure 4. (a) conventional granular; (b) bituminous sub-ballast [adapted from Di Mino, G. et al. 2012] 58
Figure 5. Purpose of the mixtures with recycled rubber: optimize the compaction curve in SGC 59
Figure 6. A graphic diagram of the bituminous sub-ballast solution. Components and materials 59
Figure 7. (a) Desirable aggregate shape and angularity; (b) Typical particle size distribution limits 61
Figure 8. (a) Maximum density curves (0.45 Power gradation graph); (b) Fuller's curves 62
Figure 9. (a) Granulometric curve based on RFI and Fuller's curve; (b) Sieve analysis developed in the lab 62
Figure 10. Grading sieves limits; (b) Grading band comparative sub-ballast asphalt mixes [PF7-RFI] 63
Figure 11. Small, Medium and Large aggregate particles distribution. 63
Figure 12. (a) Target grading curve of the bituminous sub-ballast; (b) Different fractions of aggregates; (c) Sieve analysis of fine and coarse aggregates for sub-ballast (ISO 3310); (d) Grading curves adjusted; (e) Sacks supplied of the different fractions of aggregates; (f) Sieve analysis [ISO 3310-1:2000] 64
Figure 13. Adjusting the granulometry of the sieving curves on an Excel sheet with solver function. 67
Figure 14. (a) Portland cement used; (b) Sieve analysis for different filler fractions 67
Figure 15. (a) Sketch showing saturated, surface-dry condition in an aggregate particle; (b) Pycnometer method of determining fine aggregate specific gravity [NCHRP 673] 68
Figure 16. (a) Laboratory process of aggregates selection; (b) Pycnometer method (fine aggregate) 68
Figure 17. Maltenes in solution into different fractions: saturates, aromatics and resins 69
Figure 18. EN 12591. SHRP Grades from 20/30 to 160/220. 70
Figure 19. (a) Penetration test at 25ºC; (b) Needle depth measured; (c) Bitumen casting inside the rings; (d) Detail chassis, ring, and spheres. 70
Figure 20. (a) Brookfield viscometer; (b) Rheocalc v.3.2 software; (c) Bitumen containers [ASTM D2983-17] 72
Figure 21. (a) Viscosity-Temperature chart [ASTM D2493-16]; (b) Viscosity vs Temperature binder B50/70 73
Figure 22. (a) Under traffic the film of bitumen breaks. Asphalt mix modified with rubber increase resistance; (b) Benefits of using rubber modified bitumen. 75
Figure 23. (a) Preliminary selection; (b) The tires are inserted into the first crusher 76
Figure 24. (a) Milling of the rubber; (b) Semi-finished rubber membranes in sacks 77
Figure 25. Difference sizes of crumb rubber used 77
Figure 26. (a) Sieving process; (b) Grading curves of the rubber fractions ϕ0.4-2mm; ϕ2-4mm, and ϕ5.6-11mm 78
Figure 27. (a) Sieves rubber fractions ϕ0.4-2mm; ϕ2-4mm, and ϕ5.6-11mm; (b) Rubber densities 78
Figure 28. Classification by aggregate gradation (Adapted from LabIC.UGR publications) 79
Figure 29. Gradation types. 79
Figure 30. Comparison between Dense-grade and SMA mixes 80
Figure 31. (a) Example of HMA manufacturing in the laboratory; (b) Superpave 150x120mm samples; (c) Aggregates; (d) Binder B50/70; (e) Compacted HMA specimens. 80
Figure 32. Materials and mixtures specifications of the research 82
Figure 33. Definition of the HMA and DRY mixture gradation specification bands (% passing by weight) 85
Figure 34. (a) Hveem gyratory compactor; (b) Marshall compactor; (c) Superpave gyratory compactor. 86
Figure 35. (a) Definition of volume terms used in the volumetric analysis; (b) Density-Voids and Volume Relationships of a Compacted Asphalt Sample 87
Figure 36. (a) Superpave gyratory compactor procedure; (b) Assessment of workability with SGC 88
Figure 37. The height of SGC samples as an analogy of field conditions 89
Figure 38. (a)Performance grade; (b) Aging of bitumen (distresses and mechanical tests) 92
Figure 39. (a) Procedure to measure bulk specific gravity; (b) Weight-in-water apparatus 93
Figure 40. (a) Vacuum pycnometer test; (b) Hydrostatic Density Meter 94
Figure 41. (a)Air in asphalt concrete; (b) Dense-graded mixture; (c) VMA_NMAS relationship 95
Figure 42. Graphic design of an inhomogeneously compacted mixture 98

Figure 43. Construction procedures of HMA – DRY mixtures (Protocol) 98
Figure 44. The operational framework for RUMAC (Dry) mixtures 99
Figure 45. (a) Samples extruded from the SGC; (b) Specimens after 24h; (c) Bulk specific gravity in water 99
Figure 46. (a) SGC model AFG1; (b) Sample molds of dimensions ϕ150x250mm; (c) Mixing process of aggregates, bitumen, and filler; (d) Control of temperature and digestion time 100
Figure 47. (a) Optimal binder determination [Va-%b*]; (b) Densification curves 101
Figure 48. (a) Samples for extraction of bitumen (b.4%, Va.2%); (b) Centrifuge extractor with ignition furnace 102
Figure 49. The Marshall and Superpave mix-design procedures (Adapted from Thom, N., 2008). 102
Figure 50. Density-Voids and Volume Relationships of a Compacted Asphalt Sample. 103
Figure 51. (a) IDT device; (b) Superpave-Marshall specimens for IDT and water sensitivity tests. 103
Figure 52. (a) Wet specimens; (b) Indirect Tensile strength test [EN 12697-23]. 104
Figure 53. (a) Test frame; (b) Type of failure on ITS specimens [ASTM D6931]. 104
Figure 54. Asphalt slab roller compactor pressures per mixture 105
Figure 55. Asphalt roller compactor and slab mold design details 106
Figure 56. Manufacturer of slabs by roller compactor, unmold and cut into prisms 107
Figure 57. (a) UGR-FACT test device; (b) Stress simulation in a test specimen 108
Figure 58. UGR_FACT device with a broken sample of the HMA mixture developed 108
Figure 59. Sketch of the effort conditions induced during UGR-FACT (Adapted from [Moreno, F. 2016]) 109
Figure 60. Sketch of the displacements produced during UGR-FACT test (Adapted from [Moreno, 2016]) 110
Figure 61. Representation of Log Δε (%) as a function of the dissipated energy on an HMA mix 111
Figure 62. FFRC tests. (a) Equipment and development on an HMA sample from roller slab; (b) Illustration of the experimental setup 112
Figure 63. (a) Overlaying shooting records to set the impact signal ("triggers"); (b) Example FFRC tests by signal equipment 112

List of Tables Chapter 4

Table 1. Tasks 56
Table 2. Standard limits for the Sub-ballast mixture (RFI, 2016). 58
Table 3. Locomotive E444 technical specifications 60
Table 4. Definition of aggregate fractions and types 62
Table 5. Properties of the aggregates 65
Table 6. Commercial fractions and technical data sheets provided 65
Table 7. Sieve analysis of fine and coarse aggregates. 65
Table 8. Grading curve for sub-ballast (based on RFI, ISO 3310) 66
Table 9. Sieve weights of aggregate as a function of NMAS 66
Table 10. Asphalt Binder Grade and Viscosity Parameters (NCHRP 1-37A, 2004) 71
Table 11. Properties of bitumen B50/70 used in Sub-ballast 73
Table 12. Viscosity determination of the binder 50/70 using Brookfield viscometer 73
Table 13. Optimal equiviscosity values with Brookfield viscometer 74
Table 14. Requirements for dust/binder ratio 75
Table 15. Properties of the rubber added to the dry-process CRM mixes 78
Table 16. Aggregate Gradation for Gap-graded PlusRide mixes 81
Table 17. Aggregate Gradation for Generic Dry Mixes 81
Table 18. Aggregate, rubber and bitumen specification 83
Table 19. Design Mix Properties HMA 83
Table 20. Design Mix Properties DRY 1.5% 83
Table 21. Final Grading curves for an HMA – DRY mixtures (Adjustment of sieve fractions) 84
Table 22. Results of gradation and adjustment of the passing for each mixture. 84
Table 23. Specifications for mix-design 84
Table 24. Volumetric mix design characteristics 84
Table 25. Hierarchical Organization of the Superpave Mix-design 88
Table 26. Superpave original table (SHRP Method of Test M002, Harrigan, et al. 1994) 90
Table 27. Revised Ndesign table proposed by NCHRP (2007) 91
Table 28. Revised Ndesign table proposed by AASHTO R35 (2015). 91
Table 29. Pavement surface temperatures typical of different climates (2015). 91
Table 30. Voids in Mineral Aggregate Criteria 96
Table 31. Sample volumetric design data at Ndes (HMA mixture B50/70) [AASHTO R35] 97
Table 32. Voids Filled With Asphalt Criteria (VFA vs. ESAL) 97
Table 33. Specifications for the preparation of rubber modified asphalt mixtures 100
Table 34. Volumetric analysis of RCC recipes for laboratory 106
Table 35. Fatigue cracking (Testing plan for each mixture) 110
Table 36. Characteristics of the fatigue cracking tests 111

Chapter 4 – Methodology

4.1. Introduction

The methodology outlined in this chapter, defines the different phases followed to reach the aims of this doctoral thesis describing the methodology for mix-design, the materials used, and the work plan in various phases carried out to evaluate the mechanical performance of sustainable bituminous rubberized sub-ballast (Fig. 1).

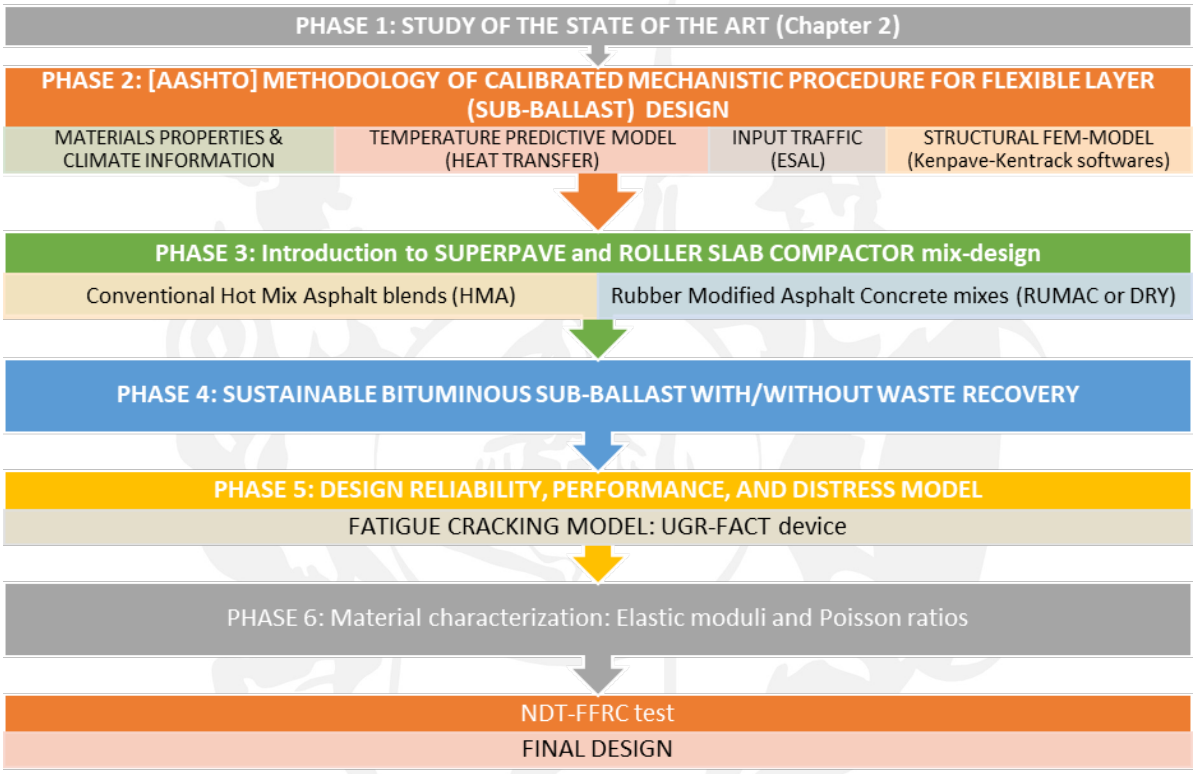


Figure 1. Work plan (methodology steps)

The use of the Superpave Gyratory Compactor (SGC)[1] for asphalt mixtures design is increasingly and currently being evaluated [Pérez-Jiménez, F. et al. 2014; Thompson, M.R. 1992; Huang Y. 2004]. The entire mix design system, including field control, is based on the use of the Volumetric mix-design with the gyratory compactor. It is the optimal laboratory tool that simulates field compaction of asphalt mixtures [Fager, G. 2001; Emery, J. 1995; Heitzman, M. 1992; Gowda, G. 1996].

The performance properties of the compacted specimens simulate the mechanical properties of flexible HMA layers. The SGC also allows the optimal compaction of the mix to be evaluated, including an estimation of the final air voids content under traffic and a measure of the structuring of the aggregate [Soto, F.M. et al. 2017]. The study is focused on evaluating the influence of the

[1] Superpave Gyratory Compactor (SGC) estimates the binder demand needed for the selected aggregate structure, and proceeds with preparing a maximum specific gravity sample and a set of 150 mm specimens for compaction in the Superpave gyratory compactor.
The gyratory simulates the mix densities achieved under the actual climate and loading conditions. This device is capable of accommodating large aggregate, recognizing potential tender mix behavior and similar compaction problems, and is well suited for mixing plant quality control operations.

compaction procedure by gyratory compactor and mechanical properties of asphalt mixtures [Harrigan, E.T. et al. 1994]. The Volumetric mix-design system is a comprehensive method of designing paving mixes tailored to the unique performance requirements dictated by the traffic, environment (climate), and a structural Railtrack section. It facilitates selecting and combining asphalt binder, aggregate, and any necessary modifier to achieve the required level of pavement performance [Cominsky, R.J. et al. 1994].

Through materials selection, it directly addresses the reduction and control of fatigue cracking, and also explicitly considers the effects of aging and moisture sensitivity in the development of the distresses. The objective of the mix design system is to define an economical blend of asphalt binder and aggregate that yields a paving mix having sufficient asphalt binder, voids in the mineral aggregate (VMA) and air voids. As requirements, it is needed excellent workability and performance characteristics over the service life [NCHRP-573, 2007; AASHTO, R35-151, 2001; Epps, J.A. 1994].

SHRP Gyratory Compactor covers the compaction of Ø100-150mm test specimens and the measurement of the density, aggregate orientation, and structural characteristics obtained in the actual sub-ballast layer [SHRP-A-407, 1994].

This chapter reports concepts about mechanical properties with HMA-RUMAC[2]mixtures for railway sub-ballast layer performed using the dry process.

The production of asphalt mixtures is now entirely an automatic process that implies an adequate mix-design procedure has the required performances within the Railtrack. These performances can be identified as *workability*, susceptibility to *mix-compaction*, and the *fatigue-cracking resistance*.

The objective of a review of Volumetric Mix-Design is to develop a lab-procedure with focused attention on better handling high-shares of rubber, and the effect of the variability of crumb rubber modifier (CRM) properties in the performance of the railway sub-ballast. Currently, no widely accepted mixture design method has been developed for rubber-modified asphalt mixtures: PlusRide® and Generic-dry© methods [Baumgardner, G.L. 2015; Ganiron, T. 2014; Huang, Y.H. et al. 1984]. In this Chapter is described the methodology, techniques of the constituent materials of the rail sub-ballast layer, and the Volumetric mix-design characterization by a review of the experimental protocol in the laboratory. Below is the scheme of ideas (Table 1):

TABLE 1. TASKS

Index	Work section	Task title
1	Constituent materials	Task 1.1 Bituminous sub-ballast mixtures. Task 1.2 Aggregates and grading curve. Task 1.3 Bitumen (composition, structure, chemistry, adhesion, modification). Task 1.4 CRM mixes.
2	Physical properties	Task 2.1 Penetration, softening point, viscosity. Task 2.2 Complex and Elastic modulus. Stiffness. Task 2.3 Ratio bitumen/filler; Dust-Asphalt ratio.
3	Mixture design	Task 3.1 Blend design validation; Mixes production in asphalt plants. Task 3.2 Superpave gyratory compactor: stability, durability, permeability, workability.
4	Superpave Mix-Design	Task 4.1 Laboratory protocol. Operational framework Task 4.2 Asphalt binder selection >> Sample preparations Task 4.3 Digestion time, compaction and densification curves Task 4.4 Optimization of compaction curves. Density correction factor. Task 4.5 Extraction of bitumen from HMA mixtures. Final design.
5	Mechanical characterization	Task 5.1 Fatigue cracking Task 5.2 Comparison of Roller slab compactor and Superpave Mix design Level III

[2] Rubber-modified hot-mix asphalt mixes (RUMAC) Plusride or Generic Dry.

4.2. Constituent materials

From the literature review, it was decided to adopt as a reference section, a granular sub-ballast made of ground aggregates with a thickness of around 19-22 cm, and a bituminous sub-ballast of 12 cm regarding performance (Fig. 2) [Signes, C. et al. 2016; Khosla, N.P. et al. 2013; Moreno F. 2013; Di Mino, G. et al. 2012; Thodesen, C. et al. 2009; Rose, J.G. et al. 2006-2011; Subhy, A. et al. 2005; Fager, G.A. 2001; Buonanno, R. 2000; Emery, J. 1995; Epps, J.A: 1994; Huang, Y. et al. 1984; CNR-BU-39, 1973].

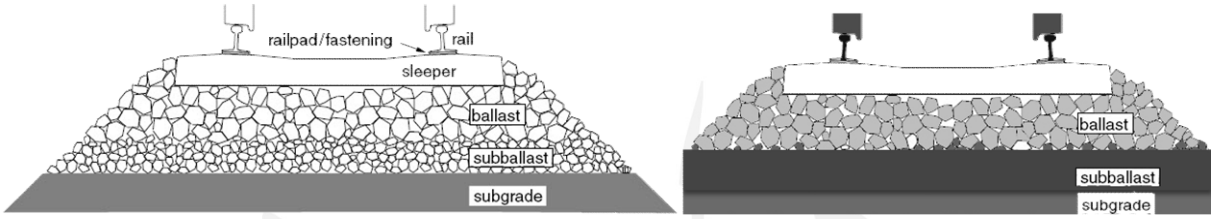


Figure 2. The confrontation between conventional and sustainable HMA sub-ballast in railways

The type of mixture commonly used within the track is a dense-graded bituminous mixture based on the Superpave specifications. Different materials have been employed to be able to design and to explore the various types of sub-ballast (Fig. 3).

BALLAST	SUB-BALLAST	AGGREGATES FOR ASPHALT	END OF LIFE TYRES	ASPHALT MIXES	RUMAC MIXTURES	RAILWAYS STRUCTURAL DESIGN
OPHITIC ROCKS	FINE-COARSE AGGREGATES	LIMESTONE (Sand-filler-gravel)	CRUMB-GROUND RUBBER (truck tires end-of-use)	HMA (B50/70) Va.±3% ; b.±4%	DRY 1.5% DRY 2% DRY 3%	Underlayment sub-ballast Trackbed
· Granulometry · Content of fine particles · Fines content · Faces of fracture · Density · Resistance to fragmentation · Flakiness index	· Granulometry · Faces of fracture · Density · Resistance to fragmentation · Flakiness index · Sand equivalent	· Granulometry · Flakiness index · Faces of fracture · Resistance to fragmentation · Sand equivalent · Density and absorption	· Granulometry · Density · Colour · Morphology · Water content · Textile fibber content · Metal content · Composition · Geometry · Bearing capacity	· Mix design · Aggregates · Bitumen · Bitumen emulsion	· Granulometry · Humidity · Bitumen content · Recovery and processing of bitumen · Recovery and processing of aggregates · Mix design	AASHTO method "Calibrated Mechanistic Structural Analysis Procedure for Flexible bituminous sub-ballast in railways" · Climate model · Input traffic · Kenpave · Kentrack

Figure 3. Materials description and methodology procedures

The asphalt mixture is designed with the similar characteristic as that used in highways, although for its application as sub-ballast the bitumen content is increased by 0,5% about the optimum for roads. Furthermore, the air void percentage is reduced to 1–3% to obtain a mix easier to densify and therefore facilitates adequate strength. The conventional granular sub-ballast analyzed is composed of ophitic aggregates with a constant granulometry from 31.5 mm to 0,063 mm according to the Italian Standard (RFI, 2006). Table 2 shows the characteristics of aggregates, bitumen, and mixture required

to for their use in railways as bituminous sub-ballast. Moreover, its maximum density and optimal moisture were determined by using the Proctor test (EN 103-500) to obtain adequate compaction of this material for its application in railway tracks (Fig. 4).

TABLE 2. STANDARD LIMITS FOR THE SUB-BALLAST MIXTURE (RFI, 2016).

	AGGREGATES
Sand equivalent (%)	> 50
Angular particles (%)	> 90
Flakiness index (%)	< 25
Los Angeles test (%)	> 25
	BITUMEN
Type	B50/70
Content (%)	> 4,75
	MIXTURE
Void content (%)	1 - 5
Filler/bitumen	0,9 - 1,2
Water sensitivity (%)	> 85
Dynamic stiffness modulus (20°C) (Mpa)	3700 - 7100

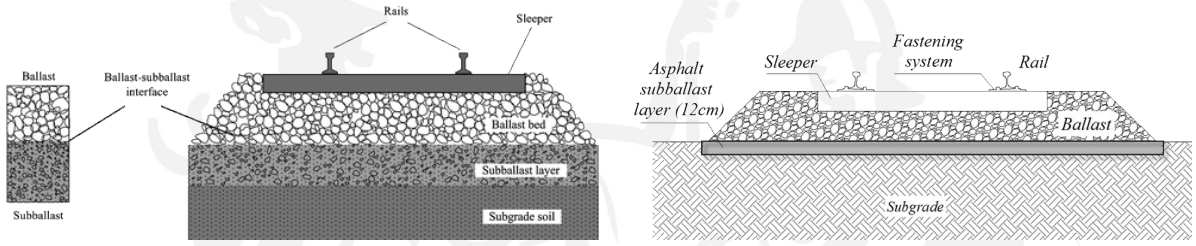


Figure 4. (a) conventional granular; (b) bituminous sub-ballast [adapted from Di Mino, G. et al. 2012]

Mixture composition, preparation, and curing are significant elements in the production phase that affect mixture performance in service. All the process of mix-design is focused on Superpave gyratory compaction technique [AASHTO R35-151, 2001-2012; AASHTO TP4, 2000; AASHTO M323, 2013; Design, S.M. 1996; SHRP-A407, 1994]. The particle size distribution of **aggregate** is one of the most influential characteristics in stiffness, stability, durability, permeability, workability, fatigue, and moisture susceptibility [Usama, H. 2013; Dessouky, S. et al. 2004]. In the case of **asphalt**, bitumens are often exposed to a wide temperature range, covering the daily and seasonal variations. The use of **CRM** has been promoted to benefit the environment [Conti Puorger, A. et al. 1976; Orlandi, D. 1984].

Therefore, a study of the RUMAC mixtures will be carried out, and their performance and improvements in the desired properties can be evaluated according to a necessary design protocol during mixing and compaction. As the material gradation and mixture design used in this study were different from other types of CRM mixtures currently available, the terms "HMA_{RFI}" and "$DRY_{1.5_2_3\%}$" were adopted as acronyms to represent the mixtures throughout this research.

Different RUMAC mixtures were designed using the Italian grading curve [RFI, 2016] but enhance with other sieves according to European standards [EN 933, 2012; EN 933-10, 2009; ISO 3310] to minimize the extra effort required in the material design stage. During the study, a high number of specimens were developed by SGC to obtain the optimum blend. Through different formulas have enhanced the percentage of asphalt binder (b.% of the total inert weight), and different quantities of rubber proportion (1-3% of the total weight of the aggregates in volumetric substitution).

In the next sections, a description of materials, HMA_DRY mixture design methodologies, sample preparation protocol, compaction methodology and a brief comparison between "Volumetric Mix-Design" and "Marshall compactor" technologies for the mixture designed is presented.

The dry process had become less popular, although it has a high potential to consume more significant quantities of scrap tires compared to the wet process (Fig. 5).

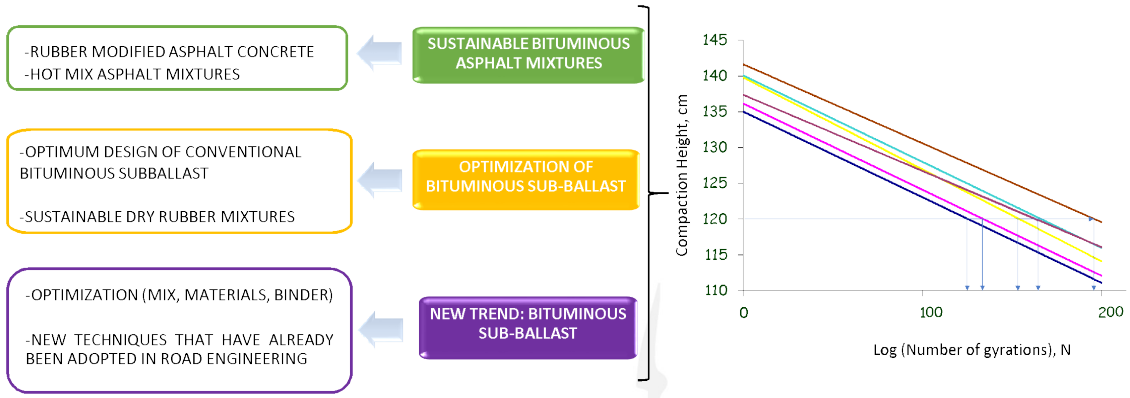


Figure 5. Purpose of the mixtures with recycled rubber: optimize the compaction curve in SGC

An outline of the adopted sustainable solution based on the materials is shown in Fig. 6. A hierarchy of the proposed multilayer rail sub-ballast model is established.



Figure 6. A graphic diagram of the bituminous sub-ballast solution. Components and materials

4.3. Technical aspects of bituminous sub-ballast: a review.

A first examination of the traditional structure, using different ballast thicknesses between 30 and 50 cm, gave the highest values of the primary loads, almost static, calculated using the *Burmister method* (Table 3). This data being analyzed, showed that there is the presence of traction effort in the ballast which, for a thickness of 35 cm, used in Italian high traffic lines, a static load reaches 0.60 daN/cm^2, affecting the ballast itself for about 1/3 of its thickness.

TABLE 3. LOCOMOTIVE E444 TECHNICAL SPECIFICATIONS

E.444		(Static loads) for sub-ballast structure			
Dimensions	16.840 x 3.020 x 4.300 mm	Thickness 35 cm; E= 1500 daN/cm^2	σ_x	σ_y	σ_z
Axle distance	3.020 mm	Wagonload freight train	0.129	0.572	-0.669
Empty mass	78,5 t (Original 83 t)	Wagonload locomotive	0.130	0.524	-0.613
Wheel diameter	1.250 mm	Wagon	0.090	0.322	-0.374
Maximum speed	180-220 km/h	Shuttle regional train	0.147	0.506	-0.589
Power supply	3 kV cc, 1.5 kV cc	Diesel railcar	0.135	0.412	-0.478

Also from the study [Orlandi, D. 1988], a 20 cm of Substrate cemented-mixed was subsequently analyzed, a structure with a little tractive strength, the features of which are given below. The value of the elasticity modulus of the cementitious conglomerate is $3 \cdot 10^4$ daN/cm^2. The value of the traction stress at almost static level is 2.4 daN/cm^2, considering cracking[3].

Finally, a sub-ballast of 12cm in a bituminous conglomerate with two different values of the elastic modulus ($5\text{-}9 \cdot 10^4$ daN/cm^2) was examined. Among the parameters that characterize the behavior of this material, subject to cyclic loads, the one providing information is the dynamic module. In fact, if the load is dynamic (moving train), the bottom of the sub-ballast is subjected to a succession of traction and compression cycles [Menichelli, S. 1995]. Sub-ballast, therefore, work unitedly, and is a viscoelastic material capable of adapting to the subsoil without cracking, and retaining the load distribution capacity on the substrate itself. From the preceding, we can state that the demands of high-speed traffic cannot be met by a traditional structure because it is subject to rapid loss of the longitudinal and transverse level. Therefore, variations, even sensitive, of the foundation and background characteristics are not influencing the rigidity, and for the evaluation of the breakdown of static loads and dynamic effects, differently to a conventional structure without sub-ballast.

4.4. Materials: Aggregates

The Volumetric mix-design system accommodates coarse aggregate up to a maximum size of 50.0mm [NCHRP-573, 2007; SHRP-A-407, 1994; SHRP-A-408, 1994]. In the case of the *sub-ballast layer* is recommended a maximum aggregate size between 25-37.5mm. The clean aggregate of local origin that meets these criteria have been chosen as a candidate material in the mix design system. The aggregate material is of natural origin, crushed and characterized by Dolomitic petrography.

In the case of the *base-road layer* is recommended a maximum aggregate size between 25-31.5mm. The particle size distribution of aggregates is usually determined and specified by performing a sieve analysis regarding grading curve limits, and these can be met by physically crushing larger rock particle, and by blending materials from more than one source.

Previous studies have shown that the use of limestone and crushed concrete enhances the resistance to permanent deformation and shear strength [Thom, N. et al. 2016]. In general, the more angular the shape of aggregate particles and the more rugged their surface texture, the higher the stability of the asphalt mixture (Fig. 7a). The more such processes are required, the more expensive the material becomes [N. Thom, 2008]. There are no requirements for a geologic type or composition other than

[3] Tests carried out in the second phase of DD Roma-Firenze on cement-based conglomerates with E±5,1-6GPa of 4 to 11 years of life, whose compressive strength at 7 days varying between 4-6MPa. In relation, it was considered [9] to assume for the module the relationship: $E = 100 \cdot K_{r7}$ MPa, with $K_{r7} = 3.11$MPa (7-day compression resistance). [1daN/cm^2=10N/cm^2=0.1MPa]

the need to meet the optional asphalt binder compatibility and the moisture sensitivity requirements for mixtures[4]. Particle size and its properties (shape, texture, strength, durability, and absorption) are determining factors in the strength of the mixture (Fig. 7b).

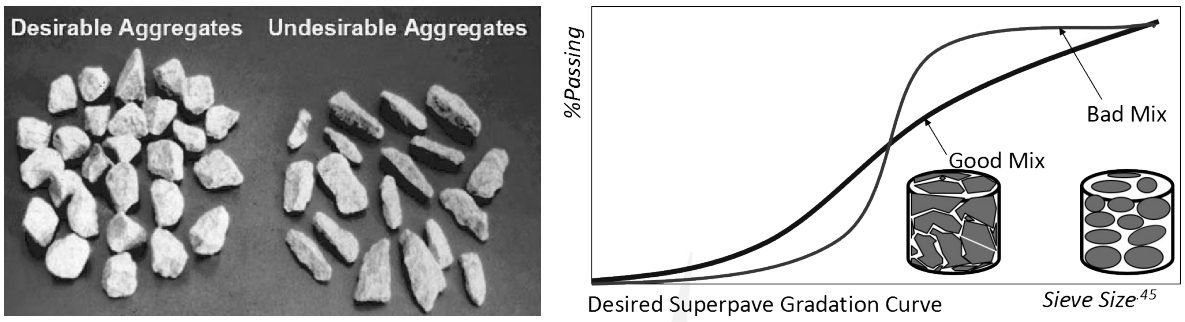


Figure 7. (a) Desirable aggregate shape and angularity; (b) Typical particle size distribution limits

Aggregate particles should be angular in shape to minimize surface area. Flat or elongated particles should be avoided. Gradation has a profound effect on material performance, which varies depending upon the material (HMA), its desired characteristics, loading, environmental, structural and mix property inputs. The best gradation is one that produces the maximum density, involving a particle arrangement where smaller particles are packed between the larger particles, which reduces the void space between particles. This fact creates more particle-to-particle contact, which in HMA would increase stability and reduce water infiltration. However, some minimum amount of void space is necessary to provide an adequate volume of the asphalt binder, and drainage to frost action for subbase course. Recent studies on aggregates for asphalt mixture design recognize the importance of the volume of coarse aggregate for improved mixture performance [Pant, T. et al. 2006; Birgisson, B. et al. 2001].

Fuller and Thompson (1907) developed a widely used equation to describe a dense aggregate gradation, called the maximum density gradation (or sometimes the *Fuller maximum density curve* [Eq. 1; Fig. 8]). Recently, a simulation algorithm was developed for modeling the dense packing of large assemblies of particulate materials [Amirjanov, A. et al. 2008].

$$\%PMD = 100 \cdot \left(\frac{d}{D}\right)^{0.45} \qquad \text{(Eq. 1)}$$

- % PMD = % passing, maximum density gradation;
- d = sieve size in question, mm;
- D = maximum sieve size, mmm_1 is the mass of the dry specimen, in grams (g).

The basis for the selection of the aggregate blend is based on achieving proper mixture volumetrics. The gradation of the aggregate is designed to ensure 1) the maximum aggregate size is appropriate for the application, 2) VMA requirements are met, and 3) a satisfactory aggregate skeleton is obtained. An aggregate interlock is needed at various levels in an asphalt mixture to resist deformation under high load repetitions. According to the requirements of the RFI specification, in the specific sub-ballast conglomerate section, the aggregate mixture to be adopted must have a granulometric composition contained in the lower/upper limits of the grading curve (Fig. 9).

[4] The SUPERPAVE system provides three levels of mix design. This permits the development of designs that will meet the demands of progressively higher levels of traffic, environmental severity and reliability. Materials selection criteria are recommended as either guidelines or requirements, depending upon the level of mix design being employed.

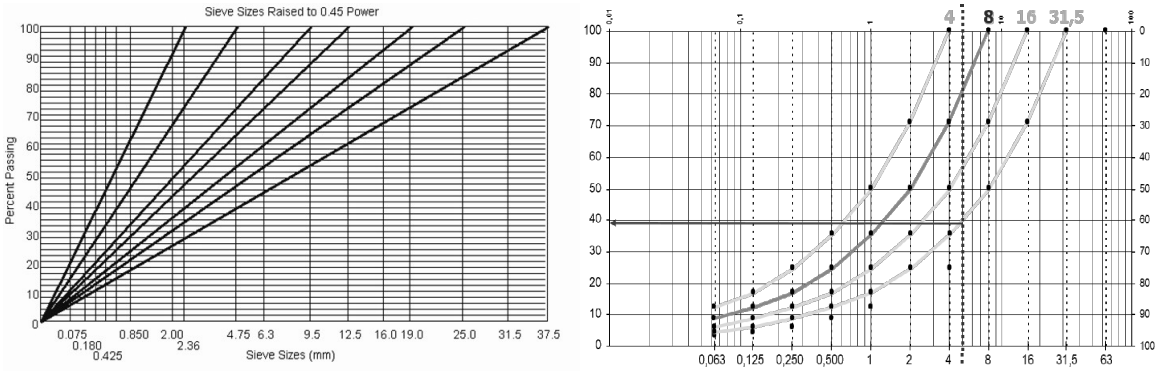


Figure 8. (a) Maximum density curves (0.45 Power gradation graph); (b) Fuller's curves

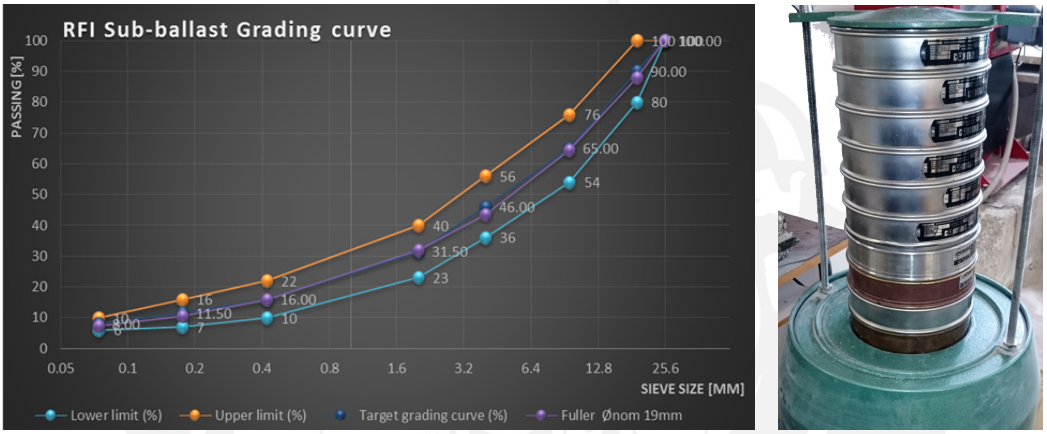


Figure 9. (a) Granulometric curve based on RFI and Fuller's curve; (b) Sieve analysis developed in the lab

In high-traffic situations, mixtures with a well-balanced gradation and an increased volume of coarse aggregates have performed the mixtures [Vavrik, W. 2000]. The following rules must be applied to the volumetric mix design system [EN 933-10, 2009; EN 933-1_2, 2012; ISO 3310, 2000] (Table 4).

TABLE 4. DEFINITION OF AGGREGATE FRACTIONS AND TYPES

Coarse aggregate	Retained on the 2.36 mm sieve
Fine aggregate	Passing the 2.36 mm sieve
Mineral Filler	Passing the 75 µm sieve
Rock	Predominately coarse gravel (retained on the 4 mm sieve)
Sand	Predominately fine aggregate (passing the 2.36 mm sieve)

Coarse aggregate is considered the primary deformation-resisting component in asphalt mixtures. *Fine aggregate* completes the aggregate structure by creating a support structure for the void spaces in the coarse aggregate. Without the inclusion of this fine aggregate, the mixture would remain open with a high percentage of voids [Al-Mosawe, H.M. et al. 2016; EN 933, 2012]. *Mineral filler* is used in the aggregate blend for developing mastic purpose, and to fill the voids in the mixture that is created by the small aggregate. It relates to stiffness and low-temperature performance [Vavrik, W.R. 2000]. The control points and restricted zone are graphed on the FHWA grading chart on which the percentage of aggregate passing a sieve size is plotted against the sieve opening size raised to the 0.45 power (Figs. 8-10)[5]. Several researchers examined the problem of improved gradation [Bassani M. et

[5] In the early 1960s, the Federal Highway Administration FHWA introduced the standard gradation graph used in the HMA industry today. This graph uses n=0.45 and is convenient for determining the maximum density line and adjusting gradation (Roberts, 1996).

This graph is slightly different than other gradation graphs because it uses the sieve size raised to the nth power (usually 0.45) as the x-axis units. Thus, n = 0.45 appears as a straight diagonal line. The maximum density line appears as a straight line from zero to the maximum aggregate size for the mixture being considered.

al. 2001; Fritz, H.W. et al. 1990; Hudson, S. et al. 1962; Nijboer, L. 1948]. The ideal gradation for maximum packing of aggregate solids occurred when the slope of the log-log gradation chart was 0.45.

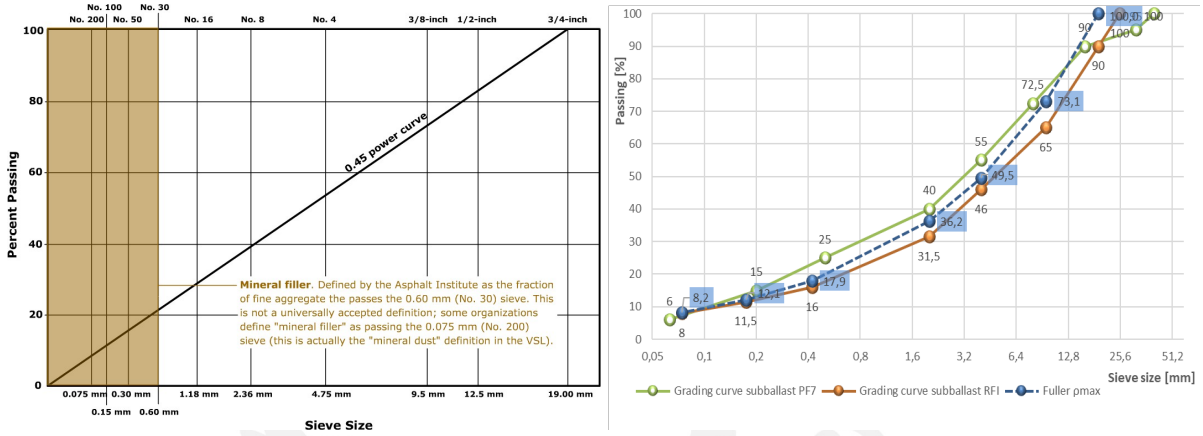


Figure 10. Grading sieves limits; (b) Grading band comparative sub-ballast asphalt mixes [PF7-RFI]

Also, a particle diameter ratio of 22mm[6] appears to be an appropriate value to study for assessing gradation of asphalt concrete. Inside this study, it was recognized that the combination of ground and angular aggregate might lead to decreased voids when compared to angular aggregate alone.

A later study of the resulting voids included an examination of aggregate packing. This study points to the fact that gradation specification bands are arbitrarily determined because of typical experience [Monismith, C.L. et al. 1985] (Fig. 11).

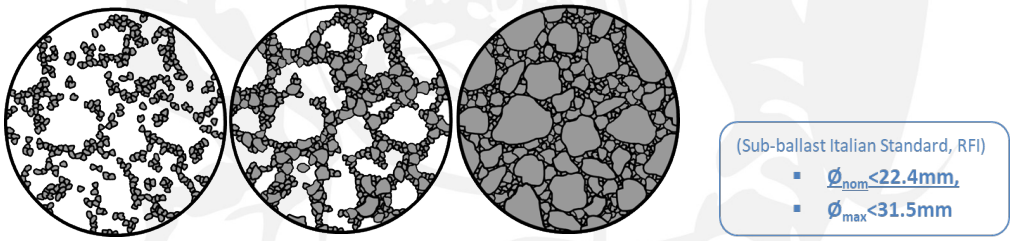


Figure 11. Small, Medium and Large aggregate particles distribution.

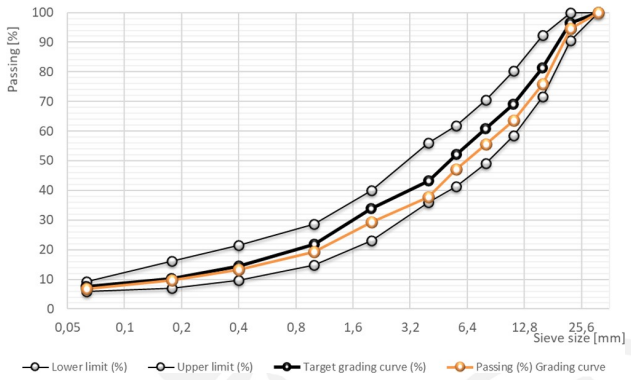
If space is to be filled with stone and structural strength is required, it is evident that a piece of stone that fills the space would have the highest structural strength. Smaller pieces of stone, no matter how well packed, will never achieve the stability of the solid piece of stone. It states that for resistance to fatigue resistance, it is advisable to have a dense gradation and high stiffness. The fatigue resistance is improved with the use of open mixtures, containing low percentages of sieve 0.075-mm material, or gap gradations with lower stiffness.

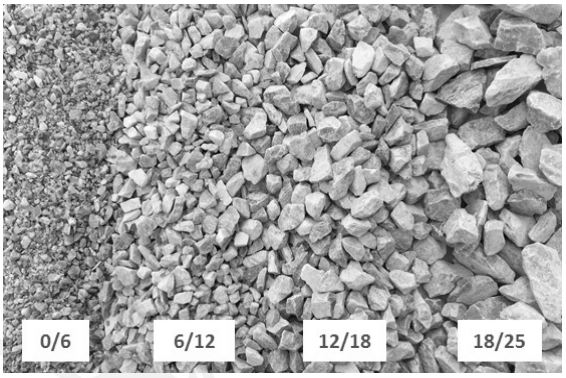
With the advent of increased traffic loading and vehicle weight, it became necessary to re-examine the aggregate structure properties that give a good performance. Figure 12a shows the extremes of the grain size curve used for bituminous sub-ballast with a maximum aggregate size of 22–25mm manufactured with characteristics that are suitable for the construction of sub-ballast for railways. The mixtures studied in this thesis were made of two primary inert part materials: filler and, fine-coarse aggregate (Fig. 12c), whose mineral skeleton is composed of limestone aggregates (Fig. 12b).

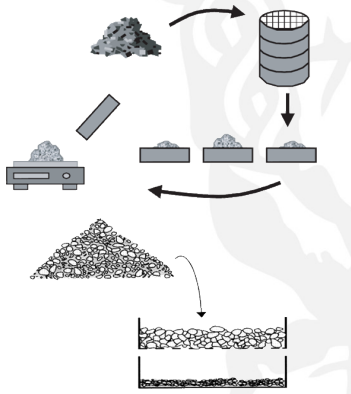
[6] As we will see in chapter 5 of experimental results, the granulometric curve responds to a maximum size of 31.5 mm (one sieve larger than the nominal max size), while the nominal size is 22.4 mm (one sieve larger than the first sieve to retain more than 10% material).

The aggregates employed to manufacture the mixes presented appropriate properties for their use in asphalt mixes by Italian regulation [RFI, 2016]. This specification relies on the results of the Marshall and water sensitivity tests, and it specifies a minimum void content between 3-5%.

This granulometric composition allows enough contact between binder and aggregates, with a nominal maximum aggregate size (NMAS), as a way of specifying the largest aggregate size, of 22.4mm, and a maximum particle size (MPS) of 31.5mm (Fig. 12d). The total combination of aggregates to develop a dense graded asphalt mix include all of the particle sizes down to, and including the filler size aggregates.







Grading curve LaB DICAM				Fuller
Sieve Sizes ISO3310 (mm)	Lower limit (%)	Upper limit (%)	Target grading curve (%)	Ønom. 22.4mm Passing (%)
31,5	100,00	100,00	*100,00*	100,00
22,4	90,48	100,00	*95,24*	85,78
16	71,59	92,23	*81,91*	73,72
11,2	58,56	80,21	*69,38*	62,79
8	49,04	70,49	*59,77*	53,97
5,6	41,22	61,80	*51,51*	45,97
4	36,00	56,00	*46,00*	39,51
2	23,00	40,00	*31,50*	28,92
1	14,77	28,61	*21,69*	21,17
0,40	9,76	21,51	*15,63*	14,02
0,177	7,02	16,05	*11,54*	9,71
0,063	5,89	9,35	*7,62*	6,10

Subballast RFI				Fuller
Sieve Size (mm)	Low limit (%)	Upper limit (%)	Target grading curve (%)	Ønom. 19mm Passing (%)
25,4	*100*	*100*	*100*	100,00
19,1	*80*	*100*	*90*	87,96
9,52	*54*	*76*	*65*	64,30
4	*36*	*56*	*46*	43,53
2	*23*	*40*	*31,5*	31,86
0,42	*10*	*22*	*16*	15,79
0,175	*7*	*16*	*11,5*	10,65
0,074	*6*	*10*	*8*	7,23



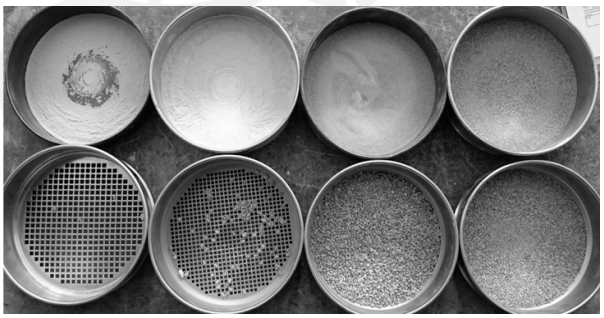


Figure 12. (a) Target grading curve of the bituminous sub-ballast; (b) Different fractions of aggregates; (c) Sieve analysis of fine and coarse aggregates for sub-ballast (ISO 3310); (d) Grading curves adjusted; (e) Sacks supplied of the different fractions of aggregates; (f) Sieve analysis [ISO 3310-1:2000].

ASTM C128:2015, EN 12620:2008, and EN 13055-2:2004 defines the aggregate size of two ways:

- Maximum size: the smallest sieve through which 100% of the aggregate sample particles pass. Superpave defines the maximum aggregate size as "one sieve larger than the nominal maximum size" [Asphalt I. 2003; Roberts, F.L. 1996].

- Nominal maximum size (NMAS): the largest sieve that retains some of the aggregate particles but not more than 10% by weight. Superpave defines nominal maximum aggregate size as "one sieve size larger than the first sieve to retain more than 10% of the material" [Freire, R.A. et al. 2017].

In the mix design procedure described in this thesis, as in the traditional Volumetric mix-design system, NMAS is defined as one sieve-size greater than the first sieve to retain ≈10% of the total aggregate by mass. Thus, it is important to specify whether "maximum size" or "nominal maximum size" is being referenced. Table 5 shows the characteristics of the aggregates. In Table 6 are shown the commercial fractions and technical data sheet requirements.

TABLE 5. PROPERTIES OF THE AGGREGATES

Properties	Standard	Results				Standard limits
	Granulometry	18/25	12/18	6/12	0/6	
Coarse aggregate shape. Flakiness index	EN 933-3:99	8	12	10	-	<25
Percentage of fractured face (UNE-EN 933-5)	EN 933-5:99	99	99	98	-	>90
Resistance to fragmentation (Los Angeles coefficient)	EN 1097-2	23	23	23	-	<25
Cleaning (organic impurity content) (<0,5%)	EN 146130	0,2	0,4	0,4	-	<0,5
Sand equivalent (>50)	EN 933-8	-	-	-	77	>50
Relative density and absorption						
-Apparent density (Mg/m3)		2,86	2,85	2,86	3,01	-
-Saturated density (Mg/m3)	EN 1097-6:01	2,83	2,81	2,81	2,96	-
-Density after drying (Mg/m3)		2,84	2,83	2,83	2,97	-
-Water absorption after immersion (%)		0,39	0,49	0,62	0,56	-

TABLE 6. COMMERCIAL FRACTIONS AND TECHNICAL DATA SHEETS PROVIDED

Components	Standard	Composition	Particle size Ø(mm)	Bulk Specific gravity (g/cm³)
Coarse aggregate	EN 1097-3:1998	Limestone	Ø25-30	2.815
	EN 1097-3:1998	Limestone	Ø20-25	2.810
	EN 1097-3:1998	Limestone	Ø10-15	2.835
	EN 1097-3:1998	Limestone	Ø5-10	2.830
Sand	EN 1097-6:2013	Limestone	Ø<5	2.840
Filler	EN 1097-7:2009	Limestone	Ø≤0.063	2.705

Properties	Standard	Value
Los Angeles abrasion loss [% by weight]<28	EN 1097-2:1999	20.70
Thickness coefficient	EN 1097-8:2001	0.39
Determination of particle shape [%]	EN 933-3:2012	1.25
Flakiness index <20 [%]	EN 933-3:2004	10
Fracture face angularity [%]	EN 933-5	100
Sand equivalent (>45) [%]	EN 933-8:2000	89
Total sulphur content (<0.5) [%]	EN 1744-1	0
Cleaning of coarse aggregates [%]	EN 146130, Annex C	0.01
Resistance to the polishing coefficient	EN 146130, Annex D	44.5
Absorption coefficient [%]	NLT-153	0.58
Proctor test [%]	NLT-108/091	5.28

TABLE 7. SIEVE ANALYSIS OF FINE AND COARSE AGGREGATES.

Sieve Size(mm)	Lower passing limit (%)	Upper passing limit (%)	Target curve (%)	FILLER	SAND	Ø5-10mm	Ø10-15mm	Ø20-25mm	Ø25-30mm
Max.size: 31.5	100.00	100.00	100.00	100.000	100.000	100.000	100.000	100.000	100.000
NMAS: 22.4	90.48	100.00	92.86	100.000	100.000	100.000	100.000	100.000	64.043
16	71.59	92.23	76.75	100.000	100.000	100.000	100.000	77.439	11.875
11.2	58.56	80.21	63.97	100.000	100.000	100.000	96.425	18.859	0.467
8	49.04	70.49	54.41	100.000	100.000	100.000	67.015	3.152	0.334
5.6	41.22	61.80	46.36	100.000	100.000	83.031	32.223	0.350	0.334
4	36.00	56.00	41.00	100.000	93.393	30.641	7.959	0.350	0.334
2	23.00	40.00	27.25	100.000	62.062	0.660	0.398	0.350	0.334
1	14.77	28.61	18.23	98.038	34.334	0.660	0.398	0.350	0.334
0.40	9.76	21.51	12.69	96.077	15.115	0.660	0.398	0.350	0.334
0.177	7.02	16.05	9.28	70.615	6.206	0.660	0.398	0.350	0.334
0.063	5.89	9.35	6.75	50.038	1.802	0.329	0.199	0.350	0.334

During the sieving process of the aggregates, an average of six until twelve (e.g., sand fraction) grading curves was made for each current portion. The materials obtained from the quarry established

the following fractions: Filler (<0.063mm); Sand (0.177-4mm); Gravel (5-10mm); Fine gravel (10-15mm); Thick gravel (20-25mm); Very thick gravel (25-31.5mm). For aggregate sieve analysis, the following standard sieve sizes were used: 37.5 mm, 25.0 mm, 19.0 mm, 12.5 mm, 9.5 mm, 4.75 mm, 2.36 mm, 1.18 mm, 0.60 mm, 0.30 mm, 0.15 mm, and 0.075 mm. (Table 7). Before defining the real grain size curve, different configurations based on Italian and European standards are studied to interpolate and to fill gaps with new sieves. Table 8 shows the final grading curve adjusted by Italian RFI (2016) and ISO 3310 regulations.

TABLE 8. GRADING CURVE FOR SUB-BALLAST (BASED ON RFI, ISO 3310[7])

Sieve Sizes ISO3310 (mm)		Lower limit (%)	Upper limit (%)	Target grading curve (%)	Fuller's curve Ønom. 22.4mm Passing (%)
Max. Size:	31.5	100.00	100.00	100.00	100.00
NMAS:	22.4	90.48	100.00	92.86	85.78
	16	71.59	92.23	76.75	73.72
	11.2	58.56	80.21	63.97	62.79
	8	49.04	70.49	54.41	53.97
	5.6	41.22	61.80	46.36	45.97
	4	36.00	56.00	41.00	39.51
	2	23.00	40.00	27.25	28.92
	1	14.77	28.61	18.23	21.17
	0.40	9.76	21.51	12.69	14.02
	0.177	7.02	16.05	9.28	9.71
	0.063	5.89	9.35	6.75	6.10

(*) Granulometric grading curve based on target values from Sub-ballast mixtures (RFI, Capitolato costruzione opera civili, Sezione XV.

The weight of the test sample must be large enough to produce reliable test results. Table 9 lists permissible weights for sieve analysis according to NMAS values.

TABLE 9. SIEVE WEIGHTS OF AGGREGATE AS A FUNCTION OF NMAS

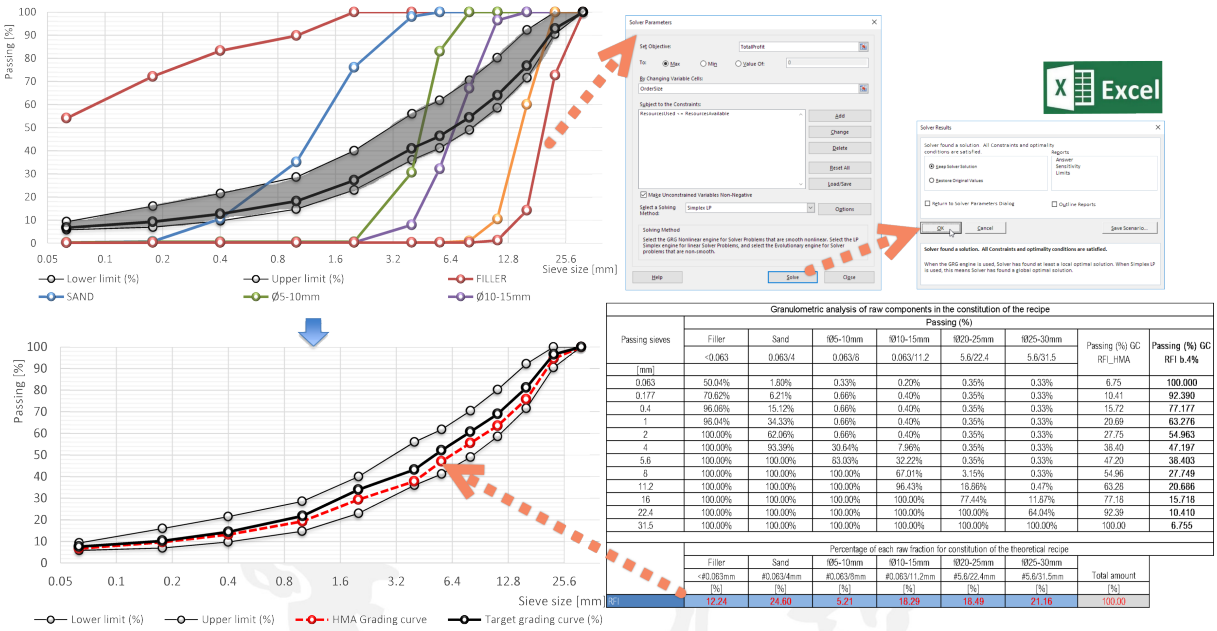
NMAS (mm)	Minimum Weight for Test Sample (kg)
9.5	1.0
12.5	2.0
19.0	5.0
25.0	10.0
37.5	15.0

The average granulometric curve of each fraction is adjusted considering the percentages retained on each sieve. The fractions were hand sieved through the ISO3310-1. The column of sieves, overlaid with mesh size decreasing from top to bottom, it is agitated to retain only the material with higher dimension than the diameter of the mesh. The column has been divided according to the commercial fractions of aggregate available, allowing to speed up the work.

Data analysis with Excel performs the representation. In this way, we can change the significant percentages of each fraction mathematically so that the final curve of the mixture is within limits defined by the objective curve. Graphically, Fig. 13 illustrates the process.

Mineral fillers (particles lying between 50 to 75 µm) consist of very fine, inert minerals that are added to an asphalt mix to improve density and strength. They form less than 6 % of HMA concrete by mass. The filler used is a Portland cement, CEM II/B-L 32,5N (EN 197-1:2011). 95% of this filler has a size smaller than 0,063 mm with an apparent density (EN 1097-3:1999) of 2.70g/cm^3 (Fig. 14).

[7] EN 933-1 (2012) Tests for geometrical properties of aggregates. Determination of particle size distribution. Sieving method.
EN 933-2 (2012) Determination of particle size distribution. Test sieves, nominal size of apertures.
EN 933-10 (2009) Tests for geometrical properties of aggregates. Assessment of fines. Grading of filler aggregates.
ISO 3310-1 (2000) Test sieves Technical requirements and testing -- Part 1: Test sieves of metal wire cloth
ISO 3310-2 (2013) Test sieves Technical requirements and testing. Part 2: Test sieves of perforated metal plate



Granulometric analysis of raw components in the constitution of the recipe

Passing sieves	Passing (%)							
	Filler	Sand	Ø5-10mm	Ø10-15mm	Ø20-25mm	Ø25-30mm	Passing (%) GC RFI_HMA	Passing (%) GC RFI b.4%
	<0.063	0.063/4	0.063/8	0.063/11.2	5.6/22.4	5.6/31.5		
[mm]								
0.063	50.04%	1.80%	0.33%	0.20%	0.35%	0.33%	6.75	100.000
0.177	70.62%	6.21%	0.66%	0.40%	0.35%	0.33%	10.41	92.390
0.4	86.08%	15.12%	0.66%	0.40%	0.35%	0.33%	15.72	77.177
1	96.04%	34.33%	0.66%	0.40%	0.35%	0.33%	20.69	63.276
2	100.00%	62.06%	0.66%	0.40%	0.35%	0.33%	27.75	54.963
4	100.00%	93.39%	30.64%	7.96%	0.35%	0.33%	38.40	47.197
5.6	100.00%	100.00%	83.03%	32.22%	0.35%	0.33%	47.20	38.403
8	100.00%	100.00%	100.00%	67.01%	3.15%	0.33%	54.96	27.749
11.2	100.00%	100.00%	100.00%	96.43%	18.86%	0.47%	63.28	20.686
16	100.00%	100.00%	100.00%	100.00%	77.44%	11.67%	77.18	15.718
22.4	100.00%	100.00%	100.00%	100.00%	100.00%	64.04%	92.39	10.410
31.5	100.00%	100.00%	100.00%	100.00%	100.00%	100.00%	100.00	6.755

Percentage of each raw fraction for constitution of the theoretical recipe

	Filler	Sand	Ø5-10mm	Ø10-15mm	Ø20-25mm	Ø25-30mm	
	<Ø.063mm	Ø.063/4mm	Ø.063/8mm	Ø.063/11.2mm	Ø5.6/22.4mm	Ø5.6/31.5mm	Total amount
	[%]	[%]	[%]	[%]	[%]	[%]	[%]
RFI	12.24	24.60	5.21	18.29	18.49	21.16	100.00

Figure 13. Adjusting the granulometry of the sieving curves on an Excel sheet[8] with solver function

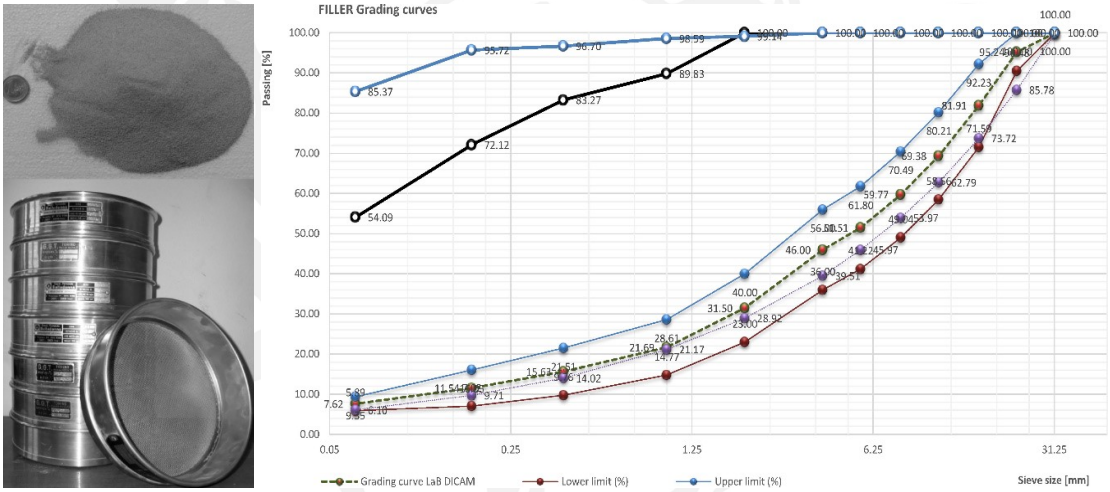


Figure 14. (a) Portland cement used; (b) Sieve analysis for different filler fractions

Mineral fillers serve a dual purpose when added to asphalt mixes. The proportion of the mineral filler that is finer than the thickness of the bitumen film forms a mortar or mastic with bitumen that contributes improving the stiffness of the binder [Usama, H. 2013; Anderson, 1996]. The particles larger than the thickness of the bitumen film behave as a mineral aggregate, thus contribute to the contact points between individual aggregate particles. The apparent specific weight of the aggregate, γ_i is the ratio between the weight of the dry aggregates and the volume occupied by it, without taking into account the air voids. The arid inert part is introduced into a previously calibrated pycnometer and determine the weight using a precision balance (Fig. 15), which is then placed in a thermostatic stove at 105°C to eliminate air bubbles remaining between the aggregates and water.

[8] Excel includes a tool called "Solver" that uses techniques from the operations research to find optimal solutions for adjusting the grading curves into on a single final curve by adjusting the quantities of each fraction within the target curve.

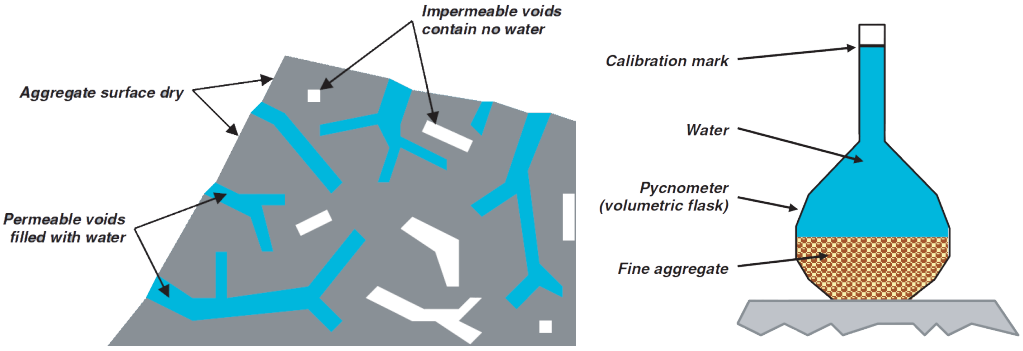


Figure 15. (a) Sketch showing saturated surface-dry condition in an aggregate particle; (b) Pycnometer method of determining fine aggregate specific gravity [NCHRP 673]

For both coarse aggregate and fine aggregate, absorption is an important property. The relative density (specific gravity) and absorption of aggregates [ASTM C127-128, 2015] are calculated using the following equations, according to Fig. 16:

$$\rho_{mh} = \frac{A}{(B + W - C)} \qquad \text{(Eq. 2)}$$

- ρ_{mh} is the bulk specific gravity, (g/cm³) to the nearest 1 kg/m³;
- A = weight of oven-dry aggregate (gr);
- B = weight of pycnometer filled with water to calibration mark (gr);
- W = weight of saturated surface-dry aggregate in the air (gr);
- C = weight of pycnometer with aggregate and filled with water to calibration mark (gr).

$$Absorption = \left(\frac{W - A}{A}\right) \cdot 100 \qquad \text{(Eq. 3)}$$

- Absorption = water absorption in weight, %;
- W = weight of saturated, surface-dry aggregate in air, gr;
- A = weight of dry (air-dry or oven-dry) aggregate in air, gr.



Figure 16. (a) Laboratory process of aggregates selection; (b) Pycnometer method (fine aggregate)

4.5. Materials: Bitumen [composition and structure]

Asphalt binder is produced from the thick, heavy residue that remains after fuels and lubricants are removed from crude oil [Pires G.M. et al. 2017; Jenks, C.W. et al. 2011]. According to [ASTM D6114M, 2009], asphalt cement is defined as a "black cementitious material occurring in nature or obtained by crude oil refining where the predominated material is mainly bitumen." The first use of bitumen as a construction material for road pavement appeared in Europe in the 1830s, simultaneously in France, England, and in the United States [Rudenskaya, J.M. 1967].

4.5.1. Bitumen Rheology.

The bitumen content typically comprises about 5 to 7 % by mass of the total asphalt mixture. The leading role of bitumen is to coat and bind the aggregate particles together. Selection of proper bitumen grade is essential for the performance of asphalt mixture under traffic and climatic conditions [Viola, F. et al. 2015; Koenders, B.G. et al. 2000]. Bitumen is a hydrogenated compound of heavy hydrocarbons. These molecules can be separated into two fractions: *Maltenes* is an oily brown like liquid, including a blend of saturates, aromatics and resins; *Asphaltenes* is a black solid composed of condensed polyaromatic molecules, including some heteroatoms like metals, nitrogen, and sulfur. This complexity of bitumen chemistry lies in the fact that many different chemicals are present (carbon and hydrogen atoms). Thanks to asphaltenes precipitation followed by chromatographic separation of maltenes in solution, the composition of bitumen are given regarding the relative quantity of its fractions for Saturates, Aromatics, Resins, and Asphaltenes (Fig. 17).

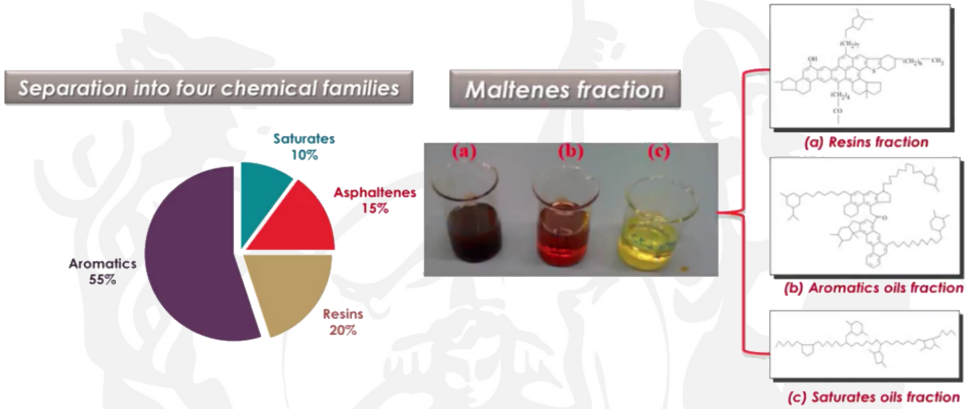


Figure 17. Maltenes in solution into different fractions: saturates, aromatics and resins

4.5.2. Performance grade of bitumen

Bitumen is a solid at ambient temperature and softens when heated, turning gradually into a viscous liquid. It is non-volatile at ambient temperature and atmospheric pressure. Optimal pump-ability is got when the viscosity is not higher than 0.2 Pas. Storage temperature must be in a range from 140ºC, (soft bitumen), to 200ºC (hard bitumen).

The **aging** (hardening) of asphalt binder is associated with the loss of volatile components and oxidation of the binder during asphalt mixture construction [Airey, 2003; Petersen, J.C. 2000; Vallerga et al. 1981]. This process is attributed to the increase in the viscosity and high molecular weight molecules of the asphalt binder [Airey, G. et al. 2003]. Further research has indicated that the amount of **physical hardening** observed in some binders is dependent on their chemical composition [Anderson et al. 1994; Claudy et al. 1992]. **Oxidation** could be considered the principal reason for bitumen aging. Consequences of severe oxidation are a separation of structural components, the rise in viscosity, embrittlement, and loss of cohesion and adhesion of the binder [Mill et al. 1992]. **Grades of bitumen** (Fig. 18) vary according to the traffic and the layer. The physical property requirements within the specifications are constant among all PG grades directly related to field performance. Thus, the greater the first (high) temperature value is, the more resistant the binder should be against high temperature distresses such as rutting. Likewise, the lower PG temperature value is, the stronger the binder should be at a low temperature cracking. The more common paving grades used in the US are

PG 64-22, PG 70-22, PG 76-22, PG58-22, PG 64-28, PG 58-28, and PG 52-34 [Fritz, H.W: et al. 1990] but this is not representative of the real conditions in other places around the world.

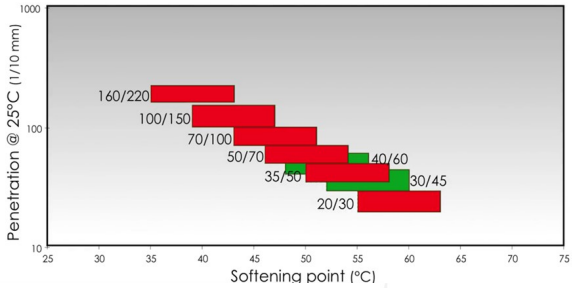


Figure 18. EN 12591. SHRP Grades from 20/30 to 160/220

Performance grading uses various measurements of the binder's flow properties to establish its grade, which is expressed as two numbers that represent high and low service temperatures for the pavement. Most of the tests used in performance grading of asphalt binders involve rheological tests. A rheological test is one that measures one or more aspects of the way in which material flows [Kandhal and Mallick, 1997, Kandhal et al. 1997]. The dynamic shear rheometer (DSR) and the bending beam rheometer (BBR) both measure the flow properties of asphalt binders, from -20 to 0°C [Hassan, N.A. et al. 2015; Kandhall, P. 1994; Esch, D. 1984].

The binder used is a 50/70 bitumen free of additives. Its characterization was carried out by the Ball-Ring test, the Penetration (SP) test, and the Viscosity test. Proper asphalt mixture functions well because they were designed in such a way as to give them specific properties contributing to the quality of workability, flexibility, and fatigue resistance. Ensuring that asphalt mixture has each of these properties is a primary objective of the mix-design.

4.5.3. Penetration & "Ring-and-ball" Softening point tests

The penetration test is a standardized test [EN 1426:2007] (Fig. 19a-19b) characterized by the consistency of bitumen during which, bitumen changes from solid state to liquid state. A standard loaded needle penetrates a sample of bitumen under specified temperature 25ºC. The "penetration" is inversely related to *viscosity*. A load of 100 grams is applied for 5 seconds on 25ºC. The depths to which the needle penetrates the surface of bitumen is measured. So, the less the needle punctures, the harder the asphalt is. Lower penetration indicated a harder bitumen. The penetration depth is measured in tenths of a millimeter. The most common way to describe a bitumen is still concerning the penetration test. Instead, the principle of the softening point test is to characterize *consistency* of asphalt at high service temperature (60/70ºC) [EN1427:2007].

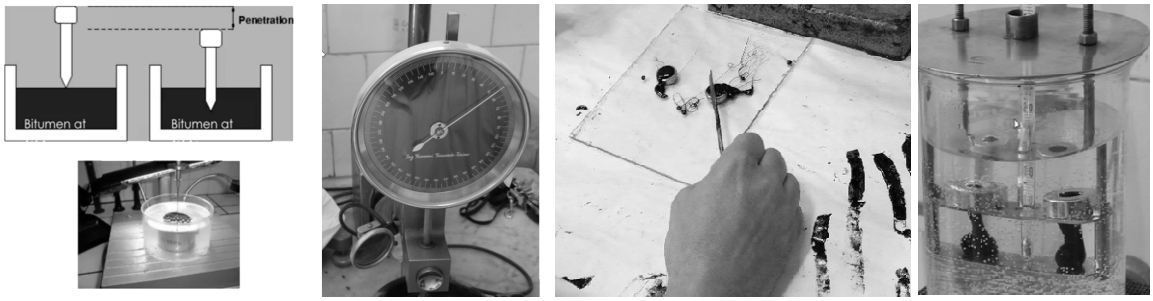


Figure 19. (a) Penetration test at 25ºC; (b) Needle depth measured; (c) Bitumen casting inside the rings; (d) Detail chassis, ring, and spheres.

The softening point is a temperature at which the bitumen has a specific viscosity (about 800 Pa · s), the thickness being that at which a steel ball drops through a prepared disk of bitumen. The bitumen sample is cast into a unique brass ring, with Ø19 mm and thickness of 6 mm placed into a thermal water bath. Two steel spheres of 3.5 grams are contacted with bitumen using a particular centering system above the rings. The temperature is raised with a thermal gradient of 5°C/min (fig. 19c-19d). Bitumen with a higher softening point is preferred in warmer places. Also in general, the higher is the softening point, the lower is the penetration grade. The softening point provides a bitumen performance index at high temperatures. The penetration index, *Ip* is calculated from the values of penetration at 25°C, 100g, 5s, determined by Eq. 4.

$$I_p = \frac{20 \cdot t_{RaB} + 500 \cdot \log P - 1952}{t_{RaB} - 50 \cdot \log P + 120} \qquad \text{(Eq. 4)}$$

- Where t_{Rab} is th softening point, °C; logP is the logarithm of the penetration at 25°C (in 0,1mm).

4.5.4. Viscosity. Brookfield viscometer

Bitumen is a very special liquid; its viscosity[9] is high. This mechanical property means that the elastic component of deformation becomes significant at in-service temperatures. It must then become viscous enough at normal air temperatures to hold the aggregate particles in place in the pavement [Takkalou, H.B. et al. 1985]. ASTM D2493-2001 determines Viscosity. Eq. 5 establishes the relationship between viscosity and temperature.

$$Log \log_{\eta} = A + VTS \log T_R \qquad \text{(Eq. 5)}$$

Where:

- η = binder viscosity, cP;
- A,VTS = regression parameters, and
- T_R = temperature, °Rankine.

Typical grades of asphalt cement and binders that have been used in rail tracks are PG 64-22, PG 70-28 and PG 76-34. For each type of asphalt binder, A and VTS values are shown in Table 10.

TABLE 10. ASPHALT BINDER GRADE AND VISCOSITY PARAMETERS (NCHRP 1-37A, 2004)

Grade	PG 64-22	PG 70-28	PG 76-34
A	10.980	9.715	8.532
VTS	-3.680	-3.217	-2.785

According [Giavarini C. et al. 1999], the apparent viscosity of Asphalt Binder is determined using a Rotational Viscometer (Brookfield), which is used at high temperatures [AASHTO-T316, 2008; EN-13302, 2010]. Temperatures above 135°C may be required for some modified asphalt binders or aged binders. The procedure implies a preheated spindle (SC4-27), after 30min of bringing the asphalt sample to the desired temperature, the viscometer speed must be at 20rpm, begins the spindle rotation during 10min of temperature equilibrium medium. The viscosity is measured during 3 min at 1min intervals, reporting the average of three readings as we have done in the laboratory (Fig. 20).

The increment of asphalt viscosity and elasticity via the crumb rubber is empirically determined [Huang, 2006; Soon, Akisetty, & Amirkhanian, 2008].

[9] Ratio between the applied shear stress and the rate of shear is called the coefficient of viscosity (Pas·s)



Figure 20. (a) Brookfield viscometer; (b) Rheocalc v.3.2 software; (c) Bitumen containers [ASTM D2983-17]

4.5.5. Thermal parameters for Superpave

Higher the softening point, lesser the temperature susceptibility. The temperature[10] susceptibility is significant; it must be fluid enough at elevated temperatures to permit it to coat the aggregate particles during mixing and to allow these particles to move past each other during compaction. The viscoelastic nature is crucial to its performance in the field (low temperatures to prevent cracking, but still be elastic enough at hot temperatures to prevent rutting) [Wang, C. 2017; Kennedy, T. 1994].

Modification of asphalt binders can enhance the overall performance in response to a particular service condition, such as a rail line carrying a high traffic volume or heavy wagons [Heitzman, M. 1992]. The modifiers are classified based on the dispersion of additives, asphalt reaction, behavior as only inert filler, and depending on their specific gravity [Wang, C. et al. 2017; Zumrawi, M. 2016; Jeong, K.D. et al. 2010; Witczak, M. et al. 1997]. The temperature of the aggregates at the time of mixing should be between 150ºC and 170ºC, whereas the binder must be 5ºC higher than that of the aggregates about the type of bitumen employed.

The bituminous binder was of type 50/70 and the optimum asphalt content, referring to the aggregate mass of aggregates, has been between 4.1% and 4.8%. The mixture must meet the RFI requirements:

- Marshall Stability value (CNR-BU n.30) performed at 60°C on compressed specimens with 75-blow per face, not less than 10 KN, and flow between 2.0 and 4.0 mm.
- Samples for which Marshall stability is determined will have from 4% to 7% of residual voids;
- Marshall Stability Loss not more than 25% (obtained by comparison of original Marshall Stability with that measured on specimens kept for 24 hours in water at 60°C); and
- Indirect traction with Brazilian test (CNR-BU n°134) not less than 0.6 N/mm^2.

The determination of *thermal parameters* (technological temperatures), mixing temperature (T^amix) and compaction temperature (T^aC), is performed by the viscosity test at four temperatures on the selected binder B50/70 [ASTM D2170-10; ASTM D4402M-15]. In the experimental investigations carried out, the grade of the bitumen was specified according to EN 1426, 2007; EN 1427, 2007; EN 12591, 2009. The type of bitumen is shown in Table 11.

[10] The temperature susceptibility of the binder is significant because it indicates the proper mixing and compaction temperatures at which to mix the binder with aggregate, and at which to compact the mixture.

TABLE 11. PROPERTIES OF BITUMEN B50/70 USED IN SUB-BALLAST

Characteristics		Standard	Required values	Observed values
Pen @25°C (in 0,1mm)	Pen	EN1426:2007	50-70	53
Penetration index [-]	Ip	EN12591 Annex A	-1.5 to +0.7	-0.575
Soft. Point (°C)	t_{RaB}	EN1427:2007	46-54	50
Kinematic viscosity (at 135°C)	Pa·s	ASTM D2196	0.379	>0.320
Equiviscosity temperatures	0.28Pa·s	EN 12695:2000	-	143.1
Brookfield (°C)	0.17Pa·s	AASHTO T316-04	-	156.2
Bulk gravity (g/cm^3)		EN 15326:2007	-	1.033

The temperature of the bituminous conglomerate at the laying stage, immediately controlled behind the paver, should not be less than 140°C. In the case of rubberized asphalt mixtures, the laying temperature shall not be less than 160°C. For binder B50/70, it was tested the standard viscosity-temperature chart through the use of a Brookfield viscometer at four different temperatures (100, 135, 150, 180°C). The temperatures at which the binder reach the optimal viscoelastic behavior were at values of 0.17Pas (mixing) and 0.28Pas (compaction) respectively. The viscosity trend is reported as a function of the temperature returned by the viscosimeter (Fig. 21; Table 12).

TABLE 12. VISCOSITY DETERMINATION OF THE BINDER 50/70 USING BROOKFIELD VISCOMETER

							Serie 1
Viscosity (Pa.s)	Speed (RPM)	% Torque	Shear Stress (N/m^2)	Shear Rate (1/sec)	T^a test (°C)	Bath (°C)	T^a desired (°C)
0.0738	200.00	2.94	50.15	68.00	180.45	180.20	180
0.1950	200.00	7.77	132.60	68.00	150.43	150.13	150
0.3792	200.00	15.18	257.83	68.00	135.11	134.87	135
3.3266	80.00	53.23	904.83	27.20	100.31	100.00	100
							Serie 2
Viscosity (Pa.s)	Speed (RPM)	% Torque	Shear Stress (N/m^2)	Shear Rate (1/sec)	T^a test (°C)	Bath (°C)	T^a desired (°C)
0.0705	200.00	2.81	47.94	68.00	180.35	180.02	180
0.1956	200.00	7.82	133.03	68.00	150.45	150.08	150
0.3938	200.00	15.74	267.75	68.00	135.17	134.88	135
3.4578	80.00	55.32	940.53	27.20	100.29	100.00	100

Mixing and compaction equivalence temperatures of bituminous conglomerates are related to specific dynamic viscosity values. Depending on the values provided by viscosity, is possible to establish the optimal temperatures for asphalt binder (Equi-viscosity temperature [NCHRP 459, 2001] (Fig. 21b):

- Optimum value of viscosity for mixing the aggregate with bitumen 0.17±0.02 [Pas];
- Optimum value of viscosity for the compaction with bitumen 0.28±0.03 [Pas];
- Optimum value of viscosity for mixing the aggregate with modified bitumen 0.34±0.02 [Pas];
- The optimum viscosity for compaction of the mixture with modified bitumen 0.58±0.03 [Pas].

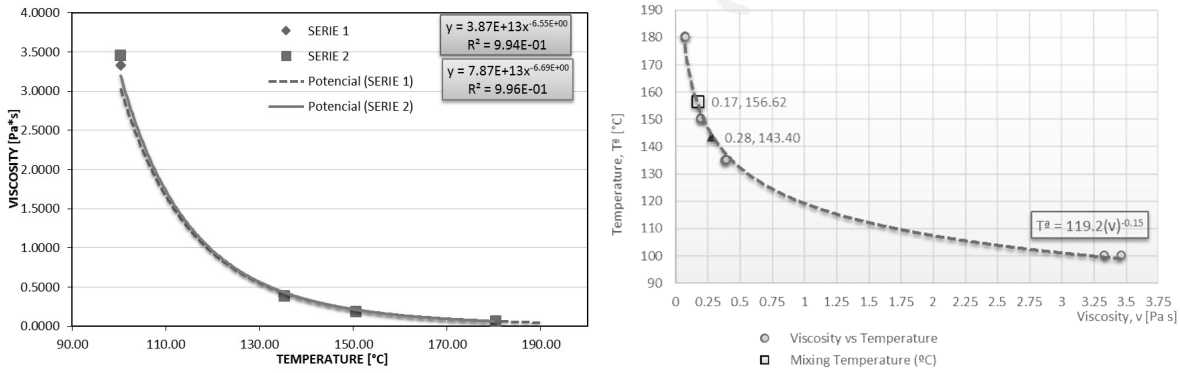


Figure 21. (a) Viscosity-Temperature chart [ASTM D2493-16]; (b) Viscosity vs Temperature binder B50/70[11]

[11] (1.0 Pa· s ≈ 1000 mm^2/s kinematic viscosity for asphalt binders)

Using the results of viscosity testing, an experimental plan was developed on HMA and rubber-modified mixtures considering that:

1. Asphalt binders can efficiently coat aggregates at a wide range of viscosity levels higher than 0.17 ± 0.02 Pas which corresponds to the temperature of 160°C;
2. Compaction effort at viscosity levels is higher than 0.28 ± 0.03 Pas corresponding to a temperature of 145°C, which is required by the Superpave design procedure.

These temperature values were determined from the regression equations of Fig.21a (Table 13).

TABLE 13. OPTIMAL EQUIVISCOSITY VALUES WITH BROOKFIELD VISCOMETER

Optimal value of viscosity for blending of aggregate with bitumen	0,17 ± 0,02 Pas	156.19
Optimal value of viscosity for the compaction of bitumen mixture	0,28 ± 0,03 Pas	143.10
	Optimal value	Final T[a]
Mixing Temperature (°C)	156.2	160
Compaction Temperature (°C)	143.1	145

4.5.6. Bitumen-filler and Dust/Asphalt ratio

The dust proportion (DP) is a parameter that measures the asphalt concrete mixtures "mastic." The mastic (asphalt binder and dust) affects the properties of the mix. Excessive dust dries out the mix reducing asphalt film thickness and durability, and insufficient dust may allow excessive asphalt films, which may result in tender, unstable mixes [Ecopneus, 2000; Buonanno, A. 2000].

Previously referred as to "*Dust to Asphalt Ratio Test*" or "dust/binder ratio" (AASHTO MP2), may be performed in the HMA mixes developed with "Volumetric mix-design." In this test, the amount of sieve Ø200 material and the percentage of asphalt cement is selected so that the Dust/Asphalt Ratio (DP) is about 0 to 2.0. Preferably, DP is about 0.6 to 1.6 [Sousa, J. et al. 1994].

The dust-to-asphalt binder ratio criterion is constant for all levels of traffic. The required range for dust/binder ratio is 0.8 to 1.6 for all mixtures larger than 4.75-mm of NMAS. However, studies in the past have reduced the requirements to a range of 0.6 to 1.2 if local materials warrant this change. For Ø4.75-mm NMAS mixtures, the required dust/binder ratio is 0.9 to 1.2, and this should not be modified[12] (Table 14). Higher dust/binder ratios provide stiffness the HMA, and also will tend to reduce the permeability. DP is computed using the effective asphalt binder content:

$$DP = \frac{P_{0.075}}{P_{be}} = \frac{\%_{filler}}{\%_{bitumen}} = 0{,}6 - 2{,}0 \qquad \text{(Eq. 6)}$$

- DP: dust proportion, calculated using effective binder content to the nearest 0.1;
- $P_{0.075}$: mineral dust content, % by total mix weight (aggregate content passing the 0.075 mm (75 μm) sieve, percent by mass of aggregate, to the nearest 0.1%) and,
- P_{be}: effective binder content, % by total mix weight (effective asphalt binder content, percent by mass of aggregate, to the nearest 0.1%.)

The weight percentage of binder and aggregate are calculated using the following equations:

$$P_b = \frac{V_b G_b}{V_{sb} G_{sb} + V_b G_b} \cdot 100\%;\ P_s = \frac{V_{sb} G_{sb}}{V_{sb} G_{sb} + V_b G_b} \cdot 100\%;\ P_{be} = \frac{V_{be} G_b}{V_{sb} G_{sb} + V_b G_b} \cdot 100\% \qquad \text{(Eq. 7)}$$

- P_b = total binder content, % by total mix weight;
- V_b = total binder content, % by total mix volume;
- V_{sb} = aggregate content, %, and; V_{be} = effective binder content, % by total mix volume;
- G_b = binder specific gravity; P_s = total aggregate content, % by total mix weight and,
- G_{sb} = overall bulk specific gravity of aggregate:

[12] The Superpave method required a range of DP. 0.6 to 1.2, but agencies can increase the requirement to 0.8 to 1.6

$$G_{sb} = \frac{P_{s1/A} + P_{s2/A} + P_{s3/A} + \ldots}{\left(\frac{P_{s1/A}}{G_{sb1}}\right) + \left(\frac{P_{s2/A}}{G_{sb2}}\right) + \left(\frac{P_{s3/A}}{G_{sb3}}\right) + \ldots} \quad \text{(Eq. 8)}$$

- $P_{s1/A}$ = volume % of aggregate 1,2…i in aggregate blend;
- G_{sb1} = bulk specific gravity for aggregate 1,2…i;

$$P_{s1} = P_s\left(\frac{P_{s1/A}}{100}\right) \rightarrow V_{sb1} = \frac{P_{s1}(100 - P_b)}{\left(\frac{P_b}{G_b}\right) + \left(\frac{P_{s1}}{G_{sb1}}\right) + \left(\frac{P_{s2}}{G_{sb2}}\right) + \left(\frac{P_{s3}}{G_{sb3}}\right) + \ldots} \quad \text{(Eq. 9)}$$

- P_{s1} = weight percent (by total mix) of aggregate 1, 2… i; P_b = weight % binder in total mix.
- V_{sb1} = volume % of aggregate 1, 2.. i in total mix;

$$P_{0.075} = \frac{\left(P_{0.075/s1} \cdot P_{s1}\right) + \left(P_{0.075/s2} \cdot P_{s2}\right) + \left(P_{0.075/s3} \cdot P_{s3}\right) + \ldots}{100} \quad \text{(Eq. 10)}$$

- $P_{0.075}$ = mineral dust content (ϕ<0.075 mm), percent by total mix weight;
- $P_{0.075/s1}$ = % passing the 0.075-mm sieve for aggregate 1, 2… i;
- P_{s1} = weight percent (by total mix) of aggregate 1, 2… i.

TABLE 14. REQUIREMENTS FOR DUST/BINDER RATIO

Mix Aggregate NMAS (mm)	Allowable range for DP (by weight)
≥4.75	0.8 to 1.6
<4.75	0.9 to 2.0

4.6. Materials: Crumb/Ground rubber modifier

Rubberised asphalt involves the use of crumb rubber to enhance the performance of the asphalt concrete mix (the dry process of producing asphalt rubber involves mixing the crumb rubber with the aggregates within the asphalt mix). Bitumens modified with crumb rubber are usually called CRMB[13]. The primary purpose of using rubber modifiers in hot mix asphalt (HMA) is to obtain a stiffer HMA at high service temperatures, a more flexible HMA to resist fatigue cracking at moderate service temperatures, and a lower or unchanged stiffness at low service temperatures to resist thermal cracking (Fig. 13).

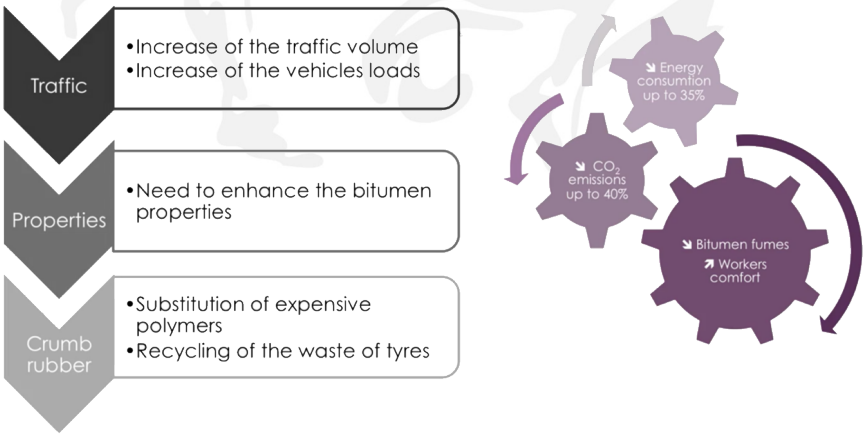


Figure 22. (a) Under traffic the film of bitumen breaks. Asphalt mix modified with rubber increase resistance; (b) Benefits of using rubber modified bitumen.

[13] In Europe there is no specific standard for Crumb Rubber Modified Bitumen. In fact, the use of that product falls under EN 14023, framework specification for polymer modified bitumen.

The rubber aggregate with gap-gradation is a two-component system in which the finest gradation is believed to interact with the asphalt cement while the coarse rubber performs as an elastic aggregate in the hot mix asphalt mixtures [Soto, F.M. et al. 2017; Hassan et al. 2014; Lee, S. 1994]. [Ayad S. et al. 2005; Hassan, N.A. et al. 2014] stated that crumb rubber that is added to dense graded mixes by using dry process is referred as Generic/RUMAC mixes while PlusRide mixes are described for incorporating the crumb rubber with gap graded mixes. The CRM used can range from 1 to 6% by weight of the total blend. However, 1 to 3% CRM is being used [Soon-Jae L. et al. 2006]. The improvement of the properties of rubberized binders depends on the interaction between the CRM and the binder, where the rubber particles swell to form a viscous gel increasing the viscosity [Airey G. et al. 2003; Thodesen, C. et al. 2009; Zanzotto L. et al. 1996; Bahia, H.U. et al. 1996].

The crumb rubber is made by shredding scrap tire, which is a particular material free of fiber and steel. The rubber particle is graded and found in many sizes and shapes. The crumb rubber is measured by the mesh screen or sieve size through which it passes during the production process. To produce CRM, it is essential to reduce the size of the tires by ambient grinding and the cryogenic processes [Becker et al. 2001; Huang, B. et al. 2002].



Figure 23. (a) Preliminary selection; (b) The tires are inserted into the first crusher

The rubber fractions considered in this research came from the trituration of heavy-truck tires (natural rubber) supplied gently by "*Baucina Recycling Tyres Srl*" located in Baucina (Palermo, Italy). At this establishment, the process began with a selection of tires, differentiating them from light vehicles, mostly from cars, motorcycles, and bicycles, heavy (trucks and self-articulated), and massively sized, constituting the volume above the previous one, including the abandoned wheels of aircraft. This distinction is tied to the size and material, as the thick rubber compound usually contains more natural rubber. For oversize tires compared to the machines, there is a volumetric reduction using a press. The tires are inserted into a first crusher, which produces quite large pieces, in the order of 30 cm, and there is a first sieve for the size of less than 40 cm (Fig. 23).

The fragments of the metal structure are removed through a magnet, below which there is a grid with a passage of 20-25mm (Fig. 24). Below 20 mm there is the so-called rubber-dust[14], which is aspirated during the process and then transported to the mill. Semi-finished products such as membranes (carpets) in rubber granules of 3-6 mm in size for molding at 300 bar at room temperature are also produced in the plant.

[14] Powder is produced in dimensions that depend solely on the customer.



Figure 24. (a) Milling of the rubber; (b) Semi-finished rubber membranes in sacks

The size of the rubber particles is graded and can be found in many shapes and sizes. The finest one can be as small as about 0.2 mm and below. The gradation used in this research is between about 0.4-2.0 mm to 2-4 mm. Crumb rubber is light in weight and also durable. It can last for an extended period in a natural environment. CRM can be categorized as a nontoxic and inert material (Fig. 25).



Rubber Powder (0.3–0.6 mm) Rubber Shred (2.36-0.85 mm) Granules (1-4 mm)

Figure 25. Difference sizes of crumb rubber used

The grain fractions, which the plant has graciously provided, had dimensions of 0.4/2 mm, 2/4 mm and 5.6/11 mm. Further sifting was carried out to study granulometry as was done for aggregates. Sieving provided the following granulometric curves, as shown in Fig. 26.

Material:	RUBBER	Data	13/05/2016

Sieves empty (kg)	Sieve Size(mm)	% Passing limit			Δmix (%) Retained	Ø0.4-2mm	Ø2-4mm	Ø5.6-11mm	Averaged
		Lower limit (%)	Upper limit (%)	Target mix (%)		%Pass.	%Pass.	%Pass.	%Passing Ø0.4-2-4mm
0.458	31.5	100.00	100.00	100.00	0.0	100.0	100.0	100.0	100.00
0.457	22.4	90.48	100.00	95.24	4.8	100.0	100.0	100.0	100.00
0.461	16	71.59	92.23	81.91	13.3	100.0	100.0	92.055	100.00
0.405	11.2	58.56	80.21	69.38	12.5	100.0	100.0	74.656	100.00
0.404	8	49.04	70.49	59.77	9.6	100.0	100.0	62.497	100.00
0.414	5.6	41.22	61.80	51.51	8.3	100.0	100.0	52.937	100.00
0.424	4	36.00	56.00	46.00	5.5	100.0	95.258	43.094	97.63
0.383	2	23.00	40.00	31.50	14.5	75.985	2.476	25.029	39.23
0.341	1	14.77	28.61	21.69	9.8	5.806	0.527	11.927	3.17
0.398	0.40	9.76	21.51	15.63	6.1	1.617	0.431	4.271	1.02
0.304	0.177	7.02	16.05	11.54	4.1	1.158	0.411	0.286	0.78
0.261	0.063	5.89	9.35	7.62	3.9	0.981	0.393	0.123	0.69
0.380	0	5.89	9.35	7.62	0.0	0.000	0.000	0.000	0.00

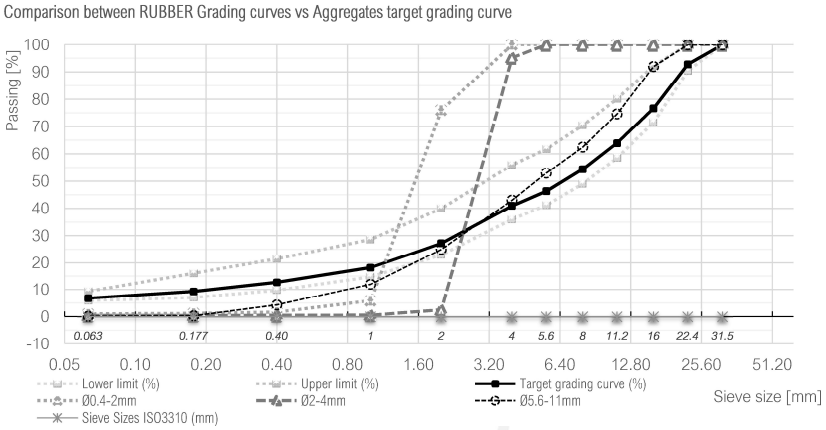


Figure 26. (a) Sieving process; (b) Grading curves of the rubber fractions ϕ0.4-2mm; ϕ2-4mm, and ϕ5.6-11mm

The specific gravity of the crumb rubber was determined using the hydrostatic procedure with pycnometer outlined in [ASTM C128, 2015; EN 12697-5, 2009] (Fig. 27; Table 15).

TABLE 15. PROPERTIES OF THE RUBBER ADDED TO THE DRY-PROCESS CRM MIXES

Color	Black
Particle morphology	Irregular, undisclosed
Moisture content (%)	<0.75%
Textile fiber content (%)	<0.65% in weight
Metal content (%)	<0.1% of the rubber weigth
Acetone extract content	7.5%-17.5%
Natural rubber content	21.0-42.0%
Polymers content (SBR)	50%
Sulfur content	0.0%-5.0%
Carbon black content	20.0%-38.0%
Ash content	0.0%-10.0%
Particle sizes from quarry	Ø0.4-2mm; Ø2-4mm; Ø5.6-11mm
Proportions of rubber studied	60% Ø0.4-2mm ; 40% Ø2-4mm
	20% Ø0.4-2mm ; 80% Ø2-4mm
Standards: C.N.R. UNI-1 ; ASTM C128 ; UNE 12597-5:2009	
Tª water: 27ºC (density 1.00025 gr/cm3)	Pycnometer test
Weight of sample (gr)	500
Weight of pycnometer, m1(gr)	767
Weight of pycnometer with sample mass, m2 (gr)	1270
Weight of pycnometer + sample ρssd + water, m3 (gr)	3106
Weight of pycnometer filled with water, m4 (gr)	3039
Maximum Specific Gravity of rubber (g/cm3)	1.1536



MAXIMUM DENSITY OF RUBBER 01 (60-40%)

$\rho_{mb} = \frac{(m_2 - m_1)}{(m_4 - m_1) - (m_3 - m_2)} \rho_w$

Standards: C.N.R. UNI 1 ; ASTM C128 ; UNE 12597-5:2009

Tª water: 0.27 ρ_w 1.0003

Material:	RUBBER	R_1 (60% Ø0.4-2mm ; 40% Ø2-4mm)
Test date:	28/07/2016	
Picnometro nº	3	
Weight of sample	500	gr
Weight of pycnometer, m1	767	gr
Weight of pycnometer with sample mass, m2	1270	gr
Weight of pycnometer+sample ssd+water to mark, m3	3106	gr
Weight of pycnometer filled of water, m4	3039	gr
Maximum Specific Gravity of rubber	1.15367	g/cm³

MAXIMUM DENSITY OF RUBBER 02 (80-20%)

Standards: C.N.R. UNI 1 ; ASTM C128 ; UNE 12597-5:2009

Tª water: 0.27 ρ_w 1.0003

Material:	RUBBER	R_2 (20% Ø0.4-2mm ; 80% Ø2-4mm)
Test date:	03/08/2016	
Picnometro nº	3	
Weight of sample	500	gr
Weight of pycnometer, m1	767	gr
Weight of pycnometer with sample mass, m2	1268	gr
Weight of pycnometer+sample ssd+water to mark, m3	3105	gr
Weight of pycnometer filled of water, m4	3039	gr
Maximum Specific Gravity of rubber	1.15172	g/cm³

Figure 27. (a) Sieves rubber fractions ϕ0.4-2mm; ϕ2-4mm, and ϕ5.6-11mm; (b) Rubber densities

4.7. Bituminous asphalt mixtures

4.7.1. Classification of asphalt mixture according to grading

Based on aggregate gradation, HMA can be categorized into dense-graded, open-graded, and gap-graded. **Dense-Graded Mixes** have a continuous particle size distribution (gradation curve does not have any abrupt slope change). Therefore, its structural performance depends mainly on the interlock between aggregate particles, with the hypothesis that smaller particles fill the voids generated by the larger particles [Roberts, F.L. et al., 1996]). The dense-graded is relatively impermeable. Fine-graded mixes have more sand-sized particles than coarse-graded mixes (Fig. 28). Traffic level is a direct consideration in the design of these mixtures. Aggregate angularity, binder grade, and some volumetric properties vary with traffic-level in dense-graded mixture procedure [HAPI, 2018].

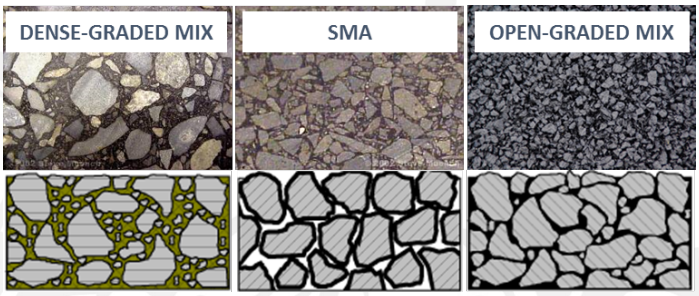


Figure 28. Classification by aggregate gradation (Adapted from LabIC.UGR publications)

Gap-graded (GGHMA) or Stone Matrix Asphalt (SMA), will be missing most medium sizes but have a relatively high proportion of fines. It is initially developed in Europe to maximize rutting resistance and durability. Since aggregates do not deform as much as asphalt binder under load, this stone-on-stone contact significantly reduces rutting. Typical SMA composition consists of 70–80% coarse aggregate, 8–12% filler, 6.0–7.0% binder, and 0.3% fiber [UTAH-MT 07-03, 2007].

Open-Graded Mixes (OG), are designed to be water permeable formulated to provide large voids (around 20%), with relatively uniform-sized aggregate typified by an absence of intermediate-sized particles. Increasing the voids in the mineral aggregate (VMA) requirement increases the useful binder content. The use of higher binder content dense-graded mixtures should be considered for base layers when the traffic level exceeds 10,000,000 ESALs. The next graph presents a detailed design procedure for the next types of HMA_DRY mixtures according to the grading curve (Fig. 29).

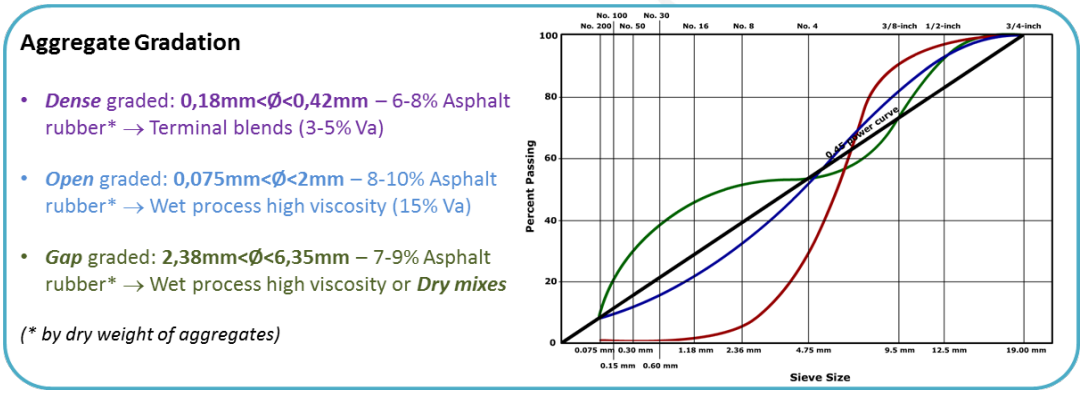


Figure 29. Gradation types

The principal design consideration in *GGHMA* is to maximize the contact between particles in the coarse aggregate fraction of the mixture. The advantages of these mixtures over *dense-graded* mixtures include an increased resistance to fatigue cracking and low-temperature performance (Fig. 30). GGHMA is considered for surface courses when the traffic level exceeds 10^6 ESALs.

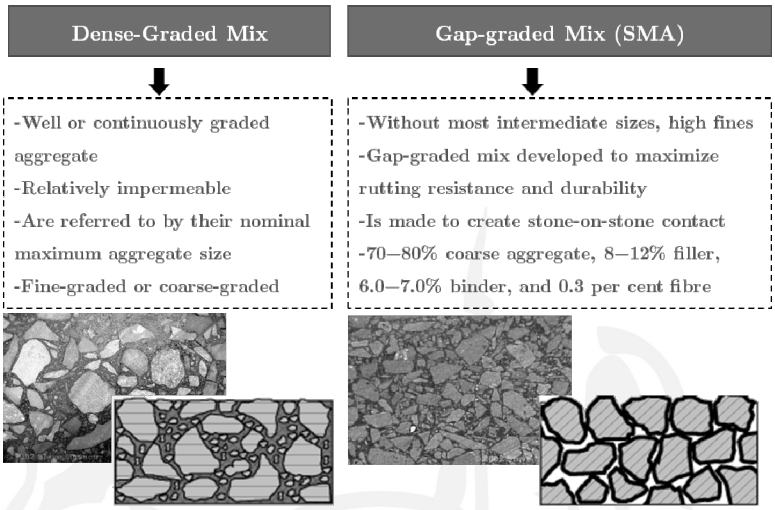


Figure 30. Comparison between Dense-grade and SMA mixes

4.7.2. Conventional Hot-Mix-Asphalt (HMA)

Hot Mix Asphalt (HMA) or Asphalt concrete is composed primarily of aggregate and asphalt binder, this is a combination of approximately 95% stone, sand, or gravel bound together by asphalt cement, a product of crude oil [Asphalt Hot Mixer, 2018]. Aggregate typically makes up about 95% of an HMA mixture by weight, whereas asphalt binder makes up the remaining 5%. By volume, a typical HMA mixture is about 95% aggregate, 4-5% asphalt binder, and 4% air voids (Fig. 31).

The asphalt binder used in HMA is stiff at room temperatures so that once this type of asphalt cools, it becomes strong enough to support heavy traffic. In the laboratory, HMA mixtures were about 4% air voids, with a range of 3 to 5%. After construction, as traffic passes over rail layers, the HMA in the wheel paths will gradually compact to air void levels approaching the design value of 3 to 4%.



Figure 31. (a) Example of HMA manufacturing in the laboratory; (b) Superpave 150x120mm samples; (c) Aggregates; (d) Binder B50/70; (e) Compacted HMA specimens.

4.7.3. Plusride[15] mixtures

Tire Rubber was introduced into asphalt mixes by blending the CRM with hot aggregates before mixing the same with asphalt to produce a rubber modified mix [Gowda, G.V. et al. 1997; Heitzman, M.A. 1992]. Pluride mixes are dry-process mixes wherein the CRM, which is primarily used as a rubber aggregate, is incorporated into aggregates with *gap gradation* before mixing with the asphalt. The finished product is referred to as "Coarse CRM Hot Mix Asphalt Concrete Mix" (Table 16).

TABLE 16. AGGREGATE GRADATION FOR GAP-GRADED PLUSRIDE MIXES

Passing sieve size (mm)	Plusride 8	Plusride 12	Plusride 16
Φ 19	-	-	100
Φ 16	-	100	100
Φ 12.5	100	60-80	50-62
Φ 9.5	60-80	30-44	30-44
Φ 1.7	23-38	20-32	20-32
Φ 0.6	15-27	13-25	12-23
Φ 0.075	8-12	8-12	7-11
%binder	8-9.5	7.5-9.0	7.5-9.0
			Rubber (% of total mix by)
Weight	1.5	2.0	3.0
Volume	3.02	3.95	5.71
			Asphalt (% of total mix by)
Weight	5.5	6.0	7.0
Maximum voids (%)	2.5	3.5	4.0

The CRM used in the PlusRide mixes can range from 1 % to 6% by weight of the total mix, with 3% rubber being commonly used. For mix-design, the trial asphalt contents were ±2% more asphalt than a conventional mixture with similar size and type of aggregates. For this study, the dry process will be applied for mixing crumb rubber into aggregates with gap gradation and dense gradation.

4.7.4. Generic dry mixtures (RUMAC)

Generic RUMAC Mixes is referred to end product by reacting crumb rubber into dense gradation (conventional for the base course in roads, and also as sub-ballast underlayment [Rose, J.G. et al. 2010,2011,2006]) to avoid direct impact of mechanical weathering and fatigue cracking. Unlike the PlusRide mixes, the gradation of CRM is a two-component system in which the crumb rubber is believed to interact with the asphalt cement while the coarse crumb rubber performs as an elastic aggregate in the Hot Mix Asphalt Concrete (HMAC) mixes [Heitzman, P.E. et al. 1992]. The finished product is referred to as "Fine Crumb Rubber Modified Hot Mix Asphalt Concrete."

TABLE 17. AGGREGATE GRADATION FOR GENERIC DRY MIXES

Passing sieve	Nominal maximum size		
(mm)	19.5mm	12.5mm	9.5mm
Φ 25	100	-	-
Φ 19	90-100	100	-
Φ 12.5	-	90-100	100
Φ 9.5	56-80	-	90-100
Φ 4.75	35-65	44-74	55-85
Φ 2.36	23-49	28-58	32-67
Φ 0.3	5-19	5-21	7-23
Φ 0.075	2-8	2-10	2-10

CRM is added to produce a dense-graded Rubber Modified Asphalt Concrete mix (Table 17). In the dry process of preparing the generic mixes, the gradation of rubber was selected that the coarse rubber particles will serve as elastic aggregates and the fine rubber will react with asphalt to produce

[15] PlusRide mix is the trade name of the mix marketed under patent by the Swedish companies Skega AB and ABV. Being a patented mix, three types of aggregate gradations are supplied by the patent company for the design of Gap Graded RUMAC Mixes.

modified binder. In this research, 1.5-3% of crumb rubber and 6.5% of asphalt content have been used in the preparation of the Generic Dry Mixes. The intimate mixing causes an increase in the viscosity of the binder when the fine crumb rubber particles reach optimum swelling.

4.7.5. Description of final mixtures studied

Before mixing, the aggregates were dried to remove moisture, and the asphalt binder was heated to 190-200°C to reduce its viscosity. During these study, different mixes were characterized by diverse amount of asphalt binder (3.5%, 4%, 5%, 5.5%, 6%, and 6.5%), and rubber proportion (0%, 1.5%, 2% and 3% of the total weight of the aggregates). Four different bituminous mixtures by SGC (HMA_{RFI} b.4%, DRY 1.5% b.5.5%, DRY 2% b. 6,5%, and DRY 3% b. 7% mixtures) were optimized.

The mix-design was developed and performed at the Laboratory of Materials and Civil Engineering of the University of Palermo. The aggregate mineral fractions used consisted of limestone obtained from the quarry "*Cava Giardinello S.N.C. Di Buttitta Francesco & C.*" (Palermo).

Through these mixtures, it was possible to assess the influence of the rubber on the performance of the rubberized asphalt materials by a dry process for a bituminous sub-ballast layer. The reference mixture is a conventional HMA without rubber as a dense-graded mixture with a lime-stone nature of aggregates, with a 4% of a conventional bitumen B50/70 (Fig. 32).

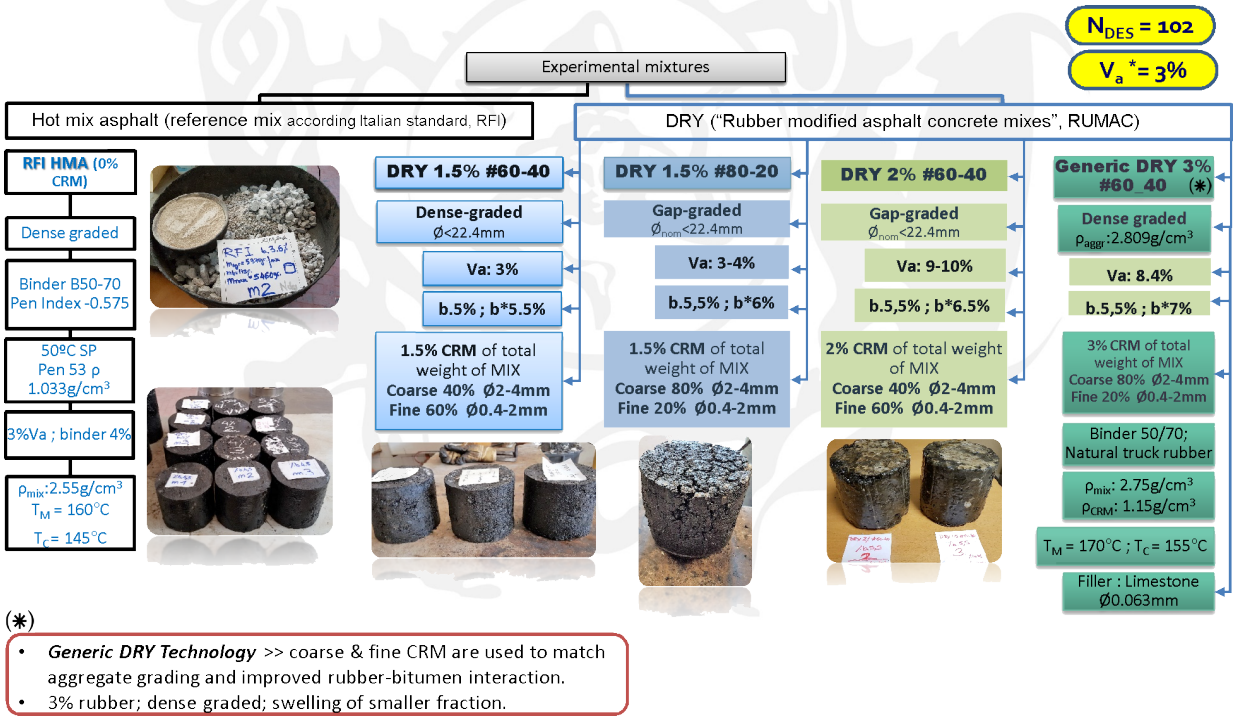


Figure 32. Materials and mixtures specifications of the research

These are mainly dense, and gap-graded asphalt concrete mixes to which scrap tire rubber is added as a part of the aggregate component [Heitzman, M. 1992; Huang, B. et al. 2002]. Rubber particles influence the effectiveness of compaction and tend to cause significant air voids [Mashaan, N.S. et al. 2013; Hamza, M.A. et al. 2005]. The type of rubber added (fibers or granules) have higher effects on the compaction behavior, and its main effects are on the stress-strain behavior during post-compaction [Fu, R. et al. 2017; Özul, Z.H. et al. 2007]. The specifications of the aggregate, filler, bitumen, and rubber are listed in Table 18.

TABLE 18. AGGREGATE, RUBBER AND BITUMEN SPECIFICATION

Component	Type	Specifications	Specific gravity (g/cm3)		
			Min	Max	Averaged
Coarse aggregate	Limestone	2mm<Ø<31.5mm	2.60	2.85	2.81
Sand	Limestone	0.177mm<Ø<2mm	2.70	3.00	2.84
Rubber	Truck tire crumb	0.2mm<Ø<5mm	1.10	1.20	1.15
Filler	Limestone	0.063<Ø<0.075mm	2.65	2.75	2.70
Bitumen	--	50/70Pen	1.00	1.10	1.03

The proper amount of binder is essential to good performance in asphalt mixtures. Once the mixture is selected (acceptable %VMA, dust-to-asphalt ratio, densification criteria, and meets the criteria for %VFA), a minimum of two specimens were compacted[16] at each of the asphalt binder content, and the estimated asphalt binder content ±0.5% and ±1.0%. The effective binder contents for the mix design were 4.2%, 4.7%, 5.2%, and 5.7% in the case of conventional HMA (a minimum of four asphalt binder contents), and at least four to six specimens were finally prepared for determination of the maximum theoretical specific gravity.

TABLE 19. DESIGN MIX PROPERTIES HMA

Mix property	Result	[SHRP A-407]
%Air voids	2.74	3.0
%VMA	12.4	<13.0
%VFA	77.9	65-75
Dust-to-Aspalt ratio	1.75	0.6-2.0
%Γmm @ Ninit =8	86.39	<89
%Γmm @ Ndes =102	96.54	96
%Γmm @ Nmax =162	97.75	<98
γ_{binder} (g/cm^3)	1.033	-
$\gamma_{aggregates}$ (g/cm^3)	2.808	-
$\Gamma_{MAX\ mixture}$ (g/cm^3)	2.634	-
$\Gamma_{SSD\ mixture}$ (g/cm^3)	2.562	-
NMAS	22.4mm	19.0mm

TABLE 20. DESIGN MIX PROPERTIES DRY 1.5%

Mix property	Result	[SHRP A-407]
%Air voids	3.37	<4.0
%VMA	15.60	13.0
%VFA	78.37	65-75
Dust-to-Aspalt ratio	1.25	0.6-2.0
%Γmm @ Ninit =10	88.87	<89
%Γmm @ Ndes =152	96.90	96
%Γmm @ Nmax =251	97.30	<98
γ_{binder} (g/cm^3)	1.033	-
$\gamma_{aggregates}$ (g/cm^3)	2.808	-
$\Gamma_{MAX\ mixture}$ (g/cm^3)	2.577	-
$\Gamma_{SSD\ mixture}$ (g/cm^3)	2.501	
NMAS	22.4mm	19.0mm

The reference HMA was designed with 4% of binder and ±3% of air voids, manufactured for a conventional B50/70 at 160ºC-145ºC mix-compaction temperatures to guarantee the workability of the mixes. Two references mixtures were proposed, one for HMA[17] (b.4%) and other for a rubberized dry mix (DRY 1.5%)[18] based on C.N.R. 39-73, RFI, 2016, and EN 12697-31 (Tables 19-20).

An aggregate weight of 5100±300gr was usually sufficient for the compacted specimens, which were mixed at the mixing temperature 160ºC-173 ºC respectively, and a compaction temperature 145ºC-150 ºC. The ambient ground rubber was processed at a standard temperature (20ºC) inside hot bituminous mixtures (160-220ºC). CRM is used as a substitute for 1.5%, 2% and 3% by weight of the total aggregates (3.2%, 4.2% and, 6.2% respectively by volumetric part of the aggregates of density equal to 2.81 g/cm^3). The proportions of rubber proposed are #60-40% for mixtures with 1.5 to 2% of rubber and, #20-80% for mixture with 3% of rubber (as, a 60% of Ø0.4-2 mm and 40% of Ø2-4 mm).

These crumb rubber particles act as a rubber-aggregate into the mixture, varying sizes between Ø0.4-2 mm and Ø2-4 mm. Ambient ground rubber with a specific gravity of 1.154 g/cm^3 is finally used. For this study, the dry process will be applied for mixing crumb rubber into aggregates with gap-graded and dense gradation. The mixes produced after incorporating rubber before mixing with the asphalt

[16] All specimens in the Superpave mix design method are conditioned as loose mix according to the short-term aging procedure in SHRP Standard Method of Test M-007.

[17] A dense-graded mix type (onwards HMA_RFI or reference mixture, with a binder content of 4% according standard EN 13108-1). The asphalt binder used was a B50/70-penetration grade having a PG70-16 (AASHTO M-320) after Superpave asphalt binder specifications.

[18] A dense-graded Plusride mixture with 1.5% of rubber and binder 5 to 5.5% (hereinafter DRY 1.5). For Plusride mixes: #60-40 (60% of fine powder-crumb rubber of Ø0.4 to 2mm and, 40% of coarse or ground rubber of Ø2 to 4mm).

cement will be called gap-graded Plusride-Rumac mixes (DRY 1.5%, DRY 2%) and dense-graded Generic dry mixes (DRY 3%). Details are shown in Tables 21 to 24, and Fig. 33.

TABLE 21. FINAL GRADING CURVES FOR AN HMA – DRY MIXTURES (ADJUSTMENT OF SIEVE FRACTIONS)

	Filler <0.063	Sand Ø0.063/4	fØ5-10mm	fØ10-15mm	fØ20-25mm	fØ25-30mm	Σcomponents
Passing	[%]	[%]	[%]	[%]	[%]	[%]	[%]
RFI_HMA	12.24	24.60	5.21	18.29	18.49	21.16	100.00
Γmix=	2.740g/cm^3					Γaggr=	2.809g/cm^3
DRY 1.5%	12.45	23.79	4.62	18.98	18.65	21.52	100.00
Γmix=	2.716g/cm^3					Γaggr=	2.808g/cm^3
DRY 2%	12.52	23.51	4.42	19.21	18.70	21.65	100.00
Γmix=	2.700g/cm^3					Γaggr=	2.808g/cm^3
DRY 3%	12.66	22.94	4.01	19.69	18.80	21.90	100.00
Γmix=	2.687g/cm^3					Γaggr=	2.808g/cm^3

TABLE 22. RESULTS OF GRADATION AND ADJUSTMENT OF THE PASSING FOR EACH MIXTURE.

Sieve	% Passing limit			Fuller's curve		HMA		DRY 1.5%		DRY 2%		DRY 3%	
Size (mm)	Lower limit	Upper limit	Avg. limits	Target (%)	Ø$_{nom.}$ 22mm (%)	Pass (%)	Retain (%)	Pass (%)	Retain (%)	Pass (%)	Retain (%)	Pass (%)	Retain (%)
31.5	100.00	100.00	100.00	100.00	100.00	100.00	0.00	100.00	0.00	100.00	0.00	100.00	100.00
22.4	90.48	100.00	95.24	92.86	85.78	92.39	7.61	92.26	7.78	92.22	7.78	92.13	7.87
16	71.59	92.23	81.91	76.75	73.72	77.18	15.21	76.82	15.51	76.70	15.51	76.46	15.67
11.2	58.56	80.21	69.38	63.97	62.79	63.28	13.90	62.77	14.11	62.59	14.11	62.24	14.22
8	49.04	70.49	59.77	54.41	53.97	54.96	8.31	54.23	8.62	53.98	8.62	53.47	8.77
5.6	41.22	61.80	51.51	46.36	45.97	47.20	7.77	46.32	7.96	46.02	7.96	45.42	8.06
4	36.00	56.00	46.00	41.00	39.51	38.40	8.79	37.72	8.53	37.49	8.53	37.02	8.39
2	23.00	40.00	31.50	27.25	28.92	27.75	10.65	27.45	10.14	27.35	10.14	27.14	9.88
1	14.77	28.61	21.69	18.23	21.17	20.69	7.06	20.61	6.76	20.59	6.76	20.53	6.61
0.40	9.76	21.51	15.63	12.69	14.02	15.72	4.97	15.80	4.76	15.82	4.76	15.88	4.66
0.177	7.02	16.05	11.54	9.28	9.71	10.41	5.31	10.51	5.28	10.54	5.28	10.61	5.27
0.063	5.89	9.35	7.62	6.75	6.10	6.75	3.66	6.85	3.66	6.88	3.66	6.94	3.67

TABLE 23. SPECIFICATIONS FOR MIX-DESIGN

	Rubber substitution (% of total mix by)		
Mixture	Asphalt (%)	Weight (%)	Volume (%)
DRY 1.5	5.5	1.5	3.02
	6.0	1.5	2.98
DRY 2.0	6.0	2.0	3.95
	6.5	2.0	3.90
DRY 3.0	7.0	3.0	5.71

TABLE 24. VOLUMETRIC MIX DESIGN CHARACTERISTICS

Characteristics of the mixtures	RFI b.4%	DRY1.5% b.5,5%	DRY2% b.6,5%	DRY3% b.7%
Mixture weight (*)	5460	5460	5460	5460
Aggregrate mass	5250	5176	5127	5103
SG Aggregates	2.809	2.808	2.808	2.808
%Inert part	96.15%	94.79%	93.89%	93.45%
Bitumen mass	210.0	284.5	333.4	357.4
S. Gravity binder	1.033	1.033	1.033	1.033
% binder	3.85%	5.21%	6.11%	6.55%
γ_{max} [g/cm^3]	2.634	2.577	2.541	2.524

(*) Optimal inert part for a specimen of Ø150x120mm

The granulometric curves that best fill the voids are those in which there is a right balance between the volume occupied by coarse grains, grains of intent, fine grains and so on. The simple addition of granular rubber to a well-graded blend would entail a significant modification of the granulometric distribution since the types of granulate that can be used do not contain all the fractions present in the lithic assortment, or at least do not include them in the same proportions [D'Andrea A. et al. 2001]. Therefore, it has been decided to introduce the rubber granulate with an ideal criterion of mutation of the mechanical characteristics of some of the elements of the granular mixture present in

the conglomerate. The benefit is the statistically good "homogeneous" distribution of the response of the material to the dynamic stresses applied by the traffic loads.

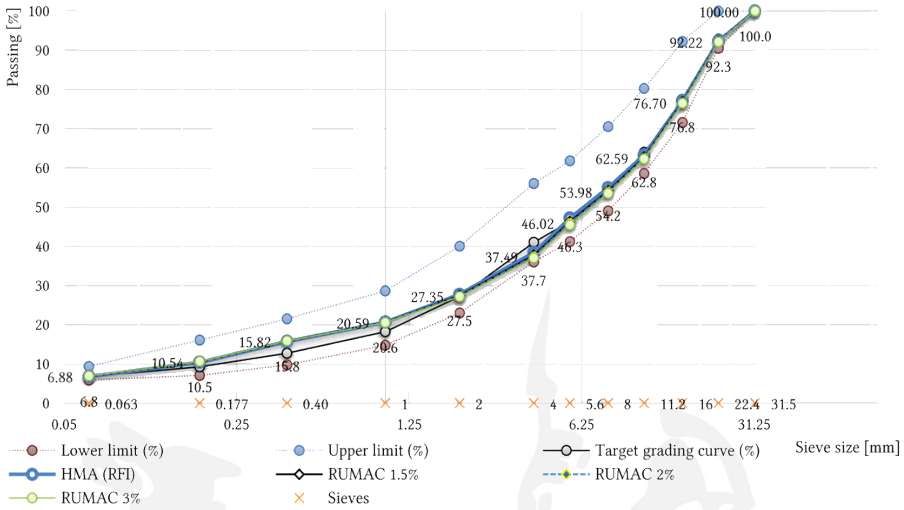


Figure 33. Definition of the HMA and DRY mixture gradation specification bands (% passing by weight)[19].

4.8. Methods

This section describes the methodology followed in the development of the research, explaining in detail the phases previously described (Fig.1), as well as the tests carried out to achieve the objectives set. The phases of the research are structured and ordered chronologically, coinciding with the objectives marked in the previous chapter. The present thesis, therefore, focuses on the analysis of the mechanical behavior of different bituminous sub-ballasts (HMA_DRY) under various conditions (temperature, frequency, and traffic loads) that are expected to produce failure of the material. When designing mixtures of rubber and aggregates in railways, all volumetric criteria are justified by what will be more accessible to develop and offer excellent performance.

CHARACTERIZATION OF THE MIXTURES:

SUPERPAVE Gyratory compactor mix-design in all blends [EN 12697-31:08]), Marshall test (only for HMA mixtures) [EN 12697-34:06], ITSR Water Sensitivity test (just for HMA) [EN 12697-12:2009], Indirect Tensile Strength (IDT) test (just for HMA) [EN 12697-23:2017], Asphalt Slab Roller Compactor [EN 12697-33:2007], and mechanical performance by Fatigue cracking UGR device and NDT-FFRC (Non destructive Free-Free Resonant Column test) [ASTM C215:2014] were applied to characterize all types of bituminous HMA_DRY blends for railway sub-ballast.

4.9. Methodology 01: "Volumetric Mixture design."

4.9.1. Superpave system: a literature review

This thesis is primarily based on the Superpave design system, including volumetric requirements, compaction levels, and specifications for aggregate properties. Also, the results and recommendations of some recent research projects have been adopted where such results have been published and

[19] NMAS – Nominal Maximum Aggregate Size – one sieve size larger than the first sieve that retains more than 10 %.

presented to the paving technology community and favorably received [Hu, W. et al. 2017; Maupin Jr. et al. 2003; Schiebel, B. 2002; Button, J. et al. 1994; Kennedy, T. 1994; Consuegra A. et al. 1989].

From the mid-2000s, the Superpave system gradually replaced the Marshall and Hveem methods. Superpave [SHRP-A-410; NCHRP-573; NCHRP-459; AASHTO R35] which is short for "SUperior PERforming PAVEments," is a pavement design system to provide durable pavements that can resist various forms of distress. It was developed to design mixtures correctly for different temperatures and traffic loadings. However, as it was being adopted, many engineers thought that the specific requirements given in the Superpave system were not providing HMA mixtures with the best performance for their local conditions and climates. For this reason, significant research has modified the requirements for the Superpave system [Khosla, N. et al. 2013; Schiebel, B. 2003; Maupin 2003].

There have been many mixture design methods over the previous century that have furthered the understanding of asphalt mixtures. When HMA pavements first began to be constructed, mixture composition was determined based on the judgment and experience [Jenks, C.W. et al. 2011; Christopher, W. J., et al. 2011; NCHRP, 673; Hveem, F. et al. 1963; Foster, C.R. 1982; Blankenship, P.B. 2004]. In the 1930s, Marshall mix design method was developed as a rational system for designing HMA mixtures and continued to be used through the 1980s. Briefly, the Marshall mix design procedure relies on compacting specimens using a standard drop hammer over a range of asphalt binder contents. In the late 1980s, the Strategic Highway Research Program (SHRP) was conducted a research program to develop improved test methods and specifications for asphalt binder and aggregates and an improved procedure for HMA mixture design and analysis. In many ways, the Superpave system of mix design and analysis [Cominsky, R. et al. 1994; Kennedy, T. 1994] was a success. This method is similar to the Marshall system in its use of volumetrics, but laboratory specimens are prepared using a gyratory compactor (Fig. 34) rather than a drop hammer.



Figure 34. (a) Hveem gyratory compactor; (b) Marshall compactor; (c) Superpave gyratory compactor

At the moment, the techniques of mixing using Marshall and Superpave (SGC) are the common ones, but there are differences between both [AASHTO T245:15; ASTM D6927-15; EN 12697-34:12; Quasim, Z. et al. 2017; Zumrawi, M. 2016; Pérez-Jiménez, F. et al. 2014; Jitsangiam, P. et al. 2013; Swami, B.L. et al. 2004; Gowda et al. 1996; Hafez I. et al. 1984; Foster, C.R. 1982]:

- Marshall method is probably the most widely used mix design method. It is simple, and inexpensive.
- SGC integrates material selection and mix-design into procedures, it was created to make the best use of asphalt paving technology and to present a system that would optimize asphalt mixture resistance to permanent deformation, fatigue cracking and low temperature cracking.

- Superpave Performance Graded (PG) system specifies the properties of the asphalt binder, volumetric and densification characteristics determined by the Gyratory Compactor (SGC).
- Marshall impact compaction does not simulate real mixture densification.
- Marshall determinates asphalt binder content, while SGC does all element of mix design.
- Marshall method requires ±95% compaction. Superpave requires 94%±2% compaction.

Understanding the terminology used to describe the volumetric composition[20] of asphalt concrete and the ability to perform a volumetric analysis are two of the most valuable aids to develop efficient asphalt concrete mix-designs. Asphalt mixtures have traditionally been designed using a "trial and error" procedure. Aggregates were combined in percentages developed from an empirical database of information extending back to the beginning of asphalt mix-design [Hveem, F. et al. 1963].

The volumetric properties of concern in the performance of the asphalt mixture are air voids (V_a), voids in the mineral aggregate (VMA), and voids filled with asphalt (VFA). VMA is the inter-granular void space between the aggregate particles in a compacted asphalt mixture, including the air voids and the effective asphalt content. VFA is the percentage of the VMA that is filled with asphalt cement (Fig. 35) [Solyman, M. 2005].

The mix-design in this study is based on the strength and fatigue resistance of an asphalt mixture derived from coarse aggregate interlock and proper aggregate packing. The durability is ensured with proper volumetric-design, including air voids, VMA, asphalt film thickness, and dust proportion.

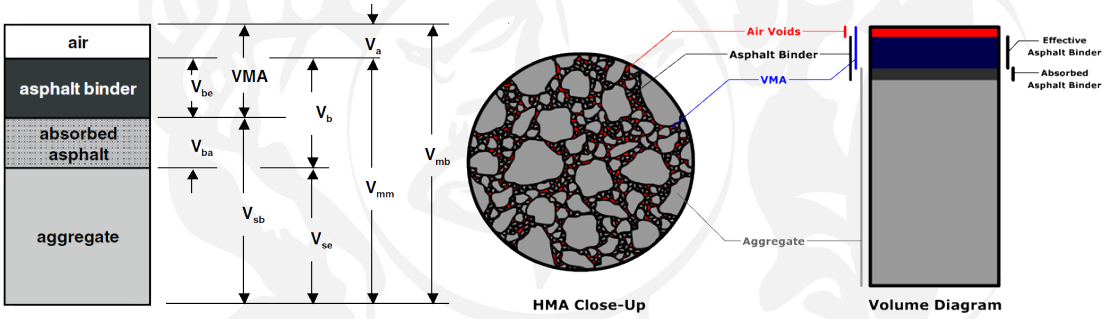


Figure 35. (a) Definition of volume terms used in the volumetric analysis; (b) Density-Voids and Volume Relationships of a Compacted Asphalt Sample

Where:

- V_{be} = Volume of effective asphalt binder; V_{ba} = Volume of absorbed asphalt binder;
- V_{ma} = Volume of voids in mineral aggregate; VMA = Voids in mineral aggregate, percent by volume;
- V_{sb} = Volume of aggregate, bulk (including all permeable surface pores);
- V_b = Total asphalt binder content, percent by volume;
- V_{se} = Effective volume of aggregate (excluding surface pores filled with asphalt);
- V_a = Air void content; V_{mm} = Volume of aggregate and asphalt; V_{mb} = Volume of the specimen.

4.9.2. Characterization of the mixtures: "SGC mix-design."

Volumetric mix design with gyratory compactor (SGC) was conceived as the optimal laboratory tool that more closely simulates field compaction of asphalt mixtures [NCHRP 464-465, 2001]. The SGC is influenced by the angle 1.25º, fixed pressure 600 kPa, and rate of gyration 30rev/min). Also depends on the amount of material (mass-height ratio), the number of gyrations, and the optimum binder to adjust the blend with a ±3% of air voids. The technique of compaction of the gyratory compactor simulates, with a high degree of likelihood, the executive process in real size. The

[20] Although composition of asphalt concrete mixtures can be given in terms of weight, traditionally the common method of describing and analyzing asphalt concrete composition is by volume.

implementing determine a phenomenon of continuous repositioning and adjustment of the materials in the mixture, generated by the rotation offset of the mold and the resulting variability, instant by instant, the number of gyrations along which the principal stresses were acting (Fig. 36a). The technical requirements are classified in two prerogatives:

- Workability: during the construction phase of the layers of the pavement (Fig. 36b);
- Durability: in the sense of guaranteeing mechanical performance over time life.

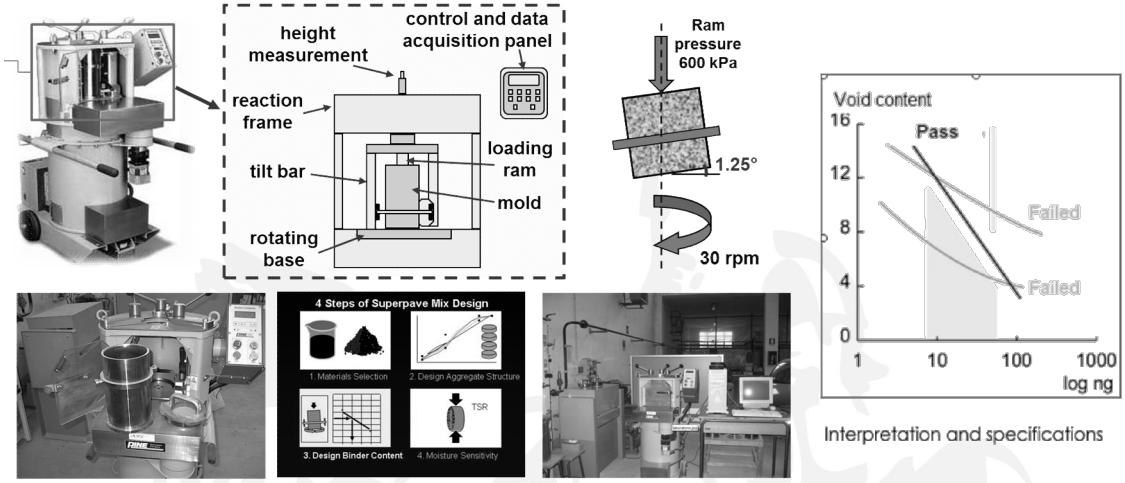


Figure 36. (a) Superpave gyratory compactor procedure; (b) Assessment of workability with SGC

Asphalt binder testing was implemented to tune the performance of the binder to the climate and traffic level. Aggregate quality specifications were established to improve the performance of the asphalt materials through the control points. The restricted zone[21] was included to prevent tender mixtures with excessive amounts of natural sand. Three distinct levels of design permit the selection of the traffic-loads (expressed as total 80 kN ESALs over the service life of the roads pavements) expected at the paving project (Table 25). Specific rules govern the treatment of the distresses in levels 2-3 for new construction. In case of railways, fatigue is the most important, where *temperature* and *traffic* are the factors that determine the mechanical evaluation[22].

TABLE 25. HIERARCHICAL ORGANIZATION OF THE SUPERPAVE MIX-DESIGN

Level 1	Level 2	Level 3
Volumetrics	Volumetrics	Volumetrics
-	Performance tests	Performance tests
-	-	Performance predictions
ESAL<10^6	10^6<ESAL<10^7	ESAL>10^7

4.9.3. Specifications of the gyratory compactor

Compaction is a central topic for asphalt mixture in that the accomplishment of mix-design depends on the required density [Hu, W. et al. 2017; Khosla, N. et al. 2003; Brown, E.R. et al. 1998; Cominsky, R. et al. 1994]. The compactor is relatively inexpensive, portable, and capable of quickly molding specimens with minimal specimen variations [Bahia, H.U. et al. 2013]. The performance properties of the compacted specimen simulate cores from pavements constructed with the same

[21] Note that the restricted zone will be eliminated by late 2002. The restricted zone refers to a particular area of the FHWA's 0.45 power gradation graph associated with Superpave mix designs.

[22] Thus, in Chapter 5 will develop this parameters for railways, and it is explained a new methodology based on AASHTO Road Test [Chandak, P. et al. 2017; Connors, M. et al. 2017; Darter, M. et al. 2001; Thompson, N.H. et al. 1992; Huang, 1984; Freeme, C. et al. 1982].

asphalt-aggregate blend. The SGC also allows an estimation of the final air voids content under traffic (the probability of the mix becoming plastic under loads) and a measure of the aggregate structure [Rahman, F. 2010].

The five primary features of the Superpave system are as follows:

1. Selection of the asphalt binder grade "PG grading" by local climate and expected traffic level.
2. Aggregate gradations are given for each aggregate size (NMAS).
3. Evaluation of trial mixtures on laboratory-compacted specimens Ø150 mm by ±120 mm thick. As in Marshall method, the level of compaction varies with the expected traffic level.
4. Volumetric requirements for design air void content (Va), VMA, and VFA.

The next step in the Superpave procedure is to define the specimens with ±Ø110mm to 150mm, and the final desirable height will correspond to the end of the test at N_{des}. Therefore, we will call it H_{Ndes}. Before the definition of the energy parameters (N_{init}, N_{des}, N_{max}), we must impose the actual height of each specimen, in correspondence with the final height that will tentatively be the closest to the H_{Ndes}. That is, our specimens after finishing the compaction process by SGC must have a height approximated to the design height (H_{Ndes}).

As a guideline, the final height will be analogous to the one we want in our actual layer of the sub-ballast, since in this way the test conditions will be similar to compaction in the field, and the mixture will be determined by the best performance [SHRP-A407, 1994; AASHTO R35; EN 12697-9]. An analogy is showed in Figure 37 for roads and railways.

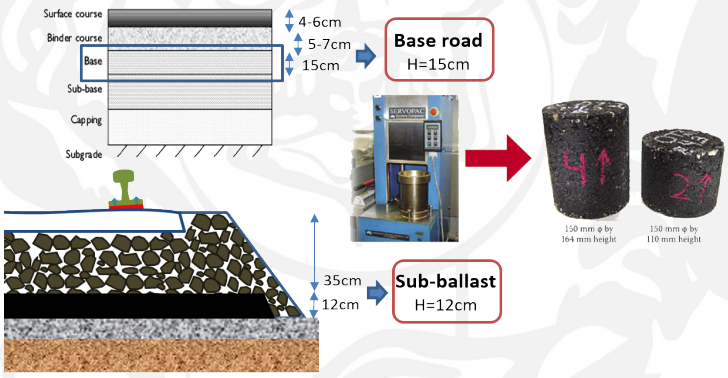


Figure 37. The height of SGC samples as an analogy of field conditions

The Superpave method of mix design was meant to include mixture test methods and an associated computer program that would predict the performance of HMA. The Mechanistic-Empirical Pavement Design Guide is in many ways a continuation of the SHRP efforts for flexible pavements.

4.9.4. Adjusting the Energetic parameters: N_{design} [23]

Compaction of specimens in the laboratory and requirements are more complicated in the Superpave system than for the Marshall method [NCHRP 673:11]. Currently, three compaction points are defined during the compaction process: $N_{initial}$, N_{design}, and N_{max}.

[23] Referenced documents:

- AASHTO M 323 2013 "Superpave Volumetric Mix Design," American Association of State Highway and Transportation Officials.
- AASHTO R35 2015 "Standard Practice for Superpave Volumetric Design for Asphalt Mixtures,".
- AASHTO T312 2015 "Standard Method of Test for Preparing and Determining the Density of Asphalt Mixture Specimens by Means of the Superpave Gyratory Compactor", American Association of State Highway and Transportation Officials.
- ASTM D6925-15, Standard Test Method for Preparation and Determination of the Relative Density of Asphalt Mix Specimens by means of the Superpave Gyratory Compactor.
- EN 12697-31:2007 "Bituminous mixtures. Test methods for hot mix asphalt. Specimen preparation by gyratory compactor".

The values of N_{max} and N_{Init} are expressed as a function of N_{DES} according to:

$$LogN_{nit} = 0,45 \cdot LogN_{des} \quad ; \quad LogN_{\max} = 1,10 \cdot LogN_{des} \qquad \text{(Eq. 11)}$$

Within the original Superpave system a maximum value of density at $N_{initial}$ was specified to help ensure proper aggregate structure since it was believed that mixtures that compacted too quickly had poor aggregate structures. N_{design} is the factor-design for compaction at which air void content, VMA, and VFA are then specified. N_{max} is the maximum number of gyrations applied to the specimen. A maximum density at N_{max} was specified in the original Superpave system to ensure that the mix would remain stable at the expected maximum traffic level [Brown, E.R: et al. 1998].

- Typically, samples are compacted to N_{design} to establish the optimum asphalt binder content and then additional samples are compacted to N_{max} as a check.

Previously, samples were compacted to N_{max} and then $N_{initial}$ and N_{design} were back calculated. However, proceeding in this way, the percentage of gaps was not real, but the maximum compacted. To reproduce the actual conditions of the mixtures in the laboratory, we must compact to N_{des} and then measure the density of the mixture once stable to 24h [NCHRP-573, 2007; Bonnot, J. 1986][24].

Some experiences were conducted to determine N_{design} [Brown, E.R: et al. 1999; Harman, T.P. et al. 1995; Blankenship, P.B. 1993]. The premises established were:

(1) there was a relationship between pavement densification and accumulated traffic;
(2) there was a relationship between the SGC sample-density compacted and in-place densities;
(3) there was a linear relationship between N_{design} and design traffic.

Flexible pavement designs and performance predictions derived from the empirical 1993 AASHTO pavement design methodology and the mechanistic-empirical NCHRP Project 1-37A approach were compared for a range of locations within the United States, each with its climate, subgrade, and other material properties and local design preferences [Carvalho, R. et al. 2006].

From this experiment, a table of N_{design} levels for three climates and seven traffic levels was developed. Later the SHRP researchers expanded this table to four climates, and the angle of gyration was changed to 1.25 degrees. The N_{design} levels were not altered at this time, even though angles had been demonstrated to affect N_{design}. After that, an evaluation was performed for the climatic zones in the N_{design} table. The argument was that the average 7-day maximum temperature was less than 39°C for the United States (Table 26).

TABLE 26. SUPERPAVE ORIGINAL TABLE (SHRP METHOD OF TEST M002, HARRIGAN, ET AL. 1994).

Design ESALs (millions)	Averaged Design Air Temperature											
	<39°C			39-40°C			41-42°C			43-44°C		
	Nini	Ndes	Nmax	Nini	Ndes	Nmax	Nini	Ndes	Nmax	Nini	Ndes	Nmax
<0.3	7	68	104	7	74	114	7	78	121	7	82	127
0.3-1	7	76	117	7	83	129	7	88	138	8	93	146
1-3	7	86	134	8	95	150	8	100	158	8	105	167
3-10	8	96	152	8	106	169	8	113	181	9	119	192
10-30	8	109	174	9	121	195	9	128	208	9	135	220
30-100	9	126	204	9	139	228	9	146	240	10	153	253
>100	9	143	233	10	158	262	10	165	275	10	172	288

(1994) SHRP A379 SUPERPAVE Mix Design. Manual of specifications, test methods, and practices
(1994) SHRP M-002 Preparation of Compacted Specimens of Modified and Unmodified HMA by SHRP Gyratory Compactor
(1994) SHRP 407 Superpave design manual for new construction and overlays

[24] This aspect, apparently irrelevant to conventional HMA mixtures, it will be different when the rubberized mixtures are studied, whose percentagge of air voids increased during the first 24h after Ndes compaction.

Finally, in 1999, the FHWA Superpave Mixtures Expert Task Group presented the new results of their respective studies on N_{design} and adopted by AASHTO in 2001. The revision from AASHTO PP28 was reduced avoiding performance graded of binder (climatic zones). In 2004, it was adopted as AASHTO M323 and AASHTO R35-2015 (Tables 27-28). The design compaction level, N_{design} is a function only of design traffic level and averaged design air temperature. This advance in the Superpave methodology has been a critical point in this thesis, since it has been possible to adapt for railways the method of SGC, initially only designed for flexible road layers.

TABLE 27. REVISED NDESIGN TABLE PROPOSED BY NCHRP (2007).

Design ESALs (millions)	Averaged Design Air Temperature				
	$N_{initial}$	N_{design}	$N_{maximum}$	% G_{mm} at $N_{initial}$	% G_{mm} at N_{max}
<0.1	6	50	74	<91.5	<98.0
0.1 to <10	7	70	107	<90.5	<98.0
1 to <30	8	100	158	<89.0	<98.0
>30	9	130	212	<89.0	<98.0

TABLE 28. REVISED NDESIGN TABLE PROPOSED BY AASHTO R35 (2015).

Design ESALs (millions)	Averaged Design Air Temperature				
	$N_{initial}$	N_{design}	$N_{maximum}$	% G_{mm} at $N_{initial}$	% G_{mm} at N_{max}
<0.3	6	50	75	<91.5	<98.0
0.3 to <3	7	75	115	<90.5	<98.0
3 to <30	8	100	160	<89.0	<98.0
>30	9	125	205	<89.0	<98.0

The literature indicates that the N_{design} levels have not been optimized to maximize performance. Due to the imprecision of N_{des} values between 100 and 125 turns (Level III), it must interpolate the ESAL values in a graph and obtain the trendline. Through the logarithm regression equation obtained, we can estimate the exact number of gyrations for railways. There is a need to verify the N_{design} road-values and relate them to railways field densification (Chapter 5).

4.9.5. Air Temperature

SUPERPAVE uses an improved system for testing, specifying, and selecting asphalt, which is the binder performance grading (PG) system selected based on the expected pavement temperature in the area of its intended use. The recent regulation does not contemplate the temperature range in which the mixture is developed, however, due to the nature of the bitumen, the selection of the performance grade is detailed below (Table 29). The binder is selected based on the climate where the bituminous layer will be placed [D'Angelo, J. A. 2001].

TABLE 29. PAVEMENT SURFACE TEMPERATURES TYPICAL OF DIFFERENT CLIMATES (2015).

Climate	Air temperature (°C)			
	Winter Low	Winter high	Summer low	Summer high
Temperature (e.g. Europe)	-10	+5	+20	+45
Cold continental (e.g. Canada)	-40	-15	+30	+50
Hot continental (e.g. India)	0	+15	+35	+60
Desert	-5	+15	+35	+65

An asphalt bituminous layer (roads-railways) is expected to perform under extreme climate conditions from the heat of summer to the frozen winter. Low temperature presents the danger of fracture and fatigue. Proper selection of the asphalt binder is critical to proper performance (Fig. 38a). The Superpave specification addresses this by testing at various aging conditions and temperatures to evaluate how the binder will perform as it ages (Fig. 38b).

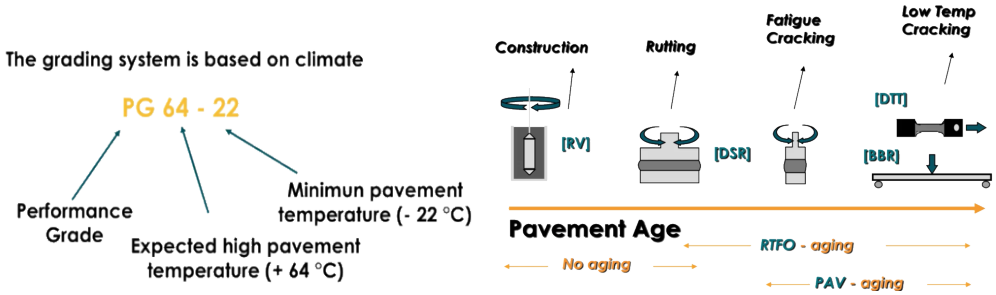


Figure 38. (a)Performance grade[25]; (b) Aging of bitumen (distresses and mechanical tests)[26]

4.9.6. Traffic levels (ESAL)

The nature of the traffic using a bituminous asphalt mixture for roads or railways is the primary design input that requires a different design because of the load magnitude, number of applications (frequency), speed of travel and cycle of life. The early-life performance of HMA mixtures under traffic should be evaluated by monitoring their deformation, surface condition, and elastic strains at the bottom of the layer [Jitareekul, P. et al. 2007].

N_{design} is established about ideal geographical area climate (maximum air temperature, design T^{a}) in which it carries out the project and traffic expected over the cycle-life (equivalent standard axle load, ESAL). Nevertheless, to use these parameters in the railway domain, it is necessary to define the Rail Equivalent Single Axle Load (R_{ESAL}), calculating the compression stress at the bottom of the base layer (roads) and the same for sub-ballast layer (to study fatigue cracking). Then, the traffic spectrum into a number of ESALs for railways is developed (Chapter 5).

The following data should be defined [Di Mascio, P. et al. 2014; Huhtala M. 1995; Robinson, 2009]:

- Traffic volume during design life[27];
- Vehicles features: type of train (e.g., high-speed or wagonload), axle number-load, and type of axle (e.g., dual, tandem or tridem wheel).

4.9.7. Bulk specific gravity and Maximum Density

The density of the compacted mix is the unit weight of the mixture (the weight of a specific volume of asphalt mixture). Mix properties are required to be measured in volumetric terms as well as weight. In mix design testing and analysis, the density of the compacted specimen is expressed in grams per centimeter cubic (g/cm^3). In this thesis, we must distinguish between:

- Bulk specific gravity: Mass per unit volume, including air voids;
- Maximum Density: Mass per unit volume, not including air voids, of a bituminous mixture at a known test temperature.

To determine the *bulk specific gravity* [EN 12697:12; AASHTO T166:16; ASTM D6925:15] (Fig. 39) of dense-graded mixtures by hydro-static method, the compacted specimens are extruded from the mold, cooled to room temperature, and the dry weight recorded (a cooling period of 10 ± 1 minutes in front of a fan is necessary before extruding the specimens to ensure the specimens are not damaged).

[25] PG 64-22. The 64 is the expected high pavement temperature, and the -22 is the expected low pavement temperature that the binder will experience based on the climate where the pavement will be built.

[26] Cracking from traffic loading happens later in life and at moderate temperature. Low temperature cracking also occurs later in the pavement's life caused by exposure to very low temperature.

[27] Railway track structure design life depends on the railway type. It is longer for the railroads with major traffic to cause the least interference to the maintenance works. The design life is 50 years for the high-speed lines and 20-25 years for the ordinary lines.

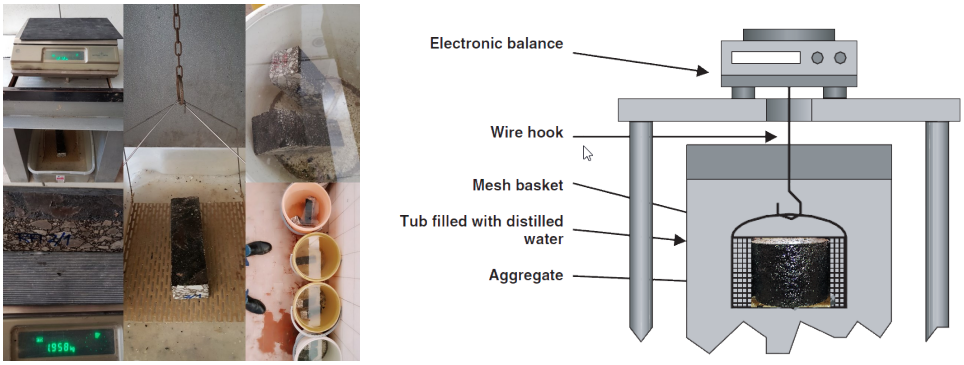


Figure 39. (a) Procedure to measure bulk specific gravity; (b) Weight-in-water apparatus

The density of the water (Mg/m^3) at the test temperature is calculated by the following formula:

$$\rho_w = 1,00025205 + \frac{7,59 \cdot T^a(^oC) - 5,32 \cdot T^{a2}}{10^6} [Mg/m^3] \quad \text{(Eq. 12)}$$

- T^a= water temperature (°C); ρ_w = water density (Mg/m^3)[28].

The bulk specific gravity of the specimen is calculated by four procedures, the choice of method to use depends on the estimated air voids in the specimen and their accessibility:

1. (A) Bulk density - dry (for samples with a very tight surface);
2. (B) Bulk dry saturated surface density (SSD), (specimens with closed surface);
3. (C) Bulk density - waterproofed specimen (for specimens with an open or rough surface);
4. (D) Apparent density by geometric method (for specimens having a natural surface).

(A) **Bulk density - dry**:

$$\rho_{bDRY} = \frac{m_1}{(m_1 - m_2)} \cdot \rho_w \quad \text{(Eq. 13)}$$

- ρ_{bDRY} is the dry bulk density, (Mg/m^3);
- m1 is the mass of the dry specimen, (gr); m2 is the mass of the specimen in water, (gr);
- ρ_w is the density of the water at the test temperature (Mg/m^3).

(B) **Bulk density - dry saturated surface (SSD) at 24h** :

$$\rho_{bSSD} = \frac{m_1}{(m_3 - m_2)} \cdot \rho_w \quad \text{(Eq. 14)}$$

- $\rho_{b_{SSD}}$ is the apparent bulk density, after 24h since the compaction (Mg/m^3);
- m1 is the mass of the dry specimen, (gr); m2 is the mass of the specimen in water, (gr);
- m3 is the mass of the specimen with dry-saturated-surface, (gr);
- ρ_w is the density of the water at the test temperature (Mg/m^3).

(C) **Bulk density - waterproofed specimen (paraffin-coated specimens):**

$$\rho_{dry} = \frac{m_1}{\left((m_2 - m_3)/\rho_w - (m_2 - m_1)/\rho_{sm}\right)} \quad \text{(Eq. 15)}$$

- ρ_{bdry} is the apparent density of the waterproofed specimen (Mg/m^3);
- m1 is the mass of the dry specimen, (gr); m2 is the mass of the specimen in water, (gr);
- m3 is the mass of the specimen with dry saturated surface, (gr);
- $\rho_w$is the density of the water at the test temperature (Mg/m^3).
- ρ_{sm} is the density of the paraffin wax at the test temperature (0.895g/cm^3).

(D_1) **Apparent density by geometric method (cylindrical-rectangular sample) [0h from compaction]**:

[28] The water density is 997,1 kg/m^3 at 25 °C. For other temperatures the water density is (997,1·K) kg/m^3 (EN 12697-5:2012).

$$\rho_{bcyl.} = \frac{m_1}{\left(\pi/4 \cdot h \cdot d^2\right)} \cdot 10^3 \; ; \; \rho_{brect.} = \frac{m_1}{\left(h \cdot l \cdot w\right)} \cdot 10^3 \qquad \text{(Eq. 16)}$$

- $\rho_{b_{dim}}$ is the geometrical bulk density, (Mg/m³);
- m1 is the mass of the dry specimen, (gr);
- H, D are the height-diameter of the cylindrical specimen, (mm);
- H, L, W are the height, length and width of the rectangular specimen, (mm).



Figure 40. (a) Vacuum pycnometer test; (b) Hydrostatic Density Meter

The *maximum specific gravity* [EN 12697:5-2009; ASTM D6925-15; AASHTO T209-12] of the specimen is calculated as follows. There are three procedures, the choice of method to use depends on the estimated air voids in the specimen and their accessibility:

(A) Volumetric procedure: maximum density of bituminous mixtures is determined from the volume of the sample without voids and from its dry mass (Fig. 40a);

(B) Hydrostatic procedure (Fig. 40b);

(C) Mathematical procedure.

(A) **Volumetric procedure**:

$$\rho_{mv} = \frac{\left(m_2 - m_1\right)}{10^6 \cdot V_p - \left(m_3 - m_2\right)/\rho_w} \qquad \text{(Eq. 17)}$$

- ρ_{mv} is the maximum density of the bituminous mixture, in (kg/m³);
- m1 is the mass of the pycnometer plus headpiece and spring, (gr);
- m2 is the mass of the pycnometer plus headpiece, spring and test sample (gr);
- m3 is the mass of the pycnometer, test sample, and water or solvent (gr);
- V_P is the volume of the pycnometer, when filled up to the reference mark (m³);
- ρ_w is the density of the water or solvent at test temperature (kg/m³).

(A) **Hydrostatic procedure**:

$$\rho_{mh} = \frac{\left(m_3 - m_1\right)}{\left(m_3 - m_1\right) - \left(m_4 - m_2\right)} \rho_w \qquad \text{(Eq. 18)}$$

- ρ_{mh} is the maximum density of the bituminous mixture, (kg/m³);
- m_1 is the mass of the container in air, (gr); m_2 is the mass of the container suspended in water, (gr);
- m_3 is the mass of the container plus test sample in air, (gr); m_4 is the m_3 suspended in water, (gr);

(A) **Mathematical procedure**:

$$\rho_{mc} = \frac{100}{\left(\frac{p_a}{\rho_{aggr}}\right) + \left(\frac{p_b}{\rho_b}\right)} \qquad \text{(Eq. 19)}$$

- ρ_{mc} is the maximum density of the mixture by calculation (kg/m³);
- p_a is the percentage of aggregate in the mixture to the nearest 0,1 % (m/m);
- ρ_{aggr} is the apparent density of the aggregate, in kg/m³;

- p_b is the percentage of binder in the mixture to the nearest 0,1 % (m/m);
- ρ_b is the density of the binder at 25 °C, in kg/m³;
- $p_a + p_b = 100{,}0$ % (m/m).

When aggregates with different densities are used, calculate the maximum density as follows:

$$\rho_{mc} = \frac{100}{\left(\frac{\%a_1}{\rho_{a1}}\right) + \left(\frac{\%a_2}{\rho_{a2}}\right) + \ldots + \left(\frac{\%b}{\rho_b}\right)} \qquad \text{(Eq. 20)}$$

- ρ_{mc} is the maximum density of the mixture (kg/m³);
- $p_{a1,2,\ldots}$ is the apparent density of aggregate 1,2,…,(kg/m³).

4.9.8. Air voids, V_a

"Air voids," when applied to asphalt concrete, means small pockets of air that exist within the asphalt binder and between aggregate particles. Air void content does not include pockets of air within individual aggregate particles, or air contained in microscopic surface voids or capillaries on the surface of the aggregate. Figure 41a shows the different ways in which air exists in asphalt mixtures.

When air void contents are too high, the pavement may be too permeable to air and water, resulting in significant moisture damage and rapid age hardening. When air void contents are too low, the asphalt binder content may be too high, resulting in a mixture prone to rutting and shoving.

In the Superpave method of designing HMA, the air void content (Va) in laboratory mix-design is held constant at 4.0%. Some agencies have, however, expanded the allowable range for air void content to 3.0-5.0%, which was the design range used in the Marshall mix design method.

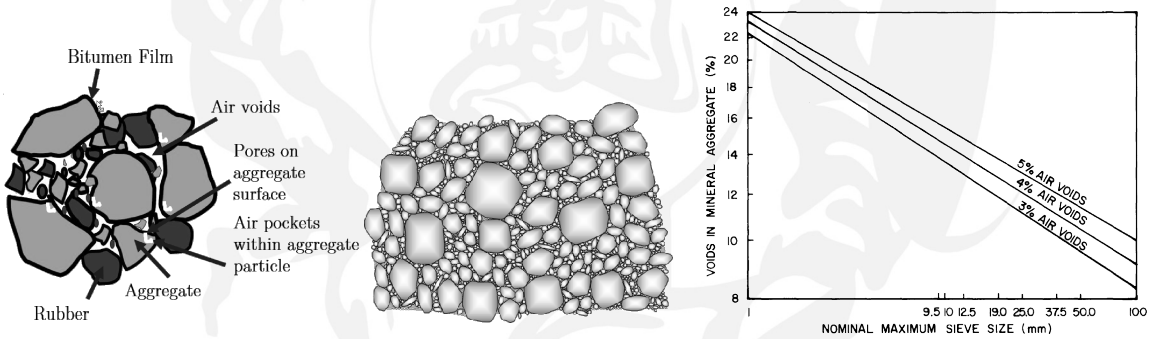


Figure 41. (a)Air in asphalt concrete[29]; (b) Dense-graded mixture; (c) VMA_NMAS relationship

In dense-graded bituminous sub-ballast, the quantity of bitumen is increased of 0.5% compared to the base course, and Va decreased to 1-3% to avoid the permeability of the layer [EN 12697:8-03].

Once the bulk specific gravity and maximum specific gravity of the asphalt mixture have been determined, the %Va is calculated as follows [AASHTO R35-12]:

$$V_a = 100 \cdot \left(\frac{\Gamma_{mm} - \Gamma_{mb}}{\Gamma_{mm}} \right) \qquad \text{(Eq. 21)}$$

- Γ_{mm} is the Maximum Specific Gravity of asphalt mixture; Γ_{mb} is the Bulk Density of asphalt mixture.

According to another formulation [C.N.R.-B.U. n. 39 (23/3/73)], the %Va is determined as:

[29] Air can exist in pores on the aggregate surface, pockets within aggregate particles, or voids within the asphalt binder or between the binder and aggregate particles. Only the last type of air is included in the air void content of asphalt concrete mixtures.

$$V_a = 1 - \frac{\gamma_{app}}{1 + \frac{b}{100}} \left(\frac{1}{\gamma_i} + \frac{\frac{b}{100}}{\gamma_b} \right) \quad [\%] \qquad \text{(Eq. 22)}$$

- γ_{app} is the bulk density of the sample, (kg/m³); γ_i is the density of the aggregates, (±2808kg/m³);
- γ_b is the density of the bitumen, (±1033kg/m³); b is the percentage of binder content in the mixture (%).

4.9.9. Voids in the Mineral Aggregates, VMA

Voids in the mineral aggregate (VMA) are the void spaces that exist between the aggregate particles in the compacted paving asphalt mixture, including the space filled with the binder. VMA represents the space that is available to accommodate the effective volume of binder (i.e., all of the binder except the portion lost by absorption into the aggregate) and the volume of air voids necessary in the asphalt mixture [Kandhal, P., Foo, K., & Mallick, R. 1998]. The more VMA in the dry aggregate, the more space is available for the binder. Since a thick binder film on the aggregate particles results in a more durable asphalt mixture, specific minimum requirements for VMA are recommended and specified as a function of the aggregate size (Fig. 41b).

Minimum VMA values are required so that a durable binder film thickness may be achieved. Increasing the density of the asphalt mixture by changing the gradation of the aggregate may result in minimum VMA values with thin films of binder and a dry looking, low durability asphalt mixture.

The voids in the mineral aggregate (VMA) is determined by bulk specific gravity of the aggregate as a percentage of the bulk volume of the compacted mix as follows:

$$VMA = 100 - \left(\frac{G_{mb} \cdot P_s}{G_{sb}} \right) = V_a + V_{be} \rightarrow P_s = 100 - P_b \qquad \text{(Eq. 23)}$$

- G_{sb} is the Bulk Specific Gravity of aggregate; G_{mb} is the Bulk Specific Gravity of asphalt mixture;
- P_s is the aggregate, percent by total weight of asphalt mixture;
- V_a is the air voids percent; V_{be} is the effective binder percent;
- P_b = Total asphalt binder content, % by mix mass.

Table 30 and Fig. 41c shows guidance values of %VMA based on NMAS [Cooley, L.A. et al. 2002].

TABLE 30. VOIDS IN MINERAL AGGREGATE CRITERIA

Nominal maximum size (NMAS)	Minimum voids in the mineral aggregate, VMA (%)
12.5mm	14.0
19.0mm	13.0
25.0mm	12.0
37.5mm	11.0

4.9.10. Voids Filled with Asphalt, VFA

Voids filled with asphalt (VFA) are the void spaces that exist between the aggregate particles in the compacted paving asphalt mixture that are filled with binder. Including the VFA requirement in a mix-design helps prevent the design of asphalt mixture with acceptable VMA.

The main effect of the VFA is to limit maximum levels of VMA and subsequently maximum levels of binder content. The VFA is the percentage of the VMA that contains binder (Table 31, Eq. 24):

$$VFA = \left(\frac{VMA - V_a}{VMA} \right) \cdot 100 \leftrightarrow VFA = 100 \cdot \left(\frac{V_{be}}{VMA} \right) \quad [\%] \qquad \text{(Eq. 24)}$$

TABLE 31. SAMPLE VOLUMETRIC DESIGN DATA AT NDES (HMA MIXTURE B50/70) [AASHTO R35]

Pb(%)	Va(%)	VMA(%)	VFA(%)	Density (kg/m³)
4.3	9.5	15.9	40.3	2320
4.8	7.0	14.7	52.4	2366
5.3	6.0	14.9	59.5	2372
5.8	3.7	13.9	73.5	2412

Acceptable values for increasing traffic are shown in Table 32 [SHRP-A407, 1994]

TABLE 32. VOIDS FILLED WITH ASPHALT CRITERIA (VFA VS. ESAL)

Traffic levels (ESALs)	Design VFA (%)
$<3\cdot10^5$	70-80
$<3\cdot10^6$	65-78
$<1\cdot10^8$	65-75

4.9.11. Effective Binder content, V_{be}

Effective binder content[30] is the volume of the binder not absorbed by the aggregate, i.e., the amount of binder that effectively forms a bonding film on the aggregate surfaces.

V_{be} is calculated based on the aggregate bulk specific gravity (G_{sb}) and the aggregate effective specific gravity (G_{se}). The higher the aggregate absorption, the higher the difference between G_{se} and G_{sb}. First, calculate the overall aggregate bulk specific gravity:

$$G_{sb}=\frac{P_{s1}+P_{s2}+P_3+\ldots}{\left(\frac{P_{s1}}{G_{sb1}}\right)+\left(\frac{P_{s2}}{G_{sb2}}\right)+\left(\frac{P_{s3}}{G_{sb3}}\right)+\ldots} \quad \text{(Eq. 25)}$$

- G_{sb} = overall bulk specific gravity for aggregate blend
- $P_{s1\ldots}$ = volume % of aggregate 1,2,3… in aggregate blend
- $G_{sb1\ldots}$ = bulk specific gravity for aggregate 1,2,3…;

$$P_b=100\left(\frac{M_b}{M_s+M_b}\right)\rightarrow V_b=\frac{P_b\cdot G_{mb}}{G_b} \quad \text{(Eq. 26)}$$

- P_b = Total asphalt binder content, % by mix *mass*;
- M_b= Mass of binder in the specimen; M_s= Mass of aggregate in the specimen;
- V_b = Total asphalt binder content, % by total mix *volume*;
- G_{mb} = Bulk specific gravity of the mixture; G_b = Specific gravity of the asphalt binder.

The absorbed asphalt binder content by volume as a percentage of total mix volume:

$$VBA=G_{mb}\cdot\left[\left(\frac{P_b}{G_b}\right)+\left(\frac{P_s}{G_{sb}}\right)-\left(\frac{100}{G_{mm}}\right)\right] \quad \text{(Eq. 27)}$$

- VBA = Absorbed asphalt content, % by total mixture volume;
- P_s = Total aggregate content, % by mix mass;
- G_{mm} = Maximum specific gravity of the mixture.

The effective asphalt by volume is found:

$$V_{be}=V_b-VBA\rightarrow P_{be}=P_b\left(\frac{V_{be}}{V_b}\right) \quad \text{(Eq. 28)}$$

- V_{be} = Effective asphalt content, % by total mixture volume;
- V_b = Total asphalt binder content, % by mixture volume;
- P_{be} = Effective asphalt binder content, % by total mass.

[30] Effective binder content should not be confused with the extracted binder content of the asphalt mixture. The effective binder content is a theoretical value and the extracted binder content is an actual test value obtained with an ignition oven or vacuum extractor.

4.9.12. Laboratory protocol of execution

Analysis of specimens and the maximum specific gravity sample were conducted to evaluate such properties as voids in mineral aggregate (VMA); voids filled with asphalt (VFA), air voids, and the dust/effective binder ratio, for determining the optimum binder content required to produce the three percent air voids at N_{des} gyrations (in railways Va±3%).

- **Manufacture of HMA mixture.**

The blended aggregate specimens and asphalt binder were placed in an oven and bring to the required mixing temperature. Heat the mixing container and all necessary mixing implements to 150-160ºC. Commonly, 4500 to 4700 gr of aggregate are required to achieve the height-sample desired for bulk specific gravities of 2.55-2.70 g/cm^3. The homogeneity of SGC samples depends on the equilibrium between granulometry (NMAS) and N_{des} (example in Fig. 42). After completing the mixing process, the mix was subjected to appropriate conditioning, removing the mix every 60±5 min to maintain consistent conditioning. At the end of the compaction process, it was removed the mold assembly from the SGC. After a suitable cooling period, the compacted specimen was extruded on a flat surface to room temperature.

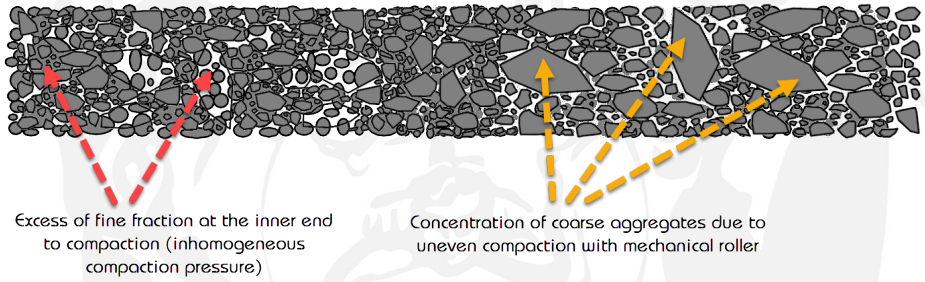


Figure 42. Graphic design of an inhomogeneously compacted mixture

In Figure 43 the work plan of the SGC procedure is developed showing the steps that must be followed for correct execution of the asphalt mixtures.

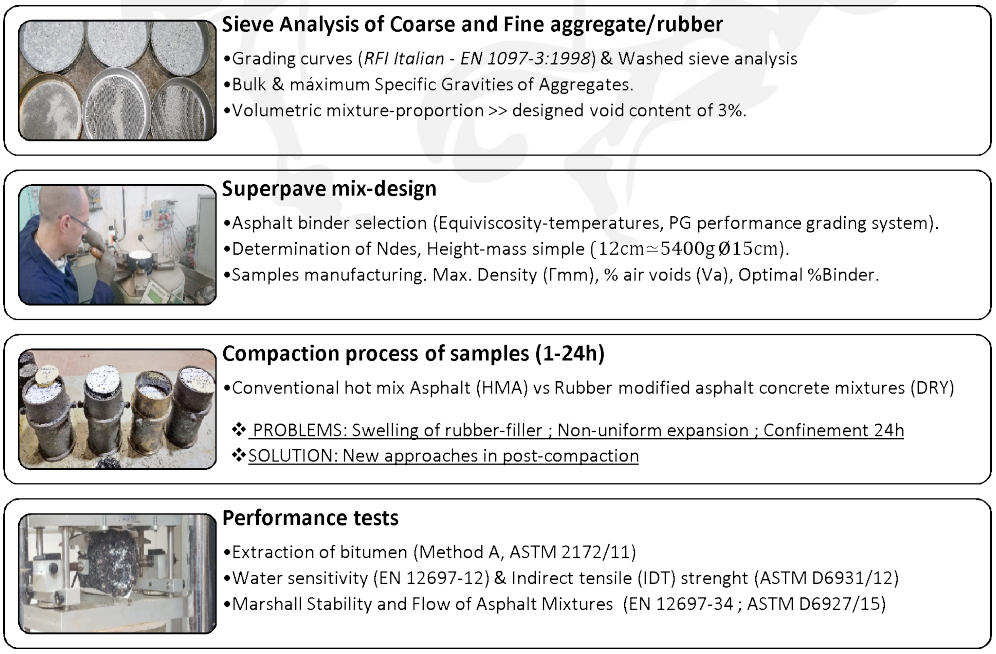


Figure 43. Construction procedures of HMA – DRY mixtures (Protocol)

In Figure 44, based on experience observed in the laboratory, an operational framework is proposed as a new protocol for the optimal procedure with rubber-aggregate modified asphalt mixtures.

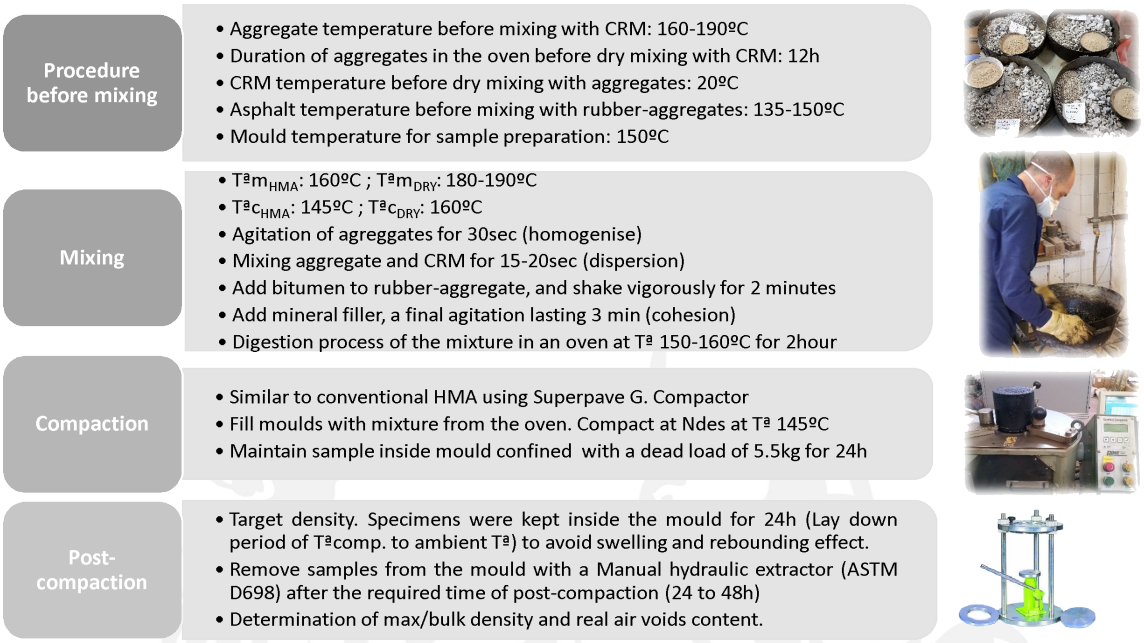


Figure 44. The operational framework for RUMAC (Dry) mixtures

- **Manufacture of the DRY mixture.**

The blended aggregate specimens and asphalt binder were placed in an oven and bring to the required mixing temperature (160-190ºC). The bituminous mixtures were then measured in the laboratory according to EN 12697-35; AASHTO T166 (Figure 45). Because of NMAS of aggregate was greater than Ø16 mm, the test pieces have been of ±Ø150 mm.



Figure 45. (a) Samples extruded from the SGC; (b) Specimens after 24h; (c) Bulk specific gravity in water

The following operations must be performed (Fig. 46):

- The supplementary plates must be kept for at least 2 hours within an enclosure which is at test temperature 145 ± 10 ° C;
- The molds are lubricated with a film of *glycerine-based soda oleate grease* or silicone oil;
- The frame and the insert plates are weighed, the mold is filled with the mixture using a funnel, and the mold is again considered with the mixture and the insert plates, to obtain the prescribed mass M of the bituminous mixture with an accuracy of 0.1%.
- Each specimen was compacted to the maximum number of gyrations. During compaction, the height of the specimen was continually monitored. The digestion temperature was fixed at 165ºC for variable times of 45, 90 and 120 min.

- During the manufacture of the CRM mixes, the temperature of the blend was increased to 180ºC to facilitate the interaction between the rubber and the bitumen, thus improving the cohesion of the mastic. This process was carefully monitored since the rubber particles could burn at temperatures higher than 190ºC. Moreover, temperatures higher than 195ºC would have led to an aging of the bitumen, which would have had a negative impact on the performance of the mix. A 10-second agitation of the natural aggregates in the mineral skeleton is needed to homogenize them better.



Figure 46. (a) SGC model AFG1; (b) Sample molds of dimensions ϕ150x250mm; (c) Mixing process of aggregates, bitumen, and filler; (d) Control of temperature and digestion time

Based on past research it was possible to identify various standards for the preparation of CRM mixes using dry process. Table 33 summarises the specifications adopted in the laboratory according to the design outlined by trial mixtures developed during this research [Soto, F. M. et al. 2017].

TABLE 33. SPECIFICATIONS FOR THE PREPARATION OF RUBBER MODIFIED ASPHALT MIXTURES

Procedures recommended	Indications	Details
Aggregate Tª before mixing with CRM	177 to 218°C	Higher aggregate temperature is said to ensure better reaction between asphalt and CRM.
Duration of aggregates in the oven before mixing with rubber	12h-24h	Aggregates will be placed in the oven for at least 12 hours before mixing.
CRM Tª before dry mixing with aggregates	Ambient Tª	CRM is maintained at room temperature will be mixed with hot aggregates.
Asphalt Tª before mixing with aggregates and CRM	135-150ºC	Asphalt will be maintained around to 150°C before mixing it with the aggregates-CRM blend.
Mould Tª for sample preparation	135ºC-150ºC	The mold temperature must comparable with the mix temperature to prevent the mix from cooling quickly.
Duration of mixing aggregate and CRM	15-20 sec	15 seconds of mixing previously
Duration of mixing aggregate and CRM with asphalt	3 minutes	Intimate mixing and mixing temperature of 135°C and above is essential.
Tª of mixing all blend	180-190ºC	During the last minutes, the mixture achieves the high temperature
Tª of compaction and hot molds	160ºC	SGC is maintained inside at 149 to 160°C
Mould treatment before adding the mix	Coat the inside of the Mould with grease	Grease is used to coat the inner side of the mold for ease in removing the sample.
Curing	160°C, 191°C, no curing	Digestion time between 60-120 min at 150ºC. 1h curing period at 160°C is recommended for PlusRide mixes.
Sample extrusion	Confinement in a mould with a dead load of 5.5kg by 24h	24 hours or min. overnight is recommended
Extraction method	Hydraulic extractor	A 5 Ton capacity hand operated, hydraulic jack mounted on a suitable frame. One plunger of mold Φ150 mm is used.

4.9.13. Densification curves [%Γmm-LogN]

A densification curve is a plot for each mixture that represents the measured relative density at N_{des} or N_{max} cycles (%Γmm) versus the logarithm of the number of gyrations. Each trend line is reported using the equation:

$$\Gamma_{mm} = \frac{\Gamma^*_{N_{des}}}{\Gamma_{\max}} \quad [\%] \quad \Leftrightarrow \quad \Gamma_{mm}(N) = \Gamma_1 + k \cdot LogN \quad [\%] \qquad \text{(Eq. 29)}$$

- Γ_{mm} is the averaged corrected specimen relative density at N_{des} (%);
- Γ_1 is the relative specific density of energy accumulated during the compaction, as an experimental factor of the trend line, decreases when increases k (%);
- k is the workability of the mixture (-).

The fundamental parameter used to characterize the volumetric variations is the relative specific weight Γ_{mm}, equal to the ratio between the specific weight of the mixture in correspondence with the number of rotations Γ_{Ndes}, and the maximum specific weight of the mixture Γ_{max} in the absence of its void volume.At the completion of compaction process, the relative density at N gyrations of interest is determined using the above equation based on the back calculation:

$$\Gamma_{mb} = \Gamma_{mbfinal} \cdot \left(\frac{h_{final}}{h_x} \right) \rightarrow \%\Gamma_{mm} = \left(\frac{\Gamma_{mb}}{\Gamma_{mm}} \right) \cdot 100 \qquad \text{(Eq. 30)}$$

- Γ_{mbx} = bulk specific gravity of the extruded specimen, at any gyration, x;
- Γ_{mm} = maximum theoretical specific gravity of the mixture;
- h_{final} = height of the specimen recorded at the final gyration, mm;
- h_x = height of the specimen recorded at any gyration, x, during the compaction process, mm; and
- $\Gamma_{mbfinal}$ = bulk specific gravity of the extruded specimen at the final gyration.

With %Va values found for each binder content, the densification curves and the diagram %b-Va are constructed as follows (Fig. 47):

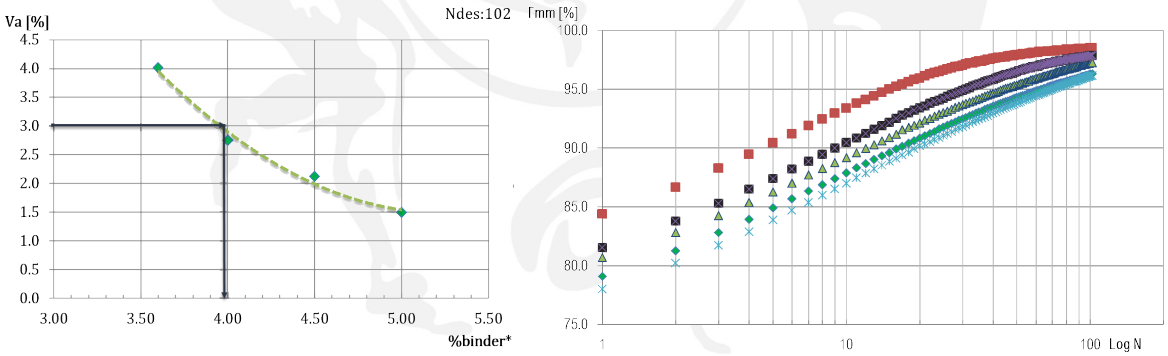


Figure 47. (a) Optimal binder determination [Va-%b*]; (b) Densification curves

4.9.14. Quantitative extraction of Asphalt Binder

This method covers the quantitative determination of asphalt cement in a bituminous mixture. The bitumen is extracted with trichloroethylene or methylene chloride solvent (Reagent grade chemical or grade of sufficiently high purity to permit use without lessening the accuracy of the determination). The bitumen content has been determined by two methods, by extraction with a centrifuge and with ignition furnace (Fig. 48).

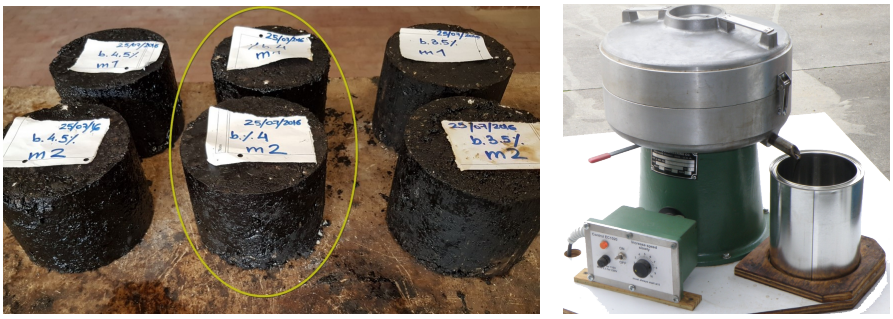


Figure 48. (a) Samples for extraction of bitumen (b.4%, Va.2%); (b) Centrifuge extractor with ignition furnace

The extracted aggregate was washed to remove fines smaller than 75 µm and the remaining aggregate was used for sieve analysis. The method involves the previous heating at 110°C of the sample to achieve sufficient workability. After the extraction of the bitumen, a new sieve analysis was done to determine the grading curve. After weighing the samples obtained and performed the calculations according to the standards codes [AASHTO T164-14; ASTM D2172-11; Qasim, Z.I., et al. 2017], it was observed that the resulting material had excess mineral filler, which produced an effect of empty closing air voids. After this test, the grading curve was adjusted, and SGC new samples were made.

4.10. Methodology 02: "Marshall mix-design"

4.10.1. Comparison SGC with Marshall methodology

The Marshall method gives optimal for stability related to stiffness and durability [ASTM D6297]. There is no measure of fatigue resistance. It is unlikely that an adhesion problem would occur at 60ºC (Fig. 49). In short, the Marshall method is a practical way of choosing the most suitable binder content, but on its own, it does not ensure adequate performance in the pavement [Zumrawi, M. 2016; Hafez, I. et al. 1994]. In Superpave, the additional checks at the end are to ensure that compaction does not occur too readily, and that void content will never fall below 2%, even under heavy traffic [Swami, B.L. et al. 2004; Buchanan M. et al. 2001]. During the development of experimental activities on laboratory, the conventional mixes HMA were developed with Superpave in samples of Ø100x · 63±2mm; then, the same mixtures were made with Marshall hammer at 75-blow obtaining cylindrical samples compacted with sizes of Ø100 · 65±5mm.

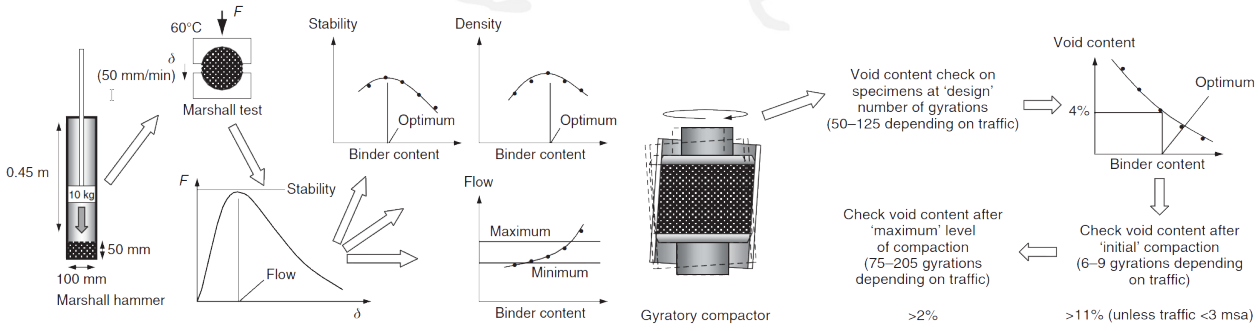


Figure 49. The Marshall and Superpave mix-design procedures (Adapted from Thom, N., 2008).

The Marshall method uses several trial aggregate-asphalt binder blends, each with a different bitumen content. Then, by evaluating each trial blend's performance, an optimum asphalt binder

content can be selected. The specimens were prepared [NLT-159/00], placed in a preheated mold and compacted with 75-blows on each side by a Marshall hammer to obtain specimens of ±60 mm in height and Ø101,6 mm. Then, the specimens were immersed in water at a temperature of 60 °C for 50±5 min. The Marshall test was also conducted to determine the percentage of voids in the mixes, along with the bulk density, deformation, and stability for the mixtures [EN 12697-34:2012] (Fig. 50).



Figure 50. Density-Voids and Volume Relationships of a Compacted Asphalt Sample.

4.10.2. Performance test: Water Sensitivity (ITSR)

Moisture damage is a complex phenomenon that involves thermodynamic, chemical, physical and mechanical processes [Sangiorgi, C. et al. 2017; Caro, S. et al. 2008]. EN12697-23:2017 describes the method for determining the effect of saturation and accelerated water conditioning on the indirect tensile strength of cylindrical specimens of bituminous mixtures [Ghazi G. et al. 2014] (Fig. 51).

The evaluation of water sensitivity is necessary because this property is directly related to the performance and durability of mixtures during the life of the layer. The characterization of water sensitivity of bituminous mixtures was performed according to standard EN 12697-12:2009.



Figure 51. (a) IDT device; (b) Superpave-Marshall specimens for IDT and water sensitivity tests.

For this test, six cylindrical specimens of the Marshall type were manufactured and compacted with 75 blows on each side. Specimens had a Ø101.6 to Ø150mm and heights from 63 to 75 mm[31]. Then the specimens were divided into two groups of three and conditioned. One subset of specimens was saturated (wet specimens) and sorted for 67-72h of immersion in a thermostatic bath at 40°C (Fig. 52a), and on a second set was maintained dry at 15°C. However, the standard indicates that the specimens are previously subjected to vacuum in water at 20°C and kept for 30 minutes under an

[31] Specimens—Cores should have smooth, parallel surfaces and conform to the height and diameter requirements specified for laboratory-molded specimens, except that a minimum height of 38 mm is permitted for specimens with a nominal diameter of 101.6 mm.

absolute pressure of 6,7 KPa (Fig. 52b). The damage caused by the immersion in water is expressed by the tensile strength ratio (ITSR), according to the formula:

$$ITSR = 100 \cdot \frac{ITS_W}{ITS_D} \quad \text{(Eq. 31)}$$

- ITSR is the indirect tensile strength ratio, in percent (%);
- ITSw is the average indirect tensile strength of the wet group, expressed in kilopascal (kPa);
- ITSd is the average indirect tensile strength of the dry group, expressed in kilopascal (kPa).

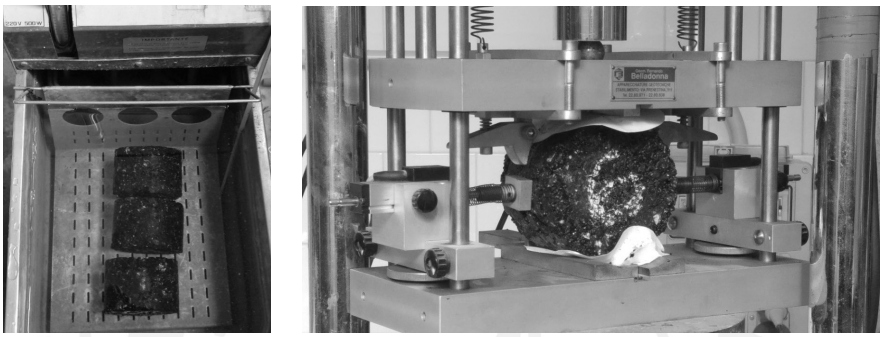


Figure 52. (a) Wet specimens; (b) Indirect Tensile strength test [EN 12697-23].

The ratio of the indirect tensile strength of the water conditioned subset compared to that of the dry subset was determined. The coefficient of indirect tensile stress (CTI) according to:

$$\mathrm{CTI} = \frac{\pi \cdot \mathrm{D} \cdot \mathrm{ITS}}{2 \cdot \delta_{\mathrm{C}}} \quad \text{(Eq. 32)}$$

- ITS = Indirect traction resistance expressed in N/mm²;
- D = sample diameter expressed in mm
- δ_{C} = breakage compression displacement expressed in mm (%);

As part of the test, three test cylinders were subjected to compressive loads between two loading strips (with a width of 12.7 mm) at a constant velocity of 50±2 mm/min (Fig. 53a). This load produced a relatively uniform tensile stress along the vertical diametric plane (Fig. 53b).

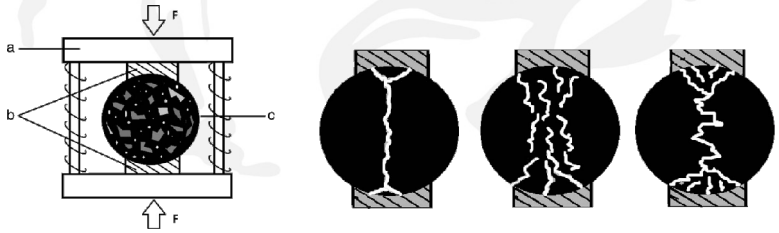


Figure 53. (a) Test frame; (b) Type of failure on ITS specimens [ASTM D6931].

The peak load at failure is recorded and used to calculate the IDT strength of the specimen. The indirect tensile strength was determined using the equation:

$$ITS = \frac{2P}{\pi \cdot D \cdot H} \quad \text{(Eq. 33)}$$

- ITS = indirect tensile strength expressed in gigapascals;
- P = breaking load (N) of the specimens under diametral compression; and
- D, H= average values of the diameter and height respectively of the specimen, mm.

4.11. Methodology 03: "Asphalt Slab Roller Compactor"

4.11.1. Equipment for Roller Compacted slabs

The Asphalt Slab Roller Compactor (ASRC)[32] [ASTM C1800M-16; ACI-325:2001; Williams, S. 2013] used in this research is a standard version that can be used for cut into beams for bending fatigue tests. The roller head freely moves by pure friction for better compaction uniformity. The vertical load should be measured and controlled to an accuracy of ±5 % of the applied load. The loading system used to achieve the required load is hydraulic, which is applied orthogonally to the axis of the travel motion with a maximum load of 350 kN/m^2 (35 kPa or 3.5 bar as pressure) [EN 12697-33:2013]. Roller compacted concrete (RCC) requires no formwork, surface finishing, dowelled joints or reinforcement. These characteristics make RCC simple, fast to construct, and high load carrying ability, early strength gain, durable and low maintenance [Bauchkar, S. et al. 2012; Brotman, I. et al. 2007; Adaska, W.S. 2006; A. Terry, 2004].

This method of test specimens requires a particular compaction procedure in predicting the performance of the material later on-site [Mohammed, H.A: et al. 2018; Muniandy, R. et al. 2008]. Roller compactor of slabs allows reproducing the actual conditions of compaction in the real field. Different studies have indicated that roller slabs compactor, which simulates real properties, is closer to field compaction [Khan, Z.A. et al. 1998; Consuerga A. et al. 1992]. The main difference between SGC and the ASRC is the difference of pressures exerted by both, while SGC is based on a constant pressure of 600 kPa, the RCC slab resulted is applied by four different pressures with different passes each one according to the type of mixture used (Fig. 54).

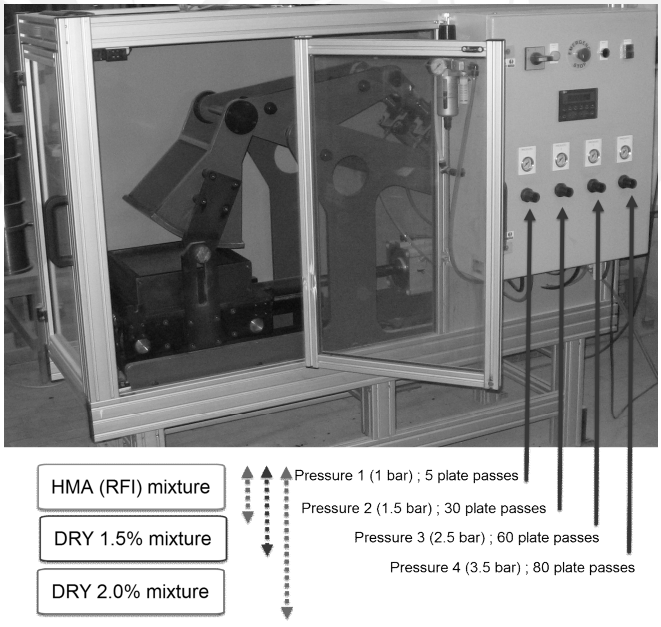


Figure 54. Asphalt slab roller compactor pressures per mixture

[32] A sample of loose asphalt mix is compacted in an automatic apparatus by the combination of vertical displacements of a segmented rolling compactor foot and horizontal movements of a rolling compactor foot relative to the compactor tray to produce a slab of compacted asphalt with a target theoretical density (that is, based on the geometric volume of the specimen).

Asphalt slabs compacted with the rolling compactor can be used to obtain specimens for further testing, including bulk specific gravity following Test Methods D1188, D2726, and D6752, fatigue performance characteristics following Test Method D7460 or AASHTO T 321, and Hamburg wheel-track testing following AASHTO T 324.

The roller performs passes at constant velocity applying different four pressures each time and changing the number of passes. The ASRC can compact asphalt slabs to a target density applying specific loads corresponding to those of pavements rollers used in the highway construction. The advantage of this method is the possibility of performing the compaction process simulating the maximum achievable field densities, while also maximizing the layer quality [Sobolev, K. et al. 2015].

A given mass of bituminous HMA or DRY blend was compacted in a rectangular mold under a direct load applied by a smooth steel roller running (Fig. 55).

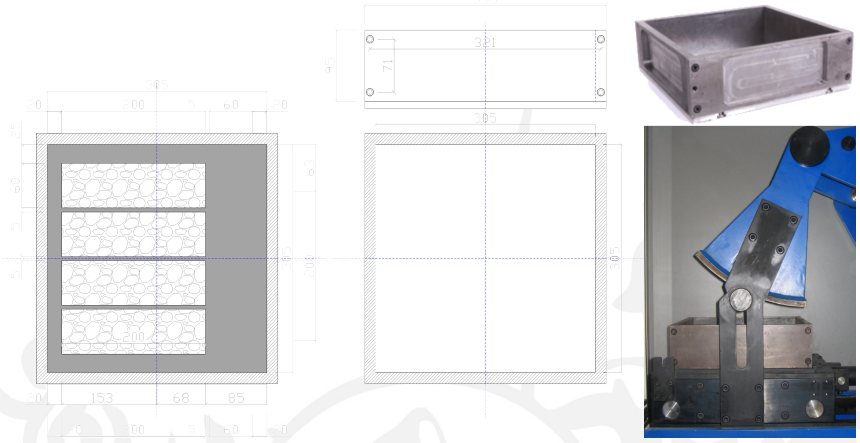


Figure 55. Asphalt roller compactor and slab mold design details

4.11.2. Sample production. Types of mixtures.

The properties of the materials used are similar to those utilized in the manufacture of cylindrical specimens for gyratory compaction. For each slab, it was possible to obtain four prismatic beams of 20x6x6cm. Nine slabs were made (3 for each mix) obtaining 12 specimens of $200 \cdot 200 \cdot 60$mm for the fatigue tests.

The blends designed to be compacted with mechanical roller were:

- An HMA (RFI) with 4% of binder content, called conventionally reference bituminous blend designed in three slabs: **HMA b.*4% and Va*3%;**
- A DRY 1.5% (binder* 5.5%) with other three slabs (mixing temperature, compaction and digestion time equals): **DRY 1.5% #60_40 b. 5.0% and b.5.5% and Va*3%;**
- A DRY 2% (binder* 6%): **DRY 2.0% #60_40 b.6.0% and b.6.5% and Va*3%.**

Dry mixes according to the protocol suggested in section 4.5.12. For a mix of a binder content 3%, in the following tables are shown the different mixtures and lab-recipes used (Table 34):

TABLE 34. VOLUMETRIC ANALYSIS OF RCC RECIPES FOR LABORATORY

Sample	H [mm]	Mass Aggreg. [gr]	Binder [%]	Theor. Mass [gr]	Binder mass [gr]	LAB Aggreg. Mass [gr]	Binder mass [gr]	Filler [gr]	Sand [gr]	fØ5-10mm [gr]	fØ10-15mm [gr]	fØ20-25mm [gr]	fØ25-30mm [gr]	CRM 60% Ø0.4-2 [gr]	CRM 40% Ø2-4 [gr]
HMA	60	13818	4.0	14371	552.74	13800	552	1605.8	3478.3	719.1	2524.3	2551.9	2920.6	-	-
DRY1.5	60	13226	5.5	13954	727.4	13526	744	1602.3	3298.5	624.8	2567.0	2522.1	2911.3	130.4	86.9
DRY1.5	60	13072	6.0	13856	784.3	13071	784	1548.4	3187.6	603.8	2480.7	2437.3	2813.5	126.6	84.4
DRY2	60	13072	6.0	13856	784.3	13272	796	1581.7	3199.5	586.2	2549.7	2481.6	2872.9	172.3	114.8
DRY2	60	12920	6.5	13760	839.8	12921	840	1539.9	3114.9	570.7	2482.3	2416.0	2796.9	168.5	112.3

Roller compactor was used to achieve the height of 60mm needed for the fatigue cracking tests. For asphalt mixes, weights between 10-15 kg have been used to make the slabs. All samples were removed from the mold after 24-36 hours of casting then left at 20ºC before testing. Then, each slab was

removed after seven days to observe the ultimate swelling effect in mixtures with rubber. The material available for fatigue testing was obtained from quadrangular beams after cutting every single slab of dimensions 300.5 · 300.5 · ±60 mm for HMA, DRY1.5%, and DRY2.0% blends (Fig. 56).



Figure 56. Manufacturer of slabs by a roller compactor, unmold and cut into prisms

The manufacturing process of the RCC slabs was identical to the manual manufacture of the blends using gyratory compactor (SGC):

- Once the mixture is ready, the entire contents of the HMA or DRY mixture are poured into a larger empty vessel, which has previously been conditioned at a temperature of 160 °C. The mixture is introduced into the oven for 90min (digestion time and reaction recycled rubber-bitumen). The mixture is then extracted and poured entirely into the mold prepared for the roller compactor, filling the voids and distributing the mixture homogeneously. With a scoop, place 1.0 to 2.0 kg of the mix in small mounds evenly spaced throughout the mold to reduce segregation and to prevent low and high-density areas.
- Due to the coarse granulometry of the mix, before the introduction of the mold into the compactor, it is vibrated for 15 seconds on a compacting vibrating table. Once all the mix has been placed, it must be spread the surface of the mix such that it is approximately level with a spatula or tine rake. Then, the mold is sliced into the roller compactor and locked to the frame. When the required vertical load or displacement is applied to the sample, compaction takes place until the selected criteria (sample height, nº cycles, or target density) are achieved.

According to EN 12697:33, the mass, M, of the blend to be introduced into the mold is a function of the maximum density of the bituminous mixture:

$$M = 10^{-6} \cdot L \cdot l \cdot e \cdot \rho_{mc} \cdot \left(\frac{100 - \%Va}{100} \right) \quad \text{(Eq. 34)}$$

- M is the mass of slab, in kilograms (kg); L is the interior length of mold, in millimeters (mm);
- l is the interior width of mold, (mm); e is the final thickness of the slab, (mm);
- ρm is the maximum density, (kg/m³); %Va is the voids content in the slab, in percent (%).

4.12. Methodology 04: "Fatigue cracking resistance."

4.12.1. Equipment: UGR_FACT

The UGR-FACT[33] method [Moreno, 2013; Moreno et al., 2013; Moreno et al., 2014-2016] was used in the present study, as it simulates the conditions that lead to the appearance of fatigue cracking in bituminous materials [Andersson, A. et al. 2015; Carpenter, S. 2006; D'Andrea, N. 2003; Baburamani, P. 1999; Bonnaure, F. 1980], using a specimen glued to two sliding supports that induce flexion, tensile and shear efforts [Moreno, F. et al. 2016] (Fig. 57).

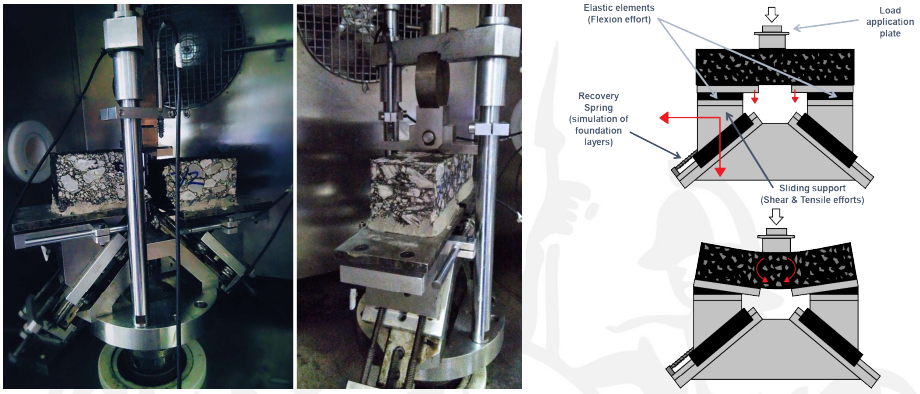


Figure 57. (a) UGR-FACT test device; (b) Stress simulation in a test specimen

Using versine cyclical loads, the device can generate and propagate a controlled fatigue cracking process, and its evolution is studied through the dissipated energy [Carpenter et al. 2003; Fatemi, A. 1998] in a representative volume where the phenomenon takes place, avoiding its random dispersion.

The test is performed at a controlled temperature inside a climate chamber by applying stress-controlled, vertical cyclic loading in versed sine. The test ends when the macro-crack propagates throughout the entire specimen (represented by failure cycle, N_f) causing its failure by fracturing it into two sections. During each loading cycle, besides the load applied, the device records horizontal and vertical deformations on both sides of the test specimen (to obtain the mean deformation value of the representative volume studied). These deformations occur near the stressed zone where the crack will develop (Figure 58).

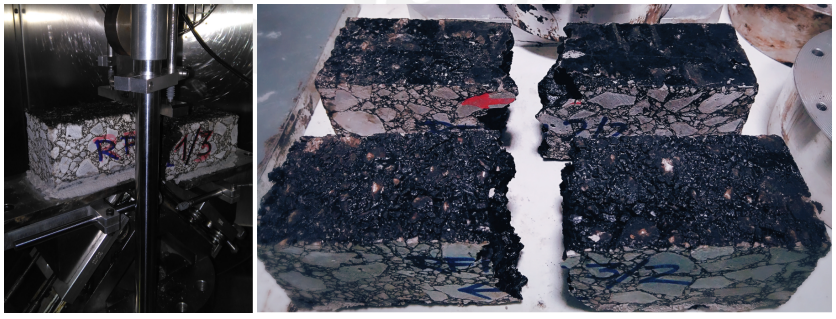


Figure 58. UGR_FACT device with a broken sample of the HMA mixture developed

Based on the values recorded, it is possible to determine the energy dissipated by the material in the volume studied, which leads to a more precise evaluation of the evolution of the damage produced by the cracking process (controlling its randomness and three-dimensional distribution).

[33] UGR_FACT device developed by the University of Civil Engineering in Granada at the Laboratory of Construction (LabIC), in Spain.

4.12.2. Test conditions of the UGR_FACT Test Method

The test conditions used to evaluate mix performance were load amplitude, frequency, and temperature [Maggiore, C. et al. 2012; Di Benedetto, H. et al. 2011; Ghuzlan, K. 2001]. Based on these considerations, each test was carried out at a constant temperature of 20ºC, a frequency of 5 Hz (high-speed trains), and three load amplitudes of 0.6, 0.8, and 1.0 kN over the specimens (200 mm in length, 60 mm in width, and 60 mm in height) of bituminous sub-ballast [Moreno-Navarro, F. et al. 2013]. In this sense, the analysis of the fatigue cracking resistance of the bituminous mixtures at 20 ºC could show the real influence of the use of crumb-ground rubber [H. Wang, et al. 2013].

The results are expressed regarding dissipated energy [Rowe, G. 1996], and the damage produced in the specimen is quantified considering that only the difference of dissipated energy from one cycle to another causes degradation in the material[34]. To provide a parameter that could be used to measure the relative damage evolution of the specimens tested (Eq. 35), the cumulative RDEC (Ratio of Dissipated Energy Change) was used to analyze the evolution of crack damage in the mixture.

$$\gamma = \frac{\sum_{i=1}^{N_f} RDEC}{N_f} = \frac{\sum_{i=1}^{N_f} \frac{\omega_{i+1} - \omega_i}{\omega_i}}{N_f} \qquad \text{(Eq. 35)}$$

- Nf is the cycle in which the macro-crack appeared at the bottom of the sub-ballast layer.

The Mean Damage Parameter (γ) was also defined to establish a quantitative reference for the resistance to fatigue cracking of the material under the conditions tested. The damage usually grows exponentially with the load. RD_n is the amount of relative damage accumulated up to n-cycle; ωi is the energy dissipation produced in loading cycle "i" (in J/m³); ωi+1 is the energy dissipation in loading cycle i+1 (in J/m³). The RD_n and RDEC are calculated as follows:

$$RD_n = \frac{\sum_{i=1}^{n} \frac{\omega_{i+1} - \omega_i}{\omega_i}}{\sum_{i=1}^{N_f} \frac{\omega_{i+1} - \omega_i}{\omega_i}} \quad ; \quad RDEC_{N+1} = \left(\omega_{n+1} - \omega_n\right) \Big/ \omega_n \qquad \text{(Eq. 36)}$$

- ω_n is the energy dissipation produced in loading cycle number n (in J/m³);
- ω_{n+1} is the energy dissipation in loading cycle "n + 1" (in J/m³).

The simple geometry of the test device is capable of generating horizontal as well as vertical deformations in the test specimen, which attempt to simulate the bending and shear stress caused by traffic loading as well as tensile strains induced by the impact of thermal gradients (Fig. 59).

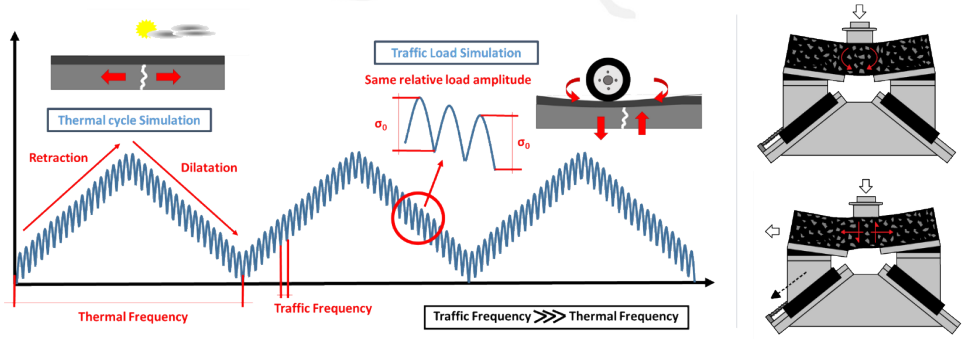


Figure 59. Sketch of the effort conditions induced during UGR-FACT (Adapted from [Moreno, F. 2016])

[34] The cumulative RDEC (Ratio of Dissipated Energy Change) is used to analyze the evolution of the damage produced in the specimen, and the Mean Damage Parameter (γ) is the value used to establish a reference in the resistance to fatigue cracking of the layer studied.

4.12.3. Fatigue Testing plan

The fatigue cracking behavior of the mixtures was analyzed using the UGR-FACT method. Different strain controlled tests were undertaken for the same material under three loading conditions, one frequency and one temperature [0.6, 0.8 and 1.0 kN of Load amplitude; two different frequencies (3 to 5 Hz), and a temperature of 20ºC], according to the European standard BS EN12697 (Table 35).

TABLE 35. FATIGUE CRACKING (TESTING PLAN FOR EACH MIXTURE)

Fatigue cracking test device	Load condition (kN)	Frequency (Hz)	Test temperature (°C)	Number of Specimens tested	Main parameters
UGR-FACT	0.6	5.0	20	3	Evolution of dissipated energy, ωi
	0.8			3	Mean damage parameter, ϒ
	1.0			3	Variation of the geometry, Δεi

Four LVDTs (one vertical and one horizontal on each side of the specimen) are used to control the vertical and horizontal displacements produced in the material in each load cycle (Fig. 60): a "permanent" displacement (h_i, v_i), and a "relative" displacement (H_i, V_i) in a load cycle.

Its evolution is studied by using a combined analysis of the dissipated energy in each load cycle (*calculated from the area of the hysteresis loop described in the "relative" displacements*) and the *variation of the geometry* ($\Delta\varepsilon i$) of the material in the zone where the fatigue phenomenon takes place (*calculated from the "permanent" displacements in both directions).*

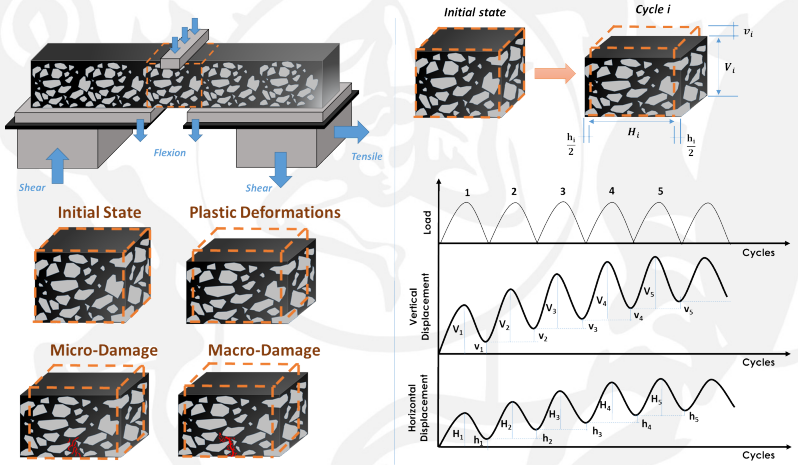


Figure 60. Sketch of the displacements produced during UGR-FACT test (Adapted from [Moreno, 2016])

Based on [Moreno-Navarro, F. et al. 2016], a methodological damage approach was developed to evaluate the movements produced at a molecular level, as well as the damage produced due to the breakage at a bonding level. The results were expressed regarding dissipated energy, a number of cycles to failure, geometrical changes, and mean damage parameter. The different stages of plastic deformations, micro-damage, and macro-damage could be identified in the material:

$$\omega_1 = \omega_{H_i} + \omega_{V_i} \rightarrow \Delta\varepsilon_i = \frac{\left|\left(1+\delta_{H_1}\right)\cdot\left(1+\delta_{V_1}\right)\right|-1}{1}\cdot 100 \qquad \text{(Eq. 37)}$$

- ωi is the dissipated energy in cycle i (in J/m³);
- ω_{Hi} is the horizontally dissipated energy in cycle i (in J/m³);
- ω_{Vi} is the vertically dissipated energy in cycle i (in J/m³);
- $\Delta\varepsilon i$ is the variation of the geometry of the specimen in cycle i for an initial unitary volume; and,
- δhi and δvi are the horizontal and vertical dimension changes measured in the specimen in cycle i.

Figure 61 shows a typical graph obtained from the representation of these two parameters (ω_i in the x-axis, and $\Delta_{\varepsilon i}$ in the y-axis).

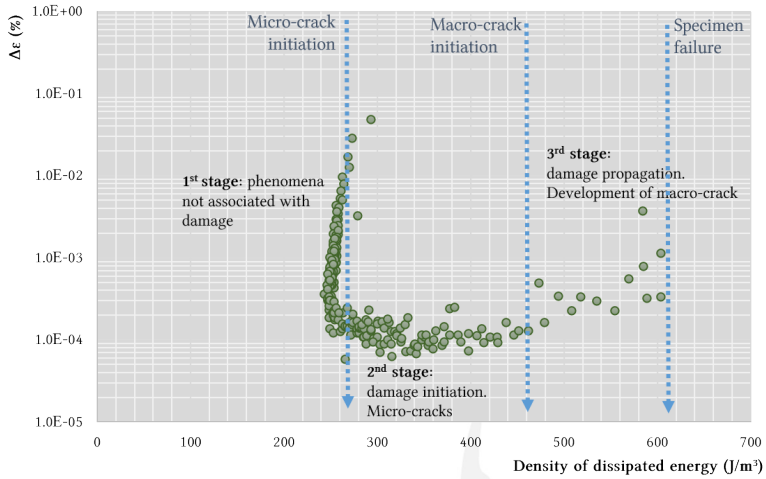


Figure 61. Representation of Log Δε (%) as a function of the dissipated energy on an HMA mix

4.12.4. Sample characteristics

From the slabs developed with Roller compactor, 9 samples of 200 · 60 · 60 mm of each type of mixture (HMA, DRY1.5, and DRY2.0%) were studied. The rest of samples obtained from slabs, 2 to 3 specimens were left in reserve for later elastic modulus test by NDT-FFRC (Table 36).

TABLE 36. CHARACTERISTICS OF THE FATIGUE CRACKING TESTS

Test	Mixture	Load condition (kN)	Frequency (Hz)	Test Temperature (°C)	Number of Specimens	Material tested
UGR-FACT (Craking resistance)	HMA b.4%	0.6	5.0	20	3	HMABituminous sub-ballast
		0.8	5.0		3	
		1.0	5.0		3	
			3.0		1	
	DRY 1.5% b.5.5%	0.6	5.0	20	3	DRY 1.5% Bituminous sub-ballast
		0.8	5.0		3	
		1.0	5.0		3	
			3.0		1	
	DRY 2% b.6%	0.6	5.0	20	3	DRY 2% Bituminous sub-ballast
		0.8	5.0		3	
		1.0	5.0		3	
			3.0		1	

4.13. Methodology 05: "NDT-FFRC."

4.13.1. Determining Stiffness, Poisson and Shear modulus from Non-Destructive testing ("FFRC," Free-free Resonant frequency test)

The use of non-destructive techniques based on the propagation of transient waves by impact is presented to evaluate the rigidity modulus and Poisson's coefficient without invading the samples destined to the fatigue tests. The complex dynamic stiffness modulus can be measured through traditional laboratory testing on cylindrical samples using steady-state uniaxial or indirect tensile tests at different temperatures (T) and frequencies (f).

The traditional procedure to determine the asphalt dynamic modulus from prepared laboratory samples is a relatively complicated, time-consuming, and expensive test [Ryden, N. 2009; Kweon, G. et al. 2006]. "Resonant frequency" (FFRC) [ASTMC215; ASTM E1876] test is widely used in many other fields of material characterization and can be used to measure the fundamental transverse, longitudinal, and torsional resonant frequencies of bituminous prisms and cylinders for the purpose of

calculating dynamic Young's modulus of elasticity, the Shear modulus, and dynamic Poisson's ratio of arbitrary sized elastic or viscoelastic samples [Martinez Soto, F. 2013; Gallego, R. et al. 2015].

The conventional dynamic modulus test using uniaxial or indirect tensile testing has not been considered because the specimens were manufactured according to dimensions only suitable for the fatigue UGR_FACT device. Instead of making new blends with cylindrical or prismatic specimens of 380 · 50 · 63mm for the 4PBDT device, nondestructive techniques are used by wave propagation to determine the small-strain Young's modulus and shear modulus in samples of 200 · 60 · 60mm.

The objective of this study is to determine the sensitivity of the natural resonance frequency method for determining the modulus of bituminous mixtures. For this purpose, it is necessary to control the quality of the signal obtained in the waves, as well as the repeatability and reproducibility of the results, given the variables that could affect the measures [Tauste, R. et al. 2017].

The principle of the test is to induce elastic excitation with an impact-hammer in one point of the specimen and to register the characteristics of the mechanical vibrations caused using one piezoelectric accelerometer in specific points of the specimen. The modal parameters (resonant frequency, modal damping and frequency response function) are measured (Figure 62).

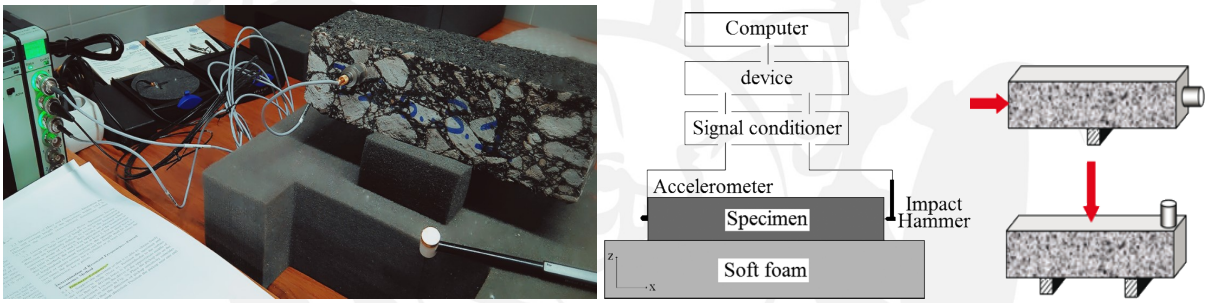


Figure 62. FFRC tests. (a) Equipment and development on an HMA sample from roller slab; (b) Illustration of the experimental setup

For vibration measurements the following equipment was used: Brüel & Kjaer, LAN-XI 6ch PULSE module 3050-A60 for signal acquisition and processing, 1 impact hammer (10Hz-65kHz), 1 uniaxial piezoelectric accelerometer model DeltaShear® 4514-B-001, a commercial software (PULSE v.16), and in-house developed software (FORTRAN and Matlab) for signal post-processing.

The FFR method is based on the analysis of the auto-spectrum of the acceleration time signals [transient pulses generated by impacts] (Figure 63).

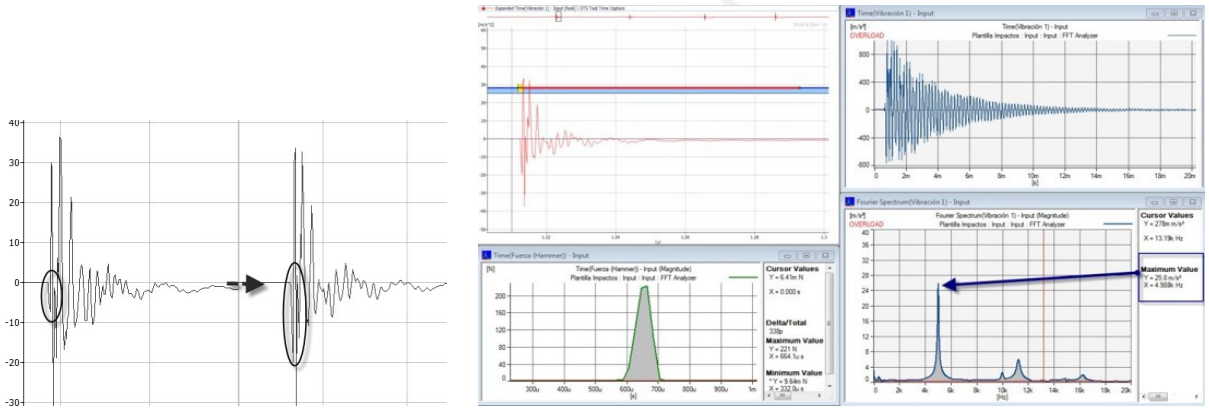


Figure 63. (a) Overlaying shooting records to set the impact signal ("triggers"); (b) Example FFRC tests by signal equipment

The free-free resonant column method (FFRC) involves signal processing techniques similar to those used in the impact-echo (IE), and Spectral Analysis of Surface Waves (SASW), but information about the internal structure of the material is extracted through the profile of velocities generated by the series of superficial impacts made. The speed of propagation is calculated according to the contact time of the impact, the broader the range of the frequencies or wavelengths, and the distance between the hammer-transducer. The wave velocity is related to Poisson's ratio, material density, and dynamic material stiffness. The advantage of this technique is that only measurements in the surface area are needed, therefore simplifying the experimental setup.

The process was performed by measuring at three different locations, to obtain the natural frequencies of the sample, called transverse, longitudinal and torsional. From these frequencies, the dynamic elastic moduli (Ed), transverse dynamic modulus (Gd) and damping coefficient (η) were obtained, using the equations:

$$\eta = (f_2 - f_1)/f \quad ; \quad E_d^T = C \cdot W \cdot f^2 \quad ; \quad E_d^L = D \cdot W \cdot f^2 \quad ; \quad G_d = B \cdot W \cdot f^2 \qquad \text{(Eq. 38)}$$

where f_i is the frequency bandwidth ranges (Hz), W is the weight of the specimen (kg) and T, C, D, B, are form and correction factors.

Then, considering the equations that relate wave speed and modulus, it was possible to determine the Poisson's ratio and to check the shear modulus estimated, using:

$$V_P = \sqrt{\frac{E(1-\upsilon)}{\rho(1+\upsilon)\cdot(1-2\upsilon)}} \quad ; \quad \mu = \left(\frac{E_s}{2G}\right) - 1 \quad 0.15 < \mu \le 0.25 \quad G_s \approx 0.832 G_d$$
$$V_S = \sqrt{\frac{E}{2\rho(1+\upsilon)}} = \sqrt{\frac{G}{\rho}} \rightarrow G = \rho(V_S)^2 \quad ; \quad V_R = \frac{0{,}87 + 1{,}12\nu}{1+\nu} \cdot V_S \qquad \text{(Eq. 39)}$$

A reference temperature of 15 ºC has been considered during the tests. The frequency range used was 51.2 kHz, with a sampling data of 3200 points, the impact-hammer digital signals had a duration of 62.5 msec and a frequency differential of 16 Hz. Each measurement was made at three different points of the specimen to avoid the wave propagation through an internal crack or air voids of the aggregate structure, concentrations of recycled rubber or possible micro-cracks or internal air voids.

4.14. Work plan

The purpose of the analysis of the developed materials, the techniques for the elaboration of samples in the laboratory, and the methodology following some specific guidelines have served to give rise to the following work plan:

- Optimization of conventional asphalt mixtures and modified with rubber by the "Superpave" Volumetric method mainly.

- Determination of the necessary parameters of temperature, rail traffic and dynamic loads (stresses) that occur in the sub-ballast layer in contrast to the base layer of roads. Through the calibrated mechanistic-empirical methodology for the design of flexible road pavements [Huan, y: 1984; Banerjee, A. et al. 2009], it is proposed to adopt the necessary parameters to the already known calculation models [Barber, E. 1957; Crispino, M. 1998; Rose, J. 2000] for the case-study of the high-speed lines of Italy.

- Having determined the optimum compaction parameters for the bituminous sub-ballast, we will proceed to develop laboratory mixtures using SGC, Marshall and ASRC techniques.

- The most representative mixtures will be designed for the mechanical characterization of the material by resistance to fatigue and elastic modulus.

- The rheological study of bitumen and its interaction with rubber from recycled tires open up the possibility of solving the problems of swelling in the compaction phase through a specific protocol for the execution of the mixtures as well as an empirical method to calibrate the parameters of energy of the SGC.

4.15. Conclusions and expectations

The methodology carried out demonstrates the need for more considerable attention to the volumetric mix design of dense-gap graded bituminous conglomerates. The study of the volumetric mix-design and the N_{des} parameter, in the context of the survey, suggest a review of the guidelines derived from international research (N_{DES} values between 3-30MESALs) the opportunity to develop the mix-design, which has a significant incidence of the development of the objectives of the thesis.

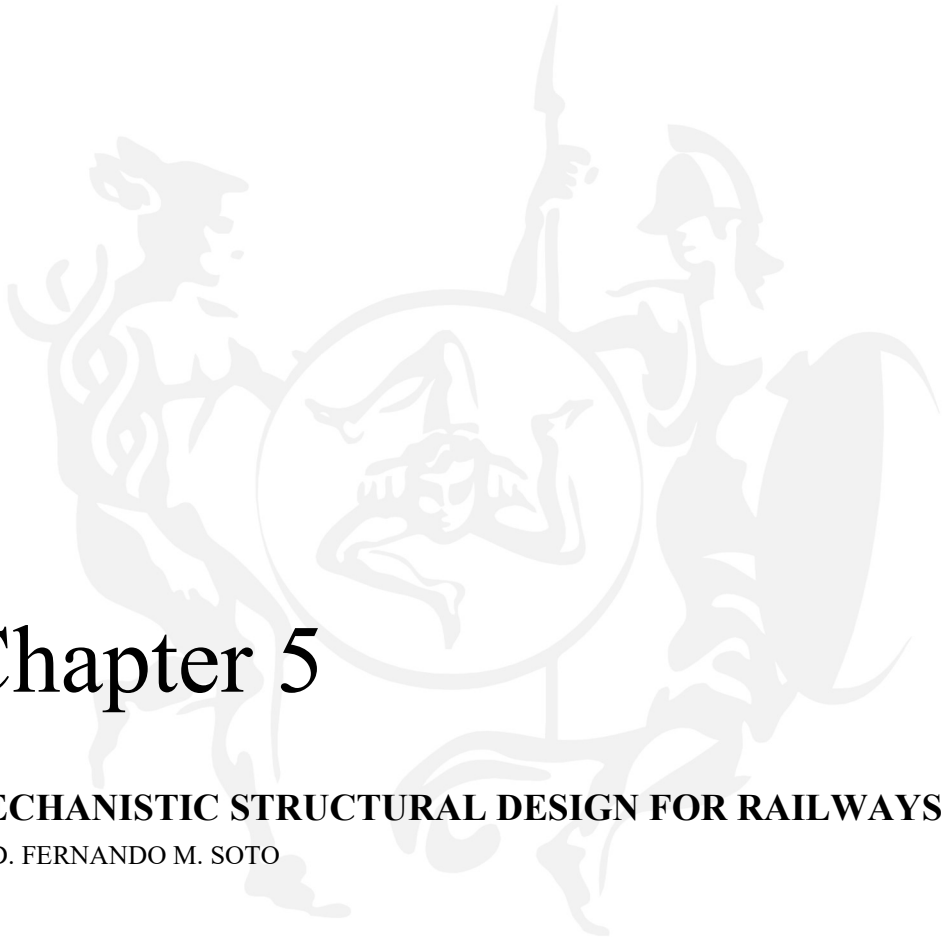
Finally, it appears to be possible to study the relationship between the N_{DES} value and the maximum temperature-traffic level combination as shown in the volumetric mix-design, by verifying whether there are significant correlations between these parameters and the compaction level. In another context, this framework can be found according to the traffic and climate characteristics, the value (N_{DES}=100) is similar than the prescription value and the experimental results. For the dense-graded blends, the specification value coincides with that shown in the case of standard compaction. However, according to the reviewed standards, it will be different during the manufacturing of rubber modified asphalt mixtures with ground rubber, where N_{des} must be increased considerably.

However, apart from the relative significance of this result, it would be profitable, on a considerably more extensive database, not to rely on a single reference value.

In the case of Volumetric mix-design, the traffic load value of MESALs>30 suggest an N_{DES} = 125. This value is lower as we will see in rubberized mixtures, where crumb rubber interacts with the bitumen and is followed by a swelling effect during post-compaction. Thus, the N_{DES} must be higher to compensate the differences in the resulting air voids content values.

It must be expressed in function of a particular climatic zone and spectrum of railway traffic lines, two parameters, perhaps the most significantly associated with distinct modes and compaction processes.

2017



Chapter 5

MECHANISTIC STRUCTURAL DESIGN FOR RAILWAYS

PH.D. FERNANDO M. SOTO

List of Figures Chapter 5

Figure 1. Underlayment HMA Trackbed by Kentrack 4.0 design program [Rose J. et al. 2006] 117
Figure 2. Research objectives developed in this chapter.....118
Figure 3. Million Gross Tons per Year Calculation (Adapted from [Rose, J. et al. 2014]).....122
Figure 4. (a) Kentrack failure criteria (Adapted from Rose and Konduri, 2006); (b) Graphical determination of design subgrade resilient modulus [AI, 1981b] 122
Figure 5. Road and railway sections for simulations with KENPAVE® and KENTRACK® 123
Figure 6. Set of wheels for a 6-axle locomotive (NTA).....124
Figure 7. Track Layout for Example Underlayment (Long/Transversal Sections).....124
Figure 8. (a) Typical train configuration; (b) Maximum number of axes for the analysis. 125
Figure 9. (a) Positioning the loads concerning the ties; (b) Ties numbering; (c) Real modelization; (d) Circular areas (equivalent radius) representing the contact between the track and underlying layers 125
Figure 10. Kentrack software interface (Example 4-layer system) 126
Figure 11. Steps procedure of Super-rail mix-design.....127
Figure 12. (a)Road and railway sections considered indicating layers applied 128
Figure 13. (a)Pandrol fast clip; (b) Technical characteristics 128
Figure 14. (a) Dynamic train configuration and load distribution; (b) Convoy Aln 501- Ale Minuetto (train for simulations); (c) Vehicle considered for road simulations.....129
Figure 15. Technical dimensions of train *ALn 501-Ale Minuetto*. Load configuration 130
Figure 16. Energy balance in railway track layers [Soto, F.M. et al. 2017].....131
Figure 17. Daily variation of T^a in the pavement at the depth z and time t [°C] between road and railways.133
Figure 18. 24hour-T^a variation at different depths [Air T^a 0°C-35ºC] between road and railways 133
Figure 19. Results obtained from the simulations carried out with KENPAVE and KENTRACK.....135
Figure 20. (a) Train main lines analyzed; (b) Types of trains in Italy (Trenitalia) 135
Figure 21. Traffic spectrum of main rail-lines [Nº axle/day vs. Axle load], [Axle load vs. %passages/day] 137
Figure 22. (a) N_{design} recommended by SGC standards; (b) Logarithmic regression by interpolation of N_{des} values 137
Figure 23. N_{design} obtained for different track-lines and different values of annual traffic growth rate.....138

List of Tables Chapter 5

Table 1. Asphalt Binder Grade and Viscosity Parameters (NCHRP 1-37A, 2004) 121
Table 2. Parameters selected for Kentrack simulations.....129
Table 3. Parameters selected for Kenpave simulations.....129
Table 4. Standard layer properties for the default case.....130
Table 5. Values adopted for Barber's equation.....132
Table 6. Results T^a pav(z,t) obtained for road base and railway sub-ballast layers 132
Table 7. Parameters inserted in the Witczak formula 133
Table 8. Deformations results at different temperatures 134
Table 9. Vehicle categories and their axle configuration for Sicilian main rail lines (2016). 135
Table 10. "Spectrum of traffic" for "Mesina-Catania" main rail line (Italy). 136
Table 11. Summary of the traffic levels expected 136
Table 12. Revised Ndesign table proposed by AASHTO R35 (2015).....137



Chapter 5 – Mechanistic Structural Design for railways

5.1. Introduction

The recent increase in traffic speeds, volumes, and loads on railroads has led to new requirements for improved stability and durability of track supports. To reduce both resilient deformations and permanent settlements, and thus to minimize maintenance costs, HMA has been used for strengthening rail structures. HMA trackbed is not only applicable for freight lines but can also be used in high-speed passenger rail lines which require tight adherence to maintaining consistent track geometry. The underlayment design is widely used and is preferred over the overlayment design, because the asphalt layer is protected from the environment and the track geometry can be easily adjusted [Rose J. et al. 2006; Wolfe S.L. et al. 2004; Huang, Y. et al. 1984], as illustrated in Fig. 1.

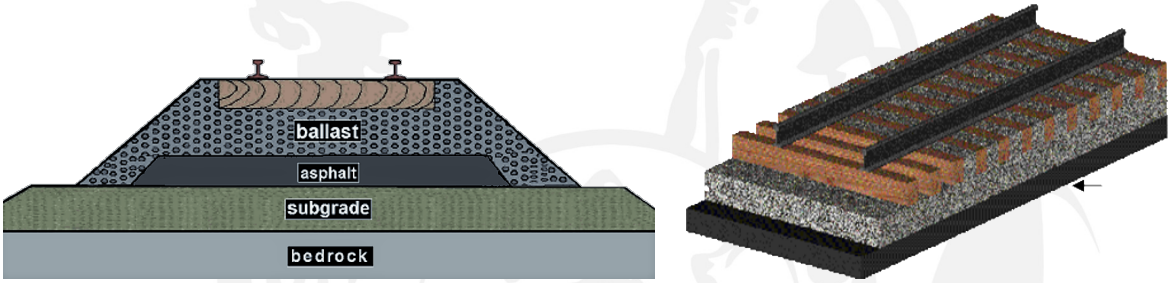


Figure 1. Underlayment HMA Trackbed by Kentrack 4.0 design program [Rose J. et al. 2006]

"Structural Design of Railway Trackbed" includes extensive literature sources already mentioned [Rose, J. et al. 2011; Teixeira, P. 2006; Asphalt I. 1998; Hensley, M. et al. 1991], however, about its performance design from the proposal of optimal mixtures is limited. There is even little adaptation of predictive models based on a mechanistic-empirical computation for the design of the railway section, widely developed in the field of roads [Banerjee, A. et al. 2009]. The AASHTO Mechanistic-Empirical Pavement Design Guide (MEPDG) [Loría-Salazar et al. 2010; Hoegh, K. et al. 2010; Schram, S. et al. 2006; Huang, Y. 2004; Darter, M. et al. 2001-2009] includes empirical distress models that have been calibrated using the North American conditions. However, the differences in material properties, traffic information, and environmental conditions for other countries make necessary to calibrate these models using local conditions. With the advent FEM analysis, it is not difficult to analyze a complex structure such as an HMA trackbed by the use of a computer model. However, a highly sophisticated railroad trackbed model, which accurately simulates the behavior of a structure in detail, would require considerable computer time to run and therefore might not be suitable for design purposes [Fateen, S. 1972]. Some simplifying assumptions must be made to provide a model of conventional design, and to keep down the computing cost within reach of general users. After reviewing several existing models, an efficient and versatile model named KENTRACK 4.0 [Rose J. 2014] was selected and applied in this thesis to study the structural analysis and design of HMA trackbeds.

The objective is to define the traffic-spectrum and environmental thermal parameters necessary to adapt the SGC methodology to the optimization of the bituminous sub-ballast layer before the mix-design of HMA_DRY blends, through compare stress levels (axle loading) to the same layer level between the base-road and railway sub-ballast layers.

5.2. Scope

The first intention of this work is to compare the base course in an asphalt roadway located under the surface layer or wearing curse under similar solicitations and binder composition as sub-ballast for railways. The FEM analysis developed with Kenpave-Kentrack computational software could predict the analytical procedure and traffic-thermal parameters that fit best with the mix-design of bituminous mixtures for Railtrack [Fang, M. et al. 2011; Iwnicki, S: 2006].

Although hot-mix asphalt (HMA) has been used for the construction of highway pavements for over a century, its use as railroad trackbeds is relatively new and, up to the present time, primarily experimental. According to the proposed research, the study of internal stresses was based on the strain-strain calculation methodology for the rail mix design. An original approach to the AASHTO-Calibrated mechanistic procedure for flexible layers (Kenpave-Kentrack [Huang, Y. 1984; Rose, J. 2014]), will determine the similarity of tensions between the road layer and the sub-ballast layer, and the parameters necessary (N_{des} to SGC) for the optimal design of HMA_DRY mixtures.

At the same time, it was needed a review of model factors, the effect of environmental conditions (thermal regime) and the study of traffic-spectrum. Other items like bitumen aging and moisture damage on the mechanical properties of HMA were implemented into the FEM analysis (Figure 2).

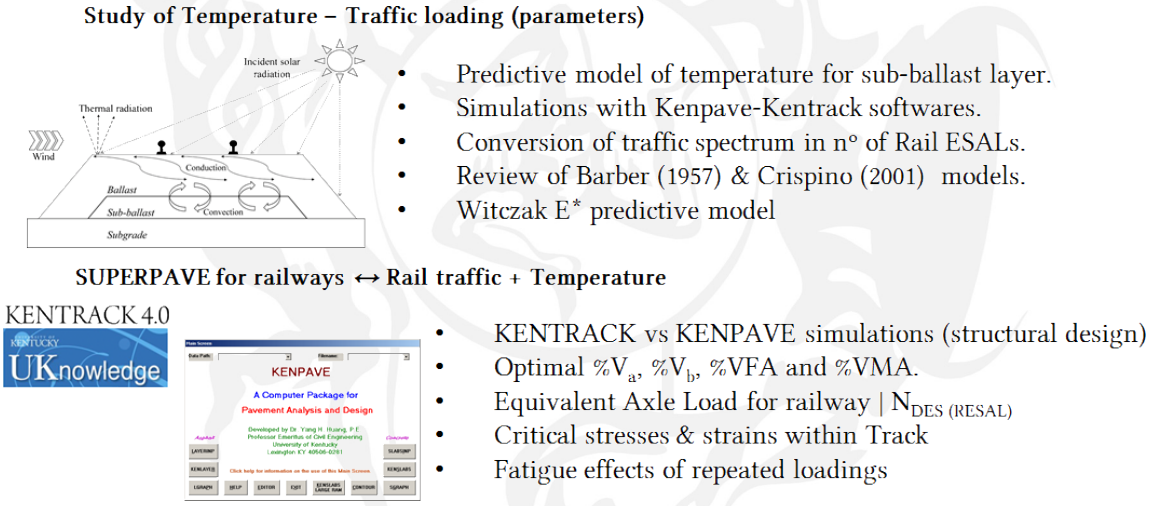


Figure 2. Research objectives developed in this chapter

5.3. A review of model factors

The development of the high-speed rail system and the increasing traffic levels have brought new technical issues of considerable importance. The higher operating speeds can result in increased noise and vibration transmitted. Also, problems with vehicle safety and the useful life of the facility itself [Khisty, C. et al. 2017; Cardona, D. et al. 2016; Dong, H. et al. 2010; Thompson, D. 2008; Esveld, C. 2001; Thompson, M. 1992]. In this context, the use of mathematical models applied to the issue of train-structure interaction has become mature over the years, representing as much as possible the complex system of structural configurations, application of static loads, strength evaluations, and vibration[1] induced on the rail structures. There is the difficulty in the choice of characteristic parameters of the superstructure as a continuous multilayer.

[1] It should be noted that the train-armament-structure interaction extends over a range of frequencies from 0.25 to 150 Hz.

Since 1967, more than thirty experimental sections of HMA trackbeds have been built in the United States. Two methods have been used to incorporate HMA in railroad trackbeds; one by placing the ties directly on the top of the HMA mat and the other by placing the HMA mat under the ballast [Huang, Y., et al. 1987; Rose, J. 1986].

The first reported use of HMA for railroad trackbeds was in 1968 [Brown, S. et al. 1967]. In 1969, the "Santa Fe Railway" placed three 213 m long asphalt test sections on a new line to service a coal mining region in northeastern New Mexico. Despite the excellent performance of these experimental sections, little work has been done on HMA trackbeds until 1981. In that date, long sections of HMA were constructed at Kentucky, where rail-ties were placed directly on top of the underlayment by an existing sub ballast [Rose, J. 1983]. Due to the lack of performance data, the thicknesses were selected arbitrarily by traffic and subgrade conditions. So far, all sections had exhibited excellent performance under widely varying traffic, roadbed, and environmental conditions.

In last decades, several authors have proposed solutions to reinforce the track-bed and mitigate sub-ballast degradation [Asphalt I. 1998; Huang, Y., et al. 1984; Rose, J. 1986; Fateen, S. 1972].

The design procedure recommended by the AASHTO is based on the results of the extensive road tests conducted in Ottawa, the 1950s, reviewed in 1993. The mechanistic-empirical performance equations are still being used as the primary models in the current guide but were modified and extended to make them applicable to other climatic regions. Several design variables are considered: time constraints, performance period, traffic, reliability, environmental effects, serviceability, effective soil resilient modulus, and the structural number (SN) [Li, N. et al. 1997; Transp. Off. 1993].

Boussinesq elastic theory is used for analyzing trackbeds based on the single-layered theory [Chandak, P.G. et al. 2017; Zang, T.W. et al. 2016; Southgate, H. et al. 1968; Sokolnikoff, I. 1956] assuming that the support layer is elastic and isotropic. Computer programs have been drawn up to design and analyze trackbeds reporting the deficiencies and limitations of the Boussinesq's method, JNR method, and Talbot's method, all based on empirical equations (Eq. 1) developed for railroad trackbed structural analysis and design:

Japanese National Railways (JNR) Talbot's equation

$$P_c = \frac{50P_m}{10+h^{1.35}} \quad \Leftrightarrow \quad P_c = \frac{16.8P_m}{h^{1.25}} \qquad \text{(Eq. 1)}$$

- Pc = subgrade pressure (kPa); Pm = applied stress on ballast (kPa); h = ballast depth (cm).

Three computer programs intended for railroad track structure analysis were developed in the United States to discourse the deficiencies in the existing design methods. These include ILLITRACK [Robnett, 1975], GEOTRACK [Chang, 1980] and KENTRACK [Huang, Y. 1984a_1986a_1987].

Therefore, it was necessary to develop a scientific rational analysis procedure to determine the stress distribution for both HMA and ballast trackbeds. The KENTRACK[2] computer program, at the University of Kentucky, was developed for this purpose, after a review made on FEARAT [Fateen, S. 1972], ILLITRACK [Tarabji, S. et al. 1976], and GEOTRACK [Chang, C. et al. 1980] models.

One critical assumption made in Kentrack is that each wheel load, when applied over a central tie, is distributed over five on each side of the central tie. Any tie away from the central tie does not carry any load. This assumption is reasonable for design purposes since the most critical stress-strain lie

[2] The KENTRACK program is based on two main theories, finite element method and multi layer system. Stresses and strains are calculated using the finite element method and multi layer system which facilitates the analysis of all types of trackbeds [Rose et al., 2003].

near the central tie. It allows the application of the simple *superposition principle* to determine the stresses and strains under multiple wheel-loads and thus saves lots of computer time. Another advantage is that the railroad is applied to the tie directly above one of the reactive points between the tie and the layered system.

In this thesis, the structural analysis of Trackbeds reviewed the computational models based on Kentrack analysis, which it was selected as a very efficient software for the design of railroad tracks and its capabilities to compare stresses and strains in HMA sub-ballast layer.

5.4. Framework of rail modeling

→ See **Annex 03**. In section "Annexes," see [Indraratna, B. 2016; Indraratna, B. et al. 2010; Rose, J.G. et al. 2014; Esveld, C. 2001; Burmister, D.M. 1943].

5.5. Materials properties

The first material properties of the structural model are the Resilient Modulus and Poisson ratios of granular ballast, HMA bituminous underlayment, and subgrade soil. These materials are considered linear-elastic and different equations are used to describe their properties. Poisson ratio was reasonably assumed as 0.45-0.50 for subgrade soils and 0.35 for all other materials [Huang, Y. 1984]. The resilient modulus of ballast was calculated using the following equation:

$$E = K_1\theta^{k_2} \rightarrow \theta = \sigma_1 + \sigma_2 + \sigma_3 + \gamma\left(1 + 2K_0\right) \qquad \text{(Eq. 2)}$$

- E= resilient modulus;
- θ=bulk stress, or the sum of three principal stresses including geostatic stresses;
- $K1$, $K2$=regression constants reflecting material properties;
- σ_1, σ_2, σ_3 = the three stresses; γ = unit weight of the material; K_0= lateral stress ratio.

A lateral stress ratio of K_0 must be specified to compute the geostatic bulk stress. When K_2=0, the material behaves linearly. Because of its small effect on stress and strain, a constant Poisson's ratio, independent of the state of stresses, is assumed for each layer. The dynamic modulus of HMA is calculated using the method developed by the Asphalt Institute [Bari, J. et al. 2006; Hwang D. & Witczak, 1979]. To accurately model the asphalt, different climatic conditions have been utilized for the various seasonal periods since the dynamic modulus is dependent on the temperature.

Witczak E* predictive model was incorporated into KENTRACK 4.0 to calculate asphalt dynamic modulus [Bari, J., & Witczak, M. 2006; Bari, J. 2005; Witczak, M. et al. 2004, 1997] expressed as:

$$\log|E^*| = -1.249937 + 0.02923\rho_{200} - 0.00167\rho_{200}^2 - 0.002841\rho_4 - 0.05809 \cdot V_a - 0.802208\, V_{beff}/(V_{beff}+V_a) + \frac{3.971977 - 0.0021\rho_4 + 0.003958\rho_{38} - 0.000017\rho_{38}^2 + 0.00547\rho_{34}}{1+e^{(-0{,}6033 - 0{,}3133\log(f) - 0{,}3935\log(\mu))}} \qquad \text{(Eq. 3)}$$

- $|E^*|$= Asphalt dynamic modulus [10^5 psi]; ρ_{200}= % passing to the sieve 0.075mm; ρ_4= % retained to the sieve 4.75mm;
- ρ_{38}= % retained to the 9.5mm sieve; ρ_{34}= % retained to the 19mm sieve;
- V_{beff}= effective binder content [% by volume]; V_a= air voids [% by volume];
- f= frequency [Hz]; and μ= binder viscosity [10^6 poise].

The characterization of the linear viscoelastic behavior of a bituminous mixture is a first step to the proper performance of rail-line tracks [Cardona, D. et al. 2016; Andrei D. et al. 1999]. Viscosity [ASTM D2493M, 2016], as one of the parameters in Eq. 3, could be determined by Eq. 4 establishing the relationship between viscosity and temperature:

$$Log_{\eta} = A + VTS \log T_R \quad \text{(Eq. 4)}$$

- η = binder viscosity, cP; A,VTS = regression parameters; T_R = temperature, °Rankine.

Typical grades of asphalt binders in trackbeds and the regression parameters "A" and "VTS" values are shown in Table 1 [Azari, H. et al. 2007].

TABLE 1. ASPHALT BINDER GRADE AND VISCOSITY PARAMETERS (NCHRP 1-37A, 2004)

Grade	PG 64-22	PG 70-28	PG 76-34
A	10.980	9.715	8.532
VTS	-3.680	-3.217	-2.785

5.6. Damage analysis: Fatigue cracking model

Pavement responses include stresses σ, strains ε, and deflections δ [AI, 1982]. Two types of damage analysis were performed in KENTRACK, tensile strains at the bottom of asphalt layer and compressive stresses at the top of the subgrade. Miner's (1945) cumulative damage concept has been widely used to predict fatigue cracking [Blasón, S: et al. 2016; Miner, M. 1945]. The fatigue cracking of asphalt was governed by the horizontal tensile strain at the bottom of asphalt layer. The relationship between tensile strain and the allowable number of load repetitions in asphalt was expressed in Eq. 5 [AI, 1981a, 1981b, 1982].

$$N_f = f_1\left(\varepsilon_t\right)^{-f_2}\left(E_1\right)^{-f_3} \rightarrow N_a = 0.0796 \cdot \varepsilon_t^{-3.291} \cdot \left|E^*\right|_a^{-0.854} \quad \text{(Eq. 5)}$$

- N_a = the allowable number of load repetitions to control fatigue cracking;
- εt = horizontal tensile strain at the bottom of asphalt;
- E_a = dynamic modulus of asphalt, psi.

The compressive stress governs the excessive permanent deformation at the top of the subgrade. The relationship between compressive stress and an allowable number of load repetitions in subgrade is expressed in Eq. 6 [22].

$$N_d = 4.837 \cdot 10^{-5} \cdot \sigma_c^{-3.734} \cdot E_s^{3.583} \quad \text{(Eq. 6)}$$

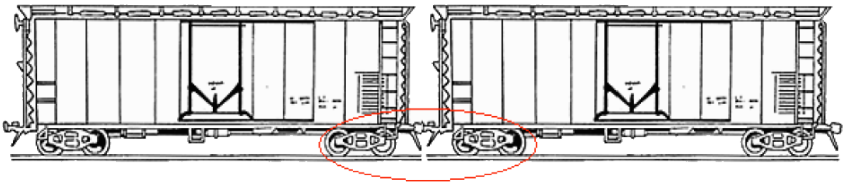
- N_d = the allowable number of load repetitions in subgrade;
- σ_c = compressive stress at the top of subgrade, psi[3];
- E_s = subgrade modulus, psi.

Equations 5-6 were developed for highway pavement where loadings and environments were entirely different from the railroad. Load pressures and temperature extremes on highway pavements are more severe than on trackbeds. Thus, the life prediction tends to be conservative when using equations developed for highway pavements.

The *predicted number of repetitions*[4] varies with the traffic that the trackbed is subjected. Assumed the predicted number of load repetitions each season is 200,000 and wheel load is 36000 lbs (16.33 tons), the traffic would be 28.6 MGT[5]. An illustration and calculations for the cargo predictions are shown in Fig. 3. With loading conditions and material properties varying throughout the year, damage may be analyzed seasonally for one year to determine the service life. Based on the maximum stress or strain in each period, the allowable nº of load repetitions was obtained from Eq. 7.

The ratio between the predicted and the allowable numbers of repetitions is computed for each period and summed to obtain the *repetition ratio* for the entire year. The *service life*, which is reciprocal of the repetition ratio, is predicted by using the minor linear damage analysis criteria.

[3] 1000 psi = 6.8947 MPa
[4] The passage of one train-car is equivalent to one load repetition
[5] Millions gross tons (1 MGT = 2 000 000 000 lbs = 907185 Tons)



Wheel load	= 36,000 lb/wheel
For one car the total weight	= 36,000 lb/wheel x 8 = 286,000 lb/rep
	= 143 ton/rep
The number of repetitions assumed per year	= 200,000 rep/yr
The traffic per year	= 200,000 rep/yr x 143 ton/rep

Figure 3. Million Gross Tons per Year Calculation (Adapted from [Rose, J. et al. 2014])

If a year is divided into four seasons, the design life for each distress mode can be written as:

$$L = \frac{1}{\sum_{i=1}^{4} \frac{N_p}{N_a}} \quad \text{(Eq. 7)}$$

- L = service life in a specific layer, years; N_p = predicted number of load repetitions each season;
- N_a = allowed number of repetitions during each period; N = number of periods.

The failure criteria in underlayment with asphalt trackbed come from two types of failure criteria. The first is the maximum vertical compressive stress or strain in a specified layer (ballast or subgrade) to control permanent deformation. The second is the maximum horizontal tensile strain at the bottom of the asphalt layer to control fatigue cracking and its service life (Fig. 4a).

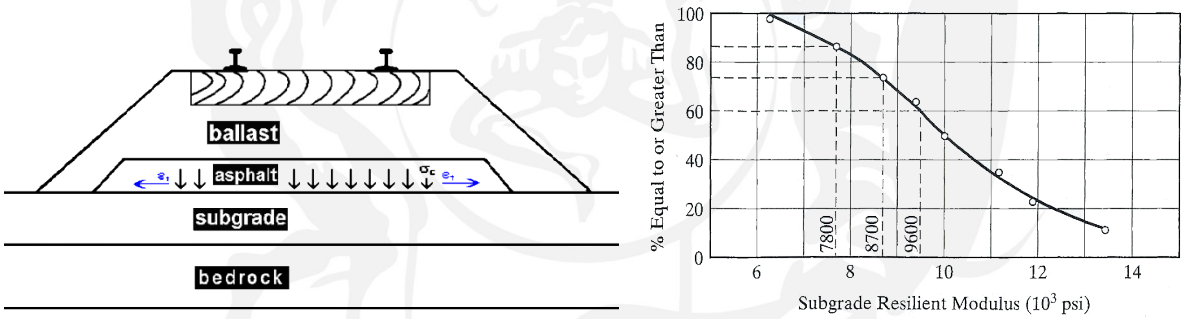


Figure 4. (a) Kentrack failure criteria (Adapted from Rose and Konduri, 2006); (b) Graphical determination of design subgrade resilient modulus [AI, 1981b]

At least six to eight test values were used to determine the *design subgrade resilient modulus*, that is defined as the modulus value for ESAL of 10^4, 10^5, and 10^6 that is smaller than 60, 75, or 87.5% of all the test values, respectively [AI, 1981a] (Fig. 4b).

5.7. Assumptions from modelization

It is necessary to understand the effects of the factors (axle load, rail size, tie type, ballast modulus-thickness, asphalt properties, sub-ballast layer thickness, and subgrade modulus) on trackbed performance to develop a rational structural design method for railroad trackbeds [Miura, S. et al. 1998]. In the design of underlayment, thickness has a significant effect on the critical stress and strain and varies according to subgrade conditions. The HMA railway trackbed has been found to impart the following benefits to the rail structure according to studies conducted [Asphalt Institute, 1998]:

- A stronger support layer below the ballast layer which distribute reduced stresses onto the subgrade;
- A resilient layer between the ballast and subgrade, eliminating the likelihood of subgrade pumping;
- An impermeable layer to divert water to the ditches, eliminating subgrade moisture fluctuations.

A softer HMA must be used in underlayment to reduce fatigue, and this is the primary objective.

Hence the proper protection of a subgrade is necessary during the construction and subsequent maintenance of the railway trackbed. HMA layers act as a waterproofing layer to the underlying subgrade layer and hence the subgrade modulus is not adversely affected [Rose, J.G. et al. 2002].

From the results of the literature review and considering the problem statement, it was decided to adopt as a reference section, a HMA bituminous sub-ballast of thickness ±12 cm. From which, the materials and properties will be investigated and compared to the conventional section on railways.

5.8. Design criteria of the HMA mix-design for sub-ballast layer

In the use of HMA trackbeds, the best resort was to study the failure criteria of asphalt highway pavements and made certain modifications to the AASHTO methodology for railways. The use of highway criteria for railroad design is considered quite conservative because of trackbed materials are more confined. Despite the importance of the presence of HMA in a sub-ballast layer, only fragmented information is available in the literature regarding the standards and procedures for its "mix -design."

Thus, thee purpose was to define reference criteria for the HMA sub-ballast to reduce the approximations caused by the inappropriate application of the "volumetric design method."

Kenpave software represented a similar real scenario in road pavements and the same for railways comparing the solicitations induced in the sub-ballast layer with the ones produced on the road base course. Both structural models were compared due to the in-depth analogy of the roads, being possible to find a parallel of ambient temperature and traffic loads at ESAL level.

The proposed methodology in this chapter aims to transform rail traffic spectrum relative to specific railway lines in the number of equivalent axes (ESALs). Subsequently, N_{design} was calculated according to the level of rail traffic (Figure 5).

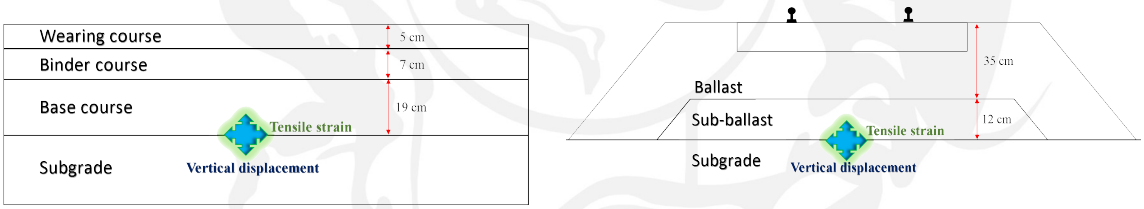


Figure 5. Road and railway sections for simulations with KENPAVE® and KENTRACK®

KENTRACK® was used for the analysis of the railway superstructure, KENPAVE® for flexible road pavements. The highlights of Kentrack are that is a computer program designed to analyze a railroad track segment as a structure, which uses *Boussinesq's Elastic Theory, Burmister's Multi-Layer System,* and *Finite Element Analysis* to perform calculations.

5.8.1. KENPAVE computer analysis

→ See **Annex 04.** In section "Annexes."

5.8.2. KENTRACK. A Railway Trackbed structural design program

KENTRACK 4.0 [Rose, J. 2014] examined the underlayment configuration for the critical horizontal tensile strain at the bottom of the HMA and the critical vertical compressive stress on the top of the subgrade. The primary factor was limiting this compressive stress on the subgrade. The program uses the Damage Analysis presented above to predict the service life of the trackbed

components for different traffic, subgrade support, and layer thicknesses. Also, it applies the relative effects of incorporating innovative materials and the thermal cracking model.

KENTRACK® considers any layer different from the substrate as nonlinear granular material, with tensions tightly connected to the elastic modulus or, as with bituminous conglomerates, even from the temperature [Rose, J. et al. 2004]. The output file generated comprises two parts: properties and results for the various periods at the different cross-sections.

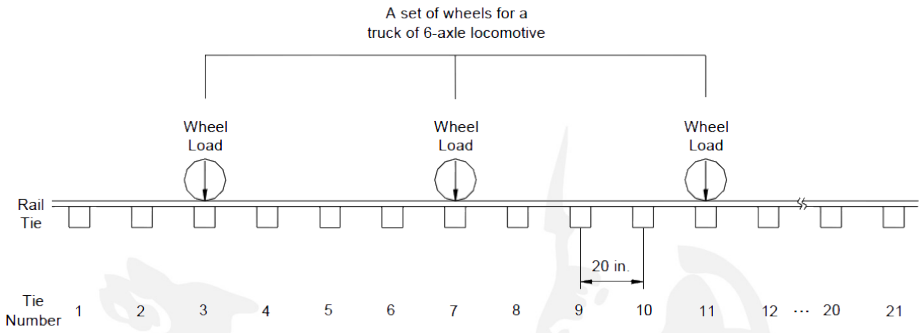


Figure 6. Set of wheels for a 6-axle locomotive (NTA)[6].

The software applies 17 subroutines to superstructures composed of six multi-layers (Nº Layers, NLS), and the calculation of tensions, deformations, and deflections can be carried out for a maximum of 10 cross-sections, as shown in Figure 6 (From crossbar 3, 7 to crossbar 11).

- **Parameters of Kentrack study. Reference values.** [Plotkin, D.E. et al. 1990]

The nº of layers (NLS=3-5) for the calculation of horizontal stresses on the lower surfaces (Nº layers for tensile strain, NLBT=0), plus the nº of layers for the calculation of vertical compression tensions (Nº layers for compressive stress, NLTC=4), must not exceed 5 (NLBT+NLTC=5). The transversal cross was divided into identifying elements (Nodal Point Locations, NPTD=7-8). Each single load was distributed over the number of rail ties (Nº ties for analysis, NTA=6). NMA (Nº Months for analysis=1). NBT (Beginning tie=2). NET (End tie=11). NLOAD (Nº of wheel loads=3). NPTD (Transverse nodal points=7). →See also Annex 05.

As an example of the output of track underlayment layout configuration[7] (Figure 7).

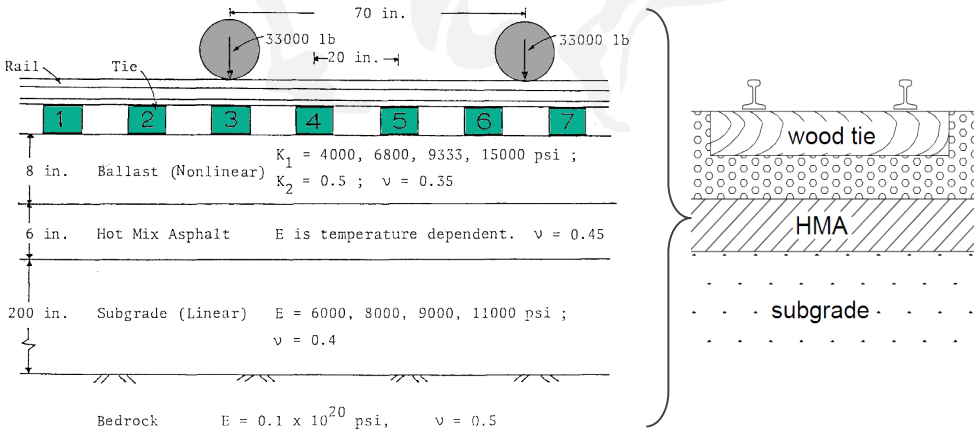


Figure 7. Track Layout for Example Underlayment (Long/Transversal Sections)

[6] Units system (1 in = 2.54cm; 1 psi = 6.9 kN/m²)

[7] The program is used for parameter initialization, for calculating the required dimensions, for the equivalent radius of the rail contact area, for the bituminous HMA elastic modulus, for distribute wheel loads for rail nodal points, and to perform nonlinearly damage analysis.

- **Axial load position concerning the rail.**

The maximum number of axes that can be used for damage analysis is 4, 2 in the back of a car and 2 in the front of the next car. The other axes of the train were considered sufficiently far away, and their presence did not affect the stresses and tensions of the four axles (Figure 8).

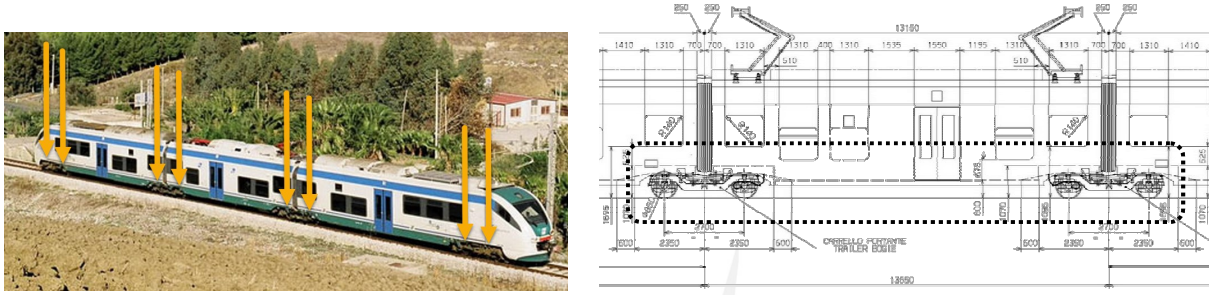


Figure 8. (a) Typical train configuration; (b) Maximum number of axes for the analysis.

- The position of the load concerning the railway sleeper.

The first rail tie where the moment was calculated is the nº2, which results from the deflection of the ties nº1, 2 and 3. Without the nº 1, the tension in the rail to the tie nº 2 would be incorrect. Once the crossbar nº1 was selected, starting from it, the axle distances must be specified.

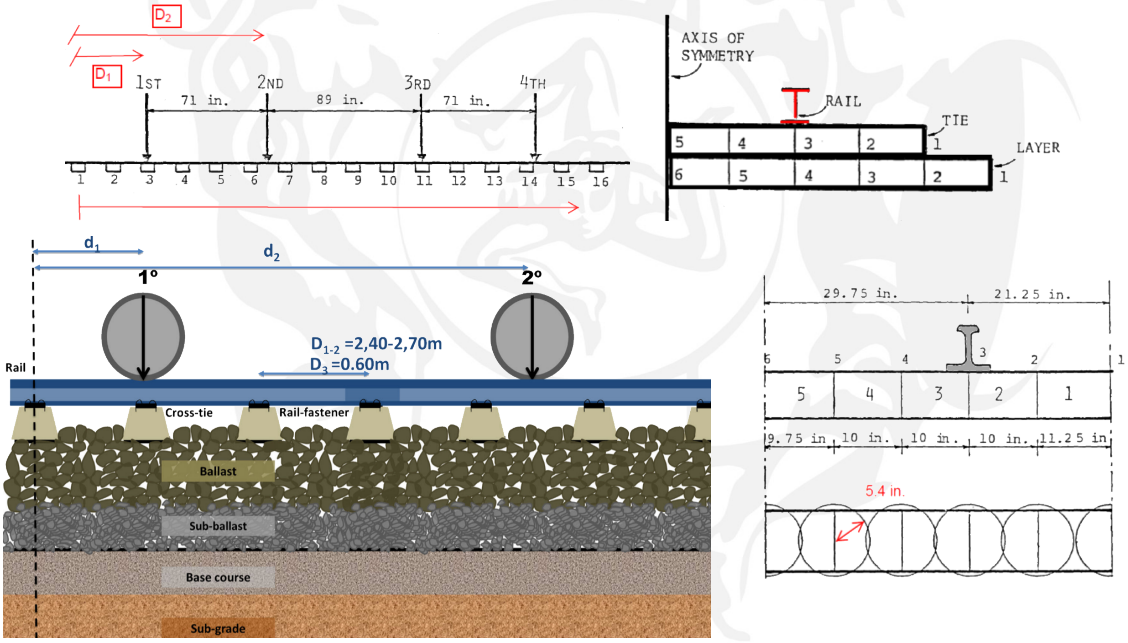


Figure 9. (a) Positioning the loads concerning the ties; (b) Ties numbering; (c) Real modelization; (d) Circular areas (equivalent radius) representing the contact between the track and underlying layers

Superposition principle is performed only in those rail ties between the *NBTs (number of beginning ties)* and the *NETs (number of end rail ties)* as specified by the user. The software adds an extra tie on each side to calculate the bending moments (Figure 9a). The selected ties must be between the nº2 to nº11. The cross-section points (NPTD=7), in the transverse direction, are shown in Figure 9b.

→If we need to calculate the superposition principle in tie nº11, the only way is to rerun the program by entering the crossbar nº1 to the right of the fourth axis[8] and increasing the number of rail ties from right to left.

[8] See Annex 03. Framework of rail modelling (3.1.2. Superposition principle)

→If the number of rail ties, NTA=6, it is necessary to select only ties nº 3-4, since the third and fourth axle loads will not have any effect on the results, having a distance of 6 ties from nº 4.

When this condition occurs, the program automatically does not consider these loads. Therefore only the results at nº 3, 4, and five must be calculated.

- **Finite Element division (FEM) of the crosstie.**

It is desirable to have a division of the elements with a cross-node beneath the rail for a more regular distribution of results (see Fig. 9d). For a wooden cross with a length of 102 in (2.59 m), width of 9 in (23 cm), and a gauge between the rails of 56.5 in (1.43 m), the crossbar was divided into 10 elements with contact area $(102 \cdot 9)/10 = 91.8$ in^2 (0.059 m^2). The equivalent radius is given by:

$$r_e = \sqrt{91{,}8/\pi} = 5.40in \text{ [9]} \qquad \text{(Eq. 8)}$$

KENTRACK 4.0 procedure is developed step by step in brief screenshots (Fig. 10):

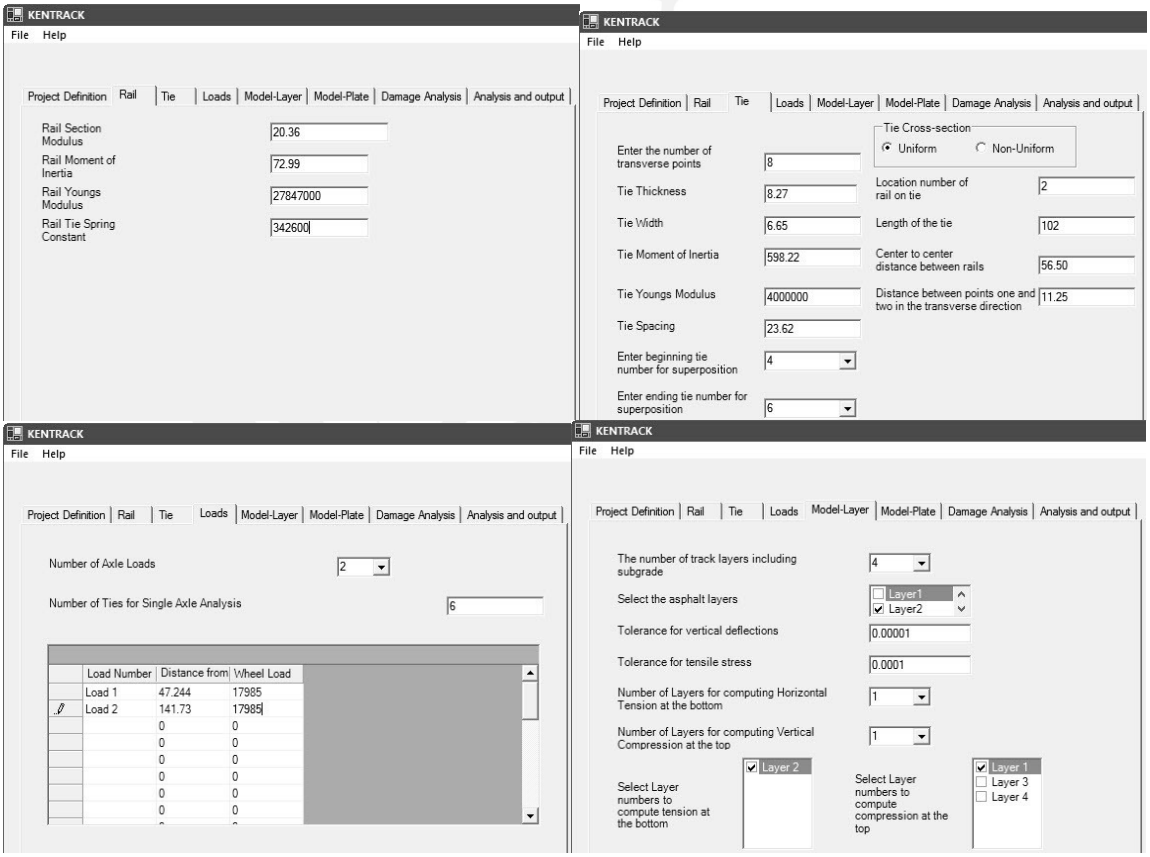


Figure 10. Kentrack software interface (Example 4-layer system)

5.9. "Volumetric Mix-Design" system in railways[10]

Rail Equivalent Single Axle Load ("RESAL") has been defined as the rail axle that produces the same vertical displacement (δ) at high temperatures, and the same horizontal tensile strain (ε_t) at low temperatures generated by the road ESAL (80 kN). Simulations were run using KENTRACK to find the "RESAL" that produces the same solicitations of the ESAL road.

[9] Input data measurement units can be inserted either with the American system (FPS) or with the International system (SI).

[10] Published articles concerning this section:
F. Martinez-Soto, G. Di Mino (2017). "Optimization of mix-design system for the sub-ballast railroad," (JTTE-E 20170721-2).
Soto, F.M. et al. 2017. "Procedure for a temperature-traffic model on rubberized asphalt layer for roads and railways," (JTTE-E 20170721-1).

The performance of asphalt pavements was influenced by temperature distribution and exposed environmental conditions [Di Mascio, P. et al. 2014; Paixao, A. et al. 2011; Mohammad, L. et al. 2004]. Climatic models included the heat transfer model [Dempsey, B.J. et al. 1970] for determining the temperature-moisture distribution and the drainage model [Liu & Lytton, 1984] in the layers.

The next section covers the methodology associated with an HMA underlayment to verify the validity of a new approach, that will be referred as "SupeRail" and consists of four steps (Fig. 11):

- Select the ESAL for rail systems, comparing the stresses induced in the sub-ballast layer with the tensions produced in the base layer of a road pavement;
- Calibration of a predictive temperature model based on Barber-Crispino [1957-2001].
- Convert the entire spectrum of traffic to an exact number of ESALs;
- Define the new N_{design} as a function of traffic and air temperature;

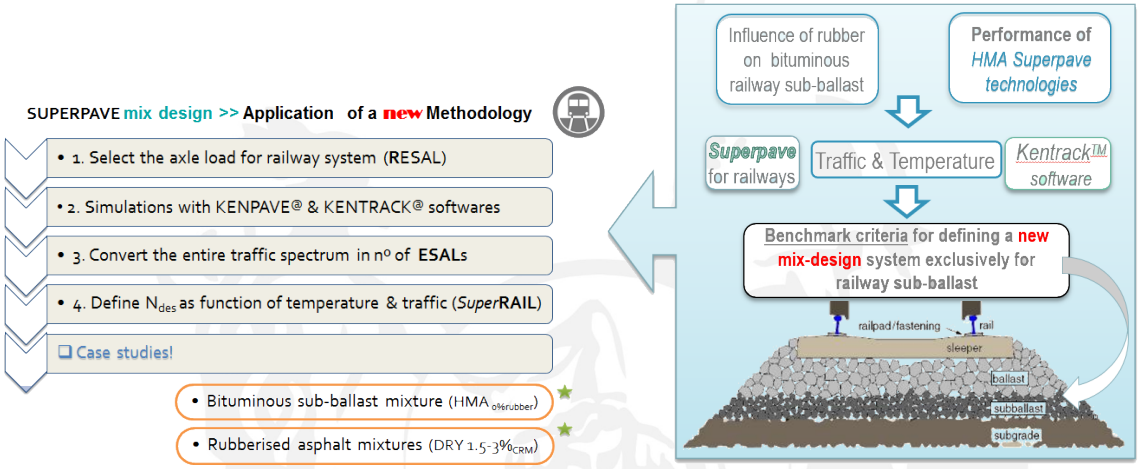


Figure 11. Steps procedure of Super-rail mix-design

Thus, it was needed to know the temperature within the layer and the relationship with the mechanical characteristics. Barber´s theory (1957) was used to determine the temperature in the road base course and, then applying the modifications purposed by Crispino M. (2001) in the sub-ballast layer. Using the average seasonal temperature analysis by simulating the thermal sub-ballast and road-base layer behavior respectively, was possible to predict the medium-layer temperatures, which obtained results are shown after different computer simulations [Soto, F. et al. 2017].

5.9.1. Comparison between sub-ballast-base road stresses

The rail-road multi-layer system requires determining the thickness layer under various conditions of traffic, subgrade, and climate. After proceeding to confront both superstructures due to the similarities of thickness and properties through FEM (*Burmister's theory*), the tensions and deformations produced by an analogous standard load have been determined (Fig. 12).

Stresses and strains in the layers of rail track structure were calculated by elastic multilayer theory, defining each layer by its thickness, Elastic Modulus, and Poisson's ratio [Andrei & Witczak, 1991]. The pressure transmitted from trains by rail, sleepers, and ballast was considered uniformly distributed over a circular area (same vertical-shear stresses, same vertical-radial displacements). The minimum thickness of an HMA depends on the subgrade support. A poor subgrade requires a thicker sub-ballast, which causes stress concentration and decreasing the fatigue life so that it can adequately compacted [Teixeira, P. et al. 2006].

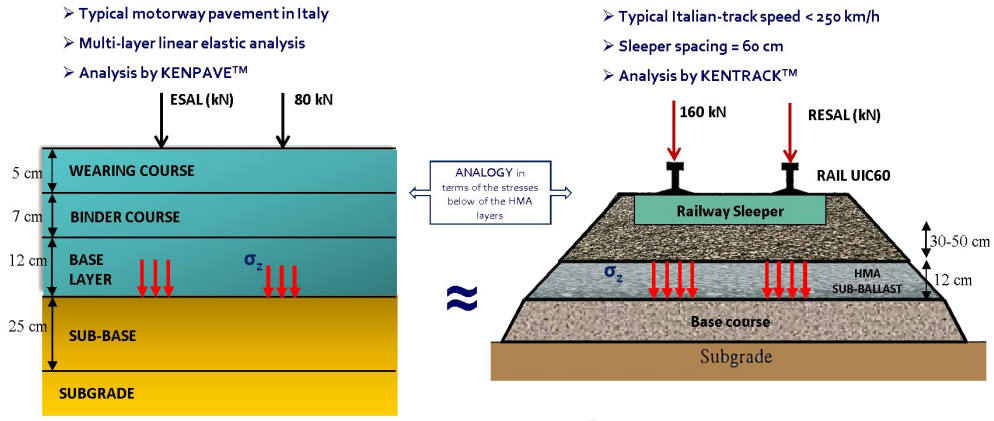


Figure 12. (a)Road and railway sections considered indicating layers applied

5.9.2. Simulations with Kenpave – Kentrack software[11]

The track system model was divided from top to bottom into rails, springs, ties, and layered support system. Rail, pads, and sleepers modeled as prismatic elements with an isotropic linear elastic constitutive FEM model for trackbed design. One hundred cycles were imposed to avoid the cumulative damage effect. The software simulations were carried out considering the air temperature range from 0°C to 35°C. Concerning finding the standard axle load, several simulations were run considering axle-passages between 80kN (roads) until 200kN (railways).

The type of rail fastener chosen, adopted by RFI (2016) in the superstructures for AV/AC, is the *Pandrol Fastclip Attack* (Fig. 13). It consists of a track anchorage system to the flexible double layer platform (constituting the second stage). The first level includes an elastomeric slotted rubber plunger of 12mm thick, interposed between the platform and a steel plate of 14mm thick, with the aim of transferring the rail loads to the tie. The second stage consists of a 4.5mm thick synthetic rubber under-rail plate. The overall rigidity, K_d is given by the sum of the contributions of the two stages. Considering the average values, the totality of the attachment member is equivalent to:

$$k_d = \frac{k_1 \cdot k_2}{k_1 + k_2} = \frac{75 \cdot 300}{75 + 300} = 60 kN/mm \qquad \text{(Eq. 9)}$$



Typical performance data				
	Value	Test method	Remarks	
Static stiffness (Rubber pad)		40 -100 MN/m	EN13146-4: 2002	Assembly secant stiffness between 5kN and 80kN
Static stiffness (Plastic pad)		> 150 MN/m	EN13146-4: 2002	Assembly secant stiffness between 5kN and 80kN
Clamping force	(FC1501)	> 16 kN	EN13146-7: 2002	Nominal toe load = 10 kN per clip
	(FC1601)	> 22.5 kN	AREMA Chapter 30	Nominal toe load = 12.5 kN per clip
Creep resistance	(FC1501)	> 9 kN	EN13146-1: 2002	Onset of slip
	(FC1601)	> 10.7 kN	AREMA Chapter 30	Proof load test
Electrical insulation		> 10 kΩ	EN13146-7: 2002	Rail-to-rail, wet, on a concrete sleeper

Figure 13. (a)Pandrol fast clip; (b) Technical characteristics

The armament was of a conventional type with 60UIC rail on crushed stone (ballast). The nominal gauge was 1.435 mm. On the high-speed rail line, there was a track type RFI-260, mass 350kg, thickness 30cm, a length of 2.60m, and an Elastic modulus of 50GPa [RFI, 2016]. The crossbars had a separation of 60 cm. The tracking platform of 13,10m with a double track at a center distance of 4.50m, and sub-ballast in a bituminous conglomerate of thickness 12cm.

[11] See Annex 03 Framework of rail modelling, and Annex 04 Kenpave computer program analysis.

Therefore, the sections in the railway platform were underlayment system. The main parameters (road-railway) used to create the reference section are in Tables 2-3.

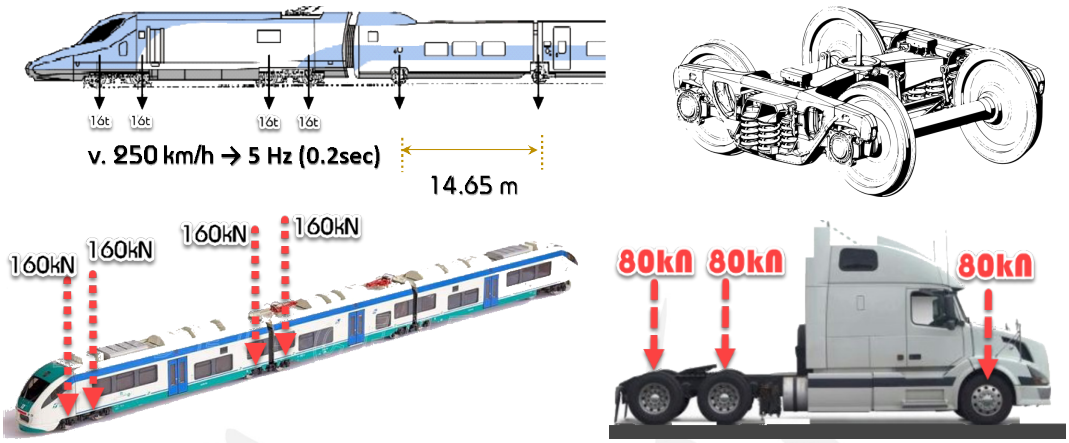


Figure 14. (a) Dynamic train configuration and load distribution; (b) Convoy Aln 501- Ale Minuetto (train for simulations); (c) Vehicle considered for road simulations

TABLE 2. PARAMETERS SELECTED FOR KENTRACK SIMULATIONS

Type of rail 60E1 (UIC) [12] 3141				Fastening system type Pandrol Fastclip	
Young's modulus [MPa]	Proportionality limit [MPa]	Resilience [MPa]	Stiffness [MN/m]	Clamping force [kN]	Creep [kN]
192000	500	600	>150	>16	>9
Sleepers in PSC[13] wires					
Sleeper thickness [cm]	Sleeper width [cm]	Sleeper weight [kg/m]	Sleeper distance [cm]	Length of the crosspiece [cm]	Rail [cm]
21	16.9	52	60	259	143.5

TABLE 3. PARAMETERS SELECTED FOR KENPAVE SIMULATIONS

Material:	Responses:	N° Periods	N° Layers
Linear	Displacement	5	4
Load information			
Load[14]	CR	CP	NR
single axle	12.62	800	1

The vehicle considered operating for the regular Italian rail lines was the *Minuetto Ale501/502-Le220*, composed of 4 bogies (16 axles) with a distance between axles (wavelength of vibration) of 14,65m. The running speed was between 160-250km/h (56-70m/s), diesel-electric power and 1,435mm standard gauge. The dimensions were $52 \cdot 2.95 \cdot 3.80$m. Load train consisted of 160kN in two wheels on each side, spaced at 60cm on centers (Fig. 15).

- It was considered a frequency f equivalent to 5Hz, that is, equal to the ratio between average train speed v, and wavelength λ (ratio between the maximum speed of a long-distance train 250km/h or 69.45m/s, and the wavelength characterized by the axle distance-tandem wheel, Eq. 10).

$$f = \vec{v}/\lambda \qquad \text{(Eq. 10)}$$

  - v= speed of the train considered (m/s);
  - λ= wavelength (axle distance between wheels), in meters.

Also, according to Celard, A.C. [Conti Puorger, A. et al. 1976] is determined by:

[12] UIC: "*Union Internationale des Chemins de fer*"
[13] Portland slag cement (special grade cement for manufacture of sleepers for Railways)
[14] CR: Contact radius of circular loaded areas [cm];
CP: Contact pressure on circular loaded areas [psi];
NR: N° of radial coordinates to be analyzed under a single wheel [-]

$$T = \left(l \cdot 3600\right) / v \rightarrow f = \frac{1}{T} \qquad \text{(Eq. 11)}$$

- T= period (sec.) or inverse of the frequency (Hz); l= length of the axle-wheels, in km; v= train speed (km/h).

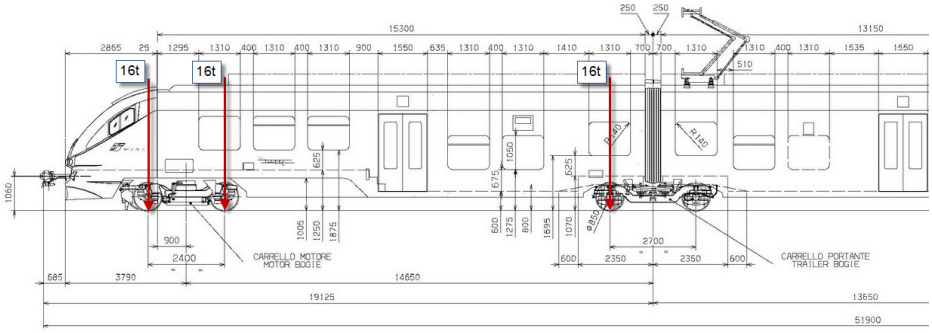


Figure 15. Technical dimensions of train *ALn 501-Ale Minuetto*. Load configuration

In the interface of Kentrack ("Loads"), are indicated 2 number of axle loads with distances from 47.244 to 141.73 inches (1.20 to 3.60m), and each load with a value of 17984 lbs (80kN). Then, the number of cross ties for single axle analysis was "six" (Table 4).

TABLE 4. STANDARD LAYER PROPERTIES FOR THE DEFAULT CASE

Layer	Thickness		Poisson's ratio[15]	Young's modulus
	mm	inches		psi(x6.89kN/m^2)
Concrete Tie	210	8.27"	0.35	4000000
Ballast	350	13.78"	0.20	18490
Sub-ballast	120	4.72"	0.40	1305000
Subgrade	300	11.81"	0.45	21350
Bedrock	---	---	0.50	10000000000

- In the "Model Layer" menu, the parameters that characterize the structure composition are the total number of layers, the tolerance of vertical deviation for the integration of the Bessel function (0.001 to 0.0001) NLTC=5. Also, the material properties (Poisson coefficient, elastic or dynamic modulus for different periods, and parameters of nonlinearity).

5.9.3. A Predictive model of temperature

The influence on the mechanical characteristics and thermal susceptibility of the bituminous conglomerate has motivated measuring the thermal cycles. Temperature was critical to the selection of the long-term grade performance values of the layer. Climatic conditions influenced the bearing capacity regarding the thermal and moisture regimes [Di Mascio, P. et al. 1999_2014]. Pavement temperatures linked with the stabilization, curing and moisture movements of the bituminous sub-ballast layer [Sol-S., M. et al. 2017; Solaimanian, M. et al. 1993].

In this research, the conventional measures of temperature, relative humidity, atmospheric pressure, wind speed-direction, precipitation, and sunlight hours during 12-months were chosen from statistics [Naude et al. 2005]. Also, the global horizontal radiation, direct standard radiation, dry-bulb temperature, and wind speed, were taken according to measures by Palermo's airport meteorology station. Considering the heat transfer based on the solar-thermal radiation between the railway and the climatic zone, and the heat-convection between the surface of the pavement and the air, an exact calculation of thermal prediction was made in the sub-ballast. So, the climatic parameters were the thermal regime of the railroad, air temperature, solar radiation, and wind speed (Fig. 16).

[15] The value adopted for the bituminous Poisson ra-tio (ν = 0.4) is the same value used by Rose et al. (2004) when validating substructure computer model stress values through in-situ measurements.

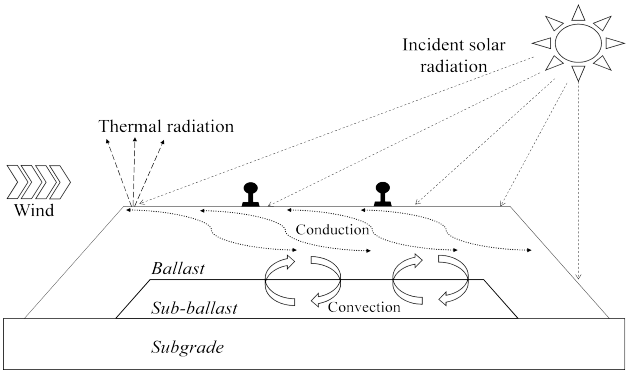


Figure 16. Energy balance in railway track layers [Soto, F.M. et al. 2017]

Straub, A.L. [1968] developed a computer model to predict pavement temperatures based on air temperature and solar radiation. Dempsey, B. et al. 1987, developed a simulation model based on the heat transfer and energy balance theories to evaluate frost action in multilayered pavements. Barber (1957) observed that pavement temperature fluctuations roughly followed a sine curve (sinusoidal functions) with a period of one day by including both the solar radiation and the air temperature in the model. Crispino, M. (2001) illustrated the results obtained after two years measuring the thermal fluctuations to evaluate the average seasonal temperature by sinusoidal functions for one day. A FEM model that predicts pavement temperatures during summer condition based on the heat transfer was presented by Hermansson (2001). Ferreira et al. (2012) analyzed through a FEM model, the long-term behavior of the deformation of the sub-ballast layer.

Thus, many models are available to define the temperature into the pavements, but in this thesis, there are both empirical took into consideration: Barber (1957) based on the theory of heat conduction in solids that solve the problem in a semi-indefinite body with the horizontal surface in contact with air, and Marchionna (M. et al. 1985), that proposed a climatic model for Italy. Thus, we proceeded to apply the ***Barber's temperature model***, used to validate pavement structures, which proved to be useful in railway. Eq. 12 expresses the layer temperature at depth z and at time t:

$$T_{pav(z,t)} = T_M + R + \left(\frac{T_V}{2} + 3R\right) \cdot F \cdot e^{-Cx} \cdot \sin\left(0.262t - C_x - arctg\left(\frac{C}{hc/K + C}\right)\right) \qquad \text{(Eq. 12)}$$

- $T_{pav(z,t)}$ = pavement temperature at the depth z and time t [°C];
- T_M = mean effective air temperature[0-35°C]; T_V = maximum variation in temperature [10.5°C];
- $R = 2/3 \cdot (b \cdot I)/24h_c$ = contribution of the solar radiation [8.35°C];
  - $h_c = 4.882 \cdot (1.3 + 0.4332 \cdot v^{3/4})$ = surface coefficient based on the wind speed [24.25 kcal/hours m²°C];
  - v = wind speed [17.25km/h]; I = average radiation [5398 kcal/m²day];
  - b = absorptivity of surface to solar radiation [0.21];
- $C = (0.131 \cdot s \cdot w)/K$ [6.71 hour$^{0.5}$/m];
  - s = specific heat [0.21 kcal/kg°C]; w = density [2500 kg/m³];
- K = thermal conductivity [1.5 kcal/mh°C]; and
- x = depth [0.47 m];

For flexible pavements in roads, and considering the warm climatic conditions of the south of Italy, it was applied the model of ***Marchionna (Kenpave simulation):***

$$T_{pm}(z) = (1.467 + 0.043z) + (1.362 - 0.005z) \cdot T_{am} \qquad \text{(Eq. 13)}$$

- $T_{m(z)}$ = monthly pavement temperature at the depth z [°C]; T_M = mean effective air temperature [°C];

In the framework of this thesis, equation 12 used the variations introduced by Crispino (1998). The difference between road-railway is the surface absorptivity to solar radiation. For the road surface layer, the absorptivity was equal to 0.9 (Barber), in the case of railways a value of 0.21 (Crispino).

5.9.3.1. Environmental conditions.

Two different temperatures within the bituminous layers were calculated as the outcome of Barber's equation using various parameters for road and railway respectively (Table 5).

TABLE 5. VALUES ADOPTED FOR BARBER'S EQUATION

Parameters	Value	Units	Parameters	Value	Units
T_M	0-10-20-30-35-40	°C	**F**	0.68	_
T_V	10.5	°C	**C**	6.71	$hour^{0.5}/m$
I	5398	$kcal/m^2h$	**R**	6.71	$hour^{0.5}/m$
v	17.25	km/h	**K**	1.5	kcal/mh°C
h_c	24.25	$hour^{0.5}/m$	**s**	0.21	Kcal/kg°C
H	16.17	1/m	**w**	2500	Kg/m^3
B_{Barber}	0.9	_	$B_{Crispino}$	0.21	_

The operating methodology to calculate the temperature gradients is composed of different stages:

- Acquisition from the last 30-years of meteorological temperature values (operated by Sicilian and meteorological Information Service, SIAS);
- Meteorological data processing, dividing the year and calculate the average max/min temperatures $T^a_{max/min}$ for each year-period.
- Calculate the average air temperature $T_a(p)$ of the seasonal periods;
- The temperature inside each layer for each period, using Barber equation.

Each simulation for various temperatures (0, 10, 20, 30, 35 and 40°C) has considered that in the case of roads and rail, the depth of interest is 31cm and 47cm, respectively. Table 6 shows the results of temperatures by *Barber-Crispino* models[16].

TABLE 6. RESULTS T^a PAV(Z,T) OBTAINED FOR ROAD BASE AND RAILWAY SUB-BALLAST LAYERS

Air T^a	0°C		10°C		20°C		30°C		35°C		40°C	
N° hour	Road	Railway	Road	Railway	Road	Railway	Road	Railway	Road	Railway	Road	Railway
0	6.68	2.04	16.68	12.04	26.68	22.04	36.68	32.04	41.68	37.04	46.68	42.04
1	6.26	1.96	16.26	11.96	26.26	21.96	36.26	31.96	41.26	36.96	46.26	41.96
2	5.99	1.88	15.99	11.88	25.99	21.88	35.99	31.88	40.99	36.88	45.99	41.88
3	5.87	1.80	15.87	11.80	25.87	21.80	35.87	31.80	40.87	36.80	45.87	41.80
4	5.93	1.73	15.93	11.73	25.93	21.73	35.93	31.73	40.93	36.73	45.93	41.73
5	6.15	1.68	16.15	11.68	26.15	21.68	36.15	31.68	41.15	36.68	46.15	41.68
6	6.52	1.64	16.52	11.64	26.52	21.64	36.52	31.64	41.52	36.64	46.52	41.64
7	7.02	1.63	17.02	11.63	27.02	21.63	37.02	31.63	42.02	36.63	47.02	41.63
8	7.60	1.64	17.60	11.64	27.60	21.64	37.60	31.64	42.60	36.64	47.60	41.64
9	8.24	1.66	18.24	11.66	28.24	21.66	38.24	31.66	43.24	36.66	48.24	41.66
10	8.89	1.71	18.89	11.71	28.89	21.71	38.89	31.71	43.89	36.71	48.89	41.71
11	9.49	1.78	19.49	11.78	29.49	21.78	39.49	31.78	44.49	36.78	49.49	41.78
12	10.02	1.85	20.02	11.85	30.02	21.85	40.02	31.85	45.02	36.85	50.02	41.85
13	10.44	1.94	20.44	11.94	30.44	21.94	40.44	31.94	45.44	36.94	50.44	41.94
14	10.71	2.02	20.71	12.02	30.71	22.02	40.71	32.02	45.71	37.02	50.71	42.02
15	10.82	2.10	20.82	12.10	30.82	22.10	40.82	32.10	45.82	37.10	50.82	42.10
16	10.76	2.17	20.76	12.17	30.76	22.17	40.76	32.17	45.76	37.17	50.76	42.17
17	10.54	2.22	20.54	12.22	30.54	22.22	40.54	32.22	45.54	37.22	50.54	42.22
18	10.17	2.25	20.17	12.25	30.17	22.25	40.17	32.25	45.17	37.25	50.17	42.25
19	9.67	2.27	19.67	12.27	29.67	22.27	39.67	32.27	44.67	37.27	49.67	42.27
20	9.08	2.26	19.08	12.26	29.08	22.26	39.08	32.26	44.08	37.26	49.08	42.26
21	8.45	2.23	18.45	12.23	28.45	22.23	38.45	32.23	43.45	37.23	48.45	42.23
22	7.80	2.18	17.80	12.18	27.80	22.18	37.80	32.18	42.80	37.18	47.80	42.18
23	7.20	2.12	17.20	12.12	27.20	22.12	37.20	32.12	42.20	37.12	47.20	42.12
Δ	**8.35**	**1.95**	**18.35**	**11.95**	**28.35**	**21.95**	**38.35**	**31.95**	**43.35**	**36.95**	**48.35**	**41.95**

The experimentation conducted has allowed the determination of the temperatures in the sub-ballast layer of the asphalt mixture (Fig. 17).

[16] Road base layer depth 31.5cm; Sub-ballast railway depth 47cm; Values of absorptivity in the case of railway = 0.21 (Crispino M. 2001) and of road = 0.9 (Barber E. 1957)

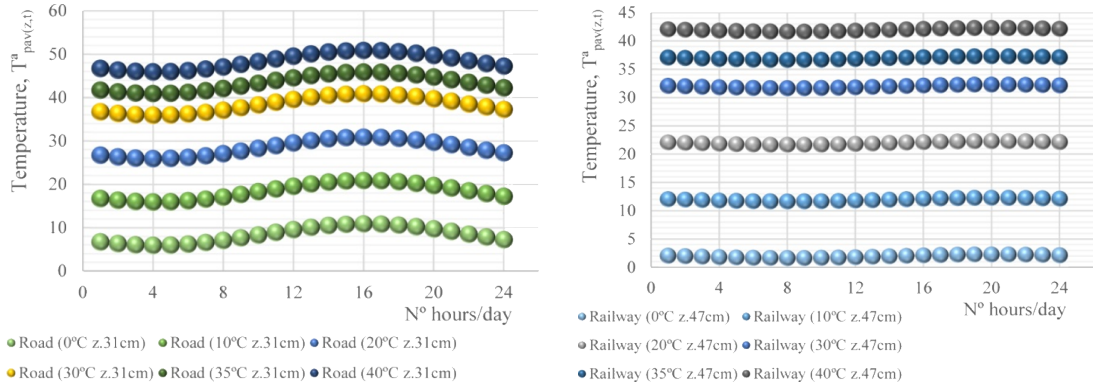


Figure 17. Daily variation of T^a in the pavement at the depth z and time t [°C] between road and railways

Based on the acquired measurements, the average seasonal temperatures in the layer (spring, summer, autumn, and winter respectively) were determined related to Sicilian climatic conditions. The following graphs show the evolution of the temperature in each layer for the most representative air temperatures (0°C and 35°C) in each section of pavement and railway, along with a sinusoidal cycle marked by the daily hours (Fig. 18).

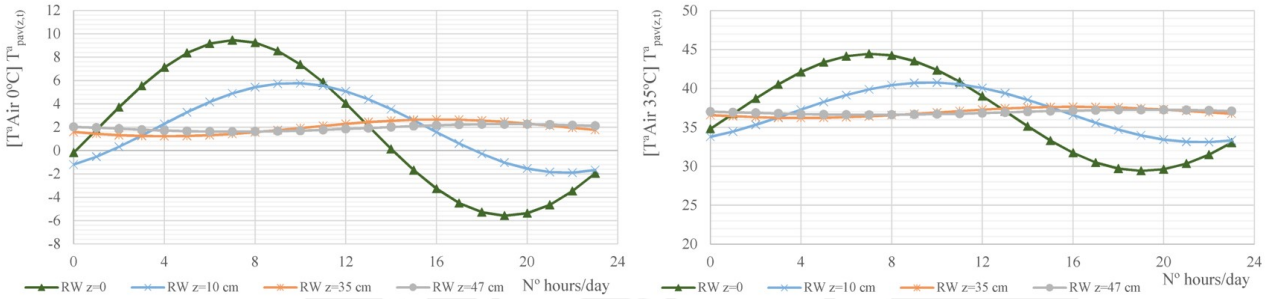


Figure 18. 24hour-T^a variation at different depths [Air T^a 0°C-35°C] between road and railways

Afterward, it was possible to calculate the mechanical characteristics of the bituminous materials with the Witczak (Andrei D. et al. 1999) predictive model based on the volumetric properties of the mixture and the characteristics of the binder (Eq. 3). It was notable that variables related to aggregate gradation (ρ_{200}, ρ_4, ρ_{38}, ρ_{34}), mix volumetric (volume of air voids, V_a and, volume of effective bitumen, V_{beff}) had the most influence on the E^* stiffness of asphalt mixes. Table 7 shows the temperatures and the properties characterizing the bituminous materials[17].

TABLE 7. PARAMETERS INSERTED IN THE WITCZAK FORMULA

Air temperature 0°C		Layer X̄ T^a [°C]	μ [10^6 poise]	log |E*|	|E*| [MPa]	ν
Road	WC	8.34	11.6057	1.174	10282.6	0.4
	BC	8.34	11.6057	1.208	11135.2	0.4
	BA	8.35	11.6057	1.283	13219.8	0.4
Rail	SB	1.94	59.5026	1.434	18929.8	0.4
Air temperature 35°C		**Layer X̄ T^a [°C]**	**μ [10^6 poise]**	**log |E*|**	**|E*| [MPa]**	**ν**
Road	WC	43.34	0.0014	-0.130	510.39	0.4
	BC	43.34	0.0014	-0.098	549.56	0.4
	BA	43.35	0.0014	-0.045	621.17	0.4
Rail	SB	36.95	0.0074	-0.235	1185.68	0.4

(*) WC: wearing course; BC: binder course; BA: base course; SB: sub-ballast layer.

[17] In applying the equation, it was assumed that the HMA has a bitumen content of 5.5 percent by volume and an air voids content of 4 percent, the mineral aggregates have 6 percent passing the No.200 sieve and, the load is applied at a frequency of 28Hz. These values are random because the objective, in this case, is to represent a point of comparison between the road model and the railroad.

The complex modulus has been identified for calculating the response of a bituminous structure to traffic loading as well as its resistance to fatigue [Benedetto, H. et al. 2016]. Properties of asphalt binders and mixes are incorporated into Witczak predictive E^* model to determine asphalt dynamic modulus as an integral step in model evaluation [Bari, J. et al. 2006; Yoder, E. et al. 1975].

5.9.4. Railway Equivalent Single-Axle load, "RESAL"

It was, therefore, necessary to study the ***rail traffic*** (*railway equivalent single axle load, RESAL*), from a particular analysis of the geographical area where the infrastructure is located. For this reason, the axle number, layout, and load have been defined as the rail axle load that produces the same vertical displacement (δ) at high temperatures and the same horizontal tensile strain (ε) at low temperatures. On the road, an ESAL of 80kN was adopted. For railways was used the passages of different types of axles: 80, 100, 120, 140, 160, 180 and 200 kN.

TABLE 8. DEFORMATIONS RESULTS AT DIFFERENT TEMPERATURES

	Wheel load (ton)	Tª [ºC]	Tensile strain [εx]	Vertical displacement, mm [δ]
Road (Base layer)	8	**0**	**2.940E-05**	4.510E-03
		10	5.230E-05	5.690E-03
		20	1.020E-04	7.540E-03
		30	2.013E-04	1.016E-02
		35	2.763E-04	1.169E-02
Railway (Sub-ballast)	8	**0**	1.380E-05	5.940E-03
	10		1.720E-05	7.400E-03
	11		1.900E-05	8.120E-03
	12		2.070E-05	8.840E-03
	14		2.410E-05	1.027E-02
	16		**2.750E-05**	1.169E-02
	18		3.110E-05	1.310E-02
	20		3.440E-05	1.450E-02
	Wheel load (ton)	**Tª [ºC]**	**Tensile strain [εx]**	**Vertical displacement, mm [δ]**
Road (Base layer)	8	0	2.940E-05	4.510E-03
		10	5.230E-05	5.690E-03
		20	1.020E-04	7.540E-03
		30	2.013E-04	1.016E-02
		35	2.763E-04	**1.169E-02**
Railway (Sub-ballast)	8	**35**	2.550E-05	6.390E-03
	10		3.190E-05	7.950E-03
	11		3.520E-05	8.720E-03
	12		3.840E-05	9.949E-03
	14		4.480E-05	1.103E-02
	16		5.130E-05	**1.256E-02**
	18		5.800E-05	1.409E-02
	20		6.440E-05	1.560E-02

The horizontal tensile strains and the deflections produced were compared (Table 8).

The values of 14.15 ton and 17.85 ton are the weights of the railway axle load that produces the same vertical displacement at high temperatures induced and the same horizontal tensile strain at low temperatures, respectively, produced by ESAL in the road structure (Figure 19).

Thus, an average of **16 ton** has been selected as the optimal value of RESAL.

- *The **tensile strain** was selected at low temperature because it is the factor governing fatigue cracking.*
- *The **vertical displacement** was selected at high temperature because it is the factor leading rutting.*

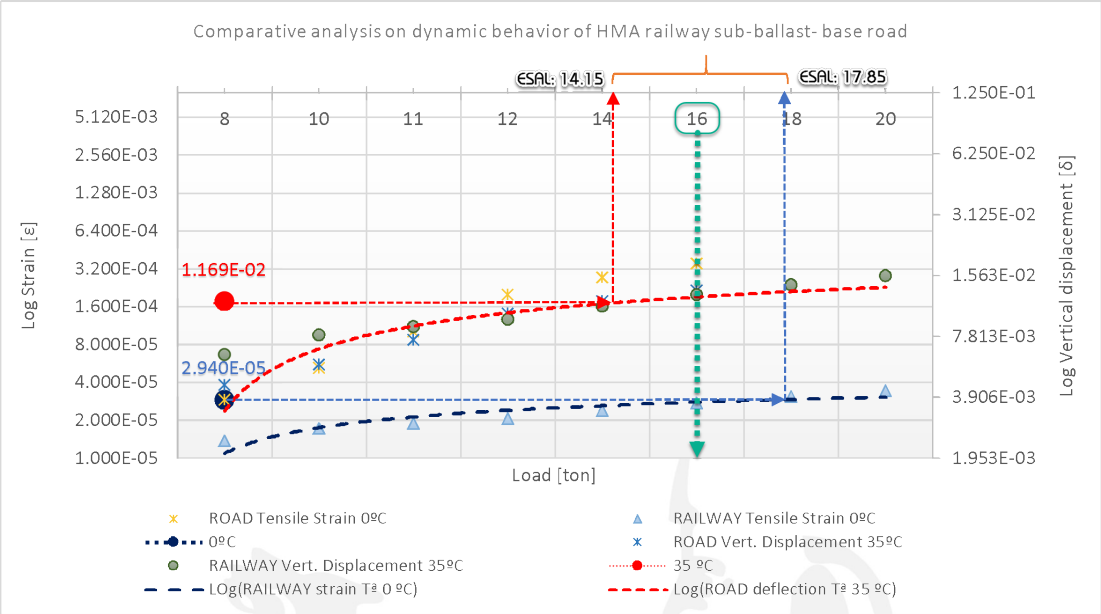


Figure 19. Results obtained from the simulations carried out with KENPAVE and KENTRACK

5.9.4.1. Conversion of traffic spectrum in "RESAL"

Above, we have calculated the compression stress at the bottom of the base layer (roads) and the same for sub-ballast layer (to study fatigue cracking), and now, the next step, is to transform the entire spectrum of traffic into the number of ESALs for railways.

The rail design life is 50-years for the high-speed lines and 30-years for the regular lines. The amount of traffic is measured regarding the number of repetitions of axle-load application, and the train passages during the service life [Sadeghi, J. et al. 2010].

The traffic information to be used for the thickness design includes the magnitude of wheel loads and the number of repetitions per year (Table 9; Fig. 20).

TABLE 9. VEHICLE CATEGORIES AND THEIR AXLE CONFIGURATION FOR SICILIAN MAIN RAIL LINES (2016).

Type of train[18]	Composition	Nº axles Loc+Coach	Distribution axle-load [Ton] (Loc+Wagons)							
			Locom.	1st	2nd	3rd	4th	5th	6th	Total ₸
Long-Distance (Intercity)	1Locom. + 4 coachs	6+16	₸20	₸13	₸13	₸13	₸13			22
	1Locom. + 5 coachs	6+20	₸20	₸13	₸13	₸13	₸13	₸13	₸13	26
Shuttle regional train	1Locom. + 3 coachs	4+12	₸18	₸12	₸12	₸12				16
	1Locom. + 4 coachs	4+16	₸18	₸12	₸12	₸12	₸12			20
Minuetto EMU	Loc.+wagon+Loc.	8	₸16							8
Diesel ALn668	1 Railcar	4		₸11						4
	2 Railcars	8		₸11						8
Wagon freight	1Locom. + 8 Wagons	6+32	₸20	₸20	₸20	₸20	₸20	₸20	₸20	38



Figure 20. (a) Train main lines analyzed; (b) Types of trains in Italy (Trenitalia)

[18] TRENITALIA, FS Italiane Group and Ferrovie Dello Stato Italiane S.p.A; RFI Rete Ferroviaria Italiana S.p.A.

Three different traffic lines in the Sicilian network (*Messina-Catania; Siracusa-Catania, and Catania-Caltanissetta)* were investigated, and their traffic spectra were converted to RESAL:

$$T_D = 365 \cdot T_{HV} \cdot [(1+r)^n - 1] / r$$
$$N_D = T_D \cdot \eta \cdot A \cdot RT = T_D \cdot (\sum_j^m f_j \cdot \mathrm{n}_j) / \sum_j^m f_j) \cdot A \quad \text{(Eq. 14)}$$
$$A = \sum_k^m f_k \cdot (P_k / P_r)^\gamma$$

- T_D = Total number of load passages expected over the entire service life [-];
- T_{HV} = Average daily traffic in the year of the construction [-];
- r = Annual growth rate of traffic (0-10%)[-]; n = Design life (30 years in case of sub-ballast) [year];
- N_D = RESALs at the end of the service life [-]; N_j = Number of passages of the j-axle;
- f_j = frequency of the j-axle; η = average number of axles for heavy wagon;
- P_k = k-axle load [kN]; P_r = Axle load of the reference axle [kN];
- γ = Coefficient that depends on the material and the pavement structure.
- For flexible and bituminous pavement is equal to 5 [see Structural Number];
- f_k = Frequency of passage of the k-axle load [-] and,
- A= coefficient of aggressiveness[19] (e.g., road highway outside the city, A=1.57).

In that way, the traffic spectrum for railways was determined (Fig. 21; Tables 10-11). Considering an average of increased rate industrial traffic of 1%, the rail equivalent single axle load (R_{ESAL}) obtained is 3.7×10^7 (Level 3 of "volumetric mix-design method").

TABLE 10. "SPECTRUM OF TRAFFIC" FOR "MESINA-CATANIA" MAIN RAIL LINE (ITALY).

Category of axes		N° Total Equal-axes	fk [%]	N° Passages x 100 trains	N°passages / N° axes	Average N° axles for train, n [%]	Coefficient of aggressiveness A
T	200	238	24.04	57.22	0.240	0.57	0.734
T	180	72	7.27	5.24	0.073	0.05	0.131
T	160	288	29.09	83.78	0.291	0.84	0.291
T	130	136	13.74	18.68	0.137	0.19	0.049
T	120	256	25.86	66.20	0.259	0.66	0.061
Total T		990	100	231.12	1.00	2.31	1.27

ESAL equivalent T	T_{HV}	R (%)	T_D	$N_{D\ (ESALs)}$
160 kN	990.00	0	1.084E+07	3.171E+07
		0.002	1.116E+07	3.265E+07
		0.004	1.149E+07	3.362E+07
		0.006	1.184E+07	3.463E+07
		0.008	1.220E+07	3.568E+07
		0.010	1.257E+07	**3.68E+07**

TABLE 11. SUMMARY OF THE TRAFFIC LEVELS EXPECTED

RESALs at the end of the service life (30 years)			
Traffic growth [%]	Catania Messina	Siracusa Catania	Caltanissetta Catania
0	3.171E+07	1.796E+07	3.131E+06
0.2	3.265E+07	1.849E+07	3.223E+06
0.4	3.362E+07	1.904E+07	3.319E+06
0.6	3.463E+07	1.961E+07	3.419E+06
0.8	3.568E+07	2.020E+07	3.523E+06
1	3.677E+07	2.082E+07	3.630E+06

$R_{ESAL} = 3.67 \times 10^7$

[19] An example, for a highway outside cities, the coefficient of aggressiveness, A, is around 1.57. For a main rail-line the value obtained is around 0.30, considering the different γ coefficient respectively. According 1993 AASHTO Guide for Flexible Pavement Structural Design.

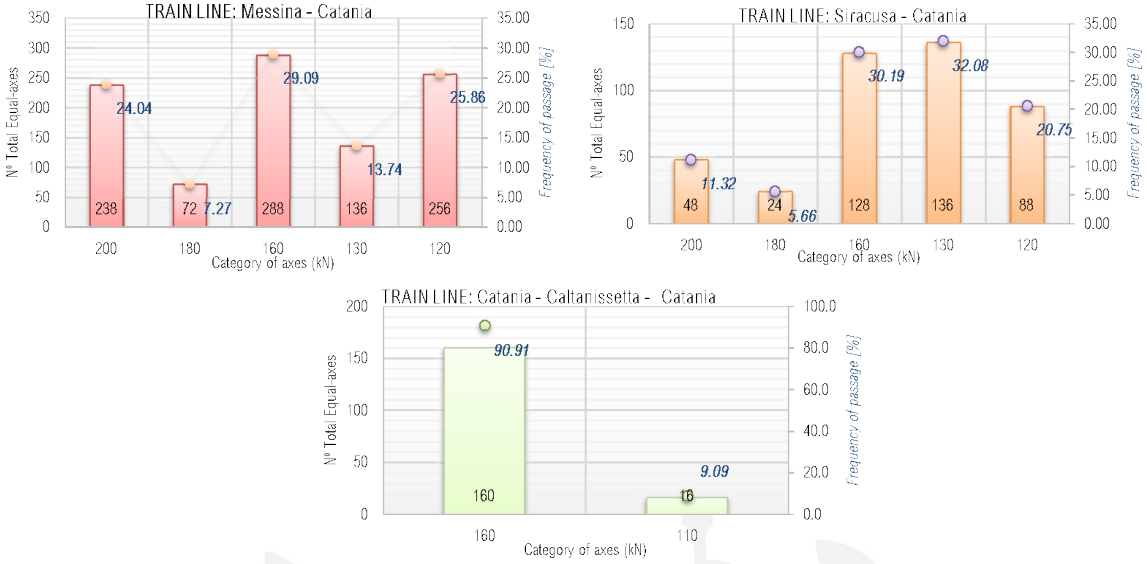


Figure 21. Traffic spectrum of main rail-lines [Nº axle/day vs. Axle load], [Axle load vs. %passages/day]

5.9.4.2. Definition of N_{design} as a function of Traffic-T[a]

Table 12 shows the recent updates of Superpave (SGC) for compaction parameters of HMA [AASHTO R35, 2001]. The number of gyrations was selected based on the traffic level calculated.

TABLE 12. REVISED NDESIGN TABLE PROPOSED BY AASHTO R35 (2015).

Design ESALs (millions)	Averaged Design Air Temperature				
	$N_{initial}$	N_{design}	$N_{maximum}$	% G_{mm} $N_{initial}$	% G_{mm} N_{max}
<0.3	6	50	75	<91.5	<98.0
0.3 to <3	7	75	115	<90.5	<98.0
3 to <30	8	**100**	160	<89.0	<98.0
>30	9	**125**	205	<89.0	<98.0

A relationship has been established between the number of maximum ESALs determined for the rail sub-ballast of the study case and the values that in recent years have been identified for the "volumetric mix-design method." Different regression curves were applied corresponding to the following standards: (1994) SHRP A-407/M-002; (2007) NCHRP-573; and (2015) AASHTO-R35 (Fig. 22a). Kentrack® examined the new asphalt grading trackbed system and their properties inside the software. Once the traffic spectrum was converted in RESAL, it was calculated the N_{design}.

Therefore, considering the recently logarithmic regression equation, correspondence between the number of N_{des} gyrations and the rail axle load value has been defined (Fig. 22b).

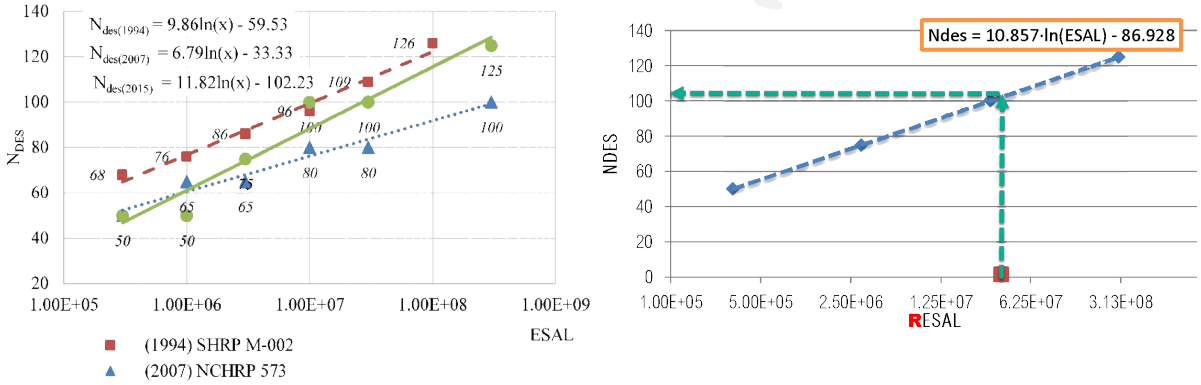


Figure 22. (a) N_{design} recommended by SGC standards; (b) Logarithmic regression by interpolation of N_{des} values

N_{des} was obtained with the maximum value of results achieved in Table 12 in the three rail-lines studied by using the regression equation: **Nd=25,10 · Log (RESAL) - 86,928** (Fig. 23). A logarithmic regression resulting from the interpolation of the N_{design} values of the "volumetric mix-design method" has been used to determine a correspondence between the nº of RESALs and the number of gyrations.

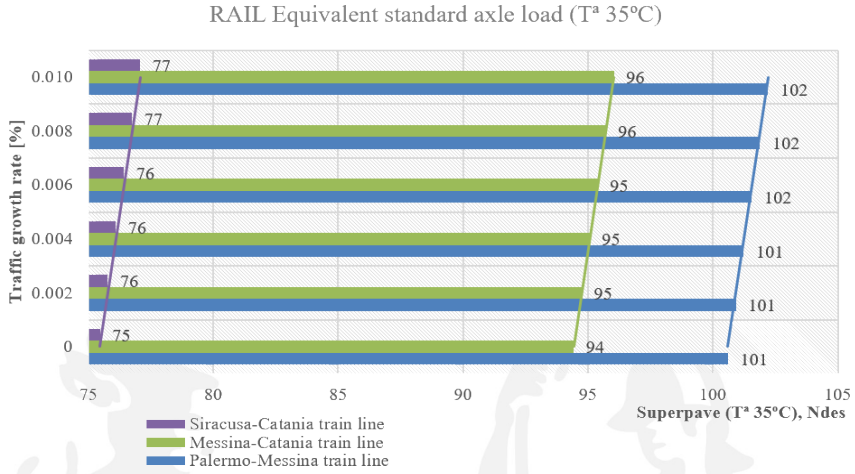


Figure 23. N_{design} obtained for different track-lines and different values of annual traffic growth rate

The values of N_{max} and N_{Init} are expressed as a function of N_{DES} according to Chapter 4.

A unique correspondence between the N_{des} - RESALs has been defined. In this lab-research, the "volumetric mix-design method" requires optimal specimen compaction with SGC at the design number of gyrations of **N_{des}=102; N_{init}=8 and N_{max}=162 gyrations.**

Once the overall procedure for the mix design was defined, and the necessary parameters are already known, a laboratory verification will be conducted in the next Chapter 6 with conventional HMA mixtures and three different rubberized asphalt blends by a dry process.

5.10. Conclusion

Thermal regime and Traffic, as the leading parameters have been studied concerning to early-life performance by monitoring mixtures under simulated trafficking [Jitareekul, P. et al. 2007].

This study has provided an advance for the development of a new methodology to adapt the Volumetric SGC, prepared for the road domain, to the railway system defining a new "RESAL," i.e., rail equivalent single axle load. According to this procedure, the standard axle for railway has been defined equal to 160 kN.

The initial objective of applying the AASHTO-Calibrated mechanistic procedure for flexible layers has been developed in several stages of calculation, allowing the similarity of the tensions between the road layer and the sub-ballast layer. The combination of the Kenpave-Kentrack calculation method and the search for the Volumetric energy parameters that allows to Superpave be adapted to the railway field have been reflected in a new methodology, called in this research as "SupeRail."

Its advantage can be applied to other railway traffic and weather conditions.

I would like to thank Professor Jerry G. Rose, from the University of Civil Engineering of Kentucky (USA) for his collaboration providing Kentrack software necessary for the performance of this research.
In gratitude to this thesis for contributing with his extensive publications that have favored the understanding of the concepts related to the modeling, structural calculation and analysis of the railway multilayer section.

2017

Chapter 6

RESULTS (LABORATORY TESTING). DISCUSSION

PH.D. FERNANDO M. SOTO

List of Figures Chapter 6

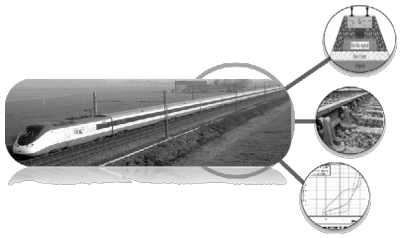
Figure 1. (a) Materials and mixtures specifications on this research; (b) HMA_DRY Specimens 144
Figure 2. HMA trial mixtures developed in a first SGC volumetric mix-design 145
Figure 3. (a) Results of HMA b.4% m1±300gr; (b) Diagram of the relationship between mass and height 146
Figure 4. (a) Relationship between %Va and height of the mixture; (b) %Va vs. Bulk specific gravity 147
Figure 5. (a) Diagram of the relationship between mass and height for all binders; (b) Interpolation %b*-%Va 147
Figure 6. (a) Densification curves for trial HMA mixtures; (b) Illustration explained strong-weak aggregate structure according to the slope of the compaction-curve 148
Figure 7. (a) HMA specimens developed as final mix-design; (b) HMA grading curve adjusted; (c) Mixtures 149
Figure 8. Air voids vs. Binder content in HMA samples (Ndes.102; ϕ150x120mm) 151
Figure 9. Densification curves for optimal HMA(RFI) mixtures ϕ150 · 120mm 151
Figure 10. (a) Marshall and SGC HMA mixtures; (b) ITSR and IDT tests; (C) SGC specimens 152
Figure 11. SGC Densification curves for optimal HMA mixtures ϕ150 · 64.5mm 153
Figure 12. Marshall results for optimal HMA(b.4%) mixtures ϕ150 · 64.5mm 154
Figure 13. Representation of substitution of granular rubber to the inert of similar granulometry 155
Figure 14. Mathematical substitution of rubber in the granulometric grading curve 155
Figure 15. (a) SGC Development of DRY 1.5% (1st trial mix-design); (b) Swelling effect 157
Figure 16. (a) Mass vs. height diagram DRY 1.5% (Ndes. 102); (b) %Va vs. Density; (c) %Va vs. %binder 158
Figure 17. (a) Densification curves DRY 1.5% (1st trial mix-design); (b) Regression values from trend-line 159
Figure 18. The inhomogeneous concentration of rubber in different sections of the DRY1.5% blend 160
Figure 19. Increase in rubber mass during curing for different specimens of trial DRY1.5% blend 160
Figure 20. Swelling effect on rubber-modified HMA samples of Ø150x120mm manufactured according SGC 160
Figure 21. Schematic representation of the swelling effect and effects 161
Figure 22. (a) Non-uniform expansion-damage due to the uncontrolled rubber recovery; (b) Hydraulic extractor 161
Figure 23. (a) Post-compaction deformation by rebound effect on DRY 1.5% by SGC; (b) Swelling and bounce-back effects of rubber particles observed in cut specimens (black points raised) 162
Figure 24. (a) Scheme of densification curve. Rebounding effect after compaction; (b)Schematic proposed solution 162
Figure 25. (a) Γmm vs. Ndes under DRY1.5% mixtures confined/unconfined in molds during 24h; (b) Results 163
Figure 26. Preliminary stage of comparison densification curves 164
Figure 27. Schematic representation of research stages and previous results 164
Figure 28. Densification curves for HMA and DRY1.5% mixtures both at N_{des}.102 165
Figure 29. Empirical "beta" approach method 166
Figure 30. Example of comparison between the compaction curves of HMA b.4%-DRY1.5 b.5% 167
Figure 31. Densification curves (HMA b.5%-DRY1.5 b.5,5%); (a) Each sample; (b) Averaged as Log(Ndes) 167
Figure 32. (a) Results of each "beta" HMA vs. DRY1.5%; (b) Averaged results adopted 168
Figure 33. (a) Specimens compacted and extruded after 24h; (b) Flowchart of DRY1.5% Ndes.152 168
Figure 34. (a) DRY1.5%. Graph %Va vs. %Binder; (b) Optimum bitumen content from the regression equation 169
Figure 35. (a) Densification curves DRY 1.5 b. 5%;5.5%; (b) Trendline and regression equations 170
Figure 36. (a) Specimens compacted and extruded after 24h; (b) Flowchart of DRY2% rubberized mixtures 170
Figure 37. (a) DRY 2%. Graph %Va vs. %Binder; (b) Optimum bitumen content from the regression equation 171
Figure 38. (a) Densification curves DRY2.0%; (b) Trendline and regression equations. Comparison DRY1.5%-2% 172
Figure 39. Flowchart of DRY3% #80-20 b.6,5% mixture (Generic-Dry) 172
Figure 40. (a) Individual Densification curves DRY3.0% b. 650%;7%; (b) Trendline and regression equations 173
Figure 41. (a) Densification curves for all SGC mixtures; (b) Trendline and regression equations 174
Figure 42. Diagram 1. Percentage ratio of voids vs. Binder content 175
Figure 43. (a) Evolution of optimal binder content after one week due to the swelling effect of rubberized compacted specimen; (b) Air voids vs. Post-compaction days 175
Figure 44. (a) First slabs compacted at b.6%-6.5%; (b) Specimens of 20 · 20 · 6cm from slabs 176
Figure 45. Manufacture and cutting of roller slabs compacted (DRY1.5% b.5.5% mixture) 177
Figure 46. Manufacture and cutting of slabs compacted with mechanical roller for DRY 2% b.6% mixture 177
Figure 47. (a) Ratio optimal binder vs. Post-compaction days; (b) Values of evolution due to swelling rubber 178
Figure 48. (a) Roller vs. SGC air voids and optimal binder relationship; (b) Ratio voids-binder content with SGC 179
Figure 49. (a) Diagram %binder and %Va; (b) Diagram %binder and %VFA-VMA for each mixture 179
Figure 50. (a) Schematic of Performance Prediction; (b) Movements due to thermal variations and traffic loads 180
Figure 51. Dissipated energy in a fatigue test with HMA and DRY mixtures 181

Figure 52. (a) HMA samples; (b) DRY 1.5% samples; (c) DRY 2.0% samples 181
Figure 53. Air voids, VMA, VFA (%); (a) HMA samples; (b) DRY 1.5% samples; (c) DRY 2.0% samples 182
Figure 54. Phenomenological approach 183
Figure 55. (a) Load 0.6 kN; (b) Load 0.8 kN; (c) Load 1.0 kN; (d) Average Nf vs. Load amplitude 184
Figure 56. Fatigue life of the mixes tested. (a) Load vs. Log Nº cycles, Nf; (b) Load vs. Duration time test 184
Figure 57. Experimental law of fatigue resistant of each blend. (a) Exponential Regression analysis; (b) Whöler log-log fatigue curve (Stress amplitude vs. Number of cycle reversals to failure, Log stress vs. Log Nf) 185
Figure 58. (a) Hysteresis loop (amount of dissipated energy) theory; (b) Different Dissipated Energy between load cycles [Adapted from Carpenter, 2006]; (c) Hysteresis loop diagram [Moreno, F. 2015] 186
Figure 59. (a) Hysteresis loops; (b) Vertical displacement vs. Nf [HMA sample 1.1 (Load 0.6 kN; Nf: 23495 cycles)] 186
Figure 60. (a) Hysteresis loops; (b) Vertical displacement vs. Nf [DRY 1.5% sample 2.3 (Load 0.6 kN; Nf: 67637 cycles)] 186
Figure 61. (a) Hysteresis loops; (b) Vertical displacement vs. Nf [DRY 2% sample 2.3 (Load 0.6 kN; Nf: 182984 cycles)] 187
Figure 62. (a) Hysteresis loops; (b) Vertical displacement vs. Nf [HMA sample 3.3 (Load 0.8 kN; Nf: 20700 cycles)] 187
Figure 63. (a) Hysteresis loops; (b) Vertical displacement vs. Nf [DRY 1.5% sample 2.4 (Load 0.8 kN; Nf: 27431 cycles)] 187
Figure 64. (a) Hysteresis loops; (b) Vertical displacement vs. Nf [DRY 2% sample 2.4 (Load 0.8 kN; Nf: 31044 cycles)] 187
Figure 65. (a) Hysteresis loops; (b) Vertical displacement vs. Nf [HMA sample 1.3 (Load 1.0 kN; Nf: 6599 cycles)] 188
Figure 66. (a) Hysteresis loops; (b) Vertical displacement vs. Nf [DRY 1.5% sample 3.3 (Load 1.0 kN; Nf: 13892 cycles)] 188
Figure 67. (a) Hysteresis loops; (b) Vertical displacement vs. Nf [DRY 2.0% sample 2.2 (Load 1.0 kN; Nf: 27347 cycles)] 188
Figure 68. Representation of Log Δε (%) as a function of the dissipated energy of the three HMA samples (Load 0.6 kN, 5 Hz) 189
Figure 69. (a) HMA $_{RFI\ 1_1}$ Load 0.6Kn, Nf. 23495 cycles; (b) HMA $_{RFI\ 2_1}$ Load 0.6Kn, Nf. 34941 cycles (c) HMA $_{RFI\ 3_1}$ Load 0.6Kn, Nf. 32400 cycles. 189
Figure 70. HMA Load 0.6kN. (a)Avg. Values of dissipated energy; (b) Horizontal displacements vs. Nf; (c) Vertical displacements vs. Nf 190
Figure 71. HMA Load 0.6 kN results (Log △εi vs. ωi) 190
Figure 72. Effect of cracking propagation. (a) HMA cleaner and larger crack; (b) DRY 2% branched fracture 191
Figure 73. Young's modulus, Load amplitude and Nf cycles, Nf; (a) HMA blend; (b) DRY 1.5% mixture; (c) DRY 2% samples 194
Figure 74. Comparative mixtures at 3-5 Hz at 1kN; (a) Relationship frequency and number of fatigue cycles, Nf; (b) Young's modulus vs. fatigue frequency 195
Figure 75. Comparative between 3-5 Hz at 1kN; (a) Shear modulus vs. Fatigue cycles, Nf; (b) Young's modulus vs. Fatigue cycles 195
Figure 76. Stress-strain hysteresis loop for controlled stress flexural fatigue testing (a) HMA mixture comparative between 3-5 Hz at 1.0 kN; (b) DRY 1.5% f.3-5 Hz at 1.0 kN; (c) DRY 2% f. 3-5 Hz at 0.8 kN 196

List of Tables Chapter 6

Table 1. HMA trial grading curve (Granulometric adjustment by fraction)....145
Table 2. HMA trial recipe for laboratory mixtures [%]....145
Table 3. Scheme of the composition of mass-height samples....145
Table 4. Verifications of the Superpave mix-design....146
Table 5. HMA Relationship Mass_Hmm Compaction....146
Table 6. Average corrected specimen relative densities (%va_%binder)....147
Table 7. Average corrected specimen relative densities (VMA_VFA)....147
Table 8. HMA effective values for mix-design....148
Table 9. HMA final grading curve....149
Table 10. HMA final recipe for laboratory mixtures....149
Table 11. HMA. Volumetric analysis of recipes for laboratory (Solver Excel)....150
Table 12. HMA final recipe. Results after compaction (Ndes.102)....150
Table 13. Determination of air voids in HMA blends....150
Table 14. Energetic parameters b.* 4% (HMA Ø150 · 120mm)....151
Table 15. HMA recipe for mixtures [SGC]....152
Table 16. HMA final recipe. Volumetric analysis....152
Table 17. HMA φ150 · 64.5mm. Results after compaction (binder 4%; Ndes.102)....152
Table 18. air voids in HMA mixes....152
Table 19. Energetic parameters (HMA φ150 · 64.5mm)....152
Table 20. HMA Marshall recipe. Volumetric analysis of recipes for laboratory....153
Table 21. HMA φ100 · 64.5mm. Results after compaction (binder 4%)....153
Table 22. Determination of air voids in HMA mixes (φ100 · 64.5mm)....153
Table 23. Marshall HMA mixture air voids and densities (75 blows; b.4%; φ100 · 63.5mm)....154
Table 24. Summary of IDT and ITSR for HMA (b.4%)....154
Table 25. Example of rubber replacement in granulometric curve ($1m^3$)....156
Table 26. DRY1.5% trial grading curve....157
Table 27. DRY1.5% trial recipe for laboratory mixtures....157
Table 28. DRY1.5% trial substitution of rubber. Adjusting mass of aggregates-binder....157
Table 29. DRY 1.5% trial recipe. Results with SGC (m_q=m_1±300gr)....158
Table 30. DRY 1.5% Air voids at Ndes (Densification curves)....158
Table 31. $DRY_{1.5\%\ \#60\text{-}40}$ Final recipe for laboratory rubberized mixtures....168
Table 32. $DRY_{1.5\%\#60\text{-}40}$ definitve recipe for laboratory manufacturing....168
Table 33. $DRY_{1.5\%\ \#60\text{-}40}$ Final recipe. Results after 24h (Ndes.152)....169
Table 34. $DRY_{1.5\%\ \#60\text{-}40}$ Final recipe. Results after 168h (Ndes.152)....169
Table 35. $DRY_{1.5\%\ \#60\text{-}40}$ Air voids vs. Binder content (0h;24h;168h), (Ndes.152)....169
Table 36. Energetic parameters ($DRY_{1.5\%\ \#60\text{-}40}$ φ150 · 120mm)....169
Table 37. Comparative HMA $_{4.0\%}$ vs. $DRY_{1.5\%\ \#60\text{-}40}$ φ150 · 120mm....170
Table 38. $DRY_{2.0\%\ \#60\text{-}40}$ Final recipe for laboratory rubberized mixtures....171
Table 39. $DRY_{2.0\%\#60\text{-}40}$ definitive recipe for laboratory manufacturing....171
Table 40. $DRY_{2.0\%\ \#60\text{-}40}$ Final recipe. Results after 24h (N_{des}.181)....171
Table 41. $DRY_{2.0\%\ \#60\text{-}40}$ Final recipe. Results after 7days (N_{des}.181)....171
Table 42. $DRY_{2.0\%\ \#60\text{-}40}$ Air voids vs. Binder content (0h;24h;168h), (N_{des}.181)....171
Table 43. Energetic parameters ($DRY_{2.0\%\ \#60\text{-}40}$ φ150 · 120mm)....171
Table 44. Comparative Energetic parameters (HMA $_{4.0\%}$ vs. $DRY_{2.0\%\ \#60\text{-}40}$ φ150 · 120mm)....172
Table 45. $DRY_{3.0\%\ \#80\text{-}20}$ recipe for laboratory rubberized mixtures....173
Table 46. $DRY_{3.0\%\#80\text{-}20}$ definitive recipe for laboratory manufacturing....173
Table 47. $DRY_{3.0\%\ \#80\text{-}20}$ Final recipe. Results after 24h (N_{des}.291)....173
Table 48. $DRY_{2.0\%\ \#60\text{-}40}$ Final recipe. Results after 7days (N_{des}.181)....173
Table 49. $DRY_{3.0\%\ \#80\text{-}20}$ Air voids vs. Binder content (0h;24h;168h), (N_{des}.291)....173
Table 50. Energetic parameters ($DRY_{3.0\%\ \#80\text{-}20}$ φ150 · 120mm)....173
Table 51. Summary of heights at N_{des} and Air voids (all mixtures)....174
Table 52. Air voids vs. Binder content in HMA_DRY samples (Optimal binder content)....175
Table 53. Trial recipes for a DRY1.5% (b. 6%) and DRY2% (b.6.5%)....176
Table 54. Disadvantageous results for roller slabs with rubber (DRY1.5 b.6%; DRY 2% b.6.5%)....176

Table 55. Roller compacted slabs results for HMA (RFI b.4%) [4 beams per slab] 177
Table 56. Roller compacted slabs results for DRY 1.5 (B.5,5%) [4 beams per slab] 177
Table 57. Roller compacted slabs results for DRY 2.0% (b.6%) [4 beams per slab] 178
Table 58. Gyratory compactor results (all mixtures) 178
Table 59. Summary of averaged results at seven days in all mixtures (Asphalt roller compactor) 179
Table 60. Roller compacted slabs results [4 beams per slab] 179
Table 61. Effective binder content vs. Air voids in SGC and Roller compacted specimens 179
Table 62. Details of "Volumetric mix-design" Gyratory Compactor 180
Table 63. Details of Standard asphalt slab roller compactor 180
Table 64. Characteristics of HMA b.4% mixture (UGR_FACT) 181
Table 65. Characteristics of DRY 1.5% b.5.5% mixture (UGR_FACT) 182
Table 66. Characteristics of DRY 2.0% b.6.0% mixture (UGR_FACT) 182
Table 67. Characteristics of reserved samples (Fatigue life at frequency 3 Hz) 182
Table 68. Specimens reserved at f. 3Hz (Fatigue life UGR_FACT) 183
Table 69. HMA b.4% (Fatigue life UGR_FACT) 183
Table 70. DRY(1.5%) b.5.5% (Fatigue life UGR_FACT) 183
Table 71. DRY(2.0%) b.6.0% (Fatigue life UGR_FACT) 184
Table 72. FFR tests for HMA specimens on anti-vibration basis and before UGR_FACT 192
Table 73. FFR tests for DRY 1.5% specimens on anti-vibration basis and before UGR_FACT 192
Table 74. FFR tests for DRY 2% specimens on anti-vibration basis and before UGR_FACT 192
Table 75. HMA samples (Young's and Shear modulus vs. Fatigue life (Nf, loads 0.6 ; 0.8 ; 1kN) 193
Table 76. DRY 1.5% samples (Young's and Shear modulus vs. Fatigue life (Nf, loads 0.6 ; 0.8 ; 1kN) 193
Table 77. DRY 2% samples (Young's and Shear modulus vs. Fatigue life (Nf, loads 0.6 ; 0.8 ; 1kN) 193
Table 78. Resume all mixtures (Young's E, Fatigue life and load amplitude) 193
Table 79. HMA b.4% (2 specimens for UGR_FACT: 1 kN; 20ºC; 3-5Hz) 194
Table 80. DRY 1.5% b.5.5% (2 specimens for UGR_FACT: 1 kN; 20ºC; 3-5Hz) 195
Table 81. DRY 2% b.6% (2 specimens for UGR_FACT: 1 kN; 20ºC; 3-5Hz) 195



Chapter 6 – Results

6.1. Introduction

The purpose is to present the laboratory testing of asphalt mixtures with/without crumb rubber modifier (CRM) in accord with the methodology studied, and the new SGC Energetic parameters developed for railways applying the AASHTO Calibrated-procedure in the last chapter[1]. The development of newly modified mixtures based on a method that refines the concrete value of N_{des} is accepted in some published research [Soto, F.M. et al. 2017-2018] for international rail sub-ballast.

This chapter includes the results for the HMA-DRY mixtures according to the methodology from the grading curve presented previously (Chapter 4). In addition to that, are explained the mix's volumetric results with SGC, Marshall (for HMA), and Roller slab compactor. Also, ITSR-IDT tests for HMA, a mechanical performance on fatigue-cracking and modulus testing for HMA-DRY optimal blends, and a new approach to solving the rubber increase, swelling, and rebound effects during the mix-design.

6.2. Phase 1: Volumetric mix-design.

The mixtures[2] analyzed and the process followed in the laboratory are described in Fig. 1.

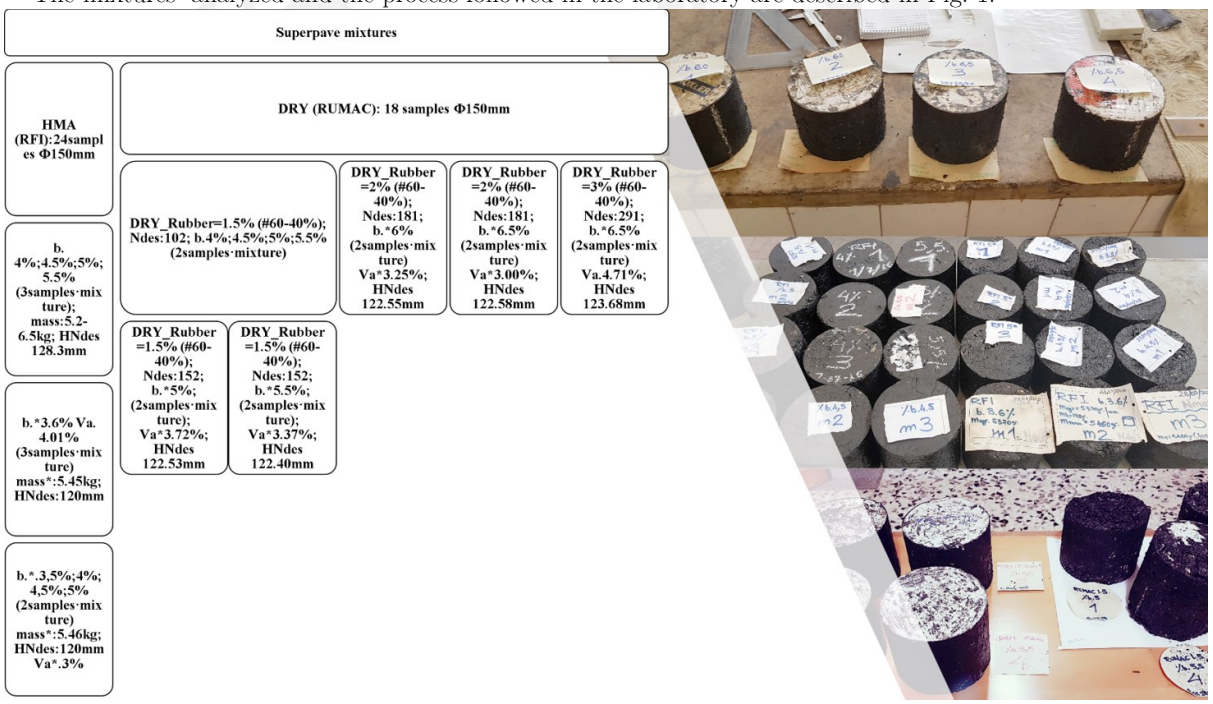


Figure 1. (a) Materials and mixtures specifications on this research; (b) HMA_DRY Specimens

Experimentally:

- For an HMA, it was needed a binder content of 4%, an aggregate mass of 5250gr, and a binder weight of 210gr of the total mixture of 5460gr.

- For a DRY blend or RUMAC at Va 3%, an aggregate mass≈5380gr, a binder content of 6% with rubber 1.5%; and a binder content of 6.5% with DRY 2%. It was observed that an open-dust content affects HMA volumetric properties such as VMA. In an attempt to minimize problems associated with extra-dust from dry sieving of two suspicious fine aggregates, was monitored by washing aggregates retained on Ø0.075mm to Ø0.6mm sieve.

[1] HMA developed at Ndes=102; Ninit=8, and Nmax=162 gyrations.

[2] Mixtures achieved a final height of 120±5mm, a Ø150mm and a target air voids of Va= 3%. Based on trial blends bitumen content from b.3.5 to 5.5%. According to AASHTO-R35 at least 4500-4700gr of aggregate is sufficient for each compacted specimen with a height of 110-120mm for aggregates with a bulk specific gravity of 2.55 to 2.70g/cm3.

6.2.1. Evaluating compacted HMA trial mixtures

The first phase of the experiment involved the study of four HMA [RFI, 2016] bituminous mixtures to determine the right mass of aggregates with 102 compaction turns. Four percentages of bitumen (4%, 4.5%, 5% and 5.5%) were established. Three samples of Ø150x120mm were done for each bitumen and different mass ±300gr, changing the binder content to determine the exact sample design mass (Fig. 2).

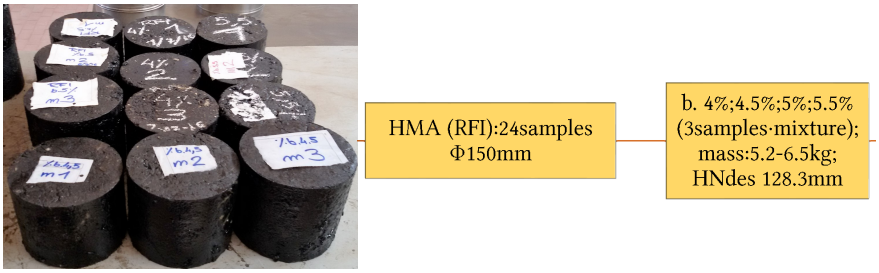


Figure 2. HMA trial mixtures developed in a first SGC volumetric mix-design

TABLE 1. HMA TRIAL GRADING CURVE (GRANULOMETRIC ADJUSTMENT BY FRACTION)

Sieve Size(mm)	% Passing limit				%Passing						TRIAL mix
	Lower limit	Upper limit	Avg. mix	Target (%)	Filler	Sand	Ø5-10mm	Ø10-15mm	Ø20-25mm	Ø25-30mm	Theoretical recipe (%)
31.5	100.00	100.00	100.00	100.00	100.00	100.00	100.00	100.00	100.00	100.00	100.00
22.4	90.48	100.00	95.24	92.86	100.00	100.00	100.00	100.00	100.00	72.68	96.53
16	71.59	92.23	81.91	76.75	100.00	100.00	100.00	100.00	60.01	14.26	81.20
11.2	58.56	80.21	69.38	63.97	100.00	100.00	100.00	96.43	10.44	1.24	68.98
8	49.04	70.49	59.77	54.41	100.00	100.00	100.00	67.01	1.00	0.35	60.73
5.6	41.22	61.80	51.51	46.36	100.00	100.00	83.03	32.22	0.40	0.35	52.15
4	36.00	56.00	46.00	41.00	100.00	98.02	30.64	7.96	0.35	0.35	43.21
2	23.00	40.00	31.50	27.25	100.00	76.08	0.66	0.40	0.30	0.35	33.96
1	14.77	28.61	21.69	18.23	89.83	35.15	0.66	0.40	0.30	0.35	21.79
0.40	9.76	21.51	15.63	12.69	83.27	10.57	0.66	0.40	0.30	0.35	14.41
0.177	7.02	16.05	11.54	9.28	72.12	0.83	0.66	0.40	0.30	0.35	10.32
0.063	5.89	9.35	7.62	6.75	54.09	0.33	0.33	0.20	0.20	0.20	7.62

→ As trial blend it was considered a HMA mixture (3 samples), with a M= 5460gr determined with the graphic mass[gr]-height[mm], a binder content of 4% to %5%±5%, air voids target value 3%, N_{des}. 102 cycles, water density: 996.7kg/m^3, aggregate density: 2808kg/m^3, and binder density: 1033kg/m^3 (Tables 2-3).

TABLE 2. HMA TRIAL RECIPE FOR LABORATORY MIXTURES [%]

Passing	Filler	Sand	fØ5-10mm	fØ10-15mm	fØ20-25mm	fØ25-30mm	Σcomponents [%]
[%]	<0.063	0.063/4	0.063/8	0.063/11.2	5.6/22.4	5.6/31.5	
HMA	12.837	21.416	7.198	20.708	18.003	19.838	100.00
Γmix=	2.747					Γaggr=	2.808

The projected mass was determined experimentally by measuring the height of the four compacted specimens and extracted from the mold, with the test stopped at N_{Design}. The values were obtained on the diagram h[mm] - M[gr], through the regression curve by interpolating the target-height of 120mm (Table 3).

TABLE 3. SCHEME OF THE COMPOSITION OF MASS-HEIGHT SAMPLES

N° sample.	Aggregate mass (gr)	Binder content (%)	Sample mass (gr)
1	m1	%b	M1 = m1(1+%b)
2	m2 = m1 + 300 gr	%b	M2 = m2(1+%b)
3	m3 = m1 - 300 gr	%b	M3 = m3(1+%b)
Q sample	mq=m1±x gr	%b	Mq=mq(1+%b)

→Initially, for conventional HMA blends, a height value between 119.3-124.2mm was achieved with a ratio of ±5480gr in specimens of Ø150mm with a bitumen percentage of 4% and different mass of aggregates (Fig. 3).

Relationship Mass_Hmm Compaction; %binder; mixture RFI						
Sample Ø150xh (mm)	H Ndes [mm]	Mass Aggr. Inert [gr]	Bitumen [%]	Sample mass [gr]	Mixture weight [gr]	Bulk spc. gravity [g/cm³]
m1	**119.3**	5200	4.0	5408.0	5475.0	
m2	**110.6**	4900	4.0	5096.0	5081.0	2.627
m3	**124.2**	5500	4.0	5720.0	5654.0	
Sub-ballast	**120**	→			**5487**	

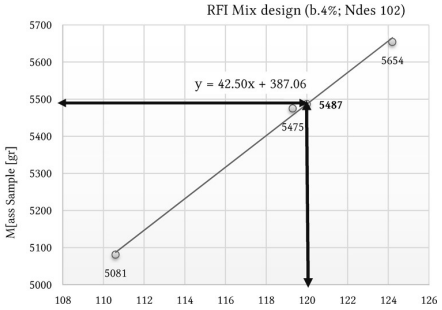


Figure 3. (a) Results of HMA b.4% m1±300gr; (b) Diagram of the relationship between mass and height

There was a difference between the calculated density and the measured density. In this way, a "correction factor," C, was introduced for the final bulk density value of the specimen, and it was possible to estimate the real density considering the variability between compaction and post-compaction:

$$C_{24h} = G_{bSSD_{24h}} \Big/ G_{b\dim_{24h}} \rightarrow G^*_{mb} = C_{24h} \cdot G_{b\dim_{Ndes}} \rightarrow \Gamma_{mm} = \frac{G^*_{mb}}{G_{\max}} \quad [\%] \qquad \text{(Eq. 1)}$$

Gmax is the Theoretical Maximum Specific Gravity of asphalt mixture;
Gmb is the Bulk Specific Gravity of each HMA sample after extrusion from SGC.

The bituminous mixtures, which at the beginning of the compaction phase showed gradual densification, reached, at the end of the test, values of $\Gamma_{mm\ (Nmax)}$ close to 100%, so they compacted too fast as an adverse effect. SGC required the threshold of $\Gamma_{mm\ (Nmax)} \leq 98\%$ so that at the end of useful life the volume of the voids was at least 2%. Auxiliary verifications were necessary to derive the Workability (densification curves) of the HMA. Also, the dust-to-asphalt binder ratio was considered to improve the mix recipes (Table 5).

TABLE 4. VERIFICATIONS OF THE SUPERPAVE MIX-DESIGN

Priority verification	%Va	$V_a = 100 - \%\Gamma_{mm(Ndes)} = 3\%$ (4% for roads)
Secondary verifications	%VMA, %VFA	$VMA = 100 - \left(\frac{\Gamma_{mb} \cdot \%P_{aggr}}{\rho_{ssd\ aggregate}} \right) \rightarrow VMA \approx 10-15\%$ (NMAS=9.5–31.5mm) $VFA = \left(\frac{VMA - V_a}{VMA} \right) \cdot 100 \rightarrow VFA \approx 65-75\%$ ($ESALs=10^7-10^8$)
Auxiliary verifications	Workability Densification (See also Chapter 4.9.13)	$V_a = 100 - \%\Gamma_{mm(Ninit)} \rightarrow \Gamma_{mm(Ninit)} \leq 89\%$ densification $V_a = 100 - \%\Gamma_{mm(N\max)} \rightarrow \Gamma_{mm(N\max)} \leq 98\%$ workability $DP = \%_{filler} / \%_{bitumen} = 0,6-2,0$

If the verifications in Table 5 were not complied with, the bitumen content was adjusted:

$$\%b^* = \%b - [0,4 \cdot (4 - V_a)] \rightarrow \Delta V_a = 4.0 - V_a \quad ; \quad \Delta P_b = -0.4 \cdot \Delta V_a$$
$$\Delta_{VMA} = -0.1 \cdot \Delta V_a \quad if \quad V_a < 4.0\% \quad ; \quad \mathrm{VMA}_{\mathrm{design}} = \mathrm{VMA}_{\mathrm{trial}} + \Delta_{VMA} \qquad \text{(Eq. 2)}$$

%b* is the design binder content (not trial), [%]; Va is the air voids percent (as n°%).

With the percentage of correct bitumen %b*, and with the mass M determined previously, the prior and auxiliary checks were carried out again. Once the aggregate plus bitumen was structured, a minimum of two-four specimens was compacted at each of the following asphalt contents: 3.5%, 4.0%, 4.5%, 5.0% and 5.5%. As an example for binder 5%, Fig. 4, and Tables 5 to 7 show the correction steps.

TABLE 5. HMA RELATIONSHIP MASS_HMM COMPACTION

Sample Ø150xh(mm)	Mass weight (gr)	Bitumen mass (gr)	H Ndes [mm]	Mass Aggr. Inert [gr]	Bitumen [%]	Sample mass [gr]	Bulk spc. gravity [g/cm³]	Maximum density [g/cm³]
m1	5436	258.6	119.5	5192	5.0	5452		
m2	5525	262.8	121.3	5292	5.0	5557	2.583	2.598
m3	5313	252.8	117.1	5092	5.0	5347		

TABLE 6. AVERAGE CORRECTED SPECIMEN RELATIVE DENSITIES (%VA_%BINDER)

N_{des}	Height $_{24h}$ [mm]	Γ_{max}	$\Gamma_{mb\ (Ndes)\ stimated}$	$\Gamma_{mb\ (Ndes)\ measured}$	Correction factor, C	Γ_{mb}^{*} (Ndes)	Γ_{mm}	% Va	%b*
102	116.33	2.598	2.574	2.561	0.997	2.567	98.5%	1.45%	3.74
102	117.50	2.598	2.578	2.544	0.993	2.561	97.9%	2.11%	4.00
102	114.50	2.598	2.568	2.569	1.000	2.568	98.9%	1.11%	3.60
Averaged	116.1	2.598	2.573	2.558	0.997	2.565	0.98	1.78%	3.78

TABLE 7. AVERAGE CORRECTED SPECIMEN RELATIVE DENSITIES (VMA_VFA)

Specimen	m_1 (gr.)	m_3 (gr.)	m_2 (gr.)	ρb_{ssd} (g/cm^3)	ρb_{DRY} (g/cm^3)	$\Gamma_{se\ geom.\ (g/cm3)}$ (g/cm^3)	Va (%)	%Water absorbed	Dev.St. $\%V_a$	VMA (%)	VFA (%)	$\Delta\%b^{*}$
1	5436	5438	3322	2.561	2.563	2.644	1.36%	0.09%	0.51%	13.24%	89.74%	3.94
2	5525	5526	3361	2.544	2.545	2.661	2.01%	0.05%		13.82%	85.44%	4.21
3	5313	5314	3253	2.569	2.571	2.626	1.02%	0.05%		12.95%	92.14%	3.81
Averaged	5425	5426.0	3312.0	2.558	2.559	2.644	1.46%	0.06%		13.34%	89.11%	4.0

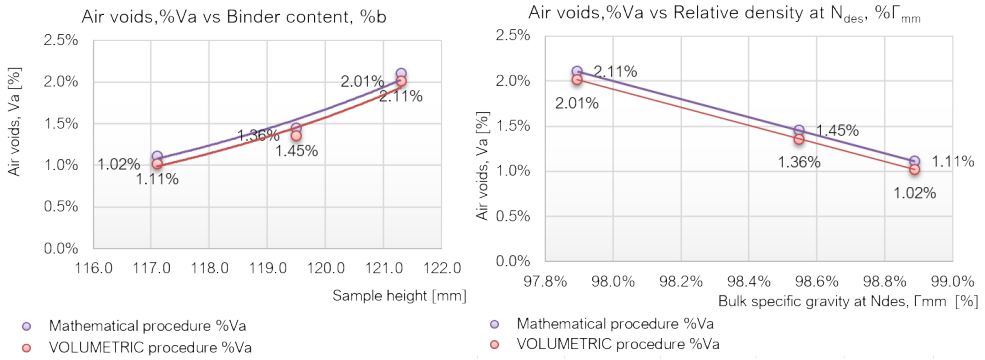


Figure 4. (a) Relationship between %Va and height of the mixture; (b) %Va vs. Bulk specific gravity

V_a, VMA, VFA, and Γ_{mm} (N_{design}) results were recorded for each sample. With the values of air voids found for each binder content, the curves "Mass of sample vs. Height (mm)," and "%b-Va" were constructed by regression interpolating the points by a polynomial equation (Fig. 5-6), resulting in the design binder content %b*.

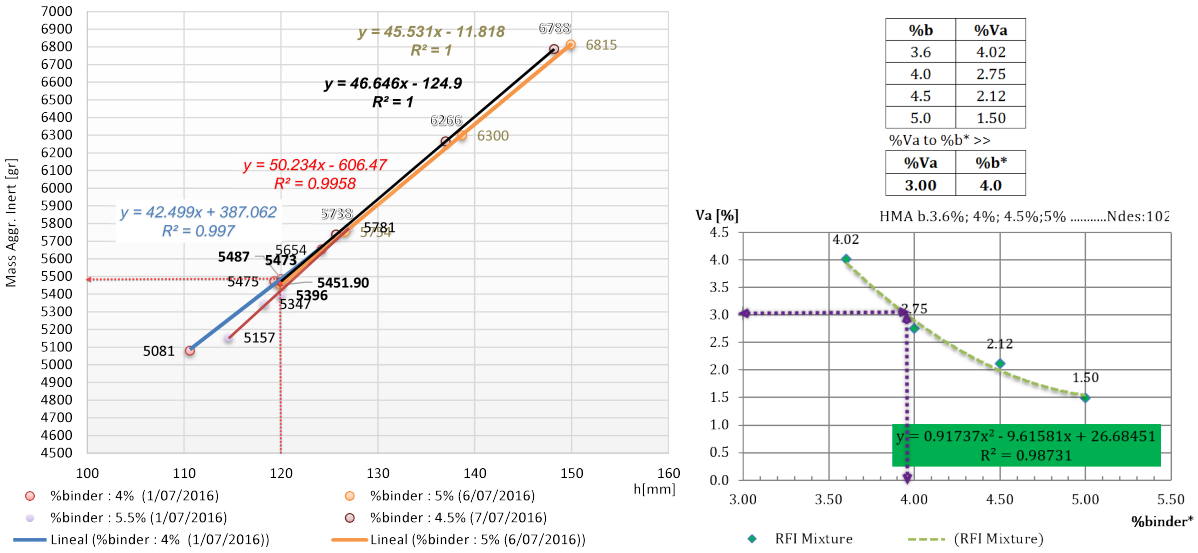


Figure 5. (a) Diagram of the relationship between mass and height for all binders; (b) Interpolation %b*-%Va

This practice was followed for all the bituminous mixtures under study. Volumetric characteristics, air voids, VMA, VFA, and density were determined for each specimen at 102 N_{design} gyrations. Next, density was checked against specification values at N_{init}, and N_{max}.

Table 8 shows the calculations made to obtain the exact amount of aggregate mass per specimen:

TABLE 8. HMA EFFECTIVE VALUES FOR MIX-DESIGN

N° sample.	Aggregate mass [gr]	Binder content (%)	Sample mass [gr]	Binder mass [gr]	$HN_{des.}$ [mm]	$H_{24h.}$ [mm]	Effective binder [gr]	M_1 24h [gr]	M_2 24h [gr]	M_3 24h [gr]	Ɣapp (g/cm³)	Γ_{max} [g/cm³]	Δ%b*	Mass-Height [-]
4.0.1	5200	4.0	5408	208	119.3	114.7	210.6	5475	3394	5477	2.622	2.637	3.01	H.120mm if m: 5487gr.
4.0.2	4900	4.0	5096	196	110.6	108.7	195.4	5081	3155	5083	2.629	2.637	2.98	
4.0.3	5500	4.0	5720	220	124.2	124.3	217.5	5654	3516	5660	2.631	2.637	3.33	
4.5.1	5500	4.5	5747	248	125.7	123.0	247.1	5738	3558	5739	2.625	2.618	4.43	H.120mm if m: 5473gr.
4.5.2	6000	4.5	6270	270	137.0	134.0	269.8	6266	3885	6268	2.624	2.618	4.36	
4.5.3	6500	4.5	6792	293	148.2	146.0	292.3	6788	4203	6789	2.619	2.618	4.30	
5.0.1	5500	5.0	5775	275	126.6	123.0	274.0	5754	3555	5756	2.622	2.608	4.32	H.120mm if m: 5452gr.
5.0.2	6000	5.0	6300	300	138.7	134.0	300.0	6300	3892	6303	2.629	2.607	4.34	
5.0.3	6500	5.0	6825	325	149.9	144.5	324.5	6815	4197	6816	2.631	2.596	4.31	
5.5.1	5200	5.5	5486	286	118.3	113.9	278.8	5347	3294	5348	2.597	2.581	4.25	H.120mm if m: 5396gr.
5.5.2	4900	5.5	5169	270	114.6	110.0	268.8	5157	3166	5157	2.584	2.581	4.43	
5.5.3	5500	5.5	5802	303	127.0	122.3	301.4	5781	3486	5781	2.513	2.581	3.97	

Finally, a densification curve was designed for each mixture (Fig. 6) that represents the measured relative density at N_{des} cycles (%Γmm) versus the logarithm of the number of gyrations. Each trend line was reported:

$$\Gamma_{mm} = \frac{\Gamma^*_{N_{des}}}{\Gamma_{\max}} \quad [\%] \quad \Leftrightarrow \quad \Gamma_{mm}(N) = \Gamma_1 + k \cdot LogN \quad [\%] \qquad \text{(Eq. 3)}$$

- Γ_{mm} is the averaged corrected specimen relative density at N_{des} (%);
- Γ_1 is the relative specific density of energy accumulated during the compaction, as an experimental factor of the trend line, decreases when increases k (%);
- k is the workability of the mixture (-).

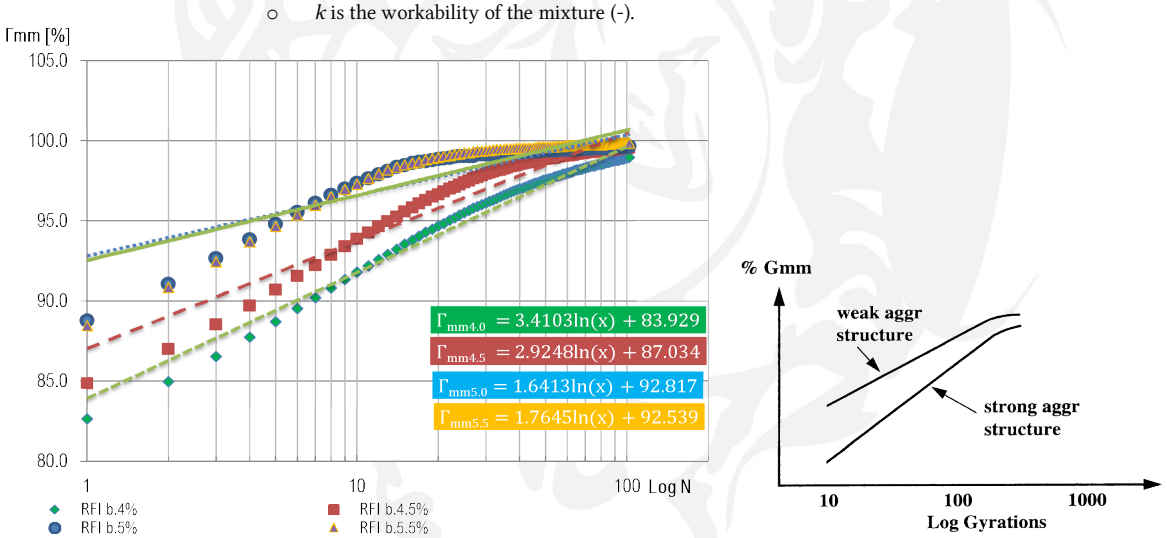


Figure 6. (a) Densification curves for trial HMA mixtures; (b) Illustration explained strong-weak aggregate structure according to the slope of the compaction-curve

Using the estimated densification curve (Fig. 6a), the density at N_{init} and N_{max} is checked against specification values. In this way, it was possible to compare sample densities through water immersion (after 24h) or using the densification curves (at N_{des}). Observing the process of compaction through the density curves, we observed the behavior of the mixture. The slope of the curve represents the parameter "k," the *workability* of the mixture (Fig. 6b), which can be interpreted as a velocity at which the bituminous conglomerate reaches a certain degree of densification. The higher this value, the better performance the blend offers during the manufacturing process. A workable blend, in turn, is economically sustainable. Mixes exhibiting relatively steep slopes and low N_{init} values are indicative of mixes that have developed a good aggregate structure or internal resistance to densification. Steeper curves indicate better aggregate structuring.

In these HMA trial mixtures, it was observed that the percentage of voids was lower than expected[3], which indicated a significant amount of unprocessed filler in the granulometric curve. Four mixtures (3 specimens per blend) it has been obtained to compact with a Va= 3%, and a height of 120mm, the optimal mass of aggregates was 5460gr, and bitumen of 3.6-4% at N_{des} = 102. T^{a}mix: 160ºC; T^{a}comp: 145ºC, and NMAS Ø22,4mm.

6.2.2. Mix-design of "optimal HMA recipes."

Next, the experimental range used for HMA-RFIs was five different binders, 3.5%, 3.6%, 4%, 4.5%, 5%. For each percentage, 2-3 specimens were packaged to determine the content of the air voids and the compaction characteristics. This phase allowed the construction of final %Va vs. %b Graph, and to determine the optimum recipe binder content. Results obtained for traditional conglomerates are reported (Fig. 7; Tables 9-10):

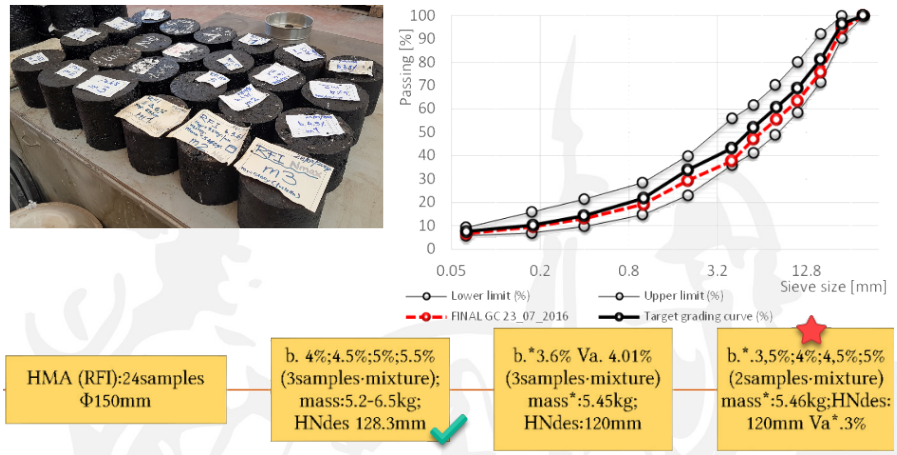


Figure 7. (a) HMA specimens developed as final mix-design; (b) HMA grading curve adjusted; (c) Mixtures

TABLE 9. HMA FINAL GRADING CURVE

Sieve Size(mm)	% Passing limit			Fuller	%Passing						HMA	
	Lower limit (%)	Upper limit (%)	Target GC (%)	Ønom. 22.4mm (%)	Filler	Sand	Ø5-10mm	Ø10-15mm	Ø20-25mm	Ø25-30mm	Passing (%)	Retained (%)
31.5	100.00	100.00	100.00	185.29	100.000	100.000	100.000	100.000	100.000	100.000	100.00	0.00
22.4	90.48	100.00	92.86	158.94	100.000	100.000	100.000	100.000	100.000	64.043	92.39	7.61
16	71.59	92.23	76.75	136.60	100.000	100.000	100.000	100.000	77.439	11.875	77.18	15.21
11.2	58.56	80.21	63.97	116.35	100.000	100.000	100.000	96.425	18.859	0.467	63.28	13.90
8	49.04	70.49	54.41	100.00	100.000	100.000	100.000	67.015	3.152	0.334	54.96	8.31
5.6	41.22	61.80	46.36	85.17	100.000	100.000	83.031	32.223	0.350	0.334	47.20	7.77
4	36.00	56.00	41.00	73.20	100.000	93.393	30.641	7.959	0.350	0.334	38.40	8.79
2	23.00	40.00	27.25	53.59	100.000	62.062	0.660	0.398	0.350	0.334	27.75	10.65
1	14.77	28.61	18.23	39.23	98.038	34.334	0.660	0.398	0.350	0.334	20.69	7.06
0.40	9.76	21.51	12.69	25.97	96.077	15.115	0.660	0.398	0.350	0.334	15.72	4.97
0.177	7.02	16.05	9.28	18.00	70.615	6.206	0.660	0.398	0.350	0.334	10.41	5.31
0.063	5.89	9.35	6.75	11.31	50.038	1.802	0.329	0.199	0.350	0.334	6.75	3.66

TABLE 10. HMA FINAL RECIPE FOR LABORATORY MIXTURES

	Filler	Sand	fØ5-10mm	fØ10-15mm	fØ20-25mm	fØ25-30mm	Σcomponents
Passing	[%]	[%]	[%]	[%]	[%]	[%]	[%]
HMA	12.236	24.605	5.211	18.292	18.492	21.164	100.00
Γmix=	2.740					Γaggr=	2.800

Each specimen was compacted to N_{max}, with data collected (height-N_{des}) during the compaction process was continually monitored. The density was monitored by knowing the initial weight of the mix, the fixed volume of the mold, and the measured height at the end of the compaction phase (Tables 11,12 and 13).

[3] This step was made applying the quantitative extraction of asphalt binder (see 4.9.14 Methodology)

TABLE 11. HMA. VOLUMETRIC ANALYSIS OF RECIPES FOR LABORATORY (SOLVER EXCEL[4])

Sample	H [mm]	Mass Aggr[gr]	Binder [%]	Sample mass [gr]	Binder mass [gr]	Recipe in laboratory ↓(+100gr.)↓	Sample mass [gr]	Binder mass [gr]	Filler [gr]	Sand [gr]	fØ5-10mm [gr]	fØ10-15mm [gr]	fØ20-25mm [gr]	fØ25-30mm [gr]
b.3.5%	120	5101	*3.5*	5280	179		5280	185	646	1162	380	1093	951	1047
b.3.6%	120	5270	*3.6*	5460	190		5370	193	657	1182	387	1112	967	1065
b.4%	120	5250	*4.0*	5460	210		5350	214	655	1178	385	1108	963	1061
b.4.5%	120	5225	*4.5*	5460	235		5325	240	652	1172	383	1103	959	1056
b.5%	120	5167	*5.0*	5425	258		5270	264	645	1160	379	1091	949	1045

TABLE 12. HMA FINAL RECIPE. RESULTS AFTER COMPACTION (NDES.102)[5]

Sample Ø150xh (mm)	Inert mass [gr]	Binder (%)	Sample mass [gr]	Binder mass [gr]	$HN_{des.}$ [mm]	$H_{24h.}$ [mm]	Effective binder [gr]	M_1 24h [gr]	M_2 24h [gr]	M_3 24h [gr]	Υapp [g/cm³]	Γ_{max} [g/cm³]	Γ_{mb^*} [g/cm³]	Γ_{mm} [%]	Va [%]	VMA[6] [%]	VFA [%]	Δ%b*
$HMA_{3.5_1}$	5101	3.5	5280	178.5	116.1	116.3	178.4	5280	3227	5284	2.557	2.656	2.565	96.6	3.65	12.10	69.87	3.36
$HMA_{3.5_2}$	5097	3.5	5275	178.4	116.4	116.1	177.7	5262	3216	5267	2.556	2.656	2.557	96.3	3.70	12.15	69.58	3.38
Averaged	5099	3.5	5277.5	178.45	116.25	116.2	178.07	5271	3221	5275	2.556	2.656	2.561	96.4	**3.68**	12.12	69.73	3.37
$HMA_{3.6_1}$	5280	3.6	5470	190.1	120.9	118.33	189.3	5454	3321	5457	2.545	2.653	2.549	96.1	3.98	12.62	68.47	3.59
$HMA_{3.6_2}$	5270	3.6	5460	189.7	121.1	119.67	189.7	5463	3326	5467	2.543	2.653	2.548	96.0	4.02	12.69	68.09	3.62
$HMA_{3.6_3}$	5270	3.6	5460	189.7	120.8	117.83	189.6	5461	3334	5462	2.558	2.653	2.558	96.4	3.46	12.15	71.53	3.38
Averaged	5099	3.6	5277.5	178.45	120.93	118.6	178.07	5259	3227	5462	2.549	2.653	2.552	96.2	**3.83**	12.49	69.37	3.60
$HMA_{4.0_1}$	5048	4.0	5250	201.9	114.3	113.33	201.3	5239	3202	5240	2.561	2.636	2.577	97.8	2.78	12.40	77.59	3.51
$HMA_{4.0_2}$	5048	4.0	5250	201.9	115.9	115.50	200.2	5209	3189	5214	2.563	2.636	2.553	96.8	2.70	12.32	78.12	3.48
Averaged	5048	4.0	5250	201.9	115.1	144.40	200.73	5224	3195	5227	2.562	2.636	2.565	97.3	**2.74**	12.36	77.86	3.49
$HMA_{4.5_1}$	5000	4.5	5225	238.5	114.3	113.3	223.8	5201	3178	5204	2.558	2.617	2.567	98.1	2.15	12.90	83.30	3.76
$HMA_{4.5_2}$	4999	4.5	5224	235.1	114.2	112.9	224.3	5214	3186	5215	2.561	2.617	2.572	98.3	2.06	12.82	83.94	3.72
Averaged	5000	4.5	5225	236.8	114.2	113.2	224.0	5208	3182	5209	2.559	2.617	2.569	98.2	**2.11**	12.86	83.62	3.74
$HMA_{5.0_1}$	5192	5.0	5452	259.6	119.5	116.33	258.6	5436	3322	5438	2.561	2.598	2.567	98.8	1.39	13.24	89.74	3.94
$HMA_{5.0_2}$	5292	5.0	5557	264.6	121.3	117.50	262.8	5525	3361	5526	2.544	2.598	2.561	98.5	2.05	13.82	85.44	4.21
$HMA_{5.0_3}$	5092	5.0	347	254.6	117.1	114.50	252.8	5313	3253	5314	2.569	2.598	2.568	98.9	1.05	12.95	92.14	3.81
Averaged	5192	5.0	5452	259.6	119.3	116.11	258.1	5425	3312	5426	2.558	2.598	2.565	98.7	**1.50**	13.34	89.11	4.07

TABLE 13. DETERMINATION OF AIR VOIDS IN HMA BLENDS

Sample	Wair (m1)	Wdry (m3)	Wwater (m2)	Υw (Kg/m³)	%b	Υb (Kg/m³)	$\Upsilon aggr$ (g/cm³)	$\Upsilon bulk$ (Kg/m³)	$\Upsilon bulk$ (Ẋ)	%Va (N_{des})	%Va	%Va (Ẍ)	%b* (Ẍ)
$HMA_{3.5_1}$	5280	5284	3227	996.30	3.5	1033.3	2807.9	2556.9	2556.30	3.65	3.65	3.67	3.37
$HMA_{3.5_2}$	5262	5267	3216					2555.7		3.69	3.70		
$HMA_{3.6_1}$	5454	5457	3321					2544.6		3.98	3.98		
$HMA_{3.6_2}$	5463	5467	3326	996.30	3.6	1033.3	2807.9	2542.7	2548.57	4.05	4.02	3.83	3.53
$HMA_{3.6_3}$	5461	5462	3334					2558.3		3.46	3.46		
$HMA_{4.0_1}$	5239	5240	3202	996.30	4.0	1033.3	2807.9	2560.7	2561.74	2.78	2.79	2.74	3.49
$HMA_{4.0_2}$	5209	5214	3189					2562.8		2.70	2.71		
$HMA_{4.5_1}$	5201	5204	3178	996.30	4.5	1033.3	2807.9	2558.1	2559.39	2.15	2.17	2.12	3.74
$HMA_{4.5_2}$	5214	5215	3186					2560.7		2.06	2.07		
$HMA_{5.0_1}$	5436	3322	5438					2560.6		1.39	1.39		
$HMA_{5.0_2}$	5525	3361	5526	996.30	5.0	1033.3	2807.9	2543.6	2557.85	2.04	2.05	1.50	4.00
$HMA_{5.0_3}$	5313	3253	5314					2569.4		1.05	1.05		

Once the experimentation on the sample range with different binder ratios was completed, the %Va-%b graph was constructed. From this relationship, exponential and polynomial regression curves, and an optimal bitumen percentage of 3.91% to 4% are obtained to get a 3% air voids (Figure 8).

Volumetric characteristics, that is, air voids, VMA, VFA, and density were determined for each specimen at 120 N_{design} gyrations. After compacting the specimens to N_{des} gyrations, it has been determined the bulk specific gravity (Γ_{mb}) and the theoretical maximum specific gravity (Γ_{mm}) of each of the five mixtures (EN 12697-6).

The densification curves for each mixture were compared (Figure 9, Table 14).

[4] The Excel tool "Solver" has allowed the calculation of the target recipe through an iterative system of linear equations, to obtain the weights of each fraction needed to pack one or more specimens, avoiding the mechanical sieving of a substantial amount of aggregate.

[5] Water temperature: 28ºC. Density water: 996.3g/cm³.

[6] Voids in the mineral aggregate (VMA) are the void spaces that exist between the aggregate particles in the compacted paving asphalt mixture, including the space filled with the binder.

Voids filled with asphalt (VFA) are the void spaces that exist between the aggregate particles in the compacted paving asphalt mixture that are filled with binder.

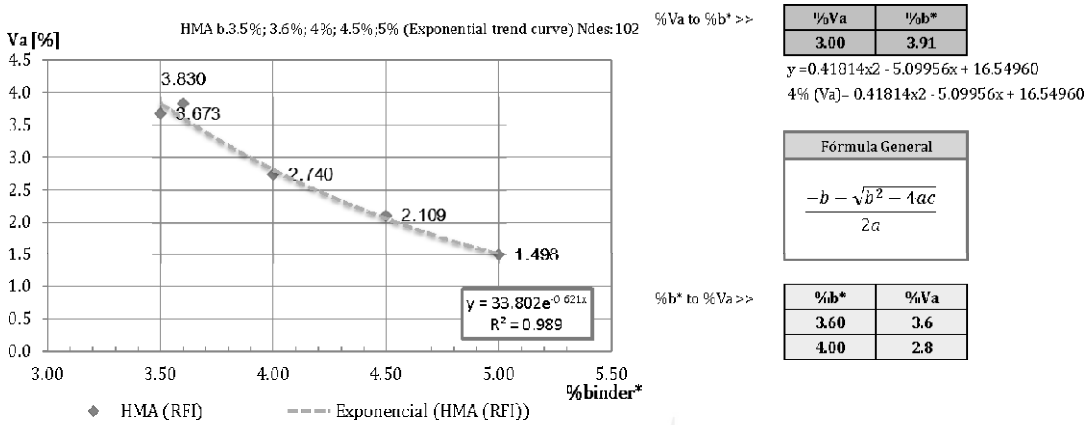


Figure 8. Air voids vs. Binder content in HMA samples (Ndes.102; ϕ150x120mm)

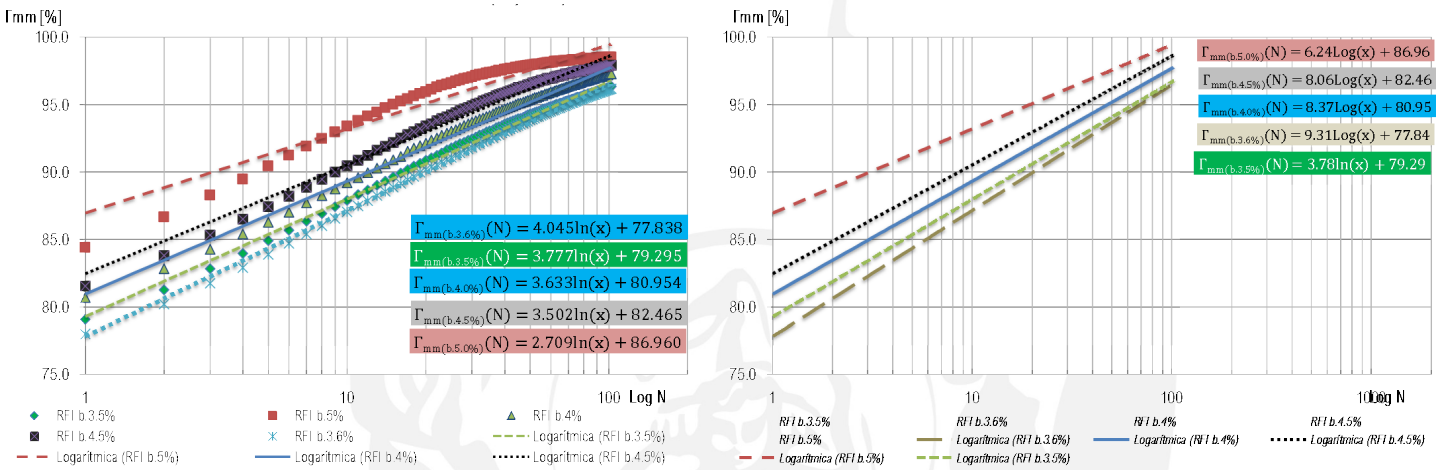


Figure 9. Densification curves for optimal HMA(RFI) mixtures ϕ150 · 120mm

TABLE 14. ENERGETIC PARAMETERS B.* 4% (HMA Ø150·120MM)

Design ESALs (millions)	Averaged Design Air Temperature							
	$N_{initial}$	N_{design}	$N_{maximum}$	% G_{mm} at $N_{initial}$	% G_{mm} at N_{des}	% G_{mm} at $N_{maximum}$	%Va (N_{des})	Dust ratio (DP)[7]
$>3\cdot10^7$	8	**102**	162	88.25	97.26	99.43	**2.74**	0.892

For an HMA with an optimal binder 4%, an air voids of 3%, the trend line was:

$$HMA_{(b.4\%)} \rightarrow \Gamma_{mm}\ (N_{des.}\ 102) = 8.365\text{Log}(x) + 80.954$$

6.3. Phase 2: Marshall method.

6.3.1. Determination of Water Sensitivity (ITSR)

The Marshall method was developed with a controlling idea that the voids achieved in the HMA mix-design must correspond with the density achieved in the field under traffic. Water sensitivity tests were conducted only for HMA to evaluate the behavior under the water susceptibility for their application as the sub-ballast layer.

→In this section, six specimens with Ø100mm with a height of ±64.5mm were studied using the SGC.

→With the same recipe, another eight samples of Ø101.6 · ±64.5mm were compacted by the Marshall hammer applying 75 blows on each side per sample. In both cases, the percentage of target voids was 3%, the same bitumen percentage of 4%, and the same grain size (Fig. 10; Tables 15 to 19).

[7] $DP=P_{0.075}/P_{be}= P_{0.075/(VMA-Va)}\rightarrow((10.41+6.75)\cdot0.5\ )/\ (12.36-2.74) = 0.892$



Figure 10. (a) Marshall and SGC HMA mixtures; (b) ITSR and IDT tests; (C) SGC specimens

TABLE 15. HMA RECIPE FOR MIXTURES [SGC]

	Filler	Sand	fØ5-10mm	fØ10-15mm	fØ20-25mm	fØ25-30mm	Σ
Passing [%]	<0.063	0.063/4	0.063/8	0.063/11.2	5.6/22.4	5.6/31.5	
RFI_HMA	12.84	21.42	7.20	20.71	18.00	19.84	100.00
Γmix=	2.744					Γaggr=	2.809

TABLE 16. HMA FINAL RECIPE. VOLUMETRIC ANALYSIS

Sample	H [mm]	φ [mm]	Mass Aggr[gr]	Sample mass [gr]	Binder mass [gr]	Filler [gr]	Sand [gr]	fØ5-10mm [gr]	fØ10-15mm [gr]	fØ20-25mm [gr]	fØ25-30mm [gr]
SGC b*.4%	120	150	5250	5460	210	640	1386	287	1006	1017	1164
	64.5	150	2740	2850	110	367	660	216	621	540	595
	65.0	100	1300	1350	52	156	281	92	264	230	253
Marshall b.4%	63.5	101.63	1275	1326	51	171	308	101	290	252	278

TABLE 17. HMA Φ150·64.5MM. RESULTS AFTER COMPACTION (BINDER 4%; NDES.102)

Sample (mm)	Inert mass [gr]	Sample mass [gr]	Binder mass [gr]	$HN_{des.}$ [mm]	$H_{24h.}$ [mm]	Vb_{eff} [gr]	M_1 24h [gr]	M_2 24h [gr]	M_3 24h [gr]	Υ_{app} [g/cm³]	Γ_{max} [g/cm³]	Γ_{mb*} [g/cm³]	Γ_{mm} [%]	Va [%]	VMA* [%]	VFA [%]	b* [%]
HMA_1	2740	2850	109.6	64.5	64.50	109.9	2861	1740	2864	2.539	2.637	2.539	96.3	3.60	13.14	72.62	3.68
HMA_2	2740	2850	109.6	64.3	64.30	109.6	2852	1742	2854	2.559		2.559	97.0	2.87	12.48	77.03	3.39
HMA_3	2740	2850	109.6	64.5	64.50	109.9	2860	1738	2863	2.536		2.536	96.2	3.71	13.24	71.96	3.73
HMA_4	2740	2850	109.6	64.5	64.50	109.6	2853	1734	2855	2.539		2.539	96.3	3.60	13.14	72.60	3.68
HMA_5	2740	2850	109.6	64.7	64.70	109.8	2858	1737	2863	2.532		2.532	96.0	3.86	13.38	71.11	3.79
HMA_6	2740	2850	109.6	64.3	64.30	109.9	2859	1732	2862	2.525		2.525	95.7	4.16	13.65	69.49	3.91
Avg.	2740	2850	109.6	64.5	64.50	109.8	2857	1737	2860	2.538	2.637	2.538	96.3	**3.63**	13.17	72.47	3.70

TABLE 18. AIR VOIDS IN HMA MIXES[8]

Mixture	Sample	$W_{air\ (m1)}$	W_{dry} (m3)	W_{water} (m2)	Υ_w (Kg/m3)	Υb (Kg/m3)	Υ_{aggr} (g/cm3)	Υ_{bulk} (Kg/m3)	Υ_{bulk} (Averaged)	$V_{a\ (Ndes)}$	$V_{a\ (\%)}$ (24h)	$V_{a\ (24h)}$	Δ%b*
HMA 4% Ndes.102 Ø150x64.5mm	HMA_1	2861.0	2864.0	1740.3	997.40	1033.3	2808.3	2539.4	2549.04	2.92%	3.60	3.23%	3.74%
	HMA_2	2852.0	2854.0	1742.3				2558.7		3.79%	2.87		
	HMA_3	2860.0	2863.0	1738.3	997.40	1033.3	2808.3	2536.4	2537.86	3.87%	3.72	3.66%	3.80%
	HMA_4	2853.0	2855.0	1734.4				2539.4		3.12%	3.60		
	HMA_5	2858.0	2863.0	1737.4	997.40	1033.3	2808.3	2532.4	2528.44	3.32%	3.87	4.02%	3.72%
	HMA_6	2859.0	2862.0	1732.4				2524.5		3.28%	4.17		
Avg.		2857	2860	1738					2538.4	**3.38%**		**3.64%**	3.75%

TABLE 19. ENERGETIC PARAMETERS (HMA Φ150·64.5MM)

Design ESALs (millions)	Averaged Design Air Temperature							
	$N_{initial}$	N_{design}	N_{max}	% G_{mm} at Ninit	% G_{mm} at Ndes	% G_{mm} at Nmax	%Va (N_{des})	Dust ratio (DP)
$>3 \cdot 10^7$	8	**102**	162	86.54	96.61	97.51	**3.38**	0.830

These first values corresponding to the mixtures by SGC. The densification curves for each mixture were traced (Figure 11). In this case study, the average regression curve of the six analyzed samples was:

[8] See 4.9.7. Bulk specific gravity and Maximum Density

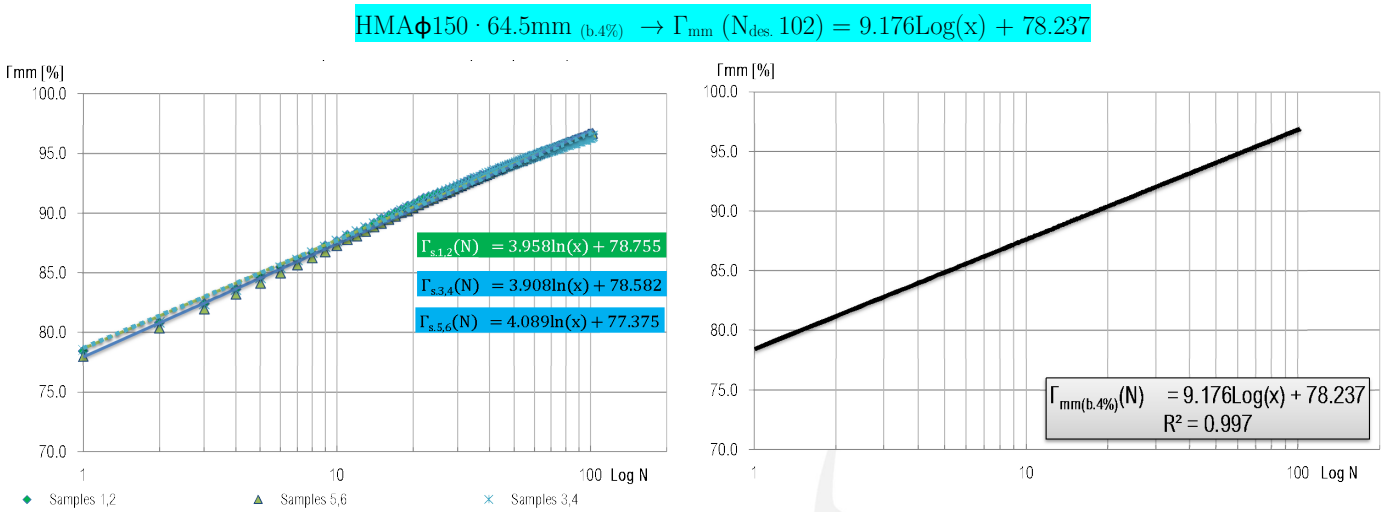


Figure 11. SGC Densification curves for optimal HMA mixtures ϕ150 · 64.5mm

In conclusion, it has been possible to improve the compaction with SGC regardless of the size of the specimen, obtaining a more excellent workability and a less densification, resulting in a more stable mixture.

Then, with the same mixture design, manufactured and following the same laboratory guidelines, Marshall specimens were compacted to size Ø100 · ±64.5mm[9] (Tables 20-22).

TABLE 20. HMA MARSHALL RECIPE. VOLUMETRIC ANALYSIS OF RECIPES FOR LABORATORY

Sample	Htarget [mm]	φ [mm]	Mass Aggr[gr]	Sample mass [gr]	Binder mass [gr]	Sample mass [gr]	Binder mass [gr]	Filler [gr]	Sand [gr]	fØ5-10mm [gr]	fØ10-15mm [gr]	fØ20-25mm [gr]	fØ25-30mm [gr]
Marshall b.4%	63.5	101.63	1275	1326	51	1400	56	171	308	101	290	252	278

TABLE 21. HMA Φ100·64.5MM. RESULTS AFTER COMPACTION (BINDER 4%)

Sample (mm)	Inert mass [gr]	Sample mass [gr]	Binder mass [gr]	Height [mm]	H_{24h} [mm]	Vb_{eff} [gr]	M_1 24h [gr]	M_2 24h [gr]	M_3 24h [gr]	Υ_{app} [g/cm³]	Γ_{max} [g/cm³]	Γ_{mb^*} [g/cm³]	Γ_{mm} [%]	Va [%]	VMA [%]	VFA [%]	Δ %b*
HMA_1	1275	1325	50.96	68.0	67.75	51.0	1326	810	1328	2.557		2.557	97.0	2.93	12.53	76.63	3.41
HMA_2	1274	1325	50.96	68.6	68.00	50.9	1324	804	1326	2.534		2.534	96.1	3.80	13.32	71.48	3.76
HMA_3	1274	1325	50.96	68.0	67.50	51.0	1328	805	1329	2.532	2.637	2.532	96.0	3.88	13.39	71.03	3.79
HMA_4	1275	1325	50.96	66.6	66.75	50.8	1323	806	1324	2.552		2.552	96.8	3.13	12.72	75.36	3.50
HMA_5	1274	1324	50.96	67.8	67.50	51.0	1328	808	1329	2.546		2.546	96.6	3.34	12.90	74.14	3.58
HMA_6	1275	1325	50.96	66.9	66.17	51.0	1326	806	1326	2.548		2.548	96.6	3.29	12.86	74.42	3.56
Avg.	1275	1325	50.96	68.2	67.28	50.9	1325	807	1327	2.545	2.637	2.545	96.5	**3.39**	12.95	73.84	3.60

TABLE 22. DETERMINATION OF AIR VOIDS IN HMA MIXES (Φ100·64.5MM)

Mixture	Sample	W_{air} (m1)	W_{dry} (m3)	W_{water} (m2)	Υ_w (Kg/m3)	Υb (Kg/m3)	Υ_{aggr} (g/cm3)	Υ_{bulk} (Kg/m3)	Υ_{bulk} (Averaged)	$V_{a\ (Ndes)}$	$V_{a\ (24h)}$	Δ%b*
HMA 4%	HMA_1	1326.0	1328.0	810.3	998.30	1033.3	2808.3	2557.0	2545.56	2.97%	3.37%	3.72%
	HMA_2	1324.0	1326.0	804.4				2534.1		3.84%		
	HMA_3	1328.0	1329.0	805.4	998.30	1033.3	2808.3	2532.0	2541.79	3.92%	3.51%	3.78%
	HMA_4	1323.0	1324.0	806.4				2551.6		3.18%		
	HMA_5	1328.0	1329.0	808.3	998.30	1033.3	2808.3	2546.3	2546.91	3.38%	3.31%	3.70%
	HMA_6	1326.0	1326.0	806.4				2547.5		3.33%		
Averaged		1326.0	1328.0	810.3					2544.76	**3.44%**	**3.40%**	3.74%

Table 23 shows the apparent density results for the two remaining specimens of the Marshall compaction. They were reserved to determine the density according to the method of paraffining samples (see chapter 4.9.7 Bulk density - waterproofed paraffin-coated specimens). Based on the results, the optimal bitumen content was ±4% for both methods, in correspondence with the Marshall test criteria for this type of mix. For instance, according to the Italian standard [RFI, section XV Sub-ballast, 2016; C.N.R.-B.U. n.30, 1973] Specifications for

[9] IDT standards [AASHTO T312; ASTM D6931] allow heights between 50.8-75mm.

Roads pavements, the air voids content in a mix must be 3–4%; the air voids content in aggregate should be higher than 14%; the stability higher than 15 kN; and the deformation of the mix between 2-3 mm (Fig. 12).

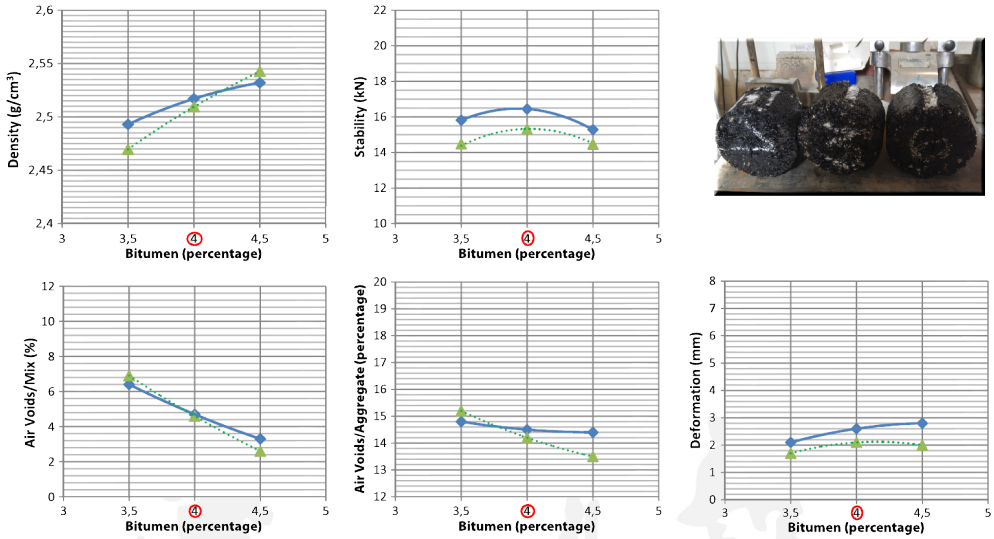


Figure 12. Marshall results for optimal HMA(b.4%) mixtures ϕ150 · 64.5mm

TABLE 23. MARSHALL HMA MIXTURE AIR VOIDS AND DENSITIES (75 BLOWS; B.4%; Φ100·63.5MM)

	Sample 1	Sample 2	
P1	1269	1261	P1, the mass of the container in air, in grams (g);
P2	1296	1289	P2, the mass of the waxed (parafinn) sample, in grams (g);
P3	763	758	P3, the mass of the paraffined sample suspended in water, in grams (g);
γmax	2.635		gr/cm3 - the Maximum density of the mixture (Procedure C EN 12697-5);
Density	2.519	2.533	gr/cm3 - the Bulk density of the mixture (Procedure C EN 12697-6);
Pb	3.96	3.96	% Binder in the mixture to the nearest 0,1 % (m/m);
Gsa(agg)	2.808		Mg/m3 = gr/cm3- Specific gravity of the aggregates;
Gb	1.033		Mg/m3 = gr/cm3- Density of the binder at 25 °C;
%Va	4.19	4.18	%Va, Air voids content
Averaged %Va	**4.21**		

As a first conclusion, the mixtures compacted by SGC reached a percentage of voids lower than those made with the Marshall methodology, which compacted less than the Volumetric gyratory compactor. Thus, a set of six Marshall cylindrical test specimens was divided into two equally sized subsets and conditioned. One subset was maintained dry at 20±5°C, while the other subset was saturated and stored in a water bath at 40±1°C for a period of 68-72h. Finally, to analyze the moisture damage, the indirect tensile strength ratio, ITSR was performed (Table 24) [see equations Chapter 4.10.2]:

TABLE 24. SUMMARY OF IDT AND ITSR FOR HMA (B.4%)

Properties (SGC specimens)	WET	DRY	Standard C.N.R. B.U. 134/91
Indirect tensile strength at 15°C (N/mm²)	1.19	1.40	≥0.6
Water sensitivity (ITSR %)	85.2		>80
Coefficient indirect tensile strength (CTI) at 25°C [EN 12697-23] (N/mm²)	123.75	91.84	30-110
Properties (Marshall specimens)	**WET**	**DRY**	**Standard**
Indirect tensile strength at 15°C (N/mm2)	1.32	1.53	≥0.6
Water sensitivity (ITSR %)	86.3		>80
Coefficient indirect tensile strength (CTI) at 25°C [EN 12697-23] (N/mm²)	66.09	77.88	30-110

The results for the HMA mixtures were optimal both by Superpave and by Marshall methodologies. The parameters of specimen dimensions and different compactions do not alter the optimal composition of the materials in the laboratory [C.N.R.-B.U. 1973]. Therefore, HMA mixtures are considered favorable for use in railway sub-ballast at the laboratory improvement level. The next step discusses the analysis of mixtures with recycled rubber adopting as a reference mixture the HMA obtained by SGC.

6.4. Phase 3.1. Mix-design of Dry rubberized mixtures

6.4.1. Substitution of rubber into a granulometric curve

For closed bituminous mixtures, a well-assorted and compact lithic structure is an essential requirement for good behavior in situ. The simple addition of rubber granulate to a well-graded mixture resulted in a significant modification of the granulometric distribution. In principle, it was assumed to adopt a volumetric replacement scheme, where it would be reasonable to assume that the volume of bitumen remains constant.

The replacement was designed in volume and not in bulk, which entailed some operational difficulties in the laboratory. It was desirable that all the results obtained were then re-translated regarding mass, to be able to carry out practical operations more efficiently. However, it is appropriate that all the results obtained are then translated again regarding mass, to be able to carry out the practical operations more efficiently [Celauro, B. et al. 2003; D'Andrea, A. et al. 2001; Buonanno, A. et al. 2000; Eco.Pne.Us, 2000]. The rubber substitution criterion is summarized in Table 25 and Figures 13-14:

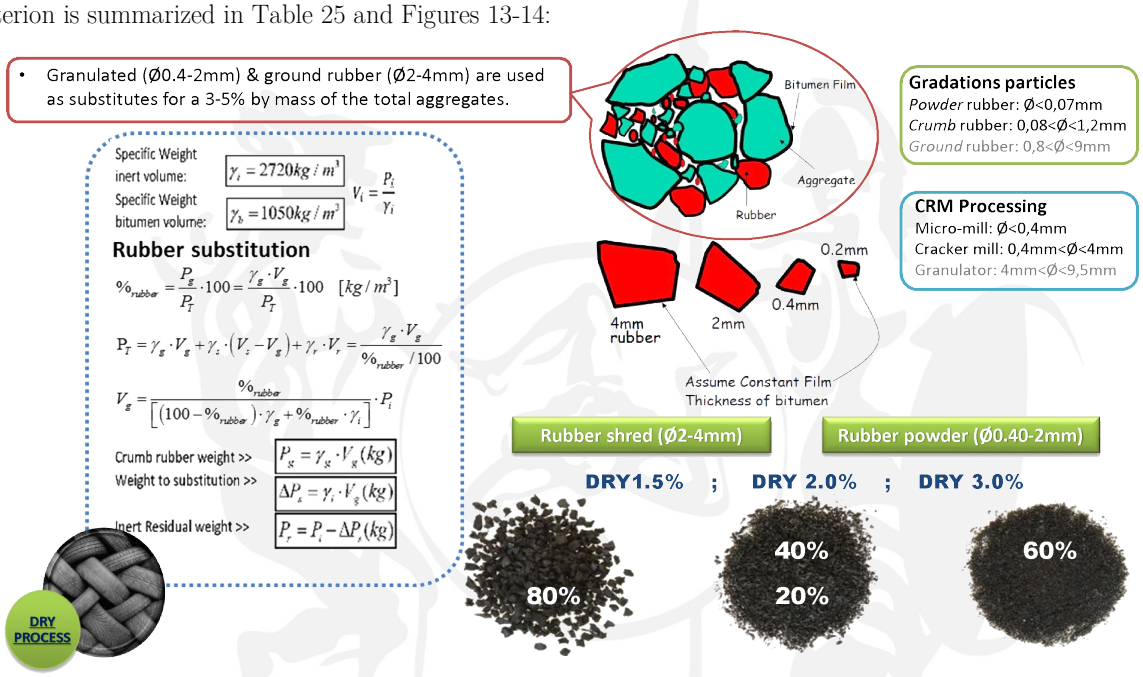


Figure 13. Representation of substitution of granular rubber to the inert of similar granulometry

Volume	1	m3	
Specific Weight Inert Vol. Yi (Kg/m3):			2808.2
Weight binder Yb (g/cm3):			1033
$V_i = \frac{P_i}{\gamma_i}$	DRY PLUSRIDE	%Binder	5.5%
		% VA:	3.0%
		%CRM:	1.5%

Inert weight > $P_i = \frac{(1 - \%Va) \cdot V_i}{\frac{1}{\gamma_i} + \frac{\%b}{\gamma_b}} = \frac{(1 - 0.03) \cdot 1}{\frac{1}{2808} + \frac{0.055}{1033}} = 2369.6 kg$

Bitumen weight > $P_b = \frac{(1 - \%Va) \cdot V_i}{\frac{1}{\gamma i} + \frac{\%b}{\gamma b}} \cdot \%b = 2369.6 \cdot 5.5\% [kg]$

Pinert (Kg)	2369.6	Vg (m3)	0.0302	Pg (Kg)	34.80	Pr (Kg)	2284.9
Pb (Kg)	130.3	Ptotal (Kg)	2319.7	Psubst (Kg)	84.70	Pmix (Kg)	2404

%CRM by Pmix	%CRM in volume	RATIO
1.50%	3.02%	0.497

Bulk density of Samples >> $\gamma_{app} = \frac{m_1}{m_3 - m_2} \cdot \gamma_w [kg/m^3]$ $\quad \%VA = 1 - \left(\frac{\gamma_{APP}}{1 + \frac{\%b}{100}} \cdot \left(\frac{1}{\gamma_i} + \frac{\%b/100}{\gamma_b} \right) \right) \rightarrow 1.5\% = 1 - \left(\frac{\gamma_{APP}}{1 + 0.055} \cdot \left(\frac{1}{2808} + \frac{0.055}{1033} \right) \right)$

Air voids % >> $\gamma_g = 1153 kg/m^3 ; \gamma_s = \gamma_i = \gamma_r = 2808 Kg/m^3$

$\%_{CRM} = \frac{P_g}{P_T} \cdot 100 = \frac{\gamma_g \cdot V_g}{P_T} \cdot 100 \rightarrow 1.5\% = \frac{1153 \cdot V_g}{P_T} \cdot 100 Kg/m^3$

$V_g = \frac{\%_{CRM}}{[(100 - \%_{CRM}) \cdot \gamma_g + \%_{CRM} \cdot \gamma_i]} \cdot P_i = \frac{1.5}{[(100 - 1.5) \cdot 1153 + 1.5 \cdot 2808]} \cdot 2369 kg$

$P_T = \gamma_g \cdot V_g + \gamma_s \cdot (V_s - V_g) + \gamma_r \cdot V_r = \frac{\gamma_g \cdot V_g}{\%_{CRM}/100} = \frac{1153 \cdot V_g}{0.015} kg$

$P_g = \gamma_g \cdot V_g$
$\Delta P_s = \gamma_i \cdot V_g$
$P_r = P_i - \Delta P_s$

Figure 14. Mathematical substitution of rubber in the granulometric grading curve

TABLE 25. EXAMPLE OF RUBBER REPLACEMENT IN GRANULOMETRIC CURVE (1M^3)

	Sieve Size(mm)	% Passing limit			RUMAC 1.5%		V: 1m^3		Volume (m^3)		Weight (kg)		
		Lower limit (%)	Upper limit (%)	Target curve (%)	Passing (%) GC	Retained (%) GC	Weight passing (Kg)	Weight retained (Kg)	V_{inert} (m^3)	V_{CRM} (1.5%) (m^3)	$W_{rubber, Pg}$	$\Delta W_{aggr, Ps}$	$W_{waste, Pr}$
Coarse aggegates (Limestone)	31.5	100.00	100.00	100.00	100.00	0.00	2808.2	0.0	0.000	0.00E+00	0.00	0.00	0.00
	22.4	90.48	100.00	92.86	92.26	7.78	2590.8	218.6	0.078	2.78E-03	3.21	7.81	210.77
	16	71.59	92.23	76.75	76.82	15.51	2157.4	435.6	0.155	5.54E-03	6.40	15.57	420.02
	11.2	58.56	80.21	63.97	62.77	14.11	1762.6	396.2	0.141	5.04E-03	5.82	14.16	382.06
	8	49.04	70.49	54.41	54.23	8.62	1522.8	242.0	0.086	3.08E-03	3.55	8.65	233.31
Fine aggegates (Limestone)	5.6	41.22	61.80	46.36	46.32	7.96	1300.7	223.5	0.080	2.84E-03	3.28	7.99	215.47
	4	36.00	56.00	41.00	37.72	8.53	1059.3	239.5	0.085	3.05E-03	3.52	8.56	230.94
	2	23.00	40.00	27.25	27.45	10.14	770.9	284.8	0.101	3.63E-03	4.18	10.18	274.64
Sand	1	14.77	28.61	18.23	20.61	6.76	578.8	189.9	0.068	2.42E-03	2.79	6.79	183.15
	0.4	9.76	21.51	12.69	15.80	4.76	443.6	133.8	0.048	1.70E-03	1.96	4.78	128.99
	0.177	7.02	16.05	9.28	10.51	5.28	295.1	148.3	0.053	1.89E-03	2.18	5.30	143.01
Filler	0.063	5.89	9.35	6.75	6.85	3.66	192.3	102.9	0.037	1.31E-03	1.51	3.68	99.21
---						6.85		2615.0	0.931	3.33E-02	38.40	93.47	2522

Apparently, this is the mathematical development to perform the rubber tire replacement by replacing one or more granulometric fractions of our aggregates. The first results of mixtures with 1.5% rubber whose usual procedure was developed by modifying the granulometric curve in different fractions are shown below. The methodology adopted was the Volumetric SGC. In this way, indicating the percentage of scrap tire rubber (STR) relative to the volume of aggregates, it was able to obtain in each case the list of required mass-materials.

6.4.2. Evaluating compacted DRY 1.5% trial mixtures

During these study, different mixes were analyzed by volumetric mix-design, obtaining optimal mixes with various amounts of asphalt binders[10]:

A dense-graded Plusride mixture with 1.5% of rubber and binder 5% to 5.5% (DRY 1.5);
A dense-graded Plusride mixture (DRY 2.0) with a binder content of 6% to 6.5% and;
A Generic dry dense-graded mixture (DRY 3.0) with a 3% of rubber and 6.5% of binder.

Initially, only coarse rubber was being used in the dry process. However, experience with the mix indicated better durability with an increase of fine rubber content [Hassan, N.A: et al. 2015; Takkalou, H. et al. 2015; D'Andrea, A. et al. 2001; Esch, D.C. 1984].

Each mixture had a different proportion of rubber, to be representative of the real conditions in the field and to ensure the homogeneity of the reaction between rubber-bitumen. Thus, the percentage of voids varied between 3.01% and 3.37%, and the distribution was:

For Plusride mixes: #60-40 (60% of fine powder-crumb rubber of Ø0.4 to 2mm and, 40% of ground rubber of Ø2 to 4mm) and;
For Generic-dry mixture: #80-20 (20% of crumb rubber of Ø0.4 to 2mm and, 80% of ground rubber of Ø2 to 4mm).

The first experimental phase consists of 4 different mixtures to determine the right mass of aggregates to reach a height of 120 mm with 102 compaction gyrations (Figure 15, Tables 26-28). Four percentages of bitumen (4%, 4.5%, 5% and 5.5%) were established. Two samples of 150x120mm per mixture were done for each bitumen tested and varied the mass ±300gr. An aggregate weight between 5100±300grams was usually sufficient for the compacted specimens, which were mixed at the appropriate mixing temperature (160ºC to 173ºC respectively) and a compaction temperature (145ºC to 150ºC). The dry-process mixes were manufactured with a digestion time between 60, 90 and 120min to enhance the interaction between binder-rubber modifying the mechanical properties of the mixes. After compaction, each sample was 24h cooled to room temperature without being removed from the mold to avoid the bounce back effect due to the swelling of rubber, because it was observed a dilatation (expansion) of the specimens after two days [Soto, F.M. et al. 2017].

[10] 1.5%, 2% and 3% of the total weight of the aggregates (3.02%, 3.90% and, 5.71% by volumetric substitution). Limestone aggregates with density value of 2.81g/cm^3 were considered.



Figure 15. (a) SGC Development of DRY 1.5% (1st trial mix-design); (b) Swelling effect

TABLE 26. DRY1.5% TRIAL GRADING CURVE

Sieve Size(mm)	% Passing limit			%Passing						TRIAL mix
	Lower limit (%)	Upper limit (%)	Target mix (%)	Filler Ø0.163mm	Sand Ø2-4mm	Ø5-10mm	Ø10-15mm	Ø20-25mm	Ø25-30mm	Theoretical recipe (%)
31.5	100.00	100.00	100.00	100.00	100.00	100.00	100.00	100.00	100.00	100.00
22.4	90.48	100.00	92.86	100.00	100.00	100.00	100.00	100.00	72.68	94.48
16	71.59	92.23	76.75	100.00	100.00	100.00	100.00	60.01	14.26	75.43
11.2	58.56	80.21	63.97	100.00	100.00	100.00	96.43	10.44	1.24	63.04
8	49.04	70.49	54.41	100.00	100.00	100.00	67.01	1.00	0.35	54.83
5.6	41.22	61.80	46.36	100.00	100.00	83.03	32.22	0.40	0.35	46.16
4	36.00	56.00	41.00	100.00	98.02	30.64	7.96	0.35	0.35	37.16
2	23.00	40.00	27.25	100.00	76.08	0.66	0.40	0.30	0.35	29.05
1	14.77	28.61	18.23	89.83	35.15	0.66	0.40	0.30	0.35	19.24
0.40	9.76	21.51	12.69	83.27	10.57	0.66	0.40	0.30	0.35	13.29
0.177	7.02	16.05	9.28	72.12	0.83	0.66	0.40	0.30	0.35	9.81
0.063	5.89	9.35	6.75	54.09	0.33	0.33	0.20	0.20	0.20	6.85

TABLE 27. DRY1.5% TRIAL RECIPE FOR LABORATORY MIXTURES

	Filler	Sand	fØ5-10mm	fØ10-15mm	fØ20-25mm	fØ25-30mm	Σcomponents
	<0.063	0.063/4	0.063/8	0.063/11.2	5.6/22.4	5.6/31.5	
Passing	[%]	[%]	[%]	[%]	[%]	[%]	[%]
DRY1.5%	13,021	20,743	6,413	21,495	18,112	20,216	100.00
Γmix=	2.746					Γaggr=	2.807

TABLE 28. DRY1.5% TRIAL SUBSTITUTION OF RUBBER. ADJUSTING MASS OF AGGREGATES-BINDER

Sample	H [mm]	Mass Aggr[gr]	Binder [%]	Sample mass [gr]	Binder mass [gr]	Filler [gr]	Sand [gr]	fØ5-10mm [gr]	fØ10-15mm [gr]	fØ20-25mm [gr]	fØ25-30mm [gr]	CRM60% Ø0.4-2 [gr]	CRM40% Ø2-4 [gr]
DRY1.5/4.0	120	5250	4.0	5350	214	655	1125	338	1133	954	1065	50	33
DRY1.5/4.5	120	5225	4.5	5325	240	651	1119	336	1127	950	1060	50	33
DRY1.5/5.0	120	5200	5.0	5300	265	648	1114	335	1122	946	1055	50	33
DRY1.5/5.5	120	5175	5.5	5275	290	645	1109	333	1117	941	1050	50	33
binder* 5%	120	5145	5.0	5600	280	685	1177	354	1186	999	1115	53	35

As an observation, it is stated how the manufacturing recipe changes in each mixture (Table 27) because the mixtures were adjusted to a dense-graded granulometric curve according to the material selected on each date. The content in bags from the quarry provided different fractions of each aggregate.

The results of the initial mixtures with recycled rubber at 1.5% showed that a bitumen content of 5.5% approached the optimum target air voids (specimens 7 and 8). All specimens were made with the same amount of aggregates (5380 gr) and a final mass of 5460 gr, based on previous studies already discussed (Table 29).

TABLE 29. DRY 1.5% TRIAL RECIPE. RESULTS WITH SGC (M_Q=M_1±300GR)[11]

Nº Φ	Aggr. mass [gr]	Binder content (%)	Sample mass [gr]	Binder mass [gr]	$HN_{des.}$ [mm]	$H_{24h.}$ [mm]	Effect. binder [gr]	M_1 24h [gr]	M_2 24h [gr]	M_3 24h [gr]	Γ_{mb^*} (g/cm³)	Γ_{mm} [%]	%Va 24h	%VMA	%VFA	Δ%b*	Mass-Height [-]
1	5200.0	4.0	5460	208	123.7	126.76	210.0	5460	3266	5552	2.342	92.6%	9.70%	18.36%	67.20%	6.52	
2	5250.0	4.0	5460	210	124.3	127.38	210.0	5461	3284	5504	2.439	88.9%	6.30%	16.28%	61.27%	5.63	
3	5224.9	4.5	5460	235	123.5	125.00	235.3	5465	3316	5467	2.529	93.3%	3.42%	13.70%	75.02%	4.48	Height
4	5225.0	4.5	5460	235	123.3	121.88	235.0	5458	3304	5473	2.504	96.8%	3.46%	14.72%	76.49%	4.95	120mm
5	5200.0	5.0	5460	260	123.0	122.50	260.2	5465	3281	5494	2.447	96.5%	5.45%	16.47%	66.92%	5.74	if m:
6	5200.0	5.0	5460	260	123.2	124.75	260.0	5461	3279	5466	2.476	94.3%	3.68%	15.86%	76.79%	5.49	**5380gr**.
7	5175.36	5.5	5460	284	123.6	123.25	284.7	5462	3272	5411	2.518	96.1%	2.44%	14.78%	83.49%	4.99	
8	5175.40	5.5	5460	285	122.2	121.00	282.1	5411	3266	5552	2.465	97.7%	2.92%	15.91%	65.38%	5.46	

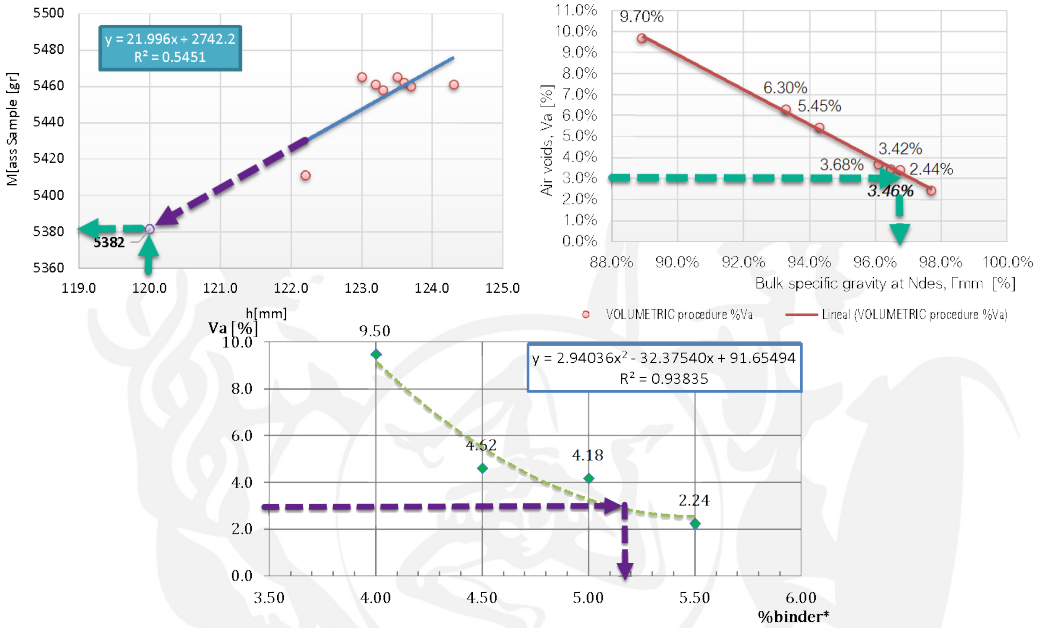


Figure 16. (a) Mass vs. height diagram DRY 1.5% (Ndes. 102); (b) %Va vs. Density; (c) %Va vs. %binder

The purpose of developing a first test mixture was to determine the right mass for a target thickness of 120mm. Even so, to fulfill this objective, we studied the densification curves because of the relevant behavior of the recycled rubber in this first test phase. The optimum bitumen content was ±5.5% when the rubber was of the order of 1.5% but lower %Va. The results of the percentage of voids are reported to N_{des} (Fig. 17; Table 30).

TABLE 30. DRY 1.5% AIR VOIDS AT NDES (DENSIFICATION CURVES)

Water temperature:		22			Water density:	997.8							
H_{Ndes} [mm]	φ 15·12cm	W_{air} (m1)	W_{dry} (m3)	W_{water} (m2)	Υ_w (Kg/m3)	%b	Υb (Kg/m3)	Υ_{aggr} (g/cm3)	Υ_{bulk} (Kg/m3)	$\Upsilon_{geom.}$ (Kg/m3)	$Va_{(\%)}$ Ndesign	$V_{a\,(\%)}$	Δ%b*
123.7	m1	5460	5552	3266	997.80	4.00%	1033.3	2807.5	2490.1	2500.6	9.49%	9.49%	6.20%
124.3	m2	5461	5504	3284					2383.6	2486.2	9.50%		
123.5	m3	5465	5467	3316	997.80	4.50%	1033.3	2807.5	2456.3	2504.1	6.12%	4.62%	4.75%
123.3	m4	5458	5473	3304					2531.8	2504.9	3.11%		
123.0	m5	5465	5494	3281	997.80	5.00%	1033.3	2807.5	2514.1	2514.3	3.22%	4.18%	5.07%
123.2	m6	5461	5466	3279					2462.3	2508.4	5.14%		
123.6	m7	5462	5411	3272	997.80	5.50%	1033.3	2807.5	2492.0	2500.7	3.32%	2.24%	4.80%
122.2	m8	5411	5552	3266					2524.1	2505.7	2.15%		

In conclusion for this DRY 1.5% trial mixture, an unstable general variation of results is observed due to the instability of the rubber and the number of turns of the compactor. The mass of aggregates to obtain specimens of height 120mm was a weight of 5380gr. Finally, a densification curve schemed for each mixture (Fig. 17):

[11] m1 = Weight of specimen in air, gr; m2 = Saturated Weight in water, gr; m3 = Weight of surface-dry specimen in air, gr
ρw = Water density at Tª test ; ρbdry = Bulk density with saturated surface dry
Γssd (Apparent Specific Gravity)=ρw[m1/(m3-m2)]
VMA= Voids in the mineral aggregate ; VFA= Voids filled of asphalt

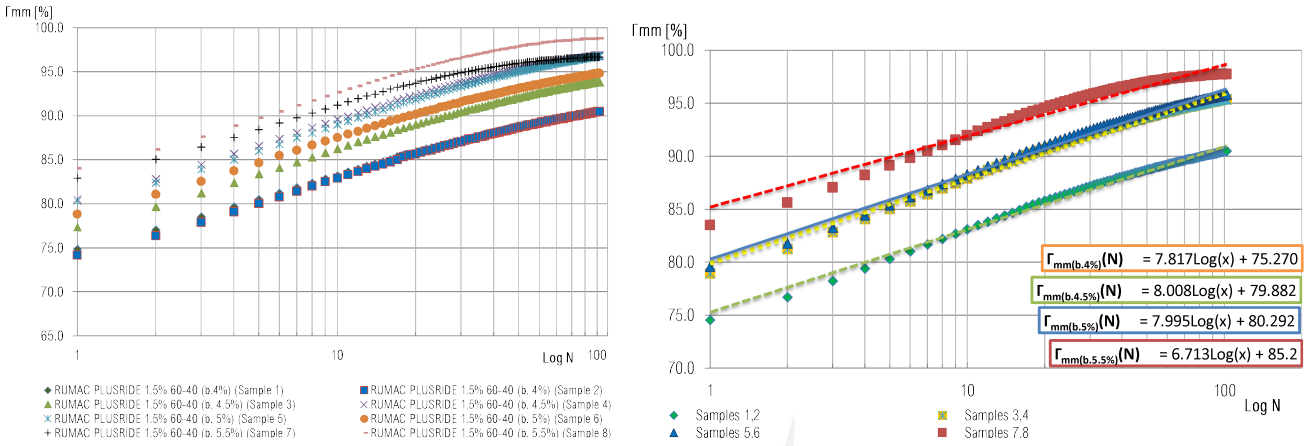


Figure 17. (a) Densification curves DRY 1.5% (1st trial mix-design); (b) Regression values from trend-line

Evidently, these DRY1.5% blends would not have then complied with the target voids at Ndes. 102 because the lack of air voids would have led to plastic deformations. Due to the resilience of the rubber, irrespective of the digestion time, we have been able to experience the swelling and rebound effects because of the accumulated residual energy of the rubber during post-compaction. The air voids of each specimen after one week were higher than desired. Numerous factors influenced in the modification, which consist of base bitumen constituents, blending time, temperature, the percentage of rubber, the gradation of crumb rubber, and the T^a mixing.

In the study carried out in the next section of this first methodology (SGC), the effects due to swelling, rebounding and non-uniform post-compaction stages were analyzed. From a possible increase in the values of Ndes as part of a new "empirical" methodological approach, based on the volumetric design of the mixture, another achievement is shown in this thesis to improve the rubber-compaction mixture.

6.4.3. Optimization of the DRY manufacturing process

6.4.3.1. Introduction

Scrap Tire Rubber (STR), used as a fraction of the coarse-fine aggregate, is the best option since it contributes to the reduction of fatigue and rutting pathologies because of the elastic behavior of the rubber [Farhan, A.H. et al. 2015; Hassan, A. 2006]. Several studies showed that the properties of binders are improved by the addition of rubber particles at ambient temperature, among which the reduction of the thermal susceptibility of bitumen and the increase of the viscosity according to the rubber-bitumen interaction [Soon-Jae, L. et al. 2008; Singleton, T. et al. 2000; Giovarini C. et al. 1999].

One of the purposes was the development of HMA_DRY mix-design but minimizing the effects derived from the rubber-bitumen interaction or reaction between asphalt and CRM (Ø2-4 mm) when blended. The rubber particles, regarding the dry process, would maintain their physical shape and properties within the asphalt mixture due to the interaction and lack of adhesion with the bitumen. This fact causes instability to the volumetric matrix due to the constant swelling of the rubber particles after compaction leading to premature cracking over the asphalt mixture [Farouk, A. et al. 2017].

6.4.3.2. Analysis of rubber-bitumen interaction

This study aims to demonstrate a different thought by controlling the rubber-bitumen interaction that causes swelling of the rubber particles [Farouk, A. 2017; Bairgi, B. 2015; Caltrans 2011; Attia, M. et al. 2009; Cao, W. 2007; Airey, G. et al. 2002; Bahia, H.U. et al. 1995; Stroup G. et al. 1993]. Depending on the proportion and density of the rubber, a diverse reaction bitumen-rubber would occur. The interaction made the b_nder stiffer and elastic and, consequently, changed the properties of the asphalt mixture [Soto, F.M. et al. 2018].

It was characteristic not to achieve uniform distribution of the rubber particles throughout the mix when adding it as a dry-filler inside an HMA mixture (120-190ºC) because there was not enough time for a reaction to

take place between binder and fine-rubber. Consequently, there was no modification of the resulting binder, in other words, diffusion or imbibition [Rahman, M. 2004]. This effect caused a concentration of "clusters of rubber" inside the mixture after compaction, because of different densities, not enough energetic gyrations during mix-design and due to a decrease of mix-temperature. In Figure 18 is shown this effect on cut specimens:



Figure 18. The inhomogeneous concentration of rubber in different sections of the DRY1.5% blend

The vulcanized natural or synthetic rubber, independently of the size of the particles, interacted with bitumen partly dissolved by imbibition or a diffusion process. However, the rubber particles in dry mixes absorbed the stresses due to the thermal changes, thereby increasing the resistance to cracking and avoiding the structural expansion. Figure 19 shows the result of bitumen absorption in the rubber–bitumen interaction for three of the trial-mixes DRY 1.5% at different rubber-bitumen ratios (b. 4.5%, b.5%, and b.5.5%):

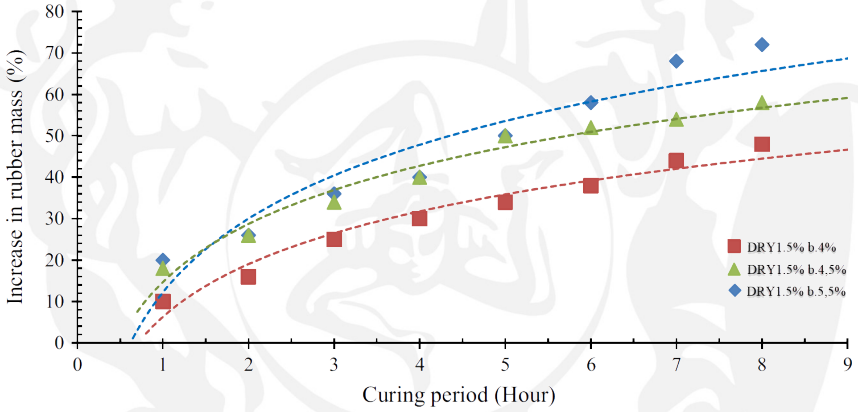


Figure 19. Increase in rubber mass during curing for different specimens of trial DRY1.5% blend

6.4.3.3. Swelling and Expansion of STR in rubberized mixes

In the dry process, the reaction time is usually short. Therefore, the rubber particles were constricted in their movement into the binder matrix limiting the free space between the rubber particles. The swelling capacity is time-dependent of rubber type, the ratio CRM-binder, and the compaction temperature. According to results in this thesis, the factors which affected the digestion process were rubber content, ground size, binder viscosity, and blending conditions. The swelling effect observed confirmed that higher temperature, the rubber absorbed lighter portions of bitumen by the diffusion process. The possible distress that could appear was the further expansion due to the energy accumulated after compaction in the mixture (Fig. 20).

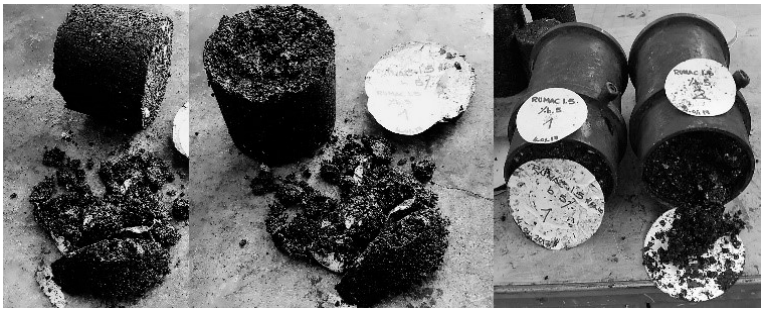


Figure 20. Swelling effect on rubber-modified HMA samples of Ø150x120mm manufactured according to SGC

Thus, swelling depends mainly on test temperature, rubber particle size, loading frequency, bitumen type, liquid-viscosity, and the amount of bitumen concentrated. Higher mixing energy would be required to maintain the molecular structure [Soto, F.M. et al. (Waset, Rome 2017)].

In Fig. 21 is explained that rubber mixture needed a curing period to complete the swelling and to stabilize:

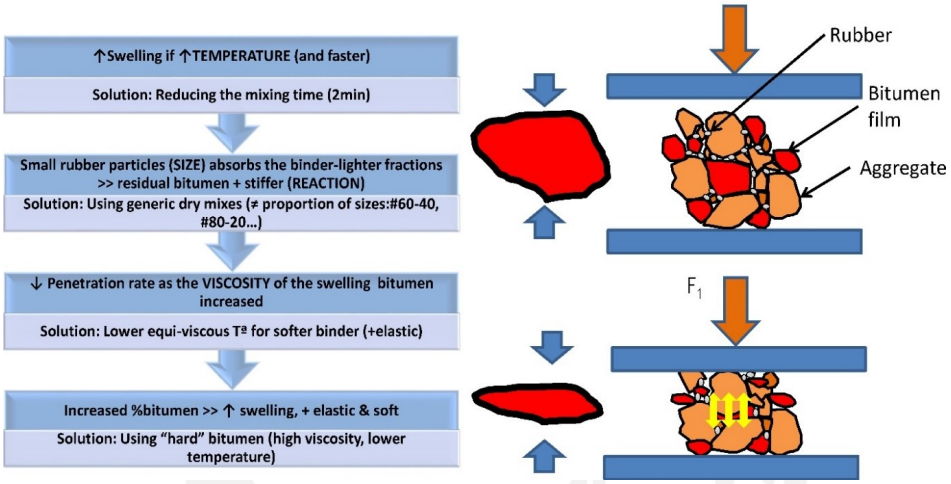


Figure 21. Schematic representation of the swelling effect and effects

During the experimental development, it was observed that the surface of the specimens was damaged due to the difficulty in cutting uniform because of coarse aggregates and rubber not-uniform expansion. Therefore, different geometrical specimens instead of being confined to 24h were found (Figure 22a). To avoid the extra-expansion due to the energy accumulated after compaction in the mixture, cylindrical split molds of Ø150mm were used to compact the specimens. It was easier to remove them after 24h with a manual hydraulic extractor [ASTM D698] without disturbing the matrix (Figure 22b).

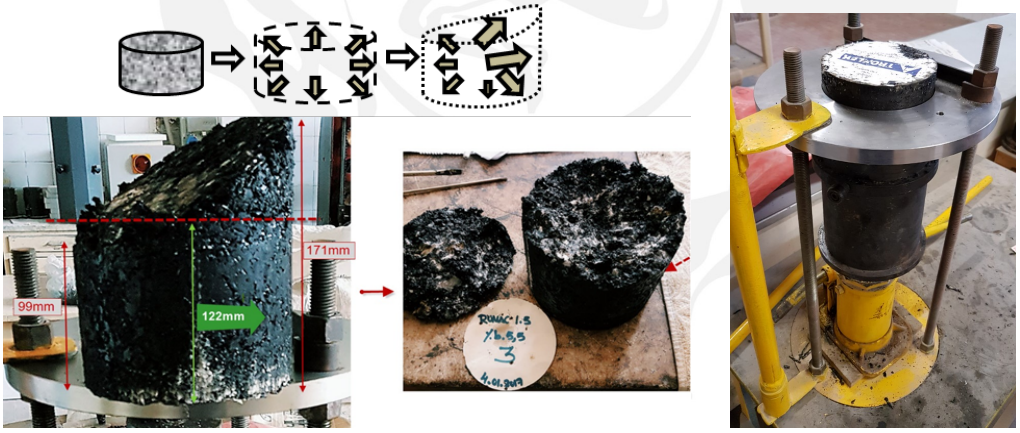


Figure 22. (a) Non-uniform expansion-damage due to the uncontrolled rubber recovery; (b) Hydraulic extractor

6.4.3.4. Rebounding effect by the recovery of storage energy

After compaction, prepared specimens undergo a dilatation (a bounce-back effect) during the curing period (first 24h) at temperature 145ºC. After compaction, the sample was cooled to lab (20ºC) temperature. The air void content was determined after extrusion, not after applied compaction at N_{des}. Rebounding of the top face on samples was a physical process observed, in which crumb rubber particles absorbed the light fractions of asphalt and swelled [Wang, S. et al. 2017; Shen, J. et al. 2017; Farouk, A. et al. 2017]. However, the interaction process between rubber and asphalt can coincide with degradation of the mixture due to the rebounding effect, whose devastating effect can be seen in Figure 23.



Figure 23. (a) Post-compaction deformation by rebound effect on DRY 1.5% by SGC; (b) Swelling and bounce-back effects of rubber particles observed in cut specimens (black points raised)

During the 12 hours after the mixing, it was observed that the rubber mixtures undergo an uncontrolled expansion in the vertical direction internal to the compacting molds (thermal stabilization phase). Thus, DRY blends required higher compaction energy to reach Va.3% during the post-compaction stabilization of the mixture to maintain thermal equilibrium and homogeneous expansion.

→Immediately after compaction, a dead load equivalent to a sample weight (±5.5kg thus limiting a possible post-compaction that reduces the final void percentage) was applied for a further 24 hours to allow the mixture to cool down to ambient temperature. In that way, bitumen gains in stiffness to reduce rubber rebounding, considering that after compaction the rubber would cause an unknown increase in volume (Fig. 24).

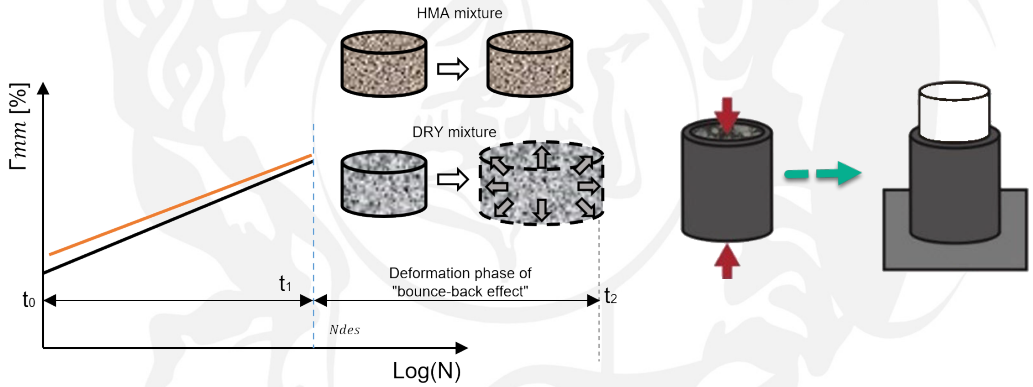
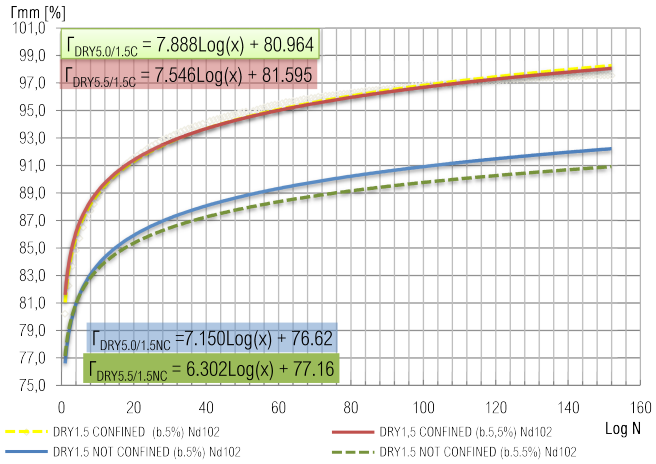


Figure 24. (a) Scheme of densification curve. Rebounding effect after compaction; (b)Schematic proposed solution

Due to the increase in compaction energy, the compactability is greater initially by having mixtures which, within the first 24 hours, experience a robust swelling effect. As an example of the consequences of not following the post-compaction process suggested, a plot of the maximum theoretical density versus the number of gyrations for the mixture made with recycled rubber at 1.5% is shown, with two percentages of bitumen at 5% and 5.5%. The difference is that both mixtures were performed with SGC but with/without the confinement of the specimen in the mold for 24 hours (Figure 25).

It is concluded that there are significant volumetric changes in the properties of each mixture directly responsible for the complex rubber-bitumen interaction, which depends on the size of the fine-coarse rubber (60-40%) and, above all, the post-compaction temperature (thermal change from 160°C to 20°C ambient).

If the specimen exhibits volume change, the final height at the end of compaction and the measured bulk-specific gravity after the sample cools cannot be used to correct the density curves because the specimen volumes differ between the Γ_{mb} measurement at the end of compaction process [Soto, F.M. et al. 2017].



(CONFINED) DRY1.5% (b.5.0% ; 5.5%) (Ndes.102 ; Ø150x120mm) 24h							
Υ_{inert}	$\Upsilon_{bitumen}$	Va	Δ%b.	%b*	Υ_{water}	VMA	VFA
(kg/m³)	(kg/m³)	(%)	(%)	(%)	Tª 21°C	(%)	(%)
2808,2	1033,3	2,79%	5,0%	4,7	0,9981	14,1%	80,3%
2808,2	1033,3	3,10%	5,5%	5,3	0,9981	15,4%	79,9%
(CONFINED) DRY1.5% (b.5.0% ; 5.5%) (Ndes.102 ; Ø150x120mm) 14d							
Υ_{inert}	$\Upsilon_{bitumen}$	Va	Δ%b.	%b*	Υ_{water}	VMA	VFA
(kg/m³)	(kg/m³)	(%)	(%)	(%)	Tª 21°C	(%)	(%)
2808,2	1033,3	3,72%	5,0%	5,1	0,9981	14,9%	75,4%
2808,2	1033,3	3,37%	5,5%	5,4	0,9981	15,6%	78,4%

(Not confined) DRY1.5% (b.5.0% ; 5.5%) (Ndes.102; Ø150x120mm) 24h							
Υ_{inert}	$\Upsilon_{bitumen}$	Va	Δ%b.	%b*	Υ_{water}	VMA	VFA
(kg/m³)	(kg/m³)	(%)	(%)	(%)	Tª 18°C	(%)	(%)
2808,2	1033,3	8,57%	5,0%	7,0	0,9987	19,2%	55,5%
2808,2	1033,3	10,05%	5,5%	8,0	0,9987	21,4%	53,1%
(Not confined) DRY1.5% (b.5.0% ; 5.5%) (Ndes.102; Ø150x120mm) 14d							
Υ_{inert}	$\Upsilon_{bitumen}$	Va	Δ%b.	%b*	Υ_{water}	VMA	VFA
(kg/m³)	(kg/m³)	(%)	(%)	(%)	Tª 13°C	(%)	(%)
2808,2	1033,3	8,56%	5,0%	7,0	0,9994	19,2%	55,5%
2808,2	1033,3	10,25%	5,5%	8,1	0,9994	21,6%	52,5%

Figure 25. (a) Γmm vs. Ndes under DRY1.5% mixtures confined/unconfined in molds during 24h; (b) Results

6.4.4. An empirical approach for the mix-design

The present section aims at proposing a novelty empirical mix-design approach tailored explicitly for rubberized asphalt (dry process) that takes into account the behavior of the CRM during the compaction and post-compaction processes. A fundamental investigation of the mechanical properties of rubber-bitumen was carried out to solve the interaction rubber-bitumen, understanding the rebounding ("bounce-back") effect, and non-uniform post-compaction, which are considerable distresses in laboratory HMA-DRY specimens.

6.4.4.1. Problem statement

The rubber increases the demand for bitumen, and this could hurt the mechanical characteristics of the asphalt mixture. The resilient modulus of the rubberized asphalt decays, and this implies an increase of layer thickness, compared with HMA mixtures [López-Moro, F. et al. 2013; Hernández-Olivares, B. et al. 2009; Moreno, F. et al. 2011]. The absorption of lighter components (maltenes) is part of the maturation process "maceration" [Dong D. et al. 2012; Silvano A. et al. 2005] that causes the swelling of the crumb rubber particles having a more viscous bitumen. Besides that, from literature review, the stiffness of the bitumen increases enhancing higher performances of the mixtures containing CRM if compared to HMA, in particular, higher resistance to rutting but cannot inhibit cracking at low temperature [Losa M. et al. 2011; Rebala, S.R. et al. 1995]. The crumb rubber gradation, the binder, rubber content, the mixing, and compaction energies, are only some of the parameters that make the process complex and unstable [Xiao, F. et al. 2009; Hafez, I.H. et al. 1994]. Despite the numerous efforts employed in improving the mix design system for bituminous mixtures, individual limitations emerge when the traditional gyratory compactor is applied to rubber-aggregate mixtures.

6.4.4.2. Empirical approach: Methodology.

CRM releases the distortion accumulated during the compaction process that may turn out in a non-negligible swelling of the asphalt mixture sample. Therefore, it is necessary to quantify the recovered deformation and the energy stored by the rubber to control the admissible voids content by modifying the compaction process adequately.

An empirical approach in the post-compaction phase has been developed to adjust the number of gyrations proposed by Volumetric mix-design with the requirement of voids content. The research steps are defined:

Preliminary phase – Comparative study of the HMA-DRY1.5% densification curves.
Compaction phase – Definition of a coefficient beta (β) for increasing N_{design} considering the elastic recovery of the rubber and calculation of the rubber storage energy.
Post-compaction phase – Thermal stabilization, confinement and curing phase defined as the time necessary for the rubber to recover its first volume after the compaction.

In the first step of the research, it was necessary to understand how the demand of bitumen increased when the rubber was added to the mixture to obtain the same workability (slope of the compaction curve) of the corresponding HMA-DRY mixtures at the same N_{design} used.

The comparative compaction curves obtained are shown as a graphical scheme in Figure 26.

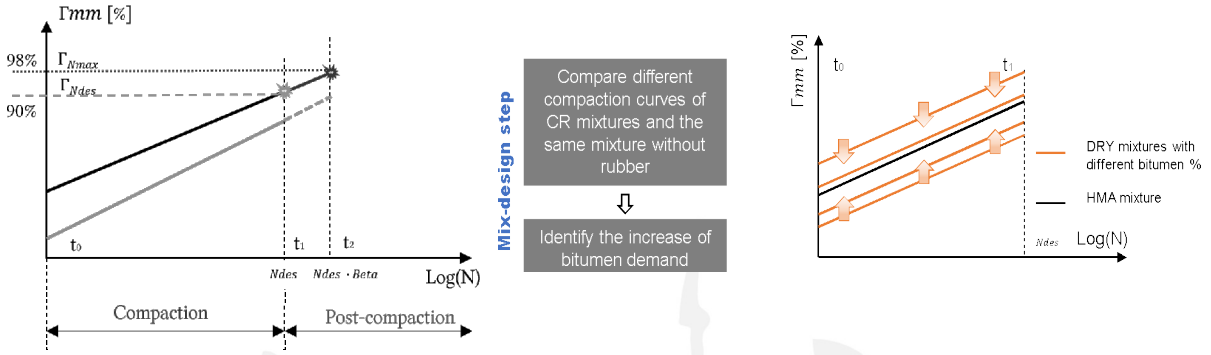


Figure 26. Preliminary stage of comparison densification curves

The basic premise was to start from each compaction curve at the point where the maximum densification was ±97% (percentage of air voids of 3%). Thus, in conventional HMA mixtures as well as those modified with CRM (DRY1.5%, and later 2-3%), it was possible to find a "beta" factor that equalized the compaction behavior. The new parameter "beta" controls the increase of turns necessary to compensate the subsequent increase of internal gaps within the established margins. The post-compaction phase leads to the definition of the coefficient "β" multiplying the standard number of gyrations (N_{des}), to achieve at the end of the curing time, the same void content obtained for an HMA mixture. In other words, an analytical-comparative method has been defined establishing a Va.3% after compaction. Figure 27 shows the schematic research stages.

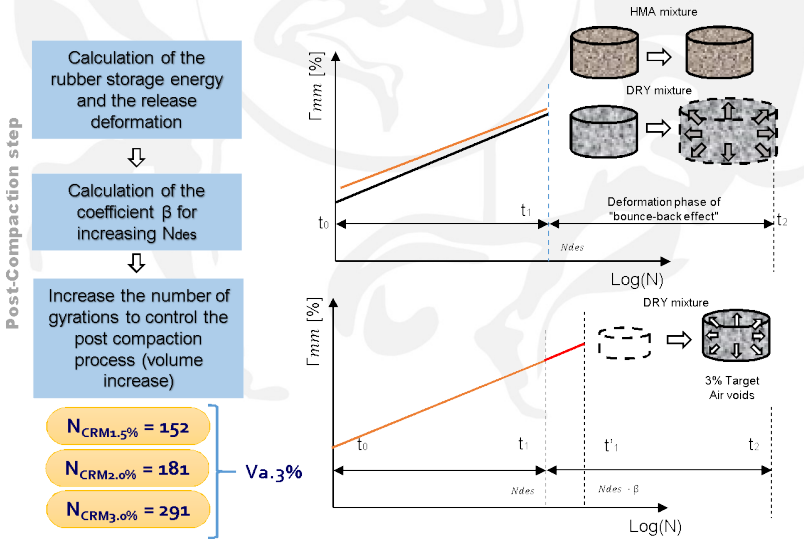


Figure 27. Schematic representation of research stages and previous results

So, for this procedure the already developed densification curves were compared for the following mixtures[12]:

- **HMA, N_{des}. 102; binder 3.5, 3.6, 4, 4.5, and 5%; Va. ±3%;**
- **DRY RUBBER 1.5% #60_40 N_{des}.102; binder 4, 4.5, 5, and 5.5%; Va. ±3%.**

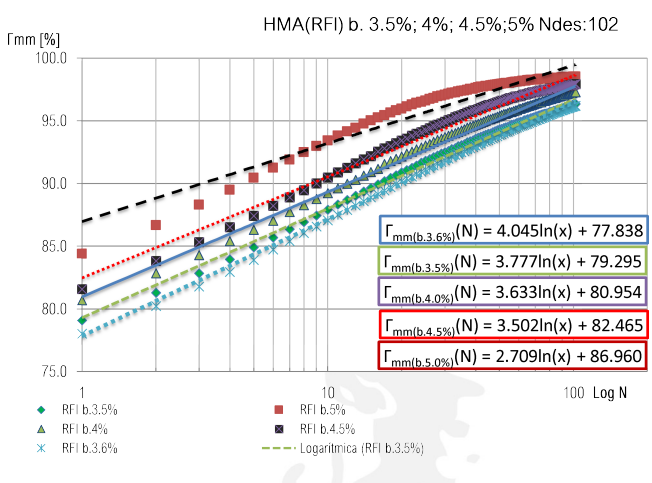
In conclusion, the average[13] regression equations were (Figure 28):

[12] For clarity and simplicity in describing the methodology within the thesis, it was decided to develop only the "beta" factor corresponding to the comparison of the densification curves of the HMA b.4% versus the DRY1.5% (N_{des}.102). Likewise, the DRY 2.0 and DRY 3.0 mixtures were subsequently applied by applying their corresponding "beta" factor.

[13] Each curve corresponds to the mean of 2 test specimens tested in the laboratory of the same mixture.

$HMA_{RFI\ (b.3.5\%)} \rightarrow \Gamma_{mm}\ (N_{des.}\ 102) = 8.697Log(x) + 79.295$
$HMA_{RFI\ (b.3.6\%)} \rightarrow \Gamma_{mm}\ (N_{des.}\ 102) = 8.314Log(x) + 77.838$
$HMA_{RFI\ (b.4.0\%)} \rightarrow \Gamma_{mm}\ (N_{des.}\ 102) = 8.365Log(x) + 80.954$
$HMA_{RFI\ (b.4.5\%)} \rightarrow \Gamma_{mm}\ (N_{des.}\ 102) = 8.065Log(x) + 82.465$
$HMA_{RFI\ (b.5.0\%)} \rightarrow \Gamma_{mm}\ (N_{des.}\ 102) = 6.238Log(x) + 86.960$

$DRY1.5_{\ (b.4.0\%)} \rightarrow \Gamma_{mm}\ (N_{des.}\ 102) = 7.817Log(x) + 75.270$
$DRY1.5_{\ (b.4.5\%)} \rightarrow \Gamma_{mm}\ (N_{des.}\ 102) = 8.008Log(x) + 79.882$
$DRY1.5_{\ (b.5.0\%)} \rightarrow \Gamma_{mm}\ (N_{des.}\ 102) = 7.995Log(x) + 80.292$
$DRY1.5_{\ (b.5.5\%)} \rightarrow \Gamma_{mm}\ (N_{des.}\ 102) = 6.713Log(x) + 85.200$



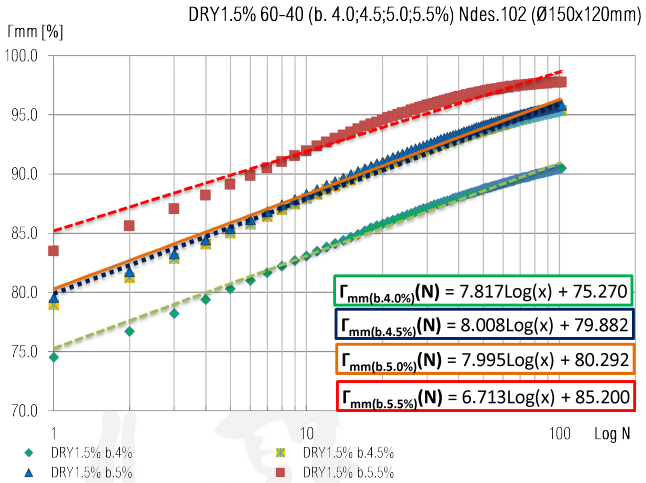


Figure 28. Densification curves for HMA and DRY1.5% mixtures both at N_{des}.102

The equations were alternated every two mixtures of each type varying the possibilities of similarity between curves and obtaining a diversity of beta parameters related to each other. In the framework of this work, "beta" was defined as the coefficient that multiplies the design number of gyrations ($\beta \cdot N_{design}$) necessary to compact a sample of HMA to obtain *the design number of gyrations required to compact a DRY sample (N_{CR})*:

$$N^{i}_{CRM} = \beta \cdot N^{i}_{des} \quad (i = 1-2 samples) \quad \Rightarrow \beta = \frac{\%V_a^{CRM}}{\%V_a^{HMA}} \ if\ Va = 3\% \rightarrow \beta = \frac{\Gamma_{mm97\%}^{CRM}}{\Gamma_{mm97\%}^{HMA}} \qquad \text{(Eq. 4)}$$

N_{CRM} = design number of gyrations optimized for rubber-aggregate mixtures;
Γ_{mm}= average specimen relative density at 97% (Va=3%).

N_{CRM} must have an upper bound (N_{limit}) defined to perform compaction with a reasonable number of turns. In fact, even if the NCR does not have a physical limit, the design of the asphalt mix cannot contemplate an infinite number of gyrations.

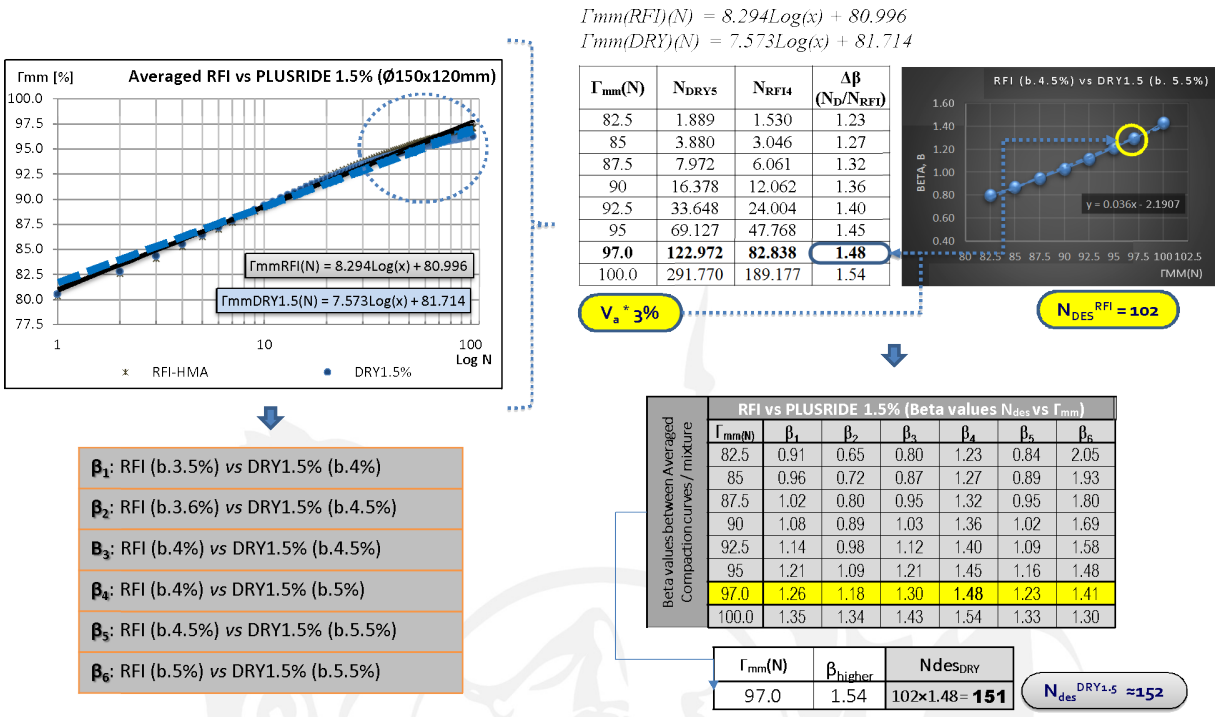
After compaction was completed, the sample was cooled to 20ºC. The real air void content was determined after extrusion, not after applied compaction at Ndes. After 24-36h the specimen was extruded and the bulk specific gravity determined (Γmb) by AASHTO T166. During the 0-24 hours after the mixing, it was observed that the rubber mixtures undergo a robust vertical expansion (thermal stabilization phase). There are previous studies that favor the fact that the mixtures need up to 24h of stabilization before compaction of a second layer [Kruntcheva, M. et al. 2006; Thom, N. et al. 2016]. Also, the surfacing material of specimens after mixing was cooled to ±115°C before being compacted.

6.4.4.3. Empirical approach: Results

The new approach-method that responds to an approximation based on laboratory (empirical) results is summarized in the following Figure 29 as an average example of both mixtures where the following process was observed. In this example, to achieve the same grade of compaction and %Va, the DRY mixture had a N_{des} equal to 102 cycles multiplied by **1.48**, resulting N^{CRM}_{des}.152 cycles to SGC. With other betas the difference was minimal, having a N_{des} between 120 to 145 cycles.

This methodology, as can be seen, allows us to determine the exact number of Ndes, provided that the mixtures we compare are the previously defined optimal ones. That is to say, those mixtures within a

homogeneous compactability, Va.3% and with bitumen optimized according to already developed methodology, it is possible to establish an empirical relation and determine the corresponding beta.



$\Gamma_{mm}(N)$	N_{DRY5}	N_{RFI4}	$\Delta\beta$ (N_D/N_{RFI})
82.5	1.889	1.530	1.23
85	3.880	3.046	1.27
87.5	7.972	6.061	1.32
90	16.378	12.062	1.36
92.5	33.648	24.004	1.40
95	69.127	47.768	1.45
97.0	**122.972**	**82.838**	**1.48**
100.0	291.770	189.177	1.54

$\Gamma_{mm(N)}$	β_1	β_2	β_3	β_4	β_5	β_6
82.5	0.91	0.65	0.80	1.23	0.84	2.05
85	0.96	0.72	0.87	1.27	0.89	1.93
87.5	1.02	0.80	0.95	1.32	0.95	1.80
90	1.08	0.89	1.03	1.36	1.02	1.69
92.5	1.14	0.98	1.12	1.40	1.09	1.58
95	1.21	1.09	1.21	1.45	1.16	1.48
97.0	1.26	1.18	1.30	1.48	1.23	1.41
100.0	1.35	1.34	1.43	1.54	1.33	1.30

RFI vs PLUSRIDE 1.5% (Beta values N_{des} vs Γ_{mm})

$\Gamma_{mm}(N)$	β_{higher}	$Ndes_{DRY}$
97.0	1.54	102×1.48= **151**

Figure 29. Empirical "beta" approach method proposed

For example, for the upper case, for a densification value of 97%, the beta factor has been determined by developing the respective regression equation by clearing the unknown "x" corresponding to the number of turns so that each mixture reaches 3% of air voids (e.g.):

$$\vdots \quad \vdots \quad \vdots \quad \vdots \quad \vdots \quad \vdots \quad \vdots \quad \vdots \quad \vdots \quad \vdots \quad \vdots$$

$$HMA_{b.4\%}: 97\% = 8.365Log(x) + 80.954 \rightarrow antiLog(x) = \left(\frac{97-80.954}{8.365}\right) = 82.838 \qquad \text{(Eq. 5)}$$

$$DRY_{b.5\%}: 97\% = 7.995Log(x) + 80.292 \rightarrow antiLog(x) = \left(\frac{97-80.292}{7.995}\right) = 122.97$$

$$\vdots \quad \vdots \quad \vdots \quad \vdots \quad \vdots \quad \vdots \quad \vdots \quad \vdots \quad \vdots \quad \vdots \quad \vdots$$

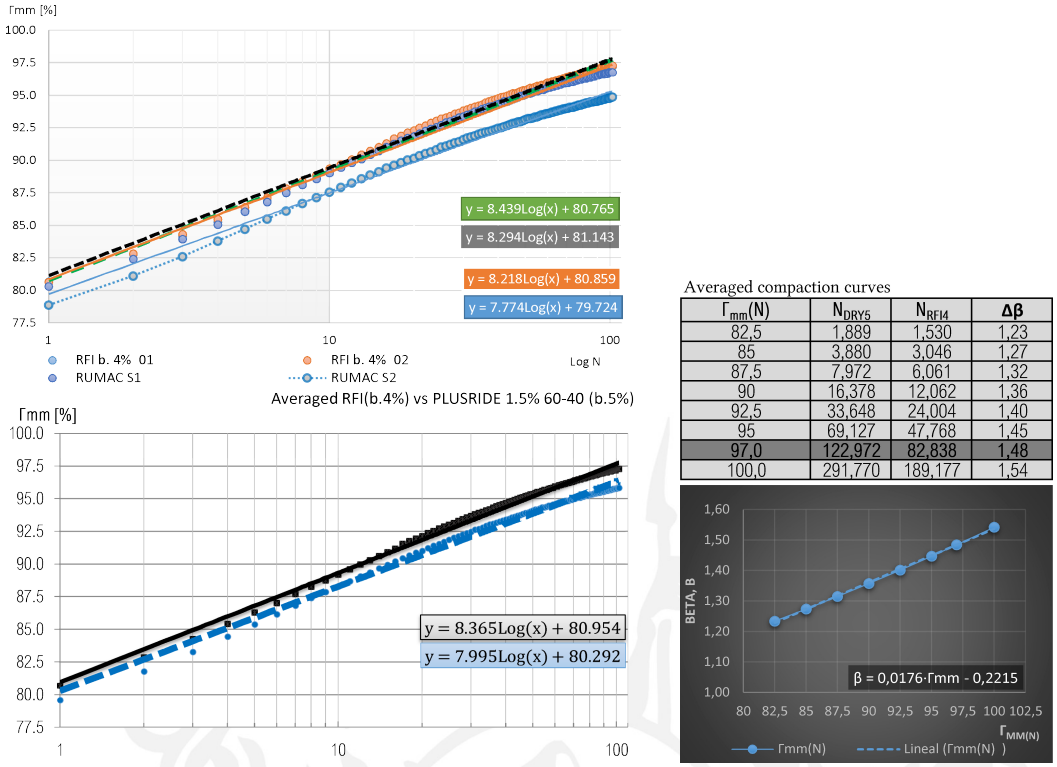
At the critical level in this thesis, two case studies (beta 4 and beta 5) are well developed since with the other combinations proceed in the same way. Also, these beta factors were the most uniform (Fig. 30).

β_4: HMA b.4% vs. DRY1.5% (b.5%)

	Va	binder
HMA	(%)	(%)
	2.74	4.00
	Va	binder
DRY	(%)	(%)
	4.13	4.00

Γmm(RFI 1 b.4%)(N) = 8.439Log(x) + 80.765
Γmm(RFI 2 b.4%)(N) = 8.294Log(x) + 81.143
Γmm(RUMAC1 b.5%)(N) = 8.218Log(x) + 80.859
Γmm(RUMAC 2 b.5%)(N) = 7.774Log(x) + 79.724
Γmm(RFI b.4%)(N)= 8.365Log(x) + 80.954
Γmm(DRY b.5%)(N)= 7.995Log(x) + 80.292

From the results obtained, with a binder content of 4%, the air voids were 2.74% in HMA mixture while in DRY 1.5% it was 4.13%, for that reason is not a valid value (higher than 3%). Above, the actual values of each mixture of %Va with b.4% to 102 cycles are shown, as well as the regression curves of each two samples per mix and its corresponding average regression curve.



Γ_{mm}(N)	N_{DRY5}	N_{RFI4}	Δβ
82,5	1,889	1,530	1,23
85	3,880	3,046	1,27
87,5	7,972	6,061	1,32
90	16,378	12,062	1,36
92,5	33,648	24,004	1,40
95	69,127	47,768	1,45
97,0	122,972	82,838	1,48
100,0	291,770	189,177	1,54

Figure 30. Example of comparison between the compaction curves of HMA b.4%-DRY1.5 b.5%

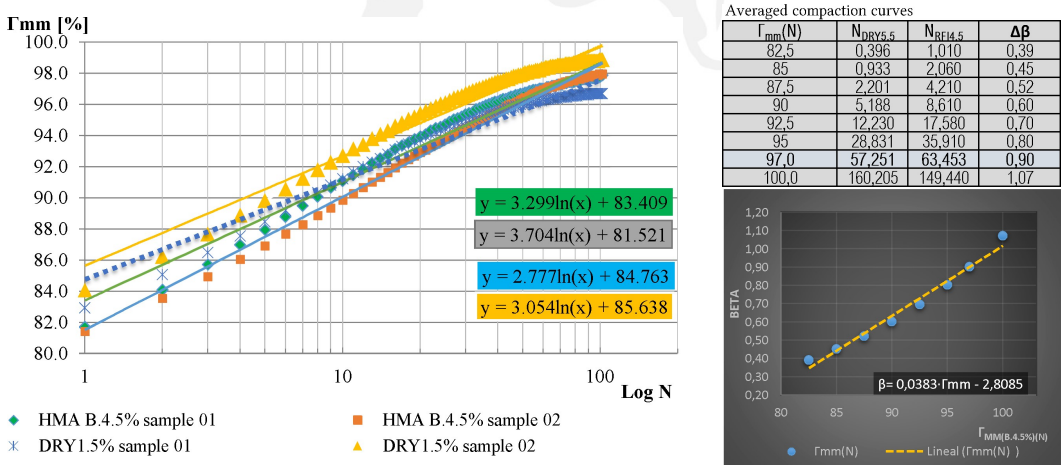
As can be seen, a first conclusion is that to obtain the same degree of compaction at the same number of gyrations with SGC, it must be considered 0.5% and 1% more bitumen content in the mixtures with the recycled rubber of 1.5% to 2%. Later, it will be shown how the beta factor grows as the rubber volume increases in the mixture, and therefore also increases the number of cycles (N_{des}) to an acceptable limit of SGC.

β_5 : HMA b.4,5% (%Va. 2.74%) vs. DRY1.5% b.5,5% (%Va. 4.13%).

	Va	binder
HMA	(%)	(%)
	1,49	5,00
	Va	binder
DRY	(%)	(%)
	2,24	5,50

Γmm(HMA 1 b.5%)(N) = 5.791Log(x) + 87.984
Γmm(HMA 2 b.5%)(N) = 6.625Log(x) + 85.670
Γmm(DRY01 b.5.5%)(N)=6.394Log(x) + 84.763
Γmm(DRY02 b.5.5%)(N)=7.032Log(x) + 85.638
Γmm(HMA b.5%)(N) = 6.238Log(x) + 86.960
Γmm(DRY b.5.5%)(N)=6.712Log(x) + 85.200

For this case study, to achieve the same grade of compaction and air voids content, the rubberized mixture showed an Ndes equal to 102 cycles multiplied by 1.33, resulting 136 cycles to SGC (Fig. 31).



Γ_{mm}(N)	$N_{DRY5.5}$	$N_{RFI4.5}$	Δβ
82,5	0,396	1,010	0,39
85	0,933	2,060	0,45
87,5	2,201	4,210	0,52
90	5,188	8,610	0,60
92,5	12,230	17,580	0,70
95	28,831	35,910	0,80
97,0	57,251	63,453	0,90
100,0	160,205	149,440	1,07

Figure 31. Densification curves (HMA b.5%-DRY1.5 b.5,5%); (a) Each sample; (b) Averaged as Log(Ndes)

"Beta" factors averaged results.

By proceeding sequentially with each combination mentioned above, and making the respective table of values "beta" for every two samples by mixing, a cloud of points is obtained. Graphically it shows the average value that must be adopted to establish a final beta between a conventional mixture HMA and a mixture with DRY1.5% rubber (Figures 32-33).

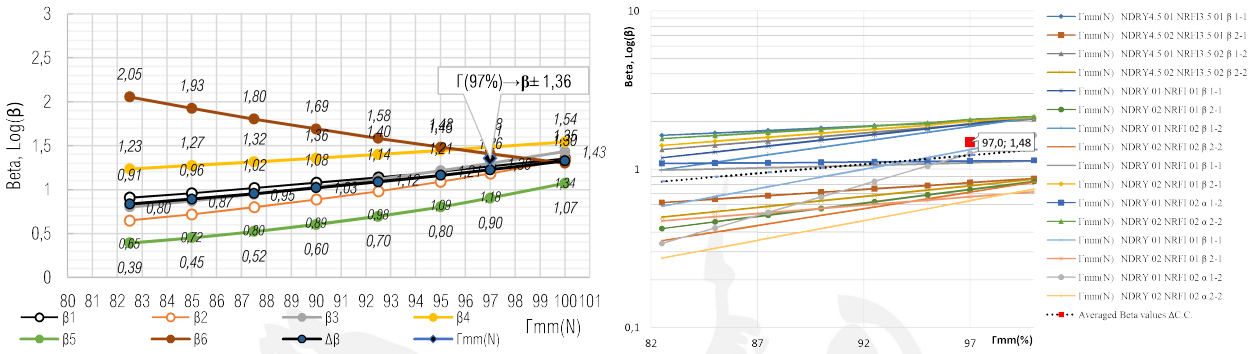


Figure 32. (a) Results of each "beta" HMA vs. DRY1.5%; (b) Averaged results adopted

Therefore, it was possible to estimate and control the final void content by applying a correction factor which adjusts the Ndes depending on the target voids to be reached.

Thus, the Ndes(CRM) was equal to $102 \cdot 1.48 = 152$ turns for a DRY 1.5%. In the same way, concerning a DRY2%, the beta factor was ±1.75-1.80 (Ndes. 181), and finally a DRY3% with beta ±2.75-2.85 (Ndes. 291).

6.5. Phase 3.2. Mix-design of DRY1.5%, N_{des}.152, b.*5-5,5%

After that new "empirical" approach, with the new parameters of Ndes for DRY blends, the final mixtures with rubber were designed. Therefore, the results already allow working in the following mixtures with optimal contents of bitumen and mass of aggregates. In the following case, the optimal DRY1.5% was studied (Fig. 33).

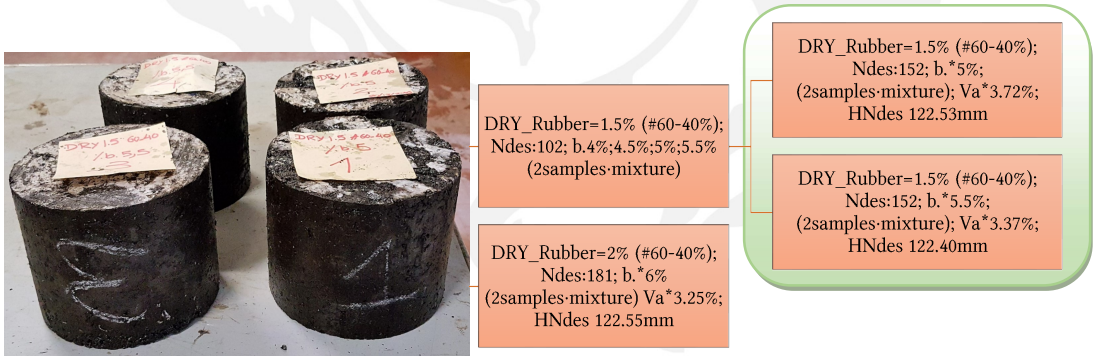


Figure 33. (a) Specimens compacted and extruded after 24h; (b) Flowchart of DRY1.5% Ndes.152

In this new experience in laboratory, mixtures respond to the following characteristics (Tables 31-36):

TABLE 31. $DRY_{1.5\%\ \#60\text{-}40}$ FINAL RECIPE FOR LABORATORY RUBBERIZED MIXTURES

	Filler	Sand	fØ5-10mm	fØ10-15mm	fØ20-25mm	fØ25-30mm	Σcomponents
	<0.063	0.063/4	0.063/8	0.063/11.2	5.6/22.4	5.6/31.5	
Passing	[%]	[%]	[%]	[%]	[%]	[%]	[%]
DRY1.5%	12.446	23.786	4.619	18.978	18.646	21.524	100.00
Γmix=	2.720					Γaggr=	2.808

TABLE 32. $DRY_{1.5\%\#60\text{-}40}$ DEFINITIVE RECIPE FOR LABORATORY MANUFACTURING

Sample	H [mm]	Mass Aggr[gr]	Binder [%]	Sample mass [gr]	Binder mass [gr]	Filler [gr]	Sand [gr]	fØ5-10mm [gr]	fØ10-15mm [gr]	fØ20-25mm [gr]	fØ25-30mm [gr]	CRM60% Ø0.4-2 [gr]	CRM40% Ø2-4 [gr]
DRY1.5/5.0	120	5142.9	5.0	5445	272	645.0	1327.8	251.5	1033.4	1015.3	1172.0	52.2	34.8
DRY1.5/5.5	120	5118.5	5.5	5420	298	642.1	1321.7	250.3	1028.6	1010.6	1166.6	52.2	34.8

TABLE 33. $DRY_{1.5\%\ \#60\text{-}40}$ FINAL RECIPE. RESULTS AFTER **24H** (NDES.152)[14]

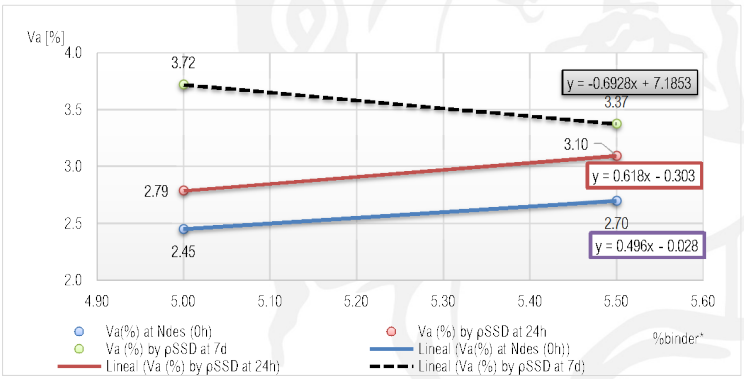
Sample Ø150xh (mm)	Inert mass [gr]	b. (%)	Sample mass [gr]	Binder mass [gr]	$HN_{des.}$ [mm]	$H_{24h.}$ [mm]	Effective binder [gr]	M_1 24h [gr]	M_2 24h [gr]	M_3 24h [gr]	Ɣapp [g/cm³]	Γ_{max} [g/cm³]	Γ_{mb^*} [g/cm³]	Γ_{mm} [%]	Va 24h [%]	VMA [%]	VFA [%]	Δ%b*
$DRY_{1.5_1}$	5143	5.0	5400	257.15	121.30	121.99	258.0	5418	3286	5421	2.533	2.596	2.533	97.58	2.76	14.10	80.42	4.67
$DRY_{1.5_2}$	5143			257.15	122.20	123.08	257.6	5410	3288	5421	2.532	2.596	2.532	97.53	2.81	14.14	80.11	4.69
Averaged	5143			257.15	121.75	122.53	257.8	5421	3287	5421	2.532	2.596	2.532	97.55	**2.79**	14.12	80.26	**4.68**
$DRY_{1.5_3}$	5118	5.5		281.49	121.70	122.62	282.0	5409	3272	5418	2.516	2.577	2.516	97.61	2.79	15.08	81.51	5.13
$DRY_{1.5_4}$	5118			281.55	121.70	121.74	282.6	5420	3264	5428	2.500	2.577	2.500	97.00	3.40	15.62	78.22	5.37
Averaged	5118			281.55	121.70	122.18	282.3	5414	3268	5423	2.508	2.577	2.508	97.30	**3.10**	15.35	79.86	**5.25**

TABLE 34. $DRY_{1.5\%\ \#60\text{-}40}$ FINAL RECIPE. RESULTS AFTER **168H** (NDES.152)[15]

Sample Ø150xh (mm)	Inert mass [gr]	b. (%)	Sample mass [gr]	Binder mass [gr]	$HN_{des.}$ [mm]	$H_{168h.}$ [mm]	Effective binder [gr]	M_1 168h [gr]	M_2 168h [gr]	M_3 168h [gr]	Ɣapp [g/cm³]	Γ_{max} [g/cm³]	Γ_{mb^*} [g/cm³]	Γ_{mm} [%]	Va 168h [%]	VMA [%]	VFA [%]	Δ%b*
$DRY_{1.5_1}$	5143	5.0	5400	257.15	121.30	121.99	258.0	5417	3286	5421	2.532	2.596	2.532	97.56	2.78	14.11	80.31	4.67
$DRY_{1.5_2}$	5143			257.15	122.20	123.08	257.6	5409	3246	5420	2.483	2.596	2.483	95.67	4.66	15.78	70.44	5.43
Averaged	5143			257.15	121.75	122.53	257.8	5413	3266	5421	2.508	2.596	2.507	96.61	**3.72**	14.95	75.38	**5.05**
$DRY_{1.5_3}$	5118	5.5		281.49	121.70	122.70	282.0	5408	3265	5420	2.505	2.577	2.505	97.19	3.21	15.45	79.21	5.30
$DRY_{1.5_4}$	5118			281.55	121.70	121.74	282.6	5420	3262	5429	2.496	2.577	2.496	96.86	3.54	15.74	77.53	5.43
Averaged	5118			281.55	121.70	122.22	282.3	5414	3263	5425	2.500	2.577	2.500	97.02	**3.37**	15.60	78.37	**5.36**

TABLE 35. $DRY_{1.5\%\ \#60\text{-}40}$ AIR VOIDS VS. BINDER CONTENT (0H;24H;168H), (NDES.152)

Mix	Specimen Ø15x12cm	H. N_{des} [mm]	H. 24h [mm]	H. 7d [mm]	Va(%) N_{des}	Va(%) 24h	Va(%) 7_{days}
Dry 1.5	$DRY^{01}_{5.0/1.5}$	121.30	121.98	121.99	2.43%	2.76%	2.78%
	$DRY^{02}_{5.0/1.5}$	122.20	123.06	123.08	2.48%	2.81%	4.66%
	$DRY^{03}_{5.5/1.5}$	121.70	122.62	122.70	2.39%	2.79%	3.21%
	$DRY^{04}_{5.5/1.5}$	121.70	121.72	121.74	3.01%	3.40%	3.54%
Mixture	**Dust-to-asphalt ratio**	**%b**	**VMA (%)**	**VFA (%)**	**Γmax g/cm³**	**Γssd g/cm³**	**Γmm (%)**
Dry 1.5%	0.716	5.0	14.95	75.38	2.596	2.508	96.61
	0.709	5.5	15.60	78.37	2.577	2.500	97.02



EXPERIMENTAL Comp. Curves results

Sample	%b	$V_{a\ (Ndes)}$	$V_{a\ (24h)}$	$V_{a\ (14d)}$
m1	5.00	2.45	2.79	3.72
m2				
m3	5.50	2.70	3.10	3.37
m4				
To 3%Va , b* :	%b*	**%b*$_{(Ndes)}$**	**%b*$_{(24h)}$**	**%b*$_{(7d)}$**
		5.08%	**5.34**	**6.04**

	%Va*	%b*$_{(24h)}$	%b*$_{(7d)}$
Dry 1.5%	3.0%	**5.4**	**6.1**
	Def. %b*	5.5	6.0

Figure 34. (a) DRY1.5%. Graph %Va vs. %Binder; (b) Optimum bitumen content from the regression equation

Avoiding to introduce greater bitumen in the mixture (typical custom in the literature of mixtures modified with rubber [Gallego, J. et al. 2000; Brown, D. et al. 1997; Gowda, G.V. et al. 1996]) it was proceeded to increase the number of cycles to N_{des}. Also, to stabilize the T^a compaction (160ºC) until the ambient temperature of 20ºC, upper confinement of the specimen was applied to the top face of the sample. A dead mass similar to a conventional core of 150 · 120mm, which confinement without exerting pressure or modifying the internal structure, for 24 hours.

TABLE 36. ENERGETIC PARAMETERS ($DRY_{1.5\%\ \#60\text{-}40}$ Φ150·120MM)

Design ESALs (millions)	%binder	$N_{initial}$	N_{design}	$N_{maximum}$	% G_{mm} at N_{init}	% G_{mm} at N_{des}	% G_{mm} at N_{max}	%Va (N_{des})	Dust ratio (DP)[16]
$>3\cdot10^7$	5.0	10	**152**	251	88.67	97.55	99.98	2.45	0.716
	5.5	10	**152**	251	88.87	97.30	99.65	2.70	0.709

[14] Water temperature: 21ºC. Density water: 998.1g/cm³.
[15] Water temperature: 12ºC. Density water: 999.6g/cm³.
[16] $DP=P_{0.075}/P_{be}= P_{0.075/(VMA-Va)} \rightarrow ((10.51+6.85)\cdot0.5) / (14.9-2.79) = 0.716$

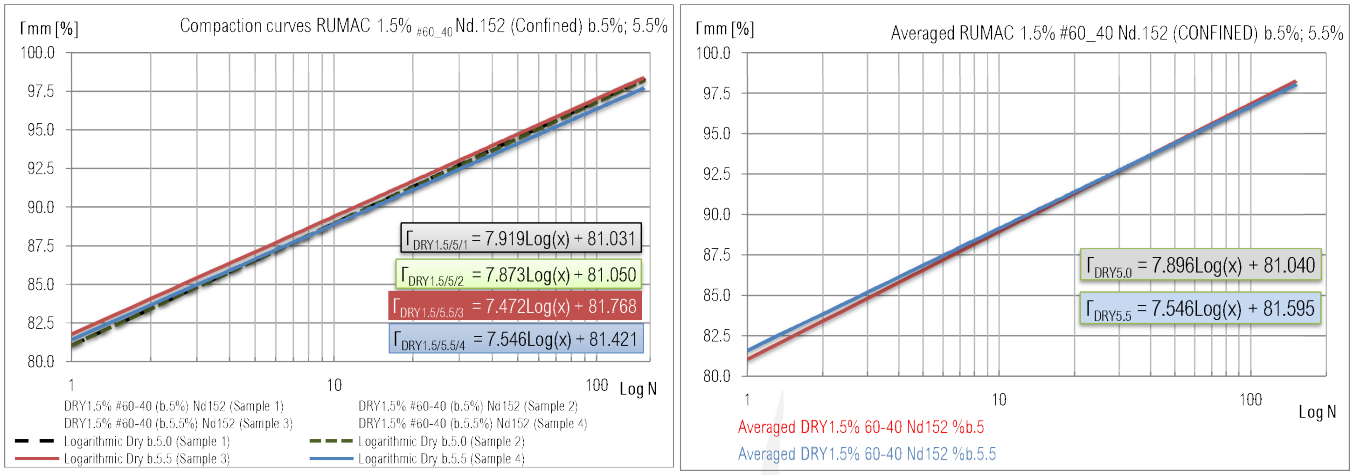


Figure 35. (a) Densification curves DRY 1.5 b. 5%;5.5%; (b) Trendline and regression equations

Densification curves were plotted for each mixture that represents the measured relative density at N_{des} or N_{max} cycles (%Gmm) versus the logarithm of the number of gyrations. For a DRY1.5 with an optimal binder 5.5%-6.0%, an air voids of ±3%, the regression equations were:

DRY1.5 $_{(b.5.0\%)}\longrightarrow \Gamma_{mm}$ ($N_{des.}$ 152) = 7.896Log(x)+81.040 ; DRY1.5 $_{(b.5.5\%)}\longrightarrow \Gamma_{mm}$ ($N_{des.}$ 152) = 7.546Log(x)+81.595

Through the results of these mixtures, it can be stated that the rubber mixtures allow lower workability of the mixture to compaction than the HMA mixture. However, due to the elasticity of the recycled rubber, the densification was more significant with the rubber content and the higher the bitumen introduced into the mix. That is, despite the increased number of gyrations (N_{des}.152 > 102), the blends at the same number of N_{des} had reached the empty content target of Va. ±3% (Table 37).

TABLE 37. COMPARATIVE HMA $_{4.0\%}$ VS. DRY $_{1.5\%\ \#60\text{-}40}$ Φ150·120MM

Design ESALs (millions)	%binder	Ndes	% Gmm at Ndes	%Va (Ndes)
>3·10^7	4.0	102	97.26	**2.74**
	5.0	152	97.55	**2.45**
	5.5	152	97.30	**2.70**

6.6. Phase 3.3. Mix-design of DRY 2.0%, N_{des}181, b*6.0-6.5%

The mixing and compaction temperatures were specified as 170±5 °C and 150±5 °C, respectively. A higher temperature will not be acceptable; it raises concerns about workers' health due to possible hazardous fumes in addition to possible thermal separation and oxidation. Therefore, the mixing and compaction temperatures were selected so that the aggregate fractions can be sufficiently coated by the binder and practically compacted to the prescribed voids content [Ayad, S. et al. 2007; Cao, W. 2007].



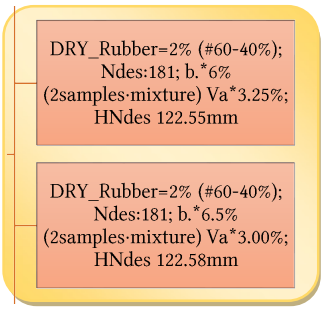


Figure 36. (a) Specimens compacted and extruded after 24h; (b) Flowchart of DRY2% rubberized mixtures

TABLE 38. $DRY_{2.0\%\ \#60\text{-}40}$ FINAL RECIPE FOR LABORATORY RUBBERIZED MIXTURES

	Filler	Sand	fØ5-10mm	fØ10-15mm	fØ20-25mm	fØ25-30mm	Σ components
	<0.063	0.063/4	0.063/8	0.063/11.2	5.6/22.4	5.6/31.5	
Passing	[%]	[%]	[%]	[%]	[%]	[%]	[%]
DRY2.0%	12.5176	23.5077	4.4173	19.2117	18.6986	21.6471	100.00

TABLE 39. $DRY_{2.0\%\#60\text{-}40}$ DEFINITIVE RECIPE FOR LABORATORY MANUFACTURING

Sample	H [mm]	Mass Aggr[gr]	Binder [%]	Sample mass [gr]	Binder mass [gr]	Filler [gr]	Sand [gr]	fØ5-10mm [gr]	fØ10-15mm [gr]	fØ20-25mm [gr]	fØ25-30mm [gr]	CRM60% Ø0.4-2 [gr]	CRM40% Ø2-4 [gr]
DRY2.0/6.0	120	5075	6.0	5375	323	640.6	1295.9	237.4	1032.7	1005.2	1163.6	69.8	46.5
DRY2.0/6.5	120	5052	6.5	5352	348	637.8	1290.2	236.4	1028.2	1000.7	1158.5	69.8	46.5

TABLE 40. $DRY_{2.0\%\ \#60\text{-}40}$ FINAL RECIPE. RESULTS AFTER 24H (N_{DES}.181)[17]

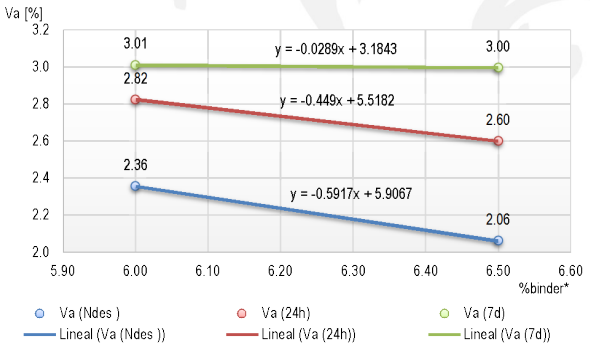
Sample Ø150xh (mm)	Inert mass [gr]	binder (%)	mass [gr]	Binder mass [gr]	$HN_{des.}$ [mm]	$H_{24h.}$ [mm]	Effective binder [gr]	M_1 24h [gr]	M_2 24h [gr]	M_3 24h [gr]	Υ_{app} [g/cm³]	Γ_{max} [g/cm³]	Γ_{mb^*} [g/cm³]	Γ_{mm} [%]	Va 24h [%]	VMA [%]	VFA [%]	Δ%b*
$DRY_{2.0_1}$	5075.5	6.0	5380	304.5	122.4	122.50	305.1	5390	3251	5403	2.503	2.559	2.496	97.54	2.67	15.92	83.20	5.53
$DRY_{2.0_2}$	5014.2		5315	300.8	120.4	121.00	299.8	5296	3194	5315	2.495	2.559	2.486	97.14	2.97	16.18	81.62	5.65
Averaged	5044.8		5347	302.7	121.4	121.75	302.4	5343	3222	5359	2.499	2.559	2.491	97.34	**2.82**	16.05	82.41	**5.59**
$DRY_{2.0_3}$	4985.9	6.5	5310	324.1	120.9	122.00	323.8	5305	3183	5310	2.492	2.541	2.476	97.44	2.48	16.67	85.11	5.90
$DRY_{2.0_4}$	4986.0		5310	324.1	120.7	121.00	324.2	5312	3194	5329	2.486	2.541	2.485	97.78	2.72	16.87	83.89	5.99
Averaged	4985.9		5310	324.1	120.8	121.50	323.9	5308	3188	5319	2.489	2.541	2.408	97.61	**2.60**	16.77	84.50	**5.94**

TABLE 41. $DRY_{2.0\%\ \#60\text{-}40}$ FINAL RECIPE. RESULTS AFTER 7DAYS (N_{DES}.181)

Sample Ø150xh (mm)	Inert mass [gr]	binder (%)	mass [gr]	Binder mass [gr]	$HN_{des.}$ [mm]	$H_{168h.}$ [mm]	Effective binder [gr]	M_1 168h [gr]	M_2 168h [gr]	M_3 168h [gr]	Υ_{app} [g/cm³]	Γ_{max} [g/cm³]	Γ_{mb^*} [g/cm³]	Γ_{mm} [%]	Va 168h [%]	VMA [%]	VFA [%]	Δ%b*
$DRY_{2.0_1}$	5075.5	6.0	5380	304.5	122.4	122.60	305.1	5392	3249	5404	2.500	2.559	2.495	97.48	2.77	16.01	82.67	5.57
$DRY_{2.0_2}$	5014.2		5315	300.8	120.4	122.91	299.8	5296	3185	5312	2.488	2.559	2.453	95.87	3.25	16.41	80.21	5.76
Averaged	5044.8		5347	302.7	121.4	122.75	302.4	5344	3217	5358	2.494	2.474	2.507	96.67	**3.01**	16.21	81.44	**5.66**
$DRY_{2.0_3}$	4985.9	6.5	5310	324.1	120.9	122.07	323.8	5299	3171	5306	2.480	2.541	2.466	97.05	2.96	17.07	82.68	6.09
$DRY_{2.0_4}$	4986.0		5310	324.1	120.7	123.10	324.2	5312	3191	5333	2.478	2.541	2.426	95.46	3.04	17.14	82.29	6.12
Averaged	4985.9		5310	324.1	120.8	122.90	323.9	5306	3181	5320	2.479	2.541	2.446	96.25	**3.00**	17.11	82.48	**6.10**

TABLE 42. $DRY_{2.0\%\ \#60\text{-}40}$ AIR VOIDS VS. BINDER CONTENT (0H;24H;168H), (N_{DES}.181)

Mix	Specimen Ø15x12cm	H. N_{des} [mm]	H. 24h [mm]	H. 7d [mm]	Va(%) N_{des}	Va(%) 24h	Va(%) 7_{days}
Dry 2.0	$DRY^{01}{}_{6.0/2.0}$	122.40	122.50	122.60	2.21%	2.67%	2.77%
	$DRY^{02}{}_{6.0/2.0}$	120.40	121.00	122.91	2.51%	2.97%	3.25%
	$DRY^{03}{}_{6.5/2.0}$	120.90	122.00	122.07	1.94%	2.48%	2.96%
	$DRY^{04}{}_{6.5/2.0}$	120.70	121.00	123.10	2.18%	2.72%	3.04%
Mixture	**Dust-to-asphalt ratio**	**%b**	**VMA (%)**	**VFA (%)**	**Γ_{max} g/cm³**	**Γ_{ssd} g/cm³**	**Γ_{mm} (%)7_{days}**
Dry 2.0%	0.670	6.0	16.21	81.44	2.559	2.494	96.67
	0.620	6.5	17.11	82.48	2.541	2.479	96.25



EXPERIMENTAL Comp. Curves results

Sample	%b	$V_{a\ (Ndes)}$	$V_{a\ (24h)}$	$V_{a\ (7d)}$
m1	6.00	2.36	2.82	3.01
m2				
m3	6.50	2.06	2.60	3.00
m4				
To 3%Va b* >>	%b*	%b*(Ndes)	%b*(24h)	%b*(7d)
		4.91	5.61	6.38

	%Va*	%b*(24h)	%b*(7d)
Dry 2%	3.0%	5.70	6.40
	Def. %b*	6.0	6.5

Figure 37. (a) DRY 2%. Graph %Va vs. %Binder; (b) Optimum bitumen content from the regression equation

TABLE 43. ENERGETIC PARAMETERS ($DRY_{2.0\%\ \#60\text{-}40}$ Φ150·120MM)

Design ESALs (millions)	%binder	$N_{initial}$	N_{design}	$N_{maximum}$	% G_{mm} at N_{init}	% G_{mm} at N_{des}	% G_{mm} at N_{max}	%Va (N_{des})	Dust ratio (DP)
$>3{\cdot}10^7$	6.0	11	**181**	304	91.785	97.643	99.690	**2.36**	0.67
	6.5	11	**181**	304	92.257	97.939	99.650	**2.06**	0.62

[17] Water temperature: 15ºC. Density water: 999.2g/cm³.

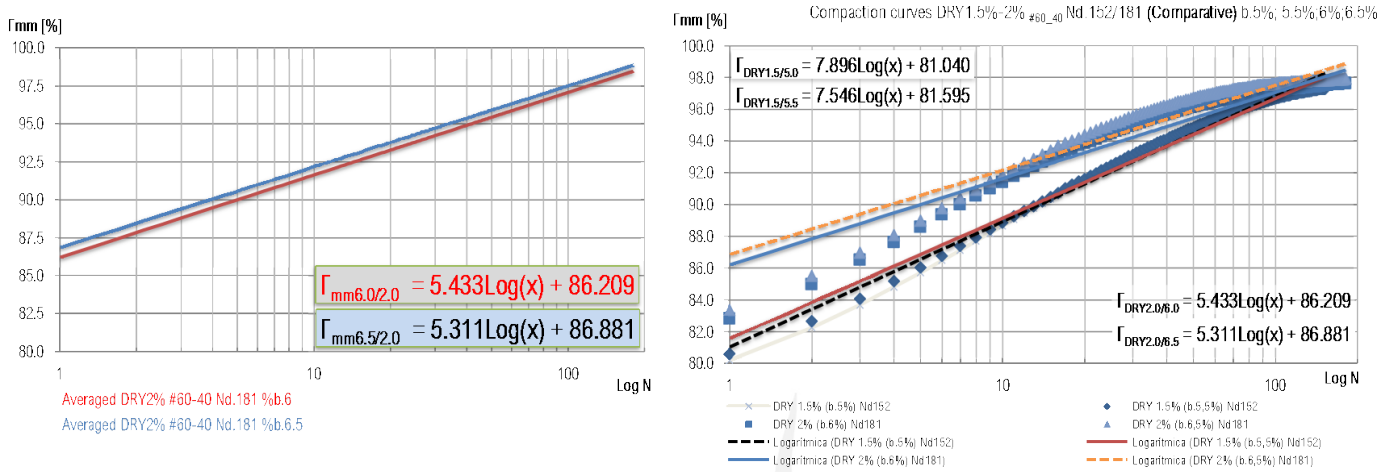


Figure 38. (a) Densification curves DRY2.0%; (b) Trendline and regression equations. Comparison DRY1.5%-2%

In conclusion, the regression equations were:

$DRY2.0_{(b.6.0\%)} \rightarrow \Gamma_{mm}(N_{des.}\,181) = 5.433Log(x)+86.209$; $DRY2.0_{(b.6.5\%)} \rightarrow \Gamma_{mm}(N_{des.}\,181) = 5.311Log(x)+86.881$

It is observed that with the new empirical beta parameter, the mixtures with rubber reach the required values for their ideal behavior after 72h. As in 1.5% mixtures, the most relevant results are compared with the reference HMA mixture (Table 44).

TABLE 44. COMPARATIVE ENERGETIC PARAMETERS (HMA $_{4.0\%}$ VS. DRY$_{2.0\%\ \#60\text{-}40}$ Φ150·120MM)

Design ESALs (millions)	%binder	N_{des}	% G_{mm} at N_{des}	%Va (N_{des})
$>3\cdot10^7$	4.0	102	97.26	**2.74**
	6.0	181	97.64	**2.36**
	6.5	181	97.94	**2.06**

6.7. Phase 3.4. Mix-design of DRY3.0%, N_{des}.291, b.6,5%

Finally, in the case of the Volumetric mix methodology, a generic dry mixture with a 3% rubber content was proposed concerning the total weight of the mix. In this case, the proportion is 80% of ground rubber and 20% of rubber powder[18] (Fig. 39-40; Tables 46-50).

Subsequently, the mechanical fatigue characterization and production of new mixtures with the roller compactor to produce prismatic specimens allowing cracking damage will be performed exclusively for HMA, DRY 1.5 and DRY 2.0% blends because they show more excellent stability and performance for the sub-ballast.

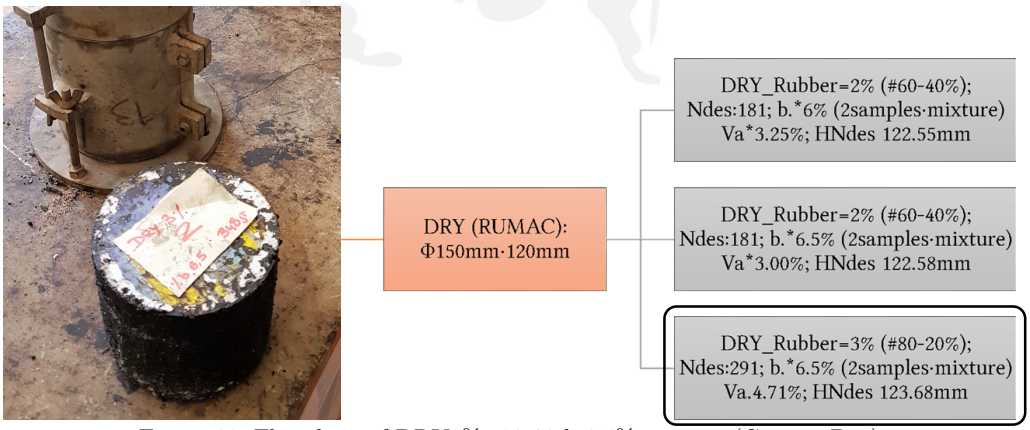


Figure 39. Flowchart of DRY3% #80-20 b.6,5% mixture (Generic-Dry)

[18] CRM affects the asphalt-rubber reaction and hence the characteristics of mixes. In the dry process of preparing the generic mixes, the gradation of rubber is so selected that the coarse rubber particles will serve as elastic aggregates and the fine rubber will react with asphalt to produce modified binder.

TABLE 45. DRY**3.0%** $_{\#80\text{-}20}$ RECIPE FOR LABORATORY RUBBERIZED MIXTURES

	Filler	Sand	fØ5-10mm	fØ10-15mm	fØ20-25mm	fØ25-30mm	Σ components
	<0.063	0.063/4	0.063/8	0.063/11.2	5.6/22.4	5.6/31.5	
Passing	[%]	[%]	[%]	[%]	[%]	[%]	[%]
DRY3.0%	12.6627	22.9422	4.0081	19.6860	18.8050	21.8960	100.00
Γmix=	2.692					Γaggr=	2.808

TABLE 46. DRY$_{3.0\%\#80\text{-}20}$ DEFINITIVE RECIPE FOR LABORATORY MANUFACTURING

Sample	H [mm]	Mass Aggr[gr]	Binder [%]	Sample mass [gr]	Binder mass [gr]	Filler [gr]	Sand [gr]	fØ5-10mm [gr]	fØ10-15mm [gr]	fØ20-25mm [gr]	fØ25-30mm [gr]	CRM20% Ø0.4-2mm [gr]	CRM80% Ø2-4mm [gr]
DRY$_{3.0_6.5}$	120	5052	*6.5*	5352	348	645.6	1259.9	214.5	1053.5	1006.4	1171.8	35.3	141.0
DRY$_{3.0_7.0}$	120	5028	*7.0*	5328	373	642.7	1254.3	213.5	1048.9	1001.9	1166.6	35.3	141.0

TABLE 47. DRY$_{3.0\%\ \#80\text{-}20}$ FINAL RECIPE. RESULTS AFTER 24H (N_{DES}.291)[19]

Sample Ø150xh (mm)	Inert mass [gr]	binder (%)	mass [gr]	Binder mass [gr]	$HN_{des.}$ [mm]	$H_{24h.}$ [mm]	Effective binder [gr]	M_1 24h [gr]	M_2 24h [gr]	M_3 24h [gr]	Υ_{app} [g/cm³]	Γ_{max} [g/cm³]	Γ_{mb^*} [g/cm³]	Γ_{mm} [%]	Va 24h [%]	VMA [%]	VFA [%]	Δ%b* to Va.3%
DRY$_{3.0_6.5}$	4957.7	6.5	5380	322.2	**121.9**	**123.58**	321.4	5266	3119	5270	2.446	2.541	2.429	95.58	**4.27**	18.19	76.53	7.01
DRY$_{3.0_7.0}$	4962.6	7.0	5310	347.7	**123.5**	**124.20**	347.1	5305	3134	5310	2.436	2.524	2.476	98.11	**4.07**	18.57	80.15	7.25

TABLE 48. DRY$_{3.0\%\ \#80\text{-}20}$ FINAL RECIPE. RESULTS AFTER 7DAYS (N_{DES}.181)

Sample Ø150xh (mm)	Inert mass [gr]	binder (%)	mass [gr]	Binder mass [gr]	$HN_{des.}$ [mm]	$H_{168h.}$ [mm]	Effective binder [gr]	M_1 168h [gr]	M_2 168h [gr]	M_3 168h [gr]	Υ_{app} [g/cm³]	Γ_{max} [g/cm³]	Γ_{mb^*} [g/cm³]	Γ_{mm} [%]	Va 168h [%]	VMA [%]	VFA [%]	Δ%b* to Va.3%
DRY$_{3.0_6.5}$	4957.7	6.5	5380	322.2	**121.9**	**123.68**	321.4	5267	3114	5270	2.436	2.541	2.415	95.04	**4.49**	18.38	75.57	7.10
DRY$_{3.0_7.0}$	4962.6	7.0	5310	347.7	**123.5**	**125.32**	347.1	5312	3194	5329	2.431	2.524	2.448	96.31	**4.09**	18.91	78.38	7.44

TABLE 49. DRY$_{3.0\%\ \#80\text{-}20}$ AIR VOIDS VS. BINDER CONTENT (0H;24H;168H), (N_{DES}.291)

Mixture	Specimen Ø15x12cm	H. N_{des} [mm]	H. 24h [mm]	H. 7d [mm]	Va(%) N_{des}	Va(%) 24h	Va(%) 7_{days}
Dry 3.0%	$DRY^{01}_{6.5/3.0}$	121.9	123.58	123.68	3.50%	4.27%	4.49%
	$DRY^{02}_{7.0/3.0}$	123.5	124.20	125.32	3.69%	4.07%	4.09%
	Dust-to-asphalt ratio[20]	***%b***	**VMA (%)**	**VFA (%)**	**Γ_{max} g/cm³**	**Γ_{ssd} g/cm³**	**Γ_{mm} (%)7_{days}**
	0.630	6.5	18.38	75.57	2.541	2.436	95.04
	0.590	7.0	18.91	78.38	2.524	2.431	96.31

TABLE 50. ENERGETIC PARAMETERS (DRY$_{3.0\%\ \#80\text{-}20}$ Φ150·120MM)

Design ESALs (millions)	%binder	$N_{initial}$	N_{design}	$N_{maximum}$	% G_{mm} at N_{init}	% G_{mm} at N_{des}	% G_{mm} at N_{max}	%Va (N_{des})	Dust ratio (DP)
$>3{\cdot}10^7$	6.5	13	**291**	513	91.186	96.497	98.014	**3.50**	0.63
	7.0	13	**291**	513	92.639	96.315	98.264	**3.69**	0.59

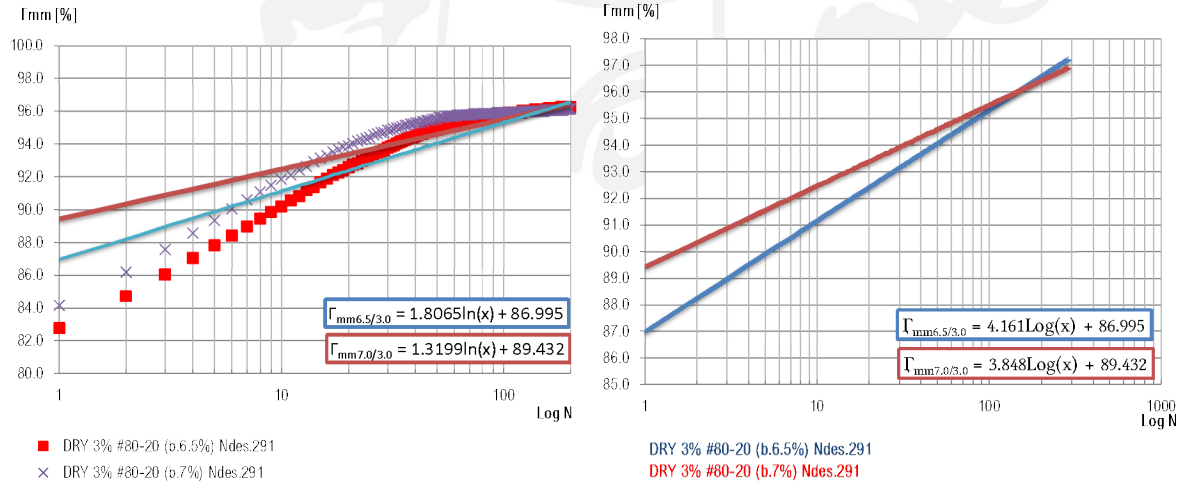


Figure 40. (a) Individual Densification curves DRY3.0% b. 6,5%-7,0%; (b) Trendline and regression equations

The high rubber content causes a sudden change in the densification graph. The higher the bitumen, the stronger structure, and the fewer internal gaps.

[19] Water temperature: 15ºC. Density water: 999.2g/cm³.

[20] DP=$P_{0.075}/Pb_{eff}$ = $P_{0.075}$/(VMA-Va)→((10.609+6.941)·0.5) / (18.38-4.49) = 0.63

For a DRY 3% rubber blend, the optimal results regarding percentage of air voids were not reached. With N_{des}. 291 gyrations, an air voids content of 3.50% at N_{des}. The drawback is that due to the "swelling" effect at seven days the mixture increases in volume and the voids amount to 4.49%.

According to the regression to obtain the percentage of suitable bitumen, the maximum percentage of asphalt would be 7% for mixtures "Generic dry" with 3% and dosage of 80-20% coarse-fine rubber.

6.7.1. Final results from SGC "Volumetric mix-design"

It was observed that the swelling effect in the specimen, in the first case studies, was greater compared to the mixtures at 1.5% and 2% of scrap tire rubber. In turn, using the empirical approach method by which the number of gyrations to N_{des} (102, 182, and 291) was increased respectively, it was adjusted each blend to the requirements of a sub-ballast layer with recycled rubber. In conclusion, the regression equations were:

HMA_{RFI} (b.4.0%) ⟶ Γ_{mm} ($N_{des.}$ 102) = 8.365Log(x) + 80.954
DRY1.5 (b.5.0%) ⟶ Γ_{mm} ($N_{des.}$ 152) = 7.896Log(x) + 81.040
DRY1.5 (b.5.5%) ⟶ Γ_{mm} ($N_{des.}$ 152) = 7.546Log(x) + 81.595
DRY2.0 (b.6.0%) ⟶ Γ_{mm} ($N_{des.}$ 181) = 5.433Log(x) + 86.209
DRY2.0 (b.6.5%) ⟶ Γ_{mm} ($N_{des.}$ 181) = 5.311Log(x) + 86.881
DRY3.0 (b.6.5%) ⟶ Γ_{mm} ($N_{des.}$ 291) = 4.161Log(x) + 86.955
DRY3.0 (b.7.0%) ⟶ Γ_{mm} ($N_{des.}$ 291) = 3.848Log(x) + 89.432

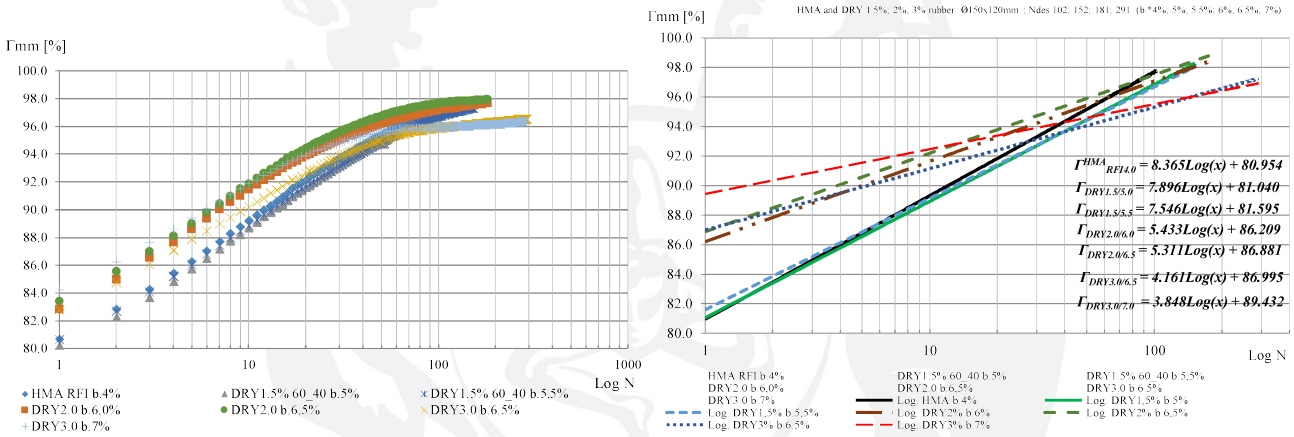


Figure 41. (a) Densification curves for all SGC mixtures; (b) Trendline and regression equations

If we analyze the results of the compaction curve for all the mixtures (Fig. 41), it is observed how the DRY blends densify before than the conventional mixture HMA, to the same number of cycles. In fact, rubberized mixes developed lower workability, higher density since the beginning of the compaction, but a higher compactability that is ensured by the increase in the number of turns induced due to the "beta" factor.

It was determined the optimum bitumen content make any mix based on the percentage of rubber required analyzing the results obtained for each mixture. Observing the regression curves (Table 51; Fig. 42), the relationship between the proportion of voids and optimum asphalt content was obtained.

TABLE 51. SUMMARY OF HEIGHTS AT N_{DES} AND AIR VOIDS (ALL MIXTURES)

Gyratory compactor	Specimen Ø150x120mm	H. N_{des} [mm]	H. 24h [mm]	H. 7d [mm]	Va(%) at N_{des} (0h)	Va(%) at 24h	Va(%) at 7days	%b.* if Va:3%	Va(%) at N_{des} (0h)	Va(%) at 24h	Va(%) at 7days	%b	VMA (%)	VFA (%)	Dust proportion (DP)
HMA (b.*4%)	$RFI^{01}_{4\%}$	114.30	113.33	113.33	2.78%	2.78%	2.78%	4.0%	2.74%	2.74%	2.74%	4.0%	12.3%	77.9%	0.892
	$RFI^{02}_{4\%}$	115.90	115.50	115.50	2.70%	2.70%	2.70%								
Dry 1.5% (b.5%)	$DRY^{01}_{5.0/1.5}$	121.30	121.99	121.99	2.43%	2.76%	2.78%	5.5%	2.45%	2.79%	3.72%	5.0%	14.9%	75.4%	0.716
	$DRY^{02}_{5.0/1.5}$	122.20	123.08	123.08	2.48%	2.81%	4.66%								
Dry 1.5% (b.*5,5%)	$DRY^{03}_{5.5/1.5}$	121.70	122.62	122.70	2.39%	2.79%	3.21%	6.0%	2.70%	3.10%	3.37%	5.5%	15.6%	78.4%	0.709
	$DRY^{04}_{5.5/1.5}$	121.70	121.74	121.74	3.01%	3.40%	3.54%								
Dry 2% (b.6%)	$DRY^{01}_{6.0/2.0}$	122.40	122.50	122.60	2.21%	2.67%	2.77%	6.5%	2.36%	2.82%	3.01%	6.0%	16.2%	81.5%	0.670
	$DRY^{02}_{6.0/2.0}$	120.40	121.00	122.91	2.51%	2.97%	3.25%								
Dry 2% (b.*6,5%)	$DRY^{03}_{6.5/2.0}$	120.90	122.00	122.07	1.94%	2.48%	2.96%	7.0%	2.06%	2.60%	3.00%	6.5%	17.1%	82.4%	0.620
	$DRY^{04}_{6.5/2.0}$	120.70	121.00	123.10	2.18%	2.72%	3.04%								
Dry 3% (b.*7%)	$DRY_{6.5/3.0}$	121.90	123.58	123.68	3.50%	4.27%	4.49%	7.5%	3.69%	4.07%	4.09%	7.0%	18.9%	78.4%	0.590
	$DRY_{7.0/3.0}$	123.50	124.20	125.32	3.69%	4.07%	4.09%								

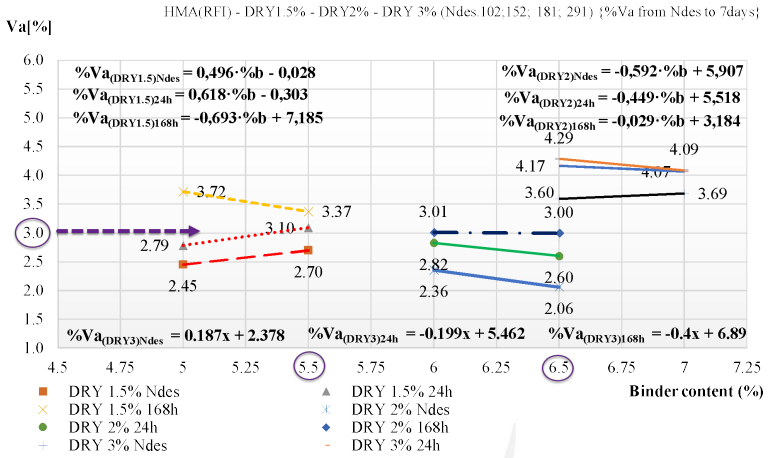


Figure 42. Diagram 1. Percentage ratio of voids vs. Binder content

In summary, if we apply the regression equations of the plotted curves (Fig. 42), we can determine the optimum real bitumen content for each mixture, from the time of post-compaction until after the seven days of expected rebound effect or swelling of the rubber. Optimal results are showed (Table 52; Figure 43):

TABLE 52. AIR VOIDS VS. BINDER CONTENT IN HMA_DRY SAMPLES (OPTIMAL BINDER CONTENT)

	%Va	%b*(Ndes)	%b*(24h)	%b*(7d)
Dry 1.5%	**3.0%**	**4.95%**	**5.34%**	**6.05%**
Dry 2%	**3.0%**	**4.91%**	**5.61%**	**6.38%**
Dry 3%	**3.0%**	**6.70%**	**7.13%**	**7.27%**

(Averaged)

	%Va*	%b*(Ndes)	%b*(24h)	%b*(7d)
Dry 1.5%	3.0%	**4.95%**	**5.40%**	**6.10%**
	Def. %b	5.0%	5.5%	**6.0%**
Dry 2%	3.0%	**5.00%**	**5.70%**	**6.40%**
	Def. %b	5.0%	6.0%	**6.5%**
Dry 3%	3.0%	**6.70%**	**7.20%**	**7.30%**
	Def. %b	7.0%	7.5%	**7.5%**

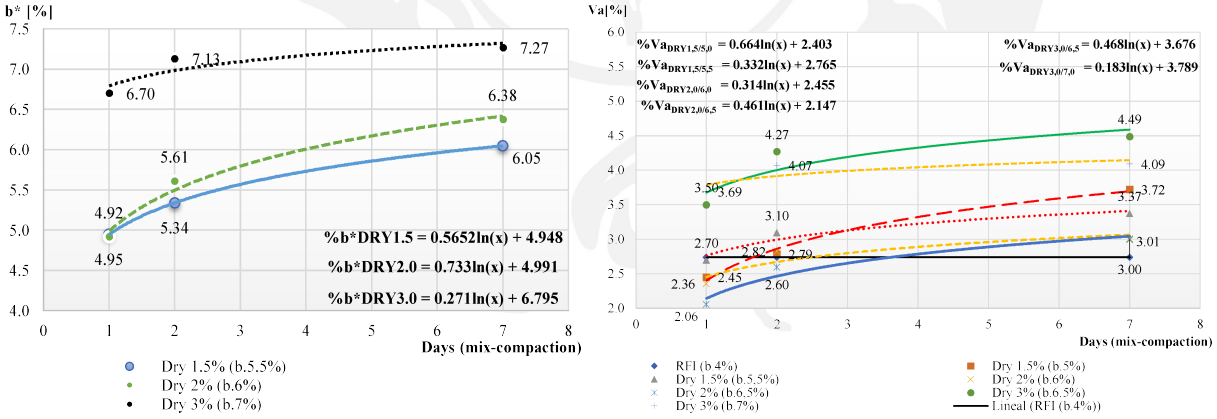


Figure 43. (a) Evolution of optimal binder content after one week due to the swelling effect of the rubberized compacted specimen; (b) Air voids vs. Post-compaction days

The compatibility of these mixes was entirely different even though 3% of air voids is the target value, being more sensitive to the gyration levels than the other. Another relevant aspect in the results was that as the rubber content in the mixture increases, the workability (slope of the trend line) decreases (higher densification).

Finally, concluding with the idea exposed by Signes, C. et al. 2016, it is possible to use unbound aggregates for the sub-ballast layer, hence reducing the cost and environmental impact of railway works. Moreover, this alternative allows reusing significant quantities of rubber as a problematic waste material, thus increasing its environmental benefits.

6.8. Phase 4: Results with Asphalt Roller compactor (ASRC)

The results with Asphalt Slab Roller Compactor focused to the next study to fatigue cracking are presented in this section to characterize the reference conventional HMA b.4%, and the rubber-aggregate blends DRY 1.5% and DRY 2% according to the optimal recipes found in the laboratory with SGC.

Previously, two mixtures with recycled rubber DRY 1.5% and DRY2%, whose bitumen contents were 6.0% and 6.5%, were studied. This first mix-design was due to the results of diagrams of %Va vs. %binder for SGC specimens the percentage of optimum air voids would be reached with those bitumen values (Table 52; Fig. 43). These test mixtures resulted in too low void percentages due to a higher bitumen content, being in the order of 1.7 to 2.6%, where the target is a minimum of 3% air voids (Fig. 44; Tables 53-54).

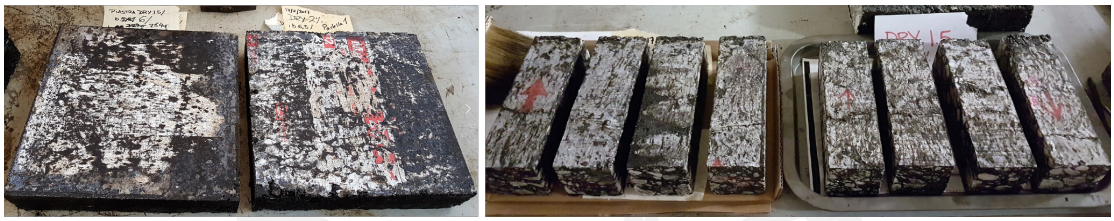


Figure 44. (a) First slabs compacted at b.6%-6.5%; (b) Specimens of 20 · 20 · 6cm from slabs

TABLE 53. TRIAL RECIPES FOR A DRY1.5% (B. 6%) AND DRY2% (B.6.5%)

Sample	H [mm]	Mass Aggreg. [gr]	Binder [%]	Theor. mass [gr]	Binder mass [gr]	Aggreg. mass [gr]	Binder mass [gr]	Filler [gr]	Sand [gr]	fØ5-10mm [gr]	fØ10-15mm [gr]	fØ20-25mm [gr]	fØ25-30mm [gr]	CRM 60% Ø0.4-2 [gr]	CRM 40% Ø2-4 [gr]
DRY 1.5%	60	13072	6.0	13856	784.3	13071	784	1548.4	3187.6	603.8	2480.7	2437.3	2813.5	126.6	84.4
DRY 2%	60	12920	6.5	13760	839.8	12921	840	1539.9	3114.9	570.7	2482.3	2416.0	2796.9	168.5	112.3

TABLE 54. DISADVANTAGEOUS RESULTS FOR ROLLER SLABS WITH RUBBER (DRY1.5 B.6%; DRY 2% B.6.5%)

Sample 20x6x6cm	Sample air mass [gr]	Weight of surface-dry specimen in air [gr]	Saturated Weight in water [gr]	$\Gamma_{(SSD)}$ [Kgr/m^3]	Va (%)	V_a *(%) (EN12697-8)*	VMA*(%)*	VFA*(%)*
	m_1	m_3	m_2	Υ_{app}	*v*			
DRY1.5/6.0/1.1	1761	1763	1063	2512	1,88	1,82%	15,59%	88,31%
DRY1.5/6.0/1.2	1775	1777	1069	2504	2,78	2,16%	15,89%	86,39%
DRY1.5/6.0/1.3	1796	1798	1083	2509	3,51	1,97%	15,72%	87,45%
DRY1.5/6.0/1.4	1874	1876	1137	2533	0,13	1,04%	14,92%	93,04%
Averaged	**1801,5**	**1803,5**	**1088,0**	**2514,4**	**2,08**	**1,75%**	**15,53%**	**88,80%**
DRY2.0/6.5/1.1	1799	1799	1065	2448	3,41	3,68%	18,14%	79,73%
DRY2.0/6.5/1.2	1801	1804	1075	2468	2,49	2,91%	17,49%	83,36%
DRY2.0/6.5/1.3	1832	1835	1103	2500	1,93	1,64%	16,41%	89,99%
DRY2.0/6.5/1.4	1771	1773	1062	2488	1,75	2,11%	16,81%	87,45%
Averaged	**1800,8**	**1802,8**	**1076,3**	**2514,4**	**2,40**	**2,58%**	**17,21%**	**85,13%**

As a first conclusion, given the results in blends with "roller compactor" the percentage of voids is reached with 0.5% less bitumen than mixtures manufactured by "Volumetric mix-design" SGC.

Three slabs of each mixture were produced, so that 12 beams of 200 · 60 · ±60mm were obtained. The amount of asphalt was adjusted to 5.5% and 6% for a DRY1.5% and DRY2%, respectively. Results of density, air voids, and weights corresponding to each one are presented in Tables 55-57 and Figures 45-46.

The following acronyms have been used to facilitate the interpretation of the results:

- For HMA mixtures (b.4%), slab 1,2...i, specimen 1,2...i: **HMA_{1_1}...HMA_{1_i}; HMA_{2_1} ... HMA_{2_i}.**
- For mixtures DRY 1.5%, bitumen 5.5%, slab 1, specimen 1: **$DRY_{1.5/5.5/1.1}$;**
- For mixtures DRY 2.0%, bitumen 6.0%, slab 2, specimen 3: **$DRY_{2/6/2.3}$;**

Based on the next results obtained from the average of 4 specimens for each of the three slabs manufactured for each mixture (12 samples), the results were satisfactory. The average height of each sample was between 60.3-61.3mm and the percentage of air voids between 2.8% and 3.4%. Finally, these specimens will be subjected to the fatigue strength test to characterize the life-cycles of mixtures under railway traffic loads mechanically.

TABLE 55. ROLLER COMPACTED SLABS RESULTS FOR **HMA (RFI B.4%)** [4 BEAMS PER SLAB]

Υ_{inert}	$\Upsilon_{bitumen}$	Voids	Binder	Υ_w	Max. density	Slab weight	ρ_{dim} (gr)	$V_{a\ slab}$						
(kg/m³)	(kg/m³)	%	%	T° 18°C	(kg/m³)	(gr)	(kg/m³)	%						
2808.6	1033.3	3.0	4.0	998.70	2.634	14324.0	2.550	3.18%						
Sample 12x6x6cm	M1	M3	M2	$\rho_{b_{SSD}}$ [Kgr/m³]	$\rho_{b\,dim}$ [Kgr/m³]	Air voids [%]	Avg. Va	H [mm]	W [mm]	L [mm]	VMA	VFA	C_V	Desv. Stand. (σ)
	[gr]	[gr]	[gr]	Υ_{app}	Υ_{sedim}	v	[%]				(%)	(%)	(%)	(%)
HMA_{1_1}	1793	1795	1105	2543.0	2538.7	3.69	3.77	59.25	59.60	200	12.94%	73.33%	10.4%	0.39
HMA_{1_2}	1842	1845	1137	2546.0	2569.2	3.58		59.35	60.40	200	12.84%	73.99%		
HMA_{1_3}	1832	1835	1129	2539.5	2574.4	3.83		59.45	59.85	200	13.06%	72.56%		
HMA_{1_4}	1865	1867	1147	2535.2	2535.1	3.99		59.52	61.80	200	13.21%	71.62%		
HMA_{2_1}	1957	1958	1212	2556.1	2556.0	2.98	3.10	62.25	60.89	202	12.49%	76.33%	12.6%	
HMA_{2_2}	1973	1974	1222	2556.4	2592.6	2.97		61.74	61.02	202	12.48%	76.41%		
HMA_{2_3}	1897	1898	1173	2549.7	2572.2	3.22		60.54	60.91	200	12.71%	74.84%		
HMA_{2_4}	1865	1867	1154	2548.9	2554.6	3.25		59.66	60.88	201	12.74%	74.65%		
HMA_{3_1}	1988	1989	1230	2553.2	2577.0	3.09	3.13	61.25	62.35	202	12.59%	75.65%	12.5%	
HMA_{3_2}	1926	1927	1195	2564.4	2593.0	2.66		61.07	60.51	201	12.21%	78.36%		
HMA_{3_3}	1913	1914	1182	2547.7	2577.6	3.30		60.41	60.82	202	12.78%	74.38%		
HMA_{3_4}	1896	1899	1172	2542.5	2511.2	3.49		60.10	62.50	201	12.96%	73.22%		
Averaged	1896	1897	1172	2548.6	2562.6	**3.34**		60.4	61.0	200.9	12.75%	74.61%	11.8%	

TABLE 56. ROLLER COMPACTED SLABS RESULTS FOR **DRY 1.5 (B.5,5%)** [4 BEAMS PER SLAB]

Υ_{inert}	$\Upsilon_{bitumen}$	Voids	Binder	Υ_w	Max. density	Slab weight	ρ_{dim} (gr)	$V_{a\ slab}$						
(kg/m³)	(kg/m³)	%	%	T° 18°C	(kg/m³)	(gr)	(kg/m³)	%						
2808.6	1033.3	3.0	5.5	998.70	2.577	14244.3	2.526	2.98%						
Sample 12x6x6cm	M1	M3	M2	$\rho_{b_{SSD}}$ [Kgr/m³]	$\rho_{b\,dim}$ [Kgr/m³]	Air voids [%]	Avg. Va	H [mm]	W [mm]	L [mm]	VMA	VFA	C_V	Desv. Stand. (σ)
	[gr]	[gr]	[gr]	Υ_{app}	Υ_{sedim}	v	[%]				(%)	(%)	(%)	(%)
$DRY_{1.5/5.5/1.1}$	1864	1866	1127	2508.1	2509.6	3.08	2.87	60.32	61.26	201	15.34%	82.53%	6.5%	0.19
$DRY_{1.5/5.5/1.2}$	1887	1890	1143	2511.8	2526.7	2.94		60.52	61.70	200	15.22%	83.34%		
$DRY_{1.5/5.5/1.3}$	1905	1907	1156	2522.2	2514.5	2.54		60.69	62.73	199	14.87%	85.65%		
$DRY_{1.5/5.5/1.4}$	1855	1857	1123	2512.9	2510.0	2.90		60.48	61.40	199	15.18%	83.58%		
$DRY_{1.5/5.5/2.1}$	1880	1882	1140	2516.9	2526.4	2.75	2.90	60.51	61.49	200	15.05%	84.45%	6.5%	
$DRY_{1.5/5.5/2.2}$	1859	1861	1127	2515.9	2511.8	2.78		60.67	60.69	201	15.08%	84.24%		
$DRY_{1.5/5.5/2.3}$	1935	1938	1172	2509.4	2509.6	3.03		60.75	63.46	200	15.30%	82.81%		
$DRY_{1.5/5.5/2.4}$	1905	1908	1154	2509.8	2538.8	3.02		60.8	61.40	201	15.28%	82.90%		
$DRY_{1.5/5.5/3.1}$	1884	1886	1140	2511.7	2502.6	2.94	2.83	60.72	61.99	200	15.22%	83.33%	6.6%	
$DRY_{1.5/5.5/3.2}$	1848	1849	1118	2514.3	2511.5	2.84		60.68	60.63	200	15.13%	83.88%		
$DRY_{1.5/5.5/3.3}$	1938	1940	1172	2509.7	2521.2	3.02		60.67	63.35	200	15.29%	82.89%		
$DRY_{1.5/5.5/3.4}$	1872	1875	1137	2522.7	2525.7	2.52		60.58	60.87	201	14.85%	85.78%		
Averaged	1886	1888	1142	2513.8	2517.4	**2.86**		60.6	61.7	200.2	15.10%	83.78%	6.53%	



Figure 45. Manufacture and cutting of roller slabs compacted (DRY1.5% b.5.5% mixture)

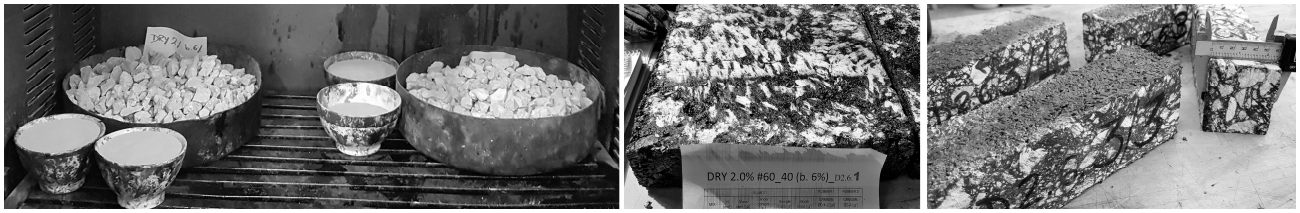


Figure 46. Manufacture and cutting of slabs compacted with a mechanical roller for DRY 2% b.6% mixture

TABLE 57. ROLLER COMPACTED SLABS RESULTS FOR **DRY 2.0% (B.6%)** [4 BEAMS PER SLAB]

Υ_{inert}	$\Upsilon_{bitumen}$	Voids	Binder	Υ_w	Max. density	Slab weight	ρ_{dim}	$V_{a\ slab}$						
(kg/m³)	(kg/m³)	%	%	T° 18°C	(kg/m³)	(gr)	(kg/m³)	%						
2808.0	1033.3	3.0	6.0	998.80	2.559	14148	2.440	3.12%						
Sample 12x6x6cm	M1	M3	M2	$\rho_{b\,SSD}$ [Kgr/m³]	$\rho_{b\,dim}$ [Kgr/m³]	Va [%]	Avg. Va	H [mm]	W [mm]	L [mm]	VMA	VFA	C_V	Desv. Stand. (σ)
	[gr]	[gr]	[gr]	Υ_{app}	Υ_{sedim}	v	[%]				(%)	(%)	(%)	(%)
$DRY_{2/6/1.1}$	1933	1935	1160	2491.2	2496.1	3.12	3.30	60.91	62.94	202	16.30%	83.73%	9.5%	0.31
$DRY_{2/6/1.2}$	1854	1854	1108	2482.3	2467.6	3.47		60.93	61.05	202	16.60%	81.92%		
$DRY_{2/6/1.3}$	1882	1884	1127	2483.1	2475.3	3.43		61.05	61.65	202	16.57%	82.09%		
$DRY_{2/6/1.4}$	1877	1879	1126	2489.7	2503.2	3.18		61.06	61.41	200	16.35%	83.42%		
$DRY_{2/6/2.1}$	1844	1846	1107	2492.3	2477.5	3.08	3.04	60.52	61.19	201	16.27%	83.95%	10.3%	
$DRY_{2/6/2.2}$	1878	1879	1128	2497.7	2474.4	2.87		60.62	61.99	202	16.09%	85.08%		
$DRY_{2/6/2.3}$	1848	1850	1108	2487.6	2479.4	3.26		60.65	61.14	201	16.43%	82.98%		
$DRY_{2/6/2.4}$	1871	1873	1124	2495.0	2483.5	2.97		60.68	61.16	203	16.18%	84.51%		
$DRY_{2/6/3.1}$	1960	1962	1173	2481.2	2476.7	3.51	3.58	62.47	63.34	200	16.64%	81.70%	8.7%	
$DRY_{2/6/3.2}$	1902	1903	1133	2467.2	2474.6	4.05		62.24	61.75	200	17.11%	79.00%		
$DRY_{2/6/3.3}$	1926	1927	1152	2482.2	2459.4	3.47		62.54	62.61	200	16.61%	81.90%		
$DRY_{2/6/3.4}$	1925	1928	1155	2487.3	2460.5	3.27		62.5	62.59	200	16.43%	82.93%		
Averaged	1892	1893	1133	2486.4	2477.4	**3.31**		61.35	61.90	201.8	16.47%	82.77%	9.4%	

6.8.1. A comparison between SGC and Slab Roller compactor

For a performance test to produce robust mechanical properties, it was necessary to ensure that laboratory specimens were fabricated based on the best distribution of aggregates and air voids inside the mix [Tashman, L.S. et al. 2000; Sousa, J. et al. 1995]. The results obtained by SGC and ASRC indicated that the different field compaction patterns used in this study produced a similar internal structure in asphalt mixtures. However, the change of the variables of compaction both with SGC (angle, pressure, height and temperature) and with the roller compactor (pressures, number of passes, mass of aggregates, binder content and temperature), has influenced the internal structure of the samples regarding the distribution of aggregates and associated air voids [Lai, J.S. et al. 1995; Roberts, F.L. et al. 1991].

At the end of the process of manufacturing slabs and specimens in each of the phases of the project, a relationship between the mixtures using the results obtained with the SGC and ASRC was established. In this case, the SGC results were (Fig. 47-48, Table 58):

TABLE 58. GYRATORY COMPACTOR RESULTS (ALL MIXTURES)

SGC blend	Specimen Ø15x12cm	H. N_{des} [mm]	H. 24h [mm]	H. 7d [mm]	Va(%) N_{des}	Va(%) at 24h	Va(%) 7days	%b.* Va:3%	Va(%) at N_{des}	Va(%) at 24h	Va(%) 7days	VMA (%)	VFA (%)	Dust prop. (DP)
HMA (b.*4%)	$HMA^{01}{}_{4\%}$	114.30	113.33	113.33	2.78%	2.78%	2.78%	4.0%	2.74%	2.74%	2.74%	12.4%	77.9%	0.89
	$HMA^{02}{}_{4\%}$	115.90	115.50	115.50	2.70%	2.70%	2.70%							
Dry 1.5% (b.*5,5%)	$DRY^{03}{}_{5.5/1.5}$	121.70	122.62	122.70	2.39%	2.79%	3.21%	6.0%	2.70%	3.10%	3.37%	15.6%	78.4%	0.71
	$DRY^{04}{}_{5.5/1.5}$	121.70	121.74	121.74	3.01%	3.40%	3.54%							
Dry 2% (b.*6%)	$DRY^{01}{}_{6.0/2.0}$	122.40	122.50	122.60	2.21%	2.67%	2.77%	6.5%	2.36%	2.82%	3.01%	16.2%	81.5%	0.67
	$DRY^{02}{}_{6.0/2.0}$	120.40	121.00	122.91	2.51%	2.97%	3.25%							

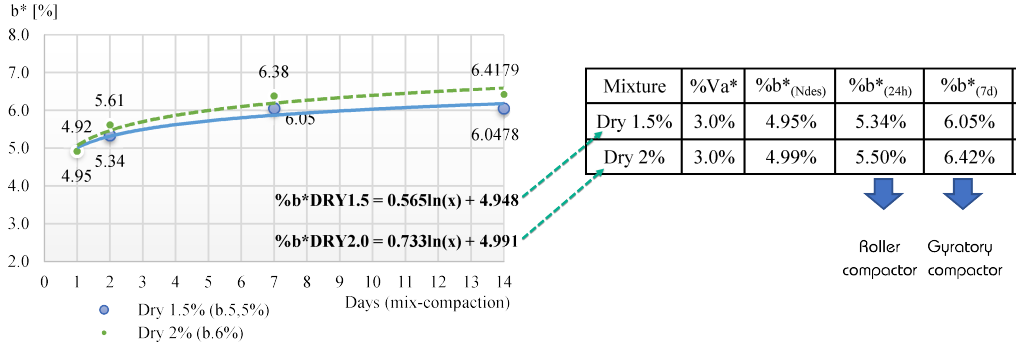


Figure 47. (a) Ratio optimal binder vs. Post-compaction days; (b) Values of evolution due to swelling rubber

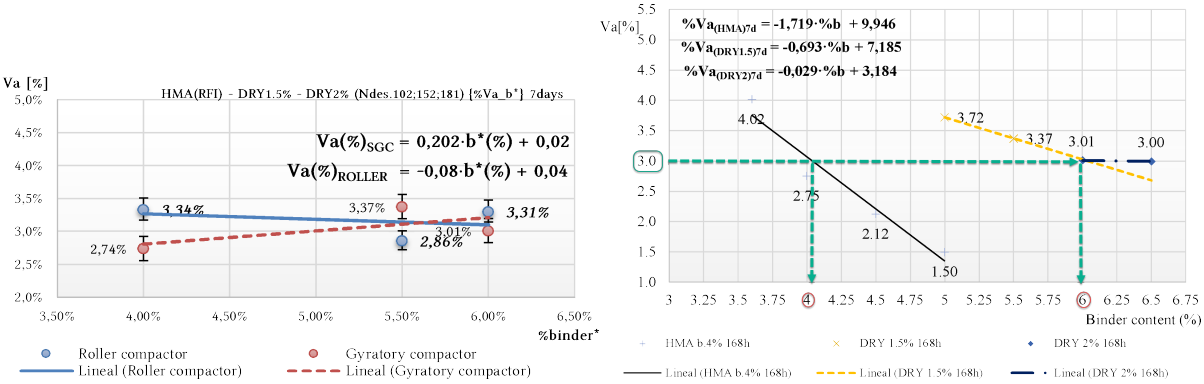


Figure 48. (a) Roller vs. SGC air voids and optimal binder relationship; (b) Ratio voids-binder content with SGC

The results show a minimum deviation since the mix-compaction process was performed under the same manufacturing conditions and continuously. In Tables 59-61, the specimens after sawing of each slab, were studied by weight, volume, and the maximum dry densities. The height at seven days was the objective factor since it affects the limit height of a 12cm thick bituminous sub-layer, and the lateral thickness of the specimens required by the UGR_FACT fatigue device. A comparative is shown in Figure 49.

TABLE 59. SUMMARY OF AVERAGED RESULTS AT SEVEN DAYS IN ALL MIXTURES (ASPHALT ROLLER COMPACTOR)

Mixture (b. %)	Ɣinert (kg/m3)	Ɣbitumen (kg/m3)	Voids %	Binder %	Ɣw (Tª 18ºC) (g/cm3)	Max. density (g/cm3)	Avg. Slabs weight (gr)	ρdim (gr) (g/cm3)	Va slab %
HMA	2808.6	1033.3	3.0	4.0	998.70	2634	14324.05	2550	3.18%
DRY1.5% b.5.5%	2808.2	1033.3	3.0	5.5	998.70	2.577	14244.33	2.526	2.98%
DRY2% b.6%	2808.0	1033.3	3.0	6.0	998.80	2.559	14148.30	2.440	3.12%

TABLE 60. ROLLER COMPACTED SLABS RESULTS [4 BEAMS PER SLAB]

Blend (%b)	Slab mixture	Height 7d [mm]	Va(%)	VMA (%)	VFA (%)	Avrg. H_{7d} [mm]	Avrg. Va(%)	Avrg. VMA (%)	Avrg. VFA (%)
HMA (b.4%)	$RFI^{01}_{4\%}$	59.39	3.77%	13.01	72.87	60.38	3.34%	12.75%	74.61%
	$RFI^{02}_{4\%}$	61.05	3.10%	12.61	75.56				
	$RFI^{03}_{4\%}$	60.71	3.13%	12.63	75.40				
Dry 1.5% (b.5,5%)	$DRY^{01}_{5.5/1.5}$	60.50	2.87%	15.15	83.78	60.62	2.86%	15.15%	83.78%
	$DRY^{02}_{5.5/1.6}$	60.68	2.90%	15.18	83.60				
	$DRY^{03}_{5.5/1.7}$	60.66	2.83%	15.12	83.97				
Dry 2% (b.6%)	$DRY^{01}_{6.0/2.0}$	60.99	3.30%	16.46	82.79	61.35	3.31%	16.47%	82.77%
	$DRY^{02}_{6.0/2.1}$	60.62	3.05%	16.24	84.13				
	$DRY^{03}_{6.0/2.2}$	62.44	3.58%	16.70	81.38				

TABLE 61. EFFECTIVE BINDER CONTENT VS. AIR VOIDS IN SGC AND ROLLER COMPACTED SPECIMENS

Mixture (%binder)	Eff. %binder	(%) Rubber	Va(%) SGC	Va(%) Roller	Va(% X̄)	Desv. Standard (V_a) [%]	CV[21]
HMA	3.85	0.00	3.82	3.34	3.58	0.34	9.5
Dry 1.5%	5.21	1.50	3.37	2.86	3.12	0.36	11.6
Dry 2%	5.66	2.00	3.04	3.31	3.18	0.19	6.0

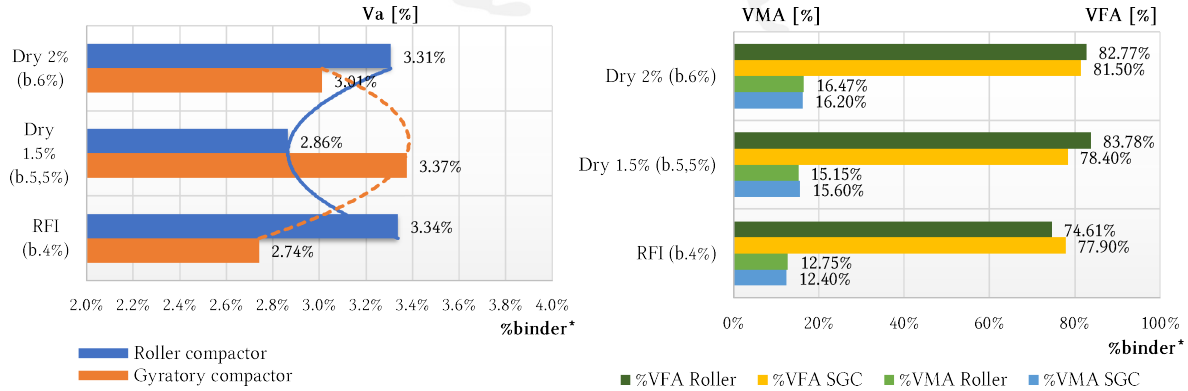


Figure 49. (a) Diagram %binder and %Va; (b) Diagram %binder and %VFA-VMA for each mixture

[21] CV: coefficient of variation also known as relative standard deviation.

The gyratory compactor was characterized by upper constant pressure of 600kPa on the head of the samples thanks to its angle of inclination of 1.25º, which combines with the speed of 30 revolutions per minute (0.5Hz) resulting in uniform and distributed compaction of the mixture [AI, 2011]. The compaction details of each of the specimens manufactured by SGC are shown in Table 62.

TABLE 62. DETAILS OF "VOLUMETRIC MIX-DESIGN" GYRATORY COMPACTOR

Mixture (%binder)	Pressure (bar)	Pressure (kN/cm²)	Ndes SGC	Area sample (cm²)	Force (kN)	Force (kN)· N_{des}	Frequency (Hz)	Duration compacting (min)	Force (Ton force)
HMA (b.4%)			102			1081.5	51.0	±7	109
Dry 1.5% (b.5,5%)	6.0	0.06	152	176.71	10.6	1611.6	76.0	±11	162
Dry 2% (b.6%)			181			1919.1	90.5	±15	193

A particular aspect of the roller compactor concerning SGC is the difference in pressure applied to the plate. Initially, for an HMA applied pressure of 1 bar exerting 15 passes on the slab, and then a second pressure of 1.5 bar followed by 30 passes. In a DRY1.5% mixture, however, the first two press programs of 1 bar and 1.5 bar were applied, and also, a third pressure of 2.5 bar followed by 60 passes. The DRY2% mixture has required the complete program of four pressures, followed by the previous ones, the last pressure of 3.5 bar and 80 passes was added. In this way, the extra-compaction ensured the air voids required and height.

According to the results, in Table 63 are shown some approximations:

TABLE 63. DETAILS OF STANDARD ASPHALT SLAB ROLLER COMPACTOR

Mixture (%binder)	Pressure (bar)	Pressure (kN/cm2)	Roller passes	Area sample (cm2)	Force (kN)	Force (kN)· Passes	Time per device pass (sec)	Duration time compacting (min)	Force (Ton-force)
HMA (b.4%)	1.0	0.010	15	930.25	9.30	139.5	120.0	6.0	14
	1.5	0.015	30		13.95	418.6	240.0		42
DRY1.5% (b.5,5%)	1.0	0.010	15		9.30	46.5	40.0	12.7	5
	1.5	0.015	30		13.95	418.6	240.0		42
	2.5	0.025	60		23.26	1395.4	480.0		140
DRY2% (b.6%)	1.0	0.010	15		9.30	46.5	40.0	23.3	5
	1.5	0.015	30		13.95	418.6	240.0		42
	2.5	0.025	60		23.26	1395.4	480.0		140
	3.5	0.035	80		32.56	2604.7	640.0		261

The disadvantage about SGC is the difficulty of controlling an exact number of passes in each bituminous mixture since the roller compactor device exerts full pressure programs. Even if the 60mm desired compaction height was imposed, it finished making passes with the roller before finishing a full program of pressure. In any case, once the height was completed, excessive roll passes caused extra-compaction that meant less densification.

6.9. Phase 5: Fatigue cracking (mechanical characterization)

The next step is to mechanically characterize the behavior of last mixtures by reducing and controlling fatigue life and cracking at service temperature [EN 12697-24:2012; Colorado APA, 2000; SHRP-A-404, 1994]. The response model of the bituminous sub-ballast layer (Fig. 50) used the properties of the predictive model and temperature calculated as a multi-layer system, and the environmental effects to predict stress and tensions caused by high-speed rail traffic (fatigue cracking).

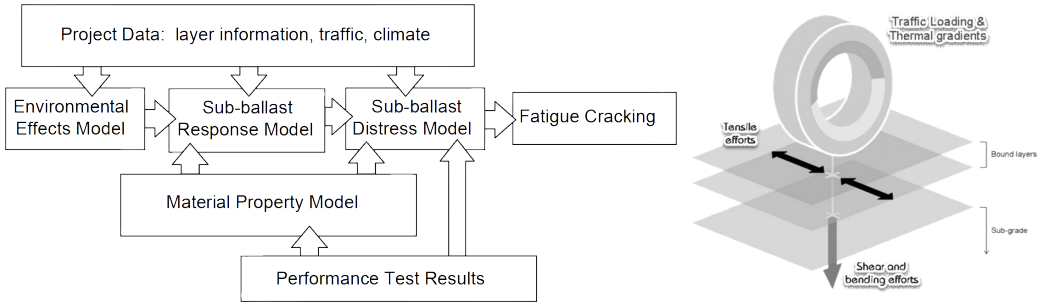


Figure 50. (a) Schematic of Performance Prediction; (b) Movements due to thermal variations and traffic loads

In the case of trackbed containing a bituminous sub-ballast layer, the calculated compressive stresses at high temperatures could be indicative of long-term track-bed settlement failure. The tensile strains at the bottom of the asphalt layer may be indicative of potential fatigue cracking at low temperatures [Moreno, F. et al. 2015; Ghuzlan, K. 2001]. Fatigue cracking was estimated using a single season (one temperature) analysis to calculate fatigue. Dissipated energy is computed for a warm season, and the cumulative dissipated energy is used to estimate fatigue-cracking. An example of the results concerning dissipation of energy inside the bituminous sub-ballast mixture is shown in Figure 51.

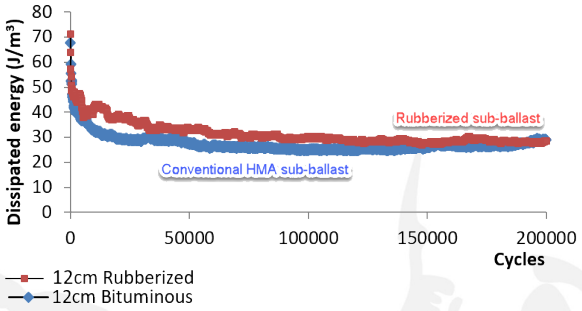


Figure 51. Dissipated energy in a fatigue test with HMA and DRY mixtures

The dimensions of $200 \cdot 60 \cdot 60$mm were selected by sawing four prism-shaped specimens per slab and previously eliminating their edges to avoid possible imperfections. Before fatigue tests, each specimen was about three hours preconditioned at the trial temperature. The results of each fatigue test are expressed in nº of cycles (Nf), load amplitude (kN) and also it was registered the duration time to control the frequency point sample.

An example of broken specimens respectively (Fig. 52).

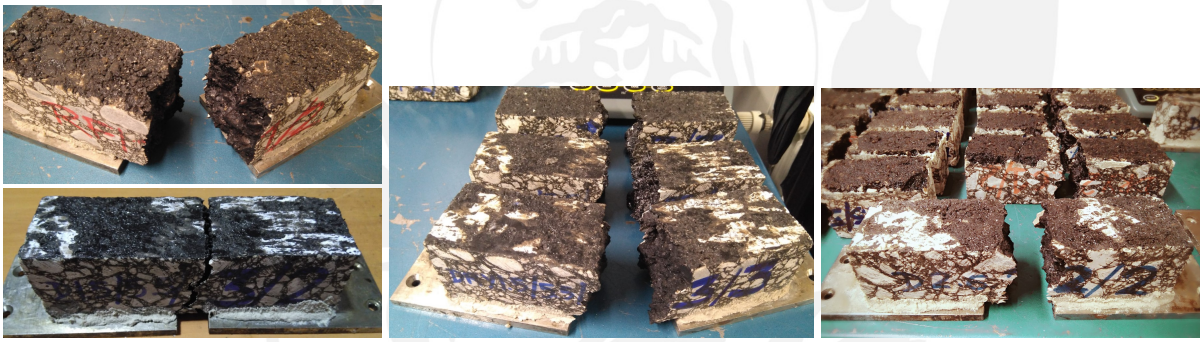


Figure 52. (a) HMA samples; (b) DRY 1.5% samples; (c) DRY 2.0% samples

The characteristics of the test specimens were already described, but they have tested again for density, the percentage of air voids and other volumetric properties during the secondment period to obtain current results before fatigue fracture tests (Tables 64-67).

TABLE 64. CHARACTERISTICS OF HMA B.4% MIXTURE (UGR_FACT)

Nº sample	Ref. 20x6x6cm	Air mass [gr]	Surface dry weight [gr]	Saturated Weight [gr]	ρ_{ssd} [Kgr/m³]	ρ_{dim} [Kgr/m³]	Air voids	Ẋ Va	H [mm]	W [mm]	L [mm]	VMA	VFA
		m_1	m_3	m_2	Υ_{app}	Υ_{sedim}	[%]	[%]				(%)	(%)
1	HMA_{1_1}	1793	1795	1105	2543.0	2538.7	3.69		59.25	59.60	200	12.94%	73.33%
2	HMA_{1_2}	1842	1845	1137	2546.0	2569.2	3.58	**3.70**	59.35	60.40	200	12.84%	73.99%
3	HMA_{1_3}	1832	1835	1129	2539.5	2574.4	3.83		59.45	59.85	200	13.06%	72.56%
4	HMA_{2_1}	1957	1958	1212	2556.1	2556.0	2.98		62.25	60.89	202	12.49%	76.33%
5	HMA_{2_2}	1973	1974	1222	2556.4	2592.6	2.97	**3.05**	61.74	61.02	202	12.48%	76.41%
6	HMA_{2_3}	1897	1898	1173	2549.7	2572.2	3.22		60.54	60.91	200	12.71%	74.84%
7	HMA_{3_1}	1988	1989	1230	2553.2	2577.0	3.09		61.25	62.35	202	12.59%	75.65%
8	HMA_{3_2}	1926	1927	1195	2564.4	2593.0	2.66	**3.02**	61.07	60.51	201	12.21%	78.36%
9	HMA_{3_3}	1913	1914	1182	2547.7	2577.6	3.30		60.41	60.82	202	12.78%	74.38%
	Avg.	**1902**	**1904**	**1176**	**2550.7**	**2572.3**	**3.26**		**60.6**	**60.71**	**201.0**	**12.68%**	**75.10%**

TABLE 65. CHARACTERISTICS OF DRY 1.5% B.5.5% MIXTURE (UGR_FACT)

N°	Ref. 20x6x6cm	Air mass [gr]	Surface dry weight [gr]	Saturated Weight [gr]	ρ_{ssd} [Kgr/m³]	ρ_{dim} [Kgr/m³]	Air voids	Ẋ Va	H [mm]	W [mm]	L [mm]	VMA	VFA
		m_1	m_3	m_2	Υ_{app}	Υ_{sedim}	[%]	[%]				(%)	(%)
1	$DRY_{1.5/5.5/1.1}$	1864	1866	1127	2508.1	2509.6	3.08		60.32	61.26	201	15.34%	82.53%
2	$DRY_{1.5/5.5/1.2}$	1887	1890	1143	2511.8	2526.7	2.94	**2.97**	60.52	61.70	200	15.22%	83.34%
3	$DRY_{1.5/5.5/1.4}$	1855	1857	1123	2512.9	2510.0	2.90		60.48	61.40	199	15.18%	83.58%
4	$DRY_{1.5/5.5/2.1}$	1880	1882	1140	2516.9	2526.4	2.75		60.51	61.49	200	15.05%	84.45%
5	$DRY_{1.5/5.5/2.2}$	1859	1861	1127	2515.9	2511.8	2.78	**2.90**	60.67	60.69	201	15.08%	84.24%
6	$DRY_{1.5/5.5/2.3}$	1935	1938	1172	2509.4	2509.6	3.03		60.75	63.46	200	15.30%	82.81%
7	$DRY_{1.5/5.5/2.4}$	1905	1908	1154	2509.8	2538.8	3.02		60.80	61.40	201	15.28%	82.90%
8	$DRY_{1.5/5.5/3.2}$	1848	1849	1118	2514.3	2511.5	2.84	**2.93**	60.68	60.63	200	15.13%	83.88%
9	$DRY_{1.5/5.5/3.3}$	1938	1940	1172	2509.7	2521.2	3.02		60.67	63.35	200	15.29%	82.89%
	Averaged	**1886**	**1888**	**1142**	**2512.1**	**2518.4**	**2.93**		**60.60**	**61.71**	**200.2**	**15.21%**	**83.40%**

TABLE 66. CHARACTERISTICS OF DRY 2.0% B.6.0% MIXTURE (UGR_FACT)

N°	Ref. 20x6x6cm	Air mass [gr]	Surface dry weight [gr]	Saturated Weight [gr]	ρ_{ssd} [Kgr/m³]	ρ_{dim} [Kgr/m³]	Air voids	Ẋ Va	H [mm]	W [mm]	L [mm]	VMA	VFA
		m_1	m_3	m_2	Υ_{app}	Υ_{sedim}	[%]	[%]				(%)	(%)
1	$DRY_{2.0/6.0/1.1}$	1933	1935	1160	2491.2	2496.1	3.12		60.32	61.26	201	15.34%	82.53%
2	$DRY_{2.0/6.0/1.2}$	1853	1854	1108	2482.3	2467.6	3.47	**3.21**	60.52	61.70	200	15.22%	83.34%
3	$DRY_{2.0/6.0/1.3}$	1882	1884	1127	2483.1	2475.3	3.43		60.69	62.73	199	14.87%	85.65%
4	$DRY_{2.0/6.0/1.4}$	1877	1879	1126	2489.7	2503.2	3.18		60.48	61.40	199	15.18%	83.58%
5	$DRY_{2.0/6.0/2.1}$	1844	1846	1107	2492.3	2477.5	3.08	**3.04**	60.51	61.49	200	15.05%	84.45%
6	$DRY_{2.0/6.0/2.2}$	1878	1879	1128	2497.7	2474.4	2.87		60.67	60.69	201	15.08%	84.24%
7	$DRY_{2.0/6.0/2.3}$	1848	1850	1108	2487.6	2479.4	3.26		60.75	63.46	200	15.30%	82.81%
8	$DRY_{2.0/6.0/2.4}$	1871	1873	1124	2495.0	2483.5	2.97	**3.25**	60.80	61.40	201	15.28%	82.90%
9	$DRY_{2.0/6.0/3.1}$	1960	1962	1173	2481.2	2476.7	3.51		62.47	63.34	200	16.64%	81.70%
	Averaged	**1883**	**1885**	**1129**	**2488.9**	**2481.5**	**3.21**		**60.99**	**61.76**	**200.1**	**16.38%**	**83.26%**

TABLE 67. CHARACTERISTICS OF RESERVED SAMPLES (FATIGUE LIFE AT FREQUENCY **3 HZ**)

N° sample	Ref. 20x6x6cm	Air mass [gr]	Surface dry weight [gr]	Saturated Weight [gr]	ρ_{ssd} [Kgr/m³]	ρ_{dim} [Kgr/m³]	Air voids	H [mm]	W [mm]	L [mm]	VMA	VFA
		m_1	m_3	m_2	Υ_{app}	Υ_{sedim}	[%]				(%)	(%)
R1	RFI_{2_4}	1865	1867	1154	2548.9	2554.6	3.25	59.66	60.88	201	12.74%	74.65%
R2	$DRY_{1.5/5.5/3.1}$	1884	1886	1140	2511.7	2502.6	2.94	60.72	61.99	200	15.22%	83.33%
R3	$DRY_{2.0/6.0/3.3}$	1926	1927	1152	2482.2	2459.4	3.47	62.54	62.61	200	16.61%	81.90%

In Figure 53, the mix-design results of these mixtures were schematized to see the homogeneity of the test specimens before the tests of NDT elastic-dynamic modulus and fatigue cracking by dissipated energy approach.

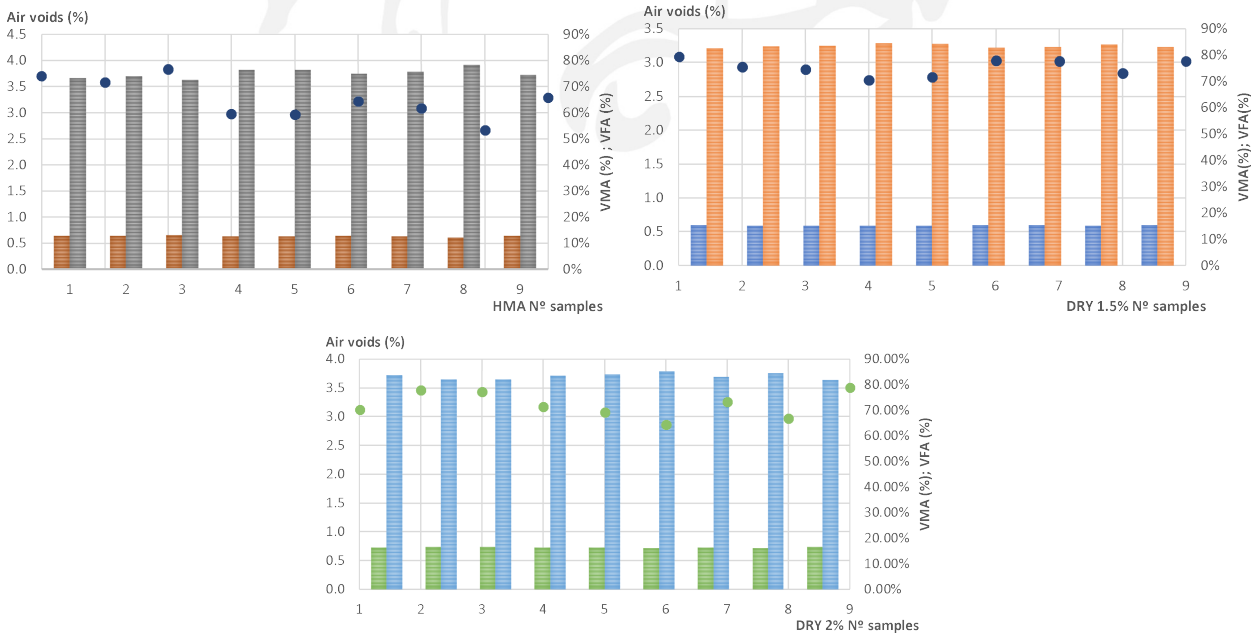


Figure 53. Air voids, VMA, VFA (%); (a) HMA samples; (b) DRY 1.5% samples; (c) DRY 2.0% samples

6.9.1. Load (kN) vs. Nf (Whöler curves)

The first step aimed to define the traditional Whöler fatigue law [Moreno, F. et al. 2014; Saunders, S. 1975] of the bituminous mixtures. The fatigue law behavior of a bituminous mixture was expressed at a given temperature and a stress-strain rate, which stress mode has this structure (Figure 54):

$$\sigma_{r(N)} = C_f^T \cdot N^{-a} \quad or \quad \varepsilon_{r(N)} = K_f^T \cdot N^{-a} \qquad \text{(Eq. 6)}$$

N^{-a} is the number of cycles to failure load when "an" is a parameter that depends on the type of stress; and **C, K** are parameters based on the mixture considered and the test conditions (temperature and frequency).

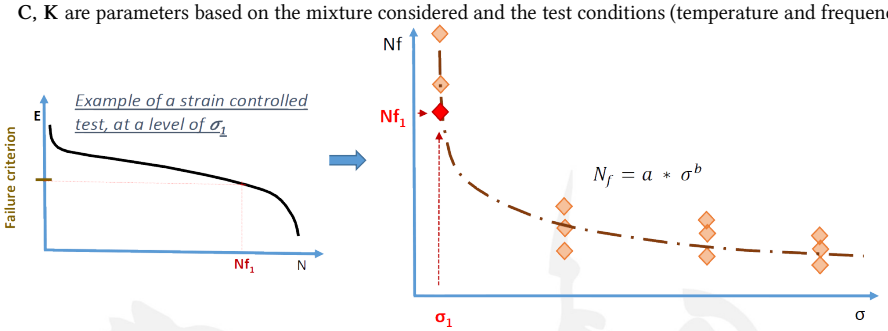


Figure 54. Phenomenological approach

For this purpose, each three specimens at the respective load amplitude of each blend (27 samples) were tested using versine load cycles with an amplitude of 0.6, 0.8 and 1 kN, a frequency of 5 Hz, and a temperature of 20 ºC, as we can see in Tables 68-71.

TABLE 68. SPECIMENS RESERVED AT F. 3HZ (FATIGUE LIFE UGR_FACT)

Specimen	Ref.	Nº cycles fatigue	Load amplitude	f	Tª	Duration test
Nº	20x6x6cm	(Nf)	(kN)	(Hz)	ºC	h:min:seg
R1	HM_{1_4}	6590	1.0	3	20	00:35:30
R2	$DRY_{1.5/5.5/3.1}$	4773	1.0			00:25:34
R3	$DRY_{1.5/5.5/2.2}$	17020	0.8			00:56:20

TABLE 69. HMA B.4% (FATIGUE LIFE UGR_FACT)

Specimen	Ref.	Nº cycles fatigue	Load amplitude	f	Tª	Duration test
Nº	20x6x6cm	(Nf)	(kN)	(Hz)	ºC	h:min:seg
1	HMA_{1_1}	23495	0.6	5	20	01:17:39
2	HMA_{1_2}	6599	1.0			00:35:34
3	HMA_{1_3}	9671	1.0			00:31:40
4	HMA_{2_1}	34941	0.6			01:56:30
5	HMA_{2_2}	27199	0.8			01:41:24
6	HMA_{2_3}	8084	1.0			00:26:20
7	HMA_{3_1}	32400	0.6			01:48:00
8	HMA_{3_2}	16720	0.8			01:10:34
9	HMA_{3_3}	20700	0.8			01:12:19
	Avg.	**30279**	**0.60**			**01:40:43**
		21540	**0.80**			**01:21:26**
		8118	**1.00**			**00:31:11**

TABLE 70. DRY(1.5%) B.5.5% (FATIGUE LIFE UGR_FACT)

Specimen	Ref.	Nº cycles fatigue	Load amplitude	f	Tª	Duration test
Nº	20x6x6cm	(Nf)	(kN)	(Hz)	ºC	h:min:seg
1	$DRY_{1.5/5.5/1.1}$	64629	0.6	5	20	03:36:45
2	$DRY_{1.5/5.5/1.2}$	19031	0.8			01:02:59
3	$DRY_{1.5/5.5/1.4}$	76656	0.6			04:15:20
4	$DRY_{1.5/5.5/2.1}$	13176	0.8			00:43:20
5	$DRY_{1.5/5.5/2.2}$	7436	1.0			00:24:20
6	$DRY_{1.5/5.5/2.3}$	67637	0.6			03:44:59
7	$DRY_{1.5/5.5/2.4}$	27431	0.8			01:31:00
8	$DRY_{1.5/5.5/3.2}$	11817	1.0			00:43:26
9	$DRY_{1.5/5.5/3.3}$	13892	1.0			00:45:40
	Avg.	**69641**	**0.60**			**03:52:21**
		23231	**0.80**			**01:05:46**
		11048	**1.00**			**00:37:49**

TABLE 71. DRY(2.0%) B.6.0% (FATIGUE LIFE UGR_FACT)

Specimen	Ref.	Nº cycles fatigue	Load amplitude	f	Tª	Duration test
Nº	20x6x6cm	(Nf)	(kN)	(Hz)	ºC	h:min:seg
1	$DRY_{2.0/6.0/1.1}$	86653	0.6	5	20	04:48:40
2	$DRY_{2.0/6.0/1.2}$	9069	1.0			00:29:40
3	$DRY_{2.0/6.0/1.3}$	11989	1.0			00:39:21
4	$DRY_{2.0/6.0/1.4}$	61402	0.6			03:24:20
5	$DRY_{2.0/6.0/2.1}$	13718	0.8			00:45:20
6	$DRY_{2.0/6.0/2.2}$	27347	1.0			01:30:39
7	$DRY_{2.0/6.0/2.3}$	182984	0.6			10:09:17
8	$DRY_{2.0/6.0/2.4}$	31044	0.8			01:42:59
9	$DRY_{2.0/6.0/3.1}$	17020	0.8			00:56:20
	Avg.	**110346**	**0.60**			**06:07:26**
		20594	**0.80**			**01:08:13**
		16135	**1.00**			**00:53:13**

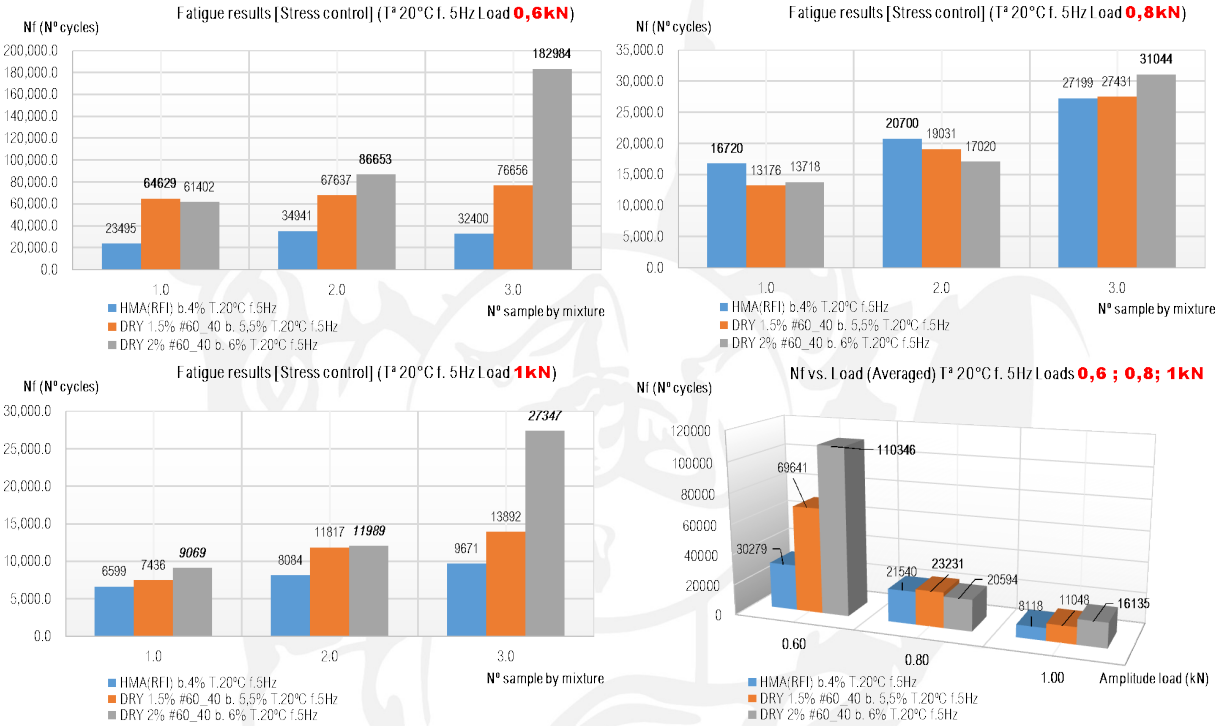


Figure 55. (a) Load 0.6 kN; (b) Load 0.8 kN; (c) Load 1.0 kN; (d) Average Nf vs. Load amplitude

The results showed the variability and inhomogeneity of some specimens with each other, even within the same type of mixture. In general, it follows that the 2% crumb rubber blend behaves better under fatigue, being more evident in the case of higher load amplitude (Figure 55).

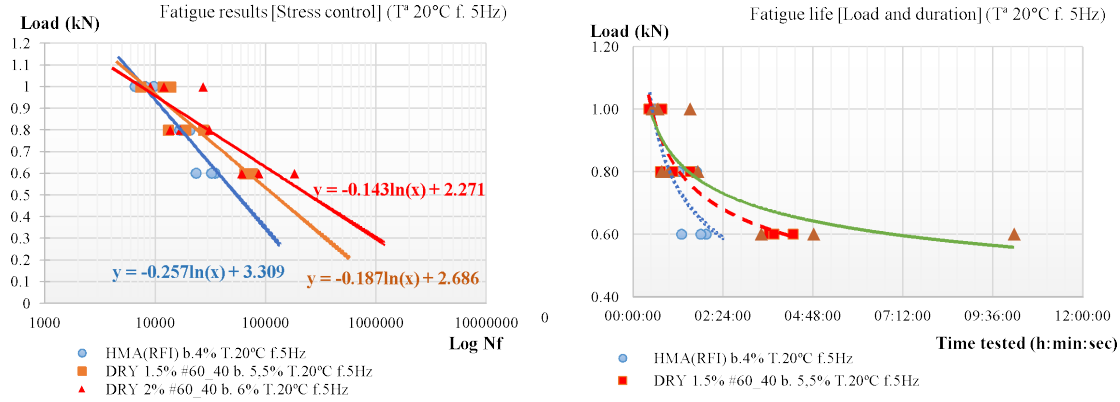


Figure 56. Fatigue life of the mixes tested. (a) Load vs. Log Nº cycles, Nf; (b) Load vs. Duration time test

The conventional HMA mixture behaved relatively homogeneously at the load of 0.8 kN being at the height of the modified mixture with 1.5% rubber. In any case, fatigue life decreased considerably as the load amplitude increased (Figure 56).

Through the graphs of the common Whöler fatigue law of fatigue behavior (Load, kN vs. Failure cycles, N_f) it can be seen that all the mixtures respond to a better long-term performance (Figure 57a). From the regression analysis of the level of load applied and the cycle of failure of each blend, it can be observed that the fatigue life of all the modified mixtures with rubber was similar. A positive difference regarding dissipated energy was observed with DRY 2%. The HMA (conventional mixture) manufactured showed a shorter fatigue life in each amplitude load. This fact reflects that the fatigue behavior of an HMA is worse than the modified rubber blends. When fatigue life was represented as a number of cycles vs. load, higher was the potential law; longer was the fatigue life. Also, in the same graph representation, less was the slope of the curve, less was affected the material by load variations.

These results demonstrate that the use of scrap tire rubber in the production of bituminous mixtures can enlarge their fatigue life and improve their behavior in the long-term (Figure 57b).

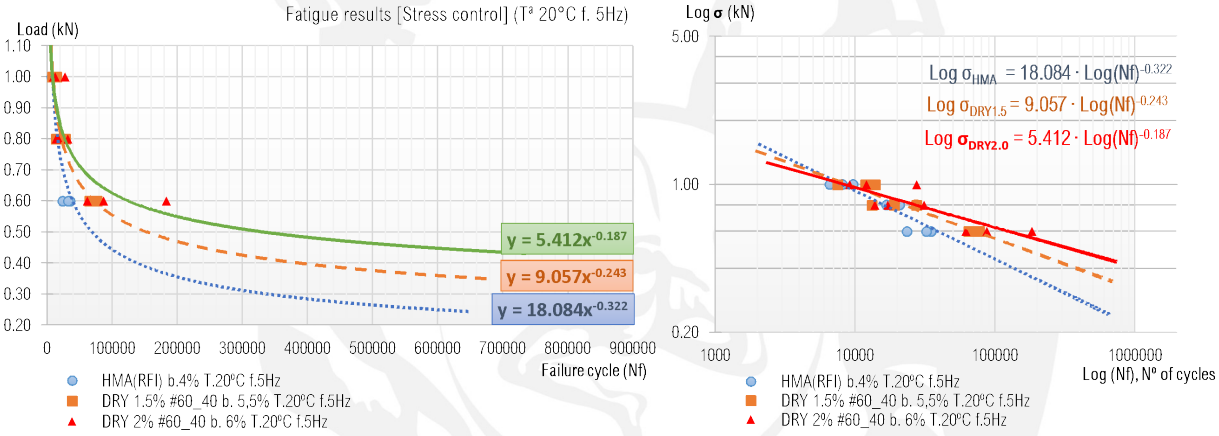


Figure 57. Experimental law of fatigue resistant to each blend. (a) Exponential Regression analysis; (b) Whöler log-log fatigue curve (Stress amplitude vs. Number of cycle reversals to failure, Log stress vs. Log Nf)

As the discussion in phenomenological approach, Wöhler's Stress-Nf curves [H. Di Benedetto et al. 2011] were based on experimental fatigue data used for life prediction of bituminous mixtures. The log-log Whöler plan curve only provides fatigue life without giving any indication about cycles needed for crack initiation and propagation. Bilogarithm Whöler plan (Logσ-LogNf) curves, therefore, don't impart sufficient confidence about failure-free performance of the component. Under specific test conditions, thanks to the bi-logarithmic diagram of Whöler, it was possible to estimate the three loads of 0.6, 0.8 and 1 kN considered optimal in this thesis for the test specimens, since they allowed to represent the fatigue behavior significantly. Consequently, the energy approach is justified in this research concerning the concepts about fatigue damage rules which look into the characteristics of fatigue curves in viscoelastic materials. However, Whöler curve has served to demonstrate the fatigue life of the mixtures, and as a conclusion, the increase in the number of cycles in mixtures with recycled rubber provides a higher yield compared to conventional mixtures, therefore, the aim of this thesis, to demonstrate the efficiency and reliability of sustainable blends with recycled tire rubber has been met.

6.9.2. Dissipated energy (ωi) [Hysteresis loops]

This methodological approach aims to evaluate the movements produced at a molecular level, as well as the damage produced due to the breakage at a bonding level. The results were expressed regarding dissipated energy, nº of cycles to failure, geometrical changes, and mean damage parameter (Fig. 58) [Moreno, F. et al.

2015-2016]. The hysteresis loop described for the "relative" displacements produced in the material is used to define the dissipated energy in each load cycle, which is obtained as the addition of the dissipated energies calculated in the vertical and horizontal directions [Carpenter, S.H. 2006].

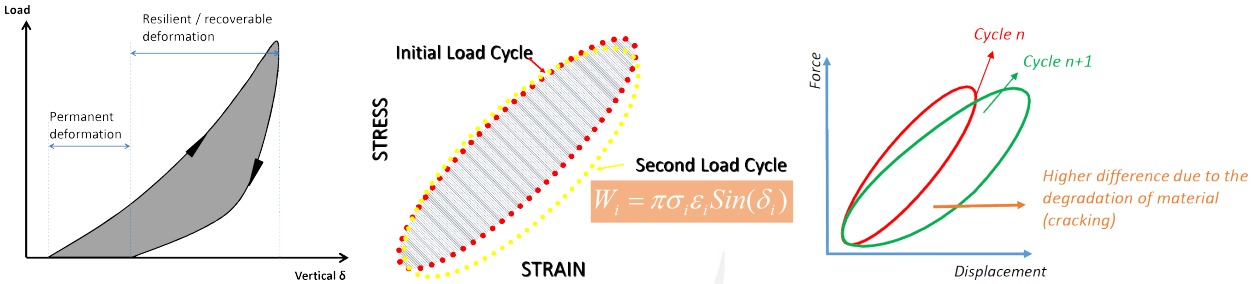


Figure 58. (a) Hysteresis loop (amount of dissipated energy) theory; (b) Different Dissipated Energy between load cycles [Adapted from Carpenter, 2006]; (c) Hysteresis loop diagram [Moreno, F. 2015]

These energies were obtained from the values of the areas inside the hysteresis loops, which is more accurate than the use of the absolute value of the "relative" displacements. From the representation of the RDEC calculated in each cycle, the RDEC value (under specific testing conditions) at the failure cycle was obtained according to the failure criterion considered (Figure 58c).

Considering the importance of hysteresis cycles in fatigue behavior, the most representative results of each mixture studied are presented (Figures 59-67). For each mixture, three samples were selected, and compared based on each load (0.6, 0.8, and 1.0 kN). Each hysteresis loop diagram represented corresponds to the first power dissipation cycle, equivalent to 104 points recorded in the device at 5 Hz, therefore, 20 seconds of duration per dissipative cycle (Load vs. Displacement curves).

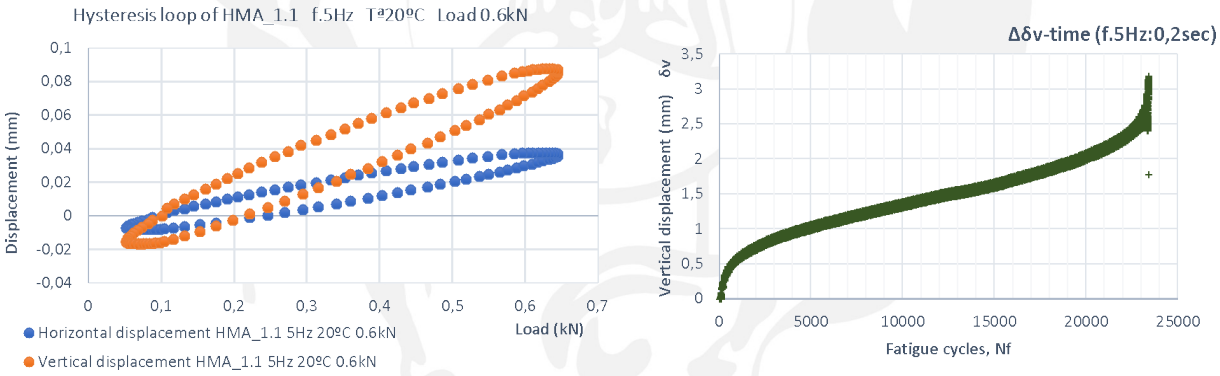


Figure 59. (a) Hysteresis loops; (b) Vertical displacement vs. Nf [HMA sample 1.1 (Load 0.6 kN; Nf: 23495 cycles)]

The hysteresis loop described for the displacements (Hi, Vi) produced is used to define the energy dissipated in each cycle, which is obtained by adding the dissipated energies calculated in the vertical-horizontal directions.

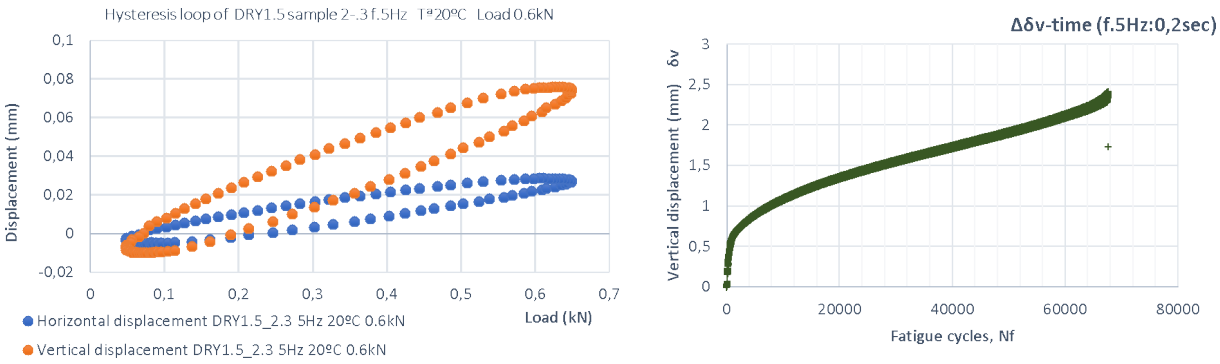


Figure 60. (a) Hysteresis loops; (b) Vertical displacement vs. Nf [DRY 1.5% sample 2.3 (Load 0.6 kN; Nf: 67637 cycles)]

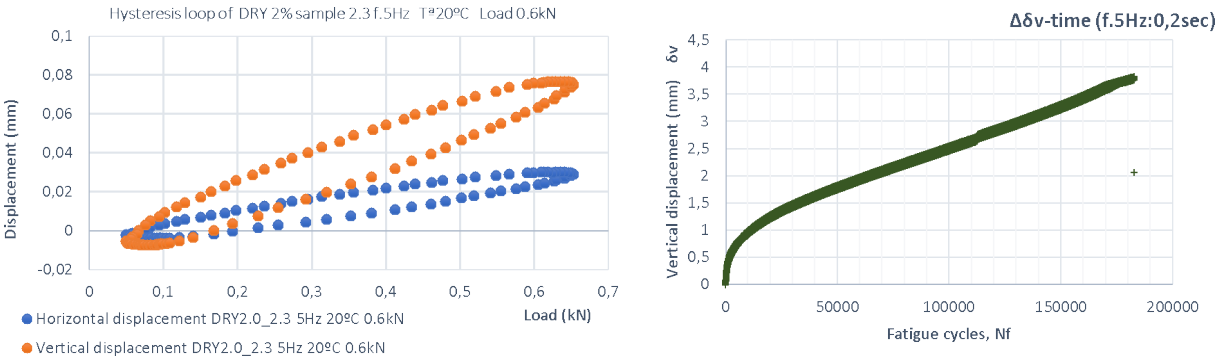


Figure 61. (a) Hysteresis loops; (b) Vertical displacement vs. Nf [DRY 2% sample 2.3 (Load 0.6 kN; Nf: 182984 cycles)]

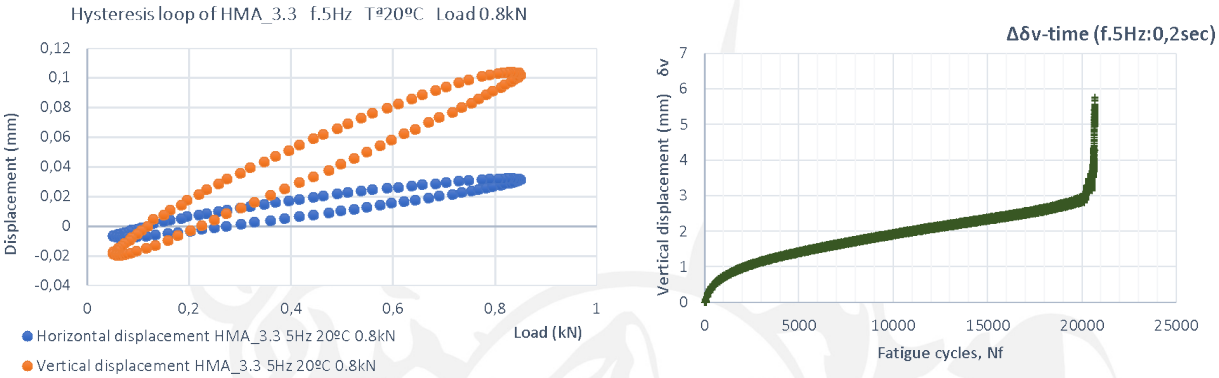


Figure 62. (a) Hysteresis loops; (b) Vertical displacement vs. Nf [HMA sample 3.3 (Load 0.8 kN; Nf: 20700 cycles)]

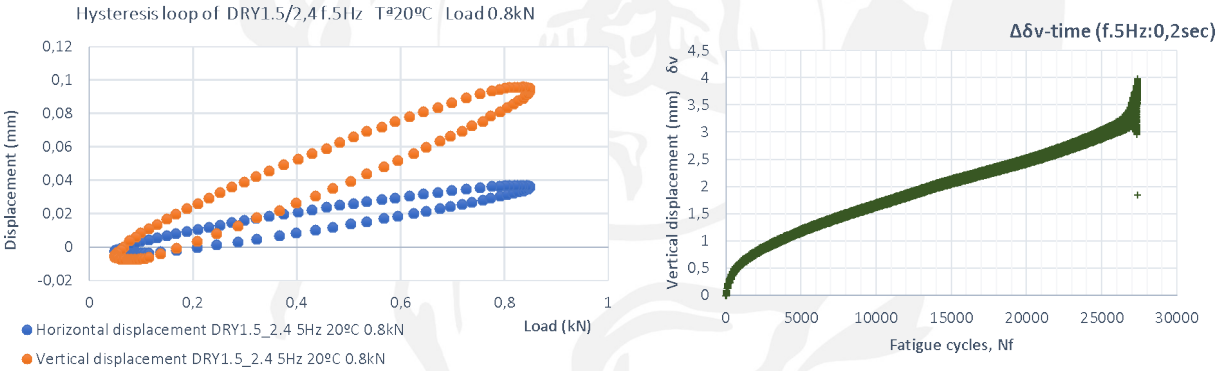


Figure 63. (a) Hysteresis loops; (b) Vertical displacement vs. Nf [DRY 1.5% sample 2.4 (Load 0.8 kN; Nf: 27431 cycles)]

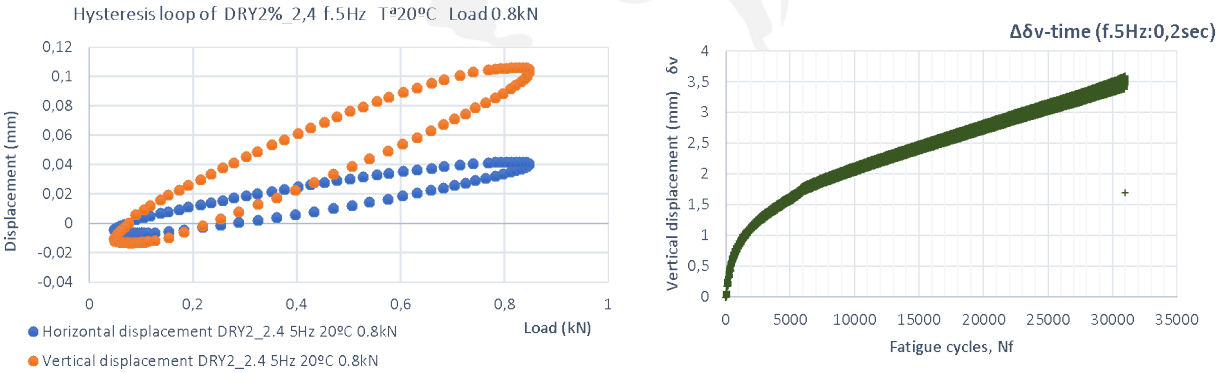


Figure 64. (a) Hysteresis loops; (b) Vertical displacement vs. Nf [DRY 2% sample 2.4 (Load 0.8 kN; Nf: 31044 cycles)]

In any mode of loading, the higher the recycled rubber content, the longer the fatigue life and the less energy dissipated due to the elasticity of the material. In conventional mixtures HMA the vertical displacements were

lower than in the rest of cases, because of the material fracture of ductile form, its greater rigidity gives plasticity to the deformations and therefore breaks before.

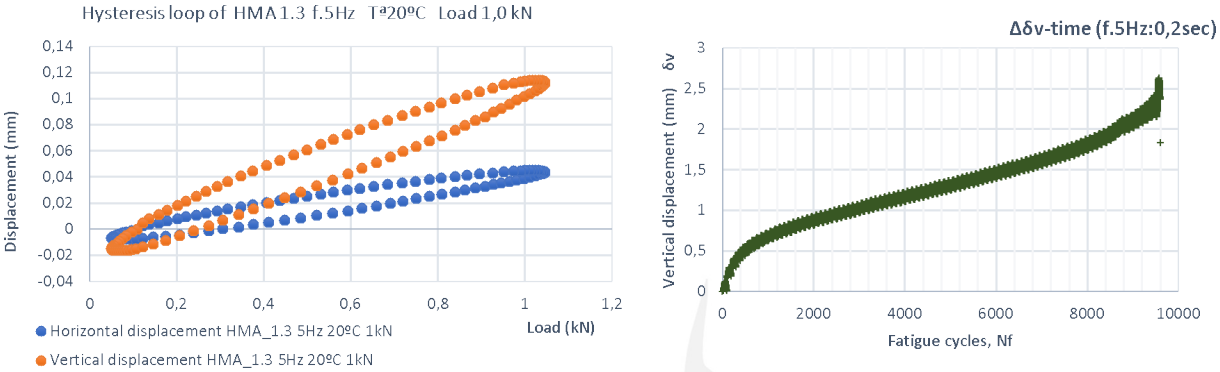


Figure 65. (a) Hysteresis loops; (b) Vertical displacement vs. Nf [HMA sample 1.3 (Load 1.0 kN; Nf: 6599 cycles)]

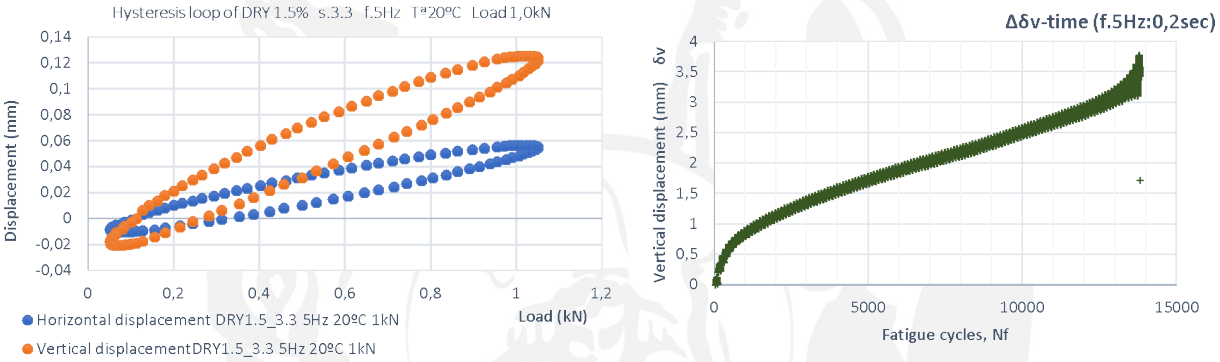


Figure 66. (a) Hysteresis loops; (b) Vertical displacement vs. Nf [DRY 1.5% sample 3.3 (Load 1.0 kN; Nf: 13892 cycles)]

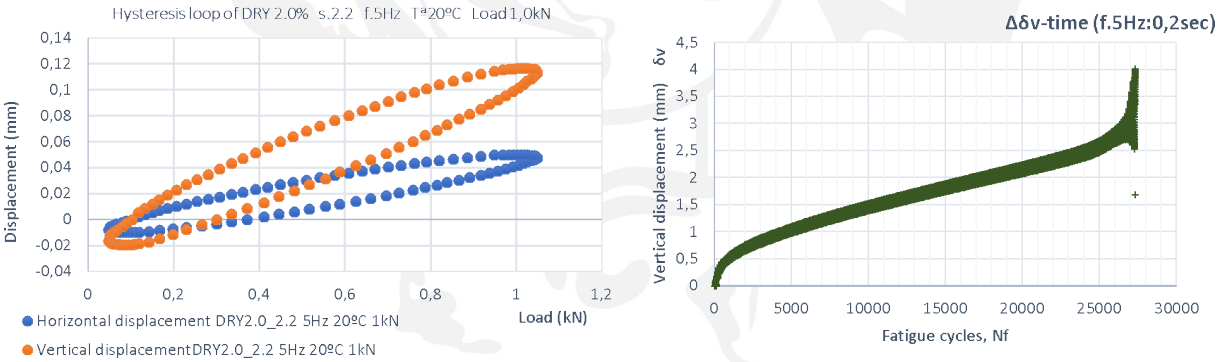


Figure 67. (a) Hysteresis loops; (b) Vertical displacement vs. Nf [DRY 2.0% sample 2.2 (Load 1.0 kN; Nf: 27347 cycles)]

The value of the closed area in each load-displacement curve represents the Dissipated energy in Joules (1J=1kNmm). The appearance of dissipated energy is due to the viscoelastic behavior of bituminous mixtures, which is related to different phenomena during cyclic loading tests.

6.9.3. Dissipated energy (ω_i) vs. Geometry variation ($\Delta\varepsilon_i$)

This methodological approach aims to evaluate the movements produced at a molecular level, as well as the damage produced due to the breakage at a bonding level. The results were expressed regarding dissipated energy, the number of cycles to failure, geometrical changes, and mean damage parameter in HMA mixes [Moreno, F. et al. 2016]. In Fig. 68 is shown the resulting graph obtained from the representation of these two parameters, being able to identify the damage in the material due to variations in the geometry.

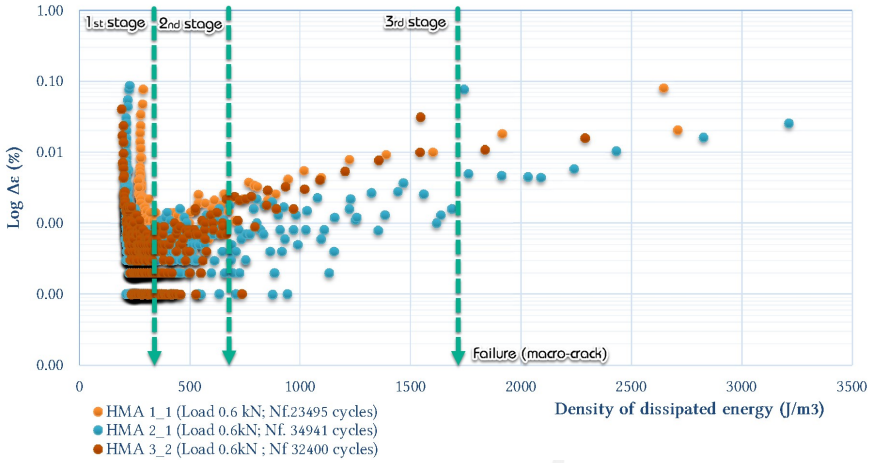


Figure 68. Representation of Log Δε (%) as a function of the dissipated energy of the three HMA samples (Load 0.6 kN, 5 Hz)

In the first stage, there are no significant changes in energy dissipated, but there are geometric variations (which become lower with increasing load cycles) as a result of plastic deformations and other phenomena such as thixotropy that is not associated with damage in asphalt mixtures. The second stage, characterized by small variations in the geometry of the material, the progressive increase of the dissipated energy is due to the initiation of damage as a result of molecular failure.The third stage was an increase in energy dissipated between the different cycles as a consequence of the development of the macro-fissure. For each sample (Fig. 69).

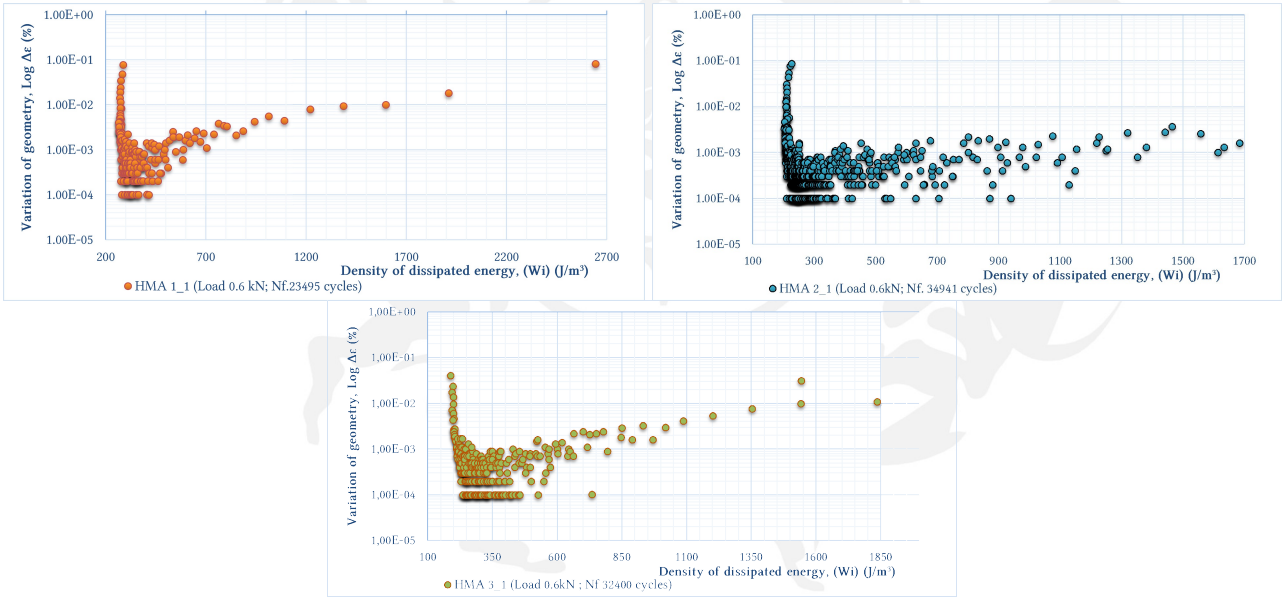


Figure 69. (a) HMA $_{RFI\ 1_1}$ Load 0.6Kn, Nf. 23495 cycles; (b) HMA $_{RFI\ 2_1}$ Load 0.6Kn, Nf. 34941 cycles (c) HMA $_{RFI\ 3_1}$ Load 0.6Kn, Nf. 32400 cycles.

In Figure 70, at the same temperature, the mean values of energy dissipated during the test for the HMA conventional mixture were studied. Also, displacements and variations in load during the fatigue life of the reference mixture are explained in the next graphs. The crucial aspect of the design was the number of load cycles that the material could support before reaching its failure, which will depend on the failure criterion selected (traditionally is chosen at 50% reduction of the stiffness modulus). Due to the viscoelastic nature of HMA mixes, the study of the dissipated energy to cycling loads offered relevant information about the fatigue behavior, which is directly related with the damage in the specimen during the fatigue test. For that reason, it was considered the study of the hysteresis loops.

Any change produced in the hysteresis loop (amount of dissipated energy) will be related to the changes produced in the material. Thus, the fatigue resistance can be characterized.

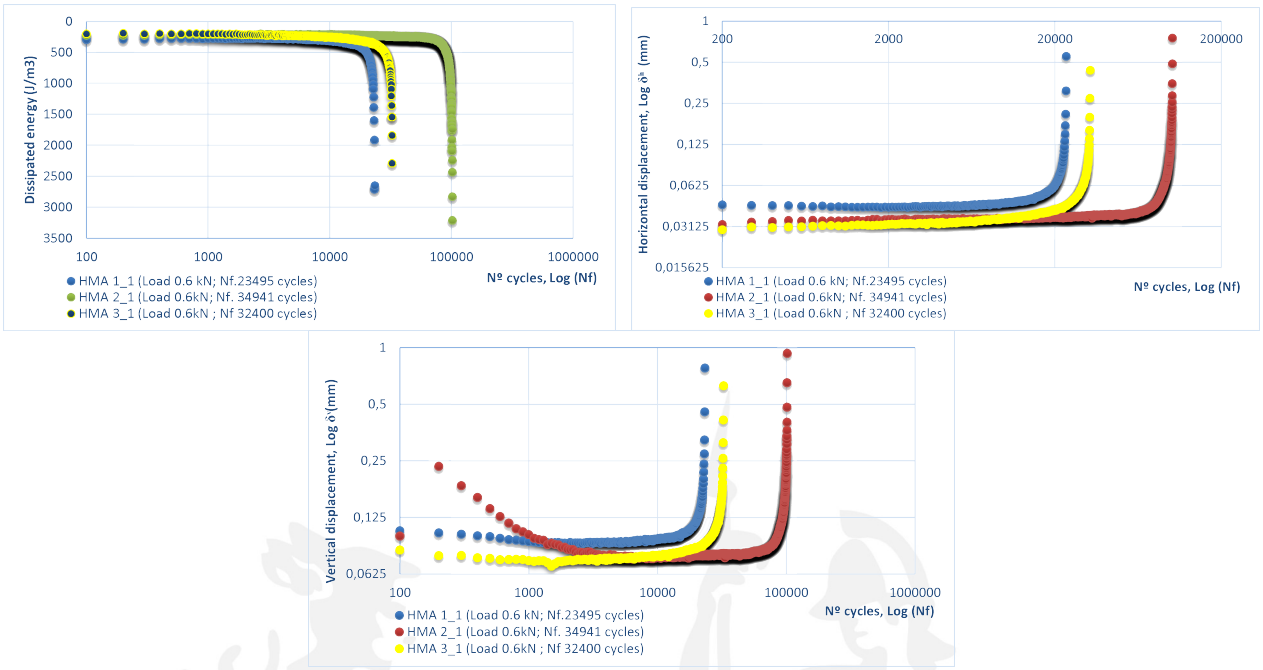


Figure 70. HMA Load 0.6kN. (a)Avg. Values of dissipated energy; (b) Horizontal displacements vs. Nf; (c) Vertical displacements vs. Nf

Figure 71 shows the results obtained when representing the two parameters achieved in each load cycle of the UGR-FACT test (dissipated energy on the x-axis, ωi, and the variation of the geometry on the y-axis, Δεi). It is clear that the different stages of the fatigue process can be identified in each sample tested. Despite the variation in the geometry, the dissipated energy measured in each initial load cycle did not change until a certain nº of cycles where due to the macro-crack the section of the curve represents a general abrupt change.

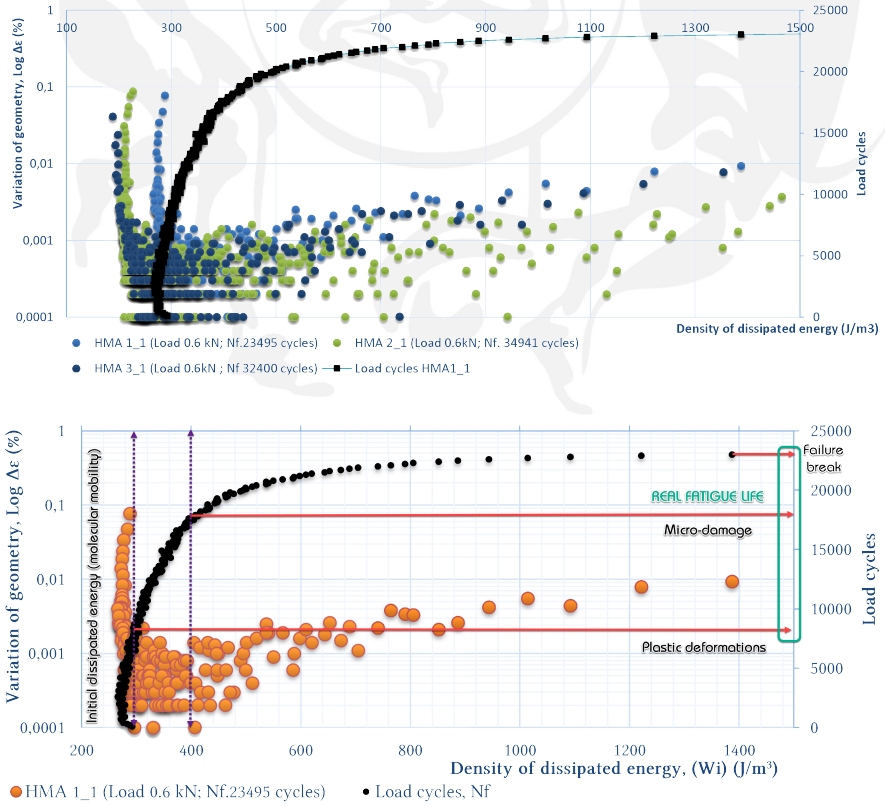


Figure 71. HMA Load 0.6 kN results (Log Δεi vs. ωi)

6.9.4. Effect of frequency, temperature, and loading

Blends were affected more by temperature than by frequency. At low temperature (10°C), the mechanical response of the mixture was more elastic (the energy dissipation values were initially lower) with a more brittle fracture (rupture was non-ductile, fragile by geometry and by the strength of the material).

When the temperature increases the response became more viscous, and the fracture was more ductile (higher values of energy dissipated, greater plasticity and ductile-plastic breakage). Because the study has been focused on the analysis of 9 samples by mixture (27 samples + 6 reserve specimens) being three samples for each amplitude of load, these are the arguments to conclude that:

The fatigue-cracking life of the DRY mixtures is considerably longer than the fatigue life of the HMA;

DRY mixtures are stiffer to fatigue than mixtures made with HMA conventional blend, but once the macro-crack has appeared, it spreads quickly through the specimen due to a more fragile response;

At higher frequencies (5 Hz), the mechanical response of the mixture is more elastic (lower values of initial dissipated energies, ωi) with a less brittle fracture (lower values of dissipated energy and variations in the geometry);

At a frequency of 3 Hz, the response was viscous; initial dissipated energy values increased, the cracking was ductile, fragile, more plastic breakage. Therefore, fewer cycles of fatigue loading could withstand, and the specimen broke earlier in all cases;

As the load-amplitude increases and the frequency decreases, resistance to fatigue becomes lower;

The break was not immediate, it happened before, but the fracture spread more slowly. At low frequency, more energy was dissipated, and damage occurred in the material causing the cracking.

Fatigue life of all the modified bitumens was very similar, independently of the DRY mixture with rubber at 2.0% (higher fatigue life) of crumb rubber added by the dry process. The mix manufactured with conventional bitumen shows a shorter fatigue life.

At the last phase of the test, the energy dissipated in each loading cycle by the DRY mixture increased until it exceeded the energy dissipated by the HMA mixture.

Mixture manufactured with crumb rubber showed a clean, thin and without ramifications cracking process, that confirms that the material was stiffer and the crack propagation was faster (Fig. 72).

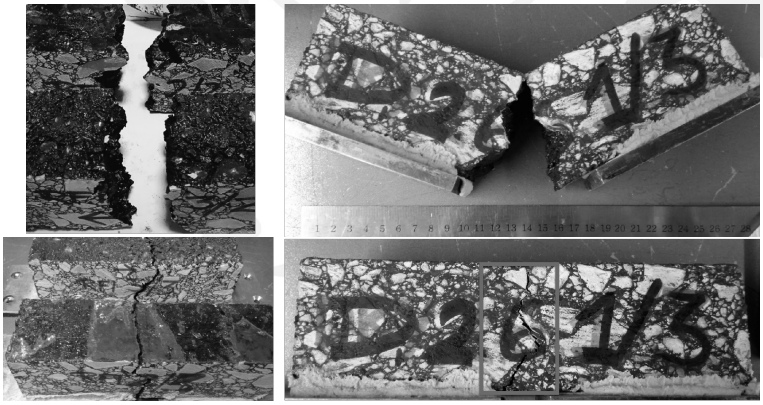


Figure 72. Effect of cracking propagation. (a) HMA cleaner and larger crack; (b) DRY 2% branched fracture

6.10. Phase 6: Non-Destructive testing (FFRC). Elastic modulus

Based on the results, Young's modulus ranges from 30 GPa for HMA blends and 20 GPa for blends with 2% of recycled rubber. Apparently, mixtures with recycled rubber show lower values of resistance modules, a higher Poisson's coefficient and wave attenuation (low wave velocity) due to the internal rubber content that attenuates the propagation of the elastic wave, respect to the HMA blends. Each value corresponds to an average of ten impacts to avoid dispersion and the suppression of signal-noise due to common rebounds because of internal heterogeneities of the material. In Tables 72-74 are summarised the NDT-FFRC values:

TABLE 72. FFR TESTS FOR HMA SPECIMENS ON ANTI-VIBRATION BASIS AND BEFORE UGR_FACT[22]

HMA Samples 20x6x6cm	Δf_T	Δf_L	Δf_G	Ed_T	Ed_L	G_D	Poison's ratio	P-wave speed	S-wave speed	R-wave speed	Young's |E|
	(Hz)	(Hz)	(Hz)	[GPa]	[GPa]	[GPa]	μ	m/s	m/s	m/s	[GPa]
HMA 1_1	4215	8928	5109	30.95	32.43	12.55	0.26	3571	2222	2057	28.48
HMA 1_2	4293	9200	5141	32.41	34.48	12.89	0.32	3680	2250	2103	30.62
HMA 1_3	4181	8997	5072	30.70	32.89	12.55	0.30	3599	2223	2072	29.34
HMA 2_1	4256	9083	5056	30.53	34.42	12.65	0.33	3669	2225	2083	30.28
HMA 2_2	4363	8141	5029	32.77	34.87	12.68	0.36	3693	2227	2095	31.11
HMA 2_3	4288	9067	4987	31.25	33.54	12.12	0.36	3627	2180	2051	29.76
HMA 3_1	4315	9045	5067	32.37	34.10	12.81	0.31	3654	2239	2091	30.28
HMA 3_2	4416	9360	5248	33.66	36.31	13.67	0.31	3763	2309	2156	32.31
HMA 3_3	4251	9040	5168	32.02	33.98	13.31	0.26	3652	2286	2118	30.26
Avg.	**4286**	**9096**	**5097**	**31.85**	**34.11**	**12.80**	**0.31**	**3656**	**2240**	**2092**	**30.27**

TABLE 73. FFR TESTS FOR DRY 1.5% SPECIMENS ON ANTI-VIBRATION BASIS AND BEFORE UGR_FACT

DRY 1.5% Samples 20x6x6cm	Δf_T	Δf_L	Δf_G	Ed_T	Ed_L	G_D	Poison's ratio	P-wave speed	S-wave speed	R-wave speed	Young's |E|
	(Hz)	(Hz)	(Hz)	[GPa]	[GPa]	[GPa]	μ	m/s	m/s	m/s	[GPa]
$DRY_{1.5/5.5/1.1}$	3749	7883	4384	23.84	25.19	9.24	0.33	3169	1919	1798	22.17
$DRY_{1.5/5.5/1.2}$	3845	8187	4528	24.72	26.94	9.84	0.35	3275	1979	1858	23.86
$DRY_{1.5/5.5/1.4}$	3856	8123	4475	24.22	26.26	9.44	0.36	3233	1938	1822	23.08
$DRY_{1.5/5.5/2.1}$	3915	8299	4629	25.61	27.73	10.27	0.32	3319	2020	1890	24.50
$DRY_{1.5/5.5/2.2}$	3861	8203	4656	25.14	27.36	10.41	0.28	3297	2035	1891	24.03
$DRY_{1.5/5.5/2.3}$	3963	8229	4491	26.04	27.19	9.64	0.38	3292	1960	1848	23.94
$DRY_{1.5/5.5/2.4}$	3840	8059	4507	25.03	26.34	9.88	0.32	3240	1984	1854	23.45
$DRY_{1.5/5.5/3.2}$	3792	7952	4437	23.79	25.44	9.36	0.33	3181	1929	1806	22.36
$DRY_{1.5/5.5/3.3}$	3717	7941	4341	23.04	25.32	9.05	0.37	3177	1899	1789	22.39
Avg.	**3838**	**8097**	**4494**	**24.60**	**26.42**	**9.68**	**0.34**	**3242**	**1963**	**1839**	**23.31**

TABLE 74. FFR TESTS FOR DRY 2% SPECIMENS ON ANTI-VIBRATION BASIS AND BEFORE UGR_FACT

DRY 2% Samples 20x6x6cm	Δf_T	Δf_L	Δf_G	Ed_T	Ed_L	G_D	Poison's ratio	P-wave speed	S-wave speed	R-wave speed	Young's |E|
	(Hz)	(Hz)	(Hz)	[GPa]	[GPa]	[GPa]	μ	m/s	m/s	m/s	[GPa]
$DRY_{2.0/6.0/1.1}$	3632	7680	4123	22.45	23.98	8.23	0.43	3103	1818	1725	21.15
$DRY_{2.0/6.0/1.2}$	3616	7707	4195	21.97	24.07	8.38	0.39	3113	1837	1736	21.03
$DRY_{2.0/6.0/1.3}$	3557	7741	4184	21.26	24.29	8.37	0.41	3127	1836	1740	21.31
$DRY_{2.0/6.0/1.4}$	3541	7499	4080	20.56	22.40	7.89	0.39	2999	1780	1682	19.81
$DRY_{2.0/6.0/2.1}$	3760	7821	4368	23.72	24.64	9.05	0.32	3144	1906	1782	21.55
$DRY_{2.0/6.0/2.2}$	3507	7675	4213	20.80	24.01	8.51	0.37	3101	1845	1737	20.92
$DRY_{2.0/6.0/2.3}$	3581	7581	4248	21.45	23.11	8.57	0.31	3048	1856	1733	20.27
$DRY_{2.0/6.0/2.4}$	3541	7560	4232	21.68	23.51	8.69	0.32	3069	1866	1743	20.59
$DRY_{2.0/6.0/3.1}$	3648	7765	4213	20.94	23.94	8.34	0.40	3106	1834	1734	21.03
Avg.	**3598**	**7670**	**4206**	**21.65**	**23.77**	**8.45**	**0.37**	**3090**	**1842**	**1735**	**20.85**

The results validate the use of FFR for mechanical properties measurement and show that the dynamic elastic modulus (Ed), shear modulus (Gd) and damping coefficient (η) can be accurately estimated using NDT. The complex shear modulus of bituminous mixtures is a fundamental property of the material.

HMA mixtures have a stiffer structure with higher amounts of fines (material <Ø75μ), with lower voids tend to have higher complex shear modulus values than rubberized mixtures.

In general, mixtures modified with rubber at 1.5% are those that show better performance and higher uniformity of results, being less dispersion of results and achieving optimal performance.

A relationship between the elastic modulus of the processed samples ($200 \cdot 60 \cdot 60$ mm) of each mixture and its resistance to fatigue has shown that depending on the number of cycles up to the macro-fracture, and as a function of the applied load, the values are homogeneous.

The remaining specimens after the fatigue tests were again subjected to NDT-FFRC tests, obviously showing, as expected, shallow values of elastic modulus due to the internal damage to the material. The results are presented for each specimen, highlighting the properties of each and their fatigue life (Tables 75-78; Fig. 73).

[22] $\Delta f_{T/L/G}$= averaged transversal/longitudinal/torsional resonant frequencies respectively;
Ed= Dynamic Young´s Modulus Elasticity; G_D= Shear modulus.

TABLE 75. HMA SAMPLES (YOUNG'S AND SHEAR MODULUS VS. FATIGUE LIFE (NF, LOADS 0.6 ; 0.8 ; 1KN)

HMA Samples 20x6x6cm	Ed_T [GPa]	Ed_L [GPa]	G_D [GPa]	Poison's ratio μ	Young's |E| [GPa]	Fatigue, Nf [n° cycles]	Load (kN) [kN]	freq. [Hz]	T[a] [GPa]
HMA 1_1	30.95	32.43	12.55	0.26	28.48	23495	0.6	5	20
HMA 1_2	32.41	34.48	12.89	0.32	30.62	6599	1.0		
HMA 1_3	30.7	32.89	12.55	0.3	29.34	9671	1.0		
HMA 2_1	30.53	34.42	12.65	0.33	30.28	34941	0.6		
HMA 2_2	32.77	34.87	12.68	0.36	31.11	27199	0.8		
HMA 2_3	31.25	33.54	12.12	0.36	29.76	8084	1.0		
HMA 3_1	32.37	34.1	12.81	0.31	30.28	32400	0.6		
HMA 3_2	33.66	36.31	13.67	0.31	32.31	16720	0.8		
HMA 3_3	32.02	33.98	13.31	0.26	30.26	20700	0.8		

TABLE 76. DRY 1.5% SAMPLES (YOUNG'S AND SHEAR MODULUS VS. FATIGUE LIFE (NF, LOADS 0.6 ; 0.8 ; 1KN)

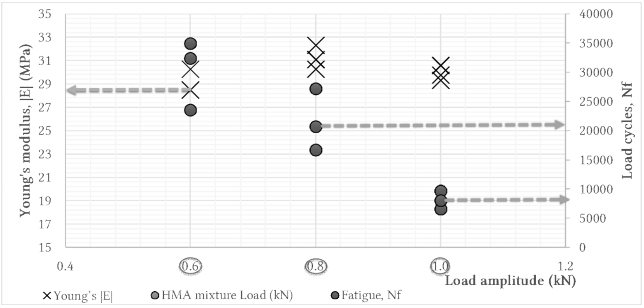
DRY 1.5% Samples 20x6x6cm	Ed_T [GPa]	Ed_L [GPa]	G_D [GPa]	Poison's ratio μ	Young's |E| [GPa]	Fatigue, Nf [n° cycles]	Load (kN) [kN]	freq. [Hz]	T[a] [GPa]
$DRY_{1.5/5.5/1.1}$	23.84	25.19	9.24	0.33	22.17	64629	0.6	5	20
$DRY_{1.5/5.5/1.2}$	24.72	26.94	9.84	0.35	23.86	19031	0.8		
$DRY_{1.5/5.5/1.4}$	24.22	26.26	9.44	0.36	23.08	76656	0.6		
$DRY_{1.5/5.5/2.1}$	25.61	27.73	10.27	0.32	24.5	13176	0.8		
$DRY_{1.5/5.5/2.2}$	25.14	27.36	10.41	0.28	24.03	7436	1.0		
$DRY_{1.5/5.5/2.3}$	26.04	27.19	9.64	0.38	23.94	67637	0.6		
$DRY_{1.5/5.5/2.4}$	25.03	26.34	9.88	0.32	23.45	27431	0.8		
$DRY_{1.5/5.5/3.2}$	23.79	25.44	9.36	0.33	22.36	11817	1.0		
$DRY_{1.5/5.5/3.3}$	23.04	25.32	9.05	0.37	22.39	13892	1.0		

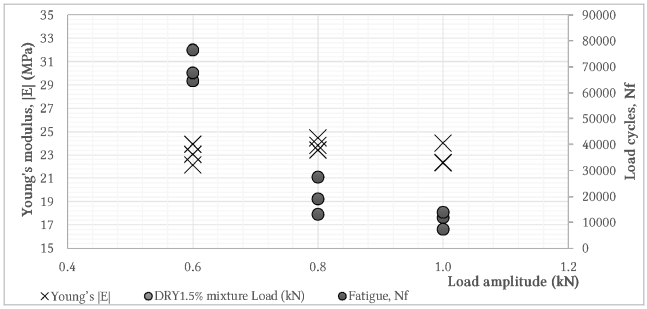
TABLE 77. DRY 2% SAMPLES (YOUNG'S AND SHEAR MODULUS VS. FATIGUE LIFE (NF, LOADS 0.6 ; 0.8 ; 1KN)

DRY 2% Samples 20x6x6cm	Ed_T [GPa]	Ed_L [GPa]	G_D [GPa]	Poison's ratio μ	Young's |E| [GPa]	Fatigue, Nf [n° cycles]	Load (kN) [kN]	freq. [Hz]	T[a] [GPa]
$DRY_{2.0/6.0/1.1}$	22.45	23.98	8.23	0.43	21.15	86653	0.6	5	20
$DRY_{2.0/6.0/1.2}$	21.97	24.07	8.38	0.39	21.03	9069	1.0		
$DRY_{2.0/6.0/1.3}$	21.26	24.29	8.37	0.41	21.31	11989	1.0		
$DRY_{2.0/6.0/1.4}$	20.56	22.4	7.89	0.39	19.81	61402	0.6		
$DRY_{2.0/6.0/2.1}$	23.72	24.64	9.05	0.32	21.55	13718	0.8		
$DRY_{2.0/6.0/2.2}$	20.8	24.01	8.51	0.37	20.92	27347	1.0		
$DRY_{2.0/6.0/2.3}$	21.45	23.11	8.57	0.31	20.27	182984	0.6		
$DRY_{2.0/6.0/2.4}$	21.68	23.51	8.69	0.32	20.59	31044	0.8		
$DRY_{2.0/6.0/3.1}$	20.94	23.94	8.34	0.4	21.03	17020	0.8		

TABLE 78. RESUME ALL MIXTURES (YOUNG'S E, FATIGUE LIFE AND LOAD AMPLITUDE)

Mixture Ref. sample	Young's |E| [GPa]	Fatigue, Nf [n° cycles]	Load (kN) [kN]	Frequency [Hz]	Temperature [°C]
HMA	29.68	30279	0.6	5	20
	31.23	21540	0.8		
	29.91	8118	1.0		
DRY 1.5%	23.06	69641	0.6		
	23.94	19879	0.8		
	22.93	11048	1.0		
DRY 2%	20.41	110346	0.6		
	21.06	20594	0.8		
	21.09	16135	1.0		





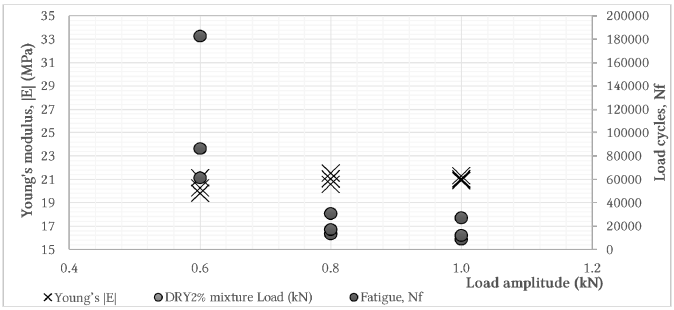


Figure 73. Young's modulus, Load amplitude and Nf cycles, Nf; (a) HMA blend; (b) DRY 1.5% mixture; (c) DRY 2% samples

In conclusion, it follows that all samples show a uniform initial modulus, being higher in the mixture without recycled HMA rubber. As the load amplitude increases, the fatigue life decreases in all mixtures besides the modulus of elasticity, being more evident in DRY blends.

The best fatigue behavior was obtained with the most elastic mixtures, i.e., DRY 2% since the rupture occurs in the long-term. The energy dissipation was lower in fatigue life (Nf) in DRY2%, despite being brittle, it withstands loads better the higher the stress amplitude at the same parity of modulus of elasticity.

Poisson's ratio was between 0.31 and 0.37, being higher in the modified mixtures with recycled rubber because of its lower value of shear modulus. In general, the HMA mixtures had a mean value of 0.35, which validates the results.

The reductions in elastic modulus were approximately 1.30% for mixtures with 1.5% CRM and as a high value of 1.45% for 2% CRM respect to the conventional HMA.

By averaging the life-to-fatigue values of each blend, regardless of the applied load, mixtures with 1.5% recycled rubber resist 1.53% more than conventional ones. Similarly, the DRY 2% withstand up to 2.20% more fatigue cycles than the conventional HMA mix.

6.10.1. Effect of frequency on Nf vs. Young's modulus

Finally, the data of the specimens reserved for the fatigue study with different frequencies were analyzed. Two samples of each mixture (HMA, DR1.5, DRY2%) were tested at the same temperature of 20 °C, a load amplitude of 1.0kN and two frequencies, 3Hz and 5Hz to fatigue cracking test.

Both specimens by mixture were chosen by selecting those related to each other regarding internal properties of the material (mass, density, the percentage of voids, VMA, VFA and final dimensions).

It was observed that the higher difference was found in the mixtures modified with 1.5% rubber, where fatigue life is tripled at 5Hz to 3Hz. The exponential regression in each of the mixtures was similar; the tendency line decreased as the number of fatigue cycles increased.

The following Tables 79-81 summarize test parameters and characteristics after manufacture. The results of fatigue and elastic modulus are compared in Figures 74-75.

TABLE 79. HMA B.4% (2 SPECIMENS FOR UGR_FACT: 1 KN; 20°C; 3-5HZ)

Ref. 20x6x6cm	Air mass [gr]	Surface dry weight [gr]	Saturated Weight [gr]	ρ_{ssd} [Kgr/m^3]	ρ_{dim} [Kgr/m^3]	Air voids	H [mm]	W [mm]	L [mm]	VMA	VFA	Load amplitude (Fatigue)
	m_1	m_3	m_2	Υ_{app}	Υ_{sedim}	[%]				(%)	(%)	(kN)
HMA_1	1865	1867	1154	2548.9	2554.6	3.25	59.66	60.88	201	12.74%	74.65%	1.0
HMA_2	1832	1835	1129	2539.5	2574.4	3.83	59.45	59.85	200	13.06%	72.56%	

2 Samples 20x6x6cm	Δf_T	Δf_L	Δf_G	Ed_T	Ed_L	G_D	Poison's ratio	Young's |E|	Fatigue, Nf	Temp.	Freq.	Duration fatigue test
	(Hz)	(Hz)	(Hz)	[GPa]	[GPa]	[GPa]	μ	[GPa]	[n° cycles)	[°C]	[Hz]	[h:min:sec]
HMA_1	4293	9200	5141	32.41	34.48	12.89	0.32	30.62	6599	20	3.0	00:35:34
HMA_2	4181	8997	5072	30.70	32.89	12.55	0.30	29.34	9671		5.0	00:31:42

TABLE 80. DRY 1.5% B.5.5% (2 SPECIMENS FOR UGR_FACT: 1 KN; 20°C; 3-5HZ)

Ref. 20x6x6cm	Air mass [gr]	Surface dry weight [gr]	Saturated Weight [gr]		ρ_{ssd} [Kgr/m^3]	ρ_{dim} [Kgr/m^3]	Air voids	H [mm]	W [mm]	L [mm]	VMA	VFA	Load amplitude (Fatigue)
	m_1	m_3	m_2		Υ_{app}	Υ_{sedim}	[%]				(%)	(%)	(kN)
$DRY_{1.5_1}$	1884	1886	1140		2511.7	2502.6	2.94	60.72	61.99	200	15.22%	83.33%	1.0
$DRY_{1.5_2}$	1848	1849	1118		2514.3	2511.5	2.84	60.68	60.63	200	15.13%	83.88%	
2 Samples 20x6x6cm	Δf_T	Δf_L	Δf_G	Ed_T	Ed_L	G_D	Poison's ratio	Young's |E|	Fatigue, Nf	Temp.	Freq.	Duration fatigue test	
	(Hz)	(Hz)	(Hz)	[GPa]	[GPa]	[GPa]	μ	[GPa]	[n° cycles)	[°C]	[Hz]	[h:min:sec]	
$DRY_{1.5_1}$	3648	7968	4560	21.93	25.51	9.88	0.26	22.38	4773	20	3.0	00:25:34	
$DRY_{1.5_2}$	3792	7952	4437	23.79	25.44	9.36	0.33	22.36	11817		5.0	00:43:26	

TABLE 81. DRY 2% B.6% (2 SPECIMENS FOR UGR_FACT: 1 KN; 20°C; 3-5HZ)

Ref. 20x6x6cm	Air mass [gr]	Surface dry weight [gr]	Saturated Weight [gr]		ρ_{ssd} [Kgr/m^3]	ρ_{dim} [Kgr/m^3]	Air voids	H [mm]	W [mm]	L [mm]	VMA	VFA	Load amplitude (Fatigue)
	m_1	m_3	m_2		Υ_{app}	Υ_{sedim}	[%]				(%)	(%)	(kN)
DRY2_1	1926	1927	1152		2482.2	2459.4	3.47	62.54	62.61	200	16.61%	81.90%	1.0
DRY2_2	1960	1962	1173		2481.2	2476.7	3.51	62.47	63.34	200	16.64%	81.70%	
2 Samples 20x6x6cm	Δf_T	Δf_L	Δf_G	Ed_T	Ed_L	G_D	Poison's ratio	Young's |E|	Fatigue, Nf	Temp.	Freq.	Duration fatigue test	
	(Hz)	(Hz)	(Hz)	[GPa]	[GPa]	[GPa]	μ	[GPa]	[n° cycles)	[°C]	[Hz]	[h:min:sec]	
DRY2_1	3456	7301	4027	18.65	21.17	7.56	0.36	18.46	10432	20	3.0	00:54:27	
DRY2_2	3648	7765	4213	20.94	23.94	8.35	0.40	21.03	17020		5.0	00:56:20	

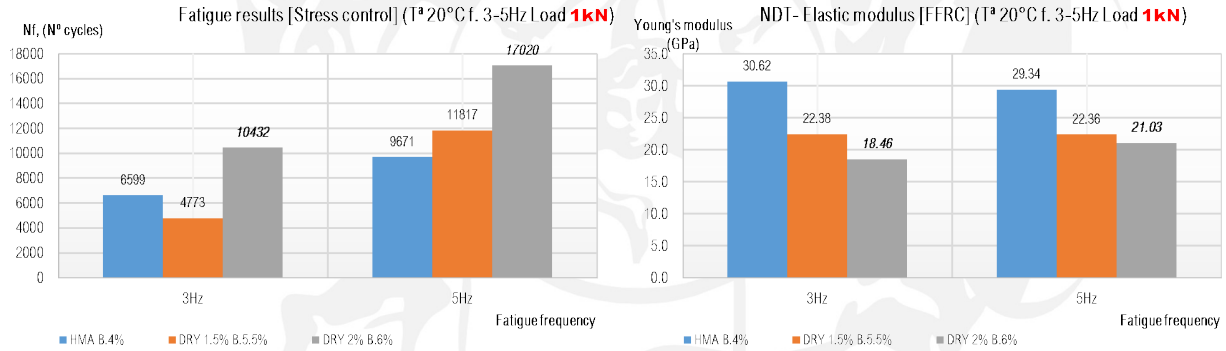


Figure 74. Comparative mixtures at 3-5 Hz at 1kN; (a) Relationship frequency and number of fatigue cycles, Nf; (b) Young's modulus vs. fatigue frequency

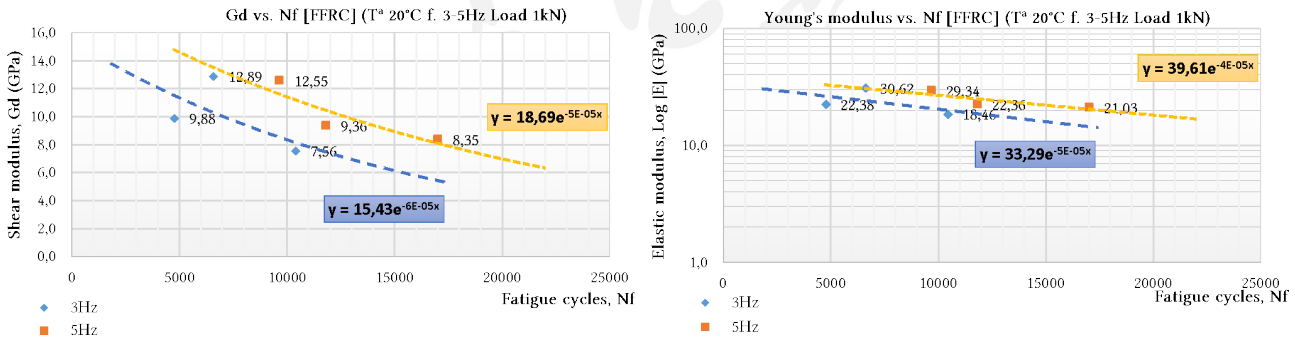


Figure 75. Comparative between 3-5 Hz at 1kN; (a) Shear modulus vs. Fatigue cycles, Nf; (b) Young's modulus vs. Fatigue cycles

The shear modulus showed the higher dispersion of results at low frequencies in the fatigue test comparing its pre-test modulus values, which corroborates that in fatigue life tests the frequency plays an important role, as the modulus decreases, the specimen behaves fracturing before, in a plastic and deformed way, due to the higher ductility.

A similar aspect is found when studying the same mixtures from the dynamic modulus of elasticity determined by FFRC. As the modulus was higher at 5Hz, the fatigue life was extended due to the elastic behavior of the material, causing the breakage to a more significant number of cycles. However, once micro-cracking of the specimen at 5Hz (high rail speed) had begun, the mixture fractured quickly in a weak way.

6.10.2. Hysteresis loops comparison

Figure 76 shows the stress-strain hysteresis obtained from controlled stress testing. If the loading and unloading curves coincide, all the energy put into the material is recovered or returned after the load is removed. If the two curves do not coincide, dissipated energy is lost in the material caused by the load cycle.

In each case, at a lower frequency, the asphalt behaves viscously, and it dissipated more energy causing the damage before in such a manner that it could not be used to return the material to its original shape.

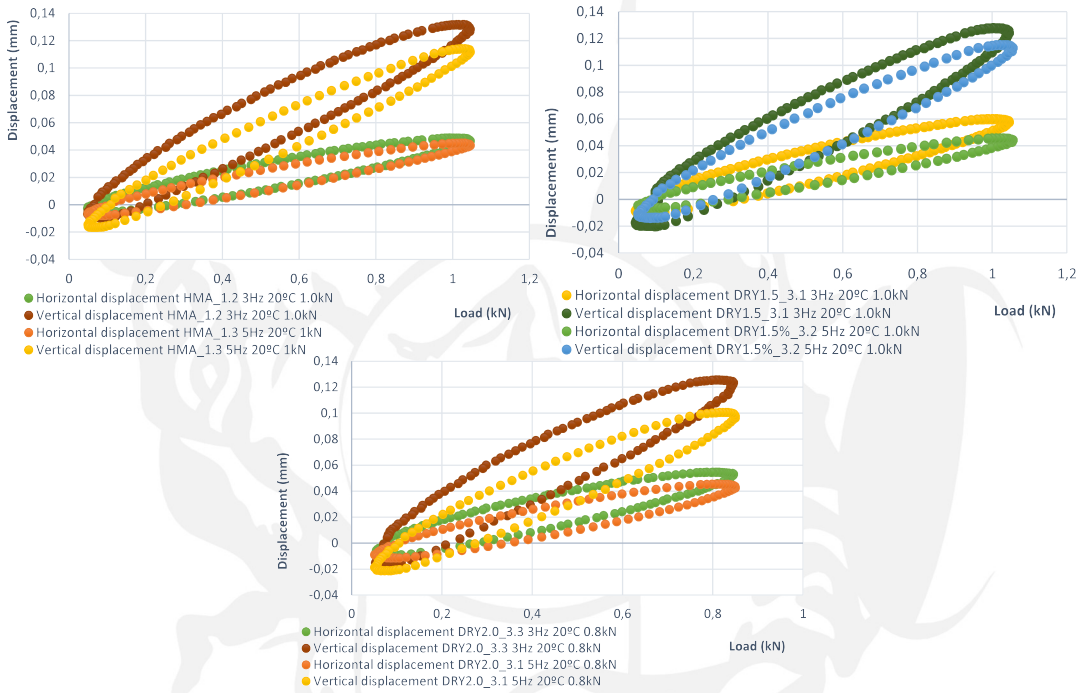


Figure 76. Stress-strain hysteresis loop for controlled stress flexural fatigue testing (a) HMA mixture comparative between 3-5 Hz at 1.0 kN; (b) DRY 1.5% f.3-5 Hz at 1.0 kN; (c) DRY 2% f. 3-5 Hz at 0.8 kN

From the final graphs of hysteresis curves, it is observed that at low frequencies all the mixtures dissipated higher energy than at 5Hz. Moreover, it occurs most clearly in the vertical displacements, associated with high energy release because the material behaves rigidly, with lower damping, experiencing high strains.

At the frequency of 3Hz, the fracture observed is ductile, more fragile due to its plasticity, responding with shorter life cycles to fatigue and experiencing rupture before. This phenomenon occurs more clearly in conventional HMA blends than rubber DRY2%.

2017

Chapter 7

CONCLUSIONS AND FUTURE LINES

PH.D. FERNANDO MARTINEZ SOTO

Chapter 7 – Conclusions

7.1. Overall conclusion

The aim of the present thesis was the optimization of bituminous sub-ballast in railways infrastructure under sustainability criteria through the reuse of SCR (scrap tire rubber), as well as the reduction of the energy consumption. So, for that and other reasons, the purpose was to develop new mixtures environmentally competitive and with an adequate mechanical behavior, in replacement of conventional materials. In that case, the primary objective has been achieved focused on the capacity of using ground rubber from discarded tires as elastic aggregate substituted in volumetric proportion inside a bituminous mixture by dry-process in the sub-ballast layer.

Mechanical performance of CRM mixtures survey has enhanced the benefits of the track, obtaining a higher capacity of dissipated energy from train passage. At first, the mechanical behavior of bituminous sub-ballast was studied, to establish a reference performance. Also, to assess the impact of the sub-ballast layer in the global behavior of the railway track, discarded tire rubber, one of the generic types of asphalt additives, has been promoted and used to reduce the problems of damage to the rail sub-ballast during the life cycle.

In this context, the use of HMA to replace granular sub-ballast is a solution that has great potential for bearing capacity and impermeability. Simultaneously the thickness of the layer is reduced to 12-15 cm, compared to the 22-25 cm used in the conventional granular design.

In general, it can be stated that the evaluation of the behavior of hot asphalt (HMA) with recycled rubber as an additive has been optimal due to the laboratory performance of conventional mixtures (standard hot mix asphalt) and mixtures modified with rubber added by the dry process (DRY). This work aimed to fundamentally identify the advantages of the addition of crumb rubber (susceptibility to temperature, elastic behavior, binder viscosity reaction, the optimal amount of rubber substituted, and a satisfactory protocol of mix-design by dry technology).

The results obtained in the laboratory with the design of different bituminous mixtures (HMA_DRY) and the use of varying compaction techniques (Volumetric mix-design, Marshall, and Asphalt Slab Roller Compactor), allowed considering their proper use for the conventional sub-ballast.

The optimization of the conventional bituminous mixture, HMA, using the gyratory compactor (SGC), Marshall hammer (indirect tensile tests and resistance to water sensitivity), and the subsequent adaptation to mixtures with the roller compactor (ASRC), simulating the real conditions on site, have demonstrated that the use of asphalt inside the sub-ballast is efficient.

Subsequently, three types of rubberized mixtures have been studied and mechanically characterized to fatigue-cracking (dissipated energy approach), and determination of the elastic-dynamic modulus by various techniques analyzed in the methodology chapter.

Finally, suitable values are obtained regarding the internal composition of the material and its mechanical performance, so that the mixtures by the dry process allow their use by favoring the damping of vibrations and noise generated in the railway section. For this reason, rubberized asphalt presents a high potential for their application as bituminous sub-ballast in railway tracks.

7.2. Conclusions of the mix design and methodology "SupeRail"

Parallel to the design of the mixtures using the Superpave methodology, there is a need to analyze the stresses and structural behavior of the sub-ballast layer to adapt the volumetric compaction to the railway sector, until then, exclusively for roads. A common purpose arises during the mix-design phase, based on a comparison of stress levels to the same degree (similarity in depth of layers) between base-course for roads and sub-ballast layer (highways vs. railway trackbed). Designs and axle loadings were studied and developed with computational software to predict the analytical procedure that fits best with the mix-design of rubberized

mixtures by dry technology. As an added factor to the innovative development of the thesis, the study was presented the AASHTO mechanistic-empirical pavement design approach to railways. The use of Kenpave-Kentrack to calculate essential strain and deformation parameters resulting in fundamental for the definition of a Railway Equivalent Standard Axle Load (RESAL) and a design number of gyrations for use in the SGC.

Thus, in Chapter 5, a new method has been confirmed that based on the rail traffic-spectrum and the predictive model of temperatures in multilayer systems, an analogy with the present stresses (road-railways) was found. It was determined the exact number of gyrations that we must be imposed to the SGC depending on the case study (climatic conditions and high-speed rail-lines). Following the Italian regulations, the case study of the railway traffic of Sicily is provided. Applying the proposed methodology were calculated the standard axle-load value of 16 tons, and a number of 102 turns for the SGC, in the case of a conventional HMA for a level III Superpave. New terminology is added in this thesis, the result of serial publications, such as "SupeRail" and "RESAL" (Railway Equivalent Standard Axle Load).

The Volumetric mix design approach is applied successfully to the railway domain for the different load configuration of the rail track system.

Subsequently, different mixtures were made with rubber in the laboratory based on the parameters of said structural methodology. Due to the pathologies derived from the energy accumulated by the compression rubber, it was observed that the effect of swelling and distribution of air gaps did not allow the manufacture of an optimum mixture for the sub-ballast.

Again, we proceed to an empirical method based on preliminary calculations and results with HMA and DRY 1.5% mixtures to provide a consistent manufacturing method (step-by-step protocol) and a "beta"[1] factor to increase the exact number of turns of the compactor depending on the percentage of rubber added.

The method offers improvements in the DRY mixtures, giving optimum values of internal composition, rubber-bitumen ratio, and thickness of 12cm according to the designed sub-ballast.

HMA rubberized mixtures by dry process is an optimal substitute for granular sub-ballast. In dry technology, we observed that the use of granulated or ground rubber instead of only powder crumb-rubber is a better solution that enhances the rubber reaction with bitumen at high temperatures.

Despite the problems of swelling and rebound of the mixtures with rubber in the post-compaction phase, it has been observed that following the manufacturing protocol suggested in this thesis; the blends are optimized for their implementation, reaching higher performance than conventional blends.

By the results obtained, the following conclusions can be drawn:

- Temperature has different reactions to swelling if rubber constitution does not change. If the temperature increases during mixing, the subsequent swelling effect increases because the rubber-bitumen composition has already occurred, because of solvent input into the network. Higher mixing energy would be required to maintain the molecular structure.
- If the constitution of rubber is changed at high temperature during the reaction, the maximum amount of swelling will be increased too and, the specimen will be weakened as the effect will cause an increase in height during post-compaction, increasing the percentage of internal voids.
- Thin or small particles of rubber will swell quickly than thicker particles. The rate of swelling is faster for smaller particles, and the maximum amount of swelling is lower for bigger particles.
- The dust/asphalt ratio and the filler content, are parameters that also influence on swelling with the effect of rubber-liquid interaction. Excessive dust or filler reduces durability and asphalt thickness film, which result in unstable mixes.
- The penetration rate of the solvent in rubber increases with decreasing viscosity of the bitumen and, this fact also depends on the degree of concentration present in the mixture.

[1] In rubberized dry mixtures, each blend has achieved a particular Ndes characteristic of the empirical factor “beta” that satisfied the volumetric mix-design requirements.

- The desired asphalt is a DRY1.5% with target air voids of 1 to 3 percent, which will quickly compact to <4% in-place air voids. It has been achieved by specifying a dense-graded mixture with a maximum aggregate size of 25.4 to 37.5mm and the asphalt binder content increased by about 0.5 percent above that considered optimum for highway applications.
- Rutting is not concerned in the insulated trackbed environment.
- The specified thickness of the superimposed ballast is 250 to 350 mm. The optimal sub-ballast solution is the "underlayment" since it is placed on a layer, typically 127-152.4 mm thick, within the structure of the track between the ballast and the subgrade.
- With hot mixing, temperatures of not less than 150 ÷ 180°C are necessary to complete the drying of the aggregates to prevent the residual moisture from causing loss of adhesion between bitumen and aggregates in the medium to long-term. Also, the high temperatures, which reduce the viscosity of the bitumen, making it possible to complete the coating of the aggregates and give the mixture the appropriate degree of workability necessary for subsequent compaction operations.
- The proposed empirical approach for the optimization of the design of the mixture made with gyratory compactor of DRY blends is considered helpful in adjusting the required N_{des} set by the Volumetric mix-design to compact rubber-aggregate asphalt blends.
- Considering a percentage of internal voids of 3%, the bitumen content must be increased by around two decimals of the binder concerning the conventional bitumen, as well as the number of gyrations, N_{des}, applying a factor of 1.2 to 1.48 for each 0.5% of rubber added (Table 1).

TABLE 1. RESULTS FOR ALL MIXTURES

Mixture	"Beta factor"	N_{des}*
HMA	1	102
DRY 1.5%	1.48	152
DRY 2%	1.77	181
DRY 3%	2.85	291

However, additional work is needed to verify the robustness of the methodology using other materials and unusual sizes of recycled rubber. Also, the procedure based on experimental approximations still lacks strong aspects of turning it into a widely accepted methodology. In fact, this thesis has considered a simplified system of a bituminous matrix (aggregates, bitumen, air voids and rubber) and has been considered the compression as the determining factor that is exerted in compaction. To establish a repeatable laboratory procedure is necessary to control all the variables to keep the mixing and compaction conditions consistent.

Even if this methodology represents the first step towards a new SCR blends design approach, it provides promising results in estimating the final void content after thermal stabilization and curing in mixtures of asphalt with rubber as we have seen during the development of this chapter.

A key point was the fact that the binder exerts a high influence on the final mechanical response of all the mixtures studied. The service life of asphalt pavements will directly depend on the type of binder used, and thus an adequate choice is crucial to constructing more durable layers. Using rubber is a sustainable solution that ensures consumption of large quantities of these waste materials.

7.3. Conclusions from Mechanical characterization

After the optimization of the mix-design by Volumetric gyratory compactor and Roller slabs, the mechanical behavior of HMA_DRY bituminous sub-ballast was studied, to establish a reference performance. This study highlights that the primary factor in the development of sub-ballast layer pathology is the fatigue cracking process associated with the passage of high-speed rail traffic and temperature gradients.

Through the investigation of different bituminous mixtures, excellent fatigue results on dry-rubberized mixtures (DRY2%) have been obtained by modifying parameters such as:

- Granulometry of the rubber-aggregates;
- Mix-compaction temperatures according to the equi-viscous T^a of the binder;
- Levels of traffic-spectrum (loads in RESALs), and (predictive temperature model) conditions;
- Frequency of step of 5Hz (v.250km / h) and loads of 0.6kN.

This mechanical study has also been associated with the dissipative energy of the HMA_DRY sub-ballast bituminous layer in question, to build a complete picture of its physical and performance characteristics. It has shown that the use of bituminous mixtures modified with recycled rubber to 2% by weight of aggregates in volumetric proportion, allows obtaining materials capable of offering a fatigue-cracking resistance higher than those made with conventional bitumen. According to this fact, some relevant conclusions are established:

- Rubberized sub-ballast could reduce the track settlement due to an increase in the stiffness of the substructure. Also, the dry mixture presented higher stress dissipation during the UGR_FACT test, which allows for more excellent protection of the track layers against the loads transmitted by trains.
- Under low frequencies (3 Hz), a decline in the cracking resistance of conventional bituminous sub-ballast was observed. Although, this finding should, therefore, be considered when applying this type of sub-ballast under adverse temperature conditions.
- The use of HMA can improve waterproofing and filter properties, preventing the contamination of both the sub-structure and the ballast layer while also offering a satisfactory coefficient of permeability.
- When tested under the standard temperatures of service expected for sub-ballast in railways tracks (20°C), the rubberized solutions presented resistance to plastic deformations profoundly better than conventional HMA sub-ballast.
- The modification of the track section caused by varying the underlayment configuration exerted the higher influence of the stiffness of the rail track.
- About mechanical behavior, the proposed sustainable alternative offer similar properties to those presented by the traditional solution but better performance to long-term.
- Regarding strength and stiffness modulus, it was found that the use of the DRY 1.5% blends induce an elastic behavior in asphalt mixes and retards the crack initiation process.
- The optimal DRY2% served to improve strength and stiffness modulus when it is compared to the traditional hot bituminous sub-ballast without crumb rubber.
- Adding at least a 2% of ground-fine rubber proportion to the bituminous sub-ballast could enhance its resistance to railway loads and thus reduced plastic deformations.
- Since the sub-ballast layer is not directly exposed to the traffic load, the problem of material losses or disintegration could be reduced.
- Although the strength of the bituminous materials and its capacity to dissipate stress are reduced with an increase in temperature or decrease in frequency, all types of bituminous mixtures presented higher fatigue resistance regarding a bibliography review.
- It has been highlighted that the DRY 2% rubberized asphalt manufactured by dry process offered a suitable long-term performance and registered higher values of load resistance transmitted by trains respect the HMA-DRY1.5% mixtures.

7.4. Overall rating

Improved blends with CRM has been achieved by substitution of the aggregates in volumetric proportion adjusting the grading curve for fine/coarse aggregates and considering the new Volumetric mix-design approach.

From the results obtained, it is evident that the best solution was the rubberized bituminous sub-ballast manufactured by a dry process with a weight of 2% of rubber of the total weight of the aggregates (4.2% by volumetric substitution) and, with a binder content of 6%. The other mixes were suitable as a bituminous sub-

ballast since it can increase the strength of the tracks and pursue at the same time sustainable development through the reduction of energy consumption.

7.5. Future lines of research

During the elaboration of this doctoral thesis, in which sustainable bituminous sub-ballast have been developed through the reuse of waste material, new lines of research have emerged as future studies to complete the sustainable bituminous sub-ballast optimization:

- Further studies are needed under a range of failure modes expected for asphalt materials, including, resistance to low-temperature cracking, which is a fundamental parameter in asphalt materials since it is of crucial importance in protecting the substructure as well as the response of full scale.
- Assess the fatigue law of the sustainable bituminous sub-ballast under several service conditions such as different temperature or humidity, analyzing the other failure distress: permanent deformation.
- Based on the technologies studied in this doctoral thesis, one of the future aims will be the evaluation of the life cycle assessment (LCA).
- It would also be of interest to analyze the mechanical response of the sustainable bituminous sub-ballast in a trial section in a high-speed line to evaluate the long-term behavior of the sub-bituminous ballast.
- It is proposed as a future line to carry out full-studies to determine the effect of aging of the binder, the temperature on the behavior of rubber and the mutual interactions between rubber and bitumen.
- Develop water susceptibility tests in rubber mixtures, indirect tensile strength, and fatigue tests after long rest periods for the optimized blends in this thesis.

2017

Bibliography

“APA” FORMAT CITATION

PH.D. FERNANDO MARTÍNEZ SOTO

References

[1] Abdelrahman, M., & Carpenter, S. (1999). Mechanism of interaction of asphalt cement with crumb rubber modifier. Transportation Research Record: Journal of the Transportation Research Board, (1661), 106-113.

[2] Abdul Hassan (2006). "Performance of Hot Mix Asphalt Using Fine Crumb Rubber", Phd Civil Engineering Malaysia, 2006/2007.

[3] Adaska, W. S. (2006). Roller-compacted concrete (RCC). In Significance of Tests and Properties of Concrete and Concrete-making Materials. ASTM International.

[4] Advanced Asphalt Technologies, LLC. (2011). A Manual for Design of Hot Mix Asphalt with Commentary (Vol. 673). Transportation Research Board.

[5] Agarwal, M. M., & Miglani, K. K. (2010). Global Heavy Haul Experience and Indian Railways. Article published in RITES Journal, 19-1.

[6] Airey, G. D., Hunter, A. E., & Collop, A. C. (2008). The effect of asphalt mixture gradation and compaction energy on aggregate degradation. Construction and Building Materials, 22(5), 972-980.

[7] Airey, G. D., Rahman, M. M. and Collop, A. C. (2003). "Absorption of Bitumen into Crumb Rubber Using the Basket Drainage Method." The International Journal of Pavement Engineering, Vol. 4(2), pp. 105-119.

[8] Airey, G. D., Singleton, T. M., & Collop, A. C. (2002). Properties of polymer modified bitumen after the rubber-bitumen interaction. Journal of materials in civil engineering, 14(4), 344-354.

[9] Aisien, F. A., Hymore, F. K., & Ebewele, R. O. (2006). Application of ground scrap tyre rubbers in asphalt concrete pavements.

[10] Alarcón D.B., (2005). "Modelo Integrado de Valor para Estructuras Sostenibles". Thesis, Universitat Politècnica de Catalunya, Escola Tècnica Superior D'Enginyers de Camins, Canals i Ports, Spain.

[11] Albalat, S. A., Domingo, L. M., Sanchis, I. V., Herráiz, J. I. R., & Segarra, A. V. (2011). Crumb Rubber Modified Bitumen for the sub-ballast layer. In Proceedings, 9 the World Congress on Railway Research, Lille, France.

[12] Albalat, S. A., Lopez, J. A., Prieto, J. M. B., Melero, J. M. M., Herraiz, J. I. R., Sanchis, I. V. (2012). Bituminous material and its use for the construction of sub-ballast. U.S. Patent Application N. 13/505,405.

[13] Al-Khateeb, G. G. (2016). Conceptualizing the asphalt film thickness to investigate the Superpave VMA criteria. International Journal of Pavement Engineering, 1-9.

[14] Al-Mosawe, H. M., Thom, N. H., Airey, G. D., & Al-Bayati, A. H. (2016). Effect of different variables on asphalt mechanical properties. In Functional Pavement Design: Proceedings of the 4th Chinese-European Workshop on Functional Pavement Design (4th CEW 2016, Delft, The Netherlands, 29 June-1 July 2016) (p. 79). CRC Press.

[15] Amirjanov, A., & Sobolev, K. (2008). Optimization of a computer simulation model for packing of concrete aggregates. Particulate Science and Technology, 26(4), 380-395.

[16] Amirkhanian, S. J. L. S. N., & Shatanawi, K. Effect of Crumb Rubber on the Aging of Asphalt Binders.

[17] Anderson, D. A. (1996). Influence of fines on performance of asphalt concrete mixtures. In Proceedings of the fourth annual aggregates symposium, Atlanta, GA.

[18] Andersson, A., O'Connor, A., & Karoumi, R. (2015). Passive and adaptive damping systems for vibration mitigation and increased fatigue service life of a tied arch railway bridge. Computer-Aided Civil and Infrastructure Engineering, 30(9), 748-757.

[19] Andrei, D., Witczak, M. W., & Mirza, M. W. (2005). Development of Revised Predictive Model for the Dynamic Complex Modulus of Asphalt Mixtures (NCHRP 1-37A). University of Maryland, College Park, Maryland..

[20] Arabani, M., Mirabdolazimi, S. M., & Sasani, A. R. (2010). The effect of waste tire thread mesh on the dynamic behavior of asphalt mixtures. Construction and Building Materials, 24(6), 1060-1068.

[21] Arnold, Terry. "Roller-Compacted Concrete Density: Principles and Practices." Portland Cement Association (2004).

[22] Aschenbrener, T. B., & McGennis, R. B. (1994). Investigation of AASHTO T 283 To Predict the Stripping Performance of Pavements in Colorado. Transportation Research Record, 26-26.

[23] Asphalt Hot Mixer (2018). Retrieved from http://www.kullumanalitourpackage.in/1162165960.html

[24] Asphalt Institute. (1998) HMA Trackbeds – Hot Mix Asphalt for Quality Railroad and Transit Trackbeds. Information Series 137, 10 pages.

[25] Assessment, M. E. (2005). Ecosystems and human well-being: wetlands and water. World resources institute, Washington, DC, 5.

[26] Attia, M., & Abdelrahman, M. (2009). Enhancing the performance of crumb rubber-modified binders through varying the interaction conditions. International Journal of Pavement Engineering, 10(6), 423-434.

[27] Ayar, P., Moreno-Navarro, F., & Rubio-Gámez, M. C. (2016). The healing capability of asphalt pavements: a state of the art review. Journal of Cleaner Production, 113, 28-40.

[28] Azari, H., Al-Khateeb, G., Shenoy, A., & Gibson, N. (2007). Comparison of Simple Performance Test| E*| of Accelerated Loading Facility Mixtures and Prediction| E*|: Use of NCHRP 1-37A and Witczak's New Equations. Transportation Research Record: Journal of the Transportation Research Board, (1998), 1-9.

[29] Baburamani, Pud. (1999). Asphalt fatigue life prediction models: a literature review. No. ARR 334.

[30] Bahia, H. U., & Davies, R. (1994). Effect of crumb rubber modifiers (CRM) on performance-related properties of asphalt binders. Asphalt paving technology, 63, 414-414.
[31] Bahia, H. U., & Davies, R. (1995). Factors controlling the effect of crumb rubber on critical properties of asphalt binders (with discussion). Journal of the Association of Asphalt paving Technologists, 64.
[32] Bahia, H. U., Coenen, A., & Tabatabaee, N. (2013). Mixture design and compaction. In Advances in Interlaboratory Testing and Evaluation of Bituminous Materials (pp. 85-142). Springer, Dordrecht.
[33] Bahia, H. U., Hanson, D. I., Zeng, M., Zhai, H., Khatri, M. A., & Anderson, R. M. (2001). Characterization of modified asphalt binders in Superpave mix design (No. Project 9-10 FY'96).
[34] Bairgi, B. K. (2015). Viability assessment of the use of ground tire rubber in asphalt pavements. Arkansas State University.
[35] Banerjee, A., Aguiar-Moya, J., & Prozzi, J. (2009). Calibration of mechanistic-empirical pavement design guide permanent deformation models: Texas experience with long-term pavement performance. Transportation Research Record: Journal of the Transportation Research Board, (2094), 12-20.
[36] Barber, E. S. (1957). Calculation of maximum pavement temperatures from weather reports. Highway Research Board Bulletin, (168).
[37] Bardesi A., (2010). "Introducción a las mezclas bituminosas." Curso de Mezclas Bituminosas: dosificación, fabricación, puesta en obra y control de calidad, Intevia, Barcelona.
[38] Bari, J. (2005). Development of a new revised version of the Witczak E* predictive models for hot mix asphalt mixtures (Doctoral dissertation, Arizona State University).
[39] Bari, J., & Witczak, M. (2006). Development of a newly revised version of the Witczak E* predictive model for hot mix asphalt mixtures (with discussion). Journal of the Association of Asphalt Paving Technologists, 75.
[40] Bassani, M.; Santagata, E.; De Palma, C. (2001). "Il metodo dei vuoti: un approccio innovativo al proporzionamento volumetrico dei conglomerati bituminosi" – XI Convegno Nazionale SIIV, Verona.
[41] Bastin R., (2005). "Development of German non-ballasted track forms." ICE. UK.
[42] Bauchkar, SD, and HS Chore. "Roller Compacted Concrete: A Litrature Review." (2012).
[43] Baumgardner, G. L. (2015). Characterization and implementation of ground tire rubber as post-consumer polymers for asphalt concrete. Mississippi State University.
[44] Becker Y, Mendez MP, Rodriguez Y (2001). Polymer modified asphalt. Vision Tecnologica, 9(1): 39-50.
[45] Berggren E., (2009). "Railway Track Stiffness Dynamic Measurements and Evaluation for Efficient Maintenance." Stockholm: Royal Institute of Technology (PhD thesis, Report TRITA AVE 2009:17, Aeronautical and Vehicle Engineering)
[46] Berggren E.G., Jahlénius Å., Bengtsson B.-E., (2002). "Continuous Track Stiffness Measurement: An Effective Method to Investigate the Structural Conditions of the Track." In Proceedings from Railway Engineering. 3-4 July, London, UK.
[47] Birgisson, B., & Ruth, B. E. (2001). Development of tentative guidelines for the selection of aggregate gradations for hot-mix asphalt. In Aggregate Contribution to Hot Mix Asphalt (HMA) Performance. ASTM International.
[48] Blankenship, P. B. (1993). "Gyratory Compaction Characteristics: Relation to Service Densities of Asphalt Mixtures,"Master's Thesis,University of Kentucky, Lexington.
[49] Blasón, S., Correia, J. A. F. O., De Jesus, A. M., Calçada, R. A., & Fernández-Canteli, A. (2016). A probabilistic analysis of Miner's law for different loading conditions. Struct. Eng. Mech, 60(1), 71-90.
[50] Bloom, E. F., Ponte, K. D., Natarajan, B. M., Ahlman, A. P., Edil, T. B., & Whited, G. (2016). State DOT Life Cycle Benefits of Recycled Material in Road Construction. In Geo-Chicago 2016 (pp. 693-703).
[51] Bonnaure, F., Gravois, A., & Udron, J. (1980). A new method for predicting the fatigue life of bituminous mixes. In Association of Asphalt Paving Technologists Proceedings (Vol. 49).
[52] Bonnot, J., "Asphalt Aggregate Mixtures," Transportation Research Record 1096: Asphalt Analysis, Sulfur,Mixes, and Seal Coats, Transportation Research Board, National Research Council, 1986.
[53] Brotman, I., Crist, M., & Gaul, J. (2007). Roller compacted concrete pavement: properties, design, and construction. In Soil and Material Inputs for Mechanistic-Empirical Pavement Design (pp. 1-10).
[54] Brown S.F., Kwan J., Thom N.H., (2007). "Identifying the key parameters that influence geogrid reinforcement of railway ballast." Geotextiles and Geomembranes, 25, pp 326-335.
[55] Brown, D., Jared, D., Jones, C., & Watson, D. (1997). Georgia's experience with crumb rubber in hot-mix asphalt. Transportation Research Record: Journal of the Transportation Research Board, (1583), 45-51.
[56] Brown, E. R., and M. S. Buchanan (1999). NCHRP Research Results Digest 237: Superpave Gyratory Compaction Guidelines, Transportation Research Board, National Research Council.
[57] Brown, E. R., and R. B. Mallick, (1998). An Initial Evaluation for Ndesign Superpave Gyratory Compactor. Journal of the Association of Asphalt Paving Technologists,Vol. 67.
[58] Brown, S. F., & Pell, P. S. (1967). An experimental investigation of the stresses, strains and deflections in a layered pavement structure subjected to dynamic loads. In Intl Conf Struct Design Asphalt Pvmts.
[59] Brundtland, G. H., & Mansour, K. The World Commission on Environment and Development (WCED). 1987. Our common future, 2010.
[60] Brunner, P. H., & Rechberger, H. (2016). Handbook of material flow analysis: For environmental, resource, and waste engineers. CRC Press.

[61] Buchanan MS, Brown ER. (2001). Effect of superpave gyratory compactor type on compacted hot-mix asphalt density. Transportation Research Record, No. 1761 pp. 50–60.
[62] Buonanno A., D'andrea Y.A., (2003). "Asphalt with rubber grains as anti-vibrating sub-ballast." Proceedings of the railway engineering 2003, April–May 2003, London.
[63] Buonanno, A., Mele, R. (2000). The use of bituminous mix sub-ballast in the Italian State Railways. In Proceedings of the paper submitted for review at 2nd Eurasphalt and Eurobitume congress, 20-22 September 2000, Barcelona, Spain.
[64] Buonanno, R. Mele, (2000). Il sub-ballast in conglomerato bituminoso nelle Ferrovie italiane. Convegno Infravia Sulle infrastrutture del trasporto terrestre, Verona 10-13 maggio 2000, quarta sessione Ambiente e infrastrutture: alternative razionali nella gestione dell'esistente, 11.5.2000, volume 1.
[65] Burmister, D.M., (1943). The Theory of Stresses and Displacements in Layered System and Applications to the Design of Airport Runways, Proceedings, Highway Research Board, Vol.23, 1943, pp.126-144.
[66] Buttlar, W. G., & Harrell, M. (2000). Development of end-result and performance-related specifications for asphalt pavement construction in Illinois. Crossroads, 195-202.
[67] Button, J.W., D. N. Little,V. Jagadam, and O. J. Pendleton, (1994). "Correlation of Selected Laboratory Compaction Methods with Field Compaction," Transportation Research Record 1454: AsphaltmMixture Design and Performance, Transportation Research Board, National Research Council.
[68] Cai, Z., Raymond, G. P., & Bathurst, R. J. (1994). Estimate of static track modulus using elastic foundation models. Transportation Research Record, 1470, 65.
[69] Calderon, A. E. U. (2013). Development of a Mechanistic-Based Approach to Evaluate Critical Conditions of Hot Mix Asphalt Mixtures. University of Nevada, Reno.
[70] Caltrans (2011) Performance survey of rubberized hot mix asphalt projects. (California Department of Transportation, 1120 N. Street Sacramento, CA 95814.
[71] Caltrans (2005). Use of scrap tire rubber. State of the technology and best practices. State of California Department of Transportation, Sacramento, CA, USA.
[72] Cao, W. (2007). Study on properties of recycled tire rubber modified asphalt mixtures using dry process. Construction and Building Materials, 21(5), 1011-1015.
[73] Cardona, D. R., Di Benedetto, H., Sauzeat, C., Calon, N., & Saussine, G. (2016). Use of a bituminous mixture layer in high-speed line trackbeds. Construction and Building Materials, 125, 398-407.
[74] Cardona, J., Arcos, R., Botello, F., Casado, J. A., & Conrado, J. (2016). End-of-life tyres prove their worth in sub-ballast applications. International Railway Journal, 56(8).
[75] Caro, S., Masad, E., Bhasin, A., & Little, D. N. (2008). Moisture susceptibility of asphalt mixtures, Part 1: mechanisms. International Journal of Pavement Engineering, 9(2), 81-98.
[76] Carpenter, S. H., & Pavements, E. L. H. (2006). Fatigue performance of IDOT Mixtures, Urbana, 51, 61801.
[77] Carpenter, S. H., & Shen, S. (2006). Dissipated energy approach to study hot-mix asphalt healing in fatigue. Transportation Research Record: Journal of the Transportation Research Board, 1970(1), 178-185.
[78] Carpenter, S., Ghuzlan, K., & Shen, S. (2003). Fatigue endurance limit for highway and airport pavements. Transportation Research Record: Journal of the Transportation Research Board, (1832), 131-138.
[79] Carrascal I., Casad, J.A., Diego S., Polanco, J.A., (2014). "Comportamiento mecánico frente a esfuerzos dinámicos de manta elastomérica para la atenuación de vibraciones en ferrocarriles". Available online: http://life2010-recytrack.com/docs/comportamientomecanico.pdf
[80] Carvalho, R., & Schwartz, C. (2006). Comparisons of flexible pavement designs: AASHTO empirical versus NCHRP Project 1-37A mechanistic-empirical. Transportation Research Record: Journal of the Transportation Research Board, (1947), 167-174.
[81] Celard, A. C. (1976). Il conglomerato bituminoso come nuova soluzione per lo strato di sottoballast nelle linee ferroviarie-Dimensionamento con metodo dinamico. Ingegneria Ferroviaria.
[82] Celauro C., Di Francisca A. (2003). L'impiego di granulato di gomma da pneumatici usati in tecnica stradale. Strade & Autostrade n. 5.
[83] Celauro, C., Di Francisca (2003). Studio sperimentale sull'impiego di CMR (Crumb Rubber Modifier) nei conglomerati bituminosi secondo processo dry, XIII Convegno Nazionale S.I.I.V. Padova 2003.
[84] Chandak, P. G., Tapase, A. B., Sayyed, S. S., & Attar, A. C. (2017, July). A State-of-the-Art Review of Different Conditions Influencing the Behavioral Aspects of Flexible Pavement. In International Congress and Exhibition" Sustainable Civil Infrastructures: Innovative Infrastructure Geotechnology" (pp. 300-312). Springer, Cham.
[85] Chang, C. W. Adegoke, E. T. Selig, (1980). "GEOTRACK Model for Railroad Track Performance," Journal ofthe Geotechnical Fngineering Division, American Society of Civil Engineers, Vol. 106, NO. GT11,1201-1218.
[86] Chen, Q., Niu, X., Zhang, Q., & Cheng, Y. (2015). Railway track irregularity measuring by GNSS/INS integration. Navigation, 62(1), 83-93.
[87] Christiansen Jr, D. W. (2010). Supporting Materials for NCHRP Report 673 (No. NCHRP Project 9-33).
[88] Christopher, W. J., Crawford, F. J., Edward, T. H., Adock, M., Delaney, E. P., & Freer, H. (2011). A Manual for Design of Hot Mix Asphalt with Commentary. Report NCHRP, 673.
[89] Claudy, P., Letoffe, J. M., King, G. N., & Plancke, J. P. (1992). Characterization of asphalts cements by thermomicroscopy and differential scanning calorimetry: Correlation to classic physical properties. Fuel science & technology international, 10(4-6), 735-765.

[90] Collop, A. C., Sewell, A. J., & Thom, N. H. (2004). Laboratory assessment of the resistance to crack propagation in high-stiffness asphaltic materials. Proceedings of the Institution of Mechanical Engineers, Part L: Journal of Materials: Design and Applications, 218(1), 55-66.
[91] Colorado Asphalt Pavement Association. (2000). Guideline for the Design and Use of Asphalt Pavements for Colorado Roadways. CAPA. Englewood, CO.
[92] Cominsky, R. J., Huber, G. A., Kennedy, T. W., & Anderson, M. (1994). The superpave mix design manual for new construction and overlays (No. SHRP-A-407). Washington, DC: Strategic Highway Research Program.
[93] Cominsky, R., Leahy, R. B., & Harrigan, E. T. (1994). Level one mix design: Materials selection, compaction, and conditioning (No. SHRP-A-408).
[94] Cong, P., Xun, P., Xing, M., & Chen, S. (2013). Investigation of asphalt binder containing various crumb rubbers and asphalts. Construction and Building Materials, 40, 632-641.
[95] Connolly, D., Giannopoulos, A., & Forde, M. C. (2013). Numerical modelling of ground borne vibrations from high-speed rail lines on embankments. Soil Dynamics and Earthquake Engineering, 46, 13-19.
[96] Connors, M., & Director, A. P. (2017). Preparation of the Implementation Plan of AASHTO Mechanistic-Empirical Pavement Design Guide (M-EPDG) in Connecticut: Phase II–Expanded Sensitivity Analysis and Validation with Pavement Management Data.
[97] Consuerga, A., Little, D. N., Quintus, H. V. and Burati, J., (1992). "Comparative Evaluation of Laboratory Compaction Devices Based on their Ability to Produce Mixtures with Engineering Properties Similar to those Produced in the Field", Transportation Research Record, TRB National Research Council, Washington, U.S.A., Vol. 1228, 80-87.
[98] Conti Puorger, A., Celard, B., Pisani, M., & Zocca, A. (1976). Il conglomerato bituminoso come nuova soluzione per lo strato di sottoballast nelle linee ferroviarie Dimensionamento con metodo dinamico. Ingegneria ferroviaria , Aprile.
[99] Cooley Jr, L. A., James, R. S., & Buchanan, M. S. (2002). Development of Mix design criteria for 4.75 mm superpave mixes (No. NCAT Report No. 2002-04).
[100] Crispino M., Festa B., Giannattasio P. (1998). "Valutazione delle temperature della sovrastruttura ferroviaria per alta velocità attraverso una sperimentazione di laboratorio". CIFI congress: la tecnologia del trasporto su ferro e l'orientamento al mercato, Napoli.
[101] Crispino, M. (2001). Valutazione delle temperature in esercizio del subballast ferroviario. Ing.Ferroviaria, 1-2.
[102] Crispino, M., D'Apuzzo, M., & Lamberti, R. (2003). Development and Experimental Validation of a Prediction Model to Assess Railway Traffic Induced Vibrations. In EURONOISE 2003, 5th European conference on Noise Control (pp. 1-10).
[103] Crockford W.W., (1995). "Recycling crumb rubber modified asphalt pavements." S.l.: Texas Transportation Institute. Report FHWA/TX-95/1333-1F.
[104] D. Orlandi, (1985). "Perché un subballast", Ingegneria Ferroviaria, pp. 447-453.
[105] D'Andrea A., Buonanno A. (2003). Asphalt with rubber grains as anti-vibrating sub-ballast Proceedings of RAILWAY ENGINEERING. Londra, 27 April 2003. London. Edinburgh: Engineering Technics Press. ISBN 0-947644-51-2.
[106] D'Andrea A., Loisi T., Urbani. L. (2006). Fenomeni vibratori da traffico stradale in presenza di strati con granulato di gomma. SIIV 2006. Cosenza. ISBN 88-7458-050-9.
[107] D'Andrea A., Mariotti T., (2001). Conglomerati bituminosi speciali con granulato di gomma. Rassegna del Bitume n. 39.
[108] D'Andrea A., Shulmann V. (2007). Recycled Tyre Materials in Roads and Civil Engineering. Edizioni Argo – Roma 2007.
[109] D'Andrea, (1999) Prototype of a low noise asphalt. 1° International colloquium on vehicle tyre road interaction. Roma.
[110] D'Andrea, A., Loprencipe, G., & Xhixha, E. (2012). Vibration induced by rail traffic: evaluation of attenuation properties in a bituminous sub-ballast layer. Procedia-Social, 53, 245-255.
[111] D'Andrea, N. Fiore. (2003). Fatigue life of asphalt concrete with rubber grains. 2003. In Fatigue Damage of Materials – Experiment and analysis. (pp. 65-74). ISBN: 1-85312-979-8: WITpress (UK).
[112] D'Andrea., L. Urbani, G. Bonin. (2004). Traffic Vibration Damping With Innovative Materials: Development And Calibration Of a Simulation Model, II Congresso Internazionale SIIV, Firenze.
[113] D'Angelo, G., Thom, N., & Presti, D. L. (2016). Bitumen stabilized ballast: A potential solution for railway track-bed. Construction and Building Materials, 124, 118-126.
[114] D'Angelo, J. A. (2001). Superpave Mix Design Tests Methods and Requirements. Federal Highway Administration, 104.
[115] Da Silva, L., Benta, A., & Picado-Santos, L. (2018). Asphalt rubber concrete fabricated by the dry process: Laboratory assessment of resistance against reflection cracking. Construction and Building Materials, 160, 539-550.
[116] Dahlberg T., (2010). "Railway Track Stiffness Variations – Consequences and Countermeasures". International Journal of Civil Engineering, vol. 8, no. 1.
[117] Darter, M., Khazanovich, L., Snyder, M., Rao, S., & Hallin, J. (2001, September). Development and calibration of a mechanistic design procedure for jointed plain concrete pavements. In Proc., 7th Int. Conf. on Concrete Pavements (Vol. 1, pp. 113-131). International Society for Concrete Pavements.
[118] Darter, M. I., Titus-Glover, L., & Von Quintus, H. L. (2009). Implementation of the Mechanistic-Empirical Pavement Design Guide in Utah: validation, calibration, and development of the UDOT MEPDG User's Guide (No. UT-09.11).
[119] De Man, A. P. (2002). DYNATRACK: A survey of dynamic railway track properties and their quality.
[120] Delaplace, M., Bazin, S., Pagliara, F., & Sposaro, A. (2014, August). High-Speed Railway System and the tourism market: between accessibility, image and coordination tool. In 54th European Regional Science Association Congress (pp. 26-29).
[121] Dempsey, B. J., & Thompson, M. R. (1970). A heat transfer model for evaluating frost action and temperature-related effects in multilayered pavement systems. Highway Research Record, (342).

[122] Dempsey, B.J., H. Hill. (1987). Characterizing Temperature Effects for Pavement Analysis and Design. Transportation Research Record, 1121: 14-22.
[123] Dessouky, S., Masad, E., & Bayomy, F. (2004). Prediction of hot mix asphalt stability using the Superpave gyratory compactor. Journal of Materials in Civil Engineering, 16(6), 578-587.
[124] Di Mascio, P. & Moretti, L. (2013). Model for estimating temperatures in concrete pavements. 1st International Journal of Pavements Conference, Brazil.
[125] Di Mascio, P., Loprencipe, G., & Moretti, L. (2014). Competition in rail transport: Methodology to evaluate economic impact of new trains on track. In Proceedings of the 3rd International Conference on Transportation Infrastructure ICTI2014–Sustainability, Eco-efficiency and Conservation in Transportation Infrastructure Asset Management, Pisa, Italy (pp. 22-25).
[126] Di Mascio, Paola; D'Andrea, Antonio (1999). Metodologia razionale per il dimensionamento delle pavimentazioni aeroportuali. SIIV–Cagliari, vol. 28, p. 29.
[127] Di Mino, G., & Di Liberto, C. M. (2008). Stato dell'arte degli interventi sulla sorgente per la mitigazione delle vibrazioni generate da sistemi di trasporto su ferro. In LE RETI DI TRASPORTO URBANO. Progettazione, Costruzione, Gestione.(pp. 1-15). Caracol snc..
[128] Di Mino, G., & Giunta, M. (2007). The volumetric mix-design of porous asphalt: An Italian study of Ndesign determination.
[129] Di Mino, G., & Tripodi, P. (2002). Studio di conglomerati bituminosi con granulato di gomma proveniente da pneumatici dismessi. In XII Convegno SIIV Riqualificazione funzionale e sicurezza del sistema viario (pp. 182-201). Università degli Studi di Parma.
[130] Di Mino, G., Di Liberto, M. (2012). Experimental survey on Dry Asphalt Rubber Concrete for Sub-ballast Layers. Journal of Civil Engineering and Architecture, ISSN 1934-7359, USA - Social and Behavioral Sciences, Volume 6, N.12(serial 61), pp. 1615-1626.
[131] Di Mino, G., Di Liberto, M., Maggiore, C., & Noto, S. (2012). A dynamic model of ballasted rail track with the bituminous sub-ballast layer. Procedia-Social and Behavioral Sciences, 53, 366-378.
[132] Di Pilato M.A., Levergood A.V., Steinberg E.I., Simon R.M., (1983). "Railroad track substructure design and performance evaluation practice," Goldberg-Zoino and Associates Inc., Newton Upper Falls, Massachusetts, Report No. FRA/ORD-83/04.2, June, p. 65.
[133] Dong D., Huang X., Li X., Zhang L. (2012). Swelling process of rubber in asphalt and its effect on the structure and properties of rubber and asphalt. Construction and Building Materials.
[134] Dubois, V., De La Roche, C., & Burban, O. (2010). Influence of the compaction process on the air void homogeneity of asphalt mixtures samples. Construction and Building Materials, 24(6), 885-897.
[135] EAPA, European Asphalt Pavement Association. (2003). Asphalt in Railway Tracks. Position Papers, 5-11.
[136] Eco.Pne.Us. (Consorzio per il riutilizzo e lo smartimento dei pneumatici usati), Pneumatici fuori uso da rifiuto a risorsa. Milano, intervento ai P.C. Mantegazza, 16 febbraio 2000.
[137] Elfgren, L., Bell, B., Nilimaa, J., Häggström, J., Tu, Y., Lundgren, K., ... & Casas, J. R. (2015). New technologies to extend the life of elderly rail infrastructure: Deliverable 1.3 in MAINLINE-a project within the EC 7th Framework Programme.
[138] Emery, J. (1995),"Evaluation of Rubber Modified Asphalt Demonstration Projects", Transportation Research Record 1515, TRB, Washington, D.C, pp 37-46.
[139] Epps, J. A., & Mason, L. S. (1994). Uses of recycled rubber tires in highways: A synthesis of highway practice. Final report (No. PB-94-197555/XAB; NCHRP--198). National Cooperative Highway Research Program, Washington, DC (United States).
[140] Esch, D. C. (1984). Asphalt Pavements Modified with Coarse Rubber Particle. Alaska P, Report No. FHWA-AK-RD-85-07. Federal Highway Administration, Washington, D.C.
[141] Esin, T., & Cosgun, N. (2007). A study conducted to reduce construction waste generation in Turkey. Building and Environment, 42(4), 1667-1674.
[142] Esveld, C. (2003). Recent developments in slab track. European Railway Review, 9(2), 81-85.
[143] Esveld, C., & Esveld, C. (2001). Modern railway track (Vol. 385). Zaltbommel, The Netherlands: MRT-productions.
[144] ETRMA-ELTs,(2015)."End-of-Life-Tyres",<http://www.etrma.org>.
[145] European Asphalt Pavement Association (www.eapa.org), Rue du Commerce 77 1040 Brussels.
[146] Evans A. and Evans R., (2006). "Rubber/Plastic Composite Rail Sleepers".
[147] Evans, A., Evans, R. (2006). The composition of a tire: typical components. The Waste & Resources Action Programme, 5.
[148] Fager, G.A. (2001),"Asphalt Rubber: A Summary of the Use of Crumb Rubber in the Hot Mixes: Kansas Experience 1990-2000", Kansas Department of Transportation, Kansas.
[149] Fang, M., Qiu, Y., Rose, J. G., West, R. C., & Ai, C. (2011). Comparative analysis on dynamic behavior of two HMA railway substructures. Journal of Modern Transportation, 19(1), 26-34.
[150] Farhan, A. H., Dawson, A. R., Thom, N. H., Adam, S., & Smith, M. J. (2015). Flexural characteristics of rubberized cement-stabilized crushed aggregate for pavement structure. Materials & Design, 88, 897-905.
[151] Farina, A., Zanetti, M. C., Santagata, E., & Blengini, G. A. (2017). Life cycle assessment applied to bituminous mixtures containing recycled materials: Crumb rubber and reclaimed asphalt pavement. Resources, Conservation and Recycling, 117, 204-212.

[152] Farouk, A. I. B., Hassan, N. A., Mahmud, M. Z. H., Mirza, J., Jaya, R. P., Hainin, et al. (2017). Effects of mixture design variables on rubber–bitumen interaction: properties of the dry mixed rubberized asphalt mixture. Materials and Structures, 50(1), 12.
[153] Fatahi B., Khabbaz H. & Indraratna, B. (2008). "Analysis of Matric Suction Effects Induced by Tree Roots on Rail Track Subgrade," Conference on Railway Engineering, Perth, WA, Australia, September 2008 in Conference Proceedings: CORE2008 Conference on Railway Engineering, ed John Goodall, Bill Singleton, RTSA, Australia, pp. 599-610.
[154] Fatemi, A., & Yang, L. (1998). Cumulative fatigue damage and life prediction theories: a survey of state of the art for homogeneous materials. International journal of fatigue, 20(1), 9-34.
[155] Feiteira Dias J L., Picado-Santos L.G., & Capitão S.D., (2014). "Mechanical performance of dry process fine crumb rubber asphalt mixtures placed on the Portuguese road network." Construction and Building Materials, 73, 247–254. http://doi.org/10.1016/j.conbuildmat.2014.09.110
[156] Ferreira, T. M., & Teixeira, P. F. (2012). Rail track performance with different subballast solutions: Traffic and environmental effects on subgrade service life. Journal of Trans-portation Engineering, 138(12), 1541-1550.
[157] Ferreira P.A., Teixeira P. F., and Cardoso M. R. (2007). "Influence of Incorporating a Bituminous Sub-Ballast Layer on the Deformations of Railway Trackbed". Dissertation for Integrated Master Degree in Civil Engineering. Instituto Superior Técnico – Technical University of Lisbon, Portugal.
[158] Ferreira, T. M., Teixeira, P. F., & Cardoso, R. (2010). Impact of bituminous subballast on railroad track deformation considering atmospheric actions. Journal of Geotechnical and Geoenvironmental Engineering, 137(3), 288-292.
[159] Fontes L., Pereira P., Pais J., Triches G. (2006). "Behavior of Asphalt Rubber Mixtures with Different Crumb Rubber and Asphalt Biner Sources." Proceedings AR2006 International Conference on Asphalt Rubber, Palm Springs, California, 2006.
[160] Foster, C. R. (1982). Development of Marshall procedures for designing asphalt paving mixtures (No. IS 84).
[161] Freeme, C. R., Maree, J. H., & Viljoen, A. W. (1982). Mechanistic design of asphalt pavements and verification using the heavy vehicle simulator. Pretoria: National Institute for Transport and Road Research.
[162] Frenzel J., Frenzel J., Fahrbahn V.J.F. (2010). "System Sato auf Asphalttragschicht, EI-Eisenbahningenieur, Heft". 9, September 2010, DVV Media Group GmbH, Hamburg, Germany.
[163] Fritz, H. W., & Eustacchio, E. (1990). Mechanical tests for bituminous mixes: characterization, design and quality control. In RILEM International Symposium, 4th, 1990, Budapest, Hungary.
[164] Fu, R., Coop, M. R., & Li, X. Q. (2017). Influence of Particle Type on the Mechanics of Sand–Rubber Mixtures. Journal of Geotechnical and Geoenvironmental Engineering, 143(9), 04017059.
[165] Gallego, J., Del Val, M. A., & Tomas, R. (2000). Spanish experience with asphalt pavements modified with tire rubber. Asphalt Rubber, 2000.
[166] GALLEGO, R., & MARTÍNEZ, F. Applicability of the technique of exploration of speed through experimental analysis NDT & simulation analytic-numerical of dispersion curve in concrete at early ages by propagation of surface waves.
[167] Ganiron Jr, T. U. (2014). Waste tire as an asphalt cement modifier for road pavement. International Journal of u-and e-Service, Science and Technology, 7(5), 181-194.
[168] Gautier, P. E. (2015). Slab track: Review of existing systems and optimization potentials including very high speed. Construction and Building Materials, 92, 9-15.
[169] Gawel I, Stepkowski R, Czechowski F (2006) Molecular interactions between rubber and asphalt. Ind Eng Chem Res 45(9):3044–3049.
[170] German Railways (1997). NGT 39. Richtlinie für die Anwendung des Leichten Fallgewichtsgerätes im Eisenbahnbau. (Directions of Application of Light Drop-Weight Tester in Railways).
[171] Ghazi G. Al-Khateeb, Khalid A. Ghuzlan (2014). The combined effect of loading frequency, temperature, and stress level on the fatigue life of asphalt paving mixtures using the IDT test configuration, International Journal of Fatigue, Volume 59, Pages 254-261, ISSN 0142-1123.
[172] Ghuzlan K. (2001). Fatigue damage analysis in asphalt concrete mixtures based upon dissipated energy concepts. Ph. D. thesis, the University of Illinois at Urbana- Champaign, Urbana, IL.
[173] Ghuzlan, K. A., & Carpenter, S. H. (2002). Traditional Fatigue Analysis of Asphalt Concrete Mixtures Transportation Research Board Annual Meeting. Washington DC.
[174] Ghuzlan, K., & Carpenter, S. (2000). Energy-derived, damage-based failure criterion for fatigue testing. Transportation Research Record: Journal of the Transportation Research Board, (1723), 141-149.
[175] Giannakos, K. (2014). Secondary stiffness of fastening's clip: Influence on the behavior of the railway track panel. Transport Research Arena.
[176] Giavarini C., Scarcella M., (1999). Rubber modified asphalt. I bitumi modificati con gomma di recupero (p. 1-2). Rassegna del Bitume n.32-33, 1999.
[177] Giunta, M., & Praticò, F. G. (2017). Design and maintenance of high-speed rail tracks: A comparison between ballasted and ballast-less solutions based on life cycle cost analysis. In Transport Infrastructure and Systems: Proceedings of the AIIT International Congress on Transport Infrastructure and Systems (Rome, Italy, 10-12 April 2017) (p. 87). CRC Press.
[178] Gmelin, H., & Seuring, S. (2014). Determinants of a sustainable new product development. Journal of Cleaner production, 69, 1-9.
[179] Gowda, G. V., Elliott, R. P., & Hall, K. D. (1997). Effects of Rubber on Asphalt Mixes (No. MBTC FR 1009, TRC-9404,).

[180] Gowda, G.V., Hall, K.D. and Elliott, R.P. (1996),"Arkansas Experience with Crumb Rubber Modified Mixes Using Marshall and Strategic Highway Research Program Level I Design Methods", Transportation Research Record 1530, TRB, Washington, D.C., pp. 25-33.
[181] Gudmarsson, A., Ryden, N., & Birgisson, B. (2012). "Characterizing the low strain complex modulus of asphalt concrete specimens through optimization of frequency response functions". The Journal of the Acoustical Society of America, 132(4), 2304-2312.
[182] Guler H., Jovanovic S., Evren G., (2011). "Modelling Railway Track Geometry Deterioration. Proceedings of the ICE" - Transport, 164(2), 65–75. doi:10.1680/tran.2011.164.2.65
[183] Gupta, R., & Narayan, S. A. (2016). Estimation of viscous and fatigue dissipation of bituminous concrete in repeated loading tests. In Functional Pavement Design: Proceedings of the 4th Chinese-European Workshop on Functional Pavement Design (4th CEW 2016, Delft, The Netherlands, 29 June-1 July 2016) (p. 319). CRC Press.
[184] Gupta, S., Degrande, G., & Lombaert, G. (2009). Experimental validation of a numerical model for subway induced vibrations. Journal of sound and vibration, 321(3), 786-812.
[185] H. Di Benedetto, Q.T. Nguyen, C. Sauzéat, (2011). Non-linearity, heating, fatigue and thixotropy during cyclic loading of asphalt mixtures, Road Mater. Pavement Des. 12 (1) 129–158.
[186] H. Wang, Z. Dang, L. Li, Z. You, Analysis of fatigue crack growth laws for crumb rubber modified (CRM) asphalt mixture, Constr. Build. Mater. 47 (2013) 1342–1349.
[187] Habib, A., Hossain, M., Kaldate, R., & Fager, G. (1998). Comparison of Superpave and Marshall mixtures for low-volume roads and shoulders. Transportation Research Record: Journal of the Transportation Research Board, (1609), 44-50.
[188] Hafeez J., Hussain K., Riaz A., Khitab S., Hussain B., Zaidi U., Farooqi A., Hayat I., Ahmed A., Asif, (2013). "Influence of time and temperature on asphalt rheological properties," Life Sci. J. 10 894–898, http://dx.doi.org/10.1002/app.21283.
[189] Hafeez, I., Kamal, M. A., Ishaq, M. A., Ahmad, N., & Khanzada, S. (2015). A Laboratory-Based Research Study to Investigate the Aggregate Packing Characteristics and Its Influence on Asphaltic Mixture's Performance. Arabian Journal for Science and Engineering, 40(11), 3119-3134.
[190] Hafez, I. H., & Witzack, M. J. (1994). Comparison of Marshall and SUPERPAVE Level I Mix Design for Asphalt Mixes. Transportation research record, 1492, 161-175.
[191] Hall, K., Dandu, S., & Gowda, G. (1996). Effect of specimen size on compaction and volumetric properties in gyratory compacted hot-mix asphalt concrete specimens. Transportation Research Record: Journal of the Transportation Research Board, (1545), 126-132.
[192] Hamza, M. A., & Anderson, W. K. (2005). Soil compaction in cropping systems: A review of the nature, causes and possible solutions. Soil and tillage research, 82(2), 121-145.
[193] HAPI (2018). A Manual For Design Of Hot-mix Asphalt With Commentary. (n.d.). Retrieved from https://www.nap.edu/read/14524/chapter/8
[194] Harman, T. P., J. D'Angelo, and J. R. Bukowski, "Evaluation of SUPERPAVE Gyratory Compactor in the Field Management of Asphalt Mixes: Four Simulation Studies," Transportation Research Record 1513: Flexible Pavement Construction, Transportation Research Board, National Research Council, 1995.
[195] Harrigan, E. T., Leahy, R. B., & Youtcheff, J. S. (1994). Superpave Manual of Specifications, Test Methods and Practices (SHRP-A-379). Washington DC, USA: National Research Council.
[196] Hassan, N. A., Airey, G. D., Jaya, R. P., Mashros, N., & Aziz, M. A. (2014). A review of crumb rubber modification in dry mixed rubberized asphalt mixtures. Jurnal Teknologi, 70(4), 127-134.
[197] Hassan, N. A., Airey, G. D., Yusoff, N. I. M., Hainin, M. R., Putrajaya, R., Abdullah, M. E., & Aziz, M. A. (2015). Microstructural characterisation of dry mixed rubberised asphalt mixtures. Construction and Building Materials, 82, 173-183.
[198] Heitzman, M. A., (1992). "State of the Practice - Design and Construction of Asphalt Paving Materials with Crumb Rubber Modifier," Transportation Research Record 1339. Federal Highway Administration, Report No. FHWA-SA-92-022.
[199] Hendriks, C. F., & Pietersen, H. S. (Eds.). (2000). Report 22: SUSTAINABLE raw materials: construction and demolition waste–state-of-the-art report of RILEM technical committee 165-SRM (Vol. 22). RILEM publications.
[200] Hensley, M. J., Rose, J.G. (1991). Performance of Hot-Mix-Asphalt Railway Trackbeds. Transportation research record, (1300).
[201] Hermansson, A. (2001). Mathematical model for calculation of pavement temperatures: comparison of calculated and measured temperatures. Journal of the Transportation Re-search Board, (n°1764), 180-188.
[202] Hernandez-Olivares B. Witoszek-Schultz, M. Alonso-Fernandez and C. Benito-Moro. 2009 Rubber-modified hot-mix asphalt pavement by dry process. International journal of pavement engineering. Vol. 10, No. 4, August 2009, 277–288.
[203] Herráiz, T. R., Domingo, L. M., Martinez, J. H. A., Prieto, J. M. B., & Herráiz, J. I. R. (2015). New environmental bituminous mixture for slab track design in tram networks. Advances in Structural Engineering, 18(12), 2117-2127.
[204] Hicks, R. G., Tighe, S., & Cheng, D. (2012, October). Rubber Modified Asphalt Technical Manual. In Proceedings, Canadian Technical Asphalt Association (Vol. 40, pp. 57-77).
[205] Hidalgo-Signes, C., Garzón-Roca, J., Grima-Palop, J. M., & Insa-Franco, R. (2017). Use of rubber shreds to enhance attenuation of railway sub-ballast layers made of unbound aggregates. Materiales de Construcción, 67(326), 115.
[206] Hidalgo-Signes, C., Martínez-Fernández, P., Garzón-Roca, J., & Insa-Franco, R. (2016). Analysis of the bearing capacity of unbound granular mixtures with rubber particles from scrap tires when used as sub-ballast. Materiales de Construcción, 66(324), 105.

[207] Hislop, V.P and Coree B.J. (2000). VMA as a design parameter in hot-mix asphalt, Proceedings of Midcontinental transportation symposium.
[208] Hoegh, K., Khazanovich, L., & Jense, M. (2010). Local calibration of Mechanistic-Empirical pavement design guide rutting model: Minnesota road research project test sections. Transportation Research Record: Journal of the Transportation Research Board, (2180), 130-141.
[209] Horvát F., Fischer S., Major Z. (2013). "Evaluation of Railway Track Geometry Stabilisation Effect of Geogrid Layers Under Ballast on the Basis of Laboratory Multi- 99 level Shear Box Tests". Acta Technica Jaurinensis, 6(2), 21–44. Retrieved from http://acta.sze.hu/index.php/acta/article/view/48.
[210] Hosseingholian M., Froumentin M., Levacher D. (2009). "Continuous Method to Measure Track Stiffness A New Tool for Inspection of Rail Infrastructure". World Applied Sciences Journal, 6(5), 579–589. Retrieved from http://www.idosi.org/wasj/wasj6(5)/1.pdf
[211] Hu, W., Jia, X., Huang, B., & Park, H. (2017). Evaluation of compactability of asphalt mixture utilizing asphalt vibratory compactor. Construction and Building Materials, 139, 419-429.
[212] Huang Y.H. Pavement analysis and design. USA: Prentice Hall, University of Kentucky; 1993.
[213] Huang, B., Mohammad, L., Graves, P., & Abadie, C. (2002). Louisiana experience with crumb rubber-modified hot-mix asphalt pavement. Transportation Research Record: Journal of the Transportation Research Board, (1789), 1-13.
[214] Huang, Y. H., Lin, C. H. I. A. N. G., & Deng, X. U. E. J. U. N. (1984). Hot Mix Asphalt for Railroad Trackbeds-Structural Analysis and Design. In Association of Asphalt Paving Technologists Proceedings (Vol. 53).
[215] Huang, Y. H., Rose, J. G., & Khoury, C. J. (1987). Thickness Design for Hot-Mix Asphalt Railroad Trackbeds, Annual Journal AAPT, Miscellaneous V.56-87, (pp.427-453).
[216] Huang, Y. H.; Lin, C.; Deng, X. J. and Rose, J. (1984). KENTRACK, A Computer Program for Hot-Mix Asphalt and Conventional Ballast Railway Trackbeds, Asphalt Institute (Publication RR-84-1) and National Asphalt Pavement Association (Publication QIP-105), 164 pages.
[217] Huang, Y., Bird, R. N., & Heidrich, O. (2007). A review of the use of recycled solid waste materials in asphalt pavements. Resources, Conservation and Recycling, 52(1), 58-73.
[218] HUANG, Y. H., C. LIN, and J. G. RosE, 1984a . "Asphalt Pavement Design: Highway versus Railroad," *Journal of Transportation Engineering, ASCE*, Vol. *110*, pp. 276-282.
[219] HUANG, Y. H ., J. G. Rose, and C . J. KHOURY, 1986a . "Hot-Mix Asphalt Railroad Trackbeds, " *Transportation Research Record 1095*, pp. 102-110, Transportation Research Board .
[220] Hudson, S. B., and Davis, R. L., "Relationship of Aggregate Voidage to Gradation," Proceedings of the Association of Asphalt Paving Technologists, Vol. 31, 1962.
[221] Huhtala Matti. (1995). "The Effect Of Wheel Loads On Pavements". Road transport technology-4. University of Michigan Transportation Research Institute, Ann Arbor.
[222] Humphrey DN, Blumenthal M (2010). The use of tire-derived aggregate in road construction applications. Green Streets Highway 2010:299-313.
[223] Hveem, F. N., Zube, E., & Skog, J. (1963). Proposed new tests and specifications for paving grade asphalts. In Association of Asphalt Paving Technologists Proceedings (Vol. 32).
[224] Hwang, D., & Witczak, M. W. (1979). Program DAMA (Chevron), User's Manual. Department of Civil Engineering, University of Maryland, MD.
[225] Ibrahim, I. M., El Rhman, A. A., & El-Shafie, M. (2015). Effect of Irradiated Crumb Rubber on Cold Recycled Bitumen Emulsion Mixes Properties. American Scientific Research Journal for Engineering, Technology, and Sciences (ASRJETS), 15(1), 76-87.
[226] Ibrahim, M. R., Katman, H. Y., Karim, M. R., Koting, S., & Mashaan, N. S. (2013). A review on the effect of crumb rubber addition to the rheology of crumb rubber modified bitumen. Advances in Materials Science and Engineering, 2013.
[227] Indraratna B., Salim W., Rujikiatkamjorn C., (2011). "Advanced Rail Geotechnology – Ballasted Track". London: Taylor & Francis Group. Retrieved from http://ro.uow.edu.au/ engpapers/900/.
[228] Indraratna, B., Nimbalkar, S., Christie, D., Rujikiatkamjorn, C., & Vinod, J. (2010). Field assessment of the performance of a ballasted rail track with and without geosynthetics. Journal of Geotechnical and Geoenvironmental Engineering, 136(7), 907-917.
[229] Indraratna, B., Khabbaz, H., Salim, W., & Christie, D. (2006). Geotechnical properties of ballast and the role of geosynthetics. Institution of Civil Engineers. Proceedings. Ground.
[230] Indraratna, B. (2016). 1st Proctor Lecture of ISSMGE:: Railroad performance with special reference to ballast and substructure characteristics. Transportation Geotechnics, 7, 74-114.
[231] International Union of Railways. (2005). UIC Code 518 – "Testing and Approval of Railway Vehicles from the Point of View of Their Dynamic Behaviour" – Safety – Track Fatigue – Ride Quality. Paris, France.
[232] Ionescu D. (2004). "Evaluation of the Engineering Behaviour of Railway Ballast." Ph.D. Dissertation, Civil Mining, and Environmental Engineering, University of Wollongong, Wollongong, New South Wales, Australia. Retrieved from http://ro.uow.edu.au/cgi/viewcontent.cgi?article=1421&context=theses.
[233] Iwnicki, S. (Ed.). (2006). Handbook of railway vehicle dynamics. CRC press.
[234] J. Feiteira Dias, L. Picado-Santos (2009). Avaliação de Desempenho de Misturas Betuminosas Rugosas com Incorporação de Alta Percentagem de Granulado de Borracha de Pneus Usados, In: XV Congresso Ibero-Latino Americano do Asfalto.

[235] J. Feiteira Dias, L. Picado-Santos, S.D. Capitão, (2014). Mechanical performance of dry process fine crumb rubber asphalt mixtures placed on the Portuguese road network, Constr. Build. Mater. 73, pp. 247–254.
[236] Jenks, C. W., Jencks, C. F., Harrigan, E. T., Adcock, M., Delaney, E. P., & Freer, H. (2011). NCHRP Report 673: A manual for design of hot mix asphalt with commentary. Transportation Research Board, Wahington, DC.
[237] Jensen, J. S., Sloth, M., Linneberg, P., Paulsson, B., & Elfgren, L. (2014). MAINLINE: MAINtenance, renewaL, and Improvement of rail transport infrastructure to reduce Economic and environmental impact. In International Conference of Bridge Maintenance, Safety and Management: 07/07/2014-11/07/2014 (pp. 1056-1063). CRC Press, Taylor & Francis Group.
[238] Jensen, W., & Abdelrahman, M. (2006). Use of crumb rubber in performance-graded binder (No. SPR-01 (05) P585).
[239] Jeong, K. D., Lee, S. J., Amirkhanian, S. N., & Kim, K. W. (2010). Interaction effects of crumb rubber modified asphalt binders. Construction and Building Materials, 24(5), 824-831.
[240] Jiang, R. N., Zhu, B. L., & Chang, L. (2016). The design of Superpave compared with Marshall design method. In MATEC Web of Conferences (Vol. 63, p. 02007). EDP Sciences.
[241] Jitareekul, P., Sunarjono, S., Zoorob, S. E., & Thom, N. H. (2007, June). Early life performance of cement and foamed bitumen stabilized reclaimed asphalt pavement under simulated trafficking. International Conference on Sustainable Construction Materials and Technologies (pp. 11-13).
[242] Jitsangiam, P., Chindaprasirt, P., & Nikraz, H. (2013). An evaluation of the suitability of SUPERPAVE and asphalt mix designs as they relate to Thailand's climatic conditions. Construction and Building Materials, 40, 961-970.
[243] Jovanovic S., (2006). "Railway Track Quality Assessment and Related Decision Making".
[244] Kaewunruen, S., & Remennikov, A. M. (2009). Dynamic flexural influence on a railway concrete sleeper in track system due to a single wheel impact. Engineering Failure Analysis, 16(3), 705-712.
[245] Kaewunruen, S., & Remennikov, A. M. (2010). Dynamic properties of railway track and its components: recent findings and future research direction. Insight-Non-Destructive Testing and Condition Monitoring, 52(1), 20-22.
[246] Kaewunruen, S., Lewandrowski, T., & Chamniprasart, K. (2017). Dynamic Responses of Interspersed Railway Tracks to Moving Train Loads. International Journal of Structural Stability and Dynamics, 1850011.
[247] Kaloush, K. E. (2014). Asphalt rubber: Performance tests and pavement design issues. Construction and Building Materials, 67, 258-264.
[248] Kandhal, P. S. (1994). Field and laboratory investigation of stripping in asphalt pavements: State of the art report. Transportation Research Record, (1454).
[249] Kandhal, P. S., & Foo, K. Y. (1997). Designing recycled hot mix asphalt mixtures using Superpave technology. In Progress of Superpave (Superior Performing Asphalt Pavement): Evaluation and Implementation. ASTM International.
[250] Kandhal, P., Foo, K., & Mallick, R. (1998). Critical review of voids in mineral aggregate requirements in Superpave. Transportation Research Record: Journal of the Transportation Research Board, (1609), 21-27.
[251] Kavussi, A., & Hicks, R. G. (1997). Properties of bituminous mixtures containing different fillers. Journal of the Association of Asphalt Paving Technologists, 66.
[252] Kazi, T. (2017). Study on the performance of crumb rubber modified bitumen by varying the sizes of crumb rubber.
[253] Kazmee, H., & Tutumluer, E. (2015). Evaluation of aggregate subgrade materials used as pavement subgrade/granular subbase. Illinois Center for Transportation/Illinois Department of Transportation.
[254] Kennedy, T. (1994). SHRP-A-410, Superior Performing Asphalt Pavements (Superpave). Transportation Research Board; Background of Superpave Asphalt Mixture Design and Analysis, Federal Highway Administration, Report number FH\VA-SA-95-003, 1995.
[255] KENTRACK Version 2.0.1, (2006) Program, Help File and Example Data Files, Department of Civil Engineering, University of Kentucky.
[256] Kerr, A. D. (1972). On the stability of the railroad track in the vertical plane (No. NYU-AA-72-35).
[257] Kerr, W. O., & Ryan, B. A. (1987). Avoiding the pitfalls of life cycle cost analysis. Report, Washington Economic Research Consultants.
[258] Khan, N., Nafees, A., Hussain, A., Zaidi, G., Osama, M., & Ghaffar, S. (2017). Exploring the Properties of Recycled Tyre Rubber for Flexible Asphalt Pavement. Journal of Basic & Applied Sciences, 13, 335-339.
[259] Khan, Z. A., Wahab, H. I., Asi, I. and Ramadhan, R. (1998). "Comparative Study of Asphalt Concrete Laboratory Compaction Methods to Simulate Field Compaction", Construction and Building Materials, Vol. 12, 373-384.
[260] Khisty, C. J., & Lall, B. K. (2017). Transportation engineering. Pearson Education India.
[261] Khodary Moalla Hamed, F. (2010). Evaluation of fatigue resistance for modified asphalt concrete mixtures based on dissipated energy concept (Doctoral dissertation, Technische Universität).
[262] Khosla, N. P., & Ayyala, D. (2013). A Performance-based Evaluation of Superpave Design Gyrations for High Traffic Surface Mixes. Procedia-Social and Behavioral Sciences, 104, 109-118.
[263] Khosla, N., Birdsall, B., & Kawaguchi, S. (2000). Evaluation of moisture susceptibility of asphalt mixtures: conventional and new methods. Transportation Research Record: Journal of the Transportation Research Board, (1728), 43-51.
[264] Kim H., Lee S.J., Armikhanian S.N., (2011). "Rheology of warm mix asphalt binders with aged binders." Constr Build Mater;25:183–9.
[265] Koenders, B. G., Stoker, D. A., Bowen, C., De Groot, P., Larsen, O., Hardy, D., & Wilms, K. P. (2000, September). Innovative process in asphalt production and application to obtain lower operating temperatures. In 2nd Eurasphalt & Eurobitumen Congress, Barcelona, Spain.

[266] Kök, B. V., & Çolak, H. (2011). Laboratory comparison of the crumb-rubber and SBS modified bitumen and hot mix asphalt. Construction and Building Materials, 25(8), 3204-3212.
[267] Kraemer C., Del Val M.A., Pardillo J.M., Rocci S., Romana M.G., Sánchez V., (2004). "Ingenieria de Carreteras". Vol II Mc Graw Hill. Madrid.
[268] Kruntcheva, Mariana R., Andrew C. Collop, and Nicholas H. Thom. "Properties of asphalt concrete layer interfaces." Journal of Materials in Civil Engineering 18.3 (2006): 467-471.
[269] Kumnuantip, C., & Sombatsompop, N. (2003). Dynamic mechanical properties and swelling behavior of NR/reclaimed rubber blends. Materials Letters, 57(21), 3167-3174.
[270] Kweon, G., Kim,Y. R. (2006). "Determination of asphalt concrete complex modulus with impact resonance test", Transportation Research Record, Vol. 1970, pp.151-160.
[271] Lai, J. S., & Shami, H. (1995). Development of rolling compaction machine for preparation of asphalt beam samples. Transportation Research Record, 18-25.
[272] Larsson, D. (2004). A study of the track degradation process related to changes in railway traffic (Doctoral dissertation, Luleå tekniska universitet).
[273] Lastra-González, P., Calzada-Pérez, M. A., Castro-Fresno, D., Vega-Zamanillo, Á., & Indacoechea-Vega, I. (2016). Comparative analysis of the performance of asphalt concretes modified by dry way with polymeric waste. Construction and Building Materials, 112, 1133-1140.
[274] Lastra-González, P., Calzada-Pérez, M. Á., Castro-Fresno, D., Vega-Zamanillo, Á., & Indacoechea-Vega, I. (2017). Porous asphalt mixture with alternative aggregates and crumb-rubber modified binder at reduced temperature. Construction and Building Materials, 150, 260-267.
[275] Lee S.-H., Lee J.-W., Park, D.-W., & Vo, H. V. (2014). "Evaluation of asphalt concrete mixtures for railway track". Construction and Building Materials, 73, 13–18.
[276] Lee Soon-Jae, Amirkhanian S., Kwon S. (2008) The effects of compaction temperature on CRM mixtures made with the SGC and the Marshall compactor. Construction and Building Materials 22 (2008) 1122–1128.
[277] Lee, S. J., Akisetty, C. K., & Amirkhanian, S. N. (2008). The effect of crumb rubber modifier (CRM) on the performance properties of rubberized binders in HMA pavements. Construction and Building Materials, 22(7), 1368-1376.
[278] Li, D., & Selig, E. T. (1995). Wheel/track dynamic interaction: track substructure perspective. Vehicle System Dynamics, 24(sup1), 183-196.
[279] Li, D., & Selig, E. T. (1998). Method for railroad track foundation design. II: Applications. Journal of geotechnical and geoenvironmental engineering, 124(4), 323-329.
[280] Li, M. X. D., Berggren, E. G., & Berg, M. (2009). Assessment of vertical track geometry quality based on simulations of the dynamic track—vehicle interaction. Proceedings of the Institution of Mechanical Engineers, Part F: Journal of Rail and Rapid Transit, 223(2), 131-139.
[281] Li, N., Haas, R., & Xie, W. C. (1997). Development of a new asphalt pavement performance prediction model. Canadian Journal of Civil Engineering, 24(4), 547-559.
[282] Li, P., Ding, Z., Zou, P., & Sun, A. (2017). Analysis of physicochemical properties for crumb rubber in the process of asphalt modification. Construction and Building Materials, 138, 418-426.
[283] Liang, R., & Lee, S. (1996). Short-term and long-term aging behavior of rubber modified asphalt paving mixture. Transportation Research Record: Journal of the Transportation Research Board, (1530), 11-17.
[284] Liu, S. J., & Lytton, R. L. (1984). Rainfall infiltration, drainage, and load-carrying capacity of pavements. Transportation research record, (993).
[285] Lichtberger B., (2005). Track compendium, First edition. Eurail Press.
[286] Loizos, A., Al-Qadi, I., & Scarpas, T. (Eds.). (2017). Bearing Capacity of Roads, Railways, and Airfields: Proceedings of the 10th International Conference BCRRA 2017, June 28-30, 2017, Athens, Greece. CRC Press.
[287] Loizos, A., Partl, M. N., Scarpas, T., & Al-Qadi, I. L. (Eds.). (2009). Advanced Testing and Characterization of Bituminous Materials, Two Volume Set. CRC Press.
[288] López Pita A. (2006). "Infraestructuras ferroviarias". Barcelona, Spain: Edicions UPC.
[289] López Pita A. and Teixeira P. F., (2001). "Resistant track homogeneity: a way to reduce maintenance costs." Proceedings of the 4th International Conference Railway Engineering, London, April-May 2001.
[290] López Pita A., Teixeira P. F., Casas C., Ubalde L. and Robusté F., (2007). "Evolution of track geometric quality in high-speed lines: the 10-year experience of the Madrid-Seville line". Proceedings of the Institution of Mechanical Engineers, Part F, Journal of Rail and Rapid Transit, Volume 221, Number 2, 2007, pp. 147-155 (9). ISSN 0954-4097.
[291] López Pita, A., & Teixeira, P. F. (2003, January). New criteria in embankment-bridge transitions on high-speed lines. In IABSE Symposium Report (Vol. 87, No. 3, pp. 8-14). International Association for Bridge and Structural Engineering.
[292] López-Moro F., Moro M., Hernández-Olivares F., Witoszek-Schultz B., Alonso-Fernández M. (2013). Microscopic analysis of the interaction between crumb rubber and bitumen in asphalt mixtures using the dry process. Construction and Building Materials.
[293] Loría-Salazar, L. G., Badilla-Vargas, G., Elizondo-Arrieta, F., Jiménez-Acuña, M., & Aguiar-Moya, J. P. (2010). EXPERIENCES IN THE CHARACTERIZATION OF MATERIALS USED IN THE CALIBRATION OF THE AASHTO MECHANISTIC-EMPIRICAL PAVEMENT DESIGN GUIDE (MEPDG) FOR FLEXIBLE PAVEMENT FOR COSTA RICA.

[294] Losa M., Leandri P., Bacci R. (2011). Mix design and performance evaluation of crm-modified asphalt concrete mixtures. 5th INTERNATIONAL CONFERENCE BITUMINOUS MIXTURES AND PAVEMENTS Thessaloniki, Greece, 1-3 June 2011.
[295] M.C. Zanetti; S. Fiore; B. Ruffino; E. Santagata; D. Dalmazzo; M. Lanotte (2014). CHARACTERIZATION OF CRUMB RUBBER FROM END-OF-LIFE TYRES FOR PAVING APPLICATIONS. In: Second Symposium on Urban Mining, Old Monastery of Saint Augustine, Bergamo, Italy, 19-21 May 2014.
[296] Ma, T., Ye, Q., Wu, C., & Huang, X. (2016). Characterization of stable crumb rubber asphalt and mixture. In Functional Pavement Design: Proceedings of the 4th Chinese-European Workshop on Functional Pavement Design (4th CEW 2016, Delft, The Netherlands, 29 June-1 July 2016) (p. 277). CRC Press.
[297] Machin, E. B., Pedroso, D. T., & de Carvalho Jr, J. A. (2017). Energetic valorization of waste tires. Renewable and Sustainable Energy Reviews, 68, 306-315.
[298] Maggiore C., Di Mino G., Di Liberto M., Airey G., Grenfell J. (2012) Mechanical characterization of dry asphalt rubber concrete for base layers by means of the four bending points tests. Four-Point Bending - Proceedings of the 3rd Conference on Four-Point Bending.
[299] Maggiore, C., Airey, G., Di Mino, G., Marsac, P., Collop, A., & Di Liberto, M. (2012). Fatigue resistance: is it possible having a unique response?. Four Point Bending, 239.
[300] Maggiore, C., Grenfell, J., Airey, G., & Collop, A. C. (2012). Evaluation of fatigue life using dissipated energy methods. In 7th RILEM International Conference on Cracking in Pavements (pp. 643-652). Springer, Dordrecht.
[301] Marais, H. I., Botha, C., Hofsink, W., Muller, J., & van Heerden, J. (2017, August). Latest developments in crumb rubber modified bitumen for use in asphalt and seals: the South African experience. In AAPA International Flexible Pavements Conference, 17th, 2017, Melbourne, Victoria, Australia.
[302] Marchionna, M. Cesarini, M.G. Fornaci (1985). Modello di degradazione strutturale (pavimentazioni) Autostrade 1/85.
[303] Martínez-Casas, J., Baeza, L., Di Gialleonardo, E., & Bruni, S. (2016). A dynamic model of the track-railway vehicle interaction on curves.
[304] Martínez Soto, F. (2013). Análisis experimental de la curva de disperisón de velocidades de ondas superficiales en morteros a edad temprana. (http://hdl.handle.net/10481/25172)
[305] Martinho, F. C. G., Picado-Santos, L. G., & Capitão, S. D. (2017). Mechanical properties of warm-mix asphalt concrete containing different additives and recycled asphalt as constituents applied in real production conditions. Construction and Building Materials, 131, 78-89.
[306] Mashaan, N. S., Ali, A. H., Karim, M. R., & Abdelaziz, M. (2012). An overview of crumb rubber modified asphalt. International Journal of Physical Sciences, 7(2), 166-170.
[307] Mashaan, N. S., Ali, A. H., Koting, S., & Karim, M. R. (2013). Performance evaluation of crumb rubber modified stone mastic asphalt pavement in Malaysia. Advances in Materials Science and Engineering, 2013.
[308] Matthews, J. M., Monismith, C. L., & Craus, J. (1993). Investigation of laboratory fatigue testing procedures for asphalt aggregate mixtures. Journal of Transportation Engineering, 119(4), 634-654.
[309] Maupin Jr, G. W. (2003). Additional Asphalt to Increase the Durability of Virginia's Superpave Surface Mixes (No. FHWA/VTRC 03-R15,).
[310] McCann, M. and Sebaaly, P. (2001). A Quantitative Evaluation of Stripping Potential in Hot Mix Asphalt Using Ultrasonic Energy for Moisture Accelerated Conditioning, Transportation Research Record 1767, Washington, D.C., Pp. 48 – 59.
[311] Menichelli, S. (1995). Il ruolo del conglomerato bituminoso nella sovrastruttura delle linee ad alta velocità. Rassegna del bitume, 24.
[312] Mill, T., Tse, D. S., Loo, B., Yao, C. C. D., & Canavesi, E. (1992). Oxidation pathways for asphalt. Prepr. ACS Div. Fuel Chem, 37(3).
[313] Miner, M. A., 1945. "Cumulative Damage in Fatigue," Transactions of the ASME, Vol. 67, pp. A159-A164.
[314] Miró Recasens, J. R., Pérez Jiménez, F. E., Moreno Navarro, F., & Rubio Gámez, M. D. C. (2015). Estudio del comportamiento a fatiga de mezclas bituminosas empleadas en rehabilitación de carreteras: influencia de la temperatura de servicio. In XVIII CILA: Congreso Ibero Latinoamericano del Asfalto 2015 (pp. 1-13).
[315] Miura, S., Takai, H., Uchida, M., & Fukada, Y. (1998). The mechanism of railway tracks. Japan Railway & Transport Review, 3, 38-45.
[316] Modarres, A., & Aloogar, A. (2017). Comparison between the fatigue response of hot and warm mix asphalts based on the dissipated energy approach. International Journal of Pavement Engineering, 18(1), 60-72.
[317] Mohammad, L., Wu, Z., Zhang, C., Khattak, M., & Abadie, C. (2004). Variability of air voids and mechanistic properties of plant-produced asphalt mixtures. Transportation Research Record: Journal of the Transportation Research Board, (1891), 85-97.
[318] Mohammed, H. A., Thom, N. H., & Dawson, A. R. (2018). Evaluating Mechanical Properties and Fatigue in Two-Layer Roller-Compacted Concrete Pavements (No. 18-01463).
[319] Momoya, Y., & Sekine, E. (2007). Performance-based Design Method for Railway Asphalt Roadbed, Doboku Gakkai Ronbunshuu E, Vol. 63, (pp. 608-619).
[320] Monismith, C. L., Epps, J. A., & Finn, F. N. (1985). Improved asphalt mix design. In Proceedings, Association of Asphalt Paving Technologists Technical Sessions, San Antonio, Texas (pp. 347-406).

[321] Moreno F., Rubio M., Martinez-Echevarria M. (2011). Analysis of digestion time and the crumb rubber percentage in dry-process crumb rubber modified hot bituminous mixes. Construction and Building Materials.
[322] Moreno F., Sol M., Martín J., Pérez M., Rubio M.C., (2011). "The effect of crumb rubber modifier on the resistance of asphalt mixes to plastic deformations". Mater Des; 47:274–80.
[323] Moreno Navarro, F.M. (2013). Diseño de un método de ensayo de laboratorio para el análisis de la resistencia a fisuración de mezclas bituminosas. Granada: Universidad de Granada, 543 p. [http://hdl.handle.net/10481/29505]
[324] Moreno, F., & Rubio, M. C. (2013). Effect of aggregate nature on the fatigue-cracking behavior of asphalt mixes. Materials & Design, 47, 61-67.
[325] Moreno-Navarro F., Sol-Sánchez M., Rubio-Gámez M.C., & Segarra-Martínez, M. (2014). "The use of additives for the improvement of the mechanical behavior of high modulus asphalt mixes." Construction and Building Materials, 70, 65–70. https://doi.org/10.1016/j.conbuildmat.2014.07.115
[326] Moreno-Navarro, F., & Rubio-Gámez, M. C. (2013). UGR-FACT test for the study of fatigue cracking in bituminous mixes. Construction and Building Materials, 43, 184-190.
[327] Moreno-Navarro, F., & Rubio-Gámez, M. C. (2014). Mean damage parameter for the characterization of fatigue cracking behavior in bituminous mixes. Materials & Design (1980-2015), 54, 748-754.
[328] Moreno-Navarro, F., & Rubio-Gámez, M.C. (2016). A New Approach for the Study of Fatigue Cracking Phenomenon in Bituminous Mixtures. In 8th RILEM International Conference on Mechanisms of Cracking and Debonding in Pavements (pp. 193-198). Springer, Dordrecht.
[329] Moreno-Navarro, F., & Rubio-Gámez, M.C. (2016). A review of fatigue damage in bituminous mixtures: Understanding the phenomenon from a new perspective. Construction and Building Materials, 113, 927-938.
[330] Moreno-Navarro, F., Rubio-Gámez, M. C., & Jiménez Del Barco-Carrión, A. (2016). Tire crumb rubber effect on hot bituminous mixtures fatigue-cracking behaviour. Journal of Civil Engineering and Management, 22(1), 65-72.
[331] Moreno-Navarro, F., Sol-Sánchez, M., & Rubio-Gámez, M. C. (2015). The effect of polymer modified binders on the long-term performance of bituminous mixtures: the influence of temperature. Materials & Design, 78, 5-11.
[332] Moreno-Navarro, F., Sol-Sánchez, M., Jimenez del Barco, A., & Rubio-Gámez, M. C. (2017). Analysis of the influence of binder properties on the mechanical response of bituminous mixtures. International Journal of Pavement Engineering, 18(1), 73-82.
[333] Muniandy, R., Jakarni, F. M., Hassim, S., & Mahmud, A. R. (2008). A newly developed laboratory slab roller compactor (turamesin): An overview. International Journal of Engineering-Transactions A: Basics, 21(2), 133.
[334] N.A. Hassan et al., Microstructural characterization of dry mixed rubberized asphalt mixtures, Constr. Build. Mater. 82 (2015) 173–183.
[335] National Asphalt Pavement Association (1982). Development of Marshall Procedures for Designing Asphalt Paving Mixtures, Info. Series 84. National Asphalt Pavement Association. Lanham, MD.
[336] Naude, F., Fröhling, R. & Theron, N. (2005). Development of a methodology to calculate stresses in track components. Proceedings of the Institution of Mechanical Engineers, Part F: Journal of Rail and Rapid Transit, 219(4), 213-224.
[337] Nazarian, S., Yuan, D., & Celaya, M. (2010, August). Stress Wave Methods for Quality control and Quality assurance of Pavement Layers during construction. In Structural Materials Technology 2010.
[338] Newcomb, D., Stroup-Gardiner, M., Kim, J. R., Allen, B., & Wattenhoffer-Spry, J. (1994). Polymerized crumb rubber modified mixtures in Minnesota.
[339] Nguyen, H. T., & Tran, T. N. (2017). Effects of crumb rubber content and curing time on the properties of asphalt concrete and stone mastic asphalt using dry process. International Journal of Pavement Research and Technology.
[340] Nijboer, L. W. (1948). "Plasticity as a Factor in the design of Dense Bituminous Road Carpets," Elsevier.
[341] Nishiura, D., Sakaguchi, H., & Aikawa, A. (2017). Development of Viscoelastic Multi-Body Simulation and Impact Response Analysis of a Ballasted Railway Track under Cyclic Loading. Materials, 10(6), 615.
[342] Norouzi, A., & Richard Kim, Y. (2017). Mechanistic evaluation of fatigue cracking in asphalt pavements. International Journal of Pavement Engineering, 18(6), 530-546.
[343] Oliveira, J., Zoorob, S., Thom, N. H., & Pereira, P. A. (2007). A simple approach to the design of pavements incorporating grouted macadams.
[344] Orlandi, D. (1984). "I fenomeni di fatica nella struttura sotto binario," Ingegneria Ferroviaria, 6/1984, pp. 317-322.
[345] Orlandi, D. (1985). Perchè un subballast. Ingegneria Ferroviaria, Agosto.
[346] Orlandi, D. (1988). Tipi di armamento per l'alta velocità Esperienze e problemi delle varie amministrazioni. Ingegneria Ferroviaria.
[347] Oteiza I. and Tenorio J.A., (2007). "La innovación en las técnicas, los sistemas y los materiales de construcción". Jornada J7: Evaluación de la sostenibilidad en la Edificación, XVII Edición Curso de Estudios Mayores de la Construcción (CEMCO) Instituto Eduardo Torroja, Madrid.
[348] Ozer, H., Al-Qadi, I. L., Singhvi, P., Bausano, J., Carvalho, R., Li, X., & Gibson, N. (2018). Prediction of pavement fatigue cracking at an accelerated testing section using asphalt mixture performance tests. International Journal of Pavement Engineering, 19(3), 264-278.
[349] Özkul, Z. H., & Baykal, G. (2007). Shear behavior of compacted rubber fiber-clay composite in drained and undrained loading. Journal of geotechnical and Geoenvironmental engineering, 133(7), 767-781.
[350] Page G. (1989). Florida's initial experience utilizing ground tire rubber in asphalt concrete mixes. Research Report FL/DOT/MO89-366. Florida Department of Transportation, Materials Office; September 1989.

[351] Paixão, A., Fortunato, E., Fontul, S., & Martins, F. (2011). A case study in construction optimization for the sub-ballast layer. In Proceedings of 11th International Conference on Railway Engineering.
[352] Palikowska, K. M. (2014). Modelling of curvature of the railway track geometrical layout using particle swarm optimization. Logistics and Transport, 21(1), 73-82.
[353] Pan, T., Tutumluer, E., & Carpenter, S. H. (2006). Effect of coarse aggregate morphology on the permanent deformation behavior of hot mix asphalt. Journal of transportation engineering, 132(7), 580-589.
[354] Panadero C, Sanz JL (2010). Analysis of sub-ballast properties: Contradictions and processes that affect their performance. Revista Ingeopres 196:14-21.
[355] Paris, P. C., & Erdogan, F. (1963). A critical analysis of crack propagation laws. ASME.
[356] Pehlken, A., & Müller, D. H. (2009). Using information of the separation process of recycling scrap tires for process modeling. Resources, Conservation and Recycling, 54(2), 140-148.
[357] Pell, P. S. (1988). Pavement materials. In International Conference on the Structural Design of Asphalt Pavements, 6th, 1987, Ann Arbor, Michigan, USA (Vol. 2).
[358] Pell, P. S., & Cooper, K. E. (1975). The effect of testing and mix variables on the fatigue performance of bituminous materials. Journal of the Association of Asphalt Paving Technologists, 44, 1-37.
[359] Peña M. (2003). Slab track test sites in the Mediterranean Corridor for high-speed use. Revista de Obras Públicas 3431:57-68.
[360] Peralta, E. J. F. (2009). Study of the Interaction between Bitumen and Rubber (Doctoral dissertation).
[361] Pérez, A., and Páez, A. (2007). "Medida de la estabilidad del betún polvo de neumáticos por solubilidad en disolventes orgánicos." Revista Carreteras, 151(1), 45–52.
[362] Pérez, F., Miró, R., Martínez, A., Martínez, C., and Páez, A. (2006). "Evaluación de la cohesión de betunes modificados con polvo de neumáticos." Materiales de Construcción, 56(284), 43–54.
[363] Pérez, F., Miró, R., Martínez, A., Paje, S. E., Bueno, M., and Terá, F. (2010). "Acoustic field evaluation of asphalt mixtures with crumb rubber." Appl. Acoust., 71(6), 578–582.
[364] Pérez-Jiménez, F., Martínez, A. H., Miró, R., Hernández-Barrera, D., & Araya-Zamorano, L. (2014). Effect of compaction temperature and procedure on the design of asphalt mixtures using Marshall and gyratory compactors. Construction and Building Materials, 65, 264-269.
[365] Perpetual Bituminous Pavements (2001). Transportation Research Circular 503, TRB, Washington, D.C.
[366] Petersen, J. C. (2000). Chemical composition of asphalt as related to asphalt durability. In Developments in Petroleum Science (Vol. 40, pp. 363-399). Elsevier.
[367] Pires, G. M., del Barco Carrión, A. J., Airey, G. D., & Presti, D. L. (2017). Maximising asphalt recycling in road surface courses: The importance of a preliminary binder design.
[368] Pirozzolo, L. (2017) Optimization of bituminous sub-ballast in railways infrastructures under sustainability criteria. Universidad de Granada.
[369] Pita, A. L., Teixeira, P. F., & Robuste, F. (2004). High speed and track deterioration: the role of vertical stiffness of the track. Proceedings of the Institution of Mechanical Engineers, Part F: Journal of Rail and Rapid Transit, 218(1), 31-40.
[370] Plotkin, D. E., Wagers, S. K., & Prose, G. (1990). A Railroad Track Structural Analysis Method for Work Planning: Development and Example Application (No. CERL-TR-M-91/07). CONSTRUCTION ENGINEERING RESEARCH LAB (ARMY) CHAMPAIGN IL.
[371] Poel, V., & Der, C. (1954). A general system is describing the visco-elastic properties of bitumens and its relation to routine test data. Journal of Chemical Technology and Biotechnology, 4(5), 221-236.
[372] Policicchio F., (2008). "Lineamenti di Infrastrutture Ferroviarie". Firenze University Press.
[373] Presti, D. L. (2013). Recycled tyre rubber modified bitumens for road asphalt mixtures: a literature review. Construction and Building Materials, 49, 863-881.
[374] Presti, D. L., Airey, G., Rubio, M. C., & Marsac, P. (2017, March). SUP&R ITN: An international training network on sustainable pavements and railways. Proceedings of the AIIT International Congress on Transport Infrastructure and Systems (Rome, Italy, 10-12 April 2017) (p. 47). CRC Press.
[375] Presti, D. L., Fecarotti, C., Clare, A. T., & Airey, G. (2014). Toward more realistic viscosity measurements of tire rubber–bitumen blends. Construction and Building Materials, 67, 270-278.
[376] Profillidis V., A. (2000). "Railway Engineering (2nd Edition)". Chippenham, Wiltshire: Ashgate Publishing Company.
[377] Putman, B. J., & Amirkhanian, S. N. (2010). Characterization of the interaction effect of crumb rubber modified binders using HP-GPC. Journal of Materials in Civil Engineering, 22(2), 153-159.
[378] Qasim, Z. I., Abbas, A. S., & Qasim, Z. I. (2017). "Effect of Filler Content on Properties of Asphaltic Mixtures for Marshall and Superpave Gyratory Compactor". Al-Nahrain Journal for Engineering Sciences, 20(1), 183-193.
[379] Rahman MM, Airey G., Collop AC. (2010). Moisture susceptibility of high and low compaction dry process crumb rubber modified asphalt mixtures. TRB; 2010 [annual meeting].
[380] Rahman MM, Airey GD, Collop AC. The mechanical properties of the dry process CRM asphalt mixtures following short-term and long-term ageing. Recycled materials in road and airfield pavements. Norway, Workshop; 2005.
[381] Rahman, F. (2010). Performance evaluation of 4.75-mm NMAS superpave mixture. Kansas State University.
[382] Rahman, Mujibur. (2004). "Characterisation of dry process crumb rubber modified asphalt mixtures". Diss. University of Nottingham, 2004.
[383] Raymond, G. P. (1984). Research on geotextiles for heavy haul railways. Canadian Geotechnical Journal, 21(2), 259-276.

[384] Rebala, S.R. and Estakhri, C.K. (1995). Laboratory evaluation of crumb rubber modified mixtures designed using TXDOT mixture design method. Transportation Research Record, 1515, 1–10.
[385] Rezaie, F., Shiri, M. R., & Farnam, S. M. (2012). Experimental and numerical studies of longitudinal crack control for pre-stressed concrete sleepers. Engineering Failure Analysis, 26, 21-30.
[386] Rhayma N., Bressolette P., Breul P., Fogli M., Saussine G., (2013). "Reliability Analysis of Maintenance Operations for Railway Tracks". Reliability Engineering & System Safety, 114, 12–25.
[387] Roberts, F.L., Kandhal, P.S., Brown, E.R., Lee, D.Y., and Kennedy, T.W. (1996). Hot Mix Asphalt Materials, Mixture Design, and Construction. National Asphalt Paving Association Education Foundation. Lanham, MD.
[388] Roberts, F.L., Mohammad, L.N., Wang, L.B. (2002). History of Hot Mix Asphalt Mixture Design in the United States J. Mat. in Civ. Engrg., Volume 14, Issue 4, pp. 279-293.
[389] Robinet, A. and A. Cuccaroni. (2010) Subballast Layer Made of Bituminous Material, Proceedings 7th World Congress on High Speed Rail, Beijing, December 2010, pages 727-730.
[390] Robinson M. and Kapoor A. (2009). "Fatigue in railway infrastructure". Woodhead publishing limited. Elsevier.
[391] Romero, M. J. G., Edwards, J. R., Barkan, C. P., Wilson, B., & Mediavilla, J. (2010). Advancements in Fastening System Design for North American Concrete Crossties in Heavy-Haul Service. In Proceedings of the AREMA 2010 Annual Conference & Exposition.
[392] Roque R., Birgisson B., Sangpetnagam B., Zhang Z. (2002). "Hot Mix Asphalt Fracture Mechanics: A Fundamental Crack Growth Law for Asphalt Mixtures", Journal of the Association of Asphalt Paving Technologists (AAPT), Kansas city, Vol. 71, pp. 816-827.
[393] Rose J., Liu S., Souleyrette R.R. (2014). "Kentrack 4.0: a railway trackbed structural design program". Proceedings of the 2014 Joint Rail Conference JRC 2014 April 2-4, 2014, Colorado Springs, USA.
[394] Rose J.G., Li D., Walker L.A., (2002). "Tests and evaluations of in-service asphalt trackbeds." American Railway Engineering and Maintenance-of-Way Association, Annual Conference & Exposition, Washington, D.C., USA.
[395] Rose J.G.; Bryson L.S., (2009). "HMA railway trackbeds: trackbed materials, performance evaluations, and significant implications". International Conference on Perpetual Pavements, Columbus, Ohio, USA.
[396] Rose, J. and Stith, J., (2004) Tekscan Sensors: Rail/Tie Interface Pressure Measurement in Railway Trackbeds. Proceedings of Railway Engineering - 7th International Conference and Exhibition, London, United Kingdom, June, 21 pages.
[397] Rose, J. G. (1983). "Hot-Mix Asphalt Trackbed Construction," Proceedings of tbe 95th Annual Conference of the Roadmasters' and Maintenance of Way Association of America, pp. 61-81.
[398] Rose, J. G. (1986). "Performance and Economic Evaluation of Hot-Mix Asphalt Trackbeds. An Update," Proceedings of tbe 98th Annual Conference of tbe Roadmasters and Maintenance of Way Association of America, 14 pages.
[399] Rose, J. G. (2000). Asphalt Trackbeds: Selection, Design, Installation Pratices, Long-Term. Proceedings of Railway Engineering-2000, 3rd International Conference and Exhibition, London, July, 12 p.
[400] Rose, J. G. (2014). Railway Trackbeds: In-Track Tests. Evaluations, and Performances–A Global Perspective.
[401] Rose, J. G., & Konduri, K. C. (2006). KENTRACK—A railway trackbed structural design program. In AREMA 2006 Annual Conference (pp. 17-20).
[402] Rose, J. G., Agarwal, N. K., Brown, J. D., & Ilavala, N. (2010). KENTRACK, A Performance-Based Layered Elastic Railway Trackbed Structural Design and Analysis Procedure–A Tutorial. In Proceedings of the 2010 Joint Rail Conference (pp. 73-110).
[403] Rose, J. G., Souleyrette, R. R., McHenry, M., Greenwell, T., Peng, X., Brown, M., & LoPresti, J. (2015). Tie-Ballast Interaction (No. NURAIL2013-UKY-R05).
[404] Rose, J. G., Su, B., & Long, W. B. (2003). Kentrack: a structural analysis program for heavy axle load railway trackbed designs. In PROCEEDINGS OF THE INTERNATIONAL CONFERENCE AND EXHIBITION RAILWAY ENGINEERING 2003, HELD LONDON, UK, 30 APRIL-1 MAY 2003-CDROM.
[405] Rose, J. G., Teixeira, P. F., & Ridgway, N. E. (2010, January). Utilization of asphalt/bituminous layers and coatings in railway trackbeds: a compendium of international applications. In 2010 Joint Rail Conference (pp. 239-255). American Society of Mechanical Engineers.
[406] Rose, J. G., Teixeira, P. F., & Veit, P. (2011). International design practices, applications, and performances of asphalt/bituminous railway trackbeds. In GEORAIL 2011—International symposium, Paris, France (pp. 19-20).
[407] Rose, J. G., Trella, M. C., & Agarwal, N. K. (2011, January). Structural Design of Railway Trackbeds: Relative Effects of Various Factors. In 2011 Joint Rail Conference (pp. 45-64). American Society of Mechanical Engineers.
[408] Rose, J. G., Y. H. Huang, and V. P. Drnevich, (1986). "Hot-Mix Asphalt Underlayments for Heavy-Haul Trackbeds," Proceedings 3rd International Heavy Haul Railway Conference, 11 pages.
[409] Rose, J., Brown, E., & Osborne, M. (2000). Asphalt trackbed technology development: the first 20 years. Transportation Research Record: Journal of the Transportation Research Board, (1713), 1-9.
[410] Rose, J., Chang, K., Brown, S., Perkins, R., Boyle, L., Cofer, W. (2016). Rail Engineering and Education Symposium Materials (No. NURail2012-UKY-E01).
[411] Rowe, G. M. (1996). Application of the dissipated energy concept to fatigue cracking in asphalt pavements (Doctoral dissertation, University of Nottingham).
[412] Rowe, G. M. (1993). Performance of Asphalt Mixtures in the Trapezoidal Fatigue Test. Proceedings of the Association of Asphalt Paving Technologist (AAPT), 62.
[413] Ruano Gomez A., (2007). "Las líneas de alta velocidad frente a las líneas convencionales".

[414] Rudenskaya, I. M. (1967). Rheological Properties of Bitumen.
[415] Ryden, N. (2009). Determining the asphalt mastercurve from free-free resonant testing on cylindrical samples. In Proc. of the 7 th Int. Symp. on Non-Destructive Testing in Civil Engineering (NDTCE'09), Ed by A. Odile and D. Xavier.
[416] S. D. Tarabji, M. R. Thompson (1976). "Finite Element Analysis of a Railway Track Support System, User's Manual," Report No. FRA-OR & 0-76-257, U.S. Department of Transportation.
[417] S. Fateen (1972). "A Finite Element Analysis of Full Depth Asphalt Railroad Track," Master's Thesis, Department of Civ il Engineering, University of Maryland.
[418] Sadeghi, J. & Barati, P. (2010). Evaluation of conventional methods in analysis and design of railway track system. International Journal of Civil Engineering, 8(1), 44-55.
[419] Sadeghi, J. M., & Babaee, A. (2006). Structural optimization of B70 railway prestressed concrete sleepers. Iranian Journal of Science & Technology, Transaction B: Engineering, 30(B4), 461-473.
[420] Sadeghi, J., Liravi, H., & Esmaeili, M. H. (2017). Experimental investigation on loading pattern of railway concrete slabs. Construction and Building Materials, 153, 481-495.
[421] Salgado R, Yoon S, Zia Siddiki N (2003). Construction of tire shreds tests embankment. Joint Transportation Research Program. Technical Report Nº: FHWA/IN/JTRP-2002/35. Available at: http://docs.lib.purdue.edu/jtrp/42/. Accessed 11 February 2013.
[422] Sangiorgi, C., Eskandarsefat, S., Tataranni, P., Simone, A., Vignali, V., Lantieri, C., & Dondi, G. (2017). A complete laboratory assessment of crumb rubber porous asphalt. Construction and Building Materials, 132, 500-507.
[423] Santiago E, García JL, González P (2010). Comparison of different subballast compaction control methods. CEDEX.
[424] Santoyo-Castelazo, E., & Azapagic, A. (2014). Sustainability assessment of energy systems: integrating environmental, economic and social aspects. Journal of Cleaner Production, 80, 119-138.
[425] Saunders, S. C. (1975). A Synthesis of Crack Growth Theories in Fatigue into Some Statistical Distributions of Fatigue Life. WASHINGTON STATE UNIV PULLMAN DEPT OF PURE AND APPLIED MATHEMATICS.
[426] Schiebel, B. (2003). Final Recommendation to Address Gyratory Angle and In-Place Voids Studies, Discussion with CDOT/Industry Group on October 18, 2002. Accessed at www.coasphalt.com/asphalt_news/cdot_issues/, April 1, 2003.
[427] Schram, S., & Abdelrahman, M. (2006). Improving prediction accuracy in mechanistic-empirical pavement design guide. Transportation Research Record: Journal of the Transportation Research Board, (1947), 59-68.
[428] Sefidmazgi, N. R. (2014). Hot mix asphalt design to optimize construction and rutting performance properties (Doctoral dissertation, The University of Wisconsin-Madison).
[429] Selig, E. T., & Waters, J. M. (1994). Track geotechnology and substructure management. Thomas Telford.
[430] Shafabakhsh, G. H., Sadeghnejad, M., & Sajed, Y. (2014). A case study of rutting performance of HMA modified with waste rubber powder. Case Studies in Construction Materials, 1, 69-76.
[431] Shahraki, M., Warnakulasooriya, C., & Witt, K. J. (2015). Numerical study of the transition zone between ballasted and ballastless railway track. Transportation Geotechnics, 3, 58-67.
[432] Shao, H., Sun, L., Liu, L., You, Z., & Yang, X. (2017). A novel double-drum mixing technique for plant hot mix asphalt recycling with high reclaimed asphalt pavement content and rejuvenator. Construction and Building Materials, 134, 236-244.
[433] Shell International Petroleum Company, ltd. (1978). Shell Pavement Design Manual: Asphalt Pavements and Overlays for Road Traffic. Shell International Petroleum Company.
[434] Shen S, Carpenter SH. (2007). Dissipated energy concepts for HMA performance: fatigue and healing. In: Center of excellence for airport technology, COE Report No. 29. Technical Report of Research. Federal Aviation Administration. Urbana-Champaign, Urbana, IL: University of Illinois.
[435] Shen, J., & Xie, Z. (2012). Comprehensive evaluation of the long-term performance of rubberized pavement: Phase I: Laboratory study of rubberized asphalt mix performance (No. FHWA-GA-12-1119).
[436] Shen, J., Amirkhanian, S., Xiao, F., & Tang, B. (2009). Influence of surface area and size of crumb rubber on high temperature properties of crumb rubber modified binders. Construction and Building Materials, 23(1), 304-310.
[437] Shen, J., Li, B., & Xie, Z. (2017). Interaction between crumb rubber modifier (CRM) and asphalt binder in a dry process. Construction and Building Materials, 149, 202-206.
[438] Shen, S. and S. H. Carpenter, "Dissipate Energy Concepts for HMA Performance: Fatigue and Healing," Department of Civil and Environmental Engineering, the University of Illinois at Urbana-Champaign, 2007.
[439] Shen, S., & Carpenter, S. (2007). Development of an asphalt fatigue model based on energy principles. Asphalt Paving Technology-Proceedings, 76, 525.
[440] Sheng, X., Jones, C. J. C., & Thompson, D. J. (2004). A theoretical model for ground vibration from trains generated by vertical track irregularities. Journal of sound and vibration, 272(3), 937-965.
[441] Shu, X., & Huang, B. (2014). Recycling of waste tire rubber in asphalt and portland cement concrete: An overview. Construction and Building Materials, 67, 217-224.
[442] Shuler, T. S., Pavlovich, R. D., Epps, J. A., & Adams, C. K. (1985). Investigation of materials and structural properties of asphalt-rubber paving mixtures. Technical Rep. Prepared for Federal Highway Administration, Washington, DC.
[443] Shulman V.L., (2000). "Tyre Recycling After 2000: Status and Options", European Tyre Recycling Association, Paris, France.
[444] Siddique, R., & Naik, T. R. (2004). Properties of concrete containing scrap-tire rubber–an overview. Waste management, 24(6), 563-569.

[445] Sienkiewicz, M., Borzędowska-Labuda, K., Wojtkiewicz, A., & Janik, H. (2017). Development of methods improving the storage stability of bitumen modified with ground tire rubber: A review. Fuel Processing Technology, 159, 272-279.
[446] Signes, C. H., Fernández, P. M., de la Torre, M. G., & Franco, R. I. (2016). Unbound Granular Materials for Sub-Ballast Layers and their Mixing with Rubber Particles from Scrap Tyres.
[447] Silva H., Oliveira J., Peralta J., Zoorob S., (2010). "Optimization of warm mix asphalts using different blends of binders and synthetic paraffin wax contents." Constr Build Mater;24:1621–31.
[448] Silvrano A. Dantas Neto, Márcio Muniz de Farias and Luiz Guilherme R. Mello Paulo Pereira and Jorge Carvalho Pais (2005). The use of crumb rubber in asphalt mixtures using the dry process. 2005 international symposium on pavement recycling são paulo –Brazil.
[449] Singleton, T. M., Airey, G. D., & Collop, A. C. (2000). "Effect of rubber-bitumen interaction on the mechanical durability of impact absorbing asphalt". In Proceedings submitted for review at 2nd Eurasphalt and Eurobitume congress, 2000, Barcelona, Spain. Book 1 session 4.
[450] Singleton, T. M., Airey, G. D., Collop, A. C., & Widyatmoko, I. (2000). Residual bitumen characteristics following dry process rubber-bitumen interaction. In Proceedings of the Asphalt Rubber Conference (pp. 463-482). Portugal: Vilamoura.
[451] Smith, R. A. (2005). Railway fatigue failures: an overview of a long-standing problem. Materialwissenschaft und Werkstofftechnik, 36(11), 697-705.
[452] Smutny J.M., (2004). "Measurement and analysis of dynamic and acoustic parameters of rail fastening", NDT&E International, 37, 119-129.
[453] Sobolev, K., Moini, M., Muzenski, S., Rani Pradoto, D., Kozhukhova, M., Flores-Vivian, I., & Faheem, A. (2015). Laboratory Study of Optimized Concrete Pavement Mixtures (No. WHRP 0092-13-04). Wisconsin Highway Research Program.
[454] Soimakallio, S., & Koponen, K. (2011). How to ensure greenhouse gas emission reductions by increasing the use of biofuels? European Union sustainability criteria. Biomass and Bioenergy, 35(8), 3504-3513.
[455] Sokolnikoff, I. S. (1956). Mathematical theory of elasticity. McGraw-Hill Book Company.
[456] Solaimanian, M., & Kennedy, T. W. (1993). Predicting maximum pavement surface temperature using maximum air temperature and hourly solar radiation. Transportation Research Record, 1-1.
[457] Sol-Sánchez, M. (2014). Desarrollo de elementos elásticos a partir de capas de neumáticos fuera de uso para su aplicación en vías de ferrocarril. Universidad de Granada.
[458] Sol-Sánchez, M., & D'Angelo, G. (2017). Review of the design and maintenance technologies used to decelerate the deterioration of ballasted railway tracks. Construction and Building Materials, 157, 402-415.
[459] Sol-Sánchez, M., Moreno-Navarro, F., & Rubio-Gámez, M. (2014). The use of deconstructed tires as elastic elements in railway tracks. Materials, 7(8), 5903-5919.
[460] Sol-Sánchez, M., Moreno-Navarro, F., & Rubio-Gámez, M. C. (2014). Viability of using end-of-life tire pads as under sleeper pads in railway. Construction and Building Materials, 64, 150-156.
[461] Sol-Sánchez, M., Pirozzolo, L., Moreno-Navarro, F., & Rubio-Gámez, M. C. (2016). A study into the mechanical performance of different configurations for the railway track section: A laboratory approach. Engineering Structures, 119, 13-23.
[462] Sol-Sánchez, M., Pirozzolo, L., Moreno-Navarro, F., & Rubio-Gámez, M. C. (2015). Advanced characterisation of bituminous sub-ballast for its application in railway tracks: The influence of temperature. Construction and Building Materials, 101, 338-346.
[463] Sol-Sánchez, M., Thom, N. H., Moreno-Navarro, F., Rubio-Gámez, M. C., & Airey, G. D. (2015). A study into the use of crumb rubber in railway ballast. Construction and Building Materials, 75, 19-24.
[464] Solyman, M. (2005). Classification of recycled sands and their applications as fine aggregates for concrete and bituminous mixtures. Doktor-Ingenieurs Dissertation, Fachbereich Bauingenieurwesen der Universität Kassel, Kassel.
[465] Soto, F. M. (2018). "Volumetric Mix-Design optimization of bituminous rubber-mixtures in railway sub-ballast," (IJESRT/Q080/17) International Journal of Engineering Sciences and Research Technology, ISSN: 2277-9655, DOI: 10.5281/zenodo.1158653 [Volume 7, Issue 1, N°61, pp. 483-507, January 2018].
[466] Soto, F. M. (2018). "Eco-Sustainable optimization of the mix-design methodology in modified bituminous mixtures with high percentage of recycled tire rubber," (GJESRM/A008/18) Global Journal of Engineering Science and Research Management, ISSN: 2349-4506, DOI: 10.5281/zenodo.1156460 [Volume 5, Issue 1, N°5, pp. 37-59, January 2018].
[467] Soto, F. M. , Mino, G. D. (2017). 'Increased Stability of Rubber-Modified Asphalt Mixtures to Swelling, Expansion and Rebound Effect during Post-Compaction'. World Academy of Science, Engineering and Technology, International Science Index, Transport and Vehicle Engineering, 11(7), 334. urn:dai:10.1999/1307-6892/73683.
[468] Soto, F. M., & Di Mino, G. (2017). Empirical Superpave Mix-Design of Rubber-Modified Hot-Mix Asphalt in Railway Sub-Ballast. World Academy of Science, Engineering and Technology. International Journal of Civil and Environmental Engineering, Vol. 4, N°(9). DOI:10.1999/1307-6892/69025.
[469] Soto, F. M., & Di Mino, G. (2017). Optimization of mix-design system for the sub-ballast railroad. Journal of Traffic and Transportation Engineering, 5, 246-259. DOI: 10.17265/2328-2142/2017.05.002 David Publishing Company, Valley Cottage, NY, USA [Volume 5, N° 5, Sept-Oct 2017, pp.246-259].
[470] Soto, F. M., & Di Mino, G. (2017). Procedure for a Temperature-Traffic Model on Rubberized Asphalt Layers for Roads and Railways. Journal of Traffic and Transportation Engineering, 5, 171-202. DOI: 10.17265/2328-2142/2017.04.001 David Publishing Company, Valley Cottage, NY, USA [Volume 5, N°4, July-August 2017, pp.171-202].

[471] Soto, F. M., & Di Mino, G. (2018). "Characterization of rubberized asphalt for railways," (IJESRT/R067/17) International Journal of Engineering Sciences and Research Technology, ISSN: 2277-9655, DOI:10.5281/zenodo.1173468 [Volume 7, Issue 2, N°41, pp. 284-303, February 2018].
[472] Soto, F. M., & Di Mino, G. (2018). "Improvements in the mix-design, performance features and rational methodology of rubber modified binders for the thermal evaluation of the railway sub-ballast," (IJRSM/F09/17) International Journal of Research Science & Management, ISSN: 2349-5197, DOI:10.5281/zenodo.1175219 [Volume 5, Issue 2, N°7, pp. 90-108, February 2018].
[473] Soto, F. M., Di Mino, G., & Acuto, F. (2017) Effect of Temperature and traffic on mix-design of bituminous asphalt for railway sub-ballast layer. Loizos, A., Al-Qadi, I., & Scarpas, T. (Eds.). Bearing Capacity of Roads, Railways and Airfields: Proceedings of the 10th International Conference (BCRRA 2017), June 28-30, 2017, Athens, Greece. CRC Press.
[474] Soto, F. M., Di Mino, G., & Di Liberto, C. M. (2016). "Evaluation of Dry Asphalt Rubber Concrete in Railway Sub-Ballast using the Four Point Bending Test", in J. Pombo, (Editor), "Proceedings of the Third International Conference on Railway Technology: Research, Development and Maintenance", Civil-Comp Press, Stirlingshire, UK, Paper 37, 2016. doi:10.4203/ccp.110.37.
[475] Sousa JB, Weissman SL (1994). Modeling permanent deformation of asphalt-aggregate mixes. J. Assoc. Asphalt. Paving. Technol., 63: 224-257.
[476] Sousa, J. B., Way, G., Harvey, J. T., & Hines, M. (1995). Comparison of mix design concepts. Transportation Research Record, 1492, 151.
[477] Southgate, H. F., & Deen, R. C. (1968). Temperature Distribution Within Aspalt Pavements and its Relationship to Pavement Deflection.
[478] Straub, A. L., Schenck Jr, H. N., & Przbycien, F. E. (1968). Bituminous pavement temperature related to climate. Highway Research Record, (256).
[479] Stroup-Gardiner, M., Newcomb, D. E., & Tanquist, B. (1993). Asphalt-rubber interactions. Transportation research record, 1417, 99.
[480] Su, B. (2005). Effects of railroad track structural components and subgrade on damping and dissipation of train-induced vibration.
[481] Subhy A., Gordon Airey and Davide Lo Presti (2005), "An investigation of the mechanical properties of rubber modified asphalt mixtures using a modified dry process," June 2017, DOI: 10.1201/9781315100333-50, Conference Paper Bearing Capacity of Roads, Railways and Airfields, Athens, Greece.
[482] Sun, Y. Q., & Dhanasekar, M. (2002). A dynamic model for the vertical interaction of the rail track and wagon system. International Journal of Solids and Structures, 39(5), 1337-1359.
[483] Susmel, L., & Lazzarin, P. (2002). A bi-parametric Wöhler curve for high cycle multiaxial fatigue assessment. Fatigue & Fracture of Engineering Materials & Structures, 25(1), 63-78.
[484] Sutharsan, T. (2010). Quantification of cohesive healing of asphalt binder based on dissipated energy analysis (Doctoral dissertation, Washington State University).
[485] Swami, B. L., Mehta, Y. A., & Bose, S. (2004). A comparison of the Marshall and Superpave design procedure for materials sourced in India. International Journal of Pavement Engineering, 5(3), 163-173.
[486] Swapna, V. P., & Stephen, R. (2016). Recycling of Rubber. Recycling of Polymers: Methods, Characterization and Applications.
[487] Takallou, H. B., R. G. Hicks, and D. C. Esch. (1986). Effect of mix ingredients on the behavior of rubber-modified asphalt mixtures. Transportation Research Record 1096.
[488] Takkalou, H. B., Hicks, R. G. and ESCH, D. C. (1985). Behaviour of Rubber-Modified Mixes. Report No. FHWA-AK-RD-86-05A. Federal Highway Administration, Washington, D.C.
[489] Takallou, H., Bahia, H., Perdomo, D., & Schwartz, R. (1997). Use of Superpave technology for design and construction of rubberized asphalt mixtures. Journal of the Transportation Research Board, (1583), 71-81.
[490] Tang, J., Liu, Q., Wu, S., Ye, Q., Sun, Y., & Schlangen, E. (2016). Investigation of the optimal self-healing temperatures and healing time of asphalt binders. Construction and Building Materials, 113, 1029-1033.
[491] Tashman, L. S., Masad, E., Peterson, B., & Saleh, H. (2000). Internal structure analysis of asphalt mixes to improve the simulation of superpave gyratory compaction to field conditions (Master's thesis, Washington State University).
[492] Tauste, R., Moreno-Navarro, F., Gallego, R., & Rubio-Gámez, M. C. (2017). Analysis of the sensitivity of the impact resonance frequency test as a tool to determine the elastic properties of bituminous materials. Materiales de Construcción, 67(327), 131.
[493] Tayebali, A. A., Coplantz, J. S., Harvey, J. T., & Monismith, C. L. (1992). Interim report on fatigue response of asphalt-aggregate mixtures. SHRP project A-003A, TM-UCB-A-003A-92-1, Asphalt research program, Institute of Transportation Studies, University of California-Berkeley, CA.
[494] Teixeira P.F., López Pita A., Casas C., Bachiller A., & Robusté, F., (2006). "Improvements in high-speed ballasted track design: benefits of bituminous subballast layers," TRB, Journal of the Transportation Research Board N° 1943, (pp.43-49).
[495] Teixeira, P. F. (2004). Contribución a la reducción de los costes de mantenimiento de vías de alta velocidad mediante la opitimización de su rigidez vertical. Universitat Politècnica de Catalunya.
[496] Teixeira, P. F., Ferreira, P. A., Pita, A. L., Casas, C., & Bachiller, A. (2009). The use of bituminous sub-ballast on future high-speed lines in Spain: structural design and economic impact. International Journal of Railway, 2(1), 1-7.

[497] Teixeira, P. F., Lopez Pita, A., & Ferreira, P. A. (2010). New possibilities to reduce track costs on high-speed lines using a bituminous sub-ballast layer. International Journal of Pavement Engineering, 11(4), 301-307.
[498] Teixeira, P.F. (2009) State of the Art on the Use of Bituminous Subballast on European High-Speed Rail Line. Workshop on Railroad Track Design Including Asphalt Trackbed, BCR2A conference - Eight International Conference on Bearing Capacity of Roads, Railways and Airfields. The University of Illinois at Urbana-Campaign (USA), June-July 2009.
[499] Thodesen, C., Shatanawi, K., & Amirkhanian, S. (2009). Effect of crumb rubber characteristics on crumb rubber modified binder viscosity. Construction and Building Materials, 23(1), 295-303.
[500] Thom N. H., Brown S.F., McDowell G.R., Konietzky H., Harireche O., (2006). "Discrete element modelling of geogrid-reinforced aggregates". Proceedings of The Institution of Civil Engineers-geotechnical Engineering, 159, pp. 35-48.
[501] Thom, N. (2006). Asphalt cracking: a Nottingham perspective. Ingenieria Civil/Civil Engineering, 26, 75-84.
[502] Thom, N. (2008). Principles of pavement engineering (p. 470). London: Thomas Telford.
[503] Thom, N. H., & Brown, S. F. (1987). Effect of moisture on the structural performance of a crushed-limestone road base (No. 1121).
[504] Thom, N. H., & Brownt, S. F. (2016). 17 The mechanical properties of unbound aggregates from various sources. Unbound aggregates in roads, 130.
[505] Thompson, M. R. (1992). Calibrated Mechanistic Structural Analysis Procedures for Pavements: Appendices (Vol. 2). National Cooperative Highway Research Program.
[506] Thompson, D. (2008). Railway noise and vibration: mechanisms, modelling and means of control. Elsevier.
[507] Tomioka, T., Takigami, T., & Aida, K. (2017). Experimental investigations on the damping effect due to passengers on flexural vibrations of railway vehicle carbody and basic studies on the mimicry of the effect with simple substitutions. Vehicle System Dynamics, 55(7), 995-1011.
[508] Torretta, V., Rada, E. C., Ragazzi, M., Trulli, E., Istrate, I. A., & Cioca, L. I. (2015). Treatment and disposal of tires: Two EU approach. A review. Waste management, 45, 152-160.
[509] Troy K, Sebaaly P, Epps J. Evaluation systems for crumb rubber modified binders and mixtures. Transportation Research Record, No. 1530. Washington, DC: TRB, National Research Council; 1996.
[510] Tutumluer, E., & Al-Qadi, I. L. (Eds.). (2009). Bearing Capacity of Roads, Railways, and Airfields, Two Volume Set: Proceedings of the 8th International Conference (BCR2A'09), June 29-July 2 2009, Unversity of Illinois at Urbana-Champaign, Champaign, Illinois, USA. CRC Press.
[511] Tzanakakis, K. (2013). The railway track and its long-term behavior: a handbook for a railway track of high quality (Vol. 2). Springer Science & Business Media.
[512] Usama, H. (2013). Effect of the repeated recycling on hot mix asphalt properties (Doctoral dissertation, Ph. D. thesis, Univ. of Nottingham, Nottingham, UK).
[513] UTAH-MT-07.03 (2007). TECHNICAL BULLETIN. Department of Transportation, https://www.udot.utah.gov
[514] Vaitkus A., Cygas A., Laurinavicius A., Perveneckas Z., (2009). "Analysis and evaluation of possibilities for the use of warm mix asphalt in Lithuania". The Baltic Journal of Road and Bridge Engineering 4 (2).
[515] Vallerga, B. A. (1981). Pavement deficiencies related to asphalt durability. In Association of Asphalt Paving Technologists Proceedings (Vol. 50).
[516] Van Dijk, W. (1975). Practical fatigue characterization of bituminous mixes. Journal of the Association of Asphalt Paving Technologists, 44, 38-72.
[517] Van Kirk, J. L. (1991). CalTrans experience with rubberized asphalt concrete. Proceedings of the Technology Transfer Session of an Introduction to Rubberized Asphalt Concrete, Topeka, Kansas.
[518] Vavrik, W. R. (2000). Asphalt mixture design concepts to develop aggregate interlock (Doctoral dissertation, the University of Illinois at Urbana-Champaign).
[519] Vijayaram, T. R. (2009). A technical review on rubber. Int. J. Design Manufact. Tech, 3, 25.
[520] Viola, F., & Celauro, C. (2015). Effect of climate change on asphalt binder selection for road construction in Italy. Transportation Research Part D: Transport and Environment, 37, 40-47.
[521] Wang, C., Zhao, L., Cao, W., Cao, D., & Tian, B. (2017). Development of paving performance index system for selection of modified asphalt binder. Construction and Building Materials, 153, 695-703.
[522] Wang, H., Silvast, M., Markine, V., & Wiljanen, B. (2017). Analysis of the Dynamic Wheel Loads in Railway Transition Zones Considering the Moisture Condition of the Ballast and Subballast. Applied Sciences, 7(12), 1208.
[523] Wang, Shifeng, Dingxin Cheng, and Feipeng X. (2017). "Recent developments in the application of chemical approaches to rubberized asphalt" Construction and Building Materials 131 (2017): 101-11.
[524] Way, G., Carlson, D., Sousa, J., Kaloush, K., and Biligiri, K. (2010). "Introduction to asphalt-rubber pavement noise reducing characteristics," 39th International Congress on Noise Control Engineering, Lisbon, Portugal, pp. 7408–7417.
[525] Wayne, J., UNL, Abdelrahrnan, M., Use of Crumb Rubber in Performance Graded Binder. University of Nebraska-Lincoln, 2006.
[526] Wei, K., Wang, F., Wang, P., Liu, Z. X., & Zhang, P. (2017). Effect of temperature-and frequency-dependent dynamic properties of rail pads on high-speed vehicle–track coupled vibrations. Vehicle System Dynamics, 55(3), 351-370.
[527] Williams, S. (2013). Comparison of the Superpave Gyratory and Proctor Compaction Methods for the Design of Roller-Compacted Concrete Pavements. Transportation Research Record: Journal of the Transportation Research Board, (2342), 106-112.

[528] Witczak, M. W., Von Quintus, H. L., & Schwartz, C. W. (1997). Superpave support and performance models management: Evaluation of the SHRP performance models system. In Eighth International Conference on Asphalt PavementsFederal Highway Administration (No. Volume III).
[529] Witczak, M.W. (2004) "Development of a mastercurve (E*) database for lime modified asphaltic mixtures", Arizona State University, Department of Civil and Environmental Engineering.
[530] Witzcak, M. W. (2002). Simple performance test for superpave mix design (Vol. 465). Transportation Research Board.
[531] Woertz, I. C., Benemann, J. R., Du, N., Unnasch, S., Mendola, D., Mitchell, B. G., & Lundquist, T. J. (2014). Life cycle GHG emissions from microalgal biodiesel–a CA-GREET model. Environmental science & technology, 48(11), 6060-6068.
[532] Wolfe SL, Humphrey DN, Wetzel EA (2004). Development of tire shred underlayment to reduce ground-borne vibration from LRT track. Geotechnical Engineering for Transportation Projects: Proceedings of the Geo-Trans 2004:750-759.
[533] Wulandari, P. S., & Tjandra, D. (2017). Use of crumb rubber as an additive in asphalt concrete mixture. Procedia engineering, 171, 1384-1389.
[534] Xiangwu D. Z., (2005). "Rubber-Modified Asphalt Concrete for High-Speed Railway Roadbeds; Final Report for High-Speed Rail". IDEA Project 40, Transportation Research Board, USA.
[535] Xiao F., Amirkhanian S., Shen J., Putman B. (2009). Influences of crumb rubber size and type on reclaimed asphalt pavement (RAP) mixtures. Construction and Building Materials.
[536] Yang, L. A., Powrie, W., & Priest, J. A. (2009). Dynamic stress analysis of a ballasted railway trackbed during train passage. Journal of Geotechnical and Geoenvironmental Engineering, 135(5), 680-689.
[537] Yang, Y. B., & Hsu, L. C. (2006). A review of researches on ground-borne vibrations due to moving trains via underground tunnels. Advances in Structural Engineering, 9(3), 377-392.
[538] Yin, J., Wang, S., & Lv, F. (2013). Improving the short-term aging resistance of asphalt by addition of crumb rubber radiated by microwave and impregnated in epoxidized soybean oil. Construction and Building Materials, 49, 712-719.
[539] Yoder, E. J., & Witczak, M. W. (1975). Principles of pavement design. John Wiley & Sons.
[540] Yoon S, Prezzi M, Zia Siddiki N, Kim B (2005). Construction of a test embankment using a sand-tire shred mixture as fill material. Waste Management 26:1033-1044.
[541] Yu, M., Wu, G., Zhou, J., & Easa, S. (2014). Proposed compaction procedure for dry process crumb rubber modified asphalt mixtures using air void content and expansion ratio. Journal of Testing and Evaluation, 42(2), 328-338.
[542] Z. Xie, J. Shen (2016). Performance of porous European mix (PEM) pavements added with crumb rubbers in a dry process, Int. J. Pavement Eng. 17 (7) pp.637–646.
[543] Zanetti, M. C., Fiore, S., Ruffino, B., Santagata, E., Dalmazzo, D., & Lanotte, M. (2015). Characterization of crumb rubber from end-of-life tyres for paving applications. Waste Management, 45, 161-170.
[544] Zanzotto L, Kennepohl G. (1996). Development of Rubber and asphalt binders by depolymerization and devulcanization of scrap tires in asphalt. Trans. Res. Board, 1530. Washington (DC): TRB, National Research Council; 1996. p. 51–9.
[545] Zaumanis et al. (eds.), Climate Change, Energy, Sustainability and Pavements, Green Energy and Technology, Springer-Verlag, (2014), DOI: 10.1007/978-3-662-44719-2_10.
[546] Zaumanis M., Mallick R.B., (2015). "Review of very high-content reclaimed asphalt use in plant-produced pavements: state of the art", Int. J. Pavement Eng. 16 (1) 39–55.
[547] Zaumanis, M., Poulikakos, L. D. and Partl, M. N. (2018) "Performance-based design of asphalt mixtures and review of key parameters," Materials and Design. Elsevier Ltd, 141, pp. 185–201. doi: 10.1016/j.matdes.2017.12.035.
[548] Zeng, X. (2005). Rubber-Modified asphalt concrete for high-speed railway roadbeds. Department of Civil Engineering, Case Western Reserve University.
[549] Zeng, X., Rose, J. G., & Rice, J. S. (2001). Stiffness and damping ratio of rubber-modified asphalt mixes: Potential vibration attenuation for high-speed railway trackbeds. Journal of Vibration and Control, 7(4), 527-538.
[550] Zhai, W., Wei, K., Song, X., & Shao, M. (2015). Experimental investigation into ground vibrations induced by very high-speed trains on a non-ballasted track. Soil Dynamics and Earthquake Engineering, 72, 24-36.
[551] Zhang, T. W., Cui, Y. J., Lamas-Lopez, F., Calon, N., & D'Aguiar, S. C. (2016). Modelling stress distribution in substructure of French conventional railway tracks. Construction and Building Materials, 116, 326-334.
[552] Zhang, Z., Roque, R., & Birgisson, B. (2001). Evaluation of laboratory-measured crack growth rate for asphalt mixtures. Transportation Research Record: Journal of the Transportation Research Board, (1767), 67-75.
[553] Zhang, Z., Zhang, X., Qiu, H., & Daddow, M. (2016). Dynamic characteristics of track-ballast-silty clay with irregular vibration levels generated by high-speed train based on DEM. Construction and Building Materials, 125, 564-573.
[554] Zhao, C., & Ping, W. (2018). Effect of elastic rubber mats on the reduction of vibration and noise in high-speed elevated railway systems. Proceedings of the Institution of Mechanical Engineers, Part F: Journal of Rail and Rapid Transit, 0954409717752201.
[555] Zhong X.G., Xiangwu D.Z., and Rose J.G., (2002). "Shear modulus and damping ratio of rubber-modified asphalt mixes and unsaturated subgrade soils". Journal of Materials in Civil Engineering, 14 (6), 496–502.
[556] Zhou, H., Holikatti, S., & Vacura, P. (2014). Caltrans use of scrap tires in asphalt rubber products: a comprehensive review. Journal of Traffic and Transportation Engineering (English Edition), 1(1), 39-48.
[557] Zoorob S.E., Suparma L.B., (2000). "Laboratory design and investigation of the properties of continuously graded asphaltic concrete containing recycled plastic aggregate replacement (Plastiphalt)". Compos; 22:2.
[558] Zumrawi, M. M. (2016). International Journal of Scientific and Technical Advancements Comparison of Marshall and Superpave Asphalt Design Methods for Sudan Pavement Mixes.

Normative (Standards)

[1] AASHTO M 323 (2013). Standard specification for Superpave volumetric mix design.
[2] AASHTO PP2 (1999). Standard Practice for Short and Long Term Aging of Hot Mix Asphalt. Washington, DC, 1994.
[3] AASHTO R 35 (2012) Standard Practice for Superpave Volumetric Design for Asphalt Mixtures. American Association of State Highway and Transportation Officials. Standard specifications for transportation materials and methods of sampling and testing (30th ed.). American Association of State Highway and Transportation Officials (AASHTO).
[4] AASHTO R35-151 (2001). "Superpave Volumetric Design for Asphalt Mixtures." (American Association of State Highway and Transportation Officials). 444 North Capitol Street N.W., Suite 249 Washington, D.C.
[5] AASHTO T 164 (2014) Quantitatie extraction of asphalt binder from HMA.
[6] AASHTO T 209 (2012) Standard Method of Test for Theoretical Maximum Specific Gravity and Density of HMA.
[7] AASHTO T 245: Resistance to Plastic Flow of Bituminous Mixtures Using Marshall Apparatus.
[8] AASHTO T 316 (2008). Standard Method of Test for Viscosity Determination of Asphalt Binder Using Rotational Viscometer. American Association of State Highway and Transportation Officials.
[9] AASHTO T166 (2016)."Bulk Specific Gravity of Compacted Hot Mix Asphalt using Saturated Surface-Dry Specimens." Standard Specifications for Transportation Materials and Methods of Sampling and Testing, 27th Edition, American Association of State Highway and Transportation Officials, Washington, DC.
[10] AASHTO T275 (2017) Bulk Specific Gravity of Compacted Hot Mix Asphalt (HMA) Using Paraffin-Coated Specimens.
[11] AASHTO T283 (2014) "Resistance of Compacted Bituminous Mixture to Moisture Induced Damage".
[12] AASHTO TP4 (2000). Standard method for preparing and determining the density of hot mix asphalt (HMA) specimens using the SHRP Gyratory Compactor. FHWA Multi-Regional Asphalt Training and Certification Group, 14.
[13] Asphalt Institute (2003) Superpave Performance Graded Asphalt Binder Specifications and Testing, 3rd Ed.,72 pp.
[14] Asphalt Institute. SUPERPAVE mix design series no. 2 (SP-2). Lexington (KY): Asphalt Institute Research Center; 2001.
[15] AI, 1981a . Thickness Design—Asphalt Pavements for Highways and Streets, Manual Series No. 1; Asphalt Institute.
[16] AI, 1981b. Asphalt Pavement Thickness Design, Information Series No. 181; Asphalt Institute.
[17] AI, 1982. Research and Development of The Asphalt Institute's Thickness Design Manual (MS-1), 9th ed., Report 82-2.
[18] ASTM C127-04, Test Method for Relative Density (Specific Gravity) and Absorption of Coarse Aggregate.
[19] ASTM C128-15, Standard Test Method for Relative Density (Specific Gravity) and Absorption of Fine Aggregate, ASTM International, West Conshohocken, PA, 2015.
[20] ASTM C215-14, Standard Test Method for Fundamental Transverse, Longitudinal, and Torsional Resonant Frequencies of Concrete Specimens, ASTM International, West Conshohocken, PA, 2014.
[21] ASTM C1800 / C1800M-16, Standard Test Method for Determining Density of Roller-Compacted Concrete Specimens Using the Gyratory Compactor, ASTM International, West Conshohocken, PA, 2016.
[22] ASTM D2170 / D2170M-10, Standard Test Method for Kinematic Viscosity of Asphalts (Bitumens), ASTM International, West Conshohocken, PA, 2010.
[23] ASTM D2172M (2017) Standard Test Method for Quantitative Extraction of Bitumen From Bituminous Paving Mixtures.
[24] ASTM D2493M-16, Standard Practice for Viscosity-Temperature Chart for Asphalt Binders, ASTM International, 2016.
[25] ASTM D2983-17, Standard Test Method for Low-Temperature Viscosity of Automatic Transmission Fluids, Hydraulic Fluids, and Lubricants using a Rotational Viscometer, ASTM International, West Conshohocken, PA, 2017.
[26] ASTM D4402 / D4402M-15, Standard Test Method for Viscosity Determination of Asphalt at Elevated Temperatures Using a Rotational Viscometer, ASTM International, West Conshohocken, PA, 2015.
[27] ASTM D4867 (2014) "Effect of Moisture on Asphalt Concrete Paving Mixtures".
[28] ASTM D6114M-09, Standard Specification for Asphalt-Rubber Binder, ASTM International, 2009.
[29] ASTM D6925 (2015) Standard Test Method for Preparation and Determination of the Relative Density of Asphalt Mix Specimens by Means of the Superpave Gyratory Compactor, ASTM International, West Conshohocken, PA, 2015.
[30] ASTM D6927 (2015) Standard Test Method for Marshall Stability and Flow of Asphalt Mixtures, ASTM International.
[31] ASTM D8079-16, Standard Practice for Preparation of Compacted Slab Asphalt Mix Samples Using a Segmented Rolling Compactor, ASTM International, West Conshohocken, PA, 2016.
[32] ASTM E1876-15, Standard Test Method for Dynamic Young's Modulus, Shear Modulus, and Poisson's Ratio by Impulse Excitation of Vibration, ASTM International, West Conshohocken, PA, 2015.
[33] Asphalt Institute. (1981). Thickness design--asphalt pavements for highways and streets (No. 1). Asphalt Institute.
[34] BS 1377-9 (1990). Methods for test for soils for civil engineering purposes. In-situ tests: determination of the vertical deformation and strength characteristics of soil by the plate loading. British Standards Institution.
[35] C.N.R.-B.U. n.30 (15/03/73) - Determinazione della stabilità e dello scorrimento di miscele di bitume e inerti lapidei a mezzo dell'apparecchio Marshall.
[36] C.N.R.-B.U. 39 (23/03/1973) - Determinazione della porosità o percentuale dei vuoti di miscele di aggregati lapidei con bitume. RFI Capitolato Costruzione Opere Civili, sezione XV Sub-ballast.
[37] C.N.R.-B.U. n.134 (19/12/91) - Norme sulle miscele di aggregati e leganti idrocarburici. Determinazione della resistenza a trazione indiretta e della deformazione a rottura di miscele di aggregati lapidei e bitume.
[38] C.N.R.-B.U. n.8 (21/03/73). Determinazione del contenuto di legante di miscele di bitume e aggregati lapidei.

[39] Design, S. M. (1996). Superpave Series No. 2 (SP-2). Asphalt Institute, Lexington, KY.
[40] EN 12620:2002+A1:2008. Aggregates for concrete.
[41] EN 12697-10 (2017) Bituminous mixtures. Test methods. Compactability.
[42] EN 12697-12 (2008) Bituminous mixtures. Test methods for hot mix asphalt. Determination of the water sensitivity.
[43] EN 12697-2 (2015) Bituminous mixtures. Test method. Determination of particle size distribution.
[44] EN 12697–23 (2017) Bituminous mixtures. Determination of the indirect tensile strength of bituminous specimen.
[45] EN 12697-24 (2012) Bituminous mixtures. Test method for hot mix asphalt. Resistance to fatigue.
[46] EN 12697-26 (2012) Bituminous mixtures - Test method for hot mix asphalt, Part 26: Stiffness.
[47] EN 12697-29 (2002) Bituminous mixtures. Test method for HMA. Determination of the dimensions of specimen.
[48] EN 12697-30 (2012) Bituminous mixtures - Test method for hot mix asphalt. Specimen preparation by impact compactor.
[49] EN 12697-31 (2007) Bituminous mixtures. Test method for hot mix asphalt. Specimen preparation by gyratory compactor.
[50] EN 12697-33 (2013) Bituminous mixtures — Test method for hot mix asphalt: Specimen prepared by roller compactor.
[51] EN 12697-34 (2012) Bituminous mixtures — Test method for hot mix asphalt: Marshall test.
[52] EN 12697-35 (2016) Bituminous mixtures — Test method for hot mix asphalt: Laboratory mixing.
[53] EN 12697-5 (2009) Bituminous mixtures. Test method for hot mix asphalt. Determination of the maximum density.
[54] EN 12697-6 (2012) Bituminous mixtures. Test method for hot mix asphalt. Determination of bulk density.
[55] EN 12697-8 (2003) Bituminous mixtures. Test methods for hot mix asphalt. Determination of void characteristics.
[56] EN 12697-9 (2003) Bituminous mixtures. Test methods for hot mix asphalt. Determination of the reference density.
[57] EN 13055-2:2004. Lightweight aggregates. Lightweight aggregates for bituminous mixtures and surface treatments and for unbound and bound applications.
[58] EN 13302:2010, BS 2000-505:2010. Bitumen and bituminous binders. Determination of dynamic viscosity of bituminous binder using a rotating spindle apparatus.
[59] EN 1426 (2007) Bitumen and bituminous binders—determination of needle penetration. British Standards.
[60] EN 1427 (2007) Bitumen and bituminous binders—Determination of the softening point—Ring and Ball method.
[61] EN 933-1 (2012) Tests for geometrical properties of aggregates. Determination of particle size distribution. Sieving.
[62] EN 933-10 (2009) Tests for geometrical properties of aggregates. Assessment of fines. Grading of filler aggregates.
[63] EN 933-2 (2012) Determination of particle size distribution. Test sieves, nominal size of apertures.
[64] EN-12591 (2009) Bitumen and bituminous binders—Specifications for paving grade bitumens.
[65] EN-12595 (2007) Bitumen and bituminous binders. Determination of kinematic viscosity.
[66] EN-12596 (2014) Bitumen and bituminous binders. Determination of dynamic viscosity by vacuum capillary.
[67] EN13848-5:2008 Railway Applications – Track Geometry Quality – Part 5: Geometric Quality Levels. Brussels, CEN.
[68] ISO 3310-1 (2016) Test sieves - Technical requirements and testing - Part 1: Test sieves of metal wire cloth. Technical Committee ISO/T24/SC8 International Organization for Standardization.
[69] ISO 3310-2 (2013) Test sieves Technical requirements and testing. Part 2: Test sieves of perforated metal plate.
[70] LCPC-SETRA, 1997, Chaussée en béton, French guideline, 134 pp. Assessing the Results of the Strategic Highway Research Program. Publication No. FHWA-SA-98-008. Federal Highway Administration. Washington D.C.
[71] LP-4 (2004) Determination of Dust Proportion (Previously referred to as the Dust/Asphalt ratio) May 27, 2004. DEPARTMENT OF TRANSPORTATION. ENGINEERING SERVICE CENTER. Office of Flexible Pavement Materials. 5900 Folsom Blvd. Sacramento, California 95819-4612.
[72] Mechanistic-Empirical Pavement Design Guide, Int. Edition: A Manual of Practice. AASHTO, Washington, D.C., 2008.
[73] NCHRP-459 (2001). Characterization of Modified Asphalt Binders in Superpave Mix Design (National Cooperative Highway Research Program).
[74] NCHRP-464 (2001). The Restricted Zone in the Superpave Aggregate Gradation Specification (National Cooperative Highway Research Program Report).
[75] NCHRP-465 (2002). Simple Performance Test for Superpave Mix Design (National Cooperative Highway Research Program Report).
[76] NCHRP-573 (2007). Superpave Mix Design: Verifying Gyration Levels in the Ndesign Table (National Cooperative Highway Research Program).
[77] NCHRP Report 673 (2011). A manual for design of hot mix asphalt with commentary, Washington, DC: TRB.
[78] RFI (Rete Ferroviaria Italiana, 2016). Gruppo Ferrovie dello Stato Italiane. Capitolato costruzioni opere civili. sezione XV sub-ballast - pavimentazioni stradali.
[79] SHRP-A-404 1994. Fatigue Response of Asphalt-Aggregate Mixes. Washington, DC: Asphalt Research Program Institute of Transportation Studies University of California. Strategic Highway Research Program National Research Council.
[80] SHRP-A-407 (1994). The Superpave Mix Design Manual for New Construction and Overlays. Strategic Highway Research Program, National Research Council, Washington, DC, USA.
[81] SHRP-A-408 (1994) "Level One Mix Design: Materials Selection, Compaction, and Conditioning," Cominsky, R., R. B. Leahy, and E. T. Harrigan, Strategic Highway Research Program, National Research Council.
[82] Spanish Ministry of Public Works (2006). General Technical Specifications for Railway Materials PF-7: Subballast.
[83] Transportation Officials. (1993). *AASHTO Guide for Design of Pavement Structures, 1993* (Vol. 1). AASHTO.
[84] UIC Code 719R (2008). Earthworks and Track-Bed Layers for Railway Lines. International Union of Railways, France.

2017

Glossary

LIST OF TERMS

PH.D. FERNANDO M. SOTO



Glossary of terms

[1] **Absorbed asphalt volume (V_{ba})**: is the volume of asphalt binder absorbed into the aggregate. It is equal to the difference between the aggregate volume when calculated with bulk specific gravity and with effective specific gravity.

[2] **Aggregate Control Points**: max/min limits which are established at specified sieve sizes for each set of aggregate gradation controls, including the maximum size, the nominal maximum size, and the restricted zone.

[3] **Aggregate Restricted Zone**: A zone which lies on the maximum density line and extends from the 300 µm sieve to the 2.36 mm sieve through which it is usually undesirable for the gradation to pass. For 25 and 37.5 mm nominal maximum size gradations, the restricted zone extends to the 4.75 mm sieve.

[4] **Air voids (V_a)**: the percent by volume of small air pockets between the coated aggregate particles throughout a compacted paving mixture (% of the bulk volume of the compacted paving mixture).

[5] **Aggregate**: collective term for the mineral materials such as sand, gravel and crushed stone that are used as a binding medium (such as water, bitumen, portland cement, lime, etc.) to form compound materials (such as asphalt concrete and portland cement concrete).

[6] **Ambient grinding**: method of processing where scrap tire rubber is ground or processed at or above ordinary room temperature. Ambient processing is typically required to provide irregularly shaped, torn particles with relatively large surface areas to promote interaction with the asphalt cement.

[7] **Ambient Ground Rubber**: processing where scrap tire rubber is ground or processed at or above ordinary room temperature.

[8] **Apparent Specific Gravity (G_{sa})**: density that includes only the volume of the aggregate particle. It does not contain the void volume that becomes filled with water during the test soak period.

[9] **Asphalt**: dark brown to black, highly viscous, a hydrocarbon produced from petroleum distillation residue. "Asphalt cement" refers to asphalt that has been prepared for use in HMA and other paving applications.

[10] **Asphalt-Aggregate Compatibility**: the ability of an asphalt binder, as measured by the net adsorption test (SHRP Test M-001, Measurement of Initial Asphalt Adsorption and Desorption in the Presence of Moisture), to adhere to the surface of the fine aggregate portion of the total aggregate and to maintain this adherence in the presence of moisture.

[11] **Asphalt Binder**: an asphalt-based cement that is produced from petroleum residue either with or without the addition of organic modifiers.

[12] **Asphalt (Binder) Content**: the percent by weight of asphalt binder in the total paving mix including both the asphalt binder and aggregate.

[13] **Asphalt Modifier**: any organic material of suitable manufacture, used in either virgin or recycled condition, which is dissolved, dispersed or reacted in asphalt cement to enhance its performance.

[14] **Asphalt Rubber (AR)**: asphalt cement modified with crumb rubber modifier. By definition, asphalt rubber binder is prepared using the "wet process." The asphalt cement and CRM are mixed and interacted at elevated temperatures and under high agitation to promote the physical interaction of the asphalt cement and CRM constituents (See Wet Process).

[15] **Asphalt-rubber blend**: a mixture of ground tire rubber (generally φ1.2-0.707mm finely ground crumb rubber) and asphalt cement, which is used as the "binder" in various types of pavement construction. It consists of 18 to 26 percent ground tire rubber by total weight of the blend. The blend is formulated at elevated temperatures to promote the chemical and physical bonding of the two constituents.

[16] **Asphalt rubber concrete**: a mixture that implies the use of an asphalt-rubber blend (binder) with dense-graded aggregates in a hot-mix application.

[17] **Asphalt-rubber hot-mix**: involves the use of an asphalt-rubber binder with open, dense or gap-graded aggregates in a hot-mix application.

[18] **Automobile tires**: tires with an outside diameter less than 66cm used on cars, pickups, and light trucks.

[19] **Average Annual Daily Traffic**: mean number of trains that passes a rail section everyday during a year.

[20] **Bending Beam Rheometer**: a low-temperature test device which measures the mid-point deflection of a simply-supported prismatic beam of asphalt binder subjected at low temperature to a constant load applied at the mid-point of the beam.

[21] **Binder content (Vb)**: the percent by mass of binder in the total mixture, including binder and aggregate.

[22] **Buffing waste**: high-quality scrap tire rubber which is a byproduct from the conditioning of tire carcasses in preparation for retreading.

[23] **Bulk Specific Gravity (Gsb)**: density that includes the volume of the aggregate particle plus the void volume that becomes filled with water during the test soak period. Since it includes the void volume, bulk specific gravity will be

less than apparent specific gravity.

[24] **Bulk Saturated-Surface Dry Specific Gravity (SSD)**: volume measurement includes the overall volume of the aggregate particle as well as the volume of the water permeable voids. The mass measurement includes the aggregate particle as well as the water within the water permeable voids. It is formally defined as the ratio of the mass of a unit volume of aggregate, including the weight of water within the voids filled to the extent achieved by submerging in water for approximately 15 hours, to the mass of an equal volume of gas-free distilled water at the stated temperature.

[25] **Clay content**: a measure of the amount of clay material which is present in the portion of aggregate that passes the 4.75 mm sieve.

[26] **Coarse Aggregate**: aggregate which is retained on the 2.36 mm sieve.

[27] **Coarse Aggregate Angularity**: the percent by weight of aggregate particles larger than 4.75 mm with one or more fractured faces.

[28] **Crackermill**: a process that tears apart scrap tire rubber by passing the material between rotating corrugated steel drums, reducing the size of the rubber to a crumb particle (generally 0.42 to 4.75 mm).

[29] **Critical Temperature (T_c)**: a test temperature higher than the effective temperature (T_{eff}) for permanent deformation which is selected to reduce testing time to reasonable levels for projects with very high predicted ESALs.

[30] **Crumb rubber modifier (CRM)**: a general term for scrap tire rubber that is reduced in size and is used as a modifier in asphalt paving materials.

[31] **Cryogenic grinding**: process that uses liquid nitrogen to freeze the scrap tire rubber until it becomes brittle and then uses a hammer mill to shatter the frozen rubber into smooth particles with relatively small surface area. This method is used to reduce particle size prior to grinding at ambient temperatures.

[32] **Cryogenically ground rubber**: a process that freezes the scrap tire rubber and crushes the rubber to the particle size desired.

[33] **Dense-graded**: refers to a continuously graded aggregate blend typically used to make hot-mix asphalt concrete (HMA) pavements with conventional or modified binders.

[34] **Design Aggregate Structure**: an aggregate gradation selected through the Superpave level 1 (volumetric) mix design procedure which meets all aggregate and volumetric requirements at an initial trial asphalt content.

[35] **Design Asphalt Content**: the asphalt content determined for the design aggregate structure through the Superpave level 1 (volumetric) mix design procedure which produces compacted specimens with four percent air void at N_{design} and which meets relevant air void requirements at N_{init} and N_{max}.

[36] **Devulcanized rubber**: rubber that has been subjected to treatment by heat, pressure, or the addition of softening agents after grinding to alter properties of the recycled material.

[37] **Direct Tension Test Device**: a low temperature, non-contact test device which measures the strain and stress at failure of an asphalt binder specimen pulled at a constant rate of elongation.

[38] **Dry process**: any method that mixes the crumb rubber modifier with the aggregate before the mixture is charged with asphalt binder. This method applies only to hot-mix asphalt production (Care must be taken during the mix design to make appropriate adjustments for the low specific gravity of the CRM compared to the aggregate material to assure proper volumetric analysis).

[39] **Dust Proportion**: by mass, the ratio between the percent passing the 0.075 mm (No. 200) sieve (P0.075) and effective binder content (P_{be}).

[40] **Dynamic Shear Rheometer (DSR)**: high and intermediate temperature test device which measures the complex shear modulus and phase angle of a binder specimen placed between two parallel plates which are oscillated concerning each other at preselected frequencies and rotational deformation amplitudes.

[41] **Effective binder volume (Vbe)**: the volume of binder that is not absorbed into the aggregate.

[42] **Effective Specific Gravity (Gse)**: Volume measurement includes the volume of the aggregate particle plus the void volume that becomes filled with water during the test soak period minus the volume of the voids that absorb asphalt. Effective specific gravity lies between apparent and bulk specific gravity.

[43] **Effective Temperature (T_{eff})**: a single test temperature at which an amount of permanent deformation or fatigue cracking would occur equivalent to that which would be measured by considering the seasonal fluctuation of temperature throughout the year.

[44] **Environmental Conditioning System**: a modified triaxial test unit in which the dynamic resilient modulus of a cylindrical/prismatic mixture specimen can be continually measured as moisture is forced through it. Moisture susceptibility is characterized by the resilient modulus ratio of conditioned to unconditioned specimens.

[45] **ESAL**: Equivalent Single Axle Load.

[46] **Extender oil**: an aromatic oil used to supplement the reaction of the asphalt and the crumb rubber modifier.

[47] **Extraction**: the process of removing asphalt binder from a sample of HMA leaving the aggregate behind (ASTM D2172-2011).

[48] **Fatigue Cracking**: fatigue failure of the HMA surface (or stabilized base) under repeated traffic loading. In thin layers, cracking initiates at the bottom of the HMA layer where the tensile stress is the highest then propagates to the surface as one or more longitudinal cracks. It is commonly referred to as "bottom-up" or "classical" fatigue cracking.

[49] **Filler or Mineral Filler**: aggregate, predominately mineral dust, which passes the 75μm sieve.

[50] **Fine Aggregate**: aggregate which passes the 2.36 mm sieve.

[51] **Fine Aggregate Angularity**: the percent of air voids of loosely compacted aggregate as measured in the National Aggregate Association Test Method A. This test is done on the portion of blended aggregates are passing the 2.36 mm sieve.

[52] **Gap-graded**: aggregate that is not continuously graded for all size fractions but is typically missing or low on some of the finer size fractions (<2.36 mm or finer). Such gradations typically plot below the maximum density line on a 0.45 power gradation chart. Gap grading is used to promote stone-to-stone contact in HMA and is similar to the gradations used in stone matrix asphalt (SMA), but with relatively low percentages passing the 75 µm sieve size. This type of gradation is most frequently used to make rubberized asphalt concrete gap graded (RAC-G) paving mixtures.

[53] **Generic dry**: mixes in which the gradation of crumb rubber is adjusted to suit the aggregate gradation. Unlike the Plusride mixes, the gradation of rubber is a two component system in which the powder rubber interacts with the asphalt cement while the coarse rubber performs as an elastic aggregate in HMA.

[54] **Granulated crumb rubber modifier**: cubical, uniformly shaped, cut crumb rubber particle with a low surface area, which is produced by a granulator.

[55] **Granulation**: produces cubical, uniformly shaped, cut crumb rubber particles with a low surface area.

[56] **Granulator**: a process that shears apart the scrap tire rubber, cutting the rubber with revolving steel plates that pass at close tolerance, reducing the rubber to particles 9.5 mm to 2.0 mm in size.

[57] **Ground crumb rubber modifier**: irregularly shaped, torn crumb rubber particles with a large surface area, generally produced by a cracker mill.

[58] **Guideline**: a specification value which is provided as design guidance, but to which conformance is not mandatory.

[59] **Gyratory compactor (SGC)**: compactor introduced by Superpave (Superior Performing Asphalt Pavements) for densifying mixtures in the laboratory at different levels based on studies in the field. The Superpave mix design maintained the volumetric properties used in the Marshall design system with a new compactor and more defined aggregate requirements based on traffic loading.

[60] **High Air Temperature**: the maximum annual 7-day average air temperature recorded at a weather station.

[61] **Hot Mix Asphalt**: is a combination of stone, sand, or gravel bound together by asphalt cement, a product of crude oil. Asphalt cement is heated aggregate, combined, and mixed with the aggregate at an HMA facility.

[62] **Indirect Tensile Creep Test**: a test in which a 150 mm diameter specimen is subjected in the indirect tensile test device to a diametral preconditioning load to obtain uniform deformation.

[63] **Indirect Tensile Strength Test**: a test in which a compressive load is applied along the diametral axis of 150 mm diameter specimen in the indirect tensile test device at a controlled vertical deformation rate until failure occurs.

[64] **Interaction**: the physical exchange between asphalt cement and CRM when blended at elevated temperatures which include swelling of the rubber particles and development of specified physical properties of the asphalt and CRM blend to meet requirements. Although often referred to as reaction, interaction is not a chemical reaction but rather a physical interaction in which the CRM absorbs aromatic oils and light fractions (small volatile or active molecules) from the asphalt cement, and releases some of the similar oils used in rubber compounding into the asphalt cement. The interaction may be more appropriately defined as polymer swell.

[65] **Laying**: the action consisting in throwing the asphalt mix on the road surface by a paver machine.

[66] **Life-cycle assessment (LCA)**: is a technique to assess environmental impacts associated with all the stages of a product's life from raw material extraction through materials processing, manufacture, distribution, use, repair and maintenance, and disposal or recycling.

[67] **Life Cycle Cost Assessment (LCCA)**: tools that facilitate proper decision-making by applying economics and operations. It improves the estimation of the total long-term economic viability of different investment options.

[68] **Lightweight aggregate**: porous aggregate with a very low density such as expanded shale, which is typically manufactured. It has been used in chip seals to reduce windshield damage.

[69] **Long-Term Aging**: an optional procedure for paving mixes in which compacted specimens are placed in a forced draft oven at 85°C. The time of exposure in the oven varies depending on the length of pavement service that is simulated. The recommended exposure time is 2 days which is equivalent to about 10 years of pavement service.

[70] **Low Air Temperature**: the minimum annual air temperature recorded at a weather station.

[71] **Material Property**: a characteristic of a material which does not depend upon the testing apparatus, procedure or condition, and from which its behavior under load can be predicted.

[72] **Maximum Aggregate Size**: one size larger than nominal value maximum aggregate size.

[73] **Maximum Density Line**: a line which is drawn from the origin of the 0.45 power chart to the point at which the maximum sieve size intersects the 100 percent passing line.

[74] **Maximum Pavement Design Temperature**: maximum temperature at 20 mm depth determined from high air temperature for any given location.

[75] **Micro-mill**: a process that further reduces a crumb rubber to a very fine ground particle, reducing the size of the crumb rubber below 425 microns.

[76] $\mathbf{N_{init}}$: Number of initial gyrations: indicates a potential for tenderness in the mix during construction,

[77] **N_{Design}**: Design number of gyrations for which the mix is designed to produce 4% air content.

[78] **N_{max}**: Maximum number of gyrations that should never be exceeded, designed to simulate the post-compaction densification due to traffic. An air content <2% would be susceptible to rutting.

[79] **Nominal max. aggregate size**: one size larger than the first sieve that retains more than 10% aggregate (for HMA Surface courses 4,75mm<Ø<19mm, Base Ø<35mm).

[80] **Open-graded**: aggregate gradation that is intended to be free draining and consists mostly of 2 or 3 nominal sizes of aggregate particles with few fines and 0 to 4 percent by mass passing the (0.075 mm) sieve. Open grading is used in hot-mix applications to provide a relatively thin surface or wearing courses with good frictional characteristics that quickly drain surface water to reduce hydroplaning, splash and spray.

[81] **Optimum Binder Content**: the asphalt content determined for the design aggregate structure through Superpave level 2 or level 3 performance testing of compacted specimens which satisfies agency requirements for acceptable, predicted levels of permanent deformation, fatigue cracking and (or) low-temperature cracking at the designated pavement design life.

[82] **Performance grading (PG) system**: Superpave categorize asphalt binders by one or more shorthand grading systems according to their physical characteristics. The PG system is based on the idea that an HMA asphalt binder's properties should be related to the conditions under which it is used. For asphalt binders, this involves expected climatic conditions as well as aging considerations.

[83] **Performance Prediction Model**: a computer algorithm which provides realistic predictions of future pavement performance from the material properties of the paving mix; the predicted traffic; the climatic history of the pavement site; and the pavement structure.

[84] **PlusRide**: a patented form of a rubber-modified asphaltic mix. The product was developed in 1960 in Sweden and patented under the name PlusRide in the United States and Rubit in Sweden. It uses coarse rubber particles (6 mm to 0.6 mm) as rubber-filled aggregates, generally about 3 percent weight of the mix. The rubber is added directly to a gap-graded aggregate so that a relatively dense-grading between the aggregate and rubber is obtained.

[85] **Reaction**: the interaction between asphalt cement and crumb rubber modifier when blended. The reaction, more appropriately defined as polymer swell, is not a chemical reaction. It is the absorption of aromatic oils from the asphalt into the polymer chains of the crumb rubber (see Interaction).

[86] **Reclaimed asphalt pavement (RAP)**: asphalt paving material milled or scrapped off an existing bituminous pavement, consisting of aggregate and asphalt binder.

[87] **Recycled mixture**: finished mixture of RAP, new binder and new aggregates.

[88] **Recycled tire rubber**: rubber obtained by processing used automobile, truck, or bus tires.

[89] **Requirement**: a specification value which a material must always meet.

[90] **Rheology**: is the study of deformation and flow of matter. Deformation and flow of the asphalt binder in HMA is important in pavement performance. HMA pavements that deform and flow too much may be susceptible to rutting and bleeding, while those that are too stiff may be susceptible to fatigue cracking. HMA pavement deformation is closely related to asphalt binder rheology.

[91] **Rock**: predominately coarse aggregate which is retained on the 2.36 mm sieve.

[92] **Rubber Aggregate**: crumb rubber modifier added to hot-mix asphalt mixture using the dry process, which retains its physical shape and rigidity.

[93] **Rubber-modified asphalt concrete (RUMAC)**: a hot-mix asphalt-concrete mixture with dense-graded aggregates using a rubber-modified asphalt.

[94] **Rubber-modified friction course**: a hot-mix asphalt mixture with open-graded aggregates using a rubber-modified asphalt.

[95] **Rubber-modified hot-mix asphalt**: hot-mix asphalt mixture that incorporates crumb rubber modifier primarily as rubber aggregate.

[96] **Rubberized asphalt**: same meaning as a wet process. Asphalt cement modified with CRM that may include less than 15 percent CRM by mass and thus may not comply with the ASTM definition of asphalt rubber (ASTM D 8, Vol. 4.03). In the past, terminal blends (wet process, no agitation CRM-modified asphalt binders including Modified Binder materials) have typically fallen into this category.

[97] **Rubberized asphalt concrete (RAC)**: material produced for hot mix applications by mixing asphalt rubber or rubberized asphalt binder with graded aggregate. RAC may be dense-, gap-, or open-graded.

[98] **Rutting**: Surface depression in the wheel path. In railways, it is evident after poor drainage. Mix rutting occurs when the subgrade does not rut yet the pavement surface exhibits wheel path depressions as a result of compaction/mix design problems.

[99] **Sand**: predominately fine aggregate which passes the 2.36 mm sieve.

[100] **Shredding**: a process that reduces scrap tires to pieces 0.15 m2 and smaller before granulation or ambient grinding.

[101] **Short-Term Aging**: A procedure for paving mixes in which loose mix is placed in a tray (immediately after mixing) to a uniform depth. The mix is held in a forced draft oven for 4 hours at 135°C, after which the mix is brought to the appropriate compaction temperature and the material compacted. This procedure simulates the aging that takes place during HMA production and the pavement construction process.

[102] **Stability**: a term often used to describe an HMA's ability to resist deformation under loading.

[103] **Stone Mastic Asphalt (SMA)**: a dense wearing course material which was developed on the continent to overcome the issue of rutting due to the action of studded tires on road surfaces. The mineral aggregate skeleton of SMA is gap-graded, and the voids are filled with a mastic of fine aggregate, filler, and binder.

[104] **Stripping**: distress in flexible layers due to loss of bond between aggregates and asphalt binder that typically begins at the bottom of the HMA layer and progresses upward.

[105] **Superpave mix design system**: is a comprehensive method of designing paving mixes tailored to the unique performance requirements dictated by the traffic, environment (climate), and a structural section at a particular pavement site. It facilitates selecting and combining asphalt binder, aggregate, and any necessary modifier to achieve the required level of pavement performance.

[106] **Susceptibility to compaction**: the property of the mixed asphalt consisting in being compacted by mechanical effort rather than by own weight.

[107] **Terminal blend**: See Wet Process, No Agitation.

[108] **Thin, Elongated Particle**: a coarse aggregate particle which has a ratio of maximum to minimum dimensions greater than five (5).

[109] **Toughness**: the weight percent of material which is lost from the blended aggregate during the Los Angeles Abrasion Test.

[110] **Tread rubber**: rubber that consists primarily of tread rubber with less than approximately 5 percent sidewall rubber.

[111] **Truck tires**: tires with an outside diameter greater than 66 cm and less than 152 cm; used on commercial trucks and buses.

[112] **Viscosity**: is the property of resistance to flow (shearing force) in a fluid or semi-fluid. Thick, stiff fluids such as asphalt rubber have high viscosity; water has low viscosity. Viscosity is specified as a measure of field quality control for asphalt rubber production and its use in RAC mixtures.

[113] **Voids in the mineral aggregates (VMA)**: the volume of the intergranular void space between the aggregate particles that includes the air voids (Va) and the effective binder content (Vbe).

[114] **Voids filled with asphalt (VFA)**: is the percentage of VMA filled with asphalt binder. It is the effective asphalt volume divided by the voids in the mineral aggregate, Vbe/VMA.

[115] **Vulcanized rubber**: rubber that has been subjected to treatment to heat, pressure, or the addition of softening agents after grinding to alter properties of the recycled material.

[116] **Warm Mix Asphalt**: technologies that allow producers of Hot Mix Asphalt (HMA) pavement material to lower temperatures at which the material is mixed and placed on the road.

[117] **Wet process**: any method that blends crumb rubber modifier with the asphalt cement before incorporating the binder in the asphalt paving project. The wet process requires thorough mixing of the crumb CRM in hot asphalt cement (190°C to 224°C) and holding the resulting blend at elevated temperatures (190°C to 218°C) for a designated minimum period (typically 45 minutes) to permit interaction between the CRM and asphalt.

[118] **Wet Process-High Viscosity**: CRM-modified binders that maintain or exceed the minimum rotational viscosity threshold of 1500 cPs at 190°C over the interaction period should be described as "wet process–high viscosity" binders to distinguish their physical properties from those of wet process-no agitation materials. These binders need agitation to keep the CRM particles evenly distributed.

[119] **Wet Process-No Agitation**: a form of the wet process where CRM is blended with hot asphalt cement at the refinery or an asphalt storage and distribution terminal and transported to the HMA mixing plant or job site for use. The term "terminal blend" is often used to describe such materials, although they may also be produced in the field.

[120] **Whole tire rubber**: rubber that includes tread and sidewalls in proportions that approximate the respective weights in an average tire.

[121] **Workability**: the ability of a mixture to be handled and the ease with which it can be placed in the field.

2017

Annexes

Annex 01. Complex and Stiffness modulus
Annex 02. Densification data file (Vol. Mix-design)
Annex 03. Framework of rail modeling: Kentrack
Annex 04. Kenpave computer program
Annex 05. Kentrack example

Annex 01. Complex and Stiffness modulus

1.1.1. Complex modulus

When an elastic solid is subjected to a shearing force, the stress is proportional to the displacement, called strain. The constant of proportionality is called the modulus. Moreover, this is similar to the viscosity of liquids. In viscous fluids, however, the stress is proportional to the rate of the strain. Bitumens exhibit both elastic and viscous qualities, so they are viscoelastic materials. Viscoelastic materials have an elastic modulus, which corresponds to in-phase deformation, as well as a viscous modulus corresponding to out-of-phase deformation (Figure 1). The complex modulus, G* is the vector sum of the elastic and the viscous modulus, which gives an idea of the stiffness of bitumen at a given temperature and loading rate. The angle of the triangle formed mathematically by this expression is called the phase angle delta, δ, that represents the offset between applied stress and the resulting strain movement (the related viscous and elastic components of behavior). In an entirely elastic material, stress and strain will be entirely in phase – which means that the angle of 0° implies fully elastic behavior; 90° represents fully viscous behavior.

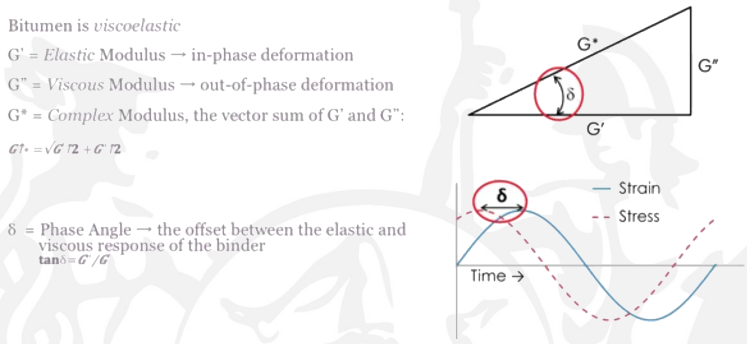


Figure 1. Complex modulus (Viscoelastic materials).

The US 'Superpave' specification is, regarding direct visco-elastic measurements, carried out in the DSR, and may, therefore, be considered much more scientifically based than tests that use penetration and softening point. Lower limits are placed on $G^*\cdot\sin\delta$ (to protect against rutting) and, $G^*/\sin\delta$ (to protect against fatigue cracking).

1.1.2. Stiffness modulus

A complex stiffness modulus is a number that relates stress to strain for linear visco-elastic material subjected to apply sinusoidal loading in the frequency domain continuously. A hot mix asphalt (HMA) mixture can be considered as linear viscoelastic material under small strain levels (≤100με). To resist fatigue cracking, an asphalt binder should be elastic, able to dissipate energy by rebounding and not cracking. Therefore, the complex shear modulus viscous portion should be minimum. When fatigue cracking is worrying, a maximum value for the viscous component of the shear modulus is specified. Thus, the HMA stress-strain relationship under continuous sinusoidal loading in the linear viscoelastic region can be defined by the complex dynamic modulus ($\pm T^a$) as the ratio of the amplitude of the sinusoidal stress (±time and load-frequency) and sinusoidal strain (at the same time-frequency) that results in a steady state response.

$$E^* = \frac{\sigma(t)}{\varepsilon(t)} = \frac{\sigma_0 sin(\omega t)}{\varepsilon_0 sin(\omega t - \phi)} = \frac{\sigma_0}{\varepsilon_0}\cdot e^{i\phi} = |E^*|\cdot e^{i\phi} \rightarrow |E^*|\cdot e^{i\cdot\phi} = |E^*|\cdot(\cos\phi + i\cdot sin\phi) = E_1 + iE_2 \quad \text{(Eq. 1)}$$

$$E_1 = |E^*|\cdot\cos\phi = |E^*|\cdot\cos(arctg(E_2/E_1)); E_2 = |E^*|\cdot sin\phi = |E^*|\cdot sin(arctg(E_2/E_1))$$

- |E*| = complex modulus; σ_{0v}= peak (maximum) stress; ε_0 = peak (maximum) stress;
- ω = angular velocity; f = load frequency; t = time; i = imaginary unit
- ∅= phase angle that represents the lag time between stress and strain;

The real component E_1 represents the elastic property of the material while the imaginary component E_2 describes the viscous behavior. The absolute value of the complex modulus is called stiffness modulus:

$$|E^*| = \sqrt{(E_1^2 + E_2^2)} \quad \text{(Eq. 2)}$$

EN12697-26 European Standard "*Determination of the stiffness of bituminous mixture*" Annex B, describes the procedure for evaluating the real component E_1 and the imaginary component E_2 of the complex modulus, the stiffness modulus and the phase angle using four-point bending test on prismatic specimens.

With the aim of this work, the accurate evaluation of the phase angle is significant because it plays a decisive role for the attenuation of the borne vibrations by traffic. The interpretation of a bending test is based on the solution of the motion equation of an elastic beam subjected to a force F, in which Young's modulus is replaced by the stiffness modulus. The solution, regarding vertical displacement v of a point at x position and a given time t, is:

$$v_{(x,t)} = \frac{q_n}{m\left(\omega_n^2 - \omega^2\right)} \cdot sin\frac{n\pi x}{L}\left[sin(\omega t) - sin\left(\omega_n t\right)\right] \quad \text{(Eq. 3)}$$

Where:

- $\omega_n = \omega_n^* = \frac{n^2 \cdot \pi^2}{L^2}\sqrt{\frac{E^* I}{m}}$, frequency of the n-harmonic wave;
- I, moment of inertia of the cross section (Fig.1);
- $q_n = 2P/L \cdot \left[\left(sin\, n\pi/3\right) + \left(sin\, 2n\pi/3\right)\right]$;
- P, applied load (Fig. 2);
- ω, angular velocity for unit of length;
- m, mass for unit of length;
- L, length of the beam [m];

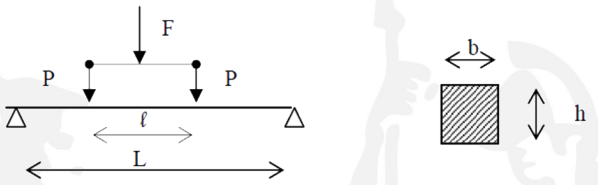


Figure 2. Loading scheme and cross section (b · h) [1][1].

The complex mechanical impedance is defined as:

$$Z^* = \frac{2P}{v_{\max}} e^{i\phi} = \frac{E^* I \pi^4}{L^3\left[\sum_i \frac{1}{i^4\left(1-\omega^2/\omega_1^2\right)}\right]}\left(sin\frac{i\pi}{3} + sin\frac{2i\pi}{3}\right) \cdot sin\frac{i\pi}{2} \quad \text{(Eq. 4)}$$

$$v_{\max} = 2PL^3 \Big/ E^* I \pi^4 \cdot \left[\sum_i \frac{1}{i^4\left(1-\omega^2/\omega_1^2\right)} \cdot \left(sin\, i\pi/3 + sin\, 2i\pi/3\right) \cdot sin\, i\pi/2\right] \quad \text{(Eq. 5)}$$

The maximum vertical displacement, v_{max} that occurs at $x=L/2$. The complex modulus is rewritten as:

$$E^* = E_1 + iE_1\theta \quad \text{(Eq. 6)}$$

- $\theta = \tan\varphi$, is the damping factor.

We have:

$$Z^* = \frac{\frac{\pi^4 E_1 I}{L^3} + iE_1\frac{\pi^4 I}{L^3}\theta - \omega^2 Lm}{\left(sin\,\pi/3 + sin\,2\pi/3\right) \cdot sin\,\pi/2} = \frac{\pi^4 E_1 I}{\sqrt{3}L^3} + iE_1\frac{\pi^4 I\theta}{\sqrt{3}L^3} - \frac{\omega^2 Lm}{\sqrt{3}} \quad \text{(Eq. 7)}$$

It is possible to get E_1 imposing the equality of the real parts:

$$\frac{2P}{\upsilon_{\max}}\cos\theta = \frac{\pi^4 E_1 I}{\sqrt{3}L^3} - \frac{\omega^2 Lm}{\sqrt{3}} \rightarrow E_1 = \left(\frac{2P}{\upsilon_{\max}}\cos\theta + \frac{M}{\sqrt{3}}\right) \cdot \frac{\sqrt{3}L^3}{\pi^4 I} \quad \text{(Eq. 8)}$$

Known E_1 is possible to obtain E_2 through the equation:

$$E_2 = E_1\theta = E_1\tan\theta = \left(\frac{2P}{v_{\max}}\cos\phi + \frac{mL}{\sqrt{3}}\left(2\pi f\right)^2\right)\frac{\sqrt{3}L^3}{\pi^4 I}\tan\theta \quad \text{(Eq. 9)}$$

The relations to calculate the components of the complex modulus suggested by the EN 12697-26:

[1] F. Martinez-Soto, et al. (2016) "Evaluation of Dry Asphalt Rubber Concrete in Railway Sub-Ballast using the Four Point Bending Test", in J. Pombo, (Editor), "Proceedings of the 3rd International Conference on Railway Technology: Research, Development and Maintenance", Civil-Comp Press, Stirlingshire, UK. DOI:10.4203/ccp.110.37.

$$E_1 = \gamma\left(\frac{F}{D}\cos(\phi) + \frac{\mu}{10^3}(2\pi f)^2\right); E_2 = \gamma\left(\frac{F}{D}sin(\phi)\right) \quad \text{(Eq. 10)}$$

- F = 2P is load amplitude (peak-peak); D is the vertical displacement measured;
- γ is a form factor that depends on the type of sample and its geometry;

$$\gamma = \frac{L^2 \cdot A}{b \cdot h^3}\left(\frac{3}{4} - \frac{A^2}{L^2}\right); A = \frac{L-l}{2} \quad \text{(Eq. 11)}$$

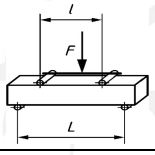
- L, space between outside clamps; l, the distance between the points of load application;
- b, width; h, the height of the prismatic specimen;
- μ, a mass factor related to the sample mass M and the moving parts masses;

$$\mu = R(X)\left(\frac{M}{\pi^4} + \frac{m}{R(A)}\right); R(X) = \frac{12 \cdot L}{A}\left[\frac{1}{\left(3X/L - 3X^2/L^2 - A^2/L^2\right)}\right] \quad \text{(Eq. 12)}$$

- X is the coordinate on which the displacement is measured.

It is noted that the equations 10 and 11 correspond to the regulations reflecting "*EN12697-26:2012 Bituminous mixtures - Test methods for hot mix asphalt – Part 26: Stiffness*". The mechanical material characteristics shall be derived from the measurements using the specific factors given in Table 1:

TABLE 1. PHYSICAL AND RHEOLOGICAL SPECIFICATIONS OF THE BINDER 50/70

Bending test	Load type	Form factor, γ mm^{-1}	Mass factor, μ (g)
4PB-PR		$\frac{AL^2}{bh^3}\left(\frac{3}{4} - \frac{A^2}{L^2}\right)$	$R\cdot\left(\frac{M}{\pi^4} + \frac{m}{R_A}\right)$

At 20ºC and 10 Hz (a frequency typical of pavement loading), G^* is typically 10–30 MPa.

Annex 02. Densification data file (SGC)

A data file example of the mix-design by SGC is reported for the HMA mixture (b.4%).

TABLE 2. EXAMPLE OF DENSIFICATION DATA FILE (HMA B. 4%)

Gyration	Height (mm)	Angle (Deg)	Pressure (kPa)	Shear Ratio	Perform. Factor	γ(N) [gr/cm3]	γ(N)*C [gr/cm3]	γmm (N) (%)	Va (%)
1	137.7	----	569	0.66888	915.6	2.158	2.126	80.70%	19.30%
2	134.2	1.29	569	0.82713	633.1	2.214	2.181	82.81%	17.19%
3	132	1.27	581	0.871	574.7	2.251	2.217	84.19%	15.81%
4	130.3	1.27	587	0.9004	555.2	2.280	2.246	85.28%	14.72%
5	129	1.27	591	0.92151	516.2	2.303	2.269	86.14%	13.86%
6	127.9	1.27	593	0.93819	487	2.323	2.288	86.88%	13.12%
7	126.9	1.27	593	0.95835	569.8	2.341	2.306	87.57%	12.43%
$N_{init.}$ 8	126.1	1.27	593	0.96339	657.5	2.356	2.321	**88.12%**	**11.88%**
9	125.4	1.26	590	0.96358	759.7	2.369	2.334	88.62%	11.38%
10	124.8	1.26	592	0.9741	789	2.381	2.345	89.04%	10.96%
11	124.2	1.26	593	0.98648	789	2.392	2.357	89.47%	10.53%
12	123.7	1.26	594	0.99535	750	2.402	2.366	89.83%	10.17%
13	123.3	1.26	595	0.99986	730.5	2.409	2.374	90.13%	9.87%
14	122.8	1.26	595	1.003	832.8	2.419	2.383	90.49%	9.51%
15	122.4	1.26	596	1.0126	862	2.427	2.391	90.79%	9.21%
16	122.1	1.26	596	1.02299	847.4	2.433	2.397	91.01%	8.99%
17	121.6	1.26	593	1.02307	1814.2	2.443	2.407	91.39%	8.61%
18	121.3	1.26	601	1.02264	1939.9	2.449	2.413	91.61%	8.39%
19	121.1	1.26	598	1.03538	1930	2.453	2.417	91.76%	8.24%
20	120.8	1.26	595	1.04236	1721.9	2.459	2.423	91.99%	8.01%
21	120.5	1.26	597	1.03588	1640.3	2.465	2.429	92.22%	7.78%
22	120.3	1.26	598	1.04184	1619	2.470	2.433	92.37%	7.63%
23	120.1	1.26	598	1.04014	1704.5	2.474	2.437	92.53%	7.47%
24	119.9	1.26	599	1.03931	1702.7	2.478	2.441	92.68%	7.32%
25	119.7	1.26	599	1.04051	1665.1	2.482	2.445	92.84%	7.16%
26	119.5	1.26	599	1.04764	1718.7	2.486	2.449	92.99%	7.01%
27	119.3	1.26	600	1.04887	1670.2	2.490	2.453	93.15%	6.85%
28	119.1	1.26	599	1.05269	1611.3	2.494	2.457	93.30%	6.70%

29	118.9	1.26	600	1.04529	1580	2.499	2.462	93.46%	6.54%
30	118.8	1.26	599	1.05356	1672.8	2.501	2.464	93.54%	6.46%
31	118.6	1.26	600	1.0522	1555.2	2.505	2.468	93.70%	6.30%
32	118.5	1.26	600	1.05038	1542.9	2.507	2.470	93.78%	6.22%
33	118.4	1.26	599	1.05415	1575.6	2.509	2.472	93.86%	6.14%
34	118.2	1.26	600	1.05391	1410.5	2.513	2.476	94.01%	5.99%
35	118.1	1.26	600	1.05682	1471.5	2.516	2.478	94.09%	5.91%
36	118	1.26	599	1.05977	1530.4	2.518	2.480	94.17%	5.83%
37	117.8	1.26	601	1.05139	1362	2.522	2.485	94.33%	5.67%
38	117.7	1.26	598	1.05887	1478.4	2.524	2.487	94.41%	5.59%
39	117.6	1.26	602	1.05692	1331.9	2.526	2.489	94.49%	5.51%
40	117.5	1.26	598	1.05421	1403.8	2.528	2.491	94.57%	5.43%
41	117.4	1.26	602	1.05539	1367.6	2.531	2.493	94.65%	5.35%
42	117.3	1.26	599	1.05793	1389.8	2.533	2.495	94.74%	5.26%
43	117.2	1.26	601	1.05893	1406.8	2.535	2.497	94.82%	5.18%
44	117.1	1.26	601	1.05817	1266.2	2.537	2.499	94.90%	5.10%
45	117	1.26	598	1.05424	1349	2.539	2.502	94.98%	5.02%
46	116.9	1.26	602	1.05885	1297.3	2.541	2.504	95.06%	4.94%
47	116.8	1.26	599	1.0612	1389.1	2.544	2.506	95.14%	4.86%
48	116.8	1.26	600	1.0589	1400.5	2.544	2.506	95.14%	4.86%
49	116.7	1.26	600	1.06137	1285.7	2.546	2.508	95.22%	4.78%
50	116.6	1.26	599	1.06142	1373.4	2.548	2.510	95.30%	4.70%
51	116.5	1.26	601	1.06069	1430.4	2.550	2.512	95.39%	4.61%
52	116.4	1.26	600	1.05416	1305.2	2.552	2.514	95.47%	4.53%
53	116.4	1.26	598	1.05868	1349	2.552	2.514	95.47%	4.53%
54	116.3	1.26	600	1.0533	1335.3	2.555	2.517	95.55%	4.45%
55	116.2	1.26	599	1.05424	1285.7	2.557	2.519	95.63%	4.37%
56	116.2	1.26	598	1.05207	1363.6	2.557	2.519	95.63%	4.37%
57	116.1	1.26	599	1.05261	1359.5	2.559	2.521	95.71%	4.29%
58	116	1.26	599	1.05216	1280.8	2.561	2.523	95.80%	4.20%
59	116	1.26	598	1.05317	1368.5	2.561	2.523	95.80%	4.20%
60	115.9	1.26	599	1.05199	1389.1	2.563	2.525	95.88%	4.12%
61	115.9	1.26	599	1.05442	1290.6	2.563	2.525	95.88%	4.12%
62	115.8	1.26	598	1.05331	1305.2	2.566	2.527	95.96%	4.04%
63	115.7	1.26	598	1.04699	1368.5	2.568	2.530	96.05%	3.95%
64	115.7	1.26	599	1.04999	1305.2	2.568	2.530	96.05%	3.95%
65	115.6	1.26	598	1.04602	1276	2.570	2.532	96.13%	3.87%
66	115.6	1.26	597	1.04619	1368.5	2.570	2.532	96.13%	3.87%
67	115.5	1.26	598	1.0434	1329.5	2.572	2.534	96.21%	3.79%
68	115.5	1.26	598	1.03888	1290.6	2.572	2.534	96.21%	3.79%
69	115.4	1.26	598	1.03888	1276	2.574	2.536	96.30%	3.70%
70	115.4	1.26	598	1.0409	1310.1	2.574	2.536	96.30%	3.70%
71	115.3	1.26	598	1.03277	1314.9	2.577	2.538	96.38%	3.62%
72	115.3	1.26	598	1.03932	1276	2.577	2.538	96.38%	3.62%
73	115.2	1.26	598	1.03783	1271.1	2.579	2.541	96.46%	3.54%
74	115.2	1.26	598	1.0329	1319.8	2.579	2.541	96.46%	3.54%
75	115.1	1.26	599	1.02974	1276	2.581	2.543	96.55%	3.45%
76	115.1	1.26	599	1.02572	1222.4	2.581	2.543	96.55%	3.45%
77	115.1	1.26	599	1.02894	1237	2.581	2.543	96.55%	3.45%
78	115	1.26	599	1.0262	1256.5	2.583	2.545	96.63%	3.37%
79	115	1.26	599	1.02114	1227.3	2.583	2.545	96.63%	3.37%
80	114.9	1.26	598	1.02265	1256.5	2.586	2.547	96.71%	3.29%
81	114.9	1.26	599	1.01966	1222.4	2.586	2.547	96.71%	3.29%
82	114.9	1.26	600	1.01502	1212.7	2.586	2.547	96.71%	3.29%
83	114.8	1.26	598	1.01515	1183.4	2.588	2.550	96.80%	3.20%
84	114.8	1.26	599	1.01504	1271.1	2.588	2.550	96.80%	3.20%
85	114.8	1.26	600	1.01383	1202.9	2.588	2.550	96.80%	3.20%
86	114.7	1.26	600	1.00719	1159.1	2.590	2.552	96.88%	3.12%
87	114.7	1.26	599	1.00381	1178.6	2.590	2.552	96.88%	3.12%
88	114.7	1.26	599	1.00642	1266.2	2.590	2.552	96.88%	3.12%
89	114.6	1.26	600	1.00311	1164	2.592	2.554	96.97%	3.03%
90	114.6	1.26	600	0.99631	1105.5	2.592	2.554	96.97%	3.03%
91	114.6	1.26	599	0.99469	1100.6	2.592	2.554	96.97%	3.03%
92	114.6	1.26	599	0.99798	1237	2.592	2.554	96.97%	3.03%
93	114.5	1.26	600	0.99028	1217.5	2.595	2.556	97.05%	2.95%
94	114.5	1.26	600	0.99044	1100.6	2.595	2.556	97.05%	2.95%
95	114.5	1.26	599	0.98377	1144.5	2.595	2.556	97.05%	2.95%
96	114.4	1.26	599	0.98705	1222.4	2.597	2.558	97.14%	2.86%
97	114.4	1.26	601	0.98066	1120.1	2.597	2.558	97.14%	2.86%
98	114.4	1.26	599	0.97746	1081.2	2.597	2.558	97.14%	2.86%
99	114.4	1.26	598	0.96993	1202.9	2.597	2.558	97.14%	2.86%
100	114.3	1.26	601	0.97499	1173.7	2.599	2.561	97.22%	2.78%
101	114.3	1.26	600	0.97047	1061.7	2.599	2.561	97.22%	2.78%
$N_{des.}$ 102	**114.3**	**1.26**	**599**	**-------**	**-------**	**2.5992**	**2.561**	**97.22%**	**2.78%**

Annex 03. Framework of rail modeling

3.1. Kentrack theory

The loading conditions in HMA tracks are different from those in asphalt highway pavements, the parameter values used for the design of highway pavements may not apply to HMA trackbeds. However, in the absence of experience and field data on HMA track, highway criteria can serve as a guide for the design of HMA trackbeds. When several loads are applied to the rail, the stress, strain, and deflection of rail and tie can be obtained by superimposing the effect of each load. The vertical stress between the tie and the layered system is distributed over circular areas of equal diameter, so the *Burmister's layered theory* [1943] can be used (Figure 3).

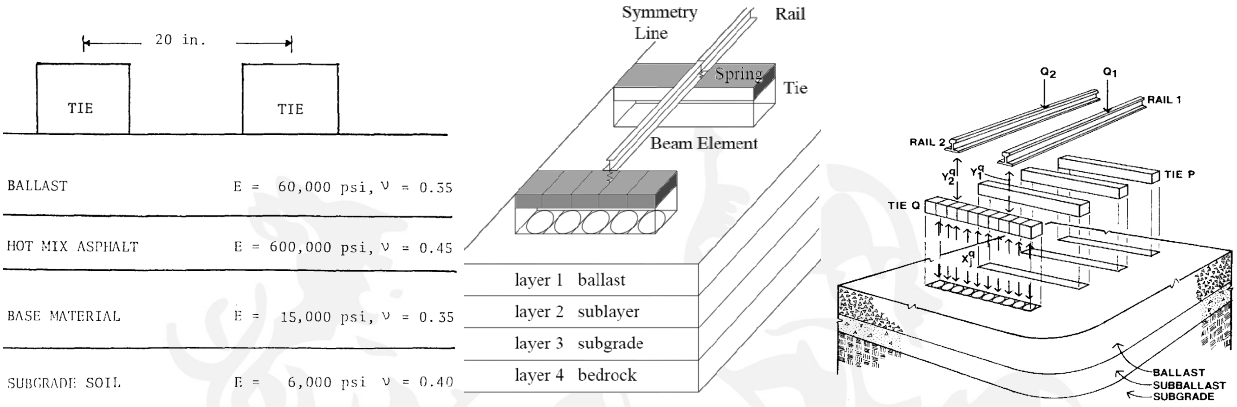


Figure 3. (a) Material Properties Used for Analysis; (b) Scheme of rail tie division; (c) Geotrack Railtrack

Static modeling of the superstructure is partial modeling, which divides the global system into its essential elements, it focuses on the calculation of subsets and elements and determines the forces.

There are several templates used in literature to describe the railway superstructure [Indraratna, B. 2016; Indraratna, B. et al. 2010; Rose, J.G. et al. 2014; Chang, C. et al. 1980], and everyone points to an area of expertise, although the theories of reference belong to the study of the problem of the beam placed on a half-space continuous elastic. The model called "Winkler" is infinite is a schematic drawing as a bed of parallel springs, independent, characterized by the same spring constant C which is independent of the shape of the support surface and the behavior of adjacent elements in those loaded [Esveld, C. (2001) Modern railway track; Cai, Z. et al. 1994] (Figure 4).

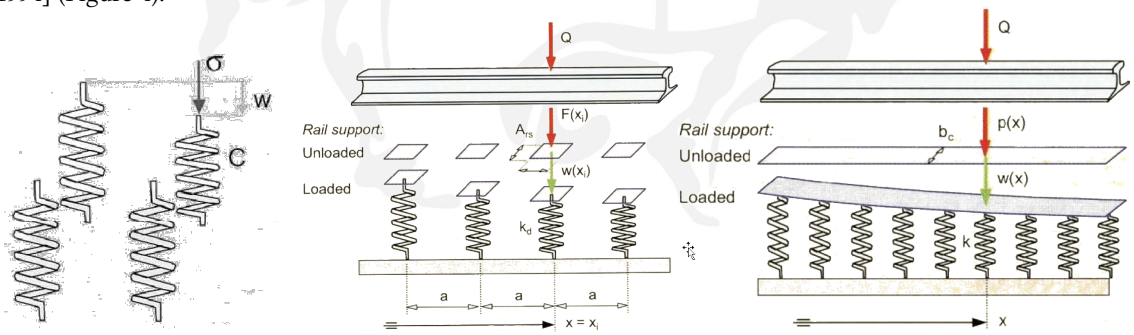


Figure 4. (a) Winkler model; (b) Discrete elastic model; (c) Continuous elastic support model

Given the symmetry found in both directions, transversal and longitudinal, only the analysis of a quarter of the system was considered. The application of finite element theory begins with the disconnection of the structure in a set of trajectory elements, numbered and schematized (Figure 5). All nodes are numbered transversely from one section to another, from top to bottom and from the outside edge to the center of the section, thus proceeding for all the others. The beam elements are longitudinally numbered along the rails and the attachment elements, and in the transverse direction for the crossbars.

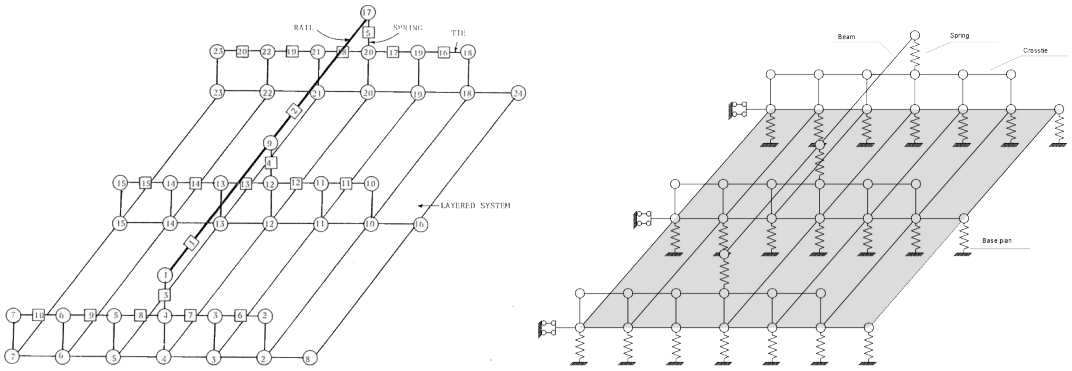


Figure 5. (a) Schematization of node elements; (b) Structural modelization

The stiffness matrix for the rail can be written as:

$$\begin{bmatrix} \frac{12EI}{L^3} & \frac{6EI}{L^2} & -\frac{12EI}{L^3} & \frac{6EI}{L^2} \\ \frac{6EI}{L^2} & \frac{4EI}{L} & -\frac{6EI}{L^2} & \frac{2EI}{L} \\ \frac{12EI}{L^3} & -\frac{6EI}{L^2} & \frac{12EI}{L^3} & -\frac{6EI}{L^2} \\ \frac{6EI}{L^2} & \frac{2EI}{L} & -\frac{6EI}{L^2} & \frac{4EI}{L} \end{bmatrix} \cdot \begin{bmatrix} w_i \\ \vartheta_{y_i} \\ w_j \\ \vartheta_{y_j} \end{bmatrix} = \begin{bmatrix} P_i \\ M_{y_i} \\ P_j \\ M_{y_j} \end{bmatrix} \quad \text{(Eq. 13)}$$

- E = Young's modulus;
- I = moment of inertia of the rail;
- L = the distance between node i and j,
- wi = vertical deflection at node i;
- -Pi = vertical force applied at node i;
- M_{yi} = moment about y-axis at node i.

Rails and ties, considered as beam elements, are orthogonal to each other. Figure 6 shows a beam element for a rail and a tie.

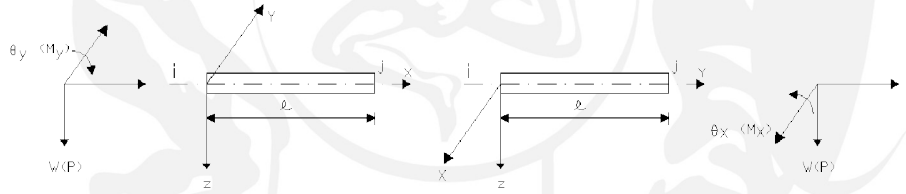


Figure 6. (a) Rail; (b) Tie

The stiffness matrix of the cross member is obtained by changing the y-axis with x, while the stiffness matrix of the spring element is as follows:

$$\begin{bmatrix} C_s & -C_s \\ -C_s & C_s \end{bmatrix} \cdot \begin{bmatrix} w_i \\ w_j \end{bmatrix} = \begin{bmatrix} P_i \\ P_j \end{bmatrix} \quad \text{(Eq. 14)}$$

- Cs= spring elastic constant;
- Wi, Wj = vertical deflection at Node i and Node j respectively.

Based on the calculations, loads below ties can be determined. Burmister's multi-layered system theory [Burmister, D.M., (1943) The Theory of Stresses and Displacements in Layered System and Applications to the Design of Airport Runways, Proceedings, Highway Research Board, Vol.23, 1943, pp.126-144], can be applied to calculate stresses and strains in the trackbed. However, due to the necessity of the multi-layered theory, the loads are simplified as intent circular loads. After calculating the stiffness matrices of every single element, the whole stiffness matrix of the structure is assembled. In the layered system, the reactive foundation forces are applied to the bottom of the ties. The overall equilibrium equations can be written as Eq. 15 (Huang et al. 1984, "Hot Mix Asphalt for Railroad trackbeds- Structural Analysis and design," Asphalt Pavement Technology, 53):

$$\left[\underline{\underline{K}}\right] \cdot \begin{bmatrix} \underline{\delta}_{rail} \\ \underline{\delta}_{crossbar} \end{bmatrix} = \begin{bmatrix} \underline{F}_{rail} \\ 0 \end{bmatrix} - \begin{bmatrix} 0 \\ \underline{F}_{crossbar} \end{bmatrix} \quad \text{(Eq. 15)}$$

- $\left[\underline{\underline{K}}\right]$ = matrix of global rigidity of the armament excluding the foundation;

- $\underline{\delta}_{rail}$ = vector shift and rotation over y-axis of all nodes of the rail;
- $\underline{\delta}_{crossbar}$ = vector displacements and rotations over x-axis of all cross nodes;
- F_{rail} = response on the rail due to the load per single wheel;
- $F_{crossbar}$ = reaction of the laying plane on the crossbar due to single wheel load.

To determine F_{rail}, Burmister's theory is used, where the vertical lowering of a point on the upper surface is given by a unit force applied to the center of a circular surface constituting a node, located at a distance "r" from the adjacent one. The flexibility matrix of the foundation is given by:

$$\left[\underline{\underline{G}}\right]\cdot\begin{bmatrix}P_1\\..\\P_i\\..\\P_n\end{bmatrix}=\begin{bmatrix}w_1\\..\\w_i\\..\\w_n\end{bmatrix}\rightarrow\left[\underline{F_{tie}}\right]=\begin{bmatrix}P_1\\..\\P_i\\..\\P_n\end{bmatrix}=\left[\underline{\underline{G}}\right]^{-1}\begin{bmatrix}w_1\\..\\w_i\\..\\w_n\end{bmatrix}\Rightarrow\left[\underline{\underline{K}}\right]\cdot\left[\underline{\delta}\right]=\left[\underline{F}\right] \quad \text{(Eq. 16)}$$

- [G] = flexibility matrix of foundation;
- Pi = vertical force at node i;
- Wi = vertical deflection to node I;
- $[F_{tie}]$= the reactive forces at the tie;
- $\left[\underline{\underline{K}}\right]$= overall stiffness of the structure;
- {δ }= overall displacement;
- {F}=overall reactive forces.

Once the movements are determined, it is possible to determine the tensions and deformations. Because the stresses and link elements are not the same, the average value is considered.

3.1.1. Multilayer modelization

For the calculation of the tensions and deformations of the layers forming the system, the theory of elastic multilayer is used. In the multilayer system shown in Figure 7, the n^{th} layer has an infinite thickness, and the elasticity modulus and Poisson coefficient of the j^{th} layer are respectively E_j and ν_j respectively.

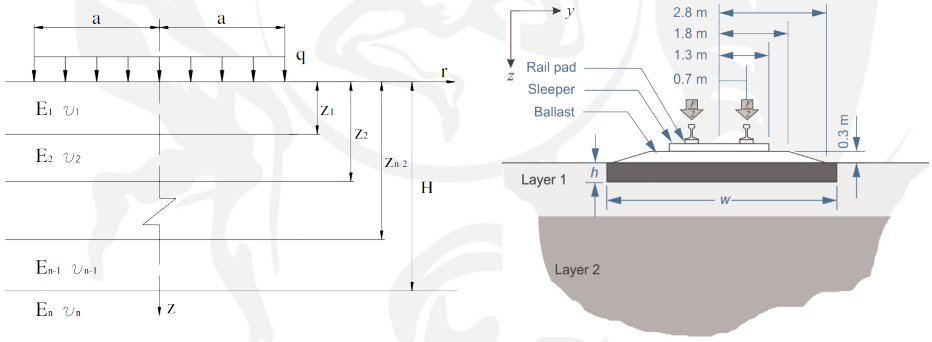


Figure 7. (a) Circular load bearing surface on the multilayer system; (b) Example sketch of track section at layered soil site with soil stiffening at the surface

A unit load ***q*** is distributed on a circular radius ***a***. Tensions and deformations at any point in the system are determined by the equation of the elastic multilayer written in cylindrical coordinates. The radius of the loading area is determined by the contact area of the crossbar and the multi-level system; If the crossbar is fractionated in a finite number of elements, the area of each circular surface is *A/m*.
By using the general equation of Burmister's multi-layered theory as shown in Eq. 17, the stresses in vertical, tangential and radial directions, the shear stresses, and the strains (displacements) in radial and vertical directions can be expressed and calculated.

$$\nabla_{\sigma}^{4}=\left(\frac{\partial_{\sigma}^{2}}{\partial_{r^2}}+\frac{\partial_{\sigma}}{r\partial_{r}}+\frac{\partial_{\sigma}^{2}}{\partial_{r^2}}\right)\cdot\left(\frac{\partial_{\sigma}^{2}}{\partial_{r^2}}+\frac{\partial_{\sigma}}{r\partial_{r}}+\frac{\partial_{\sigma}^{2}}{\partial_{Z^2}}\right)\rightarrow\alpha=\frac{a}{H};\quad\rho=\frac{r}{H};\quad\lambda=\frac{z}{H} \quad \text{(Eq. 17)}$$

- r and z, are the radial and vertical coordinates of the stress-point;
- H the distance from the surface to the top of the lower layer. The four vertical and horizontal strain and vertical deformation components of the j^{th} layer.

However, these values are not the real stresses and displacements resulting from a uniform load q distributed over a circular area. Hankel transform method is used to find the actual stresses and displacements under a uniform load over a circular area. Then, the results obtained from the above equations can be converted to stresses and displacements by using Eq. 18. To ensure that the circular surfaces are uniformly spaced along the crossbar, the length of the finished elements must be kept as uniform as possible. Eq. 19 to Eq. 24 are reported as a solution of the Eq. 16 using the Hankel transformation method (Eq. 18).

$$R = \frac{q \cdot a}{H} \int_0^{\infty} \frac{R^*}{m} J_1\left(\frac{m \cdot a}{h}\right) dm \quad where \quad R^* = -m \cdot J_o(m \cdot \alpha) \tag{Eq. 18}$$

- R^* = the stress or displacement due to the loading;
- R = the stress or displacement due to load q;
- J = Bessel function;
- m = a parameter.

$$(\sigma_z)_j = q \cdot \alpha \int_0^{\infty} J_o \cdot (m \cdot \rho) \cdot J_1 \cdot (m \cdot \alpha) \left\{ \left[A_j - C_j (1 - 2 \cdot \upsilon_j - m \cdot \lambda) \right] \cdot e^{-m \cdot (\lambda_j - \lambda)} + \right.$$
$$\left. + \left[B_j + D_j (1 - 2 \cdot \upsilon_j + m \cdot \lambda) \right] \cdot e^{-m \cdot (\lambda - \lambda_{j-1})} \right\} \cdot dm \tag{Eq. 19}$$

$$(\sigma_r)_j = -q \cdot \alpha \int_0^{\infty} J_1 \cdot (m \cdot \alpha) \left\{ \begin{array}{l} \left[J_o \cdot (m \cdot \rho) - \frac{J_1 \cdot (m \cdot \rho)}{m \cdot \rho} \right] \cdot \left\{ \left[A_j + C_j (1 + m \cdot \lambda) \right] \cdot e^{-m \cdot (\lambda_j - \lambda)} + \right. \\ \left. + \left[B_j - D_j (1 - m \cdot \lambda) \right] \cdot e^{-m \cdot (\lambda - \lambda_{j-1})} \right\} + 2\upsilon_j \cdot J_o \cdot (m \cdot \rho) \cdot \left[C_j \cdot e^{-m \cdot (\lambda_j - \lambda)} - D_j \cdot e^{-m \cdot (\lambda - \lambda_{j-1})} \right] \end{array} \right\} \cdot dm \tag{Eq. 20}$$

$$(\sigma_t)_j = -q \cdot \alpha \int_0^{\infty} J_1 \cdot (m \cdot \alpha) \left\{ \begin{array}{l} \frac{J_1 \cdot (m \cdot \rho)}{m \cdot \rho} \left\{ [A_j + C_j (1 + m \cdot \lambda)] \cdot e^{-m \cdot (\lambda_j - \lambda)} + [B_j - D_j (1 - m \cdot \lambda)] \cdot e^{-m \cdot (\lambda - \lambda_{j-1})} \right\} + \\ 2\upsilon_j \cdot J_o \cdot (m \cdot \rho) \cdot \left[C_j \cdot e^{-m \cdot (\lambda_j - \lambda)} - D_j \cdot e^{-m \cdot (\lambda - \lambda_{j-1})} \right] \end{array} \right\} \tag{Eq. 21}$$

$$(\tau_{rz})_j = -q \cdot \alpha \int_0^{\infty} J_1 \cdot (m \cdot \rho) \cdot J_1 \cdot (m \cdot \alpha) \cdot \left\{ [A_j + C_j (2 \cdot \upsilon_j + m \cdot \lambda)] \cdot e^{-m \cdot (\lambda_j - \lambda)} - \right.$$
$$\left. [B_j - D_j (2 \cdot \upsilon_j - m \cdot \lambda)] \cdot e^{-m \cdot (\lambda - \lambda_{j-1})} \right\} \cdot dm \tag{Eq. 22}$$

$$(w)_j = \frac{(1 + \upsilon_j) \cdot q \cdot a}{E_j} \int_0^{\infty} \frac{J_0 \cdot (m \cdot \rho) \cdot J_1 \cdot (m \cdot \alpha)}{m} \cdot \left\{ \left[A_j - C_j \cdot (2 - 4 \cdot \upsilon_j - m_\lambda) \right] \cdot \right.$$
$$\left. e^{-m \cdot (\lambda - \lambda_{j-1})} - [B_j + D_j (2 - 4\upsilon_j + m \cdot \lambda)] \cdot e^{-m \cdot (\lambda - \lambda_{j-1})} \right\} \cdot dm \tag{Eq. 23}$$

$$(u)_j = \frac{-(1 + \upsilon_j) \cdot q \cdot a}{E_j} \int_0^{\infty} \frac{J_0 \cdot (m \cdot \rho) \cdot J_1 \cdot (m \cdot \alpha)}{m} \cdot \left\{ \left[A_j + C_j \cdot (1 + m_\alpha) \right] \cdot \right.$$
$$\left. e^{-m \cdot (\lambda_j - \lambda)} + [B_j - D_j (1 - m \cdot \lambda)] \cdot e^{-m \cdot (\lambda - \lambda_{j-1})} \right\} \cdot dm \tag{Eq. 24}$$

- σ_z = vertical tension in the direction z;
- σ_r = long radial tension;
- σ_t = tangential tension along the direction t;
- τ_{rz} = shear strength;
- λ = vertical displacement;
- u = radial displacement;
- Jo = Bessel's function;
- J1 = 1st Bessel's function;
- m = parameter;
- A, B, C, D =integration constants.

The parameter j is the j[th] layer, and λj indicates the dimensional distance from the surface to the base of the j[th] layer. For a multilayer system, there are four integration constants per layer. However, the A_n and C_n constants for the deeper layer are set to zero, which is because the coefficient λ is infinite. Consequently, the number of constants is reduced to $4 \cdot (n-2)$, and the system can be solved with two contour conditions and $4 \cdot (n-1)$ conditions of congruence. The two contour conditions on the surface of the first layer imply that:

- the vertical voltage must be equal to q within the load area and zero to the outside;
- the cutting effort on the surface is null.

The four equations in each interface (n-1) between two layers are vertical tension, shear stress, vertical movement, and continuous radial displacement in the interface.

3.1.2. Superposition principle

Because KENTRACK is a linear elastic model with the layered foundation extended infinitely in the horizontal direction, the superposition principle can be applied. A standard case with a single wheel load P is always analyzed first. Stresses, strains, and deflections in the track system due to multiple wheel loads are obtained by superposing the results of the single wheel load (Figure 8). The load P is distributed over 6 ties to assume that the wheel load gives reliable results. The variable S_i is the deflection in the i^{th} tie due to load P.

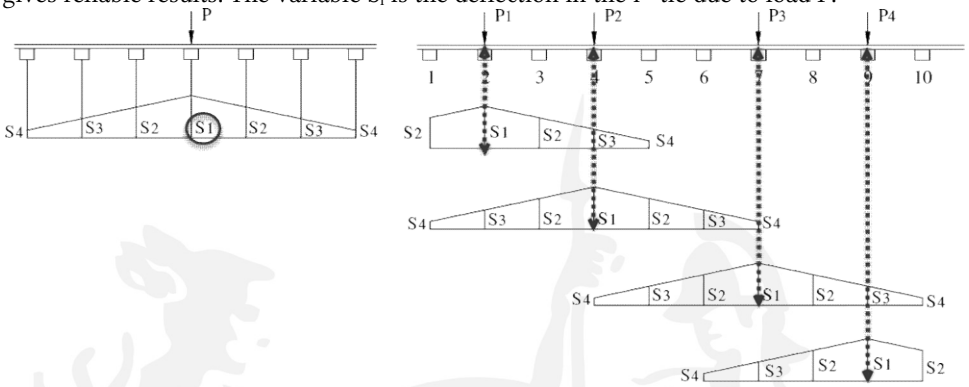


Figure 8. Superposition of Multiple Loads

The deflections in the rail-ties due to each of loads P_1 to P_4 are shown in the figure. After superposing, the deflection at the first rail tie can be calculated as Eq. 25 (Huang et al. 1984).

$$S_1^{'} = S_2 \cdot (\frac{P_1}{P}) + S_4 \cdot (\frac{P_2}{P}) \qquad \text{(Eq. 25)}$$

- S_i is the deflection in the i^{th} rail tie due to load P.

Annex 04. KENPAVE computer program

4.1 KENPAVE. A computer package for Pavement Analysis

Kenpave is a software developed by Dr. Yang H. Huang offered in his second edition of Pavement Analysis and Design published in 1993. The original four separate computer programs, LAYERINP, KENLAYER, SLABSINP, KENSLABS, were combined and integrated with some other graphics programs to form this new software. KENPAVE was written in Visual Basic. Details on the use of the software can be found on the computer screens.

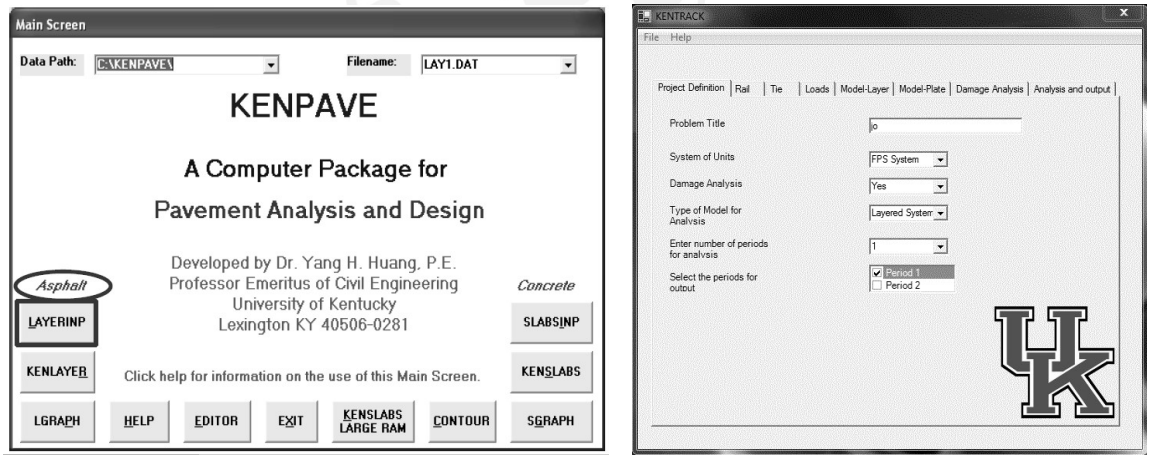


Figure 9. (a) Kenpave interface (Dr. Huang); (b) Kentrack software (Dr. Jerry Rose).

Figure 9a shows the main screen of KENPAVE, consisting of two input boxes at the top and 11 command buttons at the bottom. The left three buttons are used for flexible or asphalt pavements, the right five for rigid or concrete pavements, and the remaining three for general purposes. This software available for design of flexible pavements in roads is used for the analysis of stress-strain state in a 5-layer elastic system (Figure 10). In road pavements, the *subgrade* is of course aggregates or soil substrate. *Capping* is a subgrade improvement layer, as it is uneconomical to place high-value materials straight onto a weak soil. Capping itself is cheap, locally available material, sometimes the subgrade soil treated with lime, cement or some other hydraulic binder.

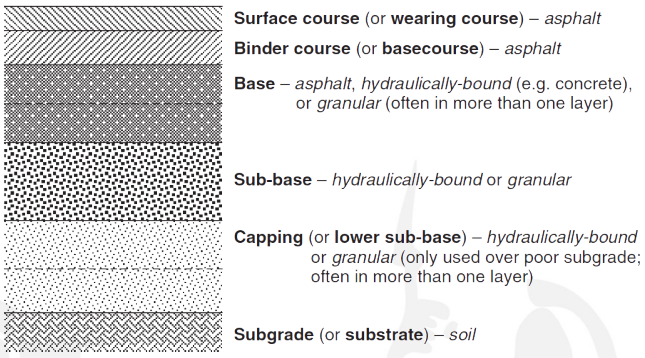


Figure 10. Pavement layer terminology (N. Thom "Principles of Pavement Engineering")

The *surface course* is a high-quality (and therefore expensive) material, tough enough to withstand direct loading, and with surface properties designed to achieve adequate skid resistance. As it is expensive, it is not a thick layer, 20–50 mm being typical. The *base layer* is the layer that gives the pavement most of its strength. It is usually relatively thick (often 200 mm or more) and therefore has to be as inexpensive as possible within the constraints of the required mechanical properties. The result is that large aggregate size tends to be used, whether the layer is asphalt, concrete or granular material. In concrete, this presents no problem; however, a likely side-effect of large aggregate size in an asphalt or roller-compacted hydraulically-bound base is a relatively uneven finish.

The *binder course* material is often very similar to the base, but with a smaller aggregate size, which means it can be laid to a typical thickness of 50–80 mm. Finally, the sub-base is much more than just a fill-in layer. The performance of an asphalt base is critically dependent on the stiffness of the layer immediately beneath, because of its influence on the flexure of the base under traffic load. Sub-bases, therefore, vary from high-quality granular materials to even stiffer hydraulically-bound layers. A typical thickness is 150 mm.

4.2 KENPAVE. Example.

The first step is to determine the state of stress and strains under a standard 80 kN single axle load, with a medium value of 85 psi (bar) tire pressure and 12.62" (32cm) spacing between the dual tires. For the road simulations (because we need to compare with railway loads) heavy trucks loads are considered and for a typical construction of pavement for major high-speed highways (Figure 11).

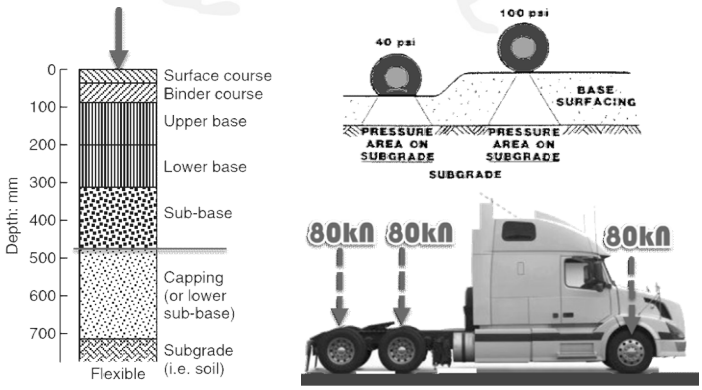
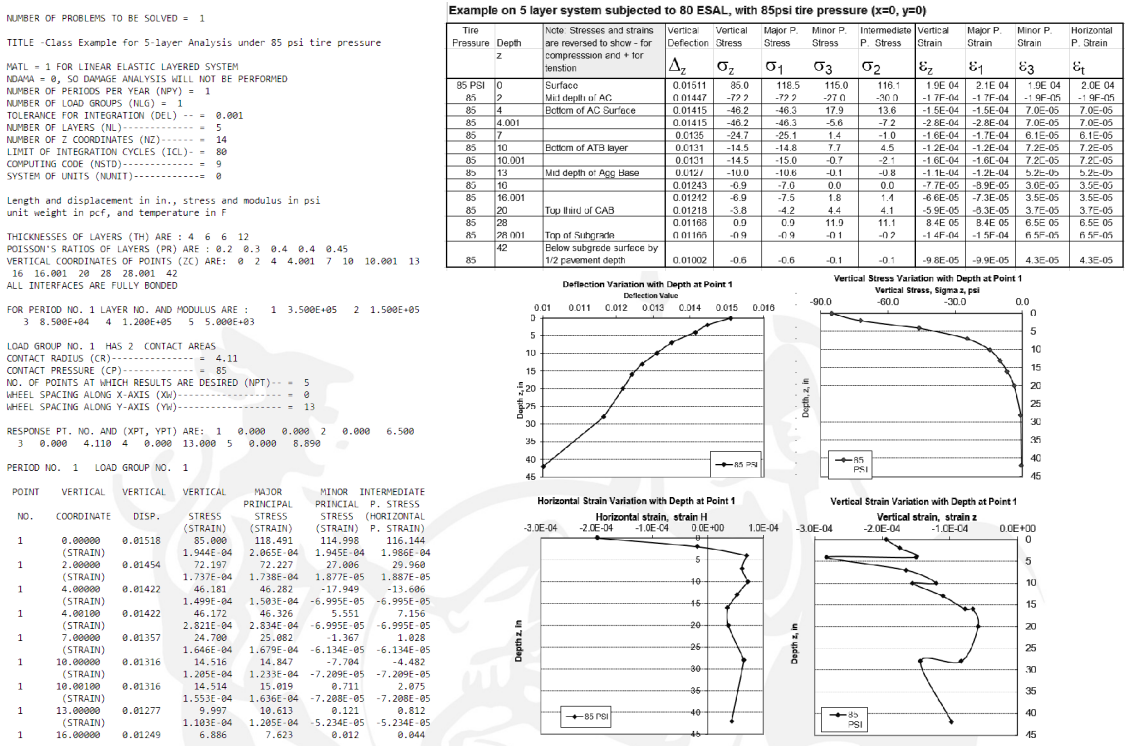


Figure 11. (a) Road section; (b) Importance of tire pressure; (c) Vehicle considered for road-load simulation

The data is divided into groups and can be found by clicking the appropriate command. Instructions follow each menu during the process. Once the input parameters are entered into the program interface, we proceed systematically with each program label.

The process continues introducing the TNLR (Total number of load repetitions for each load group during each period, and then, saving all the input data. After completing this form, click 'OK' to return to the primary form, and we obtain an output file.txt (Figure 12).



```
NUMBER OF PROBLEMS TO BE SOLVED =  1

TITLE -Class Example for 5-layer Analysis under 85 psi tire pressure

MATL = 1 FOR LINEAR ELASTIC LAYERED SYSTEM
NDAMA = 0, SO DAMAGE ANALYSIS WILL NOT BE PERFORMED
NUMBER OF PERIODS PER YEAR (NPY) =  1
NUMBER OF LOAD GROUPS (NLG) =  1
TOLERANCE FOR INTEGRATION (DEL) -- =  0.001
NUMBER OF LAYERS (NL)---------- =  5
NUMBER OF Z COORDINATES (NZ)----- =  14
LIMIT OF INTEGRATION CYCLES (ICL)- =  80
COMPUTING CODE (NSTD)---------- =  0
SYSTEM OF UNITS (NUNIT)----------=  0

Length and displacement in in., stress and modulus in psi
unit weight in pcf, and temperature in F

THICKNESSES OF LAYERS (TH) ARE :  4  6  6  12
POISSON'S RATIOS OF LAYERS (PR) ARE :  0.2  0.3  0.4  0.4  0.45
VERTICAL COORDINATES OF POINTS (ZC) ARE:  0  2  4  4.001  7  10  10.001  13
 16  16.001  20  28  28.001  42
ALL INTERFACES ARE FULLY BONDED

FOR PERIOD NO. 1 LAYER NO. AND MODULUS ARE :    1  3.500E+05    2  1.500E+05
   3  8.500E+04    4  1.200E+05    5  5.000E+03

LOAD GROUP NO. 1  HAS 2  CONTACT AREAS
CONTACT RADIUS (CR)------------- =  4.11
CONTACT PRESSURE (CP)----------- =  85
NO. OF POINTS AT WHICH RESULTS ARE DESIRED (NPT)-- =  5
WHEEL SPACING ALONG X-AXIS (XW)------------------ =  0
WHEEL SPACING ALONG Y-AXIS (YW)------------------ =  13

RESPONSE PT. NO. AND (XPT, YPT) ARE:  1   0.000   0.000  2   0.000   6.500
  3   0.000   4.110  4   0.000  13.000  5   0.000   8.890

PERIOD NO.  1   LOAD GROUP NO.  1

 POINT     VERTICAL     VERTICAL     VERTICAL      MAJOR       MINOR   INTERMEDIATE
                                                PRINCIPAL   PRINCIAL   P. STRESS
  NO.     COORDINATE      DISP.       STRESS      STRESS      STRESS   (HORIZONTAL
                                     (STRAIN)    (STRAIN)    (STRAIN)   P. STRAIN)
  1         0.00000     0.01518      85.000      118.491     114.998     116.144
            (STRAIN)                1.944E-04   2.065E-04   1.945E-04   1.986E-04
  1         2.00000     0.01454      72.197      72.227      27.006      29.960
            (STRAIN)                1.737E-04   1.738E-04   1.877E-05   1.887E-05
  1         4.00000     0.01422      46.181      46.282      -17.949     -13.606
            (STRAIN)                1.499E-04   1.503E-04   -6.995E-05  -6.995E-05
  1         4.00100     0.01422      46.172      46.326      5.551       7.156
            (STRAIN)                2.821E-04   2.834E-04   -6.995E-05  -6.995E-05
  1         7.00000     0.01357      24.700      25.082      -1.367      1.028
            (STRAIN)                1.646E-04   1.679E-04   -6.134E-05  -6.134E-05
  1         10.00000    0.01316      14.516      14.847      -7.704      -4.482
            (STRAIN)                1.205E-04   1.233E-04   -7.209E-05  -7.209E-05
  1         10.00100    0.01316      14.514      15.019      0.711       2.075
            (STRAIN)                1.553E-04   1.636E-04   -7.208E-05  -7.208E-05
  1         13.00000    0.01277      9.997       10.613      0.121       0.812
            (STRAIN)                1.103E-04   1.205E-04   -5.234E-05  -5.234E-05
  1         16.00000    0.01249      6.886       7.623       0.012       0.044
```

Example on 5 layer system subjected to 80 ESAL, with 85psi tire pressure (x=0, y=0)

Tire Pressure	Depth z	Note: Stresses and strains are reversed to show - for compression and + for tension	Vertical Deflection Δ_z	Vertical Stress σ_z	Major P. Stress σ_1	Minor P. Stress σ_3	Intermediate P. Stress σ_2	Vertical Strain ε_z	Major P. Strain ε_1	Minor P. Strain ε_3	Horizontal P. Strain ε_t
85 PSI	0	Surface	0.01511	85.0	118.5	115.0	116.1	1.9E-04	2.1E-04	1.9E-04	2.0E-04
85	2	Mid depth of AC	0.01447	-72.2	-72.2	-27.0	-30.0	-1.7E-04	-1.7E-04	-1.9E-05	-1.9E-05
85	4	Bottom of AC Surface	0.01415	-46.2	-46.3	17.9	13.6	-1.5E-04	-1.5E-04	7.0E-05	7.0E-05
85	4.001		0.01415	-46.2	-46.3	-5.6	-7.2	-2.8E-04	-2.8E-04	7.0E-05	7.0E-05
85	7		0.0135	-24.7	-25.1	1.4	-1.0	-1.6E-04	-1.7E-04	6.1E-05	6.1E-05
85	10	Bottom of ATB layer	0.0131	-14.5	-14.8	7.7	4.5	-1.2E-04	-1.2E-04	7.2E-05	7.2E-05
85	10.001		0.0131	-14.5	-15.0	-0.7	-2.1	-1.6E-04	-1.6E-04	7.2E-05	7.2E-05
85	13	Mid depth of Agg Base	0.0127	-10.0	-10.6	-0.1	-0.8	-1.1E-04	-1.2E-04	5.2E-05	5.2E-05
85	16		0.01243	-6.9	-7.0	0.0	0.0	-7.7E-05	-8.9E-05	3.6E-05	3.5E-05
85	16.001		0.01242	-6.9	-7.5	1.8	1.4	-6.6E-05	-7.3E-05	3.5E-05	3.5E-05
85	20	Top third of CAB	0.01218	-3.8	-4.2	4.4	4.1	-5.9E-05	-6.3E-05	3.7E-05	3.7E-05
85	28		0.01168	0.9	0.9	11.9	11.1	8.4E-05	8.4E-05	6.5E-05	6.5E-05
85	28.001	Top of Subgrade	0.01165	-0.9	-0.9	-0.1	-0.2	-1.4E-04	-1.5E-04	6.5E-05	6.5E-05
85	42	Below subgrade surface by 1/2 pavement depth	0.01002	-0.6	-0.6	-0.1	-0.1	-9.8E-05	-9.9E-05	4.3E-05	4.3E-05

Figure 12. (a) "LAYERINP" Main Screen; (b) Layer thicknesses and general information; (c) Layer modulus and nº periods; (d) Type of axle combination; (e)Damage analysis.

Afterward, it was possible to calculate the mechanical characteristics of the bituminous materials with the Witczak [Andrei D. et al. 1999] predictive model based on the volumetric properties of the mixture and the characteristics of the binder (Equation 21).

$$log\,|E^*| = -1.249 + 0.029\rho_{200} - 0.002\rho_{200}^{\ 2} - 0.0028\rho_4 - 0.058V_a - 0.802\cdot\left(V_{b_{eff}}/(V_{b_{eff}}+V_a)\right) +$$

$$((3.97 - 0.002\rho_4 + 0.004\rho_{38} - 0.00002\rho_{38}^{\ 2} + 0.0055\rho_{34})/(1+e^{(-0{,}603-0.313log(f)-0.393log(\mu))})) \qquad \text{(Eq. 26)}$$

- $|E^*|$= Asphalt dynamic modulus [10^5 psi]; ρ200= % passing to the sieve 0.075mm;
- ρ4= % retained to the sieve 4.75mm; ρ38= % retained to the 9.5mm sieve;
- ρ34= % retained to the 19mm sieve; Vb_{eff}= effective binder content [% by volume];
- Va= air voids [% by volume]; f= frequency[2] [Hz]; and μ= binder viscosity [10^6 poise].

According to Equation 26, the viscosity is determined based on temperature (climatic zone). In this case, we considered an Italian highway as climatic zone (speed 70km/h; frequency 28Hz; CBR 15; 20-year design life). The operating methodology to calculate the temperature gradients is composed of different stages:

- Acquisition from the last 30-years of temperature values;
- Meteorological data processing, dividing the year and calculate the Tmax_min for each year-period;
- The average air temperature T^a_M (i.e., T^a_{airPE}=24.6°C; T^a_{airAI}=15.4°C)[3];
- Temperature inside each layer.

Finally, is reported the results proposed with Kenpave methodology for flexible pavements behind heavy wheels in high-speed highways (Tables 3-4)[4].

[2] Klomp's equation, f= 0.4·V (70km/h) = 28 Hz

[3] Operated by Sicilian Information Service (SIAS) by the Regional Agriculture and Forestry

TABLE 3. KENPAVE (LAYER CHARACTERISTICS)

	E (kg/cmq)	E (Mpa)	E (Kpa)	ν
SUB-BASE	1500	147.09	147090	0.5
CAPPING LAYER	-	363.5158672	363515.8672	0.35
SUB-GRADE	-	394.5980484	394598.0484	0.35
SOIL	-	394.5980484	394598.0484	0.35

TABLE 4. KENPAVE RESULTS APPLIED IN SICILIAN ROAD PAVEMENTS (3 STAGES)

Flexible pavement (Stage 01)		*(PE_Spring-Summer; AI_Autumn_Winter)*					
		Tpav (°C)	η (10^6 poise)	log |E*|	|E*| (psi)	|E*| (KPa)	ν
SURFACE COURSE (A)		21.07	0.435371807	5.70075376	502058.5599	3461572.818	0.3
BINDER COURSE	(PE)	15.79	1.694904872	5.911191539	815063.6768	5619667.692	0.3
BASE LAYER		7.59	13.9343629	6.216791132	1647369.92	11358218.72	0.3
SURFACE COURSE (A)		10.84	6.036341595	6.019086506	1044928.336	7204529.141	0.3
BINDER COURSE	(AI)	8.49	11.05318774	6.118939052	1315040.269	9066885.843	0.3
BASE LAYER		4.84	28.2288926	6.284559577	1925571.177	13276349.37	0.3
Flexible pavement (Stage 02)							
		Tpav (°C)	η (10^6 poise)	log |E*|	|E*| (psi)	|E*| (KPa)	ν
SURFACE COURSE (A)		21.07	0.435371807	5.700754376	502058.5599	3461572.818	0.3
BINDER COURSE	(PE)	15.79	1.694904872	5.911191539	815063.6768	5619667.692	0.3
BASE LAYER		0.71	81.55632535	6.376543906	2379818.883	16408277.87	0.3
SURFACE COURSE (A)		10.84	6.036341595	6.019086506	1044928.336	7204529.141	0.3
BINDER COURSE	(AI)	8.49	11.05318774	6.118939052	1315040.269	9066885.843	0.3
BASE LAYER		1.78	61.97573719	6.353847247	2258641.206	15572786.98	0.3
Flexible pavement (Stage 03)							
		Tpav (°C)	η (10^6 poise)	log |E*|	|E*| (psi)	|E*| (KPa)	ν
SURFACE COURSE (A)	(PE)	21.60	0.38004218	5.682350194	481227.2304	3317945.82	0.3
BINDER COURSE		16.58	1.382300847	5.886313847	769686.4597	5306802.712	0.3
BASE LAYER		4.68	29.42685714	6.288383158	1942598.986	13393752.01	0.3
SURFACE COURSE (A)		11.08	5.682015768	6.012595686	1029427.311	7097653.307	0.3
BINDER COURSE	(AI)	8.84	10.09439944	6.10976301	1287546.76	8877324.726	0.3
BASE LAYER		3.55	39.37190219	6.314658005	2063754.364	14229089.15	0.3

⇩

%Passing sieves	**P 3/4**	**P3/8**	**P4**	**P200**
SURFACE COURSE	0	15	32	8
BINDER COURSE	0	10	20	6
BASE LAYER	8	10	10	6

TABLE 5. KENPAVE CALCULATIONS

	G (N)	Va (%)	%b	ϒS (N/mc)	ϒSa (N/mc)	ϒb (N/mc)
SURFACE COURSE	31.5	4.5	5.5	29000	28500	10300
BINDER COURSE	30	5	5	29000	28500	10300
BASE LAYER	29	6	4.6	28500	28000	10100

	Gs (N)	Gb (N)	Vs (mc)	Vb (mc)	V (mc)	Vba (mc)	Vbe (mc)	Vbeff (mc)
SURFACE COURSE	29.85782	1.64218009	0.00102958	0.000159435	0.001245042	1.8063E-05	0.00014137	11.35481147
BINDER COURSE	28.57143	1.42857143	0.000985222	0.000138696	0.001183072	1.7285E-05	0.00012141	10.26241135
BASE LAYER	27.72467	1.27533461	0.000972795	0.000126271	0.001169219	1.7371E-05	0.0001089	9.313857556

[4] The last tables correspond to manual calculations made by having the values of air temperature and daily traffic in the road section considered. This output data has been used during the Chapter 5 for the analogy with the road-railway section. This example of a conventional highway will be adopted for the comparison of stresses in the case of a bituminous sub-ballast on the Italian railway lines.

Annex 05. KENTRACK computer program

5.1 Example of an "output-file" with Kentrack software

The output file consists of:

- A summary of input data, reactions and stresses of the rail structure (cross-ties);
- Deflection, deformation, and tension in the sections of the analyzed superstructure (rail, tie, elastic multilayer) for each temperature considered;
- Key results concerning maximum and minimum tensions, deformations and case of damage analysis during the service life of the superstructure.

As an example, an axle 160 Kn and 30-year service life output file ".txt" is reported:

```
********** INPUT DATA **********
**********************************
SYSTEM OF UNIT:  1.000000
    ++++++++
    + RAIL +
    SECTION MODULUS OF RAIL ------------------- (RSM) =      20.36
    MOMENT OF INERTIA OF RAIL ----------------- (RMOI) =      72.99
    ELASTIC MODULUS OF RAIL ------------------- (RYM) =  .2785E+08
    SPRING CONSTANT BETWEEN RAIL AND TIE -------- (RTK) =  .3426E+06
    +++++++
    + TIE +
    THICKNESS OF TIE  (THIGH) = 8.2700
    MOMENT OF INERTIA OF TIE  (TMOI) = 598.22
    WIDTH OF TIE (TWID) =  6.6500
    CENTER TO CENTER TIE SPACING (TSPA) = 23.6200
    ELASTIC MODULUS OF TIE  (TYM) =  0.4E+07
    NON-UNIFORM TIE (NONUT) = 0
    TOTAL NUMBER OF NODAL POINTS IN  TRANSVERSE DIRECTION (NPTD) = 7
    LOCATION NUMBER OF RAIL ON TIE  (LNRT) = 2
    DISTANCES FROM NODAL POINTS TO FIRST NODAL POINT(EDGE) (Y(NPTD)) =  0.   11.250  22.625   34.00     43.4170  52.833   62.250
    THICHNESS  AND  MOMENT  OF  INERTIA  AT  EACH  NODAL                  6          8.2700          598.22
POINT IN TIE :                                                  MOMENT OF INERTIA FOR EACH ELEMENT IN TIE :
        NODAL POINT      THICKNESS     MOMENT OF INERTIA                ELEMENT NO.      MOMENT OF INERTIA
          (I)        (THIGHP(I))       (TMOIP(I))                        (I)           (TMOIE(I))
           1           8.2700           598.22                          1             598.22
           2           8.2700           598.22                          2             598.22
           3           8.2700           598.22                          3             598.22
           4           8.2700           598.22                          4             598.22
           5           8.2700           598.22                          5             598.22
    ++++++++++++++++++++++++++++++++++++++++                    NUMBER OF LAYERS FOR TENSILE STRAIN
    + OPTIONS +                                                   ANALYSIS ------------------------------ (NLBT) =1
    NUMBER OF LOADS ------------------------- (NLOAD) =2       NUMBER OF LAYERS FOR COMPRESSIVE STRESS
    NUMBER OF MONTHS FOR OUTPUT -------------- (NMOUT) =5        (OR STRAIN) ANALYSIS ------------------- (NLTC) = 1
    NUMBER OF TIES FOR ANALYSIS ---------------- (NTA) = 3     BEGINNING TIE NUMBER FOR ANALYSIS ---------- (NBT) =
    LAYERED SYSTEM MODEL ---------------------- (LAYER) = 1    ENDING TIE NUMBER FOR ANALYSIS ------------- (NET) =6
    NUMBER OF MONTHS FOR ANALYSIS -------------- (NMA) =5      NUMBER OF CROSS SECTIONS(TIES) FOR OUTPUT - (NXOUT) =1
    DAMAGE ANALYSIS ------------------------- (IDAMA) =1
    +++++++++
    + LOADS +
    +++++++++
         LOAD       DISTANCE FROM       MAGNITUDE
        NUMBER         FIRST TIE          OF LOAD
          (I)          (QXD(I))          (Q(I))
           1            47.2440          17637.00
           2           141.7300          17637.00
    ++++++++++++++++++
    + OUTPUT CONTROL +
    ++++++++++++++++++
    MONTH NUMBERS FOR OUTPUT(MNOUT(NMOUT)) ARE:    1    2    3    4    5
    CROSS SECTION NUMBERS FOR OUTPUT ARE :    3
    ++++++++++++++++++++++++
    + LAYERED SYSTEM MODEL +
    ++++++++++++++++++++++++
```

```
 NUMBER OF LAYERS IN THIS SYSTEM ------------ (NLS) =          4
 NUMBER OF ASPHALT LAYERS ----------------- (NLTEMP) =          1
 TOLERANCE FOR VERTICAL DEFLECTION --------- (TORVD) =  .1000E-04
 TOLERANCE FOR TENSILE STRESS -------------- (TORTS) =  .1000E-03
 LAYER NUMBER ------------------------ (I) :       1          2          3          4
 NONLINEAR COEF. FOR PERIOD  1 - (K1( 1,I)) :   .1849E+05   .1640E+07   .2133E+05   .2133E+05
 NONLINEAR COEF. FOR PERIOD  2 - (K1( 2,I)) :   .1849E+05   .8347E+06   .2133E+05   .2133E+05
 NONLINEAR COEF. FOR PERIOD  3 - (K1( 3,I)) :   .1849E+05   .3624E+06   .2133E+05   .2133E+05
 NONLINEAR COEF. FOR PERIOD  4 - (K1( 4,I)) :   .1849E+05   .1400E+06   .2133E+05   .2133E+05
 NONLINEAR COEF. FOR PERIOD  5 - (K1( 5,I)) :   .1849E+05   .5202E+05   .2133E+05   .2133E+05
 NONLINEAR EXPONENT ---------------- (K2(I)) :      .5000      .0000      .0000      .0000
 POISSON'S RATIO ------------------- (PR(I)) :      .2000      .4000      .5000      .5000
 THICKNESS OF LAYERS ------------- (HIGH(I)) :    13.7800     4.7200    11.8100
 ++++++++++++++++++++
 + HOT MIX ASPHALT +
 ++++++++++++++++++++
 LAYER NO. FOR TEMP. ANALYSIS -- (LNTEMP(NLTEMP)) :       2
 TEMPERATURE FOR PERIOD  1 ---- (TEMP( 1,NLTEMP)) :    35.0
 TEMPERATURE FOR PERIOD  2 ---- (TEMP( 2,NLTEMP)) :    53.0
 TEMPERATURE FOR PERIOD  3 ---- (TEMP( 3,NLTEMP)) :    71.0
 TEMPERATURE FOR PERIOD  4 ---- (TEMP( 4,NLTEMP)) :    89.0
 TEMPERATURE FOR PERIOD  5 ---- (TEMP( 5,NLTEMP)) :   107.0
 AGGREGATE PASSING =200 SIEVE(() - (P200(NLTEMP)) :      6.0
 VOLUME OF VOID(() ------------------ (VA(NLTEMP)) :      6.0
 VOLUME OF BITUMEN(() --------------- (VB(NLTEMP)) :      4.6
 ASPHALT VISCOSITY AT 70'F
    (10**6 POISES) -------------- (AVIS(NLTEMP)) :      4.5
 EXPECTED LOADING FREQUENCY(HZ) :      4.65
 ++++++++++++++++++++++++++++++++++++
 + PARAMETERS FOR DAMAGE ANALYSIS +
 ++++++++++++++++++++++++++++++++++
 NO. OF LOAD REPETITIONS (PNLR(NMA)) ARE :      100.00      100.00      100.00      100.00      100.00
      LAYER NO.              FATIGUE  PARAMETERS
   (LNBT(NLBT))    (FT4(NLBT))   (FT5(NLBT)),   (FT6(NLBT))
        2             .7950       3.2910        .8530
      LAYER NO.           DEFORMATION PARAMETERS
   (LNTC(NLTC))    (FT1(NLTC))   (FT2(NLTC))   FT3(NLTC))
        3          .4837E-02       3.7340       3.5830
 **ITERATION IN NONLINEAR ANALYSIS ( FOR PERIOD NO.  1 ) :
  ITERATION NUMBER :    1
   LAYER NO.                    MODULUS          BULK STRESS
        1                      .5730E+05          .9604E+01
  ITERATION NUMBER :    2
   LAYER NO.                    MODULUS          BULK STRESS
        1                      .6049E+05          .1070E+02
  ITERATION NUMBER :    3
   LAYER NO.                    MODULUS          BULK STRESS
        1                      .6069E+05          .1077E+02
 ******************************************************
 * OUTPUT LIST *
++++++++++++++++++++++++++++++++++++++++++++
+ DEFLECTION, STRESS + STRAIN FOR EACH CROSS SECTION +
 L    : LAYER NUMBER                                          S2   : MINIMUM HORIZONTAL PRINCIPAL STRESS
 I    : NODAL POINT NUMBER IN TRANSVERSE DIRECTION            EZ   : STRAIN IN Z DIRECTION
 W    : VERTICAL DEFLECTION                                   EX   : STRAIN IN X DIRECTION
 SZ   : STRESS IN Z DIRECTION                                 EY   : STRAIN IN Y DIRECTION
 SX   : STRESS IN X DIRECTION                                 EXY  : SHEAR STRAIN IN XY DIRECTION
 SY   : STRESS IN Y DIRECTION                                 E1   : MAXIMUM HORIZONTAL PRINCIPAL STRAIN
 SXY  : SHEAR STRESS IN XY DIRECTION                          E2   : MINIMUN HORIZONTAL PRINCIPAL STRAIN
 S1   : MAXIMUM HORIZONTAL PRINCIPAL STRESS
 ******************************************************************
 CROSS SECTION NUMBER   :    3
 ++++++++
 + RAIL +
 DEFLECTION OF RAIL, W= 0.0419 ;  MOMENT OF RAIL,  M= 131316.50;  SHEAR FORCE OF RAIL ( LEFT ), Q = 5121.77
 SHEAR FORCE OF RAIL ( RIGHT ), Q = 12513.18;   MAX. BENDING STRESS OF RAIL, S1=  6449.73
 +++++++
 + TIE +
          POINT     VERTICAL          BENDING         SHEAR        BENDING        SHEAR
          NO.    DEFLECTION           MOMENT          FORCE         STRESS        STRESS
           2        .02036               0.09       -2248.30          0.00        -32.13
           3        .01541          -25574.25       -1210.21       -176.77        -17.29
           4        .01164          -27531.91          78.10       -190.31          1.12
           5        .00960          -24440.12         372.06       -168.93          5.32
           6        .00847          -20525.16         303.16       -141.87          4.33
```

```
                7        .00811                    -18730.98          0.00        -129.47              0.00
   ++++++++++++++++++++++++
   + AT BOTTOM OF LAYERS +
   ++++++++++++++++++++++++
L I     W       SZ      SX      SY      SXY     S1      S2      EZ        EX        EY        EXY       E1        E2
2 1   .01029  -3.190  68.063  58.113   -.002  68.063  58.113 -1.63E-05  1.40E-05  9.76E-06 -1.92E-09  1.40E-05  9.76E-06
2 2   .01161  -4.426 113.079 134.180   -.001 134.180 113.079 -3.13E-05  1.86E-05  2.75E-05 -7.28E-10  2.75E-05  1.86E-05
2 3   .01169  -4.108  98.335 103.644    .001 103.644  98.335 -2.58E-05  1.78E-05  2.00E-05  9.46E-10  2.00E-05  1.78E-05
2 4   .01076  -2.793  55.066  29.428    .002  55.066  29.428 -1.11E-05  1.35E-05  2.58E-06  1.68E-09  1.35E-05  2.58E-06
2 5   .00972  -1.696  25.264 -14.110   .002  25.264 -14.110 -1.87E-06  9.58E-06 -7.14E-06  1.52E-09  9.58E-06 -7.14E-06
2 6   .00909  -1.050   8.636 -38.565   .001   8.636 -38.565  3.31E-06  7.43E-06 -1.26E-05  8.86E-10  7.43E-06 -1.26E-05
2 7   .00886   -.830   2.956 -46.836   .000   2.956 -46.836  5.07E-06  6.68E-06 -1.45E-05 -1.31E-13  6.68E-06 -1.45E-05
   ********************************************************************
   + AT TOP OF LAYERS +
   ++++++++++++++++++++
L I     W       SZ      SX      SY      SXY     S1      S2      EZ        EX        EY        EXY       E1        E2
3 1   .01029  -3.190  -2.653  -2.713   .000  -2.653  -2.713 -2.37E-05  1.40E-05  9.76E-06 -1.92E-09  1.40E-05  9.76E-06
3 2   .01161  -4.426  -3.507  -3.380   .000  -3.380  -3.507 -4.61E-05  1.86E-05  2.75E-05 -7.28E-10  2.75E-05  1.86E-05
3 3   .01169  -4.108  -3.319  -3.287   .000  -3.287  -3.319 -3.78E-05  1.78E-05  2.00E-05  9.46E-10  2.00E-05  1.78E-05
3 4   .01076  -2.793  -2.373  -2.528   .000  -2.373  -2.528 -1.61E-05  1.35E-05  2.58E-06  1.68E-09  1.35E-05  2.58E-06
3 5   .00972  -1.696  -1.525  -1.763   .000  -1.525  -1.763 -2.44E-06  9.58E-06 -7.14E-06  1.52E-09  9.58E-06 -7.14E-06
3 6   .00909  -1.050  -1.018  -1.304   .000  -1.018  -1.304  5.19E-06  7.43E-06 -1.26E-05  8.86E-10  7.43E-06 -1.26E-05
3 7   .00886   -.830   -.846  -1.147   .000   -.846  -1.147  7.78E-06  6.68E-06 -1.45E-05  8.69E-15  6.68E-06 -1.45E-05
   **ITERATION IN NONLINEAR ANALYSIS ( FOR PERIOD NO.  2 ) :      ITERATION NUMBER :    1
     LAYER NO.          MODULUS          BULK STRESS
         1          .6067E+05          .1077E+02
   ****************************
   * SUMMARY OF ANALYSIS *
   ****************************
   MAXIMUM VALUES FOR RAIL AND TIE +
   +++++++++++++++++++++++++++++++++
   PERIOD  RAIL VERT.(TIE   RAIL BEND.(TIE   TIE VERT.(TIE NO.,  TIE BEND.(TIE NO.,  TIE SHEAR(TIE NO.,   TRACK
     NO.  DEFLECTION NO.)    STRESS   NO.) PRESSURE  PT. NO.)   STRESS   PT. NO.)   STRESS   PT. NO.)  MODULUS
       1     .04193 ( 3)    6449.73 ( 3)    75.82  ( 3 , 2)      .00  ( 2 , 2)   -32.13  ( 3 , 2)   6218.69
       2     .04214 ( 3)    6469.36 ( 3)    75.77  ( 3 , 2)      .00  ( 3 , 2)   -31.98  ( 3 , 2)   6176.88
       3     .04238 ( 3)    6491.11 ( 3)    75.64  ( 3 , 2)      .00  ( 5 , 2)   -31.87  ( 3 , 2)   6130.61
       4     .04256 ( 3)    6516.11 ( 3)    75.51  ( 3 , 2)      .00  ( 2 , 2)   -31.73  ( 3 , 2)   6096.52
       5     .04288 ( 3)    6545.54 ( 3)    75.21  ( 3 , 2)      .00  ( 3 , 2)   -31.71  ( 3 , 2)   6035.82
   +++++++++++++++++++++++++++++++++++++
   + MAXIMUM VALUES FOR SUPPORT SYSTEM +
   +++++++++++++++++++++++++++++++++++++
   AT BOTTOM OF LAYERS :                                          5     2    .431E+06   38.288 ( 3, 2)    .647E-04 ( 3, 2)
PERIOD  LAYER   ELASTIC   TENSILE(TIE NO.,   TENSILE (TIE NO.,          AT TOP OF LAYERS :
     NO.   NO.   MODULUS    STRESS PT. NO.)    STRAIN  PT. NO.)        1     3    .213E+05   -4.426   ( 3, 2)    -.461E-04  ( 3, 2)
       1     2    .330E+07  134.180 ( 3, 2)    .275E-04 ( 3, 2)       2     3    .213E+05   -4.750   ( 3, 2)    -.541E-04  ( 3, 2)
       2     2    .226E+07  107.401 ( 3, 2)    .325E-04 ( 3, 2)       3     3    .213E+05   -5.122   ( 3, 2)    -.659E-04  ( 3, 2)
       3     2    .141E+07   80.687 ( 3, 2)    .396E-04 ( 3, 2)       4     3    .213E+05   -5.518   ( 3, 2)    -.832E-04  ( 3, 2)
       4     2    .810E+06   57.214 ( 3, 2)    .498E-04 ( 3, 2)       5     3    .213E+05   -5.932   ( 3, 2)    -.109E-03  ( 3, 2)
**********************************************************************************************************
```

2017

Appendix

Appendix 01. Fellow individual research project (ESR8, SUPRITN)
Appendix 02. Secondment plan
Appendix 03. Overview of research and accomplishments
Appendix 04. ESR8 Research Timeline
Appendix 05. Main full contributions

Appendix 01. ESR8 – Fellow Research

This annex mentions the general aspects required by the European project SUPRITN, in which the doctoral Fernando Martínez Soto has carried out his research work. An overview of the objectives, methodology, and tasks, which in 2014 were expected are shown. SUP&R ITN has guided the ESR8 researcher on his multidisciplinary training-through-research pathway by jointly investigating railway technologies with practical methods, models, and tools for estimating their sustainability.

Fellow ESR8	Host institution *University of Palermo*	Duration *36 months*	Start date *1st Sept. 2014*
Project title: 2.2 Characterization of rubberized asphalt for railways sub-ballasts (WP2) Supervisor name: Gaetano Di Mino (University of Palermo)			
Objectives: - Provide expertise on asphalt mix-design and materials; - Define the representative test set for characterization of the investigated materials; - Determine the performance of rubberized asphalt for railways sub-ballast in terms both of mechanical behavior and of ground-borne vibrations; - Determine useful parameters for the Sustainable tool developed inside the project.			
Tasks and methodology: - An updated review of state of the art on mechanical characterization of bituminous sub-ballast; - An updated review of rubberized asphalt for railways sub-ballast; - Compare the performances amongst the analyzed types through the experimental test.			
Results: - Report on review existing rubberized asphalt technologies; - Report on experimental survey of rubberized asphalt mixture design; - Report on experimental survey of fatigue test over rubberized asphalt mixture; - A final report containing the summary of the previous reports and mechanical data.			
Dissemination: The publication linked to each report provides papers in journals and conference proceedings.			
Planned secondment: LabIC. Ugr; University of Granada (Proff. Mª Carmen Rubio Gámez)			
Risk assessment: In light of the project will be mainly carried out in the laboratory, the risk could be the temporary lack of technicians or, more likely, the failure of test devices and the interruption of the preliminary survey due to maintenance activities of test devices. As regards to risks mentioned above, the possible solution consists of keeping on the experimental investigation in the laboratory of other academic partners such as the University of Granada that have the specific test devices.			
B.3.2. Network-wide training events, schools, conferences, workshops • Road and Railway Infrastructure Management (Master Degree Course); • Dynamic Structures. Railway and Airport Infrastructure (Master Degree Course); • Pavement Management System (Post Graduate Course); • Ground Bourne Vibrations by Rail Traffic (Post Graduate Course); • LCA of Road Pavement, Distresses, and Mix-Design of Dry Asphalt Rubber Concrete (Workshop).			

Appendix 02. Secondment Plan, 3 months (ESR8, SUPRITN)

1. The first letter of admission as visiting student.

From Host Supervisor: Prof. Gaetano Di Mino (UNIPA)
Department of Civil, Environmental, and Materials Engineering,
Università degli Studi di Palermo, Viale delle Scienze - Ed. 8 90128 Palermo

To Secondment institution: Mª Carmen Rubio Gámez - Directora LaBiC Granada (UGR)
University of Granada (Spain), LaBiC Laboratorio Ingeniería de la Construcción ETSICCP C/Severo Ochoa s/n 18071

Secondment Proposal

Recently you advertised a secondment opportunity inside SUP&R ITN Project.
Congratulations on your secondment to the University of Granada within the date for the secondment is about **March-July 2017**. The expected duration is **three months**.
This letter is to confirm the current state of your entitlements with the Laboratory Engineering Construction (LabIC.ugr). Under the terms of this secondment arrangement, you will continue to be a Doctoral Researcher at the University of Palermo for the duration of the agreement.
Once your agreement is given, I will work with you to set up a formal secondment agreement. Should the terms of the secondment alter from any outlined in this letter, the terms and conditions agreed in the secondment agreement will override this letter. All entitlements and expenses accrued through your secondment will be paid out upon completion of the secondment. Further information on this has been provided to you in Marie Curie Guide for applicants 1.4.2. Secondments.
During the secondment will be expected to be accomplished this activities and trainings:

- *Develop quick and straightforward nondestructive tests to measure the complex dynamic modulus of rubberized asphalt for railway sub-ballast layer over a wide frequency/Tª range.*
- *The fatigue life, based on the modulus and linear elastic tensile strain at the bottom of each modeled layer, will be estimated and compared with the Dissipated Energy approach for modified and conventional homogeneous asphalt sub-ballast layer.*
- *Evaluate the development of improved asphalt mixes modified with crumb rubber elaborated at the University of Palermo during the first months of 2016:*
  - *Study of a conventional mixture, two RUMAC Plusride mixes with gap-graded and 1-3% of crumb rubber and a generic hybrid mixture with dense-graded. According to Italian standard for sub-ballast, binder 50/70, limestone aggregates.*
  - *Superpave mix design and fatigue life, based on the modulus and linear elastic tensile strain at the bottom of the sub-ballast layer, will be estimated and compared to the modified mixtures, performing the UGR-FACT tests.*

This letter also confirms that you will not relinquish your position in the *Department of Construction Engineering of University of Granada (Spain)* and your substantive position will be retained for the duration of the secondment. At the conclusion of the secondment, you will return to your current position at UNIPA (2016-2017). I hope that the secondment proves to be a fruitful and rewarding experience. We see this as a great opportunity and look forward to working with you.

Yours sincerely
Prof. Mª. Carmen Rubio 21/04/2015
University of Granada, Spain. Laboratory Engineering Construction
Department of Construction and Engineering Projects. School of Civil Engineering (Polytechnic Building Granada).

Signed by doctoral candidate and supervisor as follows:

Fernando Martinez Soto

Gaetano Di Mino

María del Carmen Rubio Gámez
Professor of Construction Engineering
University of Granada

2. Secondment Certificates



MRS. MARÍA DEL CARMEN RUBIO GÁMEZ, PROFESSOR AT THE DEPARTMENT OF CONSTRUCTION ENGINEERING ENGINEERING AND ENGINEERING PROJECTS AT THE UNIVERSITY OF GRANADA

CONFIRMS:

That Mr. FERNANDO MARTINEZ SOTO, with Passport number AAI996135 Doctorate student, beneficiary of mobility towards the University of Granada under the Marie Skłodowska Curie Program, is staying in our Institution from 26/03/2017 until 26/06/2017.

In witness whereof, I hereby sign this certificate in Granada, 22 June 2017

María del Carmen Rubio Gámez
Professor of Construction Engineering
University of Granada



UNIVERSIDAD DE GRANADA

CERTIFICATE OF DEPARTURE

ACADEMIC YEAR 2016/ 2017

PROGRAMME: FP7-PEOPLE-2013-ITN - Marie-Curie Action: "Initial Training Networks", Sustainable Pavements & Railways Initial Training Network, ID 607524
Name of the home Institution: University of Granada (Spain), Department of Construction Engineering, LabIC (Mª Carmen Rubio Gámez, Professor of Civil Eng.)

IT IS HEREBY CERTIFY THAT:
Mr. FERNANDO MARTINEZ SOTO, with passport number AAI996135, as doctoral student, with DNI 74672020J (ES) and/or MRTFNN79M21Z131F (IT), beneficiary of mobility from University of Palermo (Italy), has registered as a mobility student at University of Granada, Laboratorio de Ingeniería de la Construcción (LabIC.ugr), for 3 month, since 26/03/2017 until 26/06/2017.

The Department(s)/ Faculty of Construction Engineering, University of Granada

Date
22/06/2017

Stamp and Signature

Appendix 03. Overview of the research project (ESR8, SUPRITN)

3.1. An overview of the project and significant accomplishments.

The general objectives are the development of representative tests for characterization of asphalt mix-design and bituminous materials for sub-ballast, involving the performance of rubberized asphalt regarding mechanical behavior regarding both the fatigue resistance and the stiffness modulus.

Critical points of research training:

- The study of bituminous rubber-modified HMA exposed to fatigue-cracking on railway-sub ballast;
- Performing tests on coarse-rubber from tires of heavy vehicles. Optimization by dry mixing process loads considering the new methodology conducted by Kentrack software for rail traffic in Sicily, Italy (for example) using the N_{des} determined for a Superpave methodology for railways developed in the Univ. of Palermo;
- Marshall and Superpave Gyratory Compactor for (Volumetric Mix Design), techniques and procedures with crumb rubber modified asphalt by a dry process at high temperature with different sizes, types, and percentages of rubber.
- Defining the criteria for the bituminous sub-ballast mix design to reduce the approximations involved in the recipe optimization due to an inappropriate application of the Superpave system in railways.

This research is focused on an experimental survey by mechanical fatigue tests on dry-rubberized mixtures for the sub-ballast layer on railways. For developing this application is necessary, also, to study the differences between bibliography and standards, to analyze a new mix-design approach, and to evaluate dissipated energy fatigue tests explaining the fatigue life and cracking of these mixtures.

The most relevant accomplishments are both the formulation of fatigue law and optimal mix-design procedures of the rubberized asphalt using the UGR_FACT device (University of Granada) on Superpave mixtures for railway sub-ballast layer.

3.2. Detail Research Activities Pursued. Results.

- New values of conventional parameters to define bituminous mixtures to improve the characterization of rubberized asphalt by advanced tests; on the evaluation of the performance of rubberized asphalt sub-ballasted rail track through original approaches;
- A case study of bituminous sub-ballast mix design has been investigated for a first verification of the methodology proposed: “SUPERPAVE for railways”;
- Performing tests on rubber from tires of heavy vehicles. Optimization by dry mixing process loads considering the new method found conducted by Kentrack software for rail traffic; and
- A relation between traffic and sub-ballast layer temperature depending on depth on railway model.

Fernando Martinez Soto

Gaetano Di Mino

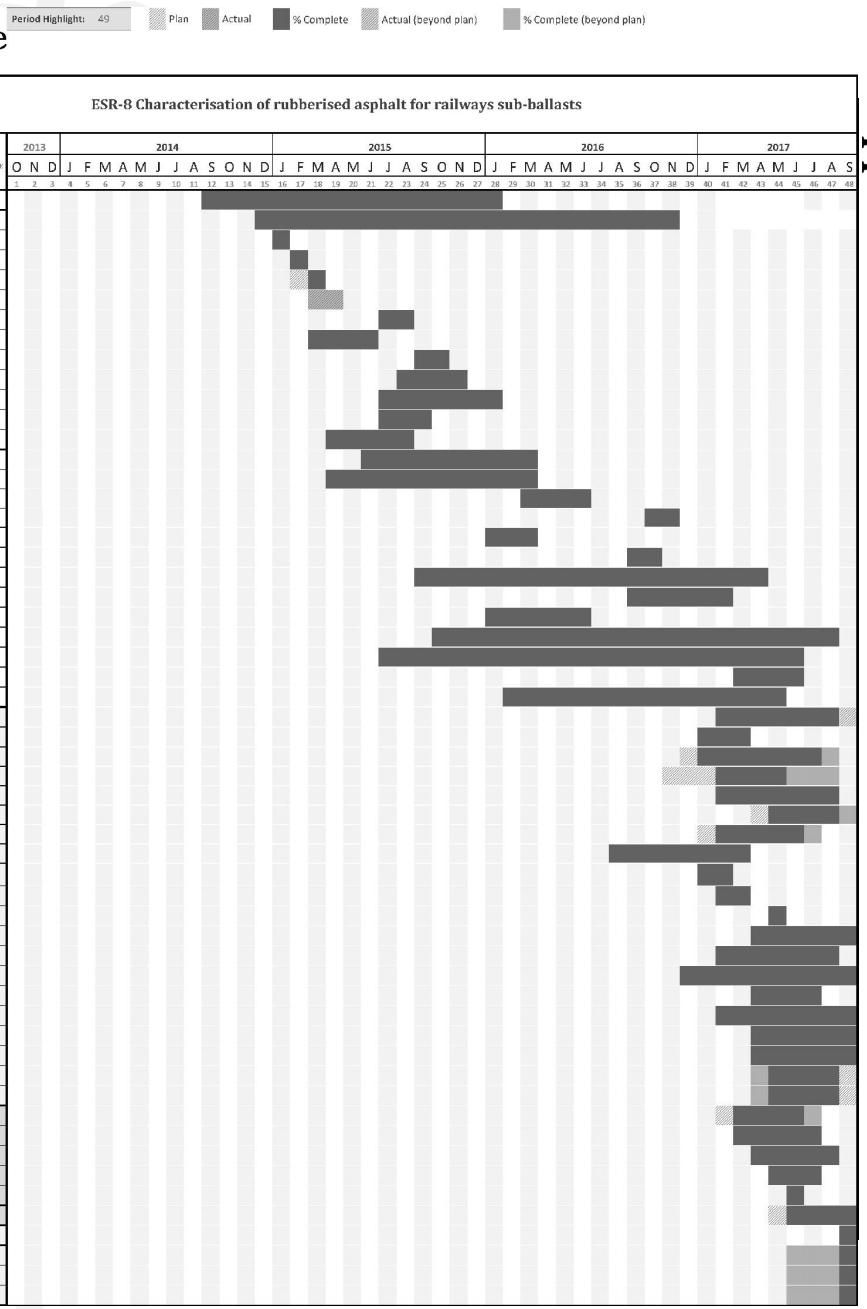
ESR8 (Fernando Martínez Soto)_____ Timeline

SUP&R ITN Sustainable Pavement & Railway Internal Training Network

The University of Nottingham UNITED KINGDOM • CHINA • MALAYSIA

ugr Universidad de Granada

ESR leader		Prof. Gaetano Di Mino, UNIPA	Project:	ESR-8 Characterisation of rubberised asphalt for railways sub-ballasts				
TASKS		ACTIVITIES		PLAN START	PLAN DURATION	ACTUAL START	ACTUAL DURATION	% COMPLETE
Tasks 2014	Task 1	*Become acquainted with literature in the field, specifications on bituminous mixtures*	UNIPA	12	17	12	17	100%
Tasks 2015	Task 2	*Experience in laboratory for testing Asphalt mixtures and equipment*	UNIPA	15	24	15	24	100%
	Workshop 1	*NOTTINGHAM: Science Outreach programme + complementary skills*	UNOTT	16	1	16	1	100%
	Workshop 2	*DUBLIN: Winter Workshop with focus on Sustainable Railway Infrastructures*	UCD	17	1	17	1	100%
	Workshop 3	*NOTTINGHAM: Outreach activities British Science day*	UNOTT	17	2	18	1	50%
	Spring School	*DELFT: 1st - 5th June 2015, Micromechanical Analysis of Asphalt Concrete course*	Delft	19	0	19	0	0%
	Workshop 4	*PALERMO: Summer School with focus on sustainability Assessment + Open Day*	UNIPA	22	2	22	2	100%
	Conference 1	*Railway Engineering 2015 29th June – 1st July, Edinburgh*	UED	18	4	28	4	100%
	Conference 2	*ANCONA: RILEM SIB conference - Official SUP&R ITN dissemination event*	UNIVPM	24	2	24	2	100%
	Conference 3	*RAILWAY TRACK SCIENCE & ENGINEERING INTERNATIONAL WORKSHOP Dec.2015, Edinburgh*	UED	23	4	23	4	100%
	Meetings	*Scientific topics evaluation: Mix design basics and fatigue tests*	UNIPA	22	7	22	7	100%
	Summer School	*SIIV SUMMER SCHOOL 2015 (Rome, Italy 7th–11th September 2015)*	Univ. Sapienza	22	3	22	3	100%
	Dissemination 1	*"Resistance to fatigue of dry asphalt rubber concrete for sub-ballast layer"*	_	19	5	29	5	100%
Tasks 2016	Conference 4	*CCRailways 2016: Research, Development and Maintenance (Sardinia, Italy April 2016)*	Sardinia	21	10	21	10	100%
	Conference 5	*TRA2016: 6th European Transport Research Conference (Poland, 18-21 April 2016)*	Poland	19	12	29	12	100%
	Conference 6	*COMPRAIL2016(15th Int. Conference on Railway Eng. Design, Madrid 19-21 July 2016)*	Madrid	30	4	30	4	100%
	Autumn School	*1° SIIV AREN, Spazio di confronto PhD. (DICAM, UNIBO, Bologna29 November 2016)*	Bologna	37	2	37	2	100%
	Workshop 5	*GRANADA Winter school 8th-12th February 2016*	UGR	28	3	28	3	100%
	Workshop 6	*SUPRITN Summer school MADRID-HUELVA 3-7 October 2016*	REPSOL-UHV	36	2	36	2	100%
	Meetings	*Scientific topics evaluation: Mix design basics and rubber mixtures. Superpave review.*	UNIPA	24	20	24	20	100%
	Dissemination 2.1	*"Benchmark parameters for defining a new mix design system for railway bituminous sub-ballast"*	-	36	6	36	6	100%
	Dissemination 2.2	*"Evaluation of Dry Asphalt Rubber Concrete in Railway Sub-Ballast using the Four Point Bending Test"*	-	28	6	28	6	100%
	Task 3	*Mix Design of dry asphalt rubber and determination of mechanical performances*	UNIPA	25	23	25	23	100%
	Task 4	*Experience in laboratory for testing the designed dry asphalt rubber mixtures*	UNIPA	22	24	22	24	100%
	Task 5	*Measurement of the fatigue properties of crumb rubberized asphalt in railways*	UNIPA	42	4	42	4	100%
	Task 7	*"Benchmark criteria for defining a new mix design system for railway sub-ballast (KENTRACK)"*	UNIPA	29	16	29	16	100%
Tasks 2017	Task 8	*This task will deal with write the thesis, revision of draft and preparation for defense*	UNIPA	41	9	41	9	100%
	Task 9	*Mixture final design (Specimens preparation with optimal %rubber, %binder, %Va)*	UNIPA	40	3	40	3	100%
	Conference 7	*BCRRA 2017 International Conference on the Bearing Capacity of Roads & Railways*	Greece	39	8	40	8	100%
	Conference 8	*WCPAM2017 (12-16 June 2017, Milan, Italy)*	Milan	38	7	41	7	100%
	Conference 9	*ICRE 2017: 19th International Conference on Railway Engineering, LONDON*	London	41	7	41	7	100%
	Conference 10	*ICRT 2017: 19th International Conference on Rail Transportation, ROME*	Rome, IT	43	5	44	5	100%
	Conference 11	*Railway Engineering RW2017, 21th-22nd June, Edinburgh (Scotland)*	UK	40	6	41	6	100%
	Conference 12	*AIIT-IC TIS Roma (April 10-12th 2017)*	Rome, IT	35	8	35	8	100%
	Workshop 7	*Winter SCHOOL 2017 NANTES (IFFSTAR, 23rd to Friday 27th of January)*	IFFSTAR	40	2	40	2	100%
	Workshop 8	*MCCA 2017 Salamanca (Spain) Marie Curie Alumni Association General Assembly and Conference*	Spain	41	2	41	2	100%
	Workshop 9	*Green Pavements Lisbon 2017, Cost Effective parameters today for a greener tomorrow*	Lisbon, PT	44	1	44	1	100%
	Conference 13	*WIIT 2017 Urban Transport, 23rd Int. Conference on Urban Transport and the Environment*	Rome, IT	43	6	43	6	100%
	Dissemination 3.1	*"Analytical approach for the mix design optimization of bituminous materials with crumb rubber"*	_	41	7	41	7	100%
	Dissemination 3.2	*"Effect of temperature and traffic on mix-design of bituminous asphalt for railway sub-ballast layer"*	_	39	10	39	10	100%
	Dissemination 3.3	*"Increased Stability of Rubber-Modified Asphalt Mixtures to Swelling, Expansion and Rebound Effect"*	_	43	4	43	4	100%
	Dissemination 3.4	*"Empirical Superpave Mix-Design of Rubber-Modified Hot-Mix Asphalt in Railway Sub-Ballast"*	_	41	8	41	8	100%
	Dissemination 3.5	*"Effective parameters to define an optimal mix-design system for the sub-ballast railroad" TJRT-2017-0019*	_	43	6	43	6	100%
	Dissemination 3.6	*"Methodology for the dimension of bituminous mixtures in railway sub-ballast" GPAV-2017-0208*	_	43	6	43	6	100%
	Dissemination 3.7	*"Optimization of mix-design system for the sub-ballast railroad" David publishing*	_	44	5	43	5	100%
	Dissemination 3.8	*"Procedure for a temperature-traffic model on rubberized asphalt layer for roads and railways" David publish*	_	44	5	43	5	100%
	Secondment	*LaBiC, Laboratory of Construction Engineering, University of GRANADA, SPAIN (4 months)*	UGR	41	5	42	5	100%
	Task 10	*Laboratory tests procedure (ITS, UGR-FACT device for fatigue cracking tests, Water sensitivity).*	UGR	42	5	42	5	100%
	Task 11	*Further investigations including more variables (CRM size, reaction time vs temperature…)*	UGR	43	5	43	5	100%
	Task 12	*Mechanical characterization of fatigue cracking: UGR_FACT device (fatigue - cracking tests)*	UGR	44	3	44	3	100%
	Workshop 10	*H. Di Benedetto (LabIC, Granada): Thermo-rheological behaviour of bit. Materials (Fatigue session)*	UGR	45	1	45	1	100%
	Dissemination 5	*Writing and publication on journal: "Fatigue resistance of crumb rubber modified mixtures" (LabIC.ugr)*	UGR	44	5	45	5	100%
	Thesis PhD.	*Presentation and doctoral dissertation on Rubber modified asphalt mixtures for railway sub-ballast*	UNIPA	48	1	48	1	100%
Tasks 2018	Conference 14	*TRA2018 "Mechanical characterization of dry-rubberized asphalt in railway sub-ballast"*	Vienna	48	4	45	4	100%
	Conference 15	*COMPRAIL2018 "Development of RUMAC for railway sub-ballast using FFRC technique"*	Lisbon, PT	48	4	45	4	100%
	Conference 16	*RAR2018 Rubberized Asphalt Rubber*	South Africa	48	4	45	4	100%



Appendix 05. Main full contributions

To develop as a full doctoral researcher in the areas of knowledge in asphalt materials and sustainability for roads and railways, during the three years of doctorate, comprehensive training was provided through research work in academic and industrial sites through the joint recruitment of the academy and the secondment to another research center. This thesis is the result of a program of complementary skills training and network-wide training events to develop competencies and career options.

This document will detail the dissemination, scientific findings and outreach presented to the International audience, and highlight the various activities that are built into the project to ensure maximum dissemination and to increase the understanding of the importance of designing and maintaining projects with sustainability.

The training activities, are aimed at enhancing the research capacities in asphalt modified mixtures with crumb rubber. Training programmed is introduced into the doctoral student to build up his team spirit and to deliver the essential scientific training. Furthermore, workshops, outreach activities and summer schools were included in it.

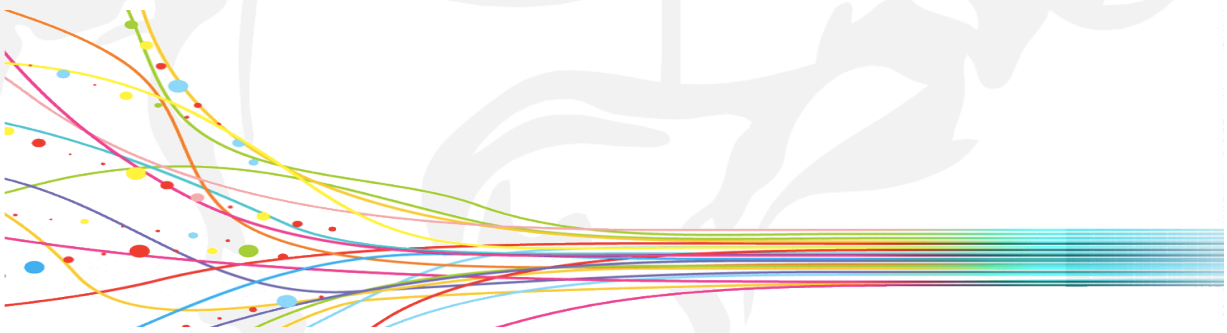
In detail, events as:

- Sustainability & LCCA applied in Railways Infrastructures;
- Scientific skills in mix-design;
- Use of techniques to test bituminous materials and performance assessment of transport infrastructure;
- Environmental Issues in Transport Infrastructures;
- Pavement Design & Construction, Transport Policy & Planning;
- Pavement Evaluation & Maintenance;
- Sustainable pavement construction, Recyclable materials for transport infrastructures;
- Introduction to Rheology and Rheometry of materials.

In addition to the public dissemination of information, the author of the thesis provides with his project website. Marie Curie website of the Supr&itn project for project dissemination has an accessible material and a database of private documents that will be accessible externally such as presentations, public deliverables and research reports, and links to media updates and other news[1].

Full contributions for future followers, please visit:

- https://unipa.academia.edu/FernandoMARTINEZSOTO
- https://www.researchgate.net/profile/Fernando_Martinez_Soto
- http://superitn.eu/wp/?page_id=865
- https://www.linkedin.com/in/fernando-martinez-soto-87322025/



[1] Intellectual Property Rights will be managed in such a way that the dissemination of knowledge can be maximized without compromising the intellectual property of any of the partners.

UNIVERSITÀ DEGLI STUDI DI PALERMO

Ingegneria Civile Ambientale – Indirizzo Infrastrutture Viarie
Dipartimento di Ingegneria Civile, Ambientale, Aerospaziale, dei Materiali - DICAM
Ingegneria Civile e Architettura – Strade, ferrovie e aeroporti - ICAR/04

2014 - 2017

CHARACTERIZATION OF RUBBERIZED ASPHALT FOR RAILWAY SUB-BALLASTS

FERNANDO MARTINEZ SOTO

Report of APA citations format

Characterization of rubberized asphalt for railway sub-ballast

Fernando Martínez Soto
PhD. Researcher, Department of Civil Engineering, University of Palermo, Italy.
E-mail: fernando.martinezsoto@unipa.it

1. Context and Relevance

The thematic area covered by this research during 2014-2017 is important from a practical point of view, since several railway authorities are considering the use of asphalt sub-ballast modified with recycled rubber, and the particular issue of the possible benefits of the inclusion of tire-dust is a reality. The subject also offers ample scope for research work at an appropriate level.

2. Scope and Content

The researcher presents an interesting study on the design and analysis of mixtures of bituminous asphalt modified with rubber, to be used as a railway sub-ballast.
The objective of increasing the load capacity of the sub-structure of the track and the ability to dampen vibrations are essential properties to ensure the durability of the railway infrastructure.
In particular, the thesis focuses on the design of asphalt mixtures that include rubber particles from waste tires through the dry process, which allows the use of significant amounts of rubber (1.5 to 3%) and then improves the durability and the mechanical performance for its application in railroads.
After the study of state of the art, the design of the mixtures is presented applying the "Volumetric mix-design" (laboratory testing applied to four mixtures) to adequately consider the effect of including considerable amounts of rubber while analyzing the influence of this component in the densification of the mixtures, which is essential to obtain an adequate mechanical behavior.
The suitable design method is the one proposed by the compaction methodology "Superpave" to be used in asphalt mixtures for rail transport, considering the equivalent axial loads for the railway lines. The last objective deals with fatigue tests using the UGR-FACT device and by means of non-destructive techniques by the NDT-FFRC (Free-Free Resonant Column) method, demonstrating that regarding applied tension, the rubberized materials showed a longer life but had a lower modulus of elasticity.
Also, the research developed is recognised into a Ph.D. thesis, that presents the study of the mechanical performance of the designed mixtures, evaluating essential properties such as resistance to cracking by fatigue, as well as a non-destructive evaluation of the features of the material.

3. Citations according to APA format

- Di Mino, G., Di Liberto, M., Noto, S., Soto, F. M., & Palermo, I. (2015). The resistance to fatigue of dry asphalt rubber concrete for sub-ballast layer. In 15th International Conference of Railway Engineering. Railway Gazette UK, July 2015, https://doi.org/10.13140/rg.2.2.11104.89606.

- Soto, F. M., Di Mino, G., & Di Liberto, C. M. (2016). "Evaluation of Dry Asphalt Rubber Concrete in Railway Sub-Ballast using the Four Point Bending Test", in J. Pombo, (Editor), "Proceedings of the Third International Conference on Railway Technology: Research, Development and Maintenance", Civil-Comp Press, Stirlingshire, UK, Paper 37, 2016. doi:10.4203/ccp.110.37

- Soto, F. M., Di Mino, G., & Acuto, F. Effect of Temperature and traffic on mix-design of bituminous asphalt for railway sub-ballast layer. Loizos, A., Al-Qadi, I., & Scarpas, T. (Eds.). (2017). Bearing Capacity of Roads, Railways and Airfields: Proceedings of the 10th International Conference on the Bearing Capacity of Roads, Railways and Airfields (BCRRA 2017), June 28-30, 2017, Athens, Greece. CRC Press.

- Soto, F. M., Mino, G. Di (2017). 'Increased Stability of Rubber-Modified Asphalt Mixtures to Swelling, Expansion and Rebound Effect during Post-Compaction'. World Academy of Science, Engineering and Technology, International Science Index, Transport and Vehicle Engineering, 11(7), 334. DOI:10.1999/1307-6892/73683
https://waset.org/abstracts/transport-and-vehicle-engineering/73683
http://thedigitaluniversity.org/Abstracts/transport-and-vehicle-engineering?&page=3

- Soto, F. M., Mino, G. D. (2017). 'Empirical Superpave Mix-Design of Rubber-Modified Hot-Mix Asphalt in Railway Sub-Ballast'. World Academy of Science, Engineering and Technology, International Science Index, Civil and Environmental Engineering, 11(9), 1905. DOI::10.1999/1307-6892/69025
https://waset.org/abstracts/civil-and-environmental-engineering/69025

- Soto, F. M., & Di Mino, G. (2017). Procedure for a Temperature-Traffic Model on Rubberized Asphalt Layers for Roads and Railways. Journal of Traffic and Transportation Engineering, 5, 171-202. DOI: 10.17265/2328-2142/2017.04.001 David Publishing Company, Valley Cottage, NY, USA [Volume 5, N°4, July-August 2017, pp.171-202].
https://www.davidpublisher.org/Public/uploads/Contribute/59acc527f2050.pdf
http://www.davidpublisher.org/Article/index?id=32566.html

- Soto, F. M., & Di Mino, G. (2017). Optimization of mix-design system for the sub-ballast railroad. Journal of Traffic and Transportation Engineering, 5, 246-259. DOI: 10.17265/2328-2142/2017.05.002 David Publishing Company, Valley Cottage, NY, USA [Volume 5, N° 5, Sept-Oct 2017, pp.246-259].
http://www.davidpublisher.org/Public/uploads/Contribute/59f2aba3819bc.pdf

- Soto, F. M. (2018) "Eco-Sustainable optimization of the mix-design methodology in modified bituminous mixtures with high percentage of recycled tire rubber," (GJESRM/A008/18) Global Journal of Engineering Science and Research Management, ISSN: 2349-4506, DOI: 10.5281/zenodo.1156460 [Volume 5, Issue 1, N°5, pp. 37-59, January 2018]
https://doi.org/10.5281/zenodo.1156460
http://www.gjesrm.com/Issues%20PDF/Archive-2018/January-2018/5.pdf

- Soto, F. M. (2018). "Volumetric Mix-Design optimization of bituminous rubber-mixtures in railway sub-ballast," (IJESRT/Q080/17) International Journal of Engineering Sciences and Research Technology, ISSN: 2277-9655, DOI: 10.5281/zenodo.1158653 [Volume 7, Issue 1, N°61, pp. 483-507, January 2018].
https://zenodo.org/record/1158653#.WoFw5OjOVHY
http://www.ijesrt.com/issues%20pdf%20file/Archive-2018/January-2018/61.pdf

- Soto, F. M., & Di Mino, G. (2018). "Characterization of rubberized asphalt for railways," (IJESRT/R067/17) International Journal of Engineering Sciences and Research Technology, ISSN: 2277-9655, DOI:10.5281/zenodo.1173468 [Volume 7, Issue 2, N°41, pp. 284-303, February 2018].
https://zenodo.org/record/1173468#.WoVvzajOWHs
http://www.ijesrt.com/issues%20pdf%20file/Archive-2018/February-208/41.pdf

- Soto, F. M., & Di Mino, G. (2018). "Improvements in the mix-design, performance features and rational methodology of rubber modified binders for the thermal evaluation of the railway sub-ballast," (IJRSM/F09/17) International Journal of Research Science & Management, ISSN: 2349-5197, DOI:10.5281/zenodo.1175219 [Volume 5, Issue 2, N°7, pp. 90-108, February 2018].
https://doi.org/10.5281/zenodo.1175219
http://www.ijrsm.com/issues%20pdf%20file/Archive-2018/February-2018/7.pdf

Signed by doctoral candidate and supervisor as follows:

Ph.D. Fernando Martinez Soto

Prof. Ing. Gaetano Di Mino

Dottorato di Ricerca in Ingegneria in Ingegneria Civile e Ambientale
Ciclo XXIX

Coordinatore: Prof. Ing. Orazio Giuffrè
Dottorando: Arch. Fernando Martinez Soto
Tutor: Prof. Ing. Gaetano Di Mino
Tesi di Dottorato: "Characterization of Rubberized Asphalt for Railway Sub-Ballast"

Relazione finale del Collegio dei Docenti

Il candidato **Fernando Martinez Soto**, nato a Granada (Spagna) il 21/08/1979, si è laureato nel mese di Giugno del 2010 in Architettura presso l'Università degli Studi di Granada con tesi dal titolo "Parque Arqueologico Periurbano y Centro de Interpretacion Museistico e Investigacion Arqueologica en Madinat Ilvira" (Relatore: Prof. Amadeo Benavent Climent – Scuola Tecnica Superiore Architettura di Granada, Correlatori: Arch. Felipe Martin Chica) con voto di laurea 7/10.

Nel 2014 ha vinto il concorso pubblico per esami per l'ammissione al XXIX ciclo (triennio Settembre 2014-Settembre 2017) del Dottorato in Ingegneria Civile, Ambientale dei Materiale (DICAM), Università degli Studi di Palermo, Viale delle Scienze, Ed. 8, 90128 PALERMO. Le attività di dottorato sono iniziate il 1 Settembre 2014.

Egli ha trascorso un periodo all'estero dal 26/03/2017 fino 26/06/2017 (3 mesi) al Laboratory Engineering Construction (LabIC UGR), Department of Construction Engineering presso la University of Granada (Spain).

I risultati degli studi compiuti sono stati pubblicati o in via di pubblicazione in riviste e conferenze internazionali.

Nell'ambito del Dottorato di Ricerca ha seguito i seguenti corsi:

- (2014) Nottingham Training Week 2014, "Scientific Introduction on Sustainable roads and railways," (8th-12th September 2014, University of Nottingham, UK).
- (2015) Nottingham (UK) Complementary skills (12th-15th January 2015, A02 Highfield House, University of Nottingham).
- (2015) Dublin Training week 2015, "Winter workshop on Railway Engineering" (2nd-6th March 2015, Irish rail & UCD, Newstead Building, University College Dublin, Belfield).
- (2015) Palermo Summer School 2015, "Sustainable assessment of transport infrastructures" (16th-23rd September 2015, University of Palermo, Italy).
- (2016) Granada Winter school 2016, "From research to Sustainable Pavement and Railway to implementation in Practical engineering Projects" (8th-12th February 2016, LaBiC at the University of Civil Engineering of Granada, Spain).
- (2016) Madrid & Huelva Summer school 2016, "Bituminous products for sustainable asphalt

technologies" (3rd-7th October 2016, Repsol Technology center in Madrid, Chemical Dpt. Pro2tes at the University of Huelva, Spain).

- (2017) Nantes Winter school 2017, "Road and railways European research" by IFFSTAR in parallel with JTR2017, Journees Techniques Route (23rd-27th January 2017, France).
- Introduction to Sustainable Development" & "The Age of Sustainable development" by Columbia University (July-August 2015).
- "How Green Is That Product? An Introduction to Life Cycle Environmental Assessment" by Northwestern University (16th June 2015, nine weeks).
- "Learning for Sustainability: Developing a personal ethic" (22nd June -26th July 2015).
- "Learning How to Learn: Powerful mental tools to help you master tough subjects" by University of California, San Diego (2016).
- "Mastering bitumen for better roads and innovative applications" (Ecole des Ponts Paris Tech. France; 4 weeks, July-August 2016).

Partecipazioni a conferenze internazionali come relatore e/o chairman:

- SIIV 2015, Summer school on Management & maintenance of civil infrastructures at the University of Sapienza (Rome), (7th-11th September 2015).
- SYB2015, 8th International RILEM Symposium, pre-conference workshops on "Testing and Characterization of Sustainable & Innovative Bituminous Materials" (Ancona, 6th October 2015, Italy).
- TRA2016, 6th EUROPEAN Transport Research conference; Marketplace Rail session, (18th-21st April 2016, Warsaw, Poland).
- Eurkind GCW 2016 Conference in Universitat Politècnica de València - Centro de Formación Permanente (Valencia, Spain, 24th-28th June 2016).
- SIIV Arena 2016, Spazio di confronto SSD ICAR/04 "Strade, Ferrovie e Aeroporti" (DICAM-UNIBO), Università di Bologna (Italy), (29th November 2016).
- JTR2017, Journees Techniques Route by IFFSTAR, (7th-8th Feb. 2017, Nantes, France).
- MCAA General Assembly & Annual Conference 2017 (Marie Curie Alumni association), (24th-25th March 2017, Salamanca, Spain).
- Green Pavements IRF/RAF Rubberized asphalt mixtures, entitled "Cost effective pavement today for a greener tomorrow," Lisbon 24th-25th May 2017 (Portugal).
- "Thermo-rheological behavior of bituminous materials and focus on Linear Viscoelasticity," about Study of Fatigue mechanical behavior of bituminous mixtures, by Professor H. Di Benedetto (University of Lyon) at Laboratory of Construction Engineering, University of Granada (29th May 2017).
- Session chairman at the ICRT2017 19th Conf. on Rail Transportation (Rome, July 2017).

Correlatore di tesi di laurea:

- Co-tutoring activity (Thesis title: "Il progetto di miscele bituminose innovative per strato di subballast ferroviario. Un nuovo approccio e indagini sperimentali", Unipa student in the department

of civil engineering, Francesco Acuto (October 2016).

- Thesis degree co-tutoring: "Studi di Lyfe cycle assessment nell'ambito delle tecnologie SUP&R ITN", Corso di Laurea in Ingegneria Civile Magistrale – Infrastrutture viarie e Trasporti, University of Palermo, Engineer student, Antonino Scaffidi Abbate (2016).

Attività didattiche integrative per i corsi di insegnamento:

- Committee Member of WASET (World Academy of Science, Engineering, and Technology).
- Session chairman at the ICRT2017 19th Conf. on Rail Transportation (Rome, July 2017).
- Ordinary member of SIIV (Società Italiana Infrastrutture Viarie).
- Ordinary member of "Marie Curie Alumni Association" (MCAA).

Le attività di Ricerca sono comprovate delle seguenti pubblicazioni:
Articoli Scientifici su riviste peer-reviewed:

- *(2015) "The resistance to fatigue of dry asphalt rubber concrete for sub-ballast layer."* Railway Gazette UK, July 2015, https://doi.org/10.13140/rg.2.2.11104.89606.
- *(2017) "Increased Stability of Rubber-Modified Asphalt Mixtures to Swelling, Expansion and Rebound Effect during Post-Compaction,"* World Academy of Science, Engineering and Technology, International Journal of Transport and Vehicle Engineering Vol: 4, Nº7, 2017, Scholar.waset.org/1999.59/73683.
- *(2017) "Empirical Superpave Mix-Design of Rubber-Modified Hot-Mix Asphalt in Railway Sub-Ballast,"* World Academy of Science, Engineering and Technology, International Journal of Civil and Environmental Engineering Vol: 4, Nº9, 2017; Scholar.waset.org/1999.20/69025.
- *(2017) "Optimization of mix-design system for the sub-ballast railroad,"* (JTTE-E 20170721-2) Journal of Traffic and Transportation Engineering, ISSN: 2328-2142, DOI: 10.17265/2328-2142/2017.05.002, David Publishing Company, Valley Cottage, NY, USA.
- *(2017) "Procedure for a temperature-traffic model on rubberized asphalt layer for roads and railways,"* (JTTE-E 20170721-1) Journal of Traffic and Transportation Engineering, ISSN: 2328-2142, DOI: 10.17265/2328-2142/2017.04.001, David Publishing Company, Valley Cottage, NY, USA.

Articoli Scientifici con status "*Under Review*"

- *(2016) "Evaluation of Dry Asphalt Rubber Concrete in Railway Sub-Ballast using the Four Point Bending Test,"* in J. Pombo, (Editor), "Proceedings of the Third International Conference on Railway Technology: Research, Development, and Maintenance," Civil-Comp Press, Stirlingshire, UK, Paper 37, 2016. doi:10.4203/ccp.110.37.
- *(2017) "Effect of temperature and traffic on mix-design of bituminous asphalt for railway sub-ballast layer,"* International Journal of Pavement Engineering (IJPE), CRC Taylor & Francis group.

Articoli Scientifici in fase di stesura

- Abstract submitted to Rubberized Asphalt Rubber 2018 (RAR2018) in South Africa at Protea Hotel Kruger Gate, September 25-28, 2018;
- TRA2018, 7th European Transport Research Conference Paper submitted entitled "Mechanical characterization of dry-rubberized asphalt in railway sub-ballast" (ID959), topic SP-7 Transport Infrastructure (16th-19th April 2018) to TRA at Vienna;
- Paper acceptance entitled "Development of dry-rubberized asphalt mixtures for railway sub-ballast using Free-Free resonant frequency technique (FFRC)" to COMPRAIL 2018 16th Intern. Conference on Railway Engineering Design, 2-4th July 2018, Lisbon Portugal).

Conference Paper – Conferenze di Rilevanza Internazionale

- Railway Engineering RW2015, paper entitled *"The resistance to fatigue of dry asphalt rubber concrete for the sub-ballast layer,"* 13th International Conference (Edinburgh, UK, 1st July 2015).
- SIIV 2015, Summer school on Management & maintenance of civil infrastructures at the University of Sapienza (Rome), Italian paper entitled "Caratterizzazione di Dry Asphalt Rubber concrete per Sub-Ballast ferroviario" (7th-11th September 2015).
- COMPRAIL 2016, 15th International Conference on Railway Engineering Design and Operation, abstract submission entitled: *"Characterization of rubberized asphalt for railway sub-ballast,"* (19-21st July 2016, Madrid, Spain).
- CCP-110 Civil-Comp. Railways 2016, 3rd International Conference on Railway Technology, Research, Development and Maintenance, paper entitled: *"Evaluation of Dry Asphalt Rubber Concrete (DARC) in railway sub-ballast using the 4PBFT",* (Cagliari, Sardinia, IT, 5-8th April 2016).
- TRA2016, 6th EUROPEAN Transport Research conference; Marketplace Rail session, ID 1587 entitled "Characterization of rubberized asphalt for railway sub-ballast" (Poster session nº 11090), topic Transport infrastructure, mode B Rails (18th -21st April 2016, Warsaw, Poland).
- SIIV Arena 2016, Spazio di confronto SSD ICAR/04 "Strade, Ferrovie e Aeroporti" (DICAM-UNIBO), Università di Bologna (Italy), Italian presentation entitled "Indagine sperimentale sul Dry Rubberized Asphalt per strato di sub-ballast ferroviario (Un nuovo approccio sul MIX DESIGN)," (29th November 2016).
- World Conference on Pavement and Asset Management, WCPAM 2017, ID-470, poster entitled: *"Effective parameters to define an optimal mix design system for the sub-ballast railroad"* (13th June 2017, Milan, Italy).
- Railway Engineering 2017, 14th International Conference, paper entitled: "*Criteria for a new mix-design system for railway sub-ballast*" (Edinburgh, Scotland, 21st-22nd June 2017).
- BCRRA-2017, 10th International Conference on the Bearing Capacity of Roads, Railways and Airfields, paper entitled: "*Effect of temperature and traffic on mix-design of bituminous asphalt for railway sub-ballast layer*," ID 196.1462313407 (28th-30th June 2017, Athens, Greece).
- ICRE-2017, 19th International Conference on Railway Engineering, paper entitled: "*Empirical Superpave mix-design of rubber-modified hot-mix asphalt in railway sub-ballast*," (London, UK 21st -22nd Sept. 2017).
- ICRT-2017, 19th International Conference on Rail Transportation, paper entitled: "*Increased Stability of Rubber-Modified Asphalt Mixtures to Swelling, Expansion and Rebound Effect during Post-Compaction*," (Rome, 17-18th July 2017).

- WIT Urban Transport 2017, 23rd International Conference on Urban Transport and the Environment, paper entitled: *"Optimization of the manufacturing process-compacting layers of sub-ballast rail through modified bituminous mixtures with rubber tires"* (Rome, 5-7th September 2017).

Contenuto della tesi (*max 2000 caratteri*)

Scrap tire rubber (STR) can be incorporated into asphalt mixtures in two different methods or techniques, which are referred to as the wet-dry process. The blending of recycled rubber with asphalt cement has been used for years and several manufacturing processes have been developed in Europe as well as in the United States. The use of a bituminous sub-ballast layer has been pointed out as an interesting alternative to the granular sub-ballast design traditionally applied in most European railroad tracks. Frequently, unbound granular materials are replaced by bituminous sub-ballast that provide additional benefits to the subgrade protection.
Much research has been conducted in finding other alternative material to be used as a modifier in asphalt mixes to improve its properties. Rubberized asphalt mixtures are regarded as a proper solution for improving the strength of the rail-track section. In comparison with traditional granular sub-ballast, these materials allow an increase in bearing capacity and greater protection of the substructure.
The recycled rubber has become a great enhancer of the modified bituminous mixtures, and in this work, it has been shown as a sustainable improvement option in HMA mixes due to the elastic behavior exposed by the rubber particles especially in reducing the fatigue cracking potential.
This thesis presents a study of laboratory evaluation on the performance of hot mix asphalt (HMA) using recycled crumb rubber as an additive. In this context, the research, therefore, aims to study the use of sustainable bituminous sub-ballast manufactured from a waste material, which is recycled rubber produced from scrap tires at the end of their service life. To this end, the procedures developed in the Department of Civil Engineering of the University of Palermo during 2014 to 2017, is focused on evaluating the mechanical behavior of bituminous materials in comparison to that presented by conventional sub-ballast. Mechanical performance is examined concerning the main requirements that need these materials (resistance to bearing capacity, energy dissipation, fatigue-cracking strength and, waterproof properties) for their use in railway tracks.
Inside the SUP&R ITN project, enrolled as an ESR-8 fellow, the main purpose of this laboratory research is the application of ambient crumb rubber (0.2mm to 0.4mm) and ground rubber (2mm to 4mm) recycled from discarded truck tires. Crumb rubber modifier is processed at a conventional temperature (20 ºC) inside hot bituminous mixtures (160-220 ºC) as a substitute for 1.5%, 2% and 3% by weight of the total aggregates using the Volumetric Mix-Design.
The impact of temperature on the mechanical properties and thermal susceptibility of the railway bituminous sub-ballast layer has served as motivation to develop the advanced measurement of the thermal cycles inside the rail track. Different simulations following the Kentrack and Kenpave software (Univ. Kentucky) were developed to be effective with the best mix-design for railways.
Thermal cycles in this layer and, an evaluation of the characteristic parameters (average seasonal temperatures interpolated by sinusoidal functions) were found.
The fine crumb rubber incorporated into asphalt mixes by using "dry process" method that mixes the crumb rubber with the aggregate before mixing it with asphalt binder. Two aggregate gradations were considered under this investigation, dense graded (asphaltic concrete with 22.4mm nominal maximum aggregate size)

and gap graded (stone mastic asphalt with 31.5mm max. aggregate size).
For each particle size distribution, of an aggregate sieve, the percentages of crumb rubber added varied from 1 to 3 percent by weight of the total aggregates. Italian standard as grading curve and Superpave gyratory compactor technique as mix-design were used.
The UGR_FACT device investigated the resistance to the fatigue characteristic as a performance indicator.
The results proved that the rubberized sustainable solution studied can offer advantages such as reducing greenhouse emissions, fuel consumption and, a suitable performance as sub-ballast for railways tracks from a mechanical behavior point of view. Moreover, it is a solution that guarantees to reduce pollution thanks to its ability to enhance mixing and compaction temperatures.
The purpose of using rubber modifiers in Hot Mix Asphalt to obtain a stiffer-elastic sustainable material has been achieved for the assessment of its behavior in sub-ballast/base layers.
Rubber-Asphalt mixes have shown a greater resistance to fatigue cracking compared to the conventional blend. The better overall performance and fatigue results obtained after that research were with an amount of two percent of crumb rubber and a six percent of bitumen added.

Valutazione della tesi e dell'attività di ricerca (*max 2000 caratteri*)

L'Architetto Fernando Martinez Soto ha frequentato il XXIX ciclo del Dottorato di Ricerca in Ingegneria Civile, Ambientale dei Materiale (DICAM), Università degli Studi di Palermo, Viale delle Scienze, Ed. 8, 90128 PALERMO, svolgendo una ricerca nell'ambito dello studio delle prestazioni meccaniche e della sostenibilità dei materiali bituminosi per uso ferroviario e sviluppando una tesi dal titolo *"*Characterization of Rubberized Asphalt for Railway Sub-Ballast.*"*

Il Collegio Docenti del Dottorato di Ricerca in Ingegneria Civile e Ambientale giudica quindi la tesi di Fernando Martinez Soto adeguata per il conseguimento del titolo di Dottore di Ricerca in Ingegneria Civile e Ambientale.

Data: 13/09/2017

Il dottorando	Il tutor	Il coordinatore
Fernando Martínez Soto	Prof. Gaetano Di Mino	Prof. Orazio Giuffrè



